Study of water resources in relation with climate in the Congo River Basin : integrated approach using in situ observations, remote sensing, and hydrological modeling

Benjamin Mambwe Kitambo

Université Fédérale
Toulouse Midi-Pyrénées

THÈSE

En vue de l'obtention du

DOCTORAT DE L'UNIVERSITÉ DE TOULOUSE

Délivré par : *l'Université Toulouse 3 Paul Sabatier (UT3 Paul Sabatier)*

Présentée et soutenue le *12/04/2023* **par :**

Benjamin MAMBWE KITAMBO

Étude de la ressource en eau en lien avec le climat dans le bassin du Congo : Approche intégrée utilisant des données in situ, la télédétection et la modélisation hydrologique

JURY

Gilles Belaud	Professeur des universités (Uni. Montpellier/G-Eau, France)	Rapporteur Président du jury
Doug Alsdorf	Professeur des universités (OSU, USA)	Rapporteur
Rodrigo Paiva	Professeur des universités (UFRGS, Brésil)	Examinateur
Frédérique Seyler	Directrice de recherche (IRD, France/Brésil)	Examinatrice
Florence Sylvestre	Directrice de recherche (IRD, France/Chad)	Examinatrice
Fabrice Papa	Directeur de recherche (IRD, France/Brésil)	Directeur de thèse
Adrien Paris	Ingénieur de recherche (Hydro-Matters/LEGOS, France)	Co-directeur de thèse
Raphaël Tshimanga	Professeur des universités (CRREBaC, Uni. Kinshasa, RDC)	Co-directeur de thèse

École doctorale et spécialité :
SDU2E : Surfaces et interfaces continentales, Hydrologie
Unité de Recherche :
LEGOS (UMR 5566)
Directeur(s) de Thèse :
Fabrice PAPA, *Adrien PARIS* et *Raphaël TSHIMANGA*
Rapporteurs :
Doug ALSDORF et *Gilles BELAUD*

Abstract

The Congo River Basin (CRB) is the world's second largest watershed in terms of river discharge and drainage area, and therefore plays a significant role in the global water cycle and Earth's climate. Yet, its hydrodynamic and hydroclimatic characteristics remained relatively poorly known mainly due to its complexity and a lack of adequate in situ observations. To overcome this challenge and taking the advantage of the recent advances in earth system sciences, a robust approach based on a combination of in situ measurement, remote sensing techniques associated with numerical hydrological modeling is proposed for a comprehensive characterization of the CRB surface hydrology at a large scale. Firstly, the research intends to validate the remote sensing derived products over the CRB, in particular, radar altimetry Surface Water Height (SWH) and Surface Water Extent (SWE) from multi-satellite using in situ data, historical and current observations. Afterward, both satellite long-term records, satellite-derived SWH and SWE were then used to analyze the spatiotemporal dynamics of surface freshwater, for instance, the regional relative contribution to the flow at the most downstream gauge here Brazzaville/Kinshasa station characterized by a bimodal hydrological regime. Secondly, the two validated datasets were further combined, and in complement with topographic dataset to estimate and analyze the long-term spatiotemporal variations of Surface Water Storage (SWS) in rivers, lakes, floodplains, and wetlands across the entire CRB over the period 1992–2015 and characterized extremes events such as extensive droughts. These datasets ensured therefore an improved monitoring of the CRB hydrological variables from space, and a better evaluation of the impact of climate variability on water availability in the region. Thirdly, due to the temporal and spatial limitations of the currents remote sensing derived datasets, a hydrological-hydrodynamic model namely MGB has been proposed to better understand the hydrological processes and hydroclimatic characteristics in a more spatially and temporally distributed manner. For this, the run of MGB model built a unique long-term dataset over 1981 to 2020 at daily time scale across the entire CRB of different hydrological variables such as river discharge and water level that bridges the gap between the past in situ databases and current and future monitoring of the CRB. This thesis work contributes to a better characterization of the hydrological variability in the CRB and represents a step forward to a better fundamental understanding of the CRB and its hydro-climatic processes, bringing more opportunities for other river basins in Africa to improve the management of water resources.

Résumé

Le bassin du Congo, deuxième plus grand fleuve mondial en termes de superficie et d'apports d'eau douce à l'océan et jouant ainsi un rôle important dans le cycle global de l'eau et le climat, reste l'un des bassins fluviaux le moins étudié du monde. Ceci limite les connaissances de ses caractéristiques hydro-climatologiques et de la variabilité y associée. La densité peu élevée du réseau des stations hydrométéorologiques et sa complexité physiographique sont parmi les causes de cet état critique des connaissances sur le bassin du Congo. Pour mieux caractériser son hydrologie de surface à l'échelle du bassin, cette thèse s'est proposée de prendre avantage des récents développements et améliorations des techniques de télédétection ainsi que de la modélisation hydrologique en combinaison avec les données in situ. Dans un premier temps, la recherche a visé à valider les produits dérivés de la télédétection sur le bassin du Congo, en particulier, la hauteur d'eau de surface (SWH) provenant de l'altimétrie radar et les étendues d'eau de surface (SWE) provenant du jeu de données des étendues d'inondation global, en utilisant des données in situ des observations historiques et actuelles. Ensuite, Ces deux ensembles de données long terme, SWH et SWE ont été utilisés pour analyser la dynamique spatio-temporelle de l'eau douce de surface, par exemple, la contribution relative régionale des sous-bassins au débit de la station la plus en aval du bassin, Brazzaville/Kinshasa caractérisée par un régime hydrologique bimodal. Deuxièmement, les deux ensembles de données validés ont été combinés et complétés par des données topographiques pour estimer et analyser les variations spatio-temporelles à long terme du stockage des eaux de surface (SWS) dans les rivières, les lacs, les plaines d'inondation et les zones humides dans l'ensemble du bassin sur la période 1992-2015. Ces ensembles de données ont donc permis d'améliorer le suivi des variables hydrologiques du bassin du Congo depuis l'espace, et de mieux évaluer l'impact de la variabilité climatique sur la disponibilité de l'eau dans la région. Troisièmement, en raison des limitations temporelles et spatiales des ensembles de données dérivées de la télédétection précédemment mentionnés, un modèle hydrologique-hydrodynamique, à savoir MGB, a été proposé pour mieux comprendre les processus hydrologiques et les caractéristiques hydro-climatiques d'une manière plus spatialement et temporellement distribuée. Pour cela, l'exécution du modèle MGB a permis de construire un ensemble de données inédit à long terme de 1981 à 2020 à l'échelle de temps journalier sur l'ensemble du bassin du Congo de différentes variables hydrologiques telles que le débit des rivières et le niveau de l'eau, qui a comblé le fossé entre les bases de données in situ historiques et les observations contemporaines et future du bassin du Congo dans son ensemble. Ce travail de thèse contribue ainsi à une meilleure

caractérisation de la variabilité hydrologique dans le bassin du Congo et représente une avancée majeure vers une meilleure compréhension du bassin du Congo et de ses processus hydro-climatiques, apportant de nouvelles opportunités pour d'autres bassins fluviaux en Afrique afin d'améliorer leur gestion des ressources en eau.

Acknowledgements

This thesis would never have been possible without the support of many people, to whom I wish to express my gratitude. I hope I have not forgotten any of them (Apologize if you miss…).

To my father God, for the breath of life and health without which this work would not have been accomplished.

I would like to express my greatest thanks and profound gratitude to my three supervisors Dr Fabrice Papa, Dr Adrien Paris and Professor Raphaël Tshimanga for their careful guidance and constructive comments that have contributed to the final production of this thesis. Thanks first of all for having imagined this ambitious thesis subject and for having accompanied me in the appropriation of the subject and the necessary theoretical knowledge, and then for having trusted me. Thanks for your great scientific skills, which resulted in fascinating conversations, but above all thanks for your human qualities, your patience and your kindness. Thanks for your endless encouragement during these three years which have not been easy due to the Covid-19 pandemic situation. Thanks Adrien, for having your door always wide open, ready to answer my several questions. Thanks Fabrice and professor Raphaël for being so available, even at the other side of the world (Brazil and DR Congo, respectively), for guiding and framing me, not always easy to manage.

I would also like to express my heartfelt gratitude to Florence Sylvestre and Sylvain Biancamaria for being available, your advice and guidance during the thesis committees. A special thanks to Frédéric Frappart and Mélanie Becker for fruitful discussion during the analysis of my results in the frame of the redaction of my articles, and to all the co-authors that participated with comments and suggestions.

I would like to extend my gratitude to Laetitia Gal and Sly Wongchuig for giving me the opportunity to learn and run the MGB model. Again Sly, a big thanks for your human qualities and support.

I am grateful to the DYnamique hydrologique du BAssin du coNGO (DYBANGO) project, which is wholly funded by the Centre National d'Études Spatiales (CNES) in support of my PhD thesis, funded by CNES, the Agence Française de Développement (AFD) and the Institut de Recherche pour le Développement (IRD), that gives me opportunities to attend international conferences as well as fieldwork activities in the CRB. A special thanks to the Congo Basin

Water Resources Research Center (CRREBaC) for hosting and supporting me during the fieldwork activities in the CRB.

Thank you to all the PhD students and CDDs with whom I shared so many good moments, and so many tea breaks. A big thanks to the hydro-matters team: Adrien, Laetitia, Romulo, Malick for fruitful scientific discussions every Tuesday after lunch. I extend my thanks to Sly and Daniel for participating to this scientific brainstorming.

Thanks to Brigitte, Agathe, Martine, Catherine and Sandra, to the info team, Caroline, as well as to the whole management team, past and present, Alexandre, Frédéric, Bertrand, for helping us on a daily basis. Thanks also to the whole doctoral school, and particularly to Geneviève Soucail, Tanya Robinson and Adrien Bru for the help given for the procedures and the follow-up of our thesis.

During the completion of my thesis, I have also had time to relax, recharge my batteries, and enjoy my surroundings here in France. I would like to extend my thanks to the Kemet team: Micael, Fernand, Lune de Grèce, Victor, Emmanuel, Jules for all the evening meals that have brightened up our weekend. A special thanks to Yannick, Thom, Max, and Christian.

My deepest gratitude and appreciation goes to my mum Grâce Kitambo because of you mum I have made it to fulfil my dreams; my sister Hélène Supa; my brothers Dominique, Jonathan, Vick, Amour for having supported me throughout my journey, you have listened to me and comforted me at every stage of my life, and for being there for me until my academic path. This achievement is shared with you all for your love, encouragement, and support. My stay in France being so far away from home was easy due to the presence of my sister Elisabeth Okwudi who travelled from London constantly to check in on me making sure that I had all I needed around me, thank you for the great laughs we share which have helped me get through some tough times and without my London family life would have been very tough. My first big sister Annie Kaoma for keeping me focused and grounded thank you, sis. To my only remaining dad Enock Katebe, my mum's Na Mwansa, Na Kaulu, and Na Mwape, for your constant prayers and encouragement. My brothers Kenneth Dr Stephen Chisama for getting me to London and for sharing amazing times during our time together. Lastly, thank you to Gaty for hosting me in Angoulême during my short breaks. Thank you too, sister Mamicho Mwansa and brother Jean-Marie Kileshye for your support.

I have been blessed to have such an amazing family without you all I wouldn't be the accomplished man I am today and for that I thank you all.

Publication record

Kitambo, B., Papa, F., Paris, A., Tshimanga, R. M., Calmant, S., Fleischmann, A. S., Frappart, F., Becker, M., Tourian, M. J., Prigent, C., & Andriambeloson, J. (2022). A combined use of in situ and satellite-derived observations to characterize surface hydrology and its variability in the Congo River basin. *Hydrology and Earth System Sciences*, *26*(7), 1857–1882. https://doi.org/10.5194/hess-26-1857-2022

Kitambo, B. M., Papa, F., Paris, A., Tshimanga, R. M., Frappart, F., Calmant, S., Elmi, O., Fleischmann, A. S., Becker, M., Tourian, M. J., Jucá Oliveira, R. A., & Wongchuig, S. (2022). A long-term monthly surface water storage dataset for the Congo basin from 1992 to 2015. *Earth System Science Data Discussions*, *2022*, 1–39. https://doi.org/10.5194/essd-2022-376

Papa, Fabrice, Crétaux, J.-F., Grippa, M., Robert, E., Trigg, M., Tshimanga, R. M., **Kitambo, B**., Paris, A., Carr, A., Fleischmann, A. S., de Fleury, M., Gbetkom, P. G., Calmettes, B., & Calmant, S. (2022). Water Resources in Africa under Global Change: Monitoring Surface Waters from Space. *Surveys in Geophysics*. https://doi.org/10.1007/s10712-022-09700-9

Tourian, M.J., Papa, F., Elmi, O., Sneeuw, N., **Kitambo, B.**, Tshimanga, R., Paris, A., Calmant, S. Current availability and distribution of Congo Basin's freshwater resources. Commun Earth Environ 4, 174 (2023). https://doi.org/10.1038/s43247-023-00836-z

Contents

List of Figures

List of Tables

Acronyms

CRB	*Congo River basin*
GIEMS-2	*Global Inundation Extent from Multi-Satellite version 2*
SWH	*Surface Water Height*
SWE	*Surface Water Extent*
SWS	*Surface Water Storage*
ENV	*ENVIronment SATellite*
ERS-2	*European Remote Sensing Satellite 2*
J2/3	*Jason satellite 2/3*
SRL	*Satellite with Argos and Altika*
S3A/B	*Sentinel 3-A/B*
DEM	*Digital Elevation Model*
ASTER	*Terra Advanced Spaceborne Thermal Emission and Reflection Radiometer*
MERIT	*Multi-Error-Removed Improved-Terrain*
ALOS	*Advanced Land Observing Satellite*
FABDEM	*Forest And Buildings removed Copernicus DEM*
KGE	*Kling–Gupta efficiency*
NSE	*Nash–Sutcliffe efficiency*
RMSE	*Root Mean Square Error*
MAPS	*Multi-mission Altimetry Processing Software*
TWS	*Total Water Storage*
HRU	*Hydrological Response Units*
GRDC	*Global Data Runoff Centre*
CHIRPS	*Climate Hazards Group InfraRed Precipitation with Station*
ECMWF	*European Centre for Medium-Range Weather Forecasts*
ERA5	*ECMWF Reanalysis version 5*
GRACE	*Gravity Recovery and Climate Experiment*
GRACE-FO	*Gravity Recovery and Climate Experiment Follow On*
GDR	*Geophysical Data Records*
ESA	*European Space Agency*
NASA	*National Aeronautics and Space Administration*
SWOT	*Surface Water Ocean Topography*

Acronymes français

CNES	*Centre National d'Études Spatiales*
CRREBaC	*Centre de Recherche en Ressources en Eau du Bassin du Congo*

General introduction

Freshwater on Earth's ice-free land accounts for only 1% of the total amount of water globally (Vörösmarty et al., 2010; Steffen et al., 2015; Cazenave et al., 2016; Albert et al., 2021). However, terrestrial freshwater is essential to human needs, ecosystem environments and biospheric processes. This freshwater is stored essentially in two reservoirs, the surface and subsurface ones. Surface reservoir is composed of rivers, lakes, man-made reservoirs, wetlands and inundated areas (Alsdorf et al., 2007; Cazenave et al., 2016). Subsurface reservoir consists of water in the uppermost few meters of the soil (root zones), as well as groundwater in confined and unconfined aquifers (A. Cazenave et al., 2016). Surface waters are of particular significance as they represent major components of the water cycle and deeply impact human societies (Alsdorf et al., 2007; Papa et al., 2010). They play a key role in many aspects of our lives, such as drinking water, agriculture, electricity production, transportation, and industrial purposes (Vörösmarty et al., 2010; Huang et al., 2018; Albert et al., 2021). Surface water bodies are dynamics in nature as they get narrow, extend, or change with time, inducing serious consequences. For instance, the rapid increase of surface water can provoke flooding or their shrinkage can cause severe crises such as drought (Huang et al., 2018a).

Surface waters constitute a major component of the global water cycle, ensuring exchanges with the atmosphere and oceans mass and energy fluxes through horizontal and vertical motions (Trenberth et al., 2007, 2011; Good et al., 2015; Cazenave et al., 2016). These exchanges are key players for climate variability and water resources availability across different scales. (Chahine, 1992; Oki and Kanae, 2006; Shelton, 2009; Cazenave et al., 2016; Stephens et al., 2020).

Despite their importance, surface waters (i.e., surface water storage and fluxes in rivers, lakes, reservoirs and wetlands) are currently poorly observed at the global scale (Biancamaria et al., 2016). The current knowledge about their spatial and temporal variations and changes are still not properly known, regionally and globally (Mekonnen and Hoekstra, 2016; Rodell et al., 2018; Cooley et al., 2021). This critical state of knowledge prevents the development of the implementation of sustainable strategies for water resources management and development (Oki and Kanae, 2006; Hall et al., 2014).

In particular, the African continent which is the second largest in the world both in terms of the size and population is mostly concerned with the challenge of the lack of adequate knowledge on its water resources availability and their dynamics. Africa hosts almost 1.4 billion inhabitants

as of 2022, representing ~18% of the global population. The latter is expected to double by 2050 (United Nations, 2019). The African continent is endowed with the largest freshwater systems (Fig. 0-1) in the world among which the Nile, the longest river in the world, and the Congo River Basin (CRB), the second-largest world's basin both in terms of drainage area and discharge to the ocean (Dai et al., 2009; Laraque et al., 2020). The continent hosts important lakes (Fig. 0-1) among the 10 largest freshwater lakes on Earth, in terms of area and volume. These are Victoria, Tanganyika and Malawi Lakes.

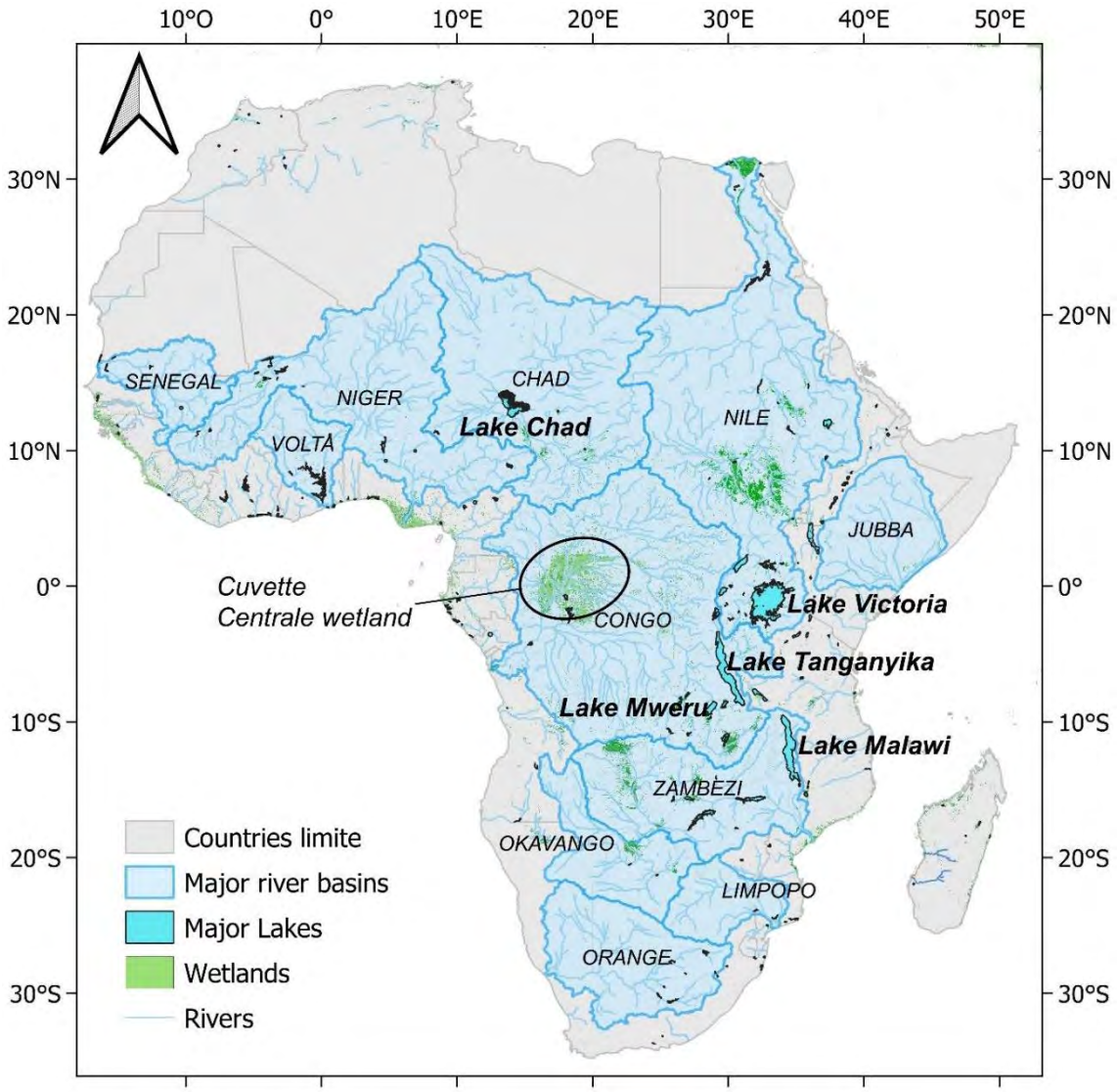

Figure 0-1. Location of major river basins, lakes and wetlands in Africa (Lehner and Grill, 2013; Gumbricht et al., 2017).

For instance, Lake Tanganyika which is located in the western part of the East African Rift system, is the largest lake in Africa by volume and second deepest (~1470 m) worldwide behind Lake Baikal (Scholz et al., 1998; Herrnegger et al., 2021). Moreover, African river systems are

surrounded by extensive wetlands and floodplains such as in the Congo (e.g., *Cuvette Centrale*), Chad, Niger, Okavango and Niles basins (Fig. 0-1), which are of global significance for biodiversity and the carbon and nutrient cycles (Simaika et al., 2021; Hastie et al., 2021).

Some regions of Africa are also home to large tropical forest that harbors incredible natural resources and acts as a carbon sink that stores billions of tons of carbon (Verhegghen et al., 2012; Dargie et al., 2017; Biddulph et al., 2021). These regions include the CRB rainforest known as the Earth's second-largest tropical forest regulating Earth's climate (White et al., 2021). Conversely, smaller water systems, such as streams, reservoirs, ponds and tanks, are also part of the African landscapes (Gardelle et al., 2010), providing water, food and natural resources for agriculture to a large portion of the population that remains mainly rural such as in the sub-Saharan region.

The hydrology of the African continent is characterized by a wide range of processes that are under the influence of complex atmosphere–land–ocean interactions and the availability of freshwater is strongly heterogeneous, generally highly seasonal and driven primarily by local or remote rainfall (Conway et al., 2009). It is subject to strong climate variability across timescales (Janicot, 1992; Hulme et al., 2001), from interannual to decadal changes (Ropelewski and Halpert, 1996; Stager et al., 2007), with alternate periods of floods or droughts (Tierney et al., 2015; Oguntunde et al., 2018). Among many examples, Lake Chad and its dramatic shrinkage since the 1980s is obviously an obvious case of how climate variability can impact African freshwater resources (Pham-duc et al., 2020).

In the past decades, the combined effect of climate change and anthropogenic pressure made freshwater availability a current global major concern (Alcamo et al., 2007; Hoekstra et al., 2012; Famiglietti, 2014; Konapala et al., 2020). In rapidly growing African economies, increasing demands for freshwater supply to sustain population growth and the needs of the agriculture and industrial sectors (Haddeland et al., 2014; Mehran et al., 2017) now pose significant threats to water resources. Environmental alterations such as land use practices, groundwater stress and deforestation, along with political conflicts, transboundary rivers, inadequate infrastructure and low adaptive capacity in many regions, make the African population particularly vulnerable to hydro-climatic variability and to any future changes in the water cycle (Inogwabini, 2020; Anderson et al., 2021).

A better understanding of hydrological processes across the continent therefore becomes fundamental for addressing these current challenges, for reducing uncertainty in future evolutions of water availability and for developing mitigation strategies (Adenuga et al., 2021).

Surprisingly, the hydrology of the African river basins, in particular the Congo River basin (CRB), remains one of the least studied worldwide and has not attracted as much attention among the scientific and international communities (Alsdorf et al., 2016; Tshimanga et al., 2022a) as has been, for instance, for other large tropical and subtropical regions such as the Amazon River basin (Fassoni-Andrade et al., 2021) or the Indian sub-continent with the Ganges–Brahmaputra (Papa et al., 2015). It currently leaves insufficient knowledge of the hydro-climatic characteristics of Africa and the CRB in particular. It is worth noting that this general introduction derived from our published paper "*Water Resources in Africa under Global Change: Role of Earth Observation and Models for Monitoring Surface Waters*" inserted in the appendix section.

Progressing on the knowledge of the CRB hydrology, hydro-climatology and its water resources is the core of this thesis.

Introduction générale

L'eau douce sur terre sans compter les glaciers et les calottes polaires ne représente que plus ou moins 1% de la quantité totale d'eau dans le monde (Vörösmarty et al., 2010 ; Steffen et al., 2015; Cazenave et al., 2016; Albert et al., 2021). Cependant, l'eau douce est essentielle à l'ensemble des besoins humains, environnementaux et des processus biosphériques. Cette eau douce est stockée essentiellement dans deux types de réservoirs, celui de surface et souterrain. Le réservoir de surface est constitué de rivières, de lacs, de réservoirs artificiels, de zones humides et de zones inondées (Alsdorf et al., 2007; Cazenave et al., 2016). Le réservoir souterrain est constitué premièrement de l'eau présente dans les quelques mètres sous la surface du sol (zone racinaire ou eau de subsurface), deuxièmement des eaux souterraines ou profondes dans les aquifères confinés et non-confinés (Cazenave et al., 2016). Les eaux de surface revêtent une importance particulière car elles représentent une des composantes majeures du cycle de l'eau et ont un impact profond sur la société humaine (Biancamaria et al., 2016). Elles touchent tous les aspects de notre vie, utilisées comme eau potable, en agriculture, dans la production d'électricité, le transport et les usages industriels (Vörösmarty et al., 2010; Huang et al., 2018; Albert et al., 2021). Les masses d'eau de surface sont dynamiques par nature, se rétrécissent ou s'étendent au fil du temps, entraînant des conséquences parfois graves. Par exemple, une augmentation rapide des eaux de surface peut provoquer des inondations ou leur rétrécissement sur une longue période peut entraîner une sécheresse grave induisant la famine (Huang et al., 2018a).

Faisant partie intégrante du cycle global de l'eau, les eaux de surface échangent avec l'atmosphère et les océans des flux de masse à travers des mouvements horizontaux et verticaux (Trenberth et al., 2007, 2011; Good et al., 2015; Cazenave et al., 2016). Ces échanges ainsi que le stockage d'eau associé sont également des acteurs clés du système climatique avec des liens importants et des rétroactions sur les variations climatiques et les ressources en eau (Chahine, 1992 ; Oki et Kanae, 2006; Shelton, 2009; Cazenave et al., 2016; Stephens et al., 2020).

Malgré leur importance, les eaux de surface (c'est-à-dire le stockage et les flux d'eau de surface dans les rivières, les lacs, les réservoirs et les zones humides) sont actuellement peu surveillées à l'échelle mondiale (Biancamaria et al., 2016). Les connaissances actuelles sur leurs variations et changements spatiaux et temporels sont encore mal connues, à l'échelle régionale et mondiale (Mekonnen et Hoekstra, 2016; Rodell et al., 2018; Cooley et al., 2021). Cet état critique des connaissances empêche le développement de stratégies adéquates et durables pour gérer les ressources en eau (Oki et Kanae, 2006; Hall et al., 2014).

Cet état actuel des connaissances concerne également l'Afrique, le deuxième plus grand continent du monde, tant par sa taille que par sa population. L'Afrique compte à peu près 1.4 milliard d'habitants à partir de 2022, soit ~18% de la population mondiale. Cette dernière devrait doubler d'ici 2050 (Nations unies, 2019). Le continent africain est aussi doté des plus grands systèmes d'eau douce (Fig. 0-1) du monde, parmi lesquels le Nil, le plus long fleuve du monde, et le fleuve Congo, le deuxième plus grand bassin du monde à la fois en termes d'aire de drainage et de débit vers l'océan (Dai et al., 2009; Laraque et al., 2020). Le continent abrite d'importants lacs (Fig. 0-1) parmi les 10 plus grands lacs d'eau douce de la planète, en termes de superficie et de volume. Il s'agit des lacs Victoria, Tanganyika et Malawi, situé dans la branche orientale du système du rift est-africain. Le lac Tanganyika est le plus grand lac d'Afrique en volume et le deuxième plus profond (~1470 m) au monde derrière le lac Baïkal (Scholz et al., 1998; Herrnegger et al., 2021). De plus, les systèmes fluviaux africains sont entourés de vastes zones humides et de plaines d'inondation, comme dans les bassins du Congo (par exemple, la *Cuvette Centrale*), du Tchad, du Niger, de l'Okavango et du Nil (Fig. 0-1), qui ont une importance mondiale pour la biodiversité et les cycles du carbone et des nutriments (Simaika et al., 2021; Hastie et al., 2021).

Au cours des dernières décennies, l'effet combiné du changement climatique et de la pression anthropique a fait de la disponibilité de l'eau douce une préoccupation majeure actuelle au niveau mondial (Alcamo et al., 2007; Hoekstra et al., 2012; Famiglietti, 2014; Konapala et al., 2020). Dans les économies africaines à croissance rapide, les demandes croissantes d'approvisionnement en eau douce pour soutenir la croissance démographique et les besoins des secteurs agricole et industriel (Haddeland et al., 2014; Mehran et al., 2017) constituent désormais des menaces importantes pour les ressources en eau. Les altérations environnementales telles que les pratiques d'utilisation des terres, le stress des eaux souterraines et la déforestation, ainsi que les conflits politiques, les rivières transfrontalières, les infrastructures inadéquates et la faible capacité d'adaptation dans de nombreuses régions, rendent la population africaine particulièrement vulnérable à la variabilité hydro-climatique et à tout changement futur du cycle de l'eau (Inogwabini, 2020; Anderson et al., 2021).

Une meilleure compréhension des processus hydrologiques à travers le continent devient donc fondamentale pour relever ces défis actuels, pour réduire l'incertitude des évolutions futures de la disponibilité de l'eau et pour développer des stratégies d'atténuation (Adenuga et al., 2021).

Étonnamment, l'hydrologie des bassins fluviaux africains, en particulier le bassin du Congo, reste l'une des moins étudiées au niveau mondial et n'a pas attiré autant d'attention de la part des communautés scientifiques et internationales (Alsdorf et al, 2016; Tshimanga et al., 2022a)

comme cela a été le cas, par exemple, pour d'autres grandes régions tropicales et subtropicales telles que le bassin du fleuve Amazone (Fassoni-Andrade et al., 2021) ou le sous-continent indien avec le Gange-Brahmapoutre (Papa et al., 2015). Elle laisse actuellement des connaissances insuffisantes sur les caractéristiques hydro-climatiques de l'Afrique et du bassin du Congo en particulier.

Le bassin du Congo est situé dans la région équatoriale de l'Afrique (Fig. 1-1). Il est le deuxième plus grand système fluvial au monde, tant en termes d'aire de drainage que de débit. Le bassin couvre ~3.7 x 10^6 km^2, et son débit annuel moyen est d'environ 40 500 m^3 s^{-1} qui est remarquablement stable (Spencer et al., 2016; Laraque et al., 2009, 2013, 2020). Le fleuve Congo s'écoule sur 4 700 km depuis la partie sud-est de la République démocratique du Congo (RDC) jusqu'à l'océan Atlantique et son bassin versant s'étend sur neuf pays, à savoir la République centrafricaine, le Cameroun, la République du Congo, l'Angola, la RDC, la Zambie, la Tanzanie, le Rwanda et le Burundi (Fig. 1-1).

Le bassin du Congo joue un rôle crucial dans les cycles hydrologiques et biogéochimiques locaux, régionaux et globaux, avec une influence significative sur la variabilité climatique régionale (Nogherotto et al., 2013; Burnett et al., 2020) et des impacts sur la croissance socio-économique à l'échelle régionale (Tshimanga et al., 2022b).

Le bassin du Congo a en effet un rôle clé dans le système terrestre en tant que l'un des trois principaux centres convectifs sous les tropiques (avec le bassin du fleuve Amazone et la région tropicale Indo-Pacifique) (Hastenrath, 1985). Couvert par plus de 45% de forêt tropicale, représentant environ 20% des forêts tropicales du monde, le bassin du Congo (Verhegghen et al., 2012; Biddulph et al., 2021), avec ses vastes plaines d'inondation et zones humides, joue un rôle crucial en tant que puits/sources de Co_2 (cycle du carbone) (Dargie et al., 2017; Becker et al., 2018; Crezee et al., 2022). Enfin, 80% de sa population vit des activités qui sont fortement dépendantes de la ressource en eau (agriculture, pêche, navigation), ce qui rend la population particulièrement vulnérable à la variabilité hydro-climatique et aux événements extrêmes (Inogwabini, 2020; White et al., 2021). Dans ce contexte, il existe un besoin évident de mieux comprendre les processus hydro-climatiques du bassin et leur impact sur les ressources en eau (Tshimanga et al., 2022a). Cependant, le bassin reste difficile à surveiller à grande échelle, le réseau des stations hydrométéorologiques étant peu dense et peu entretenu (Laraque et al., 2020). Ceci limite la compréhension de la variabilité des composantes du bilan hydrologique et des principaux facteurs contrôlant leur dynamique à des échelles spatiales et temporelles appropriées (Tshimanga, 2022).

Des efforts ont été menés pour entreprendre des études utilisant la télédétection et/ou la modélisation numérique afin de surmonter le manque d'informations d'observation dans le bassin du Congo et de mieux caractériser les différentes composantes du cycle hydrologique (par exemple, Rosenqvist et Birkett, 2002; Crowley et al., 2006; Lee et al., 2011; Becker et al., 2014, 2018; Ndehedehe et al., 2019, 2022; Fatras et al., 2021; Frappart et al., 2021; Datok et al., 2022). Certains des résultats des efforts susmentionnés sont rapportés dans Tshimanga et al. (2022a) qui présente les avancées récentes réalisées par les experts de la région et leurs collaborateurs internationaux sur les variations et les influences des précipitations, de l'hydrologie et de l'hydraulique, et de la dynamique des sédiments et du carbone dans le bassin du Congo.

La plupart des études mentionnées ci-dessus basées sur la télédétection et la modélisation hydrologique ont été validées ou évaluées par rapport à peu d'informations provenant d'autres données hydrologiques de télédétection et/ou de données de terrain historiques, ne permettant souvent que des comparaisons de signaux saisonniers (Becker et al., 2018), qui ne couvraient pas non plus la même période de disponibilité des données (Paris et al., 2022). Par conséquent, la grande taille du bassin, son hétérogénéité spatiale et le manque d'observations in situ ont rendu difficile la validation des observations à long terme dérivées par satellite des composantes de l'hydrologie de surface et la mise en place adéquate de modèles hydrologiques à grande échelle (Munzimi et al., 2019). Des résultats récents appellent à la nécessité d'une couverture spatiale complète de l'élévation de la surface de l'eau du bassin du Congo à l'aide d'observations dérivées de l'altimétrie satellitaire pour englober toute la gamme de variabilité à travers ses rivières et ses zones humides jusqu'à son exutoire (Carr et al., 2019). En outre, même si des efforts récents ont permis de caractériser la façon dont l'eau s'écoule dans le bassin du Congo, la dynamique à l'échelle du bassin est encore peu étudiée, notamment en ce qui concerne les contributions des différents sous-bassins à l'hydrologie de l'ensemble du bassin (Alsdorf et al., 2016 ; Laraque et al., 2020) et au régime annuel bimodal du débit du fleuve Congo près de son embouchure. Jusqu'à présent, seules quelques études ont examiné les différentes contributions et le transfert d'eau de l'amont vers l'aval du bassin en se basant sur quelques données in situ de débit (Bricquet, 1993 ; Laraque et al., 2020) et sur une modélisation à grande échelle (Paris et al., 2022). En ce qui concerne le stock d'eau de surface, celui du bassin du Congo reste encore largement méconnu et il y a encore beaucoup à découvrir sur sa dynamique dans le bassin sur le long terme bien que quelques efforts aient été consacrés à la caractérisation de sa variabilité spatio-temporelle sur la période 2003-2007 (Becker et al., 2018).

En ce qui concerne la modélisation hydrologique, compte tenu de la complexité naturelle et de l'étendue géographique du bassin du Congo, il est nécessaire de développer une modélisation hydrologique appropriée et adéquate pour aider à améliorer nos connaissances sur les pratiques de gestion des ressources en eau dans le bassin, et faire face aux impacts du changement environnemental. Et également, permettre de tirer des leçons des épisodes passés dans de nombreux domaines tels que les ressources en eau et les risques naturels en l'occurrence les inondations ou les sécheresses. Par conséquent, un modèle hydrologique capable de caractériser et de reproduire la variabilité hydro-climatique du bassin et qui peut être utilisé pour soutenir les décisions politiques de gestion et de développement des ressources en eau dans le bassin du Congo (Tshimanga, 2022).

Malgré les efforts déployés pour caractériser l'hydro-climatologie du bassin du Congo et sa variabilité au cours des deux dernières décennies en utilisant la télédétection et la modélisation hydrologique, il reste encore beaucoup à découvrir sur les caractéristiques hydro-climatiques, sa variabilité et les changements dans cette région (Tshimanga et al., 2022a), laissant ouvertes des questions majeures qui seront abordées dans cette thèse.

Chapter 1: Background and context

1.1 Congo River basin

The CRB is located in the equatorial region of Africa (Fig. 1-1). It is the second largest river system in the world, both in terms of drainage area and discharge. The basin covers ~3.7 x 10^6 km^2, and its mean annual flow rate is about 40 500 m^3 s^{-1} that is remarkably stable (Spencer et al., 2016; Laraque et al., 2009, 2013, 2020). The Congo River flows over 4 700 km from the southeastern part of the Democratic Republic of Congo (DRC) to the Atlantic Ocean and its drainage area spans over nine countries that are Central Africa Republic, Cameroon, Republic of the Congo, Angola, DRC, Zambia, Tanzania, Rwanda, and Burundi (Fig. 1-1). The mean temperature over the basin is estimated to be 25° C. The CRB is generally divided into six main sub-basins based on the physiography of the basin (Laraque et al., 2020). These are Lower-Congo (southwest), Middle-Congo (centre), Sangha (northwest), Ubangui (northeast), Kasai (south-centre), and Lualaba (southeast) (Fig. 1-1). Precipitation is accounted for 2 000 mm yr^{-1} in the central part of the basin and decreases to 1 100 mm yr^{-1} away from the equator. The peak annual potential evapotranspiration accounts for ~1 500 mm yr^{-1} near the equator, decreasing northwards and southwards to less than 1 000 mm yr^{-1} (Sridhar et al., 2022). The CRB plays a crucial role in the local, regional, and global hydrological and biogeochemical cycles, with significant influence on the regional climate variability (Nogherotto et al., 2013; Burnett et al., 2020) and impacts on the socio-economic growth at the regional scale (Tshimanga et al., 2022b).

The CRB is indeed one of the three main convective centres in the tropics (Hastenrath, 1985). About 45% of the CRB land area is covered by dense tropical forest (Verhegghen et al., 2012), accounting for ~20% of the global tropical forest and storing about ~80 x 10^7 t of carbon, equivalent to ~2.5 years of current global anthropogenic emissions (Biddulph et al., 2021). It is the world's largest tropical peat carbon that accounts for ~28% of the total area of tropical peat carbon (Verhegghen et al., 2012; Dargie et al., 2017; Becker et al., 2018; Crezee et al., 2022). The CRB is also characterized by a large network of rivers, along with extensive floodplains and wetlands playing a critical role in studies of habitat, biodiversity, sediment dynamics of the river, and carbon cycling (Zheng et al., 2015; Datok et al., 2022; Biddulph et al., 2021). These wetlands are located mainly in the Lualaba region in the southeastern part of the basin and the well-known *Cuvette Centrale* region as identified by Gumbricht et al. (2017) (Fig. 1-1).

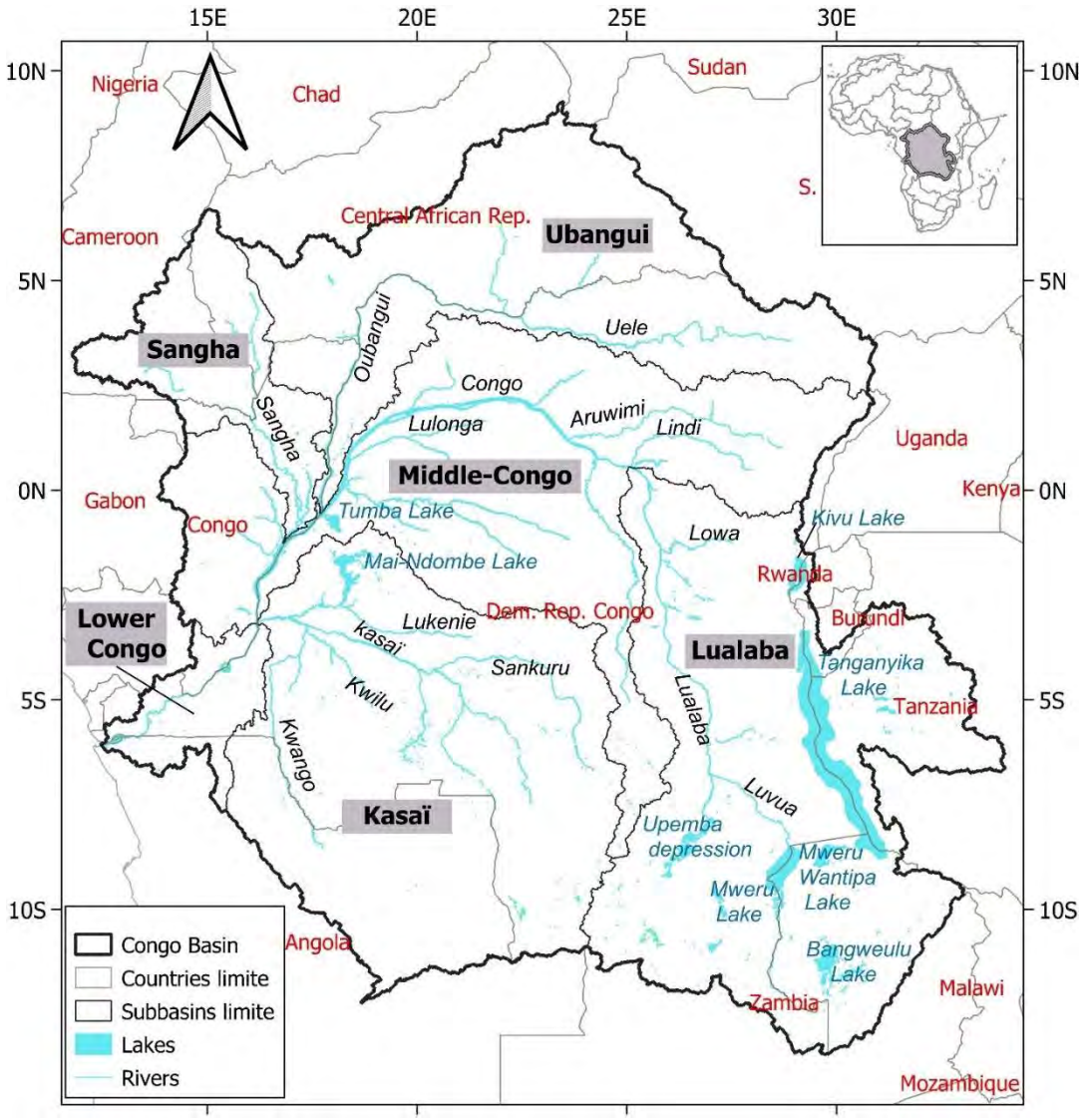

Figure 1-1. Main physiographic features of the Congo River basin. Small dark lines show the major sub-basins (name in dark bold with a grey background). Red colour indicates countries (Sources: Esri; Garmin International, Inc).

The CRB rainforest and inland waters therefore strongly contribute to the carbon cycle of the basin (Dargie et al., 2017; Fan et al., 2019; Hastie et al., 2021). Additionally, more than 80% of the human population within the CRB rely on the basin water resources for their livelihood and are particularly vulnerable to climate variability and alteration, and to any future changes that would occur in the basin water cycle (Inogwabini, 2020; White et al., 2021). Increasing evidence suggest that changes in land use practices, such as large-scale mining or deforestation, pose a significant threat to the basin water resources availability, including hydrological, ecological, and geomorphological processes in the basin (Bele et al., 2010; Ingram et al., 2011; Nogherotto et al., 2013; Tshimanga and Hughes, 2012; Plisnier et al., 2018). These

environmental alterations require a better comprehension of the overall basin hydrology across scales. Surprisingly, despite its major importance, the CRB is still one of the least studied river basin in the world (Laraque et al., 2020; Tshimanga et al., 2022a) and has not attracted as much attention among the scientific communities as, for instance, the Amazon Basin (Alsdorf et al., 2016). Therefore, there is still insufficient knowledge of the CRB hydro-climatic characteristics and processes and their spatiotemporal variability. This is sustained by the lack of comprehensive and maintained in situ data networks that keep the basin poorly monitored at a large scale, therefore limiting our understanding of the major factors controlling freshwater dynamics at proper space and timescales (Tshimanga, 2022).

1.2 Problem statement

Since the 1960s, there has been a drastic decline in the hydro-meteorologic monitoring networks in the CRB so that, currently, there are no more than 15 gauges out of 400 initially installed considered as operational (Tshimanga et al., 2016), making a substantial difficulty to understand the hydro-climate processes in the CRB (Tshimanga et al., 2022a). For more details about the problematic of the in situ gauges in the CRB, refers to the chapter three of this thesis.

Efforts have been made to undertake studies using remote sensing and/or numerical modelling to overcome the lack of observational information in the CRB and better characterize the various components of the hydrological cycle (e.g., Rosenqvist and Birkett, 2002; Crowley et al., 2006; Lee et al., 2011; Becker et al., 2014, 2018; Ndehedehe et al., 2019, 2022; Fatras et al., 2021; Frappart et al., 2021; Datok et al., 2022). Some of the results of these efforts are reported in Tshimanga et al. (2022a) that provides recent advances done by experts from the region and their international collaborators on the variations in and influences on rainfall, hydrology and hydraulics, and sediment and carbon dynamics within the CRB. For instance, Crowley et al. (2006) estimated terrestrial (surface plus ground) water storage within the CRB for the period of April 2002 to May 2006 using GRACE satellite gravity data. The result showed a significant seasonal (30 ± 6 mm of equivalent water thickness) and long-term trends, the latter yielding a total loss of ~280 km^3 of water over the 50-month span of data. Betbeder et al. (2014) used combinations of the SAR L-band and optical images to characterize the *Cuvette Centrale* land cover. They found that the wetland extent reaches 360 000 km^2 (i.e., 32% of the total area). Becker et al. (2018) combined information based on Global Inundation Extent from Multi-satellite (GIEMS; Prigent et al., 2007) and altimetry-derived water levels from Envisat (350 Virtual Stations [VSs]) to estimate Surface Water Storage (SWS) and analyzed its variability

over the period 2003–2007. Its mean annual variation was estimated at ~81 ± 24 km^3, which accounts for 19 ± 5% of the annual variations in GRACE-derived total terrestrial water storage. Ndehedehe et al. (2019), using the observed Standardized Precipitation Index (SPI) and the global sea surface temperature, examined the impact of the multi-scale ocean–atmosphere phenomena on hydro-climatic extremes, showing that 40% of the basin during 1994–2006 was affected by severe multi-year droughts. Recently, Fatras et al. (2021) analyzed the hydrological dynamics of the CRB using inundation extent estimates from the multi-angular and dual polarization passive L-band microwave signals from the Soil Moisture and Ocean Salinity (SMOS) satellite along with precipitation for 2010–2017. The mean flooded area was found to be 2.39% for the entire basin, and the dataset helped to characterize floods and droughts during the last 10 years.

In addition to remote sensing observations, hydrological modelling represents a valuable tool for studying the CRB water cycle (Tshimanga et al., 2011, 2014, 2022c; Aloysius and Saiers, 2017; Munzimi et al., 2019; O'Loughlin et al., 2019; Paris et al., 2022; Datok et al., 2022). For example, Tshimanga and Hughes (2014) used a semi-distributed rainfall–runoff model to examine runoff generation processes and the impact of future climate and land use changes on water resources availability. The magnitude and timing of high and low flows were adequately captured, with, nevertheless, an additional wetland submodel component that was added to the main model to account for wetland and natural reservoir processes in the basin. Aloysius and Saiers (2017) simulated the variability in runoff, in the near future (2016–2035) and mid-century (2046–2065), using a hydrological model forced with precipitation and temperature projections from 25 global climate models (GCMs) under two scenarios of greenhouse gas emission. Munzimi et al. (2019) applied the Geospatial Streamflow Model (GeoSFM) coupled to remotely sensed data to estimate daily river discharge over the basin from 1998 to 2012, revealing a good agreement with the observed flow but also a discrepancy in some parts of the basin where wetland and lake processes are predominant. O'Loughlin et al. (2019) forced the large-scale LISFLOOD-FP hydraulic model with combined in situ and modelled discharges to understand the Congo River's unique bimodal flood pulse. The model was set for the area between Kisangani and Kinshasa on the main stem, including the major tributaries and the *Cuvette Centrale* region. The results revealed that the bimodal annual pattern is predominantly a hydrological rather than a hydraulically controlled feature. Paris et al. (2022) demonstrated the possibility of monitoring the hydrological variables in near-real time using the hydrologic–hydrodynamic model MGB (Portuguese acronym for large basin model) coupled to the current operational satellite altimetry constellation. The model outputs showed a good consistency with

the small number of available observations, yet with some notable inconsistencies in the mostly ungauged *Cuvette Centrale* region and in the southeastern lakes' sub-basins. Datok et al. (2022) used the Soil and Water Assessment Tool (SWAT) model to understand the role of the *Cuvette Centrale* region in water resources and ecological services. Their findings have highlighted the important regulatory function of the *Cuvette Centrale* region, which receives contributions from the upstream Congo River (33%), effective precipitation inside the *Cuvette Centrale* region (31%), and other tributaries (36%).

Most of the above studies based on remote sensing (RS) and hydrological modelling were validated or evaluated against few information from other hydrological RS data and/or historical gauge data, often enabling only comparisons of seasonal signals (Becker et al., 2018), which also did not cover the same period of data availability (Paris et al., 2022). Therefore, the large size of the basin, its spatial heterogeneity, and the lack of in situ observations have made the validation of long-term satellite-derived observations of surface hydrology components and the proper set-up of large-scale hydrological models difficult (Munzimi et al., 2019). Recent results call for the need of a comprehensive spatial coverage of the CRB water surface elevation using satellite-altimetry derived observations to encompass the full range of variability across its rivers and wetlands up to its outlet (Carr et al., 2019). Additionally, even if recent efforts have been characterizing how water flows across the CRB, the basin-scale dynamics are still understudied, especially regarding the contributions of the different sub-basins to the entire basin hydrology (Alsdorf et al., 2016; Laraque et al., 2020) and to the annual bimodal pattern in the CRB river discharge near to its mouth. Up to now, only a few studies have examined the various contributions and the lag time from upstream to downstream the basin based on a few in situ discharge gauge records (Bricquet, 1993; Laraque et al., 2020) and large-scale modelling (Paris et al., 2022). Regarding the SWS, the CRB's SWS remains still widely unknown and there is still a lot to unravel about the dynamics of SWS in the basin over the long-term period though some efforts have been devoted to characterize the spatio-temporal variability of SWS over the period 2003-2007 (Becker et al., 2018).

In addition to this, during the past two decades, several hydrological modeling studies have been carried out in the CRB using statistical, process-based hydrologic and hydrodynamic models to attempt understanding the CRB's hydrologic variability and processes at the large scale. Many of these studies have faced challenges due to the lack of information/data, a thorough understanding of the CRB's hydrologic processes such as the role of lakes and wetlands in the dynamics of surface water, and the integration of this understanding in model structures (i.e., incorporating lake routing module). For instance, function related to the

representation of the natural storage of wetlands and lakes that dominate the hydrology of the CRB as well as the routing functions over the main river channels are among the issues that challenged modeling experiments (Tshimanga and Hughes, 2014; Aloysius and Saiers, 2017). Tshimanga (2022) also reported that many of these studies have been undertaken in an experimental mode, testing the models' performance in a new and data-scarce environment, and not for solving the real hydrologic and water resource issues of day-to-day life. Based on this precedent evaluation, there are still a number of issues and uncertainties that should attract the attention of future modelling studies. These issues relate to lack of appropriate data, as well as the lack of consideration of the CRB's hydrology processes in model structures. Considering the CRB's natural complexity and geographic extent, there is a need for the development of a proper and adequate hydrological modeling to help improve practices of water resources management in the basin, and address impacts of environment change. Therefore, a hydrological model able to characterize and reproduce the hydroclimate variability of the CRB and that can be used in support of policy decisions of water resources management and development in the CRB (Tshimanga, 2022) is still strongly needed.

1.3 Scientific questions and research objectives

Despites the efforts made to characterize the CRB's hydro-climatology and its variability in the past two decades using remote sensing and hydrological modeling, there is still a lot to unravel about the hydroclimatic characteristics, variability and changes in this region (Tshimanga et al., 2022a), leaving major science questions open. These questions encompass the lag time from upstream to downstream at the different locations and during the different phases of the hydrological cycle in the basin; the spatio-temporal dynamics of SWS over long-term period at different spatial scales in the basin; the way this dynamic is modulated by climate variability and the SWS behavior during exceptional drought events; the contributions of the individual components of the water balance equation and the partitioning between continental water storage variations (surface storage, groundwater and soil moisture), river discharge and evapotranspiration; and the processes governing the water dynamics in the basin and more specifically in the *Cuvette Centrale*, i.e., is it supplied mostly by local rainfall and emptying mostly by evapotranspiration? In a tropical and sparsely gauged basin such as the CRB, the advent of free and open Earth observation (EO) datasets is an unprecedented opportunity to answer these questions, as such

datasets prove to be very useful for monitoring large drainage basins climate and hydrology where in situ information is lacking (Fassoni-Andrade et al., 2021; Kitambo et al., 2022a).

The general purpose of the thesis is to provide a comprehensive hydrodynamic and hydroclimatic characteristics and their variability of the CRB surface hydrology at a large scale using a robust approach based on a combination of in situ measurement, remote sensing techniques associated with hydrological modelling.

Specifically, the study aims to achieve the following objectives:

To provide comprehensive validation of long-term remote-sensing-derived products over the entire CRB, in particular water level variations from satellite altimetry and surface water extent from multi-satellite.

We will provide newly intensive and comprehensive validations of remote sensing derived products in the CRB using an unprecedented consolidated in situ database covering the entire CRB (28 gauges of river discharge and height) of historical and current observations of rivers and floodplains dynamic acquired thanks to our collaboration with regional and national partners of the CRB and their strong will of improving knowledge and bounding research and operational communities in the CRB. We will in particular evaluate radar altimetry-derived water level variations (a total of 2311 VSs over the period of 1995 to 2020) and surface water extent from multi-satellite techniques from 1992 to 2015 (Global Inundation Extent from Multi-Satellite-2 [GIEMS-2]; Prigent et al., 2020) over the CRB.

To use the validated long-term Earth Observations (EO) datasets to analyze the dynamics of surface water and to identify hydrological patterns within the CRB.

The validated long-term satellite-derived observations will be used to analyze the spatio-temporal dynamics of the water propagation and their patterns at the sub-basins and basin scale levels. Although there is some knowledge about the characterization on how water flows across the CRB, the basin-scale dynamics are still understudied and the validated earth observations datasets will help understanding the relative contribution of different region within the CRB to the bimodal hydrological regime at Brazzaville/Kinshasa station.

To estimate and analyze the seasonal and interannual variability of the CRB water storage dynamics, especially the variability of surface freshwater volume stored in rivers, lakes, floodplains, and wetlands.

We propose to estimate and analyze the seasonal and interannual dynamics of the CRB freshwater water storage components, especially the variability of surface freshwater volume stored in rivers, lakes, floodplains, and wetlands using for the first time unprecedented long-term datasets and a trove of Digital Elevation Model (DEMs). To this end we will work on two methodologies. The first one as described in Frappart et al. (2008, 2011) combines Surface Water Extent (SWE) from the dataset GIEMS-2 and the long-term satellite-derived Surface Water Height (SWH) from multi-mission radar altimetry estimated at 160 VSs obtained during the first objective of my thesis over the period 1995 to 2015. The second one, based on the hypsometric curve approach as described in Papa et al. (2013), combines SWE from GIEMS-2 with topographic data from four DEMs, namely The Terra Advanced Spaceborne Thermal Emission and Reflection Radiometer (ASTER), Advanced Land Observing Satellite (ALOS), Multi-Error-Removed Improved-Terrain (MERIT) and Forest And Buildings removed Copernicus DEM (FABDEM) generating the SWS over the period 1992 to 2015.

To study the ability of large-scale hydrological models to properly characterize and reproduce the hydroclimate variability of the CRB. We will focus specifically on the set-up and validation of the MGB model and the comparison of model outputs to the previous hydrological datasets developed during previous objectives.

We will investigate the ability of a large-scale hydrological model (namely the MGB, Portuguese acronym Large Basin Model) to properly characterize and reproduce the long-term hydroclimate variability of the CRB. MGB is a conceptual, semi-distributed hydrologic–hydrodynamic model developed for tropical regions (Collischonn et al., 2007) intensively used in large South American basins with low-slope rivers affected by floodplains (Paiva et al., 2013), with some applications also in Africa and over the CRB (Fleischmann et al., 2018; Bogning et al., 2021; Andriambelosom et al., 2020; Paris et al., 2022). We will implement MGB over the CRB where floodplain topography, as well as basin and sub-basin discretization are extracted from the vegetation corrected MERIT DEM (Yamazaki et al., 2017) with a discretization of the basin into 50 sub-basins. The model is manually calibrated from 2001 to 2020 (for river stage and discharge) using 9 available in situ gauges spatially distributed from upstream to downstream part of the basin and 836 satellite-derived water levels from multi-missions. The first task of this third objective is to better assess MGB simulations in terms of river level height and discharge variations using the consolidated database of in situ observations from objective one. The second task is to perform an intensive comparison of

MGB outputs with the database of satellite-derived observations of surface water levels, extent and storages from the two previous objectives.

1.4 Thesis organization

This thesis document is structured as an article-based thesis and divided into 7 chapters. Following the introduction presented in this chapter, chapter 2 presents the overview of the hydrological cycle, the traditional (i.e., in situ) and contemporary (i.e., remote sensing by satellite) ways of monitoring surface water bodies. A focus is given on the satellite radar altimetry technique with its different applications and the monitoring of surface water extent from EO. The chapter will end by presenting a broad overview on hydrological modeling with a focus on the MGB model that is developed in our research study. Chapter 3 describes the dataset involved in this research, in particular the radar-altimetry-derived surface water height. Chapter 4 provides the characterization of the surface hydrology and its variability over the CRB using a combined dataset of in situ and satellite-derived observations and is organized around our published paper in Hydrology and Earth System Sciences (HESS) "*A combined use of in situ and satellite-derived observations to characterize surface hydrology and its variability in the Congo River basin"*. Chapter 5 is dedicated to present the long-term spatio-temporal variability of the CRB's SWS from multi-satellite technic, thematic leveraged in our under-review paper in Earth System Science Data (ESSD) "*A long-term monthly surface water storage dataset for the Congo basin from 1992 to 2015*". Chapter 6 presents the development of the MGB model over the basin, its assessment against in situ (i.e., discharge and water level) and satellite-derived water levels observations and the comparison with other hydrological databases from satellite-derived observations. Those analyses will be presented in our in-prep paper "*Long-term daily simulation of hydrological variables using hydrodynamic modeling in the Congo basin*". In chapter 7 we provide the conclusion of the main findings of our research and the perspectives for future research. One of them, already begun, is the step toward the development of the SWS dataset at the global scale. We will provide an example of the development of the satellite-based SWS dataset using the hypsometric curve approach at continental scale over the South America and African continent. This dataset is a benchmark product in the context of the evaluation and validation of the hydrology-oriented satellite mission product, the NASA-CNES Surface Water and Ocean Topography (SWOT) launched on the 16th of December 2022.

Chapter 2: Hydrological cycle, monitoring of continental surface water, and hydrological modeling

2.1 Hydrological cycle

Water is the only chemical compound that occurs on Earth in all its three states, or phases: liquid, solid, and gas, in various degrees of motion. The changes and transportability of water in each of its phases are the foundations of the hydrologic cycle which constantly replenishes and redistributes the relatively small volume of freshwater (Shelton, 2009). The hydrological cycle is a continuous combination of natural processes providing the mechanism for the natural redistribution of water between the hydrosphere, atmosphere, lithosphere, and biosphere (Shelton, 2009; Karamouz et al., 2013) (Fig. 2-1).

The hydrological cycle can be summarized as follows. Water evaporates from the oceans and land surfaces to become water vapor that is carried over the earth by atmospheric circulation. The water vapor condenses and precipitates on the land and oceans. The precipitated water may be intercepted by vegetation, become overland flow over the ground surface, infiltrate into the ground, flow through the soil as subsurface flow, or discharge as surface runoff. Evaporation from the land surface comprises evaporation directly from soil and vegetation surfaces, and transpiration through plants leaves. Collectively these latter processes are called evapotranspiration. Infiltrated water may percolate deeper to recharge groundwater and later become spring flow or seepage into streams to also become streamflow (Viessman and Lewis, 1995; Todd and Mays, 2005). Nevertheless, human actions influence the hydrological cycle. The United States Geological Survey (USGS) released the global water cycle diagram (https://www.usgs.gov/media/images/water-cycle-png, last access 13 February 2023) showing the impact of human water use on the water's storage, motion, and quality (Fig. 2-1). The direct human alteration of the terrestrial water cycle includes reservoir creation (e.g., dam for hydroelectricity, human consumption, irrigation, mining), redirection of rivers, water withdrawal from wetlands, lakes, groundwater aquifers to supply communities, and so on. Another aspect is water quality that is affected by returning contaminated water to rivers (Vörösmarty and Sahagian, 2000).

A general hydrologic equation or budget can be developed based on the processes illustrated above (Viessman and Lewis, 1995).

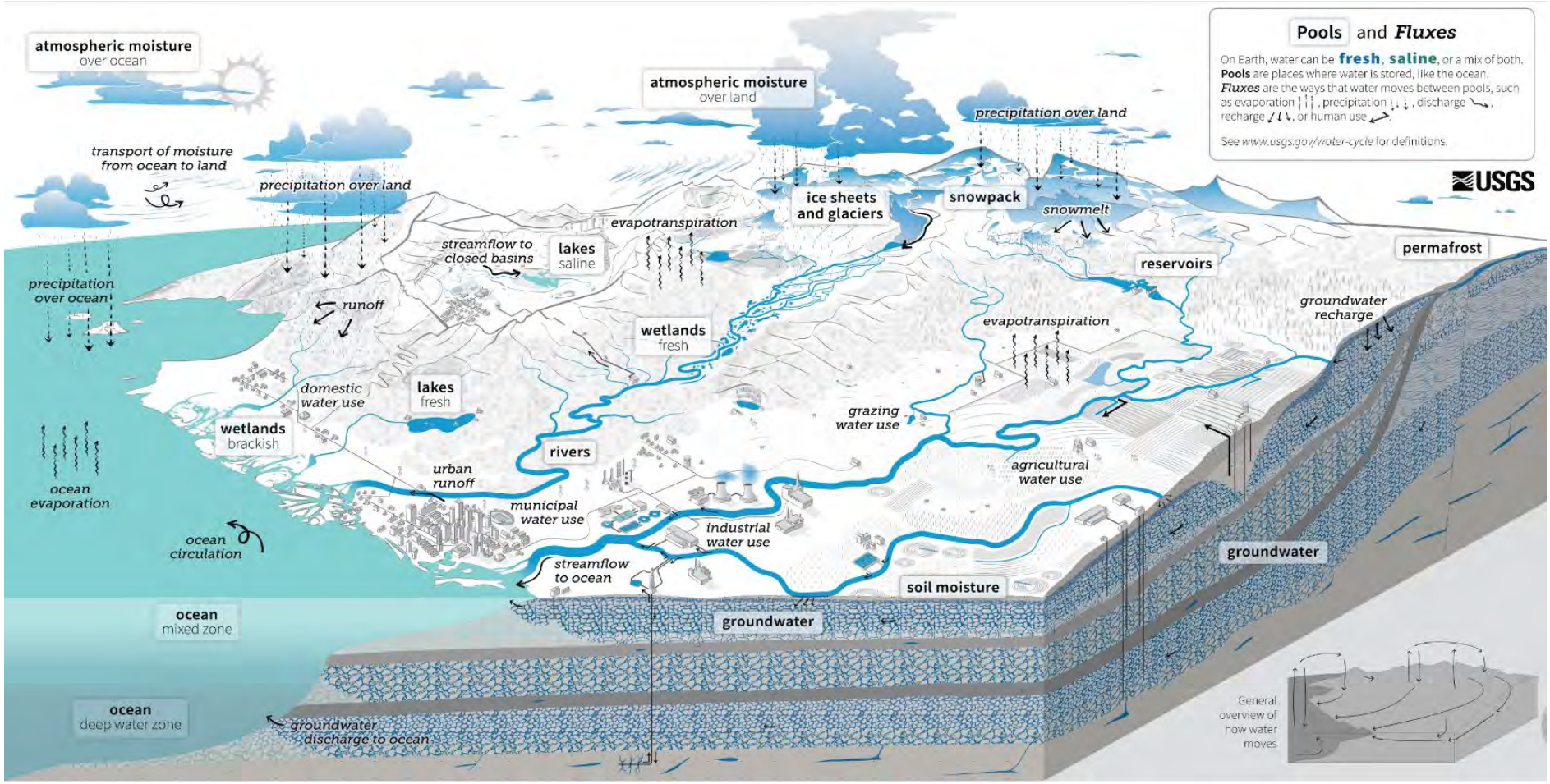

Figure 2-1. Global water cycle diagram including human impacts on water (Source: USGS).

$$\Delta S(\Delta \mathrm{SWS} + \Delta \mathrm{SM} + \Delta \mathrm{GW}) = P - R - G - E - T \quad (1)$$

where ΔS stands for the change in total water storage with ΔSWS the surface water storage, ΔSM the soil moisture, ΔGW the groundwater storage, P is the precipitation, R is the surface runoff, G is the groundwater flow, E is the evaporation, and T is the transpiration. All these various hydrologic equation terms are measurable using two major methods, in situ and remote sensing measurement. The practical problem is the inability to estimate these components properly, especially at a large scale (Viessman and Lewis, 1995). The processes of the terrestrial branch of the hydrologic cycle are strongly affected by the land-atmosphere dynamics and surface heterogeneity in soil type, topography, and vegetation (Lakshmi et al., 2015). Moreover, the expected increase in human water demand and the related change in land use, irrigation, and emission of greenhouse gases bring variations in the hydrological cycle often taking place at the local or even regional scale but can still trigger modifications that have an upscale effect possibly leading to global changes in the hydrological cycle (Viessman and Lewis, 1995; Rast et al., 2014; Bengtsson et al., 2014). To comprehend all these interactions between increasing human stresses on water, land use, and climate change, and thereby the related variations of the hydrological equation terms spatially and temporally, the understanding of the hydrological cycle needs to be advanced on all interconnected scales from local to global and this required adequate information. However, in situ systems cannot satisfactorily capture entirely the variability at the surface, as these are often point measurements and not spatial distributed. Thus, Earth Observation offers a unique opportunity to better characterize hydrological components' variability (Alsdorf et al., 2007; Meijerink et al., 2007) and to better understand the complex interactions between different terms of the hydrological cycle. In the 1990s, several space agencies (e.g., NASA, CNES, ESA, JAXA) launched numerous spaceborne sensors to study various components of the terrestrial hydrological cycle (Lakshmi et al., 2015). Advances in remote sensing enable nowadays the estimation and monitoring of the different components of the terrestrial water cycle (Fig. 2-3). Yet with different accuracies and spatio-temporal samplings.

2.2 Monitoring of land surface water

Not all hydrological variables are concerned in our research thesis. This is due to the satellite products used in our study. Our focus lies on the monitoring of land surface water, specifically water level, water extent, and discharge.

2.2.1 In situ monitoring

Historically, the monitoring of land surface water variability relies on in situ observations that quantify the movement (height, extent, discharge) and quality of water in river channels, lakes and wetlands. However, in situ networks are sparse, unevenly distributed globally, or even within a hydrological basin, particularly in remote areas with difficult access (e.g., tropical basins) or security concerns. In situ gauge networks are generally costly to maintain, especially for developing countries, and the availability of ground-based hydrological information has dramatically decreased during the last decades (Fekete et al., 2012), especially over Africa (Tramblay et al., 2021) (Fig. 2-2). For instance, the Global Data Runoff Centre (GRDC) portal provides the spatial distribution of the in situ discharge stations labelled according to the duration of the record. The remark is that there is an uneven distribution of current observations. The United States of America, western Europe, Australia, Brazil and South of Africa are countries with more contemporary observations, unlike Africa, and Asia where historical observations are predominant as shown on Figure 2-2. (https://portal.grdc.bafg.de/applications/public.html?publicuser=PublicUser#dataDownload/Home, last access: 13 February 2023). A striking example is the CRB, where hydrological monitoring can be traced back to the beginning of the 20th century (Trigg and Tshimanga, 2020). Until the end of the 1960s, more than 400 gauging sites provided observations of water level and discharge (Alsdorf et al., 2016), while today, there are only 15 gauges considered as operational (Laraque et al., 2020). In addition, in many places, even when data exist, their public access can be restricted by government agencies (Chawla et al., 2020) and they are often not available to the scientific community due to political situations or transboundary water sharing conditions (Papa et al., 2010a). Finally, in situ data are not capable of monitoring all water characteristics such as large floods events, wetland-river connectivity or the variability of numerous small lakes/ponds in a same area (Alsdorf et al., 2007).

2.2.2 Satellite monitoring

In the context of a gradual collapse of in situ water monitoring systems during the last decades, especially in Africa (Fekete et al., 2012; Tramblay et al., 2021), satellite remote sensing techniques offer a cost-effective means for monitoring the various components of the terrestrial water cycle (Fig. 2-3), with a relatively continuous, high spatio-temporal coverage and reasonable accuracy (Chawla et al., 2020).

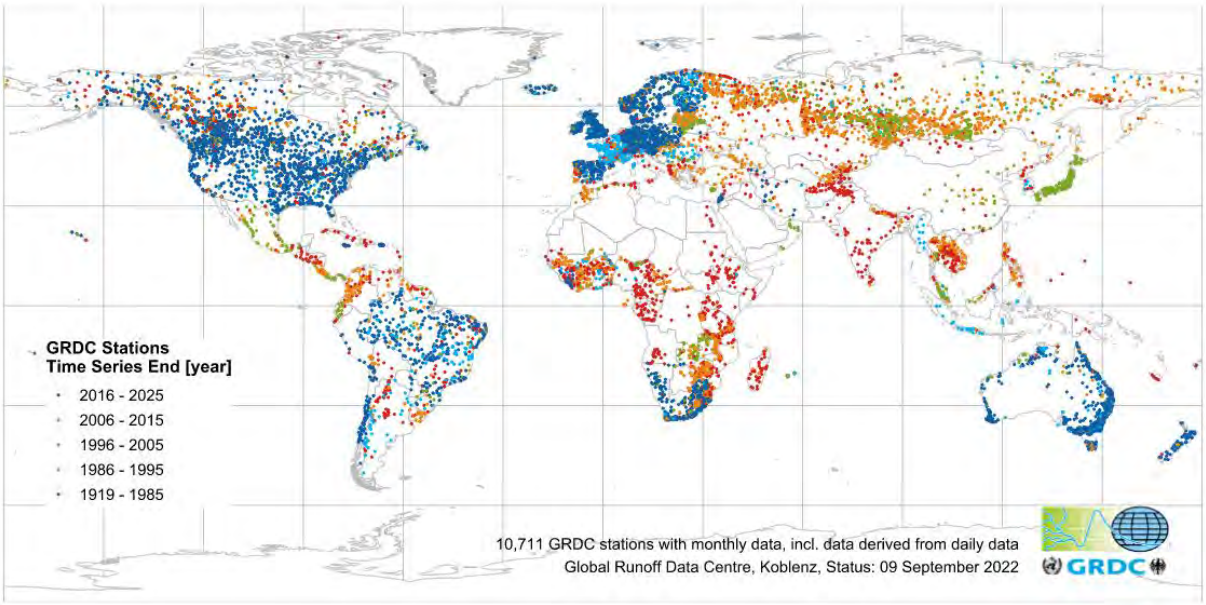

Figure 2-2. Spatial distribution of the in situ discharge stations from GRDC database labelled according to the duration of the record (GRDC Time Series End [year]) capturing historical and contemporary observations.

In our research thesis, we will focus on surface water elevation and extent. Over the last thirty years, satellite remote sensing approaches have been very useful to hydrology investigations with the advent of monitoring the extent and elevation of water bodies and their changes over time from space (Alsdorf et al., 2007; Calmant et al., 2008; Chawla et al., 2020; Fassoni-Andrade et al., 2021, among others). For instance, since the late 1990s, radar altimetry missions provide observations of water levels of lakes, rivers and floodplains (Cretaux et al., 2017; Cretaux, 2022) under their orbit tracks, now with the potential of long-term monitoring at thousands of VSs. In parallel, the use of satellite observations in a wide range of the electromagnetic spectrum (visible, infrared, and microwave, and their combination) has been developed to monitor the extent of surface water bodies for various spatial and temporal scales (Papa et al., 2010b; Leon et al., 2012; Pekel et al., 2016; Prigent et al., 2016; Huang et al., 2018b). They are often complementary to observations from the Gravity Recovery And Climate Experiment (GRACE) mission which provides, since 2002, long-term time series of the spatio-temporal variations in total terrestrial water storage (TWS) (Tapley et al., 2004) changes and helps to depict emerging changes in water availability at the global scale linked to environmental or human disturbances (Rodell et al., 2018).

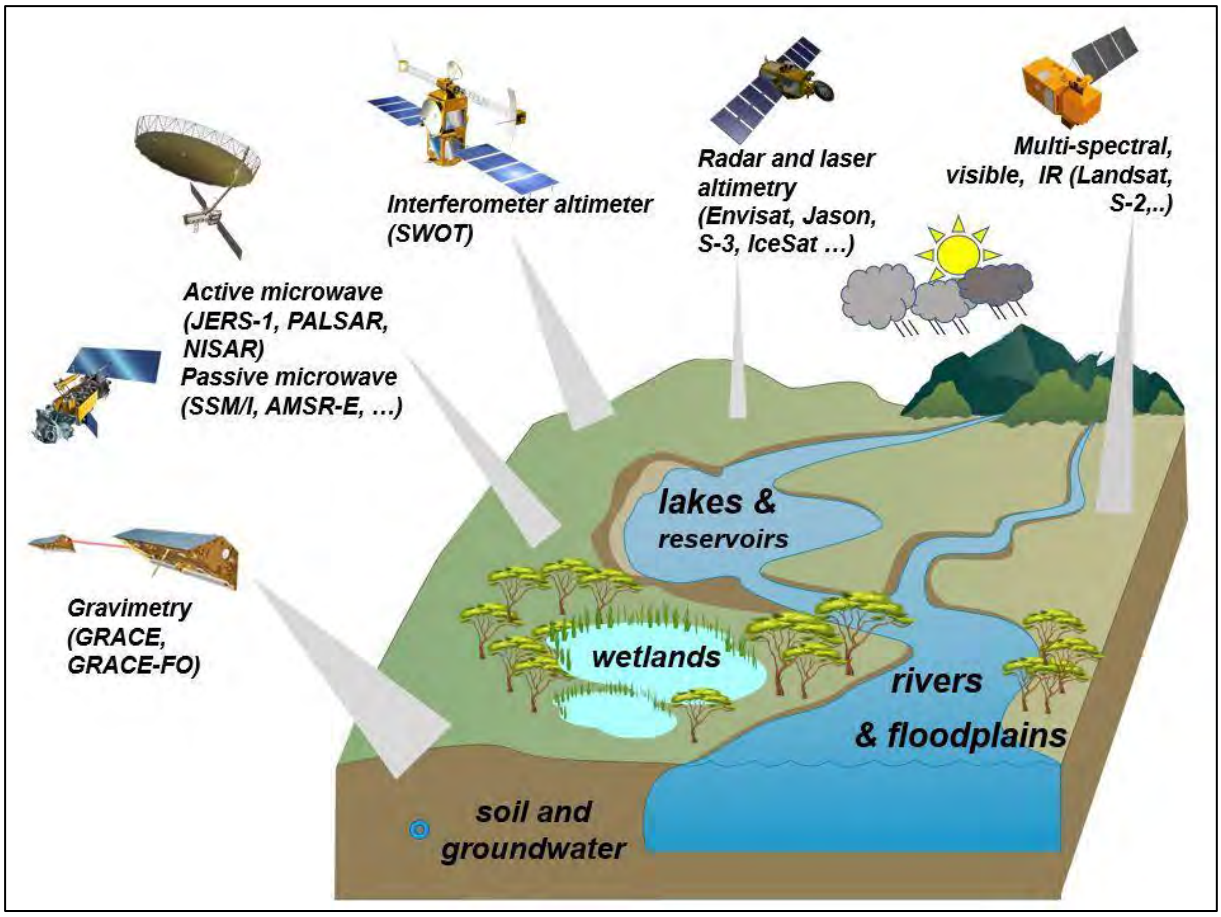

Figure 2-3. Schematic representation of surface water components and hydrological variables (e.g., water elevation and extent) and satellites that are used to monitor them are indicated (from Papa et al. [2022]).

In parallel, the availability of remote sensing observations has fostered the developments of hydrological and hydraulic modeling that helps to understand hydrological processes and their interactions and to build scenarios of past or future hydrological evolutions in the context of climate change, environmental alterations and flow/storage regulations by human interventions (Sood and Smakhtin, 2015; Lettenmaier et al., 2015; Döll et al., 2016; Tarpanelli et al., 2022). Earth Observation advances are therefore a breakthrough for surface hydrology and a unique opportunity to develop comprehensive observing systems to monitor Africa's land water and manage its water resources, specifically, in a sparse or ungauged river basin characteristic of major developing countries.

2.2.2.1 Satellite radar altimetry

Satellite remote sensing techniques, particularly, radar altimetry has been useful for several applications in geodesy, navigation, geophysics, geodynamics, oceanography and other

disciplines related to climate and environment of the Earth and in general for monitoring hydrological cycle parameters (Łyszkowicz and Bernatowicz, 2017; Stammer and Cazenave, 2018; Abdalla et al., 2021). Over inland water bodies, radar altimetry has been promising technology to monitor water levels variation of rivers and lakes at regional to global scales (Cretaux et al., 2017; Ghosh et al., 2017; Jiang et al., 2017). In this section, we will elaborate on the principle and physics of radar altimetry technique and the different satellite missions.

2.2.2.1.1 Generalities

Radar altimetry is an observation technique that measures distance with a radar altimeter on board a satellite aiming to determine the distance from the satellite to the ocean surface. The transmitter of the altimeter emits a very high frequency signal (a radar wave) in the direction of the Earth's surface, and its receiver picks up the echo, i.e., the part of the signal reflected by the sea surface. The time elapsed between transmission and receiving of the radar signal corresponds to the height of the satellite. Since the position of the satellite in its orbit and relative to the Earth's reference ellipsoid is precisely determined by other methods, the instantaneous sea level relative to the ellipsoid is measured (Cretaux, 2022). However, in practice, the electromagnetic wave is disturbed during its path and it is necessary to apply corrections to the raw measurement. These corrections will be presented later (Łyszkowicz and Bernatowicz, 2017; Stammer and Cazenave, 2018).

Primarily design for open ocean observations, radar altimetry expanded to other areas of science and the progress achieved by this spatial technique has exceed the expectations in the fields of global and coastal oceanography, hydrology, geodesy and cryospheric sciences (Abdalla et al., 2021). The level of accuracy and precision needed have largely evolved from the early beginning until now and strongly depends on the acquisition mode of the satellite and the environment characteristics for land water bodies (Jiang et al., 2020; Kittel et al., 2021; Abdalla et al., 2021; Kitambo et al., 2022a).

Geodesy is the science which studies and calculates the Earth's gravity field and its physical form. It has benefited from the observations acquired by satellite altimetry such as Topex/ Poseidon and Jason1/Jason2 (to mention the most famous ones) (Barzaghi et al., 2015). In fact, by measuring the level of the oceans, we can access the distribution of mass on the surface and in the interior of the Earth. To do this, it is necessary to extract from the altimeter measurement the component related to dynamic topography by averaging the measurements at the same point and over a long time period. This average value is close to the geoid (equipotential surface).

Therefore, the sea surface height measurements are then turned into geoid changes and subsequently into gravity field changes. By doing so, Andersen and Knudsen, (2000) developed the global marine gravity field model from satellite altimetry data by estimating ocean gravity anomalies over the sea surface (Fig. 2-4). Since this time, several models have been constructed (Łyszkowicz and Bernatowicz, 2017).

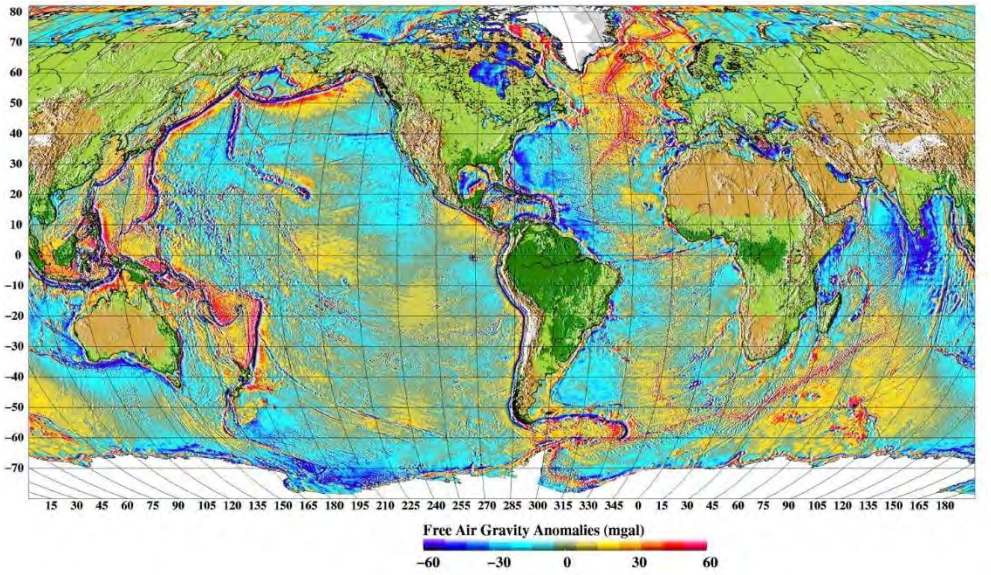

Figure 2-4. Gravity anomalies from satellite altimetry (Source: DNSC05 geoid model, Aviso).

Oceanography has benefited also greatly from the advent of satellite altimetry. The latter has substantially advanced understanding of the oceans by providing unprecedented observations of the surface topography (Fig. 2-5) at scales larger than ~200 km. This has increased the knowledge of global ocean circulation, from the role of mesoscale eddies in shaping this ocean circulation, up to global sea level rise (Cazenave et al., 2018; Abdalla et al., 2021). However, there is still challenges for modern oceanography that need to be solved regarding the observations of ocean dynamics at smaller, and faster scales (Klein et al., 2019).

Global estimates of glacier mass changes have traditionally been based on extrapolation of local geodetic and glaciological measurements. The advent of satellite altimetry in synergy with GRACE and GRACE-FO has also made it possible to measure mass changes of the ice sheets and the glaciers of the world (Fig. 2-6). Since the ERS-1 mission, scientists have been able to establish 26-year of altimetry record which has played a key role in measuring mass changes of the ice sheets (Shepherd et al., 2019) and glaciers (Gardner et al., 2013) of the world. Khan et al. (2022) showed using satellite altimetry from ICESat and ICESat-2 that mass loss from Greenland's peripheral glaciers result in a substantial contribution to sea level rise. Satellite

altimetry has thus made possible the assessment of ice thickness and the quantification of the influence of glacier melt on sea level rise.

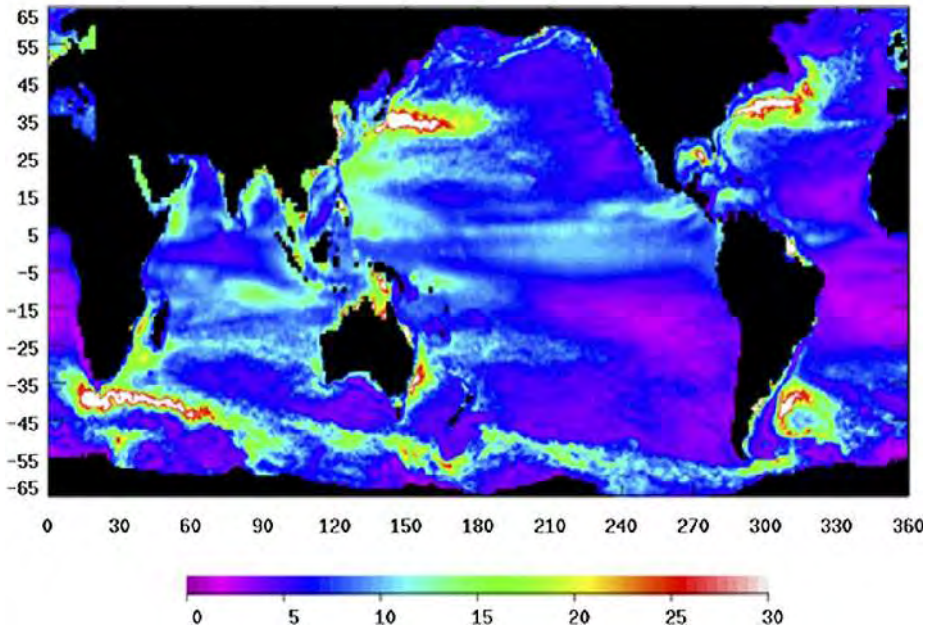

Figure 2-5. Standard deviation (in cm) of the surface height derived from altimeter data over the period of time 1992 to 2006 (Abdalla et al., 2021).

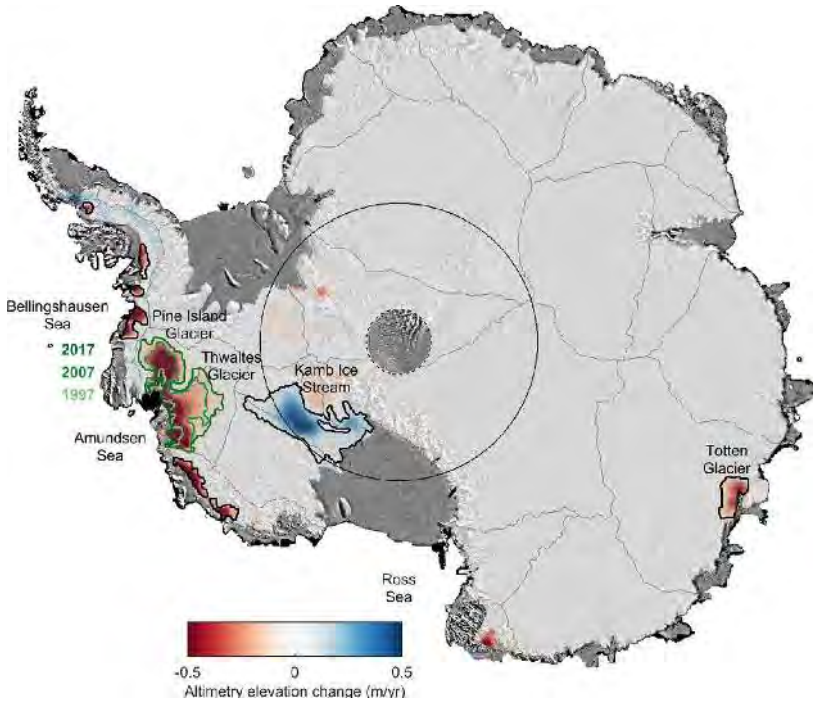

Figure 2-6. Schematic representation of the Antarctic ice sheet elevation showing its average rate change over the period 1992 to 2017 computed from ERS-1 and 2, ENVISAT, and Cryosat-2 satellite radar altimetry. Black circles around the pole indicate the southern limit of the Cryosat-2 (dashed) and other (solid) satellite orbits. The glacier drainage basins are

represented by grey boundaries. Areas of dynamical imbalance and those that have evolved over time are showing respectively by black and green boundaries (Abdalla et al., 2021).

In hydrology, with the failure of in situ gauging networks to provide spatially and temporally hydrological information on rivers, lakes, and wetlands, satellite altimetry has proved to be great tools in the monitoring of inland water bodies providing hydrological products such as time series of water stages (Fig. 2-7), discharges although it was not design primarily for hydrology (Calmant and Seyler, 2006). Radar altimetry over inland water requires specific processing as the signal is subject to other disturbances (e.g., presence of vegetation) different from those of the oceans. It is certainly in this field that altimetry has made significant progress in recent years (e.g., Synthetic Aperture Radar [SAR] technology), reaching accuracies of the order of a few tens of centimeters overs rivers (Abdalla et al., 2021; Kittel et al., 2021; Kitambo et al., 2022a). Besides monitoring water levels, altimetry also allows the quantification of many other variables associated with water level such as discharge, slope, volume (Papa et al., 2013; Paris et al., 2022; Scherer et al., 2022; Kitambo et al., 2022b). In the near future, Surface Water Ocean Topography (SWOT) satellite with its technological approach on the interferometry on large swaths will help provide better measurements and improve the global coverage and high resolution (Biancamaria et al., 2016).

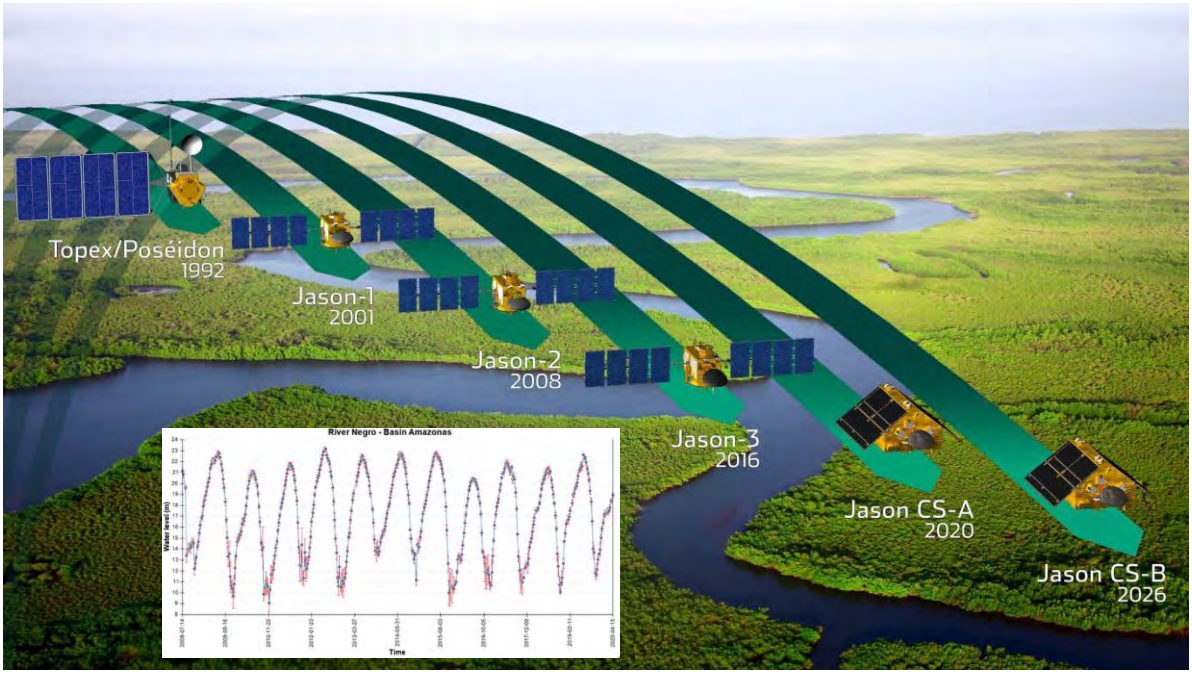

Figure 2-7. Timeline of Topex/Poseidon and Jason radar altimetry series. On bottom left side, water level time series from radar altimetry over the solimoes and Negro rivers confluence in the Amazon basin (Source: Aviso).

2.2.2.1.2 Physics of radar altimetry

Satellite altimetry is a radar technique that measures the distance, based on a simple principle of functioning. Radar altimeter on board a satellite emits a very high frequency signal (a radar wave) in the direction of the Earth's surface, which is reflected by the surface water (Stammer and Cazenave, 2017). The distance between the surface water and the altimeter (called range) is calculated by the formula:

$$R = v\,x\,\frac{t}{2} \quad (1)$$

where v stands for the speed of the radar pulse equals to light's celerity (3×10^8 m s^{-1}), t is the two-way travel time of the wave. The estimation of the satellite altitude (H) with respect to an Earth reference (i.e., ellipsoid), thanks to laser telemetry and DORIS (Nouel et al., 1988) or GPS positioning systems, enables the calculation of surface water height (SWH) by subtracting the altimetric distance to the satellite altitude as follows (Cretaux et al., 2017; Cretaux, 2022):

$$SWH = H - R + Cp + Cg + Ci \quad (2)$$

The different computational variables involved in the SW measurement are illustrated in Fig. 2-8.

Cp, Cg, and Ci refer to the corrections that must be applied for a precise determination of SWH. These corrections are essentially of three types (Cretaux et al., 2017):

- Cp stands for corrections of propagation through the atmosphere due to the presence of ions and water in the ionosphere and the troposphere. The magnitude of the error is in terms of a few centimeters.
- Cg corresponds to geophysical corrections that aim to correct for the crustal deformation due to pole and solid earth tides at the time of measurement with respect to a reference Earth.
- Ci stands for instrumental bias and an electromagnetic bias related to significant wave height and wind velocity. The error is on the order of a few centimeters on ocean. Over continental water bodies, this correction is not considered, except for very large water bodies.

SWH is provided in the geodetic frame of the orbitography systems. To convert it into an orthometric height, useful for hydrology, it must be corrected from the local undulation of the geoid N:

$$SWH_{corr} = SWH - N \quad (3)$$

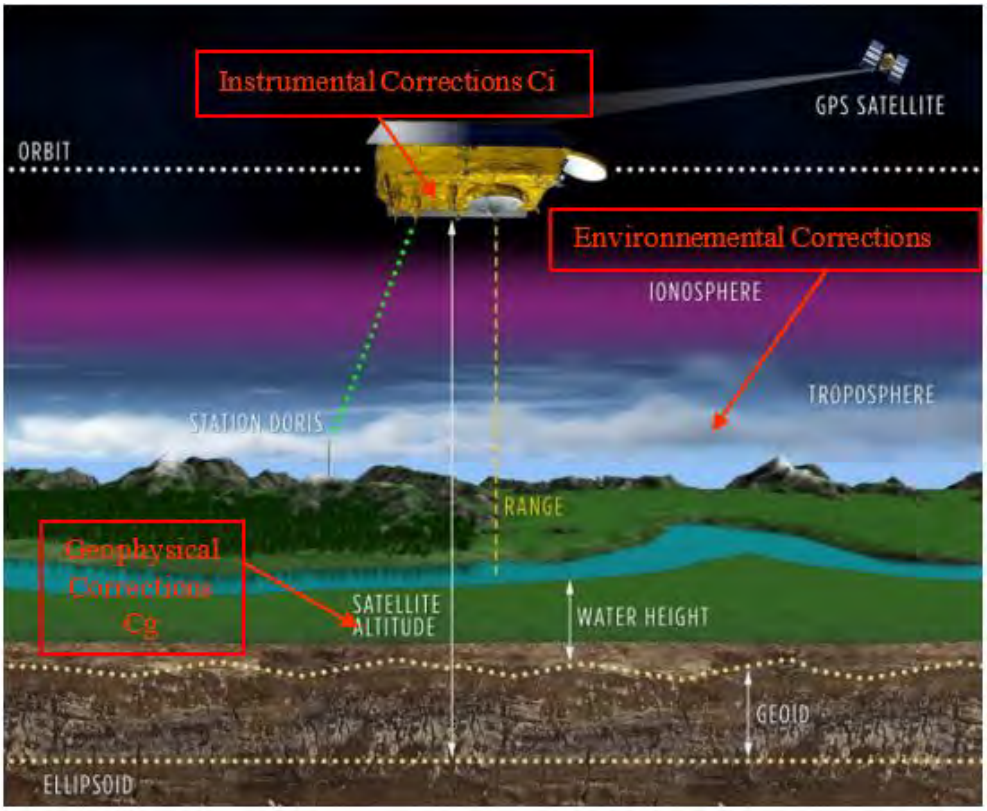

Figure 2-8. Schematic representation of the surface water height measurement from radar altimetry satellite. red rectangles represent different components of corrections to the measurement (Source: Aviso).

2.2.2.1.3 Creation of water level time series

The altimeter embedded in a satellite emits an electromagnetic wave at different frequencies (e.g., commonly used S, C, Ku, and Ka) in the direction of the Earth's surface over an area from which the radar wave will be reflected back to the altimeter. This area, called footprint or ground spot is of several tenths of square kilometers and its diameter is a function of the technical characteristics of the satellite antennas (Cretaux et al., 2017; Cretaux, 2022). The return echo does not arrive instantly at a given moment to the receiver, it lasts over time with varying amplitude defining therefore the shape of the radar echo, namely the waveform. It passes successively through the states of a point, a full circle and then a section of a cylinder whose diameter increases up to a certain threshold inherent to the instruments (Fig. 2-9). In reality, the satellite never observes a completely flat surface (calm water, Fig. 2-9a) but rather a surface with a certain amount of roughness (rougher water, Fig. 2-9b), which has the consequence of disturbing the waveforms (Fig. 2-9).

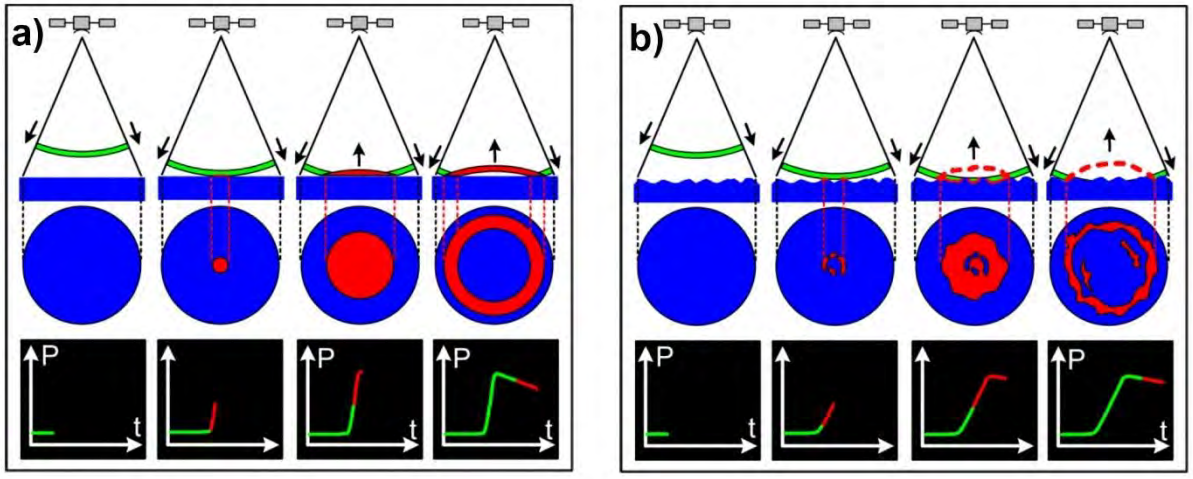

Figure 2-9. Representation of a reflected waveform of conventional altimetry echo. At the top, a representation of the satellite and emitted wave, with the reflected wave in red. In the middle, the behavior of the wave on a smooth surface (a) and rough surface (b). At the bottom, the wave form received by the altimeter (Calmant et al., 2008).

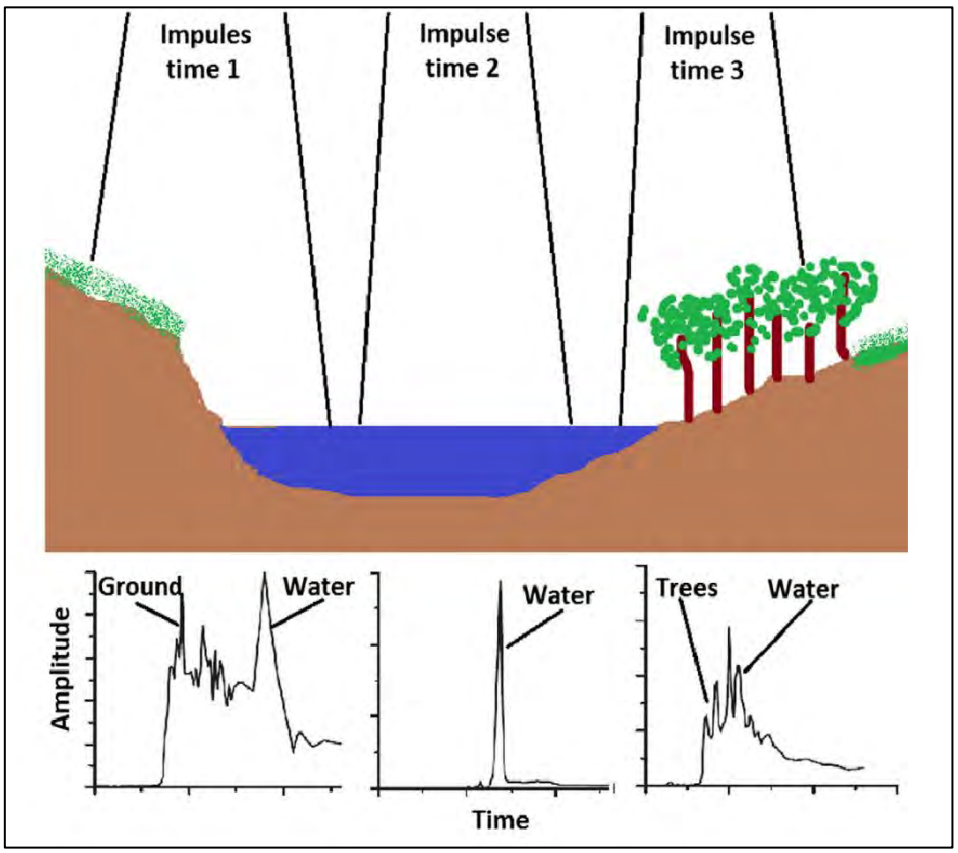

Figure 2-10. Schematic representation of waveform over inland water bodies (Maillard et al., 2015).

There is a variety of radar echo shapes depending often on the type of surface on which the electromagnetic wave is reflected. Subsequently, the radar echo shape is often a mixture of several reflectors causing the waveforms to be multipeaked (Fig. 2-10), particularly over inland water bodies. Thus, it is necessary to analyze the return echo not one by one but as a whole in order to obtain a usable and intelligible signal. This processing is called tracking when it is done on board and retracking when it is done on the ground.

ENVIronmental SATellite (ENVISAT) was the first satellite mission to propose reprocessed range in the Geophysical Data Records (GDRs) from four different retracking algorithms (i.e., Ocean, Offset Center of Gravity [OCOG] or Ice-1, Ice-2, and Sea Ice). There are several retracking algorithms (i.e., Ocean, Ice-1, Ice-2, Ice-3, Sea-Ice, Red-3, Oce-3), and Initially, altimetry data processing algorithms was developed for the open ocean (Rybushkina et al., 2012). They are classified in two categories, retracker based on the physical modeling of the waveforms by adjusting the real waveforms to the theoretical waveform models such as Ocean, Ice-2, Red-3, Oce-3 and the one that are empirical (and not based on physical laws formulated mathematically) such as Ice-1, Ice-3, and Sea-Ice. The choice of one or the other is made according to the nature of the surface observed. Over the Great Lakes, ranges derived from the ocean retracker still provide the best results (Cretaux et al., 2017). Over rivers, it is generally preferred to use the retracking algorithm Ice-1 due to its robustness although it was originally developed for polar ice caps (Frappart et al., 2006; Da Silva et al., 2010).

Based on the operation mode of radar altimeters, the latter are classified as functioning in: Low resolution mode (LRM) also called conventional altimetry (Fig. 2-11a), Synthetic Aperture Radar (SAR) also known as Delay-Doppler Altimetry (Fig. 2-11b), and SAR Interferometric (SARIn, Fig. 2-11c). All the three modes take measure only at the nadir (i.e., vertically below the satellite). With the evolution expected in spatial hydrology, a new instrument designed for wide-swath altimetry embeds in the Surface Water and Ocean Topography (SWOT) satellite will enables two-dimensional observation of rivers and water bodies on two swaths of 50 km each on both sides of the ground track of the satellite (Biancamaria et al., 2016). LRM mode used on the first generation of altimeters (European Remote Sensing [ERS]-1 and 2, Topex-poseidon [T/P], Environmental satellite [Envisat], Jason-1, Jason-2, GEOSAT Follow On [GFO], SARAL/AltiKa [SRL]), considers the reflection of the emitted beam as a whole with a footprint covers several tens of square kilometers. SAR mode, incorporated in Cryosat-2 and Sentinel-3, uses the doppler effect to distinguish where the beam is reflected, between reflections from behind and in front of the transmitted beam. This enables the slicing of the footprint in bands within the footprint with a decrease in the noise level compared to LRM

mode (i.e., much higher spatial resolution [~300 m] in along-track direction, in the direction in which the satellite is moving). In SARIn mode, operated in Sentinel-6 and Jason-CS, the spatial resolution (~50 cm) in along-track direction has increased with the capability to very precisely geolocate the reflecting point within the radar footprint.

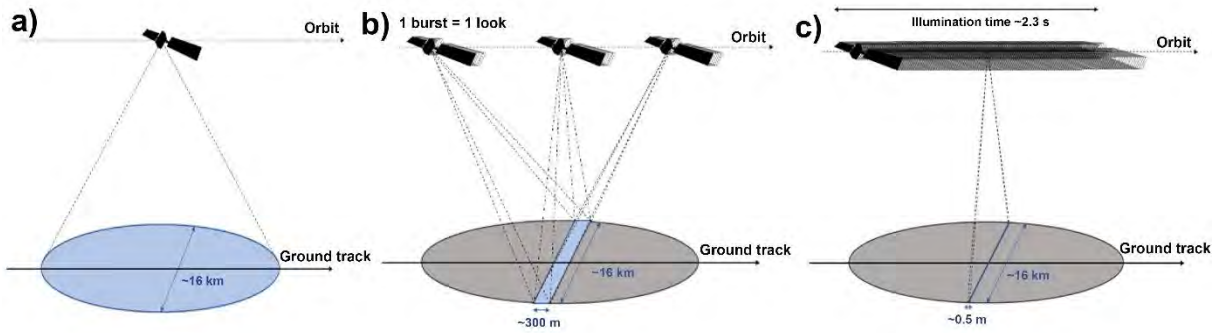

Figure 2-11. Type of operation mode of acquisition of radar altimeters. a) Low resolution mode, b) Synthetic aperture radar, and c) Synthetic aperture radar Interferometric (Source: Aviso).

Note that several initiatives have been undertaken aiming to generalize the use of altimetry for hydrology by providing homogeneous radar altimetry data sets over the whole period of observations. For instance, in the framework of the Contribution de l'Altimetrie Spatiale à l'Hydrologie (CASH) project, T/P data have been reprocessed using Envisat algorithms (Seyler et al., 2005). For European Remote Sensing (ERS) data, the reprocessing performed by the European Space Agency (ESA) for ERS-1 and 2 was done in the framework of the Reprocessing of Altimeter Products for ERs (REAPER) project (Femenias et al., 2014) and by the Centre for Topographic Studies of the Oceans (CTOH) for ERS-2 (Frappart et al., 2016). Even though primarily, the radar altimeter technique was designed for oceanography purposes, recently, more and more spatial agencies such as ESA, Centre National d'Etudes Spatiales (CNES), National Aeronautics and Space Administration (NASA), Indian Space Research Organization (ISRO) have started including hydrological objectives for the design of new altimeters. An example with SRL and Sentinel-3A missions launched for the first time with a target of monitoring continental waters. More recently, the satellite dedicated fully to both continental hydrology and oceanography mission, SWOT satellite. It is a result of the collaboration between the (US) NASA, CNES (the French Spatial Agency), the Canadian Space Agency and the United Kingdom Space Agency. Considering the hydrology capabilities of SWOT, many hydrologist scientists are calling SWOT the "golden age of water cycle observations from space" (Gallucci, 2021).

2.2.2.1.4 Radar altimetry missions

Since the 1970s, with the useful measurement of the ocean surface topography using radar equipment embedded in Seasat, Geosat, and ERS-1 satellite missions, several new radar altimetry missions were launched (Fig. 2-12) providing water level variations over oceans and land surface water bodies (Łyszkowicz and Bernatowicz, 2017) (Abdalla et al., 2021). Considering the era of radar altimetry, its timeline can be organized in two periods: past and current missions.

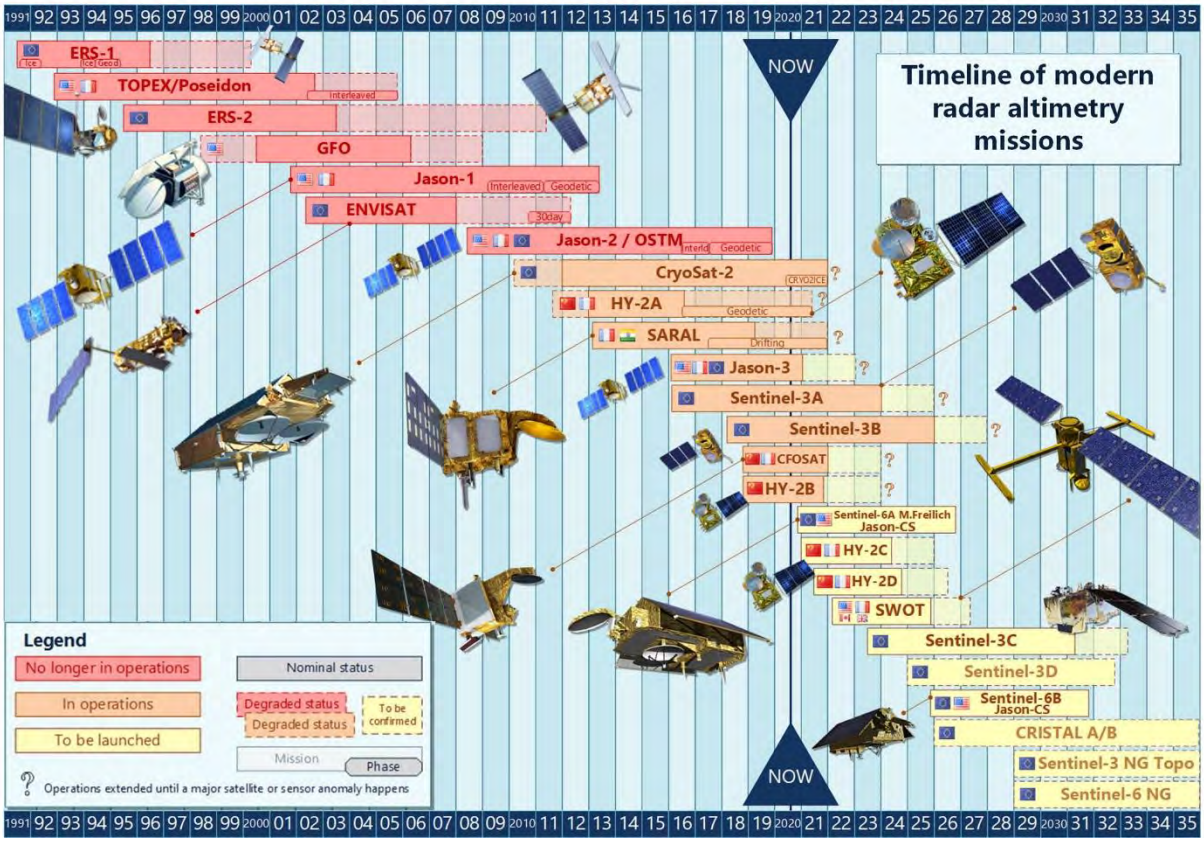

Figure 2-12. Timeline of modern radar altimetry missions (Source: Aviso+ [2022]).

2.2.2.1.4.1 History and research missions

For a short history, it was at Williamstown Symposium in 1969 where experts from solid Earth and ocean domains brainstormed about the potentiality of satellite altimetry and from that altimetry was given a high priority. This resulted in the 1970s and 1980s with the development of accurate satellite altimeter systems such as Skylab that provided for the first time the measurements of undulations in the marine geoid due to seafloor features, followed by Geos-3 that the altimeter inherited from the Skylab, gave more precise altimetric measurements. The lesson taught by this mission was the ability of such a system to measure the geoid and

oceanographic parameters. Moreover, scientists showed the capability of altimeter to derive valid measurements over land and sea ice. The last satellite to be launched in the 1970s was Seasat that paved the foundations of the next generation of ocean satellites. Its altimetric measurement design included major innovation that enables providing improved quality data (Tapley et al., 1982). In the 1980s, Geosat was the only satellite launched whose altimeter inherited the technology of Seasat.

In the 1990s, started to be launched the generation of satellite with an accurate orbitography and location system (e.g., Doppler Orbitography and Radiopositioning Integrated by Satellite [Doris]) such as T/P, in concurrent with the European Remote Sensing (ERS-1) satellite. Table 2-1 summarizes the main characteristics of some of the past and the current altimetry missions.

Table 2-1. Past and Current Altimetry Mission Characteristics (Stammer and Cazenave, 2017).

Mission	Altitude/ Repetitivity	Inclination	Altimeter frequency	Agency	Launch/End of mission	Primary objective
Skylab	440 km	50°	Ku band radar alt	NASA	1973/1974	Geodesy
Geos-3	830 km	114.98°	Ku band radar	NASA	1975/1979	Geodesy
Seasat	800 km/17 days	108°	Ku band radar	NASA	1978/1978	Ocean
Geosat	800 km/17 days	108°	Ku band radar (Seasat Heritage)	US Navy	1985/1990	Geodesy, Ocean
ERS 1	785 km/35 days, 3 days (ice), 168 days (geodetic)	Sun synchronous	Ku band radar (includes an ice mode)	ESA	1991/2000	Ocean, Ice, Geodesy
TOPEX/ Poseidon	1336 km/10 days	66°	Ku and C band radar	NASA/CNES	1992/2006	Ocean
ERS 2	785 km/35 days (as ERS-1)	Sun synchronous	Similar to ERS-1	ESA	1995/2011	Ocean, Ice
GFO	800 km/17 days, Same as Geosat	Same as Geosat	Ku band radar	US Navy	1998/2008	Ocean
Jason 1	Same as TOPEX/ Poseidon	Same as TOPEX/ Poseidon	Ku & C band radar	NASA/CNES	2001/2013	Ocean
ENVISAT	782 km/35 days 799 km/30 days (end of life)	Sun synchronous	ERS-1 heritage, Ku and S band radar alt	ESA	2002/2012	Ocean
Jason-2	Same as Jason-1	Same as Jason-1	Similar to Jason-1	NASA/CNES/ NOAA/ EUMETSAT	2008/2019	Ocean
Cryosat-2	717 km/369 days	92°	Ku nadir	ESA	2010/-	Ice

			looking radar, SAR and interferometric SAR mode			
HY 2A	971 km/14 days, first phase, 973 km/168 days geodetic, second phase	Sun synchronous	Ku & C band radar alt	CNSA/CNES	2011/2020	Ocean, Geodesy
SARAL/ Altika	Same as ENVISAT	Sun synchronous	Ka Band radar alt	CNES/ISRO	2013/-	Ocean, Hydrology, Ice
Jason-3	Same as Jason-1	Same as Jason-1	Similar to Jason-1	NASA/CNES/ NOAA/ EUMETSAT	2016/-	Ocean
Sentinel 3A	815km/27 days	Sun synchronous	Ku and C band radar alt including an along track SAR mode	EU/ESA	2016/-	Ocean
Sentinel 3B	Same as Sentinel 3A	Same as Sentinel 3A	Similar to Sentinel 3A	Same as Sentinel 3A	2018/-	Same as Sentinel 3A
CFOSAT	~500 km	97°		CNSA/CNES	2018/-	Ocean
Jason-CS/Sentinel-6MF	1336 km/10 days	66°		ESA/NASA/ EUMETSAT/EU /CNES/NOAA	2020/-	Ocean

In the context of the increasing need to observe and model the global water cycle, NASA, CNES, the Canadian Space Agency (CSA), and the United Kingdom Space Agency (UKSA) jointly developed SWOT satellite launched on the 16th of December 2022 for 3-year lifetime and it is considered as the golden age of hydrology due to its Ka-Band Radar Interferometer technique. SWOT (Fig. 2-13) is the first satellite mission with both objectives to measure ocean and land water surface topography. SWOT mission works with an unprecedented new concept combining two SAR antennas operating in Ka-Band. The radar altimeter called Ka-Band Radar Interferometer (KaRin) will provide images of water elevations within two swaths of 50 km each on both sides of the ground track of the satellite. These two swaths are separated by a band of 20 km without observations (Fig. 2-13) (Biancamaria et al., 2016).

SWOT payload is also constituted of a Ku-band nadir altimeter working in LRM, inherited from the Jason technology. The satellite flies on a non-sun-synchronous of 21-day repeat cycle at 890.6 km. One of the advantages of SWOT is the more complete ground coverage than with previous nadir-altimeters. In addition to the water height, which is measured mainly by the current altimetry mission, SWOT will also provide both width and slope measurements. The

main objective of SWOT for hydrology is to study hydrological processes and understand the role and impact of water storage change on the global water cycle and to study the sensitivity of the continental water cycles to human activities.

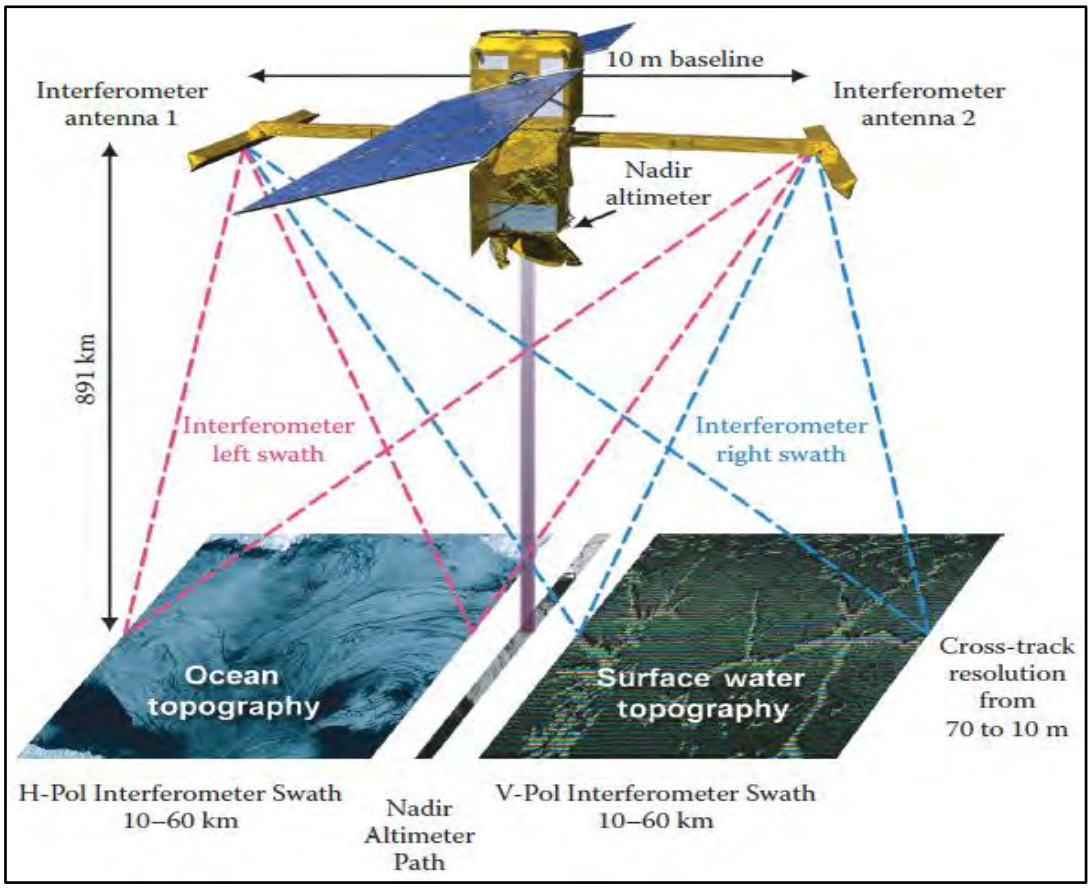

Figure 2-13. Characteristics of SWOT satellite (Source: CNES).

2.2.2.1.5 Applications of radar altimetry over land

Radar altimetry system has been developed mainly for oceanography purposes. In the early age of the development of altimetry, scientists also discovered the capability of altimeters to derive valid measurements over land. Since then, radar altimetry has been a valuable observational tool for the other hydrosphere components (e.g., rivers, lakes, wetlands) (Abdalla et al., 2021; Cretaux, 2022). Altimetric water levels are increasingly used to solve hydrological problems. Such data are particularly useful for large hydrological basins as well as for poorly monitored basins (Santos da Silva et al., 2014; Fassoni-Andrade et al., 2021; Kitambo et al., 2022a). Recently some agencies such as CNES, NASA, ESA, and ISRO have started to include hydrological objectives for the design of new altimeters.

Early after the launch of the first radar altimeter, Birkett (1994) proved that radar altimetry can be used efficiently in the monitoring of the relative lake level variations. The first altimeter (e.g., Geosat mission) showed large errors due mainly to inaccuracies in the determination of the satellite orbit. Nevertheless, ERS-2, ENVISAT, T/P showed a clear opportunity to derive lake level variations with an overall accuracy of 10 cm or even less than this, ~4 cm rms (Birkett, 1995). This capability of radar altimetry to successfully derive the accurate lake level data over a long-term period opened the opportunity of climate change studies because lake level data act as an important indirect indicator of climate change. Moreover, the accuracy of satellite altimeter to derive water level variations over river and floodplains have been successful in several river basins and different environment (Frappart et al., 2006; Seyler et al., 2008; Da Silva et al., 2010; Papa et al., 2015; Kittel et al., 2021; Kitambo et al., 2022a). Several applications have been developed using stages from radar altimetry in hydrology. Kouraev et al. (2004), Zakharova et al. (2006), Papa et al. (2012) were able to estimate river discharge of different rivers from altimetry data by merging with in situ observations. The methodology used the empirical relationship between satellite-derived water levels and daily estimations of river discharges based on rating curves (RCs). Getirana et al. (2009) showed the possibility of monitoring river discharge in poorly gauged basins, specifically the northern Amazon basin from spatial altimetry data in particular ENVISAT. The methodology is to obtain high accuracy relationships between water levels provided by radar altimetry and water discharge computed by a hydrological model. Paris et al. (2022) used the same approach over the CRB and showed the possibility of near real time monitoring of spatialize discharge from a trove of satellite altimetry (i.e., J2 and 3, S3B). On top of providing the depth and the discharge, RCs can also estimate along a given reach useful information on the shape of cross sections (Paris et al., 2016). Another study has demonstrated the possibility of inferring the discharge through the rating curve model (Tarpanelli et al., 2013). Radar altimetry in combination with other remotely sensed data has provided surface water volume variations over rivers, lakes and wetlands. Papa et al. (2015) and Becker et al. (2018) derived surface water storage over rivers and wetlands respectively in Ganges-Brahmaputra River basin and Congo by merging surface water extent from Global Inundation Extent from Multi-Satellite and satellite-derived water levels from radar altimetry. Carabajal and Boy (2021) derived relative volume variations of several lakes and reservoirs in South America by combining surface water extent of these water bodies from Moderate Resolution Imaging Spectroradiometer (MODIS) together lake water heights obtained from the Ice, Cloud and Land Elevation Satellite (ICESat). Another application in which radar altimetry is involved is the calibration/validation of hydrological and

hydrodynamic models (Sun et al., 2012; Paiva et al., 2013; Garambois et al., 2017; Corbari et al., 2019; Pujol et al., 2020). Paiva et al. (2013) used water levels derived from ENVISAT altimetry data and other remotely sensed products (e.g., monthly terrestrial water storage [TWS] anomalies derived from the Gravity Recovery and Climate Experimental mission [GRACE]) to validate the hydrologic/hydrodynamic MGB model over the Amazon River basin. Park (2020) used satellite radar altimetry data (i.e., J2) to understand the mechanism of channel-floodplain seasonal connectivity along the Amazon River. The approach is based on the concurrent measurement of water levels over river and floodplain and the analyzing of their seasonal changes in water surface height difference. This led to the identification of two indiscrete flooding processes during the rising phase that are channelized and overbank dispersion processes.

Several groups or institutions around the world have developed several databases of altimetry over inland water using different processors during the past 20 years. These databases provide time series of surface water elevation, covering a wide range of water bodies and applications. The databases are "River&Lake" providing water level time series over rivers, lakes, reservoirs (http://altimetry.esa.int/riverlake/continent/africa.html, Berry et al., 2005); "Hydroweb" provinding similar data as the first database (https://hydroweb.theia-land.fr/, Crétaux et al., 2011); "G-REALM" providing water level time series only over lakes and reservoirs (https://ipad.fas.usda.gov/cropexplorer/global_reservoir/, Birkett et al., 2011); "DAHITI" that provides a variety of hydrologial information on lakes, reservoirs, rivers, and wetlands (https://dahiti.dgfi.tum.de/en/, Schwatke et al., 2015). Recently, other iniatives have emerged such as the ESA CCI "Lakes" ECV providing lake water level and other satellite-derived products (https://climate.esa.int/fr/projects/lakes/, Woolway et al., 2020); and "GRRATS" providing water level over rivers (https://research.byrd.osu.edu/grrats /index_7.php, Coss et al., 2020).

All these databases provide time series at VSs in different river basins worldwide ready to be used in hydrological analysis. However, not all potential VSs are available in these databases, sometimes because they did not meet the requested quality standard, sometimes because they were not included in the apriori locations to be processed as it is the case for example of very narrow rivers or floodplains and marshes small streams. Altimetric observations or raw data named "Geophysical Data Records" (GDRs) can then be downloaded freely from the Center for Topographic studies of the Oceans and Hydrosphere (CTOH, http://ctoh.legos.obs-mip.fr/) and manually processed with specific software. The CTOH is a French observation service that

makes available the GDR provided by the space agencies along with additional parameters and corrections. Several software have been developed for processing GDRs data in order to create water time series such as the Virtual Altimetry Station software (VALS, Da Silva et al., 2010; Frappart et al., 2015a), Multi-mission Altimetry Processing Software (MAPS, Frappart et al., 2015b) and more recently Altimetric Time Series Software (AlTiS, Frappart et al., 2021). AlTiS V2.2.6 is the latest version of the three software developed by CTOH. It is a free software and is released as open source under the CeCill License. AlTis is an open access software (http://ctoh.legos.obs-mip.fr/applications/land_surfaces/_altimetric_data/altis, last access 13 February 2023) under python3 environment (Anaconda distribution) and tested for GNU/Linux, Windows 10 (and soon for Mac OS X).

A new era opened in the last few years with the advent of operational satellite altimetry missions. In the frame of the COPERNICUS program, ESA and EUMETSAT funded and operate a constellation of satellites (among which the Sentinel-3 and Sentinel-6 missions) with different sensors onboard and capable of monitoring in near real time and on the global scale several characteristics of Earth's surface. Through this operational service, ESA is committed to provide free and open access to data to any user on Earth. This turns possible the creation of new services based upon Copernicus data in domains as wide as hydroelectricity, humanitarian, climate change, flood forecasting, etc.

2.2.2.2 Surface water extent from Earth observation

A variety of remote sensing techniques including optical and radar sensors have been employed in a wide range of observations of the electromagnetic spectrum, including visible, infrared, or microwave observations (Alsdorf et al., 2007; Prigent et al., 2016; Li et al., 2022) to estimate and monitor the distribution of inland surface water from very fine spatial resolution (few meters) to coarser ones (~50 km) covering various temporal scales and periods (Papa et al., 2022).

Nowadays, in the field of hydrology and water resources research, there are several products with different range of space and time resolutions presenting advantages and disadvantages related to the technique of data acquisition (Li et al., 2022; Papa et al., 2022). For instance, optical and infrared sensors have good spatial/temporal resolution, sometimes with ~10 m resolution and a few days revisit, but their capabilities are limited in tropical and subtropical Africa regions because of dense clouds and vegetation, whereas, SARs show very large

capabilities to measure surface water extent at high resolution (10–100 m) but often suffer from a low temporal revisit time, making them not suitable to monitor rapid hydrological processes. For more details about the inland surface water extent from EO, refers to Li et al. (2022) and Papa et al. (2022) that is inserted in the appendix of this thesis.

2.3 Hydrological modeling

Hydrology is the science dedicated to the study of waters all over the Earth, their occurrence, circulation and distribution, their chemical and physical properties and their reaction with the environment including their relation to living things (Linsley et al., 1975). It also treats the relationship of water with the environment in each phase of the hydrological cycle. The increase in anthropogenic pressure and the climate change have caused changes in the hydrologic system balance. Different hydrologic phenomena require to be thoroughly studied in order to understand these variations. During the past decades and thanks to the increase of computational power, hydrological models have become one of the most used tools to understand and represent the complex time and space variations of physical processes (Devia et al., 2015). Large-scale hydrological models are being used to manage international conflicts related to water in transboundary basins (Andersen et al., 2001), to estimate climate change effects on streamflow (Guo et al., 2002), to assess the effects of widespread land cover change on streamflow (Matheussen et al., 2000), for hydrological forecasting (Bremicker et al., 2004), and as a tool for decision support in water resources planning and management of river basins (Tshimanga, 2022). Especially in data-scarce regions, they became one of the unique solutions to overcome the lack of in situ data.

A model is a simplified representation of a physical system through equations that symbolize the relationship between an input and an output at a given time interval (Tucci, 1986; Devia et al., 2015). As the rainfall variable is much easier to measure continuously than the hydrometric variable (Thiery, 1993), one of the main problems to be solved in hydrology is to know how precipitation is transformed into runoff taking into account various parameters used for describing watershed characteristics. One of the purpose in the field of hydrological modeling is to improve the representation of processes and interactions between the different components of the hydrological cycle. Hydrological models can be applied from small basins up to the very complex and large basins (Devia et al., 2015), and the selection of an adequate model will vary depending on the spatio-temporal scales and the type of processes to be represented. In this section, we will present different types of models and the main information needed to use a

hydrological model. Finally, we will present the MGB model that was used to derive the flow over the CRB in our research study.

2.3.1 Types of models

Various hydrological models have been developed during the past four decades and each model has got its own unique characteristics (Devia et al., 2015). Efforts have been made by hydrologists to classify hydrological models according to the way they describe processes, their capacity or not to represent the spatial variations of processes and variables, and the degree of complexity of equations (Singh, 1995; Refsgaard and Storm, 1996; Jajarmizadeh et al., 2012; Devia et al., 2015; Yoosefdoost et al., 2022). They can be separated into several classes but here we will present dominant classifications. Hydrological models, often built on mathematical structures, can be gathered by four basic categories, namely simulation basis, spatial representation, temporal representation and method of solution. Further, each category can be split in more detailed subcategories. For instance, simulation basis consists of physically-based, conceptual, and empirical models. Moreover, the spatial representation category includes lumped and distributed systems while the temporal representation category comprises steady state, steady state seasonal and continuous representations. The method of solution includes classes such as analytical and numerical solutions. Usually, these terms constitute the basis of classification of hydrological models (Devia et al., 2015). In addition, there are models with a simplified representation of flow propagation without consideration of flooded areas (Collischonn et al., 2007), with flooded areas (Yamazaki et al., 2011), to a hydrodynamic representation of propagation (Paiva et al., 2013a, b).

2.3.1.1 Classification of hydrological models

A lumped model represents a basin as a single entity without providing any information about the spatial distribution of variables. It simulates state variables and fluxes into and out of the catchment as a whole (Silberstein, 2006). Jajarmizadeh et al. (2012) reports that many conceptual models are lumped models in a sense that the basin is represented by a series of units that give spatially average treatment of the system. Contrary, distributed models consider a basin into many entities, and the state variables and fluxes between the entities are determined across the catchment. Between the two models exists a semi-distributed category which considers a basin as a series lumped models. In comparison with a fully-distributed model, a semi-distributed model requires less data.

Empirical models are generally the simplest models. They represent real systems with mathematical explanation using experimental data without considering the features and processes of the hydrological system. They are utterly dependent on the existing data, thus the name data driven models. Several primary hydrological models are empirical and have play crucial role in developing science of hydrological models. For instance, the IHACES and Instantaneous Unit Hydrograph (IUH) are empirical model that show unit hydrographs (Noorbakhsh et al., 2005). Empirical models involve statistical approach to perform a statistical analysis (e.g., linear and multiple regressions) from concurrent input and output time series.

Conceptual models describe all the components of hydrological processes as a series of moisture stores, with fluxes between the stores and out of the catchment represented by parametric equations. The conceptual parametrizations often attempt to quantify physical processes. The model parameters are assessed not only from field data but also through calibration (Silberstein, 2006). The calibration involved curve fitting between simulated variables against an observed record. One of the first and famous developed conceptual model was Stanford Watershed Model IV (SWM) with parameters ranging from 16 to 20 (Crawford and Linsley, 1966). Since then, several conceptual models have been developed with varying degree of complexity. HBV and TOPMODEL are examples of conceptual models. Conceptual models are not a physical-based processes rather they simulate the behavior of the system based on a concept. (Devia et al., 2015).

Physically-based models represent different components of the hydrological processes (e.g., evapotranspiration, infiltration) using the governing equations of motion. These models called mechanistic are a mathematically idealized representation of the real phenomenon and include the principles of physical processes. The hydrological processes related to water's motion are solved numerically using finite difference equations, however, analytical solutions can be considered (Jajarmizadeh et al., 2012). These models involve huge amounts of data (e.g., soil moisture content, initial water depth, topography, dimensions of river network, etc.) and a considerably number of parameters related to physical characteristics of the catchment are required. Note that the state variables here are wholly measurable parameters (Pechlivanidis et al., 2011) (Devia et al., 2015). As example of a physically-based models, we have MIKESHE model and SWAT models (Devia et al., 2015).

Other types of classification consider space-scale based classification. According to this, Singh (1995) reports that hydrological models can be broadly split in those of small catchments (up to 100 km^2), medium-size catchments (100-1000 km^2), and large catchments (greater than 1000 km^2) (Pechlivanidis et al., 2011). Other large-scale hydrological models exist at continental and

global scale simulating terrestrial water cycle. Such models broadly fall into two categories. Land Surface Models (LSM) and Global Hydrology Models (GHM). LSMs are numerical models that solve the coupled fluxes of water, energy, and carbon between the land surface and atmosphere. These models focus on solving the surface-energy balance. In contrast, GHMs focus on describing terrestrial water fluxes and on solving the water balance equation in the context of water resources assessment. In comparison to catchment-scale models, usually large-scale models are not calibrated (Gudmundsson et al., 2012; Siqueira et al., 2018; Fisher and Koven, 2020).

2.3.2 Input data for hydrological modeling

For hydrological modeling, the most often forcing data needed to all these models are hydrometeorological, physiographic, hydrometric, pedologic, geomorphologic, geologic, land/land cover, and agricultural data (Devia et al., 2015; Singh, 2018). Often, these data have been collected by local, state, and federal agencies for their operational and management purposes. During the past three decades, technology for data collection has undergone a revolutionary change. For instance, it is now possible to collect spatial data rather than point data and satellite technology has enabled the community to collect data in remote inaccessible areas (Singh, 2018).

2.3.3 MGB hydrological-hydrodynamic model

MGB is a conceptual, semi-distributed, large-scale hydrological model that uses physical and conceptual equations to simulate land surface hydrological processes (Collischonn et al., 2007; Paiva et al., 2013; Siqueira et al., 2018). The model discretizes the basin into unit catchments and uses the hydrological response units (HRUs) approach that combine soil type and land use within each unit catchment. The simulated vertical hydrological processes in MGB comprises soil water budget using a bucket model, energy budget and evapotranspiration, interception, soil infiltration and runoff computed based on the variable contributing area concept and also sub-superficial and groundwater flow generation.

To the original version of the MGB with propagation mode solved by a Musckingum Cunge method was added a new flow routing algorithm that simulate flood inundation and backwater effects (Paiva et al., 2011, 2013). All the executables associated to the MGB model and needed to carry out all the modelling steps are freely available on the website of the IPH "Hidrologia de Grande Escala" (https://www.ufrgs.br/lsh/, last access 13 February 2023), together with the

tutorials. In this section a brief description of the MGB hydrological-hydrodynamic model is presented.

2.3.3.1 Short model description

The MGB is a semi-distributed rainfall-runoff model that uses conceptual equations to simulate the terrestrial hydrological cycle as aforementioned above. Figure 2-14 illustrates the different components of the MGB.

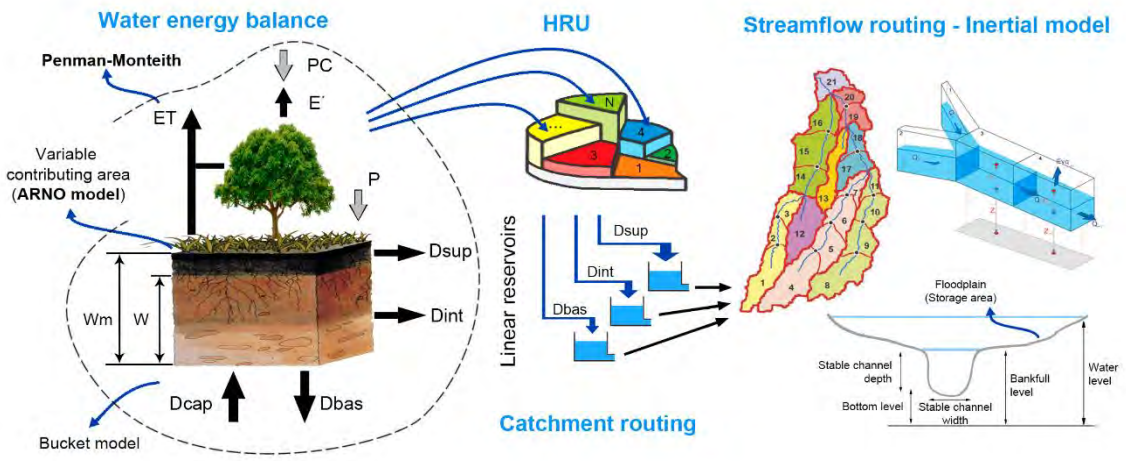

Figure 2-14. Schematic of the general structure of the MGB hydrological-hydrodynamic model (Pontes et al., 2017).

In the most recent version of the MGB model, the basin is discretized into unit-catchments, which are further divided into hydrological response units (HRU) that are usually produced by the combination of soil and land cover maps. Vertical water and energy budgets such as vegetation interception, evapotranspiration and infiltration are computed independently for each HRU of each unit-catchment to model the generation of surface, subsurface and subsurface runoff. This runoff is routed in the single river reach with an associated floodplain that is contained in each unit-catchment. Soil water balance is computed considering a single soil layer (bucket model), according to:

$$W_{i,j}^{t} = W_{i,j}^{t-1} + \left(P_i - ET_{i,j} - Dsup_{i,j} - Dint_{i,j} - Dbas_{i,j} + Dinf_{i,j}\right) \cdot \Delta t \qquad (1)$$

where: t, i and j, are indexes related to time step, unit-catchment and HRU, respectively; W is the water storage capacity in the soil layer (mm); P is the precipitation that reaches the soil (mm Δt^{-1}); ET is the evapotranspiration from soil (mm Δt^{-1}); Dsup is the surface runoff (mm Δt^{-1});

Dint is the subsurface flow (mm Δt^{-1}); Dbas is the flow to the groundwater reservoir (mm Δt^{-1}); Dinf is the infiltration of flooded areas to the soil (mm Δt^{-1}) and; Δt is the time step for water budget, usually equal to 1 day.

In each HRUs, the generated flow is routed to the stream network using three linear reservoirs representing the baseflow, subsurface flow and surface flow (Paiva et al., 2013). For surface and subsurface reservoirs, streamflow releases are controlled by the time of concentration computed with Kirpich formula similarly to (Ludwig and Bremicker, 2006).

The propagated discharge in the main network of each watershed is the sum of the flow of the upstream watershed and the flow generated in the watershed itself. Flow routing in river channels can be computed using the Muskingum–Cunge method (Collischonn et al., 2007) or the local inertial method (Pontes et al., 2017). The latter is a simplification of the 1D Saint-Venant equations in which the advective inertial term is neglected (inertial method) (Bates et al., 2010; Pontes et al., 2017), leaving equations 2 and 3 corresponding with continuity and conservation of the quantity of motion respectively, as follows:

$$\frac{\partial A}{\partial t} + \frac{\partial Q}{\partial x} = 0 \quad (2)$$

$$\frac{\partial Q}{\partial t} + gA\frac{\partial h}{\partial x} = gAS_0 - gAS_f \quad (3)$$

where Q represents the flow rate ($m^3 s^{-1}$), A is the cross-sectional area (m^2), h is the flow depth (m), n is the Manning roughness coefficient. On the other hand, t and x represent the temporal and spatial dimensions of the differential equations.
Detailed information on the internal structure of the MGB hydrologic-hydrodynamics components together with other processes that the model simulates can be found in Collischonn et al. (2007) and Paiva et al. (2013).

2.3.3.2 Pre-processing of MGB model

As aforementioned, MGB model discretizes the basin into unit catchments which are further divided into HRU. These processes are performed under the pre-processing, relevant step for generating input files compulsory to the run of the MGB model such as the Mini.gtp and other data. The Mini.gtp gathers information about each catchment discretized in the study basin, such as upstream drainage area, centroids coordinates, length of the segmented stream, among others. Originally, the preprocessing is executed using a GIS-based tool namely IPH-Hydro

Tools package (Siqueira et al., 2016). That can be downloaded freely via the following website https://www.ufrgs.br/lsh/ (last access 13 February 2023). In contrast to the GIS-based tool, Hydro-matters company (https://www.hydro-matters.fr/, last access 13 February 2023) have developed a pre-processing step working under python3 environment and tested for GNU/Linux and Windows 10.

2.3.3.3 Applications of MGB model

Since the development of the MGB model, several applications have been elaborated and here we will mention some of these applications. The latter include climate change studies (Sorribas et al., 2016; Brêda et al., 2020), prevision/forecasting studies (Fan et al., 2016; Siqueira et al., 2016; Quedi and Fan, 2020; Petry et al., 2022), reanalysis analysis studies (Wongchuig et al., 2017, 2019), and near real time monitoring (Paris et al., 2022). Brêda et al. (2020) uses MGB model to assess the potential climate change impacts on the continental water balance. An ensemble of 25 global climate models (GCM) from CMIP5 projection were used to force the model in order to evaluate the mean alterations of water balance variables and river discharge in South America. Regarding forecasting, Fan et al. (2016) develop a hydrological forecasting system based on MGB model for support in decision making of dam operation for flood control in the northern region of Brazil (i.e., Tocantins River). The Streamflow forecasts were obtained based on quantitative precipitation forecasts. Beside this study, Siqueira et al. (2016) showed the possibility of coupling a higher-resolution meteorological model with MGB model to identify flood events. The ensemble forms the Hydrological Ensemble Prediction Systems playing a crucial role in the operational flood forecasting. For this system, the hydrological forecasts showed higher sensitivity to the parameterization of the meteorological model demonstrating coupling a hydrological model to an ensemble prediction system with different physical representations can be useful to capture forecast uncertainty. Wongchuig et al. (2019) develop a consistent register of hydrological reanalysis variables called hydrological reanalysis across the 20th century (HRXX) in the Amazon Basin using MGB model. Such a dataset is important to manage water resources especially in developing countries where hydrological information is limited. Long-term climatic reanalysis of rainfall (ERA-20CM) with bias removed was used to force the model and data assimilation technique was applied. The obtained results shown that both bias correction and the data assimilation with localization method greatly improved the simulations. Finally, Paris et al. (2022) demonstrated the possibility of near real time monitoring of channel depths and discharges in the poorly gauged basin of Congo

through operational radar altimetry coupling with a large-scale hydrologic-hydrodynamic MGB model. The approach consists in developing a rating curve between the satellite-derived water level and the simulated discharge. Then, to use the rating curve together with the operational satellite altimetry constellation to infer the discharge. The latter technique has leaded to experimental platform for monitoring/predicting the flow at any point on the Niger River in near real time (https://mgb-hyfaa.pigeo.fr/site/, last access 13 February 2023). Effort of such experimentation of platform is being developed over the CRB and French-Guyana basin (https://www.hydro-matters.fr/, last access 13 February 2023).

Chapter 3: Datasets

3.1 Introduction

In order to significantly improve the knowledge about the spatial and temporal variability of the CRB's hydroclimatic patterns, heterogeneous information from in situ hydrometeorological stations, remote sensing, specifically, radar altimetry and surface water extent from multi-satellite technique, and hydrological modeling are combined and analyzed. In the following chapter, only data related altimetry and water extent are treated. The data on the hydrological modeling are presented in the chapter dedicated to the modeling part.

3.2 In situ river discharge and water level data

Hydrological monitoring in the CRB can be traced back to the year 1903, with the implementation of the Kinshasa gauging site. Until the end of 1960, which marks the end of the colonial era for many riparian countries in the basin, more than 400 gauging sites were installed throughout the CRB to provide water level and discharge data (Tshimanga, 2022). It is unfortunate that many of these data could not be accessible to the public interested in hydrological research and water resources management. Since then, there has been a critical decline in the monitoring network, so that, currently, there are no more than 15 gauges considered as operational (Fig. 3-1, Tshimanga et al., 2016; Alsdorf et al., 2016; Laraque et al., 2020; Tshimanga, 2022). Yet the latest observations are, in general, not available to the scientific community. Initiatives, such as Congo HYdrological Cycle Observing System (Congo-HYCOS), have been carried out to build the capacity to collect data and produce consistent and reliable information on the CRB hydrological cycle (OMM, 2010). Moreover, recent efforts have been carried out to conduct field measurement campaigns in the middle reach of the Congo River and the Kasai tributary using the latest equipment for investigation of large rivers (i.e., Acoustic Doppler Current profiler, Sonar, GNSS) in the context of the Congo River Hydraulics and Morphology (CRuHM) project (Fig. 3-2). During this project to which I participated, several automatic water level recorders were installed at specific sections (Fig. 3-2, e.g., installation of Kisangani (Fig. 3-2a) and Bumba (Fig. 3-2b) water level stations) to collect water level variations continuously, at hourly time step. Additionally, river bathymetry and discharge were also measured using a Garmin GT22 single-beam sonar echo sounders equipment and an Acoustic Doppler current profiler (ADCP, Teledyne RiverRay, 600 kHz) respectively. Beside the discharge, ADCP measurements enable to get other hydrodynamic

characteristics such as wetted perimeter, hydraulic depths, velocity distribution (Tshimanga et al., 2022c).

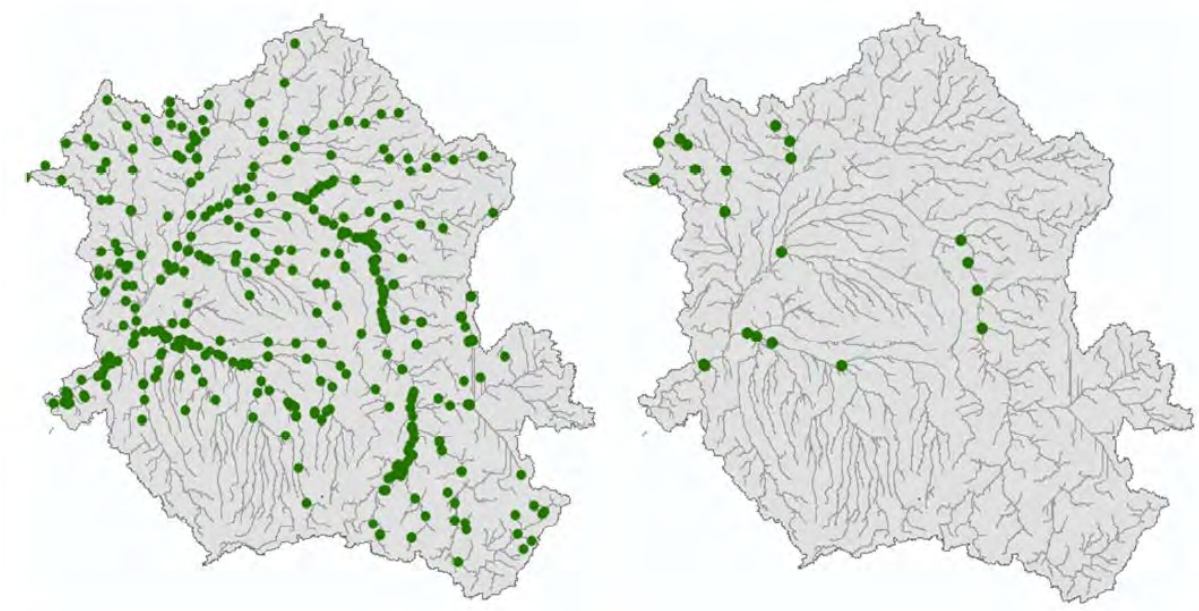

Figure 3-1. Density of streamflow gauges in the Congo River basin before the 1960s (left) and the current situation (right) (Tshimanga et al., 2016).

In this research study, we have accessed to a set of historical and contemporary observations (e.g., from CRuHM project) of river water stages (WSs) and discharge (Table 1). Those were obtained thanks to the collaboration with the regional partners of the Congo Basin Water Resources Research Center (CRREBaC, https://www.crrebac.org/, last access 13 February 2023), from the Environmental Observation and Research project (SO-HyBam, https://hybam.obs-mip.fr/fr/, last access: 13 February 2023), and from the Global Runoff Data Centre database (GRDC, https://portal.grdc.bafg.de/applications/public.html?publicuser=PublicUser#dataDownload/Stations, last access: 13 February 2023). It is worth noting that the discharge data from the gauges are generally derived from water level measurements converted into discharge using stage–discharge relationships (rating curves). Many of the rating curves related to historical gauges were first calibrated in the early 1950s, and information is not available on recent rating curves updates nor regarding their uncertainty despite recent efforts from the SO-HyBam programme and the Congo–Hydrological Cycle Observing System (Congo-HYCOS) programme from the World Meteorological Organization (WMO; Alsdorf et al., 2016).

Figure 3-2. Installation of automatic water level recorders. Kisangani (a) and Bumba (b) stations. Map of the stations installed through CRuHM projet (c).

Table 1 presents the unprecedented in situ dataset that is mapped at Fig. 3-3. Table 3-1 is organized in the following two categories: one with stations providing contemporary observations, i.e., covering a period of time that presents a long overlap (several years) with the satellite era (starting in 1995 in our research study), and another with stations providing long-term historical observations before the 1990s. In the frame of the Commission Internationale du Bassin du Congo–Ubangui–Sangha (CICOS)/CNES/IRD/AFD spatial hydrology working group, the Maluku Tréchot and Mbata hydrometric stations were set up right under Sentinel-3A (see below) ground tracks. Additionally, for Kutu–Muke, the water stages are referenced to an ellipsoid, which therefore provide surface water elevations.

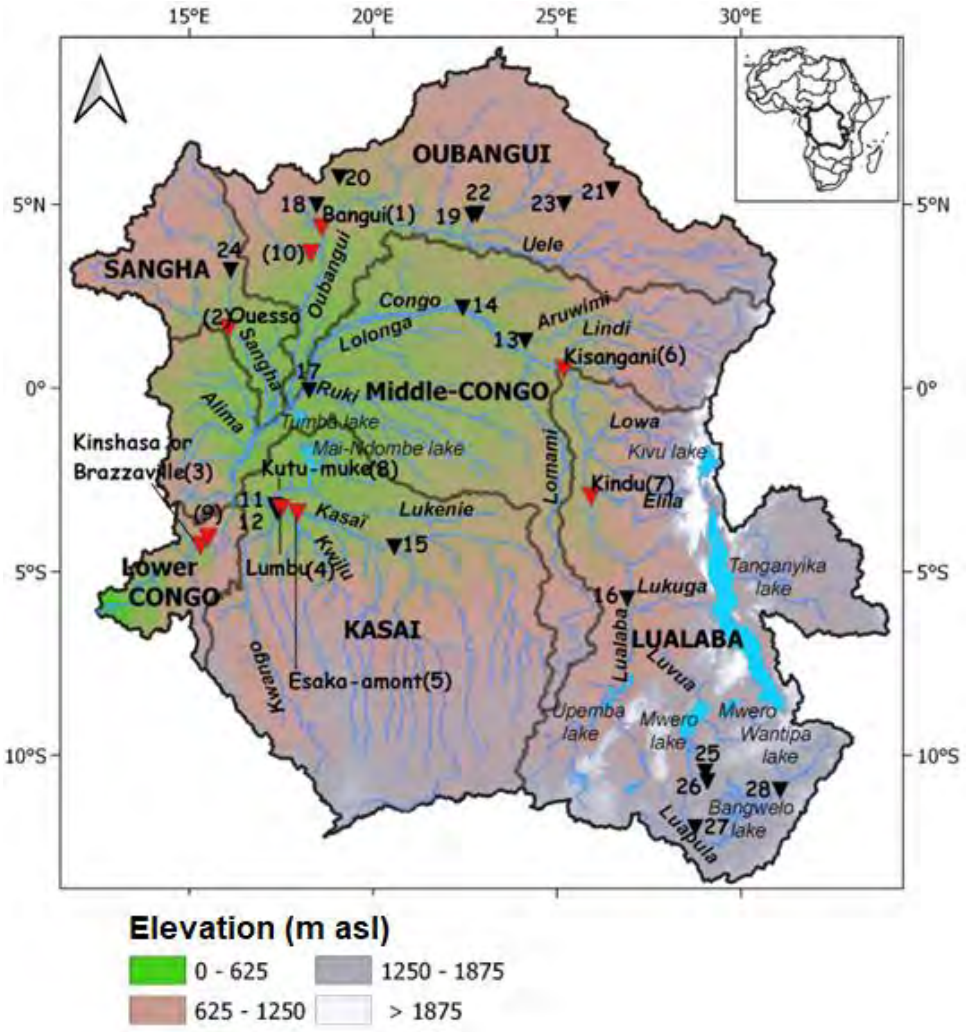

Figure 3-3. The Congo River basin. Its topography is derived from the Multi-Error-Removed Improved Terrain (MERIT) digital elevation model (DEM). Also displayed are the locations of the in situ gauging stations (triangle). Red and black triangles represent, respectively, the gauge stations with current (> 1994) and historical observations. Their characteristics are reported in Table 3-1 (Kitambo et al., 2022a).

Table 3-1. Location and main characteristics of in situ stations used in this research study. The locations are displayed in Fig. 3-3. WS: Water Stage (Kitambo et al., 2022a).

N°	Name	Lat	Lon	Sub-basin	Variable	Period	Frequency	Source
Stations with contemporary observations								
1	Bangui	4.37	18.61	Ubangui	ws/ Discharge	1936-2020	Daily/Monthly	CRREBaC/ SO-Hybam
2	Ouesso	1.62	16.07	Sangha	ws/ Discharge	1947-2020	Daily/Monthly	CRREBaC/ SO-Hybam
3	Brazzaville/ Kinshasa	-4.3	15.30	Lower-Congo	ws/ Discharge	1903-2020	Daily/Monthly	CRREBaC/ SO-Hybam

4	Lumbu-dima	-3.28	17.5	Kasaï	ws	1909-2012	Daily	CRREBaC
5	Esaka-amont	-3.4	17.94	Kasaï	ws	1977-2010	Daily	CRREBaC
6	Kisangani	0.51	25.19	Lualaba	ws/ Discharge	1967-2011/ 1950-1959	Daily/Monthly	CRREBaC
7	Kindu	-2.95	25.93	Lualaba	ws/ Discharge	1960-2004/ 1933-1959	Daily/Monthly	CRREBaC
8	Kutu-muke	-3.20	17.34	Kasaï	Surface water elevation	2017-2020	Hourly	CRREBaC
9	Maluku-Trechot	-4.07	15.51	Lower-Congo	ws	2017-2020/ 1966-1991	Hourly/Daily	CRREBaC
10	Mbata	3.67	18.30	Ubangui	ws/ Discharge	2016-2018/ 1950-1994	Hourly/ Monthly	CRREBaC
Stations with historical observations								
11	Bagata	-3.39	17.40	Kasaï	ws	1952-1990	Daily	CRREBaC
12	Bandundu	-3.30	17.37	Kasaï	ws	1929-1993	Daily	CRREBaC
13	Basoko	1.28	24.14	Middle-Congo	ws	1972-1991	Daily	CRREBaC
14	Bumba	2.18	22.44	Middle-Congo	ws	1912-1961	Daily	CRREBaC
15	Ilebo	-4.33	20.58	Kasaï	ws	1924-1991	Daily	CRREBaC
16	Kabalo	-5.74	26.91	Lualaba	ws	1975-1990	Daily	CRREBaC
17	Mbandaka	-0.07	18.26	Middle-Congo	ws	1913-1984	Daily	CRREBaC
18	Bossele-bali	4.98	18.46	Ubangui	Discharge	1957-1994	Monthly	CRREBaC
19	Bangassou	4.73	22.82	Ubangui	Discharge	1986-1994	Monthly	CRREBaC
20	Sibut	5.73	19.08	Ubangui	Discharge	1951-1991	Monthly	CRREBaC
21	Obo	5.4	26.5	Ubangui	Discharge	1985-1994	Monthly	CRREBaC
22	Loungoumba	4.7	22.69	Ubangui	Discharge	1987-1994	Monthly	CRREBaC
23	Zemio	5.0	25.2	Ubangui	Discharge	1952-1994	Monthly	CRREBaC
24	Salo	3.2	16.12	Sangha	Discharge	1953-1994	Monthly	CRREBaC
25	n.a.	-10.46	29.03	Lualaba	Discharge	1971-2004	Monthly	CRREBaC

26	n.a.	-10.71	29.09	Lualaba	Discharge	1971-2005	Monthly	CRREBaC
27	Chembe Ferry	-11.97	28.76	Lualaba	Discharge	1956-2005	Daily/Monthly	GRDC/ CRREBaC
28	Old pontoon	-10.95	31.07	Chambeshi	Discharge	1972-2004	Daily	GRDC

3.3 Radar altimetry

From the 1960s, many riparian countries of the CRB have been marked by a drastic decline in the hydro-meteorological stations, so that, within the CRB, no more than 15 gauging in situ stations are considered operational (Tshimanga et al., 2016). In this context, the recent development of radar altimetry technology can provide a viable approach to monitor at the large scale the CRB (Becker et al., 2014, 2018; Paris et al., 2022; Kitambo et al., 2022a). The technique allows to compensate in situ hydrometric data through the establishment of VSs, defined as the intersection of the satellite ground track with a water body at which surface water height (SWH) can be retrieved with temporal interval sampling provided by the repeat cycle of the orbit (Frappart et al., 2006; Da Silva et al., 2010). In the past decade, efforts have been performed to extract satellite-derived water level time series from the raw data freely distributed by CTOH in the standardized format of along-track GDRs. For instance, Becker et al. (2014, 2018) established 140 (Fig. 3-4a) and 350 (Fig. 3-4b) VSs, respectively, from ENVISAT tracks crossing the CRB using VALS and MAPS software. Paris et al. (2022) used ~1000 VSs (Fig. 3-4c) from multi-mission satellites J2 and 3, ENVISAT, Saral, and S3. These VSs were acquired from both manual (i.e., following the methodology presented in Da Silva et al. [2010, 2012]) and automated processing (based on the backscatter filtering and outlier detection, from Theia/Hydroweb website http://hydroweb.theia-land.fr/, Crétaux et al., 2011) of the raw radar echoes.

In our research study, the satellite altimetry data were obtained from (1) ERS-2 that provide observations from April 1995 to June 2003 with a 35 d repeat cycle, (2) ENVISAT, hereafter named ENV; providing observations from March 2002 to June 2012 on the same orbit as ERS-2, (3) J2 and 3, flying on the same orbit with a 10 d repeat cycle, covering June 2008 to October 2019 for J2 and January 2016 to the present for J3, (4) SARAL/Altika, hereafter named SRL; from which we use observations from February 2013 to July 2016, ensuring the continuity of the ERS-2/ENV long-term records on the orbit, with a 35 d repeat cycle, and (5) S3A and S3B; available, respectively, since February 2016 and April 2018, with a ~27 d repeat cycle. Figure 3-5 provides their ground-track over the CRB. The VSs used in this study were acquired from

the global operational dataset available on the Theia/Hydroweb website, the VOLODIA project (research and operational stations) and the manual processing (i.e., creation of new VSs), in particular ERS-2 mission using MAPS software. Ice1 retracking algorithm was used to convert the raw radar waveforms into ranges, hence SWH time series, as it was found to provide robust estimates (Frappart et al., 2006). Figure 3-6 provides an example of some manual processing we performed during our research to derive satellite-derived SWH using MAPS. This constituted my first steps in learning MAPS software dealing with GDRs signals.

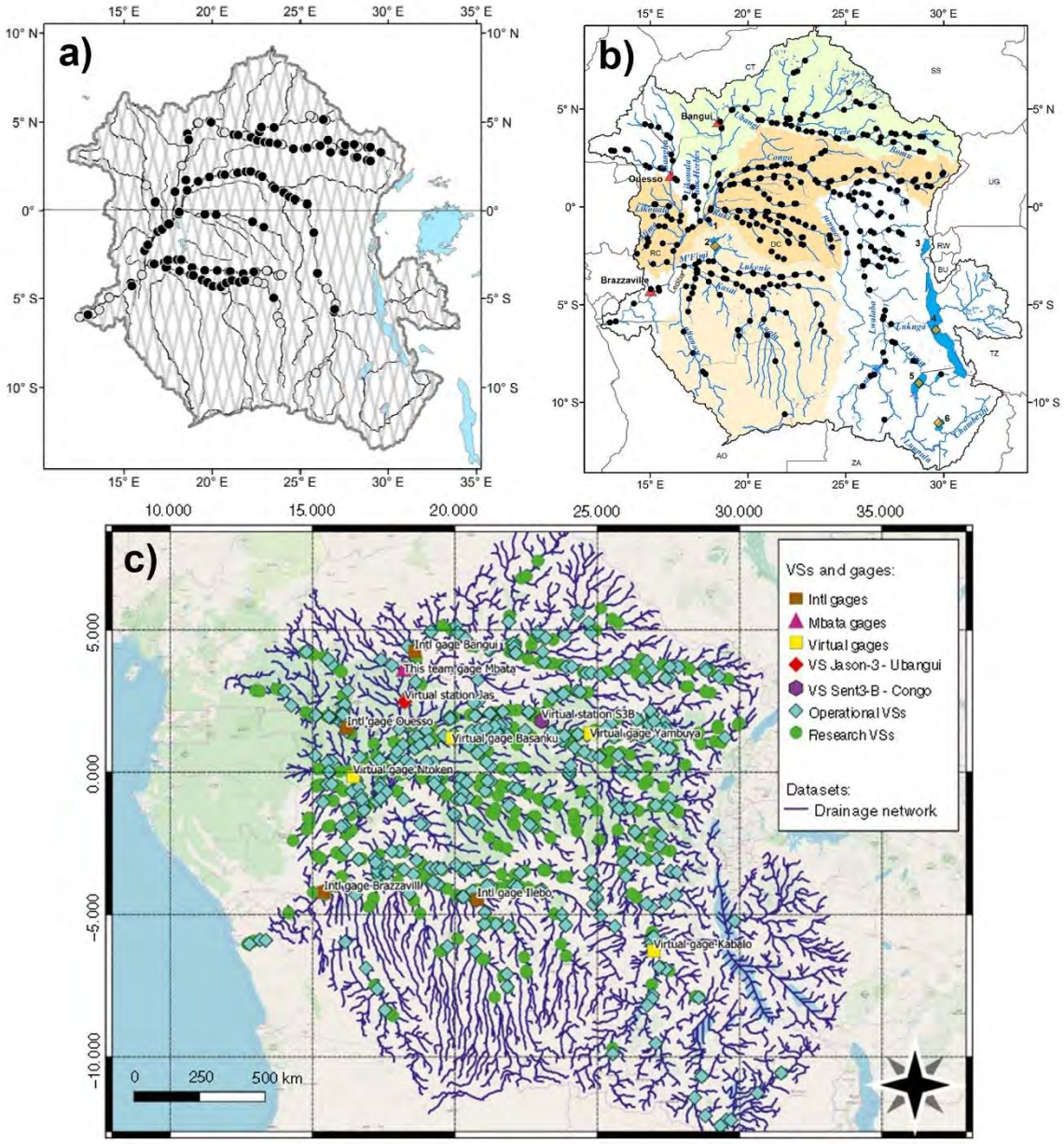

Figure 3-4. Location of multi-mission radar altimeter VSs. 140 (a) and 350 (b) VSs from ENVISAT mission (Becker et al., 2014, 2018). ~1000 VSs from J2 and 3, ENVISAT, Saral, and S3 missions (Paris et al., 2022).

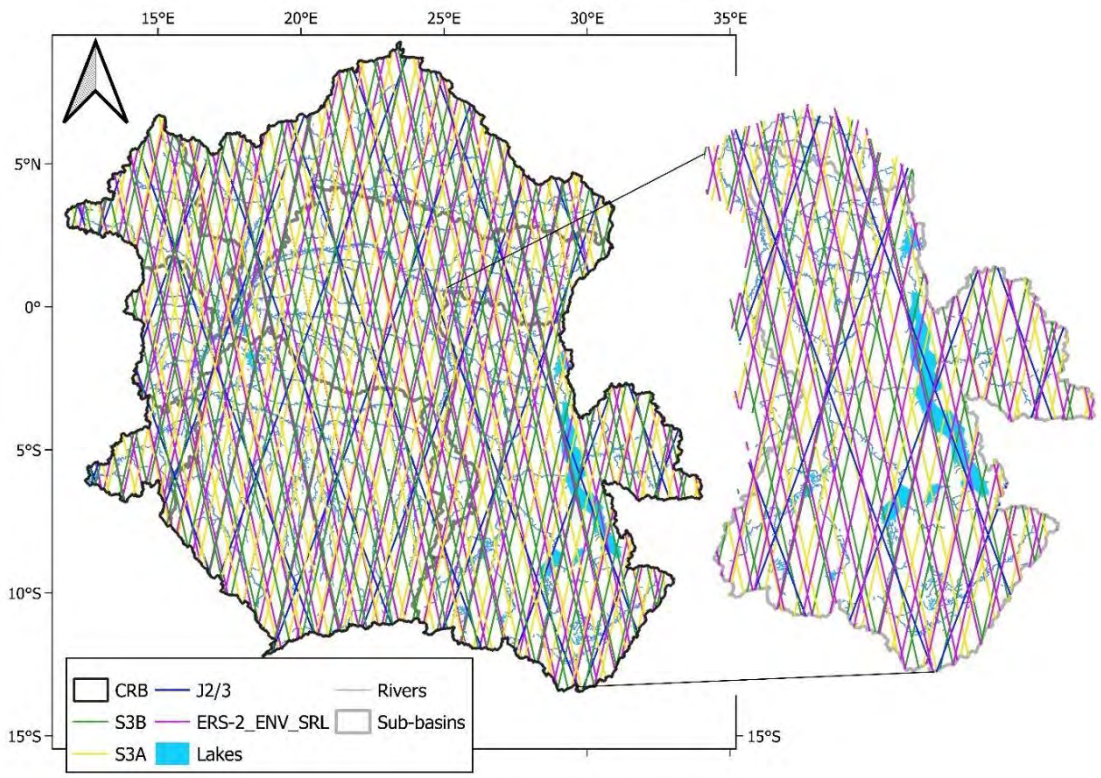

Figure 3-5. Ground-tracks of multi-mission radar altimetry over the CRB.

Overall, a number of ~2300 VSs covering the period 1995 to 2020 and spatially distributed across the CRB were analyzed during our research with a total number of 323 VSs from ERS-2, 364 and 342 VSs for ENV and ENV2 (new orbit of ENVISAT since late 2010), respectively, 146 and 98 VSs for J2 and J3, respectively, 358 VSs for SRL, 354 VSs for S3A, and 326 VSs for S3B (Kitambo et al., 2022a). All VSs passed an efficient quality control. To avoid outliers or bad time series in our dataset, we defined a criteria that allows us to identify VSs time series that do not satisfy it. The criteria is defined by the following formula:

$$C = (3 \times std) + \bar{X} \quad (4)$$

where C is the criteria, STD stands for the standard deviation of a VS time series, $\bar{X}$ stands for the mean of a VS time series.

The quality control consists of checking if the mean amplitude ($\bar{A}$) of a VS time series is bigger than C. If $\bar{A}$ is greater than C, the VS time series is set aside for an in-depth checking (i.e., visualization of the time series), else, the VS time series is kept. Figure 3-7 shows examples of time series that were excluded for the dataset (in total, 9 VSs were excluded). It is important to point out here that, in terms of single river level height measurements, there are several factors that may affect the measurement in introducing uncertainties. These are the choice of the retracking, the width of the river, and the morphology of the riverbanks (e.g., presence of

vegetation, sandbank), among other factors (Da Silva et al., 2010; Papa et al., 2012; Kitambo et al., 2022a).

The multi-mission radar altimetry dataset used in our research study enabled us to build long series over the CRB. Water levels time series were combined successively from different satellite missions (i.e., ERS-2, ENV, ENV2, J2 and 3, SRL, S3A and B). To do that, the half-width of the pulse-limited radar beam over a flat surface is ~2 km, thus the pooling of VSs is based on the principle of the nearest neighbour located at a minimum distance of 2 km (Da Silva et al., 2010; Cretaux et al., 2017). For satellite belonging to the same family of orbit (e.g., 35-day repeat cycle, ERS-2_ENV_SRL), the tandem period (i.e., period at which two satellites fly on the same orbit) is used to intercalibrate the series. For instance, considering ERS-2 and ENV, the difference in the average over the tandem period is added to ERS-2 and ENV is considered to be the reference due to the long period of observation. In the case of satellite from different family (e.g., SRL and S3A), the difference in the average over the whole period of observation is considered for intercalibration.

The thorough analysis conducted on the multi-mission radar altimetry dataset and the display of their spatial distribution are shown in the next chapter that deals with the characterization of the surface hydrology over the CRB.

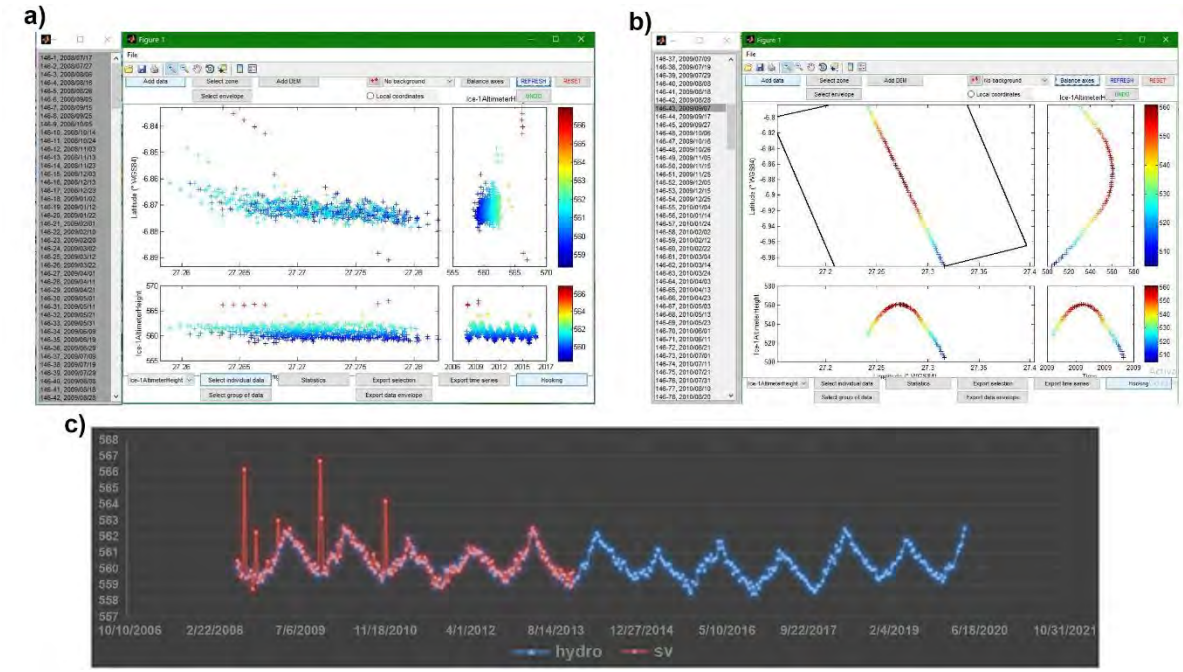

Figure 3-6. Processing of GDRs data using MAPS software. Screenshot of MAPS's graphic interface when uploading GDR's J2/3 data (a). Off-nadir effect (Hooking) at the cycle 43 of the ground track 146 of J2 (b). Comparison of satellite-derived water levels from J2/3 between the

one processed manually (in red) and the one downloaded from Hydroweb website (in blue, VS: R_CONGO_LUVUA_KM3253) (c).

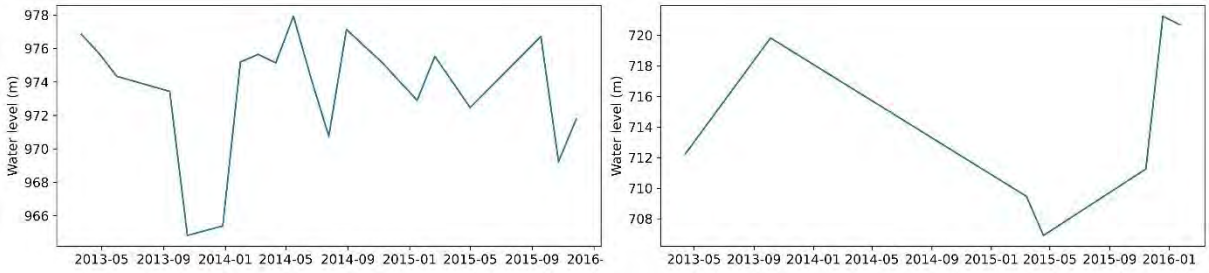

Figure 3-7. Examples of VSs time series that have been excluded from the multi-mission radar altimetry dataset.

3.4 Surface water extent

The Global Inundation Extent from Multi-Satellite (GIEMS) dataset captures the spatial and temporal dynamics of the extent of episodic and seasonal inundation, wetlands, rivers, and lakes at the global scale (Prigent et al., 2001, 2007, 2020). It is developed from complementary multiple-satellite observations (Prigent et al., 2001, 2007; Papa et al., 2010). The multi-sensor technique to estimate the surface water extent and dynamics is primarily based on passive microwave observations (19 and 85 GHz or 1.58 cm to 0.35 cm in wavelength) from the Special Sensor Microwave/Imager (SSM/I and SSMIS). It also integrates climatologies from visible (0.58-0.68 µm) and near-infrared (0.73-1.1 µm) reflectance and the derived Normalized Difference Vegetation Index (NDVI) from the Advanced Very High-Resolution Radiometer (AVHRR), and active microwaves observations (at 5.25 GHz or 5.71 cm in wavelength) from the ERS scatterometer (Papa et al., 2010). In this study, we used the current dataset called GIEMS-2 that estimates the monthly surface water extent at the global scale from 1992 to 2015 on an equal area grid of 0.25° spatial resolution at the equator (i.e., each pixel covers 773 km^2). GIEMS-2 was established following three steps. The first one is the emissivity calculation, followed by the detection of the surface water pixels, and finally the quantification of the surface water fraction per pixel. In contrast to GIEMS (Prigent et al., 2007), there was some updates for GIEMS-2 regarding the estimation of the passive microwave emissivity calculation and the quantification of the surface water fraction at pixel level in order to avoid the dependence of the development of GIEMS-2 to ancillary data (Prigent et al., 2020). Figure 3.8 displays the algorithm used to develop GIEMS-2 dataset along with the changes from GIEMS

methodology. Detailed information on each step involved in the development of GIEMS-2 can be found in Prigent et al. (2020).

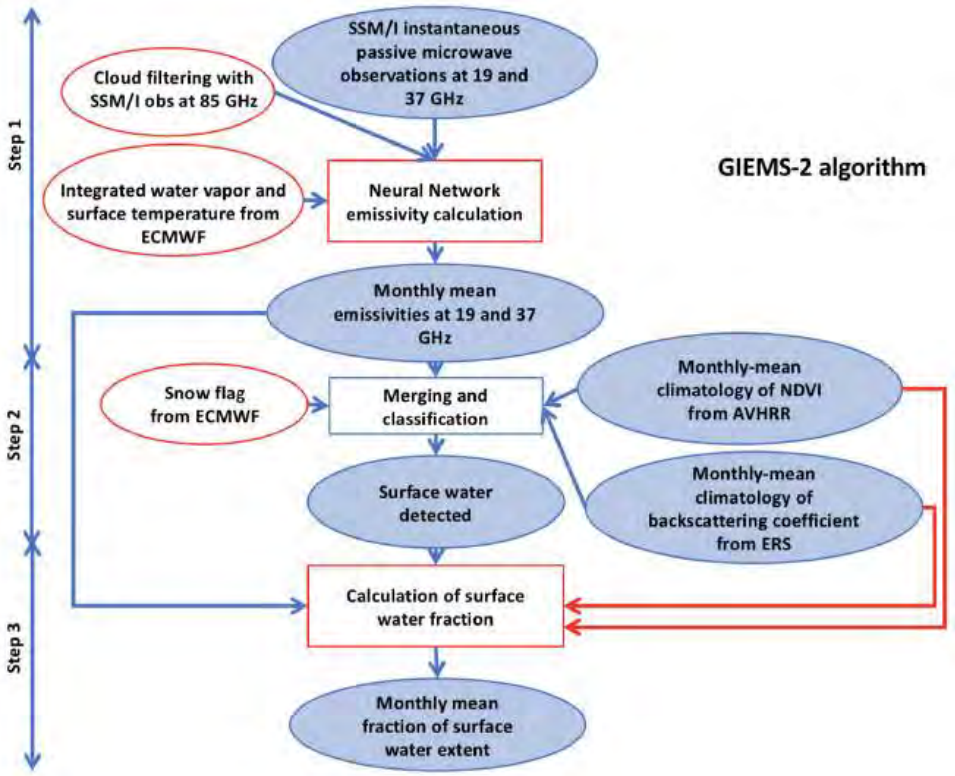

Figure 3-8. Schematic presentation of the GIEMS-2 algorithm. In red, the changes from GIEMS methodology (Prigent et al., 2020).

The seasonal and interannual dynamics of both the initial and the 24-year surface water extent have been assessed in different environments against multiple variables such as in situ and altimeter-derived water levels in wetlands, lakes, rivers, in situ river discharges, satellite-derived precipitation, or total water storage from Gravity Recovery and Climate Experiment (GRACE) (Prigent et al., 2007, 2020; Papa et al., 2008, 2010, 2013). GIEMS has been used in different hydrological and climatic applications such as methane surface emission (Ringeval et al., 2010), estimation of the spatio-temporal variations of surface water storage (Frappart et al., 2011, 2015; Papa et al. , 2013a, 2015; Becker et al., 2018) and validation of the river flooding scheme at the global scale (Decharme et al., 2008, 2011).

GIEMS-2 uncertainties are related to the underestimation of small surface water bodies comprising less than 10% of the fractional coverage in equal-area grid cells (i.e., 80 km^2 in 800 km^2 pixels; see Fig. 7 of Prigent et al., 2007, for a comparison against high-resolution 100m SAR images, Becker et al., 2018). Large freshwater bodies worldwide such as Lake Baikal, the

Great Lakes, or Lake Victoria are masked in GIEMS-2. In the CRB, this is the case for Lake Tanganyika Prigent et al., 2007. This will impact the total extent of surface water at basin-scale, but not its relative variations, as the extent of Lake Tanganyika itself shows small variations on seasonal and interannual timescales.

It is worth noting that there is not a specific product for Africa related to surface water extent. This justifies the use of products originally designed for global scale applications (Papa et al., 2022) and in our case GIEMS-2 dataset. The choice of GIEMS-2 is motivated by the fact that is a multi-satellite technique combining the strengths of the information provided by passive microwave observations with other types of satellite observations (Papa et al., 2010). Moreover, GIEMS-2 covers the period 1992 to 2015 on a monthly basis enabling to characterize the recent flood dynamics in several basins worldwide over a long-term period of 24-year (Kitambo et al., 2022a).

Chapter 4: A combined use of in situ and satellite-derived observations to characterize surface hydrology and its variability in the Congo River basin

4.1 Introduction

The first objective of my research study is dedicated to the in-depth validation over the CRB of EO datasets, and particularly radar altimetry-derived SWH and SWE from GIEMS-2, given that this validation should allow a better characterization of the CRB's surface hydrology. It is important to notice that very few studies have been undertaken with the purpose of validating radar altimetry and GIEMS-2 products over the whole CRB, and specially both together. This was due in part to the lack of availability of in situ observations that are not easily obtained from the national hydrological services. The satellite-based datasets will be used to better understand the hydrology functioning of the CRB's surface water dynamics. To date, Becker et al. (2018) and Paris et al. (2022) reported, respectively, comparison of SWE from GIEMS and radar altimetry SWH against in situ discharge and water stage from very few stations (i.e., no more than 4 stations) and often on the seasonal cycle. Bricquet (1993) examined the various contributions and the lag time from upstream to downstream the basin based on a limited number of in situ stations. Considering the large size of the basin and its spatial heterogeneity, in spite the aforementioned efforts, several questions remain still open: what is the performance of satellite-derived SWH from radar altimetry and SWE from GIEMS-2 in terms of peak-to-peak variations at the interannual scale when compared to long-term in situ data? To which extent are those two satellite products able to sample the spatial variability over surface waters within the CRB? What is the lag time of waters at different locations in the basin and during the different phases of the hydrological cycle of the CRB at the Brazzaville/Kinshasa station?

This research chapter is devoted to answer these above questions using three set of databases. 1) radar altimetry dataset from multi-mission satellites ERS-2, ENV, SRL, J2 and 3, S3A and B. 2) Global Inundation Extent from Multi-satellite dataset, and 3) In situ dataset. The results obtained from the analysis of these three datasets led to a publication in HESS of the European Geosciences Union journal. The paper is included in this chapter and titled " A combined use of in situ and satellite-derived observations to characterize surface hydrology and its variability in the Congo River basin". My contribution to this paper consisted in threefold. First, the

acquisition of the data from different platforms and regional partners in DR Congo, thanks to the collaboration with the Congo Basin Water Resources Research Center (CRREBaC). Secondly, the analysis of the datasets. For radar altimetry data that span the period 1995 to 2020, I performed an efficient quality control of the downloaded data and the ones from VOLODIA project. I build new VSs specifically from ERS-2 GDRs data using MAPS software. Several packages embedded in python are used to perform computation and analysis. In this regard, long-term series were formed by combining VSs from different satellite missions and comparison is performed between in situ and long-term satellite-derived observations along with Pearson correlation. For SWE from GIEMS-2 global dataset, the extraction of the data using the CRB mask was the first task, followed by different analysis and comparisons. In order to be confident with the results obtained from the satellite-based datasets, the same analysis carried out for satellite-based dataset have been completed with an unprecedented in situ dataset obtained from the regional partners. Lastly, the redaction of the article that has been reviewed, corrected and improved by all the co-authors. The next section gives more insight about the findings of the article.

4.2 Kitambo et al. 2022: " A combined use of in situ and satellite-derived observations to characterize surface hydrology and its variability in the Congo River basin"

Hydrol. Earth Syst. Sci., 26, 1857–1882, 2022
https://doi.org/10.5194/hess-26-1857-2022

Hydrology and Earth System Sciences
Open Access
EGU

A combined use of in situ and satellite-derived observations to characterize surface hydrology and its variability in the Congo River basin

Benjamin Kitambo[1,2,3], Fabrice Papa[1,4], Adrien Paris[5,1], Raphael M. Tshimanga[2], Stephane Calmant[1], Ayan Santos Fleischmann[6,7], Frederic Frappart[1,8], Melanie Becker[9], Mohammad J. Tourian[10], Catherine Prigent[11], and Johary Andriambeloson[12]

[1]Laboratoire d'Etudes en Géophysique et Océanographie Spatiales (LEGOS), Université de Toulouse, CNES/CNRS/IRD/UT3, Toulouse, France
[2]Congo Basin Water Resources Research Center (CRREBaC), Department of Natural Resources Management, University of Kinshasa (UNIKIN), Kinshasa, Democratic Republic of the Congo
[3]Department of Geology, University of Lubumbashi (UNILU), Route Kasapa, Lubumbashi, Democratic Republic of the Congo
[4]Institute of Geosciences, Campus Universitario Darcy Ribeiro, Universidade de Brasília (UnB), 70910-900 Brasilia (DF), Brazi
[5]Hydro Matters, 1 Chemin de la Pousaraque, 31460 Le Faget, France
[6]Instituto de Pesquisas Hidráulicas (IPH), Universidade Federal do Rio Grande do Sul (UFRGS), Porto Alegre, RS, Brasil
[7]Instituto de Desenvolvimento Sustentável Mamirauá, Tefé, AM, Brazil
[8]INRAE, Bordeaux Sciences Agro, UMR1391 ISPA, 71 Avenue Edouard Bourlaux, 33882 CEDEX Villenave d'Ornon, France
[9]LIENSs/CNRS, UMR 7266, ULR/CNRS, 2 Rue Olympe de Gouges, La Rochelle, France
[10]Institute of Geodesy, University of Stuttgart, Stuttgart, Germany
[11]LERMA, Observatoire de Paris, Sorbonne Université, CNRS, Université PSL, Paris, France
[12]Laboratoire de Géophysique de l'Environnement et de Télédétection (LGET), Institut et Observatoire de Géophysique d'Antananarivo (IOGA), Université d'Antananarivo, Antananarivo, Madagascar

Correspondence: Benjamin Kitambo (benjamin.kitambo@legos.obs-mip.fr)

Received: 9 June 2021 – Discussion started: 6 July 2021
Revised: 28 January 2022 – Accepted: 17 March 2022 – Published: 12 April 2022

Abstract. The Congo River basin (CRB) is the second largest river system in the world, but its hydroclimatic characteristics remain relatively poorly known. Here, we jointly analyse a large record of in situ and satellite-derived observations, including a long-term time series of surface water height (SWH) from radar altimetry (a total of 2311 virtual stations) and surface water extent (SWE) from a multi-satellite technique, to characterize the CRB surface hydrology and its variability. First, we show that SWH from altimetry multi-missions agrees well with in situ water stage at various locations, with the root mean square deviation varying from 10 cm (with Sentinel-3A) to 75 cm (with European Remote Sensing satellite-2). SWE variability from multi-satellite observations also shows a plausible behaviour over a ∼ 25-year period when evaluated against in situ observations from the subbasin to basin scale. Both datasets help to better characterize the large spatial and temporal variability in hydrological patterns across the basin, with SWH exhibiting an annual amplitude of more than 5 m in the northern subbasins, while the Congo River main stream and Cuvette Centrale tributaries vary in smaller proportions (1.5 to 4.5 m). Furthermore, SWH and SWE help illustrate the spatial distribution and different timings of the CRB annual flood dynamic and how each subbasin and tributary contribute to the

hydrological regime at the outlet of the basin (the Brazzaville/Kinshasa station), including its peculiar bimodal pattern. Across the basin, we estimate the time lag and water travel time to reach the Brazzaville/Kinshasa station to range from 0–1 month in its vicinity in downstream parts of the basin and up to 3 months in remote areas and small tributaries. Northern subbasins and the central Congo region contribute highly to the large peak in December–January, while the southern part of the basin supplies water to both hydrological peaks, in particular to the moderate one in April–May. The results are supported using in situ observations at several locations in the basin. Our results contribute to a better characterization of the hydrological variability in the CRB and represent an unprecedented source of information for hydrological modelling and to study hydrological processes over the region.

1 Introduction

The Congo River basin (CRB) is located in the equatorial region of Africa (Fig. 1). It is the second largest river system in the world, both in terms of drainage area and discharge. The basin covers $\sim 3.7 \times 10^6$ km^2, and its mean annual flow rate is about 40 500 m^3 s^{-1} (Laraque et al., 2009, 2013). It plays a crucial role in the local, regional, and global hydrological and biogeochemical cycles, with significant influence on the regional climate variability (Nogherotto et al., 2013; Burnett et al., 2020). The CRB is indeed one of the three main convective centres in the tropics (Hastenrath, 1985) and receives an average annual rainfall of around 1500 mm yr^{-1}. Additionally, about 45 % of the CRB land area is covered by dense tropical forest (Verhegghen et al., 2012), accounting for ~ 20 % of the global tropical forest and storing about $\sim 80 \times 10^7$ t of carbon, equivalent to ~ 2.5 years of current global anthropogenic emissions (Verhegghen et al., 2012; Dargie et al., 2017; Becker et al., 2018). The CRB is also characterized by a large network of rivers, along with extensive floodplains and wetlands, such as in the Lualaba region in the southeastern part of the basin and the well-known Cuvette Centrale region (Fig. 1). The CRB rainforest and inland waters therefore strongly contribute to the carbon cycle of the basin (Dargie et al., 2017; Fan et al., 2019; Hastie et al., 2021). Additionally, more than 80 % of the human population within the CRB rely on the basin water resources for their livelihood and are particularly vulnerable to climate variability and alteration and to any future changes that would occur in the basin water cycle (Inogwabini, 2020). Increasing evidence suggest that changes in land use practices, such as large-scale mining or deforestation, pose a significant threat to the basin water resources availability, including hydrological, ecological, and geomorphological processes in the basin (Bele et al., 2010; Ingram et al., 2011; Nogherotto et al., 2013; Tshimanga and Hughes, 2012; Plisnier et al., 2018). These environmental alterations require a better comprehension of the overall basin hydrology across scales. Surprisingly, despite its major importance, the CRB is still one of the least studied river basins in the world (Laraque et al., 2020) and has not attracted as much attention among the scientific communities as, for instance, the Amazon Basin (Alsdorf et al., 2016). Therefore, there is still insufficient knowledge of the CRB hydro-climatic characteristics and processes and their spatiotemporal variability. This is sustained by the lack of comprehensive and maintained in situ data networks that keep the basin poorly monitored at a large scale, therefore limiting our understanding of the major factors controlling freshwater dynamics at proper space- and timescales.

Efforts have been carried out to undertake studies using remote sensing and/or numerical modelling to overcome the lack of observational information in the CRB and better characterize the various components of the hydrological cycle (Rosenqvist and Birkett, 2002; Lee et al., 2011; Becker et al., 2014; Becker et al., 2018; Ndehedehe et al., 2019; Crowhurst et al., 2020; Fatras et al., 2021; Frappart et al., 2021a). For instance, seasonal flooding dynamics, water level variations, and vegetation types over the CRB were derived from JERS-1 (Rosenqvist and Birkett, 2002) or ALOS PALSAR synthetic aperture radar (SAR) data, as well as ICESat and Envisat altimetry (Betbeder et al., 2014; Kim et al., 2017). Bwangoy et al. (2010) and Betbeder et al. (2014) used combinations of the SAR L band and optical images to characterize the Cuvette Centrale land cover. They found that the wetland extent reaches 360 000 km^2 (i.e. 32 % of the total area). Becker et al. (2014) demonstrated the potential of using radar altimetry water levels from Envisat (140 virtual stations – VSs) to classify groups of hydrologically similar catchments in the CRB. Becker et al. (2018) combined information based on Global Inundation Extent from Multi-satellite (GIEMS; Prigent et al., 2007) and altimetry-derived water levels from Envisat (350 VSs) to estimate surface water storage and analyse its variability over the period 2003–2007. Its mean annual variation was estimated at $\sim 81 \pm 24$ km^3, which accounts for 19 ± 5 % of the annual variations in GRACE-derived total terrestrial water storage. Ndehedehe et al. (2019), using the observed Standardized Precipitation Index (SPI) and the global sea surface temperature, examined the impact of the multi-scale ocean–atmosphere phenomena on hydro-climatic extremes, showing that 40 % of the basin during 1994–2006 was affected by severe multi-year droughts. Recently, Fatras et al. (2021) analysed the hydrological dynamics of the CRB using inundation extent estimates from the multi-angular and dual polarization passive L-band microwave signals from the Soil Moisture and Ocean Salinity (SMOS) satellite along with precipitation for 2010–2017. The mean flooded area was found to be 2.39 % for the entire basin, and the dataset helped to characterize floods and droughts during the last 10 years.

In addition to remote sensing observations, hydrological modelling represents a valuable tool for studying the CRB water cycle (Tshimanga et al., 2011; Tshimanga and

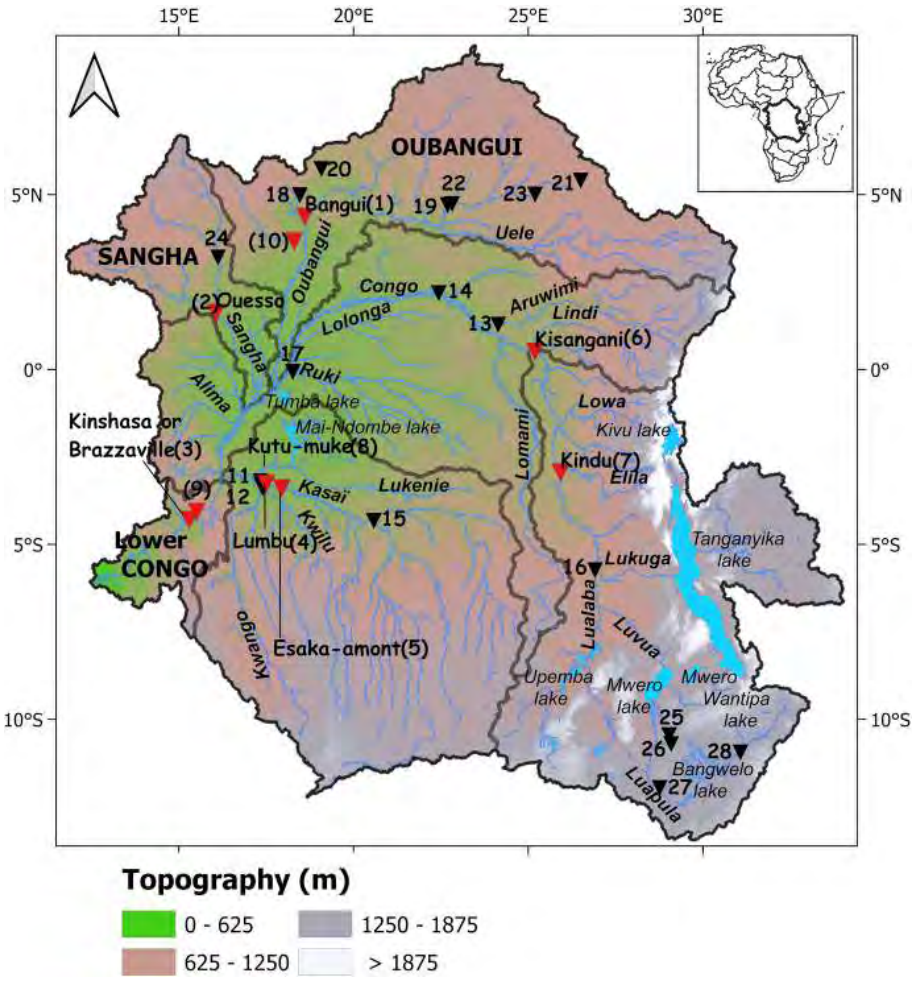

Figure 1. The Congo River basin (CRB). Its topography is derived from the Multi-Error-Removed Improved Terrain (MERIT) digital elevation model (DEM), showing the major subbasins (brown line), major rivers, and tributaries. Also displayed are the locations of the in situ gauging stations (triangle). Red and black triangles represent, respectively, the gauge stations with current (> 1994) and historical observations. Their characteristics are reported in Table 1.

Hughes, 2014; Aloysius and Saiers, 2017; Munzimi et al., 2019; O'Loughlin et al., 2019; Paris et al., 2022; Datok et al., 2022). For example, Tshimanga and Hughes (2014) used a semi-distributed rainfall–runoff model to examine runoff generation processes and the impact of future climate and land use changes on water resources availability. The magnitude and timing of high and low flows were adequately captured, with, nevertheless, an additional wetland submodel component that was added to the main model to account for wetland and natural reservoir processes in the basin. Aloysius and Saiers (2017) simulated the variability in runoff, in the near future (2016–2035) and mid-century (2046–2065), using a hydrological model forced with precipitation and temperature projections from 25 global climate models (GCMs) under two scenarios of greenhouse gas emission. Munzimi et al. (2019) applied the Geospatial Streamflow Model (GeoSFM) coupled to remotely sensed data to estimate daily river discharge over the basin from 1998 to 2012, revealing a good agreement with the observed flow but also a discrepancy in some parts of the basin where wetland and lake processes are predominant. O'Loughlin et al. (2019) forced the large-scale LISFLOOD-FP hydraulic model with combined in situ and modelled discharges to understand the Congo River's unique bimodal flood pulse. The model was set for the area between Kisangani and Kinshasa on the main stem, including the major tributaries and the Cuvette Centrale region. The results revealed that the bimodal annual pattern is predominantly a hydrological rather than a hydraulically controlled feature. Paris et al. (2022) demonstrated the possibility of monitoring the hydrological variables in near-real time using the hydrologic–hydrodynamic model MGB (Portuguese acronym for large basin model) coupled to the current operational satellite altimetry constellation. The model outputs showed a good consistency with the small number

of available observations, yet with some notable inconsistencies in the mostly ungauged Cuvette Centrale region and in the southeastern lakes' subbasins. Datok et al. (2022) used the Soil and Water Assessment Tool (SWAT) model to understand the role of the Cuvette Centrale region in water resources and ecological services. Their findings have highlighted the important regulatory function of the Cuvette Centrale region, which receives contributions from the upstream Congo River (33 %), effective precipitation inside the Cuvette Centrale region (31 %), and other tributaries (36 %).

Most of the above studies based on remote sensing (RS) and hydrological modelling were validated or evaluated against information from other hydrological RS data and/or a few historical gauge data, often enabling only comparisons of seasonal signals (Becker et al., 2018), which also did not cover the same period of data availability (Paris et al., 2022). Therefore, the large size of the basin, its spatial heterogeneity, and the lack of in situ observations have made the validation of long-term satellite-derived observations of surface hydrology components and the proper set-up of large-scale hydrological models difficult (Munzimi et al., 2019). Recent results call for the need of a comprehensive spatial coverage of the CRB water surface elevation using satellite-altimetry-derived observations to encompass the full range of variability across its rivers and wetlands up to its outlet (Carr et al., 2019). Additionally, even if recent efforts have been characterizing how water flows across the CRB, the basin-scale dynamics are still understudied, especially regarding the contributions of the different subbasins to the entire basin hydrology (Alsdorf et al., 2016; Laraque et al., 2020) and to the annual bimodal pattern in the CRB river discharge near to its mouth. Up to now, only a few studies have examined the various contributions and the water transfer from upstream to downstream the basin based on a few in situ discharge gauge records (Bricquet, 1993; Laraque et al., 2020) and large-scale modelling (Paris et al., 2022).

The aim of this study is therefore twofold. First, we provide, for the very first time, an intensive and comprehensive validation of long-term remote-sensing-derived products over the entire CRB, in particular radar altimetry water level variations (a total of 2311 VSs over the period of 1995 to 2020) and surface water extent from multi-satellite techniques from 1992 to 2015 (GIEMS-2; Prigent et al., 2020), using an unprecedented in situ database (28 gauges of river discharge and height) containing the historical and current records of river flows and stages across the CRB. Next, these long-term observations are used to analyse the spatiotemporal dynamics of the water propagation at subbasin- and basin-scale levels, significantly improving our understanding of surface water dynamics in the CRB.

The paper is organized as follows. Section 2 provides a brief description of the CRB. The data and the method employed in this study are described in Sect. 3. Section 4 is dedicated to the validation and evaluation of the satellite surface hydrology datasets, and it presents their main characteristics in the CRB. The results are presented in Sect. 5, and they focus on the use of the satellite datasets to understand the spatiotemporal variability in surface water in the CRB. Finally, the conclusions and perspectives are provided in Sect. 6.

2 Study region

The CRB (Fig. 1) is a transboundary basin that encompasses the following nine riparian countries: Zambia, Tanzania, Rwanda, Burundi, Republic of the Congo, Central Africa Republic, Cameroon, the Democratic Republic of the Congo (DRC), and Angola. The Congo River starts its course in southeastern DRC, in the village of Musofi (Laraque et al., 2020), and then flows through a series of marshy lakes (e.g. Kabwe, Kabele, Upemba, and Kisale) to form the Lualaba river. The latter is joined in the northwest by the Luvua river draining Lake Mweru (Runge, 2007). The river name becomes Congo (formerly Zaire) from Kisangani until it reaches the ocean. The Kasaï River in the southern part (left bank) and the Ubangi and Sangha rivers from the north (right bank) are the principal tributaries of the Congo River. Other major tributaries are Lulonga, Ruki on the left bank, and Aruwimi on the right bank. In the heart of the CRB stands the Cuvette Centrale region, a large wetland along the Equator (Fig. 1), which plays a crucial role in local and regional hydrologic and carbon cycles. Upstream of Brazzaville/Kinshasa, the Congo River main stem flows through a wide multi-channel reach dominated by several sand bars called Pool Malebo.

With a mean annual flow of $40\,500\,m^3\,s^{-1}$, computed at the Brazzaville/Kinshasa hydrological station from 1902 to 2019, and a basin size of $\sim 3.7 \times 10^6\,km^2$, the equatorial CRB (Fig. 1) stands as the second largest river system worldwide, behind the Amazon River, and the second in length in Africa after the Nile River (Laraque et al., 2020). The CRB is characterized by the hydrological regularity of its regime. Alsdorf et al. (2016), referring to historical studies, report that the annual potential evapotranspiration varies little across the basin, from 1100 to $1200\,mm\,yr^{-1}$. The mean annual rainfall in the central parts of the basin accounts for about $2000\,mm\,yr^{-1}$, decreasing both northward and southward to around $1100\,mm\,yr^{-1}$. The mean temperature is estimated to be about 25 °C.

The topography and vegetation of the basin are generally concentrically distributed all around the Cuvette Centrale region, which is bordered by plateaus and mountain ranges (e.g. Mayombe, Chaillu, and Batéké). In the centre of the basin stands a great equatorial forest, with multiple facies, surrounded by wooded and grassy savannas, typical of Sudanese climate (Bricquet, 1993; Laraque et al., 2020). In this study, six major subbasins are considered, based on the physiography of the CRB (Fig. 1). These are Lualaba (southeast), middle Congo (centre), Ubangui (northeast), Sangha (northwest), Kasaï (south centre) and lower Congo (southwest).

3 Data and methods

3.1 In situ data

Hydrological monitoring in the CRB can be traced back to the year 1903, with the implementation of the Kinshasa gauging site. Until the end of 1960, which marks the end of the colonial era for many riparian countries in the basin, more than 400 gauging sites were installed throughout the CRB to provide water level and discharge data (Tshimanga, 2021). It is unfortunate that many of these data could not be accessible to the public interested in hydrological research and water resources management. Since then, there has been a critical decline in the monitoring network, so that, currently, there are no more than 15 gauges considered as operational (Alsdorf et al., 2016; Laraque et al., 2020). Yet the latest observations are, in general, not available to the scientific community. Initiatives, such as Congo HYdrological Cycle Observing System (Congo-HYCOS), have been carried out to build the capacity to collect data and produce consistent and reliable information on the CRB hydrological cycle (OMM, 2010).

For the present study, we have access to a set of historical and contemporary observations of river water stages (WSs) and discharge (Table 1). Those were obtained thanks to the collaboration with the regional partners of the Congo Basin Water Resources Research Center (CRREBaC), from the Environmental Observation and Research project (SO-HyBam; https://hybam.obs-mip.fr/fr/, last access: 19 January 2022), and from the Global Runoff Data Centre database (GRDC; https://www.bafg.de/GRDC/EN/02_srvcs/21_tmsrs/210_prtl/prtl_node.html, last access: 19 January 2022). It is worth noting that the discharge data from the gauges are generally derived from water level measurements converted into discharge using stage–discharge relationships (rating curves). Many of the rating curves related to historical gauges were first calibrated in the early 1950s, and information is not available on recent rating curves updates nor regarding their uncertainty despite recent efforts from the SO-HyBam programme and the Congo–Hydrological Cycle Observing System (Congo-HYCOS) programme from the World Meteorological Organization (WMO; Alsdorf et al., 2016).

Table 1 is organized in the following two categories: one with stations providing contemporary observations, i.e. covering a period of time that presents a long overlap (several years) with the satellite era (starting in 1995 in our study), and another with stations providing long-term historical observations before the 1990s. In the frame of the Commission Internationale du Bassin du Congo–Ubangui–Sangha (CICOS)/CNES/IRD/AFD spatial hydrology working group, the Maluku Tréchot and Mbata hydrometric stations were set up right under Sentinel-3A (see below) ground tracks. Additionally, for Kutu–Muke, the water stages are referenced to an ellipsoid, which therefore provide surface water elevations.

3.2 Radar-altimetry-derived surface water height

Radar altimeters on board satellites were initially designed to measure the ocean surface topography by providing along-track nadir measurements of water surface elevation (Stammer and Cazenave, 2017). Since the 1990s, radar altimeter observations have also been used for continental hydrology studies and to provide a systematic monitoring of water levels of large rivers, lakes, wetlands, and floodplains (Cretaux et al., 2017).

The intersection of the satellite ground track with a water body defines a virtual station (VS), where surface water height (SWH) can be retrieved with temporal interval sampling provided by the repeat cycle of the orbit (Frappart et al., 2006; Da Silva et al., 2010; Cretaux et al., 2017).

The in-depth assessment and validation of the water levels derived from the satellite altimeter over rivers and inland water bodies were performed over different river basins against in situ gauges (Frappart et al., 2006; Seyler et al., 2008; Da Silva et al., 2010; Papa et al., 2010, 2015; Kao et al., 2019; Kittel et al., 2021; Paris et al., 2022), with satisfactory results and uncertainties ranging between a few centimetres to tens of centimetres, depending on the environments. Therefore, the stages of continental water retrieved from satellite altimetry have been used for many scientific studies and applications, such as the monitoring of abandoned basins (Andriambeloson et al., 2020), the determination of rating curves in poorly gauged basins for river discharge estimation (Paris et al., 2016; Zakharova et al., 2020), the estimation of the spatiotemporal variations in the surface water storage (Papa et al., 2015; Becker et al., 2018), the connectivity between wetlands, floodplains, and rivers (Park, 2020), and the calibration/validation of hydrological (Sun et al., 2012; de Paiva et al., 2013; Corbari et al., 2019) and hydrodynamic (Garambois et al., 2017; Pujol et al., 2020) models.

The satellite altimetry data used in this study were acquired from (1) the European Remote Sensing-2 satellite (ERS-2; providing observations from April 1995 to June 2003 with a 35 d repeat cycle), (2) the Environmental Satellite (ENVISAT, hereafter named ENV; providing observations from March 2002 to June 2012 on the same orbit as ERS-2), (3) Jason-2 and 3 (hereafter named J2 and J3; flying on the same orbit with a 10 d repeat cycle, covering June 2008 to October 2019 for J2 and January 2016 to the present for J3), (4) the Satellite with ARgos and ALtiKa (SARAL/Altika, hereafter named SRL; from which we use observations from February 2013 to July 2016, ensuring the continuity of the ERS-2/ENV long-term records on the orbit, with a 35 d repeat cycle), and (5) Sentinel-3A and Sentinel-3B missions (hereafter named S3A and S3B; available, respectively, since February 2016 and April 2018, with a $\sim$ 27 d repeat cycle). While ERS-2, ENV, SRL, and J2 missions are past missions, J3 and S3A/B are still ongoing missions. The VSs used in this study were either directly downloaded from the global operational database of Hydroweb

Table 1. Location and main characteristics of in situ stations used in this study. The locations are displayed in Fig. 1. WS is the water stage.

No.	Name	Lat	Long	Subbasin	Variable	Period	Frequency	Source
Stations with contemporary observations								
1	Bangui	4.37	18.61	Ubangui	WS/ discharge	1936–2020	Daily/monthly	CRREBaC/ SO-HyBam
2	Ouésso	1.62	16.07	Sangha	WS/ discharge	1947–2020	Daily/monthly	CRREBaC/ SO-HyBam
3	Brazzaville/ Kinshasa	−4.3	15.30	Lower Congo	WS/ discharge	1903–2020	Daily/monthly	CRREBaC/ SO-HyBam
4	Lumbu–Dima	−3.28	17.5	Kasaï	WS	1909–2012	Daily	CRREBaC
5	Esaka–Amont	−3.4	17.94	Kasaï	WS	1977–2010	Daily	CRREBaC
6	Kisangani	0.51	25.19	Lualaba	WS/ discharge	1967–2011/ 1950–1959	Daily/monthly	CRREBaC
7	Kindu	−2.95	25.93	Lualaba	WS/ discharge	1960–2004/ 1933–1959	Daily/monthly	CRREBaC
8	Kutu–Muke	−3.20	17.34	Kasaï	Surface water elevation	2017–2020	Hourly	CRREBaC
9	Maluku Tréchot	−4.07	15.51	Lower Congo	WS	2017–2020/ 1966–1991	Hourly/daily	CRREBaC
10	Mbata	3.67	18.30	Ubangui	WS/ discharge	2016–2018/ 1950–1994	Hourly/ monthly	CRREBaC
Stations with historical observations								
11	Bagata	−3.39	17.40	Kasaï	WS	1952–1990	Daily	CRREBaC
12	Bandundu	−3.30	17.37	Kasaï	WS	1929–1993	Daily	CRREBaC
13	Basoko	1.28	24.14	Middle Congo	WS	1972–1991	Daily	CRREBaC
14	Bumba	2.18	22.44	Middle Congo	WS	1912–1961	Daily	CRREBaC
15	Ilebo	−4.33	20.58	Kasaï	WS	1924–1991	Daily	CRREBaC
16	Kabalo	−5.74	26.91	Lualaba	WS	1975–1990	Daily	CRREBaC
17	Mbandaka	−0.07	18.26	Middle Congo	WS	1913–1984	Daily	CRREBaC
18	Bossele–Bali	4.98	18.46	Ubangui	Discharge	1957–1994	Monthly	CRREBaC
19	Bangassou	4.73	22.82	Ubangui	Discharge	1986–1994	Monthly	CRREBaC
20	Sibut	5.73	19.08	Ubangui	Discharge	1951–1991	Monthly	CRREBaC
21	Obo	5.4	26.5	Ubangui	Discharge	1985–1994	Monthly	CRREBaC
22	Loungoumba	4.7	22.69	Ubangui	Discharge	1987–1994	Monthly	CRREBaC
23	Zemio	5.0	25.2	Ubangui	Discharge	1952–1994	Monthly	CRREBaC
24	Salo	3.2	16.12	Sangha	Discharge	1953–1994	Monthly	CRREBaC
25	NA	−10.46	29.03	Lualaba	Discharge	1971–2004	Monthly	CRREBaC
26	NA	−10.71	29.09	Lualaba	Discharge	1971–2005	Monthly	CRREBaC
27	Chembe Ferry	−11.97	28.76	Lualaba	Discharge	1956–2005	Daily/monthly	GRDC/ CRREBaC
28	Old pontoon	−10.95	31.07	Chambeshi	Discharge	1972–2004	Daily	GRDC

Note: NA stands for not available.

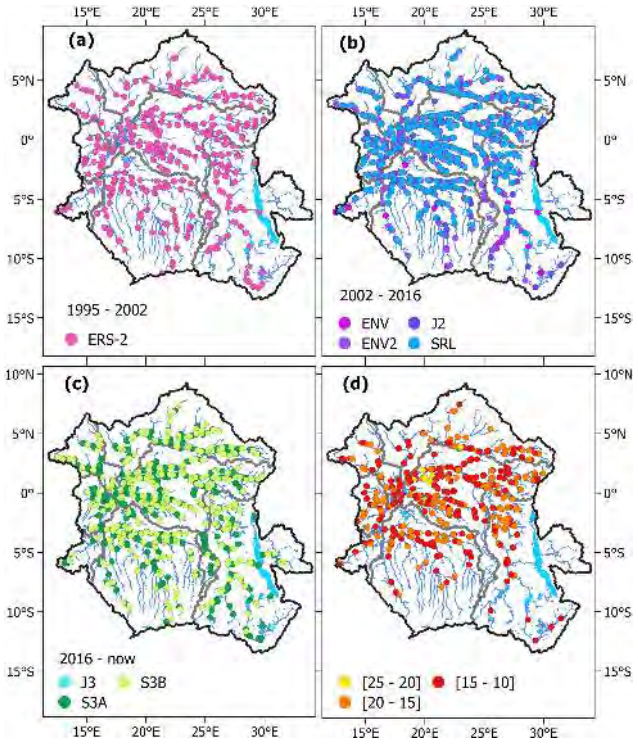

Figure 2. Locations of altimetry VSs over time within the CRB. **(a)** ERS-2 VSs, covering the 1995–2002 period. **(b)** ENV, ENV2, J2, and SRL VSs during 2002–2016. **(c)** J3, S3A, and S3B VSs from 2016 up to the present. **(d)** VSs with an actual long time series from a combination of multi-satellite missions, with the record period ranging between 25 and 20 years (yellow), 20 and 15 years (orange), and 15 and 10 years (red).

(http://hydroweb.theia-land.fr, last access: 19 January 2022) or processed manually using MAPS and ALTIS software (respectively, Multi-mission Altimetry Processing Software and Altimetric Time Series Software; Frappart et al., 2015a, b, 2021b) and GDRs (geophysical data records) provided freely by the CTOH (Center for Topographic studies of the Oceans and Hydrosphere; http://ctoh.legos.obs-mip.fr/, last access: 19 January 2022). We thus reached a total number of 323 VSs from ERS-2, 364 and 342 VSs for ENV and ENV2 (new orbit of ENVISAT since late 2010), respectively, 146 and 98 VSs for J2 and J3, respectively, 358 VSs for SRL, 354 VSs for S3A, and 326 VSs for S3B (Fig. 2).

Figure 2d shows the actual combination of VSs derived from different satellite missions with the purpose of generating long-term water level time series spatialized over the CRB. A total of 25, 20, 14, and 12 years of records were aggregated, respectively, with ERS-2_ENV_SRL_S3A, ERS-2_ENV_SRL, ENV_SRL, and, finally, J2_J3. The pooling of VSs is based on the principle of the nearest neighbour located at a minimum distance of 2 km (Da Silva et al., 2010; Cretaux et al., 2017).

The height of the reflecting water body derived from the processing of the radar echoes is subject to biases. The biases vary with the algorithm used to process the echo, called the retracking algorithm, and with the mission (e.g. orbit errors, onboard system, and mean error in propagation velocity through atmosphere). Therefore, it is required that these biases are removed in order to compose multi-mission series. We used the set of absolute and intermission biases determined at Parintins on the Amazon River, Brazil (Daniel Medeiros Moreira, personal communication, 2020). At Parintins, the orbits of all the past and present altimetry missions (except S3B) have a ground track that is in close vicinity to the gauge. The gauge has been surveyed during many static and cinematic Global Navigation Satellite System (GNSS) campaigns, giving the ellipsoidal height of the gauge as zero and the slope of the water surface. We also took into account the crustal deflection produced by the hydrological load using the rule given by Moreira et al. (2016). Therefore, all the altimetry measurements could be compared rigorously to the absolute reference provided by the gauge readings, making the determination of the biases for each mission and for each retracking algorithm possible. It is worth noting that this methodology does not take into account the possible local or regional phenomena that could have an impact on the biased values. Ideally, similar studies should be carried out at several locations on Earth to verify whether such a regional phenomenon exists or not.

Note that there is no common height reference between altimeter-derived water height (referenced to a geoid model) and the in situ water stage (i.e. the altitude of the zero of the gauges is unknown). Therefore, when we want to compare them, we merge them to the same reference by calculating the difference in the averages over the same period and adding this difference to the in situ water stage.

3.3 Multi-satellite-derived surface water extent

The GIEMS captures the global spatial and temporal dynamics of the extent of episodic and seasonal inundation, wetlands, rivers, lakes, and irrigated agriculture at $0.25° \times 0.25°$ resolution at the Equator (on an equal-area grid, i.e. each pixel covers 773 km^2; Prigent et al., 2007, 2020). It is developed from complementary, multiple satellite observations (Prigent et al., 2007; Papa et al., 2010), and the current data (called GIEMS-2) cover the period from 1992 to 2015 on a monthly basis. For more details on the technique, we refer to Prigent et al. (2007, 2020).

The seasonal and interannual dynamics of the $\sim$ 25-year surface water extent have been assessed in different environments against multiple variables, such as the in situ and altimeter-derived water levels in wetlands, lakes, rivers, in situ river discharges, satellite-derived precipitation, or the total water storage from Gravity Recovery and Climate Experiment (GRACE; Prigent et al., 2007, 2020; Papa et al., 2008, 2010, 2013; Decharme et al., 2011). The technique gener-

ally underestimates small water bodies comprising less than 10 % of the fractional coverage in equal-area grid cells (i.e. $\sim 80\,km^2$ in $\sim 800\,km^2$ pixels; see Fig. 7 of Prigent et al., 2007, for a comparison against high-resolution – 100 m – SAR images; see Hess et al., 2003 and Aires et al., 2013 for details over high and low water seasons in the central Amazon). Note that large freshwater bodies worldwide, such as Lake Baikal, the Great Lakes, and Lake Victoria are masked in GIEMS-2. In the CRB, this is the case for Lake Tanganyika (Prigent et al., 2007). This will impact the total extent of the surface water, but not its relative variations, at basin scale as the extent of Lake Tanganyika itself shows small variations across seasonal and interannual timescales.

4 Validation of satellite surface hydrology datasets and their characteristics in the CRB

4.1 Validation of altimetry-derived surface water height

Observations of in situ WS (see Fig. 1 for their locations; Table 1) over the CRB are compared to radar altimetry SWH (Figs. 3 and 4). The comparisons at nine locations cover five subbasins, including Sangha (Ouésso station; Fig. 3a), Ubangui (Bangui and Mbata stations; Figs. 3d and 4d), Lualaba (Kisangani and Kindu station; Fig. 3j and p), Kasaï (Kutu–Muke and Lumbu–Dima; Fig. 3m and g), and lower Congo (Brazzaville/Kinshasa and Maluku Tréchot stations; Figs. 3s and 4a). In order to evaluate the performance of the different satellite missions, we choose the nearest VSs located in the direct vicinity of the different gauges.

Figure 3 (left column) provides the first comparison of long-term SWH time series at seven gauging stations. It generally shows a very good agreement, presenting a similar behaviour in the peak-to-peak height variations, within a large set of hydraulic regimes (low- and high-flow seasons). Similar results in the CRB were found by Paris et al. (2022), where the comparisons were done at a seasonal timescale, with a few tens of centimetres of standard error. Note that the VSs of different missions were not located at the same distance from the in situ gauges (distance ranges between 1 and 38 km). The gauge is considered right below the satellite track when its distance is less than 2 km (as in Fig. 4a and d), as reported by Da Silva et al. (2010). This can explain some discrepancies generally observed for the VSs far away from the in situ gauges (distance > 10 km; Fig. 3a). Such discrepancies can be due to severe changes in the cross section between the gauge and the VS, such as changes in river width. For Ouésso (Fig. 3a), ENV2 overestimates the lower water level as compared to the other missions. Figure 3j, m, and p present the benefit of spatial altimetry for completing actual temporal gaps of the in situ observations. Nevertheless, for Kindu (Fig. 3p), ENV and J2 are showing different amplitudes. The difference between radar altimetry water levels and in situ observations (Fig. 3; centre column) shows values of the order of few tens of centimetres (concentration of points around zero in the histograms). The scatterplots between altimetry-derived SWH and in situ water stage presented in Fig. 3 (right column) confirm the good relationship observed in the time series. The correlation coefficient ranges between 0.84 and 0.99, with the average standard error of the overall entire series varying from 0.10 to 0.46 m. The values of root mean square deviation (rmsd) are found to be comparable to others obtained in other basins over the world (Leon et al., 2006; Da Silva et al., 2010; Papa et al., 2012; Kittel et al., 2021). The results obtained from the analysis for each satellite mission at each station are summarized in Table 2.

The highest rmsd is 0.75 m at Ouésso station on the Sangha River, related to the ERS-2 mission (Table 2), and the lowest value of rmsd is 0.10 m at Mbata station on the Lobaye River, with S3A mission (Fig. 4d). The pattern observed in Table 2 is that the rmsd decreases continuously from ERS-2 to S3A. In general, ERS-2 presents larger values of rmsd (above 40 cm) than its successor ENV and the lowest coefficient correlation (r) compared to other satellite missions.

These results are in good accordance with Bogning et al. (2018) and Normandin et al. (2018), who observed that the slight decrease in performances of ERS-2 against ENV can be attributed to the lowest chirp bandwidth acquisition mode which degrades the range resolution. The increasing performance with time (from ERS-2 to S3A) is linked to the mode of the acquisition of data from the satellite sensor. ERS-2, ENV, J2/3, and SRL operate in low-resolution mode (LRM) with a large ground footprint, while S3A/B (like other missions such as CryoSat-2) uses the synthetic aperture radar (SAR mode), also known as delay-Doppler altimetry, with a small ground spot (Raney, 1998), resulting in a better spatial resolution than the LRM missions along the track and, thus, a better performance. SRL operating at the Ka band (smaller footprint) and at a higher sampling frequency also shows good performances, as already reported (Bogning et al., 2018; Bonnefond et al., 2018; Normandin et al., 2018). As mentioned above, the accuracy of SWH depends on several factors, among them the width and the morphology of the river. For instance, at the Bangui station on the Ubangui River, S3B surprisingly presents a rmsd of 0.42 m, which is much higher than expected. This can be explained by, amongst others, the fact that its ground track intersects the river in a very oblique way over a large distance (~ 3 km) and at a location where the section presents several sandbanks, thus impacting the return signal and resulting in less accurate estimates.

These validations of radar altimetry SWH in six subbasins of the CRB provide confidence in using the large sets of VSs to characterize the hydrological dynamics of SWH across the basin. Figure 5a provides a representation of the mean maximal amplitude of SWH at each one of those VSs. The

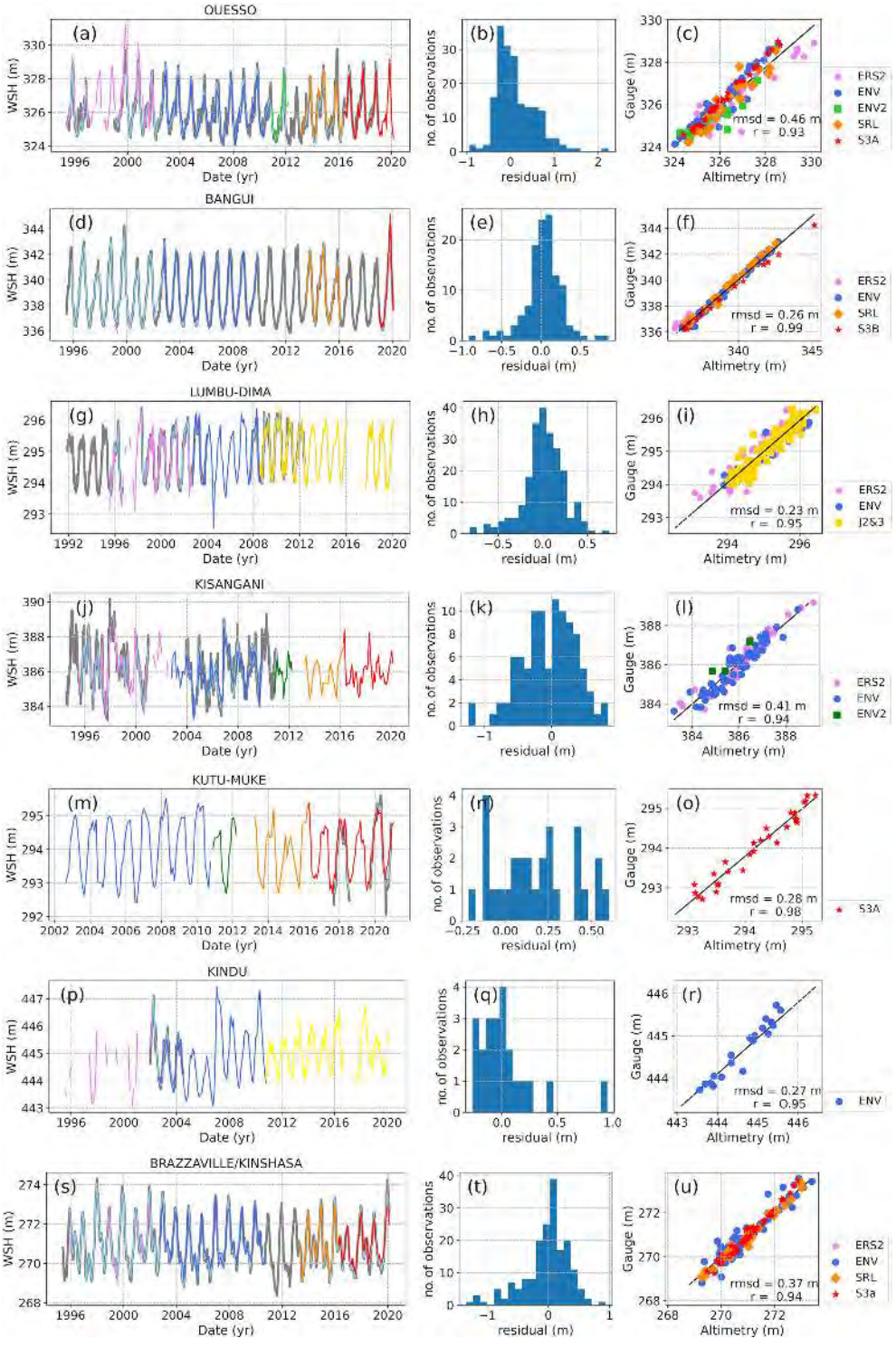

Figure 3. Comparison of the in situ water stage (Table 1) and long-term altimeter-derived SWH obtained by combining ERS-2, ENV, ENV2, SRL, J2/3, and S3A/B at different sites (see Fig. 1 for their locations). **(a, d, g, j, m, p, s)** The time series of both in situ and altimetry-derived water heights, where the grey line in the background shows the in situ daily WS variations (grey), and the sky blue line indicates the in situ WS sampled at the same date as the altimeter-derived SWH from ERS-2 (purple), ENV (royal blue), ENV2 (lime green), SRL (dark orange), J2/3 (yellow), and S3A/S3B (red) missions. **(b, e, h, k, n, q, t)** The histogram of the difference between the altimeter-derived SWH and the in situ WS. **(c, f, i, l, o, r, u)** The scatterplot between altimeter-derived SWH and in situ WS. The linear correlation coefficient r and the root mean square deviation (rmsd), considering all the observations, are indicated. The solid line shows the linear regression between both variables.

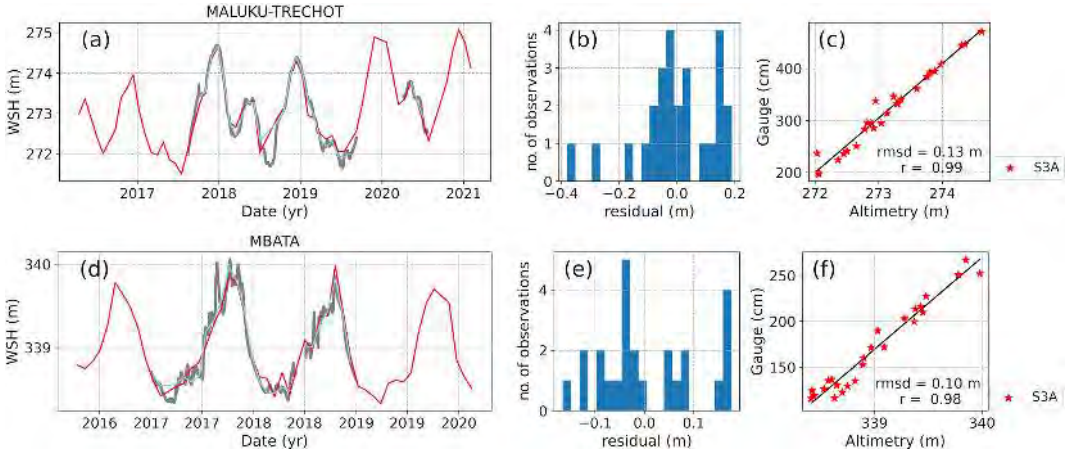

Figure 4. Similar to Fig. 3 but the in situ stations are located right below the satellite track of S3A. A comparison of the in situ water stage (Table 1) and S3A altimeter-derived SWH at different sites is shown (see Fig. 1 for their locations). **(a, d)** The time series of both in situ and altimetry-derived water heights, where the grey line in the background shows the in situ daily WS variations (grey), and the sky blue line indicates the in situ WS sampled at the same date as the altimeter-derived SWH from S3A (red) mission. **(b, e)** The histogram of the difference between the altimeter-derived SWH and the in situ WS. **(c, f)** The scatterplot between altimeter-derived SWH and in situ WS. The linear correlation coefficient r and the root mean square deviation (rmsd), considering all the observations, are indicated. The solid line shows the linear regression between both variables.

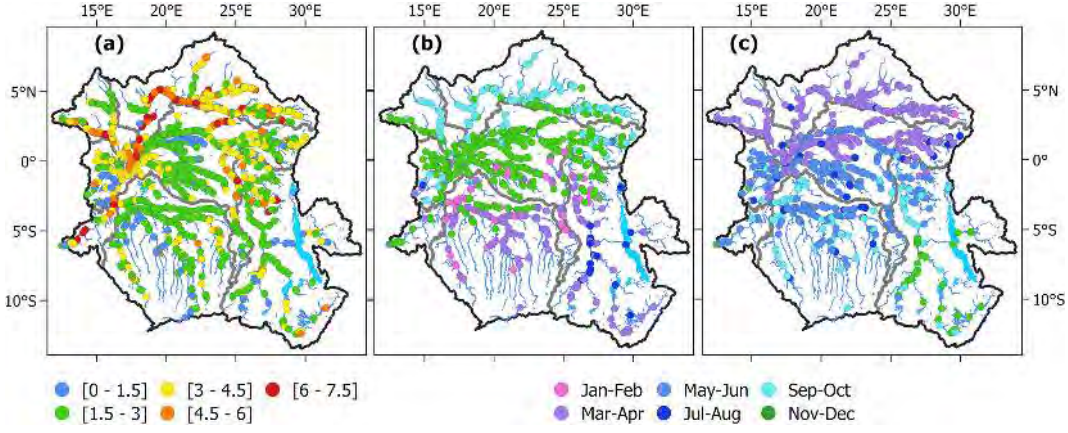

Figure 5. Statistics for radar altimetry VSs. **(a)** The maximum amplitude of SWH (in metres). **(b)** The average month of the maximum of SWH. **(c)** The average month of the minimum of SWH.

Ubangui and Sangha rivers in the northern part of the basin present the largest amplitude variations, up to more than 5 m, while the Congo River main stem and Cuvette Centrale region tributaries vary in smaller proportions (1.5 to 4.5 m). This finding aligns with previous amplitude values reported in the main stem of the Congo River (O'Loughlin et al., 2013). The variation in amplitude in the southern part is similar to the variation observed in the central part, and only a few locations present different behaviours. This is the case, for instance, for the Lukuga river (bringing water from the Tanganyika Lake to the Lualaba river), which is characterized by an amplitude lower than 1.5 m, such as some parts of the Kasaï basin (upper Kasaï, Kwilu, and Wamba rivers) and some tributaries from the Batéké plateaus. The latter are well known for the stability of their flows, due to a strong groundwater regulation.

Figure 5b and c shows the average month for the annual highest and lowest SWH, respectively, at each VS. The high period of water levels in the northern subbasins is September to October, November to December in the central part, and March to April in the southern part. Conversely, the season of low water levels in the northern subbasins is March to April, while the central part of the CRB is at the lowest in May to June, with an exception for the Lulonga river and the right bank tributaries upstream the confluence with the Ubangui (e.g. Aruwimi), for which the driest period is March to April. The Kasaï subbasin is characterized by two periods of low water level, namely September to October and May to

Table 2. The rmsd and r per satellite mission for each in situ station related to Fig. 3.

No.	In situ	ERS-2		ENV		ENV2		J2/3		SRL		S3A		S3B	
	station	rmsd (m)	r	rmsd (m)	r	rmsd (m)	r	rmsd (m)	r	rmsd (m)	r	rmsd (m)	r	rmsd (m)	r
1	Bangui	0.46	0.99	0.15	0.99	–	–	–	–	0.23	0.99	–	–	0.42	0.99
2	Ouésso	0.75	0.91	0.32	0.96	0.89	0.89	–	–	0.20	0.99	0.17	0.99	–	–
3	Brazzaville	0.66	0.87	0.33	0.95	–	–	–		0.21	0.99	0.24	0.99	–	–
4	Lumbu–Dima	0.30	0.92	0.23	0.96	–	–	0.20	0.96	–	–	–	–	–	–
6	Kisangani	0.40	0.95	0.39	0.94	0.64	0.94	–	–	–	–	–	–	–	–
7	Kindu	–	–	0.27	0.95	–	–	–	–	–	–	–	–	–	–
8	Kutu–Muke	–	–	–	–	–	–	–	–	–	–	0.28	0.98	–	–
9	Maluku Tréchot	–	–	–	–	–	–	–	–	–	–	0.13	0.99	–	–
10	Mbata	–	–	–	–	–	–	–	–	–	–	0.10	0.98	–	–

June, on the main Kasaï river stem and its other tributaries. Similarly, the major highland Lualaba tributaries (e.g. Ulindi, Lowa, and Elila), fed by the precipitation in the South Kivu region, present lowest levels in May and June. From its confluence with the Lukuga river and up to Kisangani, the Lualaba river reaches its lowest level in September to October. In the Upemba depression, the low SWH period is November–December. This evidences the strong seasonal signal of the gradual floods of the CRB, clearly illustrating the influence of the rainfall partition in the northern and southern parts of the basin and the gradual shifts due to the flood travel time along the rivers and floodplains. This will be further analysed and discussed in Sect. 5.

4.2 Evaluation of surface water extent characteristics from GIEMS-2

Figure 6 shows the surface water extent (SWE) main patterns over the CRB. Figure 6a and b display, respectively, the mean and the mean annual maximum in the extent of surface water over the 1992–2015 period. Figure 6c shows the variability in SWE, expressed in terms of the standard deviation over the period. Figure 6d provides the average month of SWE annual maximum over the record. The figures show plausible spatial distributions of the major drainage systems, rivers, and tributaries (Lualaba, Congo, Ubangui, and Kasaï) of the CRB. The dataset indeed delineates the main wetlands and inundated areas in the region such as in the Cuvette Centrale region, the Bangweulu swamps, and the valley that contains several lakes (Upemba). These regions are generally characterized by a large maximum inundation extent (Fig. 6b) and variability (Fig. 6c), especially in the Cuvette Centrale region and in the Lualaba subbasin, and are dominated by the presence of large lakes and seasonally inundated floodplains. The spatial distribution of GIEMS-2 SWE is in agreement with several other estimates of SWE over the CRB (see Figs. 3 and 6 of Fatras et al., 2021), including L-band SMOS-derived products (SWAF – surface water fraction; Parrens et al., 2017), Global Surface Water extent dataset (GSW; Pekel et al., 2016), the ESA-CCI (European Space Agency Climate Change Initiative) product and SWAMPS (Surface WAter Microwave Product Series) over the 2010–2013 time period. At the basin scale, and in agreement with the results from the altimetry-derived SWH, GIEMS-2 shows that the Cuvette Centrale region is flooded at its maximum in October–November (Fig. 6d), while the Northern Hemisphere part of the basin reaches its maximum in September–October, and the Kasaï and southeastern part reaches its maximum in January–February.

Seasonal and interannual variations in the CRB scale total SWE and the associated anomalies over 1992–2015 are shown in Fig. 6e and f. The deseasonalized anomalies are obtained by subtracting the 25-year mean monthly value from each individual month. The total CRB SWE extent shows a strong seasonal cycle (Fig. 6e), with a mean annual averaged

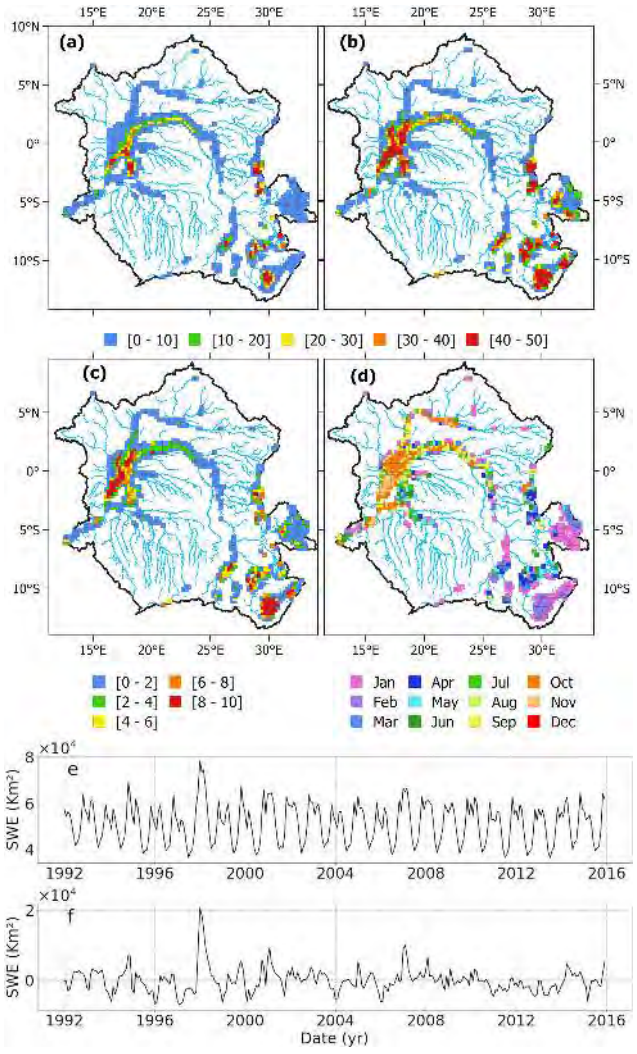

Figure 6. Characterization of SWE from GIEMS-2 over the CRB. **(a)** Mean SWE (1992–2015) for each pixel, expressed as a percentage of the pixel coverage size of 773 km^2. **(b)** SWE variability (standard deviation over 1992–2015; also in percent). **(c)** Annual maximum SWE averaged over 1992–2015 (in percent). **(d)** Monthly mean SWE for 1992–2015 for the entire CRB. **(e)** Time series of SWE. **(f)** Corresponding deseasonalized anomalies obtained by subtracting the 24 years of mean monthly values from individual months.

maximum of $\sim 65\,000$ km^2 over the 1992–2015 period, with a maximum $\sim 80\,000$ km^2 in 1998. The time series shows a bimodal pattern that characterizes the hydrological annual cycle of the CRB. It also displays a substantial interannual variability, especially near the annual maxima. The deseasonalized anomaly in Fig. 6f reveals anomalous events that have recently affected the CRB in terms of flood or drought events. As discussed in Becker et al. (2018), the positive Indian Ocean Dipole (pIOD) events, in conjunction with the El Niño events that happened in 1997–1998 and 2006–2007, triggered floods in east Africa, the western Indian Ocean, and southern India (Mcphaden, 2002; Ummenhofer et al., 2009) and resulted in the large positive peaks observed. The CRB was also impacted by significantly severe and sometimes multi-year droughts during the 1990s and 2000s, often impacting about half of the basin (Ndehedehe et al., 2019). These events can be depicted from GIEMS-2 anomaly time series with repetitive negative signal peaks.

In order to evaluate SWE dynamics at basin and subbasin scales, here we compare at the monthly time step for the seasonal and interannual variability in the GIEMS-2 estimates against the variability in the available in situ water discharge and stages (Table 1).

First, at the entire basin scale, Fig. 7 displays the comparison between the total area of the CRB SWE with the river discharge measured at the Brazzaville/Kinshasa station, which is the most downstream station available for our study near the mouth of the CRB. There is a fair agreement between the interannual variation (Fig. 7a) in the surface water extent and the in situ discharge over the period from 1992 to 2015, with a significant correlation coefficient ($r = 0.67$ with a 0-month lag; p value < 0.01) and a fair correlation for its associated anomaly ($r = 0.58$; p value < 0.01). On both the raw time series and its anomaly (Fig. 7b), SWE captures major hydrological variations, including the yearly and bimodal peaks. The seasonal comparison (Fig. 7c) shows that the SWE reaches its maximum 1 month before the maximum of the discharge in December. From January to March, the discharge decreases, while the SWE remains high. For the secondary peak, the SWE maximum is reached 2 months before the one for discharge in May. This is in agreement with the results shown with the SWE spatial distribution of the average month of the maximum inundation in October–November in the Cuvette Centrale region (Fig. 6a).

Further, the evaluation of SWE dynamics is performed at the subbasin level against available observations at the outlets of each of the 5 subbasins. Similar to Fig. 7, Fig. 8 shows the comparisons of the aggregated SWE at the subbasin scale against in situ observations at their respective outlet stations (Bangui for Ubangui, Ouésso for Sangha, Lumbu–Dima for Kasaï, Kisangani for Lualaba, and Brazzaville/Kinshasa for the middle Congo subbasin). For Lualaba and Kasaï (Fig. 9), in situ SWHs are used since no discharge observation is available. For each subbasin, we estimate the maximum linear correlation coefficient of point time records between the SWE and the other variables when lagged in time (months). The temporal shift helps to express an estimated travel time of water to reach the basin outlet. There is a general good agreement (with high lagged correlations $r > 0.8$; Figs. 8a, d, g and 9a) between both variables, and lag time ranging between 0 and 2 months, with SWE preceding the discharge, except for the Lualaba. The seasonal analysis in Ubangui and Sangha subbasins shows that the discharge starts to increase one month prior to SWE (from May), probably related to local precipitation downstream the basins, before both variables increase steadily and reach their maxi-

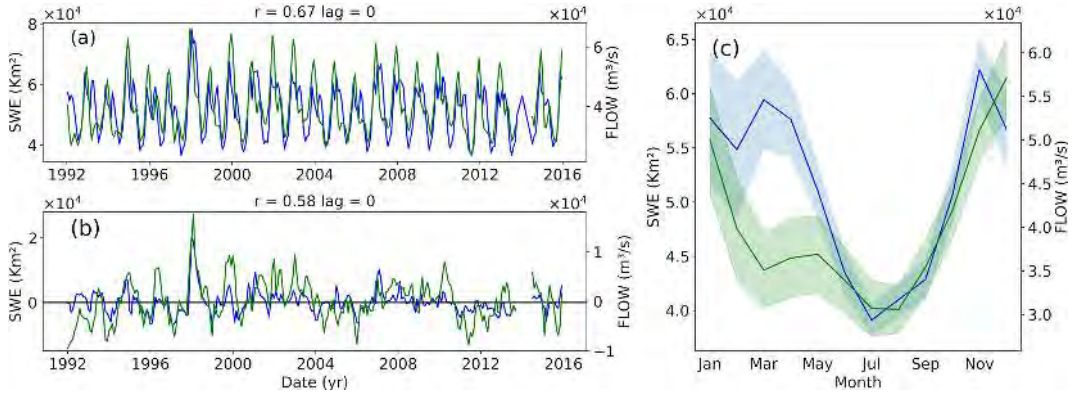

Figure 7. Comparison of monthly SWE **(a)** and its anomalies **(b)** at CRB scale against the in situ monthly mean water discharge at the Brazzaville/Kinshasa station. The blue line is the SWE, and the green line is the mean water discharge. **(c)** The annual cycle for both variables (1992–2015), with the shaded areas illustrating the standard deviations around the SWE and discharge means.

mum in October–November (Fig. 8c and f). For the Kasaï subbasin (Fig. 9c), SWE increases from July, followed within a month by the water stage, reaching a peak respectively in December and January. While SWE slowly decreases from January, only the discharge continues to increase to reach a maximum in April. For the middle Congo subbasin (Fig. 8), the variability in SWE and discharge are in good agreement ($r = 0.89$, Fig. 8g) with the SWE steadily preceding the discharge by one month (Fig. 8i). The annual dual peak is also well depicted. On the other hand, the Lualaba subbasin with a moderate correlation ($r = 0.54$ and lag = 0 month; Fig. 9d) shows a particular behaviour with the water stage often preceding the SWE (Fig. 9f). This could be explained by the upstream part of the Lualaba subbasin where the hydrology might be disconnected from the drainage system due to the large seasonal floodplains and lakes, well captured by GIEMS. These water bodies store freshwater and delay its travel time, while the outlet still receives water from other tributaries in the basin. For all subbasins, the inter-annual deseasonalized anomalies present in general positive and moderate linear correlations ($0.4 < r < 0.5$; p value < 0.01 with 0-month lag; Figs. 8b, e and 9b, e) except for the middle Congo where the correlation is greater (0.63; p value < 0.01) with temporal shift of one month (Fig. 8h). This confirms the good capabilities of satellite-derived SWE to portray anomalous hydrological events in agreement with in situ observations at the subbasin scale.

At the basin scale, we have already showed that the annual variability in the CRB discharge is in fair agreement with the dynamic of SWE, from seasonal to interannual timescales. Figure 10 investigates the comparison between water flow at the Brazzaville/Kinshasa station against the variability in SWE for each subbasin. For Ubangui, Sangha, and middle Congo (Fig. 10a, d and g), the variability in water discharge is strongly related to the SWE variations with a respective lag of 2, 1, and 0 months, related to the decreasing distance between the subbasin and the gauging station. The time series of the anomalies of the above subbasins capture also some of the large peak variations while other peaks are observed at the subbasin scale. Kasaï subbasin presents a good correspondence ($r = 0.74$ and lag = 0) between the variability in water flow and SWE, as well as for their associated anomaly ($r = 0.47$ and lag = 0). Unlike the other four sub-catchments, Lualaba presents again a low agreement ($r = 0.05$ and lag = 0) with, as already seen in Fig. 9, a non-consistent behaviour and shifted variations between SWE and discharge (Fig. 10m), related to lakes and floodplains storage which delay the water transfer to the main river. Nevertheless, anomalies like the strong one in 1998, with large floods linked to a positive Indian Ocean Dipole in conjunction with an El Niño (Becker et al., 2018) are in phase and within same order of magnitude (Fig. 10n).

A focus on the middle Congo anomaly time series reveals that it is the only subbasin where all the variations in the peak discharge are well captured in SWE. This reflects the strong influence of the middle Congo floodplains on the flow at the Brazzaville/Kinshasa station, for which the variability may be explained, at ~ 35 %, by the variations in SWE in the Cuvette Centrale region, based on the maximum lagged correlation of 0.59 for the deseasonalized anomalies of the two variables. More interestingly, while the river discharge shows a double peak in its seasonal climatology (a maximum peak in December and a secondary peak in May), it is not portrayed in the SWE in most subbasins, except for the middle Congo that also receives contributions from Sangha, Ubangui, Kasaï, and Lualaba. The next section investigates these characteristics.

5 Results: a better understanding on how CRB surface water flows

The evaluation of both SWH from radar altimetry and SWE from GIEMS-2, presented in the previous sections, provides

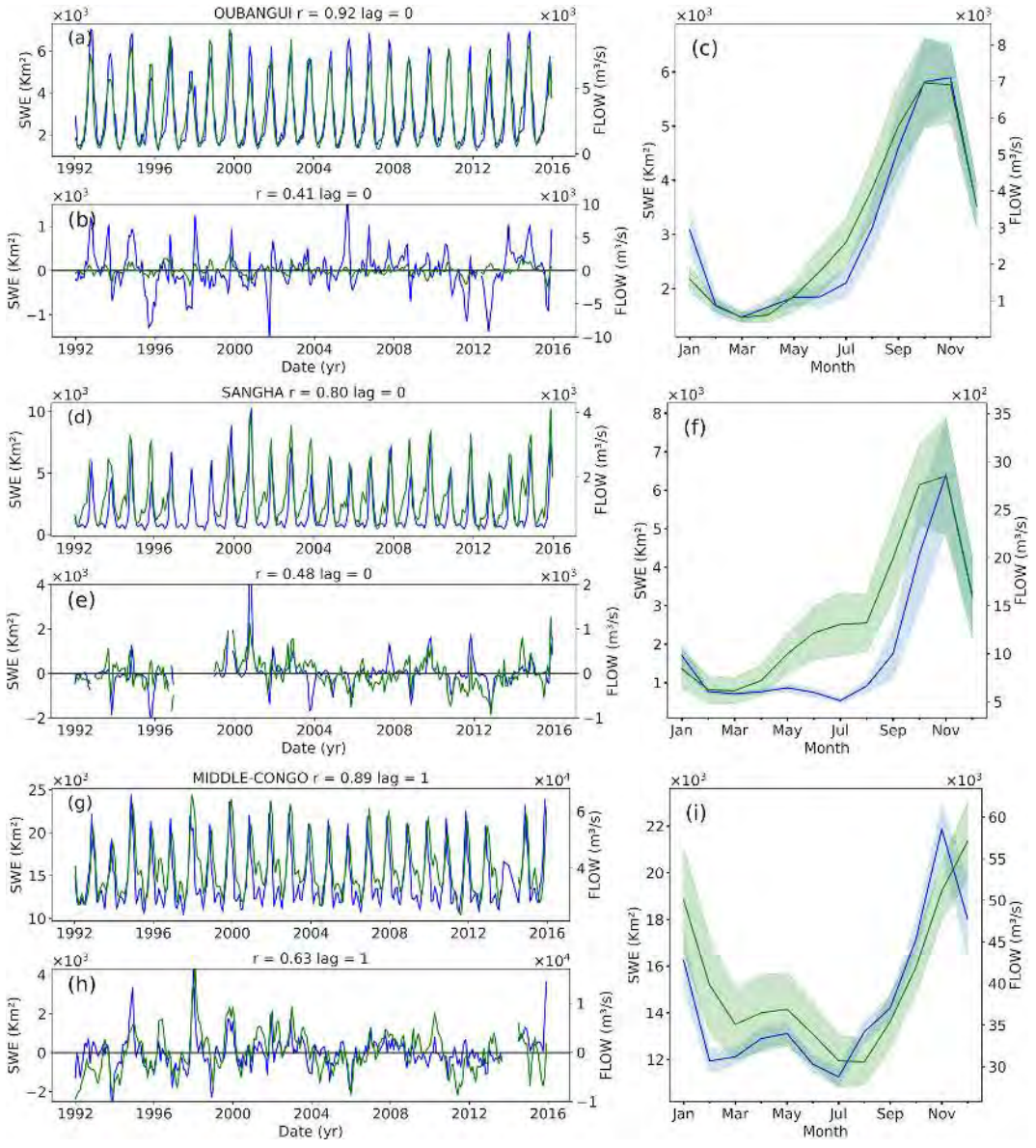

Figure 8. Similar to Fig. 7 but for each of the five subbasins. A comparison of the monthly SWE (absolute and anomaly values) against the in situ water discharge at each subbasin outlet is shown. The blue line is for the SWE, and the green line is for the water discharge. The annual cycle for both variables (1992–2015) is also displayed, with the shaded areas illustrating the standard deviations around SWE and discharge means.

the confidence to further analyse the dynamics of surface water and their patterns within the CRB.

5.1 Seasonal water travel time through the rivers and subbasins of the CRB

The water travel time through the rivers and subbasins of the CRB was previously investigated by using observations from a few in situ gauges (Bricquet, 1993). In this study, SWH and SWE datasets enable a similar analysis at the large scale, with an extended analysis to the entire CRB.

Here, we determine the maximum of the linear Pearson correlation coefficient by considering a time lag between the satellite-derived SWH at each VS (from ERS-2, ENV, J2/3, SRL, and S3A missions) and GIEMS SWE at each cell, against the Brazzaville/Kinshasa SWH and discharge, respectively. For this, we use the scipy.stats.pearsonr package from Python that also includes the computation of the p value that we use for performing the hypothesis test of the significance of the correlation coefficient. In the following, we consider the significance level to be 0.1.

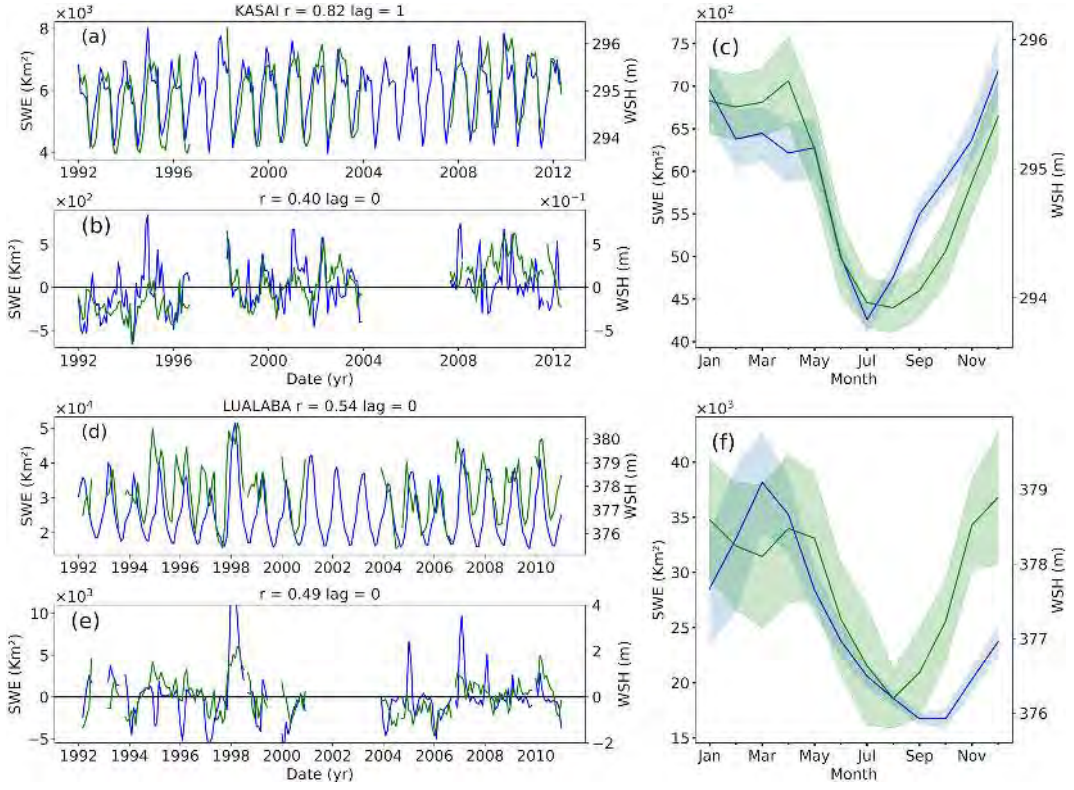

Figure 9. Similar to Fig. 8 using available in situ water stage. A comparison of the monthly SWE (absolute and anomaly values) against the in situ water stage at each subbasin outlet is shown. The blue line is for the SWE, and the green line is for the water stage. The annual cycle for both variables (1992–2015) is also displayed, with the shaded areas illustrating the standard deviations around SWE and discharge means.

Note that the temporal shift between SWH/SWE and in situ stages and discharges is constrained between acceptable values, i.e. it cannot be negative, as we are investigating the time needed by surface waters to reach the Brazzaville/Kinshasa station. For each VS, the longest possible time series is used. For GIEMS-2, the data over the 24-year record are used against the entire river discharge record (1992–2015). The maps of the highest correlations and their corresponding time shifts are provided in Fig. 11. Note that both satellite-derived datasets are jointly analysed to support and complement each other's individual result. As a validation, the linear Pearson correlation coefficients between altimeter-derived SWH and GIEMS-2 SWE for each location within a 25 km distance and a common availability of data were estimated (figure not shown). The correlations found are generally high (> 0.9) across the entire CRB.

Figure 11a and b evidences that the northern (Sangha and Ubangui) and the central (western middle Congo and downstream tributaries of Kasaï) parts are fairly well correlated ($r > 0.6$; p value < 0.1), both in terms of SWH and SWE to the discharge at Brazzaville/Kinshasa. In the eastern part of the middle Congo and downstream part of the Lualaba river, SWH and SWE show different patterns, with higher maximal correlations for SWH (> 0.6) than SWE (< 0.5). On the other hand, the southeastern part of the Lualaba subbasin presents a low correlation ($r < 0.2$) for both variables, confirming again that the discharge at the Brazzaville/Kinshasa station is not strongly influenced by the remote water dynamics from the southeastern part of the CRB. The temporal shifts (in months) associated to the maximum correlation (Fig. 11c and d) at each VS and GIEMS-2 cell (only locations where $r \geq 0.6$ are displayed) help to estimate the water travel time to the Brazzaville/Kinshasa reach. As expected, the time lag for both SWH and SWE increases with the distance from the Brazzaville/Kinshasa station from 0 up to 3 months in remote areas and small tributaries of the upper CRB. The mainstream of the Congo in the middle Congo subbasin and northern Kasaï are characterized by 0 months of lag due to their proximity with the reference station (Brazzaville/Kinshasa). However, left- and right-margin tributaries (for instance, the Likouala-aux-Herbes and Ngoko rivers) present a 1-month lag. The Ubangui and Sangha subbasins show a minimum of 2 months' lag and up to 3 months for the remote area in the far northern part of the Ubangui basin (Kotto and Mbomou rivers; Fig. 11c). Interestingly, on the downstream part of the Ubangui river, and in the Cuvette Centrale region, there is a notable 1-month difference between the lag in SWH and SWE. While SWH shows a lag time of 0–1 month, it is 1–2

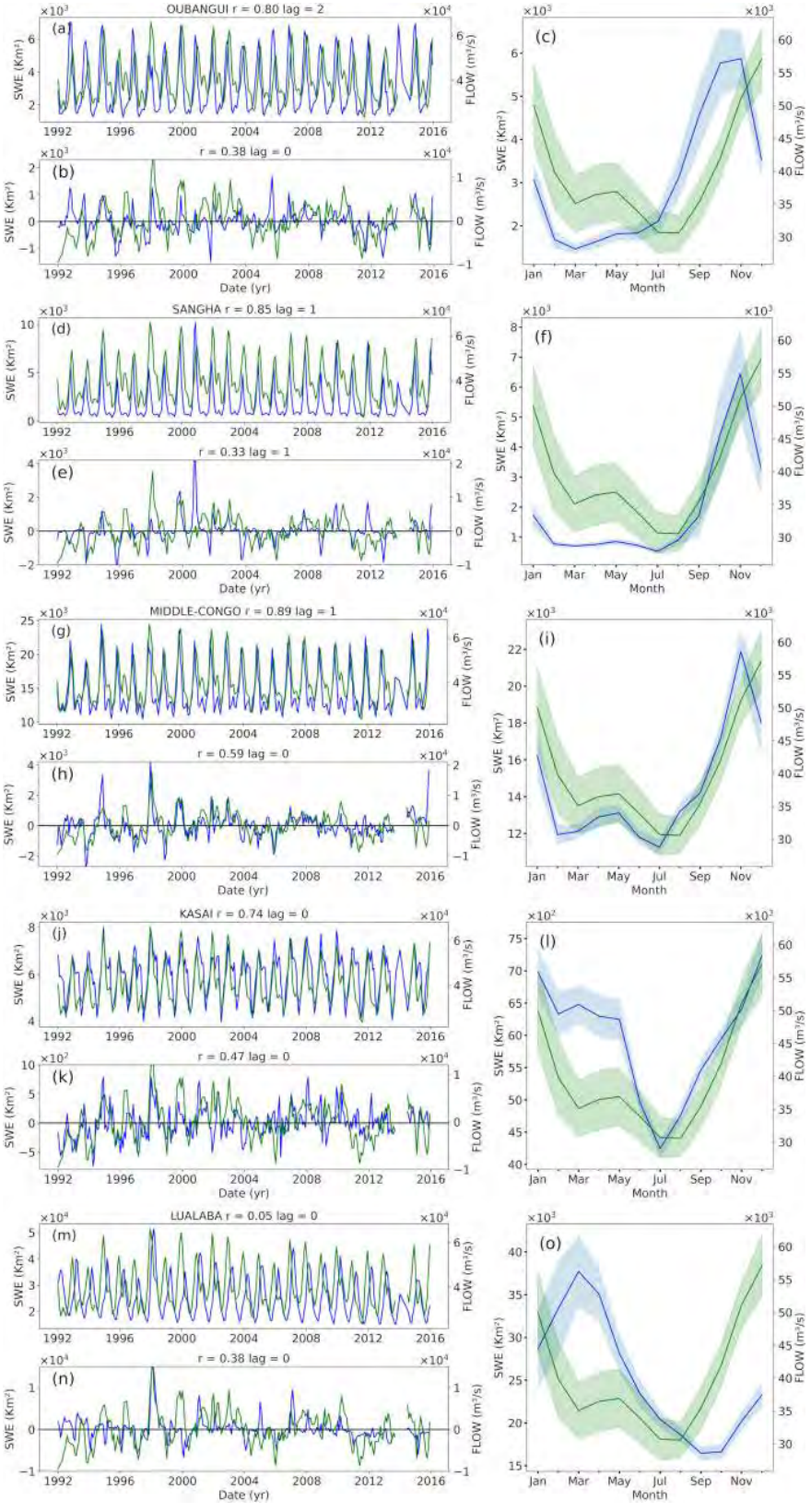

Figure 10. Similar to Figs. 7–9 but the SWE estimated at each of the five subbasins is compared against the in situ monthly mean water discharge at the Brazzaville/Kinshasa station. The blue line is for the SWE, and the green line is for the water flow at the Brazzaville/Kinshasa station. The annual cycle for each variable (1992–2015) is also displayed, with the shaded areas illustrating the standard deviations around the SWE and discharge means.

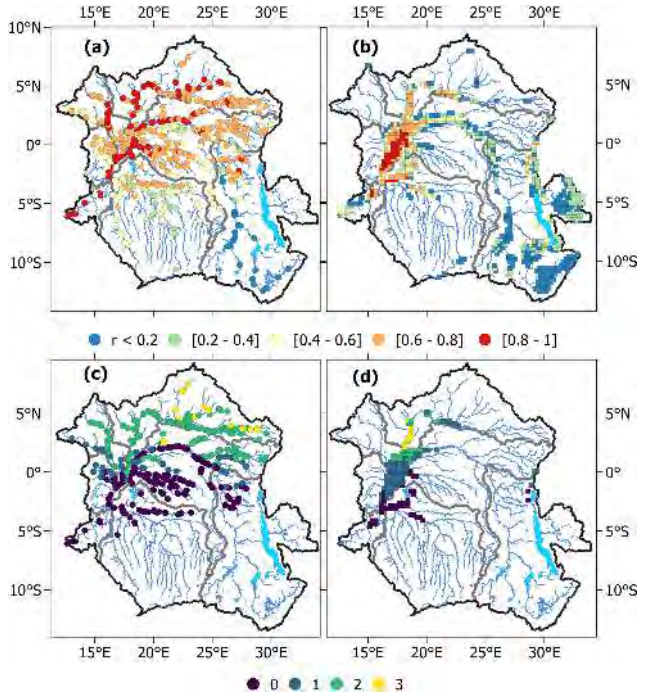

Figure 11. Maps of the optimal coefficient correlation and associated lag at each VS and GIEMS-2 cell. **(a)** Optimum coefficient correlation between altimetry-derived SWH (from ERS2, ENV, SRL, J2/3, and S3A missions) at each VS against the in situ water stage at the Brazzaville/Kinshasa station. **(b)** Same as **(a)** for each GIEMS-2 cell against the river discharge at the Brazzaville/Kinshasa station. Panels **(c)** and **(d)** show, respectively, their optimum lag in months. In panels **(c)** and **(d)**, only the time lags for which the maximum correlation has a p value < 0.05 are displayed.

months for SWE. This can be explained by specific hydrological mechanisms of wetlands and large floodplains and the processes between river and floodplains connectivity. These differences can be due, on the one hand, to the different behaviours between the water level dynamics and water extent in shallow flooded areas, where SWH in river generally increases before the surface water extent increases with riverbank overflows, while the waters stand for a longer time in the wetlands than in the rivers. The differences might also be attributed to relatively disconnected wetlands and rivers and/or to the presence of interfluvial wetlands fed directly by local precipitation instead of overbank flooding.

In order to confirm and validate the results on the dynamics of water surface flows obtained from altimeter-derived SWH and GIEMS-derived SWE, we perform a similar analysis using water level and flow observations from historical (< 1994) and current gauges, as presented in Table 2. For each station, covering all the subbasins considered, we estimated the correlation between the available observations and the observations at the Brazzaville/Kinshasa station at daily and monthly time steps. The results are presented in Table 3. In order to facilitate the comparisons, results for the VSs and SWE cells (as presented in Fig. 11) related to the nearest available in situ gauge stations are reported in Table 3, even if not covering the same period of time.

Overall, the results from the Table 3 support the general findings reported in Fig. 11, both in terms of optimum coefficient correlation and in terms of lag, with a general good agreement between in situ and satellite observations. The correlation analysis (with p value < 0.05; the change in the p value is related to the in situ record length) between observations at Brazzaville/Kinshasa and the various other stations confirms the higher positive values ($r > 0.7$; with a mean time lag of 8 d and 0 months) with increasing maximum correlation when closest to Brazzaville/Kinshasa in situ station. Lower Congo also shows very high correlations ($r > 0.8$). The Kasaï subbasin presents low to moderate positive lagged correlation (0.35 to 0.55; lag $= 0$), with values decreasing with respect to longer distance from the month, which is in agreement with the results from the satellite estimates. For the Lualaba subbasin, the results at the Kisangani outlet station present a moderate maximum correlation ($r > 0.6$), similar to the values obtained with SWH from altimetry. In agreement with the results for both SWH and SWE, in situ observations confirm that, in other upstream locations of the Lualaba, which are connected to lakes and floodplains, very low correlations ($r < 0.2$) are observed. Both Ubangui and Sangha subbasins have large positive correlations ($r > 0.7$), with a respective time lag of 2 months (65 d when using in situ daily observations) and 1 month (45 d), similar to what satellite observations provided. The difference observed in the correlation coefficient and the lag between SWH and SWE, for the Basoko station in middle Congo, for instance, also confirms the different hydrological behaviour between the adjacent wetlands and the main river channel. This is also in line with the 1-month lag observed at some locations in the Cuvette Centrale region between both satellite-derived SWH and SWE, supporting the idea that different processes drive the relation between river channel height and flood extent dynamics.

5.2 Subbasin contributions to the CRB bimodal hydrological regime

A supplementary analysis was performed in order to better illustrate the spatial distribution of the CRB flood dynamics over all the various tributaries and also their different timing and how each subbasin contributes to the peculiar bimodal pattern of the hydrological regime downstream the main stem at Brazzaville/Kinshasa (Figs. 11 and 12). Here, we reproduced the same analysis as above but now considering, individually, the two distinct periods of the year corresponding to each hydrological peak observed at Brazzaville/Kinshasa. We first consider the August–February period (the first large peak) for each time series and estimate the correlation. Then we consider the March–July period corresponding to the secondary peak. The results are shown in Fig. 12, and the com-

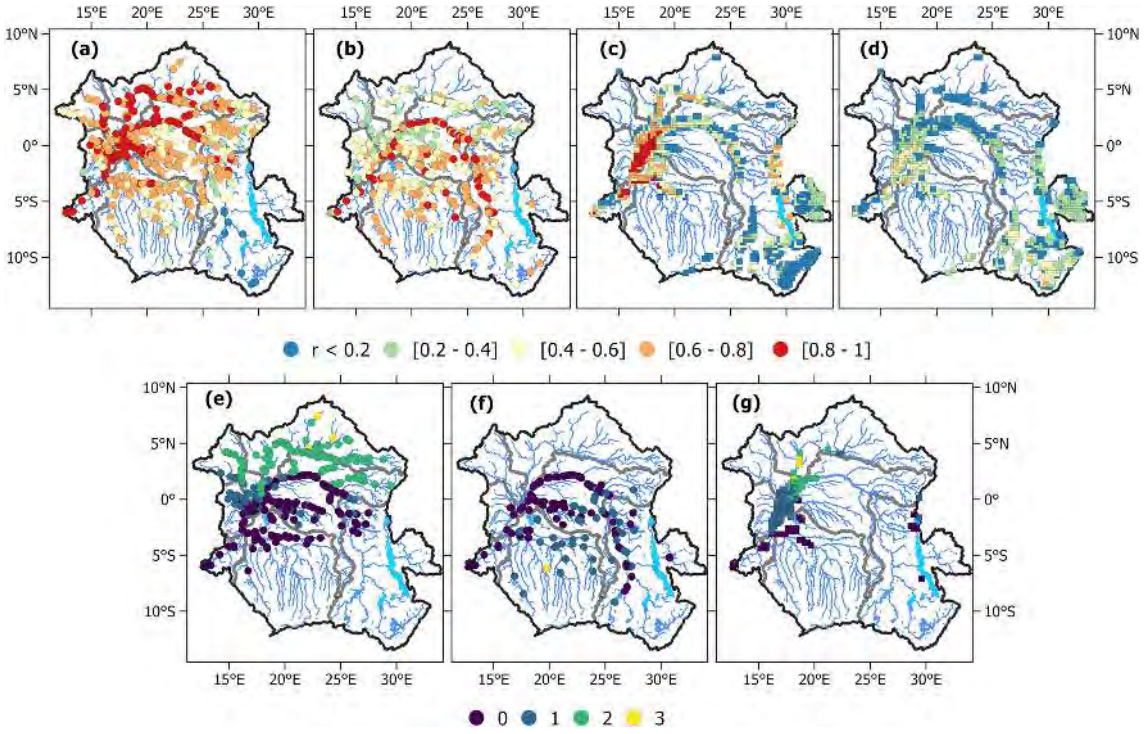

Figure 12. Similar to Fig. 11 but considering the two distinct periods of the year corresponding to each hydrological peak observed at Brazzaville/Kinshasa. **(a)** The optimum coefficient correlation between altimetry-derived SWH (from ERS2, ENV, SRL, J2/3, and S3A missions) at each VS against the in situ water stage at the Brazzaville/Kinshasa station for the period of August–February. **(b)** Same as panel **(a)** but for the period of March–July. **(c)** The optimum coefficient correlation between SWE at each GIEMS-2 against in situ discharge at the Brazzaville/Kinshasa station for the period of August–February. **(d)** Same as panel **(c)** but for the period of March–July. **(e–g)** The time lag (in months) associated, respectively, to panels **(a–c)** but only for cases where the maximum correlation has p value < 0.05. The time lag associated to panel **(d)** has too few values with a p value < 0.05 and is therefore not shown.

parison/validation of the results with historical and current in situ records are summarized in Table 4.

Figure 12 clearly depicts the relative contributions of the northern subbasins and the southern subbasins to the first peak and to the second peak, respectively. Regarding the first peak (Fig. 12a, c, e, and g), the major contribution of the Ubangui and Sangha rivers ($r > 0.6$) to the downstream main stem at Brazzaville/Kinshasa during the August–February period is evidenced, with a water transfer time to the Brazzaville/Kinshasa station ranging between 1 and 3 months (again, increasing with the distance to the gauging station). Middle Congo, northern Kasaï, and the highland of the Lualaba subbasin also show some contribution during this period but with 0 to 1 month lag. Water that supplies the second peak of the hydrograph essentially comes from the centre and the southern part of the basin (Fig. 12b, d, and f), including remote rivers in the Kasaï subbasin with a 1–2 month lag and the western part of the Lualaba. The very low correlations between the upper part of the basin (Kivu region, Luapula, and upper Lualaba) and the discharge at Brazzaville/Kinshasa suggest that the contribution in terms of discharge of this region to the hydrological cycle downstream is negligible, for both peaks, in comparison to that from other tributaries. These conclusions are supported by the similar analyses performed using the in situ observation records (Table 4). This confirms the relatively low contribution of the northern part to the second peak at the Brazzaville/Kinshasa station. On the monthly basis, the lags are found to be similar to the in situ and satellite observations, while the daily data from the in situ records help to provide a better characteristic of the travel time at a finer timescale. For instance, with the second peak of the hydrograph, the Kasaï and middle Congo subbasins are characterized, respectively, by a mean time lag of 1 month (28 d) and 0 months (7 d), depending on the data sampling interval considered.

6 Conclusion and perspectives

The present study uses a unique joint analysis of in situ and satellite-derived observations to better characterize the CRB surface hydrology and its variability. First, thanks to the availability of an in situ database of historical and contemporary observations of water levels and discharges, we provide an intensive and comprehensive validation of long-term ($\sim$ 25-year) time series from space-borne water level

Table 3. Optimal coefficient correlation and associated lag for each in situ station against SWH and discharge at the Brazzaville/Kinshasa station, with their closest VS and GIEMS-2 cell (SWE) and their latitude and longitude in parentheses (second column). In the last two columns, in parenthesis, the r and lag values are given at the daily timescale when daily observations are available. Only correlations with a 95 % significance are reported.

No.	In situ	Monthly (daily)	
		r	lag
Kasaï subbasin			
4	Lumbu–Dima	0.46 (0.46)	0 (0)
	VS (−3.26, 17.46)	0.48	0
5	Esaka–Amont	0.34 (0.35)	0 (0)
	VS (−3.40, 18.09)	0.5	0
11	Bagata	0.55 (0.54)	0 (0)
	VS (−3.39, 17.40)	0.66	0
	SWE (−3.38, 17.40)	0.49	0
15	Ilebo	0.40 (0.40)	0 (0)
	VS (−4.34, 20.49)	0.42	0
	SWE (−4.38, 20.68)	0.48	0
Middle Congo subbasin			
13	Basoko	0.72 (0.73)	0 (10)
	VS (1.26, 23.72)	0.83	1
	SWE (1.38, 23.88)	0.24	0
14	Bumba	0.72 (0.73)	0 (10)
	VS (2.19, 22.19)	0.78	0
	SWE (2.12, 22.39)	0.51	1
17	Mbandaka	0.92 (0.92)	0 (5)
	VS (−0.04, 18.40)	0.94	0
	SWE (−0.12, 18.38)	0.83	1
Lower Congo subbasin			
9	Maluku Tréchot	0.97 (0.96)	0 (0)
	VS (−4.15, 15.41)	0.97	0
	SWE (−4.12, 15.42)	0.85	0
Lualaba subbasin			
6	Kisangani	0.64 (0.61)	0 (0)
	VS (0.36, 25.38)	0.63	0
	SWE (0.38, 25.38)	0.39	3
7	Kindu	0.12 (0.13)	0 (0)
	VS (−3.14, 25.93)	0.17	0
	SWE (−2.88, 25.91)	0.32	0
16	Kabalo	−0.17 (−0.17)	3 (0)
	VS (−5.76, 26.91)	−0.3	0
	SWE (−6.38, 27.04)	0.03	0
25	15 933 300	0.42	1
	VS (−10.68, 28.68)	−0.21	0
26	1 593 210	0.42	2
	VS (−10.68, 28.68)	−0.21	0
Lualaba subbasin			
27	1 593 100	0.55	1
	VS (−11.89, 28.53)	−0.34	0
28	Old pontoon	−0.23 (0.1)	0 (0)
	VS (−10.56, 31.46)	−0.17	0
	SWE (−10.88, 31.19)	0.03	0
Ubangui subbasin			
1	Bangui	0.79 (0.78)	2 (65)
	VS (4.35, 18.57)	0.83	2
	SWE (4.38, 18.68)	0.68	2
10	Mbata	0.71	2
	VS (3.66, 18.29)	0.81	2
18	Bossele–Bali	0.53	2
	VS (4.43, 18.34)	0.83	2
19	Bangassou	0.78	2
	VS (4.72, 22.80)	0.78	2
21	Obo	0.65	2
	VS (5.15, 26.30)	0.73	2
22	Loungoumba	0.64	2
	VS (4.81, 22.93)	0.87	2
23	Zemio	0.70	2
	VS (4.90, 24.78)	0.88	2
Sangha subbasin			
2	Ouésso	0.69 (0.71)	1 (45)
	VS (1.44, 16.20)	0.81	1
	SWE (0.62, 16.62)	0.61	1
24	Salo	0.78	2
	VS (2.88, 16.24)	0.80	2

variations and surface water extent throughout the CRB. The comparison of radar-altimetry-derived water levels with the in situ water stage at the interannual scale shows an overall good agreement, with standard errors, in general, lower than 0.30 m. The analysis of the rmsd across the various missions shows an improvement over time from ERS-2 (tens of centimetres) to S3A/B (a few centimetres) missions, confirming the technological improvement in terms of sensors and data processing. A total of more than 2300 VSs covering the 1995–2020 period was used in this study and is now freely available. When compared to in situ observations, GIEMS-2 SWE also shows consistent and complementary information at the subbasin and basin scales. These two long-term records are then used to analyse the spatiotemporal dynamics of surface freshwater and its propagation at subbasin and

Table 4. Optimal coefficient correlation and associated lag for each in situ station against SWH and discharge at the Brazzaville/Kinshasa station for the two periods of time corresponding to the first and second peak and for their closest VS and GIEMS-2 cell (SWE). Their latitude and longitude are in parentheses in the second column. In parenthesis, in the last two columns, the r and lag values, using daily observations are shown. Only correlations with a 95 % significance are reported.

No.	In situ	Peak 1 (August–February) monthly (daily)		Peak 2 (March–July) monthly (daily)	
		r	lag	r	lag
Kasaï subbasin					
4	Lumbu–Dima	0.63 (0.63)	0 (0)	0.65 (0.63)	1 (30)
	VS (−3.26, 17.46)	0.67	0	0.65	1
5	Esaka–Amont	0.52 (0.52)	0 (0)	0.52 (0.38)	0 (25)
	VS (−3.40, 18.09)	0.64	0	0.49	1
11	Bagata	0.65 (0.65)	0 (0)	0.57 (0.56)	1 (20)
	VS (−3.39, 17.40)	0.77	0	0.70	0
	SWE (−3.38, 17.40)	0.55	0	0.34	1
15	Ilebo	0.59 (0.59)	0 (0)	0.59 (0.60)	1 (40)
	VS (−4.34, 20.49)	0.66	0	0.64	1
	SWE (−4.38, 20.68)	0.54	0	0.44	2
Middle Congo subbasin					
13	Basoko	0.77 (0.81)	1 (15)	0.81 (0.77)	0 (5)
	VS (1.26, 23.72)	0.82	2	0.77 1	
	SWE (1.38, 23.88)	0.45	0	0.17	3
14	Bumba	0.77 (0.80)	0 (15)	0.77 (0.77)	0 (10)
	VS (2.19, 22.19)	0.80	0	0.80	0
	SWE (2.12, 22.39)	0.54	1	0.02	3
17	Mbandaka	0.92 (0.93)	0 (5)	0.92 (0.91)	0 (0)
	VS (−0.04, 18.40)	0.96	0	0.84	0
	SWE (−0.12, 18.38)	0.84	1	0.63	0
Lower Congo subbasin					
9	Maluku Tréchot	0.97 (0.97)	0 (0)	0.92 (0.92)	0 (0)
	VS (−4.15, 15.41)	0.97	0	0.90	0
	SWE (−4.12, 15.42)	0.90	0	0.60	1
Lualaba subbasin					
6	Kisangani	0.83 (0.78)	0 (0)	0.73 (0.77)	0 (0)
	VS (0.36, 25.38)	0.75	0	0.75	0
	SWE (0.38, 25.38)	0.55	3	0.25	3
7	Kindu	0.25 (0.26)	0 (0)	0.66 (0.68)	0 (0)
	VS (−3.14, 25.93)	0.29	0	0.80	0
	SWE (−2.88, 25.91)	0.23	0	0.30	3
16	Kabalo	−0.28 (−0.30)	0 (0)	0.73 (0.74)	0 (0)
	VS (−5.76, 26.91)	−0.18	0	0.81	0
	SWE (−6.38, 27.04)	−0.09	2	0.26	0
28	Old pontoon	(0.22)	(0)	0.60 (0.56)	1 (30)
	VS (−10.56, 31.46)	–	–	0.65	1
	SWE (−10.88, 31.19)	−0.03	3	0.21	0

Table 4. Continued.

No.	In situ	Peak 1 (August–February) monthly (daily)		Peak 2 (March–July) monthly (daily)	
		r	lag	*r*	lag
Ubangui subbasin					
1	Bangui	0.87 (0.87)	2 (55)	0.23 (0.24)	3 (75)
	VS (4.35, 18.57)	0.82	2	0.41	3
	SWE (4.38, 18.68)	0.6	2	0.05	3
10	Mbata	0.62	2	–	–
	VS (3.66, 18.29)	0.82	2	–	–
18	Bossele–Bali	0.51	3	–	–
	VS (4.43, 18.34)	0.82	2	–	–
19	Bangassou	0.81	2	–	–
	VS (4.72, 22.80)	0.76	2	–	–
21	Obo	0.58	2	–	–
	VS (5.15, 26.30)	–	–	–	–
22	Loungoumba	0.54	2	–	–
	VS (4.81, 22.93)	0.92	2	–	–
23	Zemio	0.65	2	–	–
	VS (4.90, 24.78)	0.91	2	–	–
Sangha subbasin					
2	Ouésso	0.73 (0.78)	1 (40)	0.28 (0.30)	0 (20)
	VS (1.44, 16.20)	0.81	1	0.35	3
	SWE (0.62, 16.62)	0.63	1	0.17	3
24	Salo	0.81	2	–	–
	VS (2.88, 16.24)	0.7	2	–	–

basin scales, significantly improving our understanding of how surface water flows in the CRB.

The analysis of the large database of SWH from altimetry shows that the amplitude varies greatly across the basin, from more than 5 m in the Ubangui and Sangha rivers, while the Cuvette Centrale region and the southern basins display smaller annual variations (1.5 to 4.5 m). The maximum level is reached in September–October in the northern part of the basin, in November–December in the central part, and in March–April in the Lualaba region. Surface water bodies and wetlands in the Lualaba subbasin and Cuvette Centrale region present the highest variation in extent across the subbasins and reach their maximum inundation, respectively, in January–February and November–December. Then we investigate the hydrology contributions and water travel times from upstream to downstream reaches by comparing SWE and SWH to stage and discharge at the Brazzaville/Kinshasa station. In particular, the methodology permitted us to better illustrate the spatial distribution of the CRB flood dynamics on the various tributaries, their different timing, and how each subbasin contributes to the peculiar bimodal pattern of the hydrological regime downstream of the main stem in Brazzaville/Kinshasa. The time shift for both SWH and SWE increases with the distance from the Brazzaville/Kinshasa station from no time lag at the vicinity of the outlet up to 3 months in remote areas and small tributaries of the CRB. Northern subbasins and the central Congo region highly contribute to the large August–March peak, while the southern part supplies water to both peaks and in particular to the second one. These results are supported by in situ observations to confirm the findings from satellite observations and from previous studies. Our results therefore confirm the suitability of both long-term water surface elevation time series from radar altimetry and flooded areas from GIEMS-2 for monitoring the CRB surface water dynamics, potentially bridging the gap between past in situ databases and current and future monitoring as an ensemble. Their use in hydrological models will permit a better representation of local- and basin-scale hydrodynamics and ensure an improved monitoring of hydrological variables from space.

The very first use of a large dataset of VSs spread over more than 100 tributaries across the basin and spanning the

whole altimetry period permitted an unprecedented analysis in terms of both the length of the observation and number of observations, providing time series of more than 20 years over the CRB. This unique dataset of surface water levels variations, combined to the ∼ 25-year SWE from GIEMS, should permit us to generate estimates of surface water storage. Complementary to the GRACE/GRACE-FO (Gravity Recovery and Climate Experiment Follow-On) total water storage estimates, it will further permit the estimation of long-term and interannual variations in the freshwater volume in the CRB, including subsurface and groundwater storage and their link with hydro-climatic processes across the region. Furthermore, the use of both satellite datasets in the hydrological models will permit a better representation of local- and basin-scale hydrodynamics and ensure an improved real-time monitoring of hydrological variables from space, as well as a better evaluation of climate variability impacts on water availability. These datasets will also play a key role in the evaluation and validation of future hydrology-oriented satellite missions, such as the NASA-CNES Surface Water and Ocean Topography (SWOT), which is to be launched in late 2022. More generally, the use of satellite-derived observations dedicated to surface hydrology will contribute to a better fundamental understanding of the CRB and its hydro-climatic processes, bringing more opportunities for other river basins in Africa to improve the management of water resources.

Finally, the better understanding of large-scale CRB surface hydrology variability will help to improve the comprehension at the local and regional scales of the hydrological and biogeochemical cycles, as the CRB is recognized to be one of the three main convective centres in the tropics, and its inland waters strongly contribute to the carbon cycle of the basin. Our findings also highlight the large spatiotemporal variability in the surface hydrologic components within the basin that will help understand the links and feedback with regional climate and the influence of events such as El Niño–Southern Oscillation (ENSO) on water resources. The results from both long-term SWH from radar altimetry and flooded areas from GIEMS-2 have confirmed the benefits of Earth observation in characterizing and understanding the variability in the surface hydrologic components in a sparsely gauged basin such as the CRB. Since these datasets are global, our study and the methodology will benefit similar investigations in other ungauged tropical river basins.

Data availability. The altimetry data over inland water bodies are distributed via the Hydroweb website (time series of water levels in the rivers and lakes around the world, http://hydroweb.theia-land.fr/; Hydroweb, 2022). The SWH dataset over the Congo is freely available from this online platform. For GIEMS-2, the dataset is available upon request to Catherine Prigent (catherine.prigent@obspm.fr).

Author contributions. BK, FP, AP, RTM, and SC conceived the study. BK processed the data and performed the analysis. BK, FP, and AP analysed and interpreted the results and wrote the draft. RTM and CP were responsible for the data curation. All authors discussed the results and contributed to the final version of the paper.

Competing interests. The contact author has declared that neither they nor their co-authors have any competing interests.

Disclaimer. Publisher's note: Copernicus Publications remains neutral with regard to jurisdictional claims in published maps and institutional affiliations.

Acknowledgements. Benjamin Kitambo has been supported by a doctoral grant from the French Space Agency (CNES), Agence Française du Développement (AFD), and Institut de Recherche pour le Développement (IRD). This research has been supported by the CNES TOSCA project "DYnamique hydrologique du BAssin du CoNGO (DYBANGO)" (2020–2023).

Financial support. This research has been supported by the Centre National d'Etudes Spatiales (project TOSCA DYBANGO).

Review statement. This paper was edited by Shraddhanand Shukla and reviewed by Paul Bates and one anonymous referee.

References

Aires, F., Papa, F., and Prigent, C.: Along-term, high-resolution wetland dataset over the Amazon basin, downscaled from a multiwavelength retrieval using SAR data, J. Hydrometeorol., 14, 594–607, https://doi.org/10.1175/JHM-D-12-093.1, 2013.

Aloysius, N. and Saiers, J.: Simulated hydrologic response to projected changes in precipitation and temperature in the Congo River basin, Hydrol. Earth Syst. Sci., 21, 4115–4130, https://doi.org/10.5194/hess-21-4115-2017, 2017.

Alsdorf, D., Beighley, E., Laraque, A., Lee, H., Tshimanga, R., O'Loughlin, F., Mahé, G., Dinga, B., Moukandi, G., and Spencer, R. G. M.: Opportunities for hydrologic research in the Congo Basin, Rev. Geophys., 54, 378–409, https://doi.org/10.1002/2016RG000517, 2016.

Andriambeloson, J. A., Paris, A., Calmant, S., and Rakotondraompiana, S.: Re-initiating depth-discharge monitoring in small-sized ungauged watersheds by combining remote sensing and hydrological modelling: a case study in Madagascar, Hydrolog. Sci. J., 65, 2709-2728, https://doi.org/10.1080/02626667.2020.1833013, 2020.

Becker, M., Santos, J., Calmant, S., Robinet, V., Linguet, L., and Seyler, F.: Water Level Fluctuations in the Congo Basin Derived from ENVISAT Satellite Altimetry, Remote Sens., 6, 9340–9358, https://doi.org/10.3390/rs6109340, 2014.

Becker, M., Papa, F., Frappart, F., Alsdorf, D., Calmant, S., da Silva, J. S., Prigent, C., and Seyler, F.: Satellite-based estimates of surface water dynamics in the Congo River Basin, Int. J. Appl. Earth Obs. Geoinf., 66, 196–209, https://doi.org/10.1016/j.jag.2017.11.015, 2018.

Bele, Y., Mulotwa, E., Bokoto de Semboli, B., Sonwa, D., and Tiani, A.: Afrique centrale: Les effets du changement climatique dans le Bassin du Congo: la nécessité de soutenir les capacités adaptatives locales, CRDI/CIFOR, Canada, 5 pp., https://idl-bnc-idrc.dspacedirect.org/bitstream/handle/10625/45639/132108.pdf (last access; 6 April 2022), 2010.

Betbeder, J., Gond, V., Frappart, F., Baghdadi, N. N., Briant, G., and Bartholomé, E.: Mapping of Central Africa forested wetlands using remote sensing, IEEE J. Select. Top. Appl. Earth Obs. Remote Sens., 7, 531–542, https://doi.org/10.1109/JSTARS.2013.2269733, 2014.

Bogning, S., Frappart, F., Blarel, F., Niño, F., Mahé, G., Bricquet, J. P., Seyler, F., Onguéné, R., Etamé, J., Paiz, M. C., and Braun, J. J.: Monitoring water levels and discharges using radar altimetry in an ungauged river basin: The case of the Ogooué, Remote Sens., 10, 350, https://doi.org/10.3390/rs10020350, 2018.

Bonnefond, P., Verron, J., Aublanc, J., Babu, K., Bergé-Nguyen, M., Cancet, M., Chaudhary, A., Crétaux, J.-F., Frappart, F., Haines, B., Laurain, O., Ollivier, A., Poisson, J.-C., Prandi, P., Sharma, R., Thibaut, P., and Watson, C.: The Benefits of the Ka-Band as Evidenced from the SARAL/AltiKa AltimetricMission: Quality Assessment and Unique Characteristics of AltiKa Data, Remote Sens., 10, 83, https://doi.org/10.3390/rs10010083, 2018.

Bricquet, J.-P.: Les écoulements du Congo à Brazzaville et la spatialisation des apports, in: Grands bassins fluviaux périatlantiques: Congo, Niger, Amazone, Paris, ORSTOM, edited by: Boulègue, J. and Olivry, J.-C., Colloques et Séminaires, Grands Bassins Fluviaux Péri-Atlantiques: Congo, Niger, Amazone, Paris, France, 1993/11/22-24, 27–38, ISBN 2-7099-1245-7, ISSN 0767-2896, 1995

Burnett, M. W., Quetin, G. R., and Konings, A. G.: Data-driven estimates of evapotranspiration and its controls in the Congo Basin, Hydrol. Earth Syst. Sci., 24, 4189–4211, https://doi.org/10.5194/hess-24-4189-2020, 2020.

Bwangoy, J. R. B., Hansen, M. C., Roy, D. P., De Grandi, G., and Justice, C. O.: Wetland mapping in the Congo Basin using optical and radar remotely sensed data and derived topographical indices, Remote Sens. Environ., 114, 73–86, 2010.

Carr, A. B., Trigg, M. A., Tshimanga, R. M., Borman, D. J., and Smith, M. W.: Greater water surface variability revealed by new Congo River field data: Implications for satellite altimetry measurements of large rivers, Geophys. Res. Lett., 46, 8093–8101, https://doi.org/10.1029/2019GL083720, 2019.

Corbari, C., Huber, C., Yesou, H., Huang, Y., and Su, Z.: Multi-Satellite Data of Land Surface Temperature, Lakes Area, and Water Level for Hydrological Model Calibration and Validation in the Yangtze River Basin, Water, 11, 2621, https://doi.org/10.3390/w11122621, 2019.

Cretaux, J., Frappart, F., Papa, F., Calmant, S., Nielsen, K., and Benveniste, J.: Hydrological Applications of Satellite Altimetry Rivers, Lakes, Man-Made Reservoirs, Inundated Areas, in: Satellite Altimetry over Oceans and Land Surfaces, edited by: Stammer, D. C. and Cazenave, A., Taylor & Francis Group, New York, 459–504, ISBN 9781315151779, https://doi.org/10.1201/9781315151779, 2017.

Crowhurst, D., Dadson, S., Peng, J., and Washington, R.: Contrasting controls on Congo Basin evaporation at the two rainfall peaks, Clim. Dynam., 56, 1609–1624, https://doi.org/10.1007/s00382-020-05547-1, 2021.

Dargie, G. C., Lewis, S. L., Lawson, I. T., Mitchard, E. T. A., Page, S. E., Bocko, Y. E., and Ifo, S. A.: Age, extent and carbon storage of the central Congo Basin peatland complex, Nature, 542, 86–90, https://doi.org/10.1038/nature21048, 2017.

Da Silva, J., Calmant, S., Seyler, F., Corrêa, O., Filho, R., Cochonneau, G., and João, W.: Water levels in the Amazon basin derived from the ERS 2 and ENVISAT radar altimetry missions, Remote Sens. Environ., 114, 2160–2181, https://doi.org/10.1016/j.rse.2010.04.020, 2010.

Datok, P., Fabre, C., Sauvage, S., N'kaya, G. D. M., Paris, A., Santos, V. D., Laraque, A. and Sánchez-Pérez, J.-M. : Investigating the Role of the Cuvette Centrale in the Hydrology of the Congo River Basin, in: Congo Basin Hydrology, Climate, and Biogeochemistry, edited by: Tshimanga, R. M., N'kaya, G. D. M., and Alsdorf, D., AGU, https://doi.org/10.1002/9781119657002.ch14, 2022.

Decharme, B., Douville, H., Prigent, C., Papa, F., and Aires, F.: A new river flooding scheme for global climate applications: Off-line evaluation over South America, J. Geophys. Res.-Atmos., 113, 1–11, https://doi.org/10.1029/2007JD009376, 2008.

Decharme, B., Alkama, R., Papa, F., Faroux, S., Douville, H., and Prigent, C.: Global off-line evaluation of the ISBA-TRIP flood model, Clim. Dynam., 38, 1389–1412, https://doi.org/10.1007/s00382-011-1054-9, 2011.

de Paiva, R. C. D., Buarque, D. C., Collischonn, W., Bonnet, M., Frappart, F., Calmant, S., and Mendes, C. A. B.: Large-scale hydrologic and hydrodynamic modeling of the Amazon River basin, Water Resour. Res., 49, 1226–1243, https://doi.org/10.1002/wrcr.20067, 2013.

Fan, L., Wigneron, J.-P., Ciais, P., Chave, J., Brandt, M., Fensholt, R., Saatchi, S. S., Bastos, A., Al-Yaari, A., Hufkens, K., Qin, Y., Xiao, X., Chen, C., Myneni, R. B., Fernandez-Moran, R., Mialon, A., Rodriguez-Fernandez, N. J., Kerr, Y., Tian, F., and Penuelas, J.: Satellite-observed pantropical carbon dynamics, Nat. Plants, 5, 944–951, https://doi.org/10.1038/s41477-019-0478-9, 2019.

Fatras, C., Parrens, M., Peña Luque, S., and Al Bitar, A.: Hydrological Dynamics of the Congo Basin From Water Surfaces Based on L-Band Microwave, Water Resour. Res., 57, e2020WR027259, https://doi.org/10.1029/2020wr027259, 2021.

Frappart, F., Calmant, S., Cauhopé, M., Seyler, F., and Cazenave, A.: Preliminary results of ENVISAT RA-2-derived water levels validation over the Amazon basin, Remote Sens. Environ., 100, 252–264, https://doi.org/10.1016/j.rse.2005.10.027, 2006.

Frappart, F., Papa, F., Malbeteau, Y., León, J. G., Ramillien, G., Prigent, C., Seoane, L., Seyler, F., and Calmant, S.: Surface freshwater storage variations in the Orinoco floodplains using multi-satellite observations, Remote Sens., 7, 89–110, https://doi.org/10.3390/rs70100089, 2015a.

Frappart, F., Papa, F., Marieu, V., Malbeteau, Y., Jordy, F., Calmant, S., Durand, F. and Bala, S.: Preliminary assessment of SARAL/AltiKa observations over the Ganges-

Brahmaputra and Irrawaddy Rivers, Mar. Geod., 38, 568–580, https://doi.org/10.1080/01490419.2014.990591, 2015b.

Frappart, F., Zeiger, P., Betbeder, J., Gond, V., Bellot, R., Baghdadi, N., Blarel, F., Darrozes, J., Bourrel, L., and Seyler, F.: Automatic Detection of Inland Water Bodies along Altimetry Tracks for Estimating Surface Water Storage Variations in the Congo Basin, Remote Sens., 13, 3804, https://doi.org/10.3390/rs13193804, 2021a.

Frappart, F., Blarel, F., Fayad, I., Bergé-Nguyen, M., Crétaux, J. F., Shu, S., Schregenberger, J., and Baghdadi, N.: Evaluation of the Performances of Radar and Lidar Altimetry Missions for Water Level Retrievals in Mountainous Environment: The Case of the Swiss Lakes, Remote Sens., 13, 2196, https://doi.org/10.3390/rs13112196, 2021b.

Garambois, P. A., Calmant, S., Roux, H., Paris, A., Monnier, J., Finaud-Guyot, P., Samine Montazem, A., and da Silva, J. S.: Hydraulic visibility: Using satellite altimetry to parameterize a hydraulic model of an ungauged reach of a braided river, Hydrol. Process., 31, 756–767, https://doi.org/10.1002/hyp.11033, 2017.

Hastenrath, S.: Climate and circulation of the tropics, D. Reidel Publishing Company, Holland, https://doi.org/10.1007/978-94-009-5388-8, 1985.

Hastie, A., Lauerwald, R., Ciais, P., Papa, F., and Regnier, P.: Historical and future contributions of inland waters to the Congo Basin carbon balance, Earth Syst. Dynam., 12, 37–62, https://doi.org/10.5194/esd-12-37-2021, 2021.

Hess, L. L., Melack, J. M., Novo, E., Barbosa, C., and Gastil, M.: Dual-season mapping of wetland inundation and vegetation for the central Amazon basin, Remote Sens. Environ., 87, 404–428, https://doi.org/10.1016/j.rse.2003.04.001, 2003.

Hydroweb: http://hydroweb.theia-land.fr/, last access: 6 April 2022.

Ingram, V., Tieguhong, J. C., Schure, J., Nkamgnia, E., and Tadjuidje, M. H.: Where artisanal mines and forest meet: Socio-economic and environmental impacts in the Congo Basin, Nat. Resour. Forum, 35, 304–320, https://doi.org/10.1111/j.1477-8947.2011.01408.x, 2011.

Inogwabini, B.-I.: The changing water cycle: Freshwater in the Congo, WIREs Water, 7, e1410, https://doi.org/10.1002/wat2.1410, 2020.

Kao, H., Kuo, C., Tseng, K., Shum, C. K., Tseng, T.-P., Jia, Y.-Y., Yang, T.-Y., Ali, T. A., Yi, Y., and Hussain, D.: Assessment of Cryosat-2 and SARAL/AltiKa altimetry for measuring inland water and coastal sea level variations: A case study on Tibetan Plateau Lake and Taiwan Coast, Mar. Geod., 42, 327–343, https://doi.org/10.1080/01490419.2019.1623352, 2019.

Kim, D., Lee, H., Laraque, A., Tshimanga, R. M., Yuan, T., Jung, H. C., Beighley, E., and Chang, C.-H.: Mapping spatio-temporal water level variations over the central Congo River using PALSAR ScanSAR and Envisat altimetry data, Int. J. Remote Sens., 38, 7021–7040, https://doi.org/10.1080/01431161.2017.1371867, 2017.

Kittel, C. M. M., Jiang, L., Tøttrup, C., and Bauer-Gottwein, P.: Sentinel-3 radar altimetry for river monitoring - A catchment-scale evaluation of satellite water surface elevation from Sentinel-3A and Sentinel-3B, Hydrol. Earth Syst. Sci., 25, 333–357, https://doi.org/10.5194/hess-25-333-2021, 2021.

Laraque, Alain, Bricquet, J. P., Pandi, A., and Olivry, J. C.: A review of material transport by the Congo River and its tributaries, Hydrol. Process., 23, 3216–3224, https://doi.org/10.1002/hyp.7395, 2009.

Laraque, A., Bellanger, M., Adele, G., Guebanda, S., Gulemvuga, G., Pandi, A., Paturel, J. E., Robert, A., Tathy, J. P., and Yambele, A.: Evolutions récentes des débits du Congo, de l'Oubangui et de la Sangha, Geo-Eco-Trop., 37, 93–100, 2013.

Laraque, Alain, N'kaya, G. D. M., Orange, D., Tshimanga, R., Tshitenge, J. M., Mahé, G., Nguimalet, C. R., Trigg, M. A., Yepez, S., and Gulemvuga, G.: Recent budget of hydroclimatology and hydrosedimentology of the congo river in central Africa, Water, 12, 2613, https://doi.org/10.3390/w12092613, 2020.

Lee, H., Beighley, R. E., Alsdorf, D., Chul, H., Shum, C. K., Duan, J., Guo, J., Yamazaki, D., and Andreadis, K.: Remote Sensing of Environment Characterization of terrestrial water dynamics in the Congo Basin using GRACE and satellite radar altimetry, Remote Sens. Environ., 115, 3530–3538, https://doi.org/10.1016/j.rse.2011.08.015, 2011.

Leon, J. G., Calmant, S., Seyler, F., Bonnet, M. P., Cauhopé, M., Frappart, F., Filizola, N., and Fraizy, P.: Rating curves and estimation of average water depth at the upper Negro River based on satellite altimeter data and modeled discharges, J. Hydrol., 328, 481–496, https://doi.org/10.1016/j.jhydrol.2005.12.006, 2006.

Mcphaden, M. J.: El Niño and La Niña: Causes and Global Consequences, in: Encyclopedia of Global Environmental Change, edited by: MacCracken, M. C. and Perry, J. S., USA, 353–370, ISBN 0-471-97796-9, https://www.pmel.noaa.gov/gtmba/files/PDF/pubs/ElNinoLaNina.pdf (last access: 6 April 2022), 2002.

Moreira, D. M., Calmant, S., Perosanz, F., Xavier, L., Rotunno Filho, O. C., Seyler, F., and Monteiro, A. C.: Comparisons of observed and modeled elastic responses to hydrological loading in the Amazon basin, Geophys. Res. Lett., 43, 9604–9610, https://doi.org/10.1002/2016GL070265, 2016.

Munzimi, Y. A., Hansen, M. C., and Asante, K. O.: Estimating daily streamflow in the Congo Basin using satellite-derived data and a semi-distributed hydrological model, Hydrolog. Sci. J., 64, 1472–1487, https://doi.org/10.1080/02626667.2019.1647342, 2019.

Ndehedehe, C. E., Anyah, R. O., Alsdorf, D., Agutu, N. O., and Ferreira, V. G.: Modelling the impacts of global multi-scale climatic drivers on hydro-climatic extremes (1901–2014) over the Congo basin, Sci. Total Environ., 651, 1569–1587, https://doi.org/10.1016/j.scitotenv.2018.09.203, 2019.

Nogherotto, R., Coppola, E., Giorgi, F., and Mariotti, L.: Impact of Congo Basin deforestation on the African monsoon, Atmos. Sci. Lett., 14, 45–51, https://doi.org/10.1002/asl2.416, 2013.

Normandin, C., Frappart, F., Diepkilé, A. T., Marieu, V., Mougin, E., Blarel, F., Lubac, B., Braquet, N., and Ba, A.: Evolution of the performances of radar altimetry missions from ERS-2 to Sentinel-3A over the Inner Niger Delta, Remote Sens., 10, 833, https://doi.org/10.3390/rs10060833, 2018.

O'Loughlin, F., Trigg, M. A., Schumann, G. J.-P., and Bates, P. D. : Hydraulic characterization of the middle reach of the Congo River, Water Resour. Res., 49, 5059–5070, https://doi.org/10.1002/wrcr.20398, 2013.

O'Loughlin, F., Neal, J., Schumann, G. J., Beighley, R. E., and Bates, P. D.: A LISFLOOD-FP hydraulic model of the middle reach of the Congo, J. Hydrol., 580, 124203, https://doi.org/10.1016/j.jhydrol.2019.124203, 2019.

OMM: CONGO-HYCOS, Organisation météorologique mondiale, 101 pp., https://library.wmo.int/doc_num.php?explnum_id=4883 (last access: 6 April 2022), 2010.

Papa, F, Gu, A., Frappart, F., Prigent, C., and Rossow, W. B.: Variations of surface water extent and water storage in large river basins: A comparison of different global data sources, Geophys. Res. Lett., 35, 1–5, https://doi.org/10.1029/2008GL033857, 2008.

Papa, F., Prigent, C., Aires, F., Jimenez, C., Rossow, W. B., and Matthews, E.: Interannual variability of surface water extent at the global scale, 1993–2004, J. Geophys. Res.-Atmos., 115, 1–17, https://doi.org/10.1029/2009JD012674, 2010.

Papa, F., Bala, S. K., Pandey, R. K., Durand, F., Gopalakrishna, V. V, Rahman, A., and Rossow, W. B.: Ganga-Brahmaputra river discharge from Jason-2 radar altimetry: An update to the long-term satellite-derived estimates of continental freshwater forcing flux into the Bay of Bengal, J. Geophys. Res., 117, C11021, https://doi.org/10.1029/2012JC008158, 2012.

Papa, F., Frappart, F., Güntner, A., Prigent, C., Aires, F., Getirana, A. C. V., and Maurer, R.: Surface freshwater storage and variability in the Amazon basin from multi-satellite observations, 1993–2007, J. Geophys. Res.-Atmos., 118, 11951–11965, https://doi.org/10.1002/2013JD020500, 2013.

Papa, F., Frappart, F., Malbeteau, Y., Shamsudduha, M., Vuruputur, V., Sekhar, M., Ramillien, G., Prigent, C., Aires, F., Pandey, R. K., Bala, S., and Calmant, S.: Satellite-derived surface and sub-surface water storage in the Ganges-Brahmaputra River Basin, J. Hydrol. Reg. Stud., 4, 15–35, https://doi.org/10.1016/j.ejrh.2015.03.004, 2015.

Paris, Adrien, De Paiva, R. D., Da Silva, J. S., Moreira, D. M., Calmant, S., Garambois, P.-A., Collischonn, W., Bonnet, M., and Seyler, F.: Stage-discharge rating curves based on satellite altimetry and modeled discharge in the Amazon basin, Water Resour. Res., 52, 3787–3814, https://doi.org/10.1002/2014WR016618, 2016.

Paris, A., Calmant, S., Gosset, M., Fleischmann, A. S., Conchy, T. S. X., Garambois, P.-A., Bricquet, J.-P., Papa, F., Tshimanga, R. M., Guzanga, G. G., Siqueira, V. A., Tondo, B.-L., Paiva, R., da Silva, J. S., and Laraque, A.: Monitoring Hydrological Variables from Remote Sensing and Modeling in the Congo River Basin, in: Congo Basin Hydrology, Climate, and Biogeochemistry edited by: Tshimanga, R. M., N'kaya, G. D. M., and Alsdorf, D., AGU, https://doi.org/10.1002/9781119657002.ch18, 2022.

Park, E.: Characterizing channel–floodplain connectivity using satellite altimetry: Mechanism, hydrogeomorphic control, and sediment budget, Remote Sens. Environ., 243, 111783, https://doi.org/10.1016/j.rse.2020.111783, 2020.

Parrens, M., Al Bitar, A., Frappart, F., Papa, F., Wigneron, J.-P., and Kerr, Y.: Mapping dynamic water fraction under the tropical rain forests of the Amazonian basin from L-band brightness temperature, Water, 9, 350, https://doi.org/10.3390/w9050350, 2017.

Pekel, J.-F., A. Cottam, N. Gorelick, and Belward, A. S.: High-resolution mapping of global surface water and its long-term changes, Nature, 540, 418–422, https://doi.org/10.1038/nature20584, 2016.

Plisnier, P. D., Nshombo, M., Mgana, H., and Ntakimazi, G.: Monitoring climate change and anthropogenic pressure at Lake Tanganyika, J. Great Lakes Res., 44, 1194–1208, https://doi.org/10.1016/j.jglr.2018.05.019, 2018.

Prigent, Catherine, Papa, F., Aires, F., Rossow, W. B., and Matthews, E.: Global inundation dynamics inferred from multiple satellite observations, 1993–2000, J. Geophys. Res.-Atmos., 112, 1993–2000, https://doi.org/10.1029/2006JD007847, 2007.

Prigent, C., Jimenez, C., and Bousquet, P.: Satellite-Derived Global Surface Water Extent and Dynamics Over the Last 25 Years (GIEMS-2), J. Geophys. Res.-Atmos., 125, 1–21, https://doi.org/10.1029/2019JD030711, 2020.

Pujol, L., Garambois, P. A., Finaud-Guyot, P., Monnier, J., Larnier, K., Mosé, R., Biancamaria, S., Yesou, H., Moreira, D., Paris, A., and Calmant, S.: Estimation of multiple inflows and effective channel by assimilation of multi-satellite hydraulic signatures: The ungauged anabranching Negro river, J. Hydrol., 591, 125331, https://doi.org/10.1016/j.jhydrol.2020.125331, 2020.

Raney, R. K.: The delay/Doppler radar altimeter, IEEE T. Geosci. Remote, 36, 1578–1588, https://doi.org/10.1109/36.718861, 1998.

Rosenqvist, Å. and Birkett, C. M.: Evaluation of JERS-1 SAR mosaics for hydrological applications in the Congo River basin, Int. J. Remote Sens., 23, 1283–1302, https://doi.org/10.1080/01431160110092902, 2002.

Runge, J.: The Congo River, Central Africa, in: Large Rivers: Geomorphology and Management, edited by: Gupta, A., John Wiley and Sons, 293–309, https://doi.org/10.1002/9780470723722.ch14, 2007.

Seyler, F., Calmant, S., Silva, J., Filizola, N., Roux, E., Cochonneau, G., Vauchel, P., and Bonnet, M.: Monitoring water level in large trans-boundary ungauged basins with altimetry: the example of ENVISAT over the Amazon basin, in: 6th SPIE Asia Pacific Remote Sensing Conference, November 2008, Nouméa, France, https://doi.org/10.1117/12.813258, 2008.

Stammer, D. and Cazenave, A.: Satellite Altimetry over Oceans and Land Surfaces, Taylor and Francis Group, Boca Raton, London, New York, 645 pp., 2017.

Sun, W., Ishidaira, H., and Bastola, S.: Calibration of hydrological models in ungauged basins based on satellite radar altimetry observations of river water level, Hydrol. Process., 26, 3524–3537, https://doi.org/10.1002/hyp.8429, 2012.

Tshimanga, R. M.: Two decades of hydrologic modeling and predictions in the Congo River Basin: Progress and prospect for future investigations, Under press, in: Congo Basin Hydrology, Climate, and Biogeochemistry: A Foundation for the Future, edited by: Alsdorf, D., Tshimanga, R. M., and Moukandi, G. N., Wiley-AGU, ISBN 9781119656975, 2021.

Tshimanga, R. M. and Hughes, D. A.: Climate change and impacts on the hydrology of the Congo Basin: the case of the northern sub-basins of the Oubangui and Sangha Rivers, Phys. Chem. Earth, 50–52, 72–83, https://doi.org/10.1016/j.pce.2012.08.002, 2012.

Tshimanga, R. M. and Hughes, D. A.: Basin-scale performance of a semi-distributed rainfall-runoff model for hydrological predictions and water resources assessment of large rivers: the Congo River, Water Resour. Res., 50, 1174–1188, https://doi.org/10.1002/2013WR014310, 2014.

Tshimanga, R. M., Hughes, D. A., and Kapangaziwiri, E.: Initial calibration of a semi-distributed rainfall runoff model for

the Congo River basin, Phys. Chem. Earth, 36, 761–774, https://doi.org/10.1016/j.pce.2011.07.045, 2011.

Ummenhofer, C. C., England, M. H., Mcintosh, P. C., Meyers, G. A., Pook, M. J., Risbey, J. S., and Gupta, A. S., and Taschetto, A. S.: What causes southeast Australia's worst droughts?, Geophys. Res. Lett., 36, L04706, https://doi.org/10.1029/2008GL036801, 2009.

Verhegghen, A., Mayaux, P., De Wasseige, C., and Defourny, P.: Mapping Congo Basin vegetation types from 300 m and 1 km multi-sensor time series for carbon stocks and forest areas estimation, Biogeosciences, 9, 5061–5079, https://doi.org/10.5194/bg-9-5061-2012, 2012.

Zakharova, E., Nielsen, K., Kamenev, G., and Kouraev, A.: River discharge estimation from radar altimetry: Assessment of satellite performance, river scales and methods, J. Hydrol., 583, 124561, https://doi.org/10.1016/j.jhydrol.2020.124561, 2020.

4.3 Conclusion

The mains findings of this paper on the CRB's surface hydrology can be resumed as follows:

- A better performance (i.e., with Root Mean Square Error [RMSE] ranging from 10 to 75 cm) of several satellite radar altimetry (ERS-2, ENV, SRL, J2/3, and S3A/B) to derive continental water level variations within a large set of hydraulic regimes (low and high flow seasons) over long-term period ~25-year from 1995 up to 2020. The range of magnitude of RMSE is in agreement with results from other basins.
- Analyses of spatial distribution maps of the maximum amplitude and the hydrodynamic in terms of the time of maximum and minimum of SWH across the basin. Northern sub-basins present largest variations, up to more than 5 m, reaching their maximum and minimum respectively in Sep-Oct and March-April while southern sub-basins and *Cuvette Centrale* vary in smaller proportions (1.5 m to 4.5 m) with their maximum and minimum occurring respectively in March-April and September-October/November-December. This spatial distribution of the maximum amplitude is controlled by the topography of the basin. Middle and Southern sub-basins with low amplitude present in general a flat topography while in the Northern sub-basins rivers flow through the hilly terrain justifying the higher variations of amplitude.
- A better performance (i.e., with r varying between 0.54 to 0.92) of GIEMS-2 dataset in reproducing the spatial and temporal seasonal and interannual dynamics of SWE across the basin. At the basin scale, *Cuvette Centrale* flooded at its maximum in October/ November. The lowest correlation in the Lualaba sub-basin is probably due to its non-straightforward hydrology dominated by lakes and their connections with floodplains.
- The temporal shift of correlation between one side, radar altimetry and GIEMS-2, and the other side stage/discharge at Brazzaville/Kinshasa station reveals the lag time that varies from 0 to 3 months across the basin. At the sub-basin scale, northern sub-basins are characterized by 2 to 3 months lag and middle sub-basins show 0 to 1 month lag.
- The two satellite-based dataset reveal the regional relative contribution to the flow at the bimodal regime of Brazzaville/Kinshasa station. Most sub-basins show higher correlation with the peak that occurs between August and February at Brazzaville/Kinshasa while only the southern part (Kasaï) and Middle-Congo are more related to the secondary peak that happens between March and July.

Our results confirm the suitability of both long term SWH from radar altimetry and flooded areas from GIEMS-2 to monitoring the CRB flows, potentially bridging the gap between past in situ databases and current and future monitoring of the CRB as an ensemble. These unique two satellite-based dataset should permit us to generate estimates of surface water storage over the CRB. The next chapter explore the estimates of the surface water storage over river, wetlands, floodplains, lakes as well as their temporal dynamics at interannual time scale by combining SWE from GIEMS-2 and the long-term satellite-derived SWH and SWE and topographic data from global Digital Elevation Models (DEMs).

Chapter 5: A long-term monthly surface water storage dataset for the Congo basin from 1992 to 2015

5.1 Introduction

The amount of water stored and moving through rivers, wetlands, floodplains, and lakes across the CRB still remains widely unknown. The CRB is characterized by a large network of rivers, along with extensive floodplains and wetlands, such as in the Lualaba region in the southeastern part of the basin and the well-known *Cuvette Centrale* region, which stores a large amount of freshwater. Research studies conducted in different basins have highlighted the role that plays the amount of water stored through large floodplains and wetlands (Papa and Frappart, 2021; Wu et al., 2022). They help a better understanding of the exchange between the main river channel and the dissolved and particulate material (Ward et al., 2017), also act as a regulator of the hydrology of the basin due to their storage effects along the channel reaches (Wohl, 2021), and influences the biogeochemical and traces gas exchanges and transport between the atmosphere, land and the ocean (Hastie et al., 2021). Yet, such study of determining the role of SWS dynamics into the hydrological and biogeochemical cycles of CRB has not been conducted, due in part to the lack of the quantification of surface water storage across the basin over a long-term period. However, efforts have recently been devoted to estimate SWS for large rivers, floodplains, wetlands, and lakes in the CRB using satellite-derived observations. Becker et al. (2018) estimated the spatio-temporal variability of SWS by combining surface water extent from GIEMS and radar altimeter-derived surface water height of rivers at 350 virtual stations from the ENV mission over the period 2003-2007. They reported that the mean annual variations of the CRB's SWS was about 81 ± 24 km^3, contributing to 19 ± 5% of the annual variations of GRACE-derived terrestrial water storage. Hastie et al. (2021) determined the relative contribution of inlands water to the Congo basin carbon balance. He highlighted the importance of the aquatic carbon fluxes into the Congo basin global carbon balance. Its results call for long-term monitoring of carbon levels and fluxes in the rivers and further investigations. The quantification of SWS over the basin could help to better understand the carbon fluxes as the fluxes of this gas vary with the amount of water.

Despite these efforts to characterize the CRB's SWS, there is still a lot to unravel about the dynamics of SWS in the basin. Considering these knowledge gaps, this chapter addresses the following research questions: What are the spatio-temporal dynamics of SWS over long-term

period at the CRB basin and sub-basins scales? How is these dynamics modulated by climate variability and what is the SWS behavior during exceptional drought events? In order to quantify the long-term variations in rivers, wetlands and floodplains water volumes, three databases and two approaches have been explored. The databases consist of the multi-satellite-derived surface water extent from GIEMS-2, radar-altimetry-derived SWH, and various DEM. The first approach is based on the complementarity between the spatio-temporal dynamics of SWE from GIEMS-2, and satellite-derived SWH (i.e., multi-satellite approach) and the second one on the combination of SWE from GIEMS-2 with topographic data from DEM (i.e., hypsometric curve approach). The obtained results led to writing a paper that is accepted for publication in ESSD of the European Geosciences Union journal. The peprint is included in this chapter and titled " A long-term monthly surface water storage dataset for the Congo basin from 1992 to 2015". The paper deals with the acquisition of the data and processing, the computation of the water storage and the analysis of the results. In this research study, the satellite-derived SWH used are the ones spanning the record period 1995-2015 generated from the first objective of the thesis. Same for the SWE obtained from the analysis done previously in the first part of the thesis. The new dataset in this chapter are the topographic data that came from 1) the Terra Advanced Spaceborne Thermal Emission and Reflection Radiometer (ASTER), 2) Advanced Land Observing Satellite (ALOS), 3) Multi-Error-Removed Improved-Terrain (MERIT) and 4) Forest And Buildings removed Copernicus DEM (FABDEM). Some processing were carried out according to the nature of DEM that is of two types: a digital surface model (DSM) (i.e., refers to the upper surface of natural and built or artificial features of the environment) and a digital terrain model (DTM) (i.e., represents the elevation of the earth's surface removed with all natural and built features). The treatment consisted in removing the bias related to the tree height to the DSM represented by ASTER and ALOS. We then estimated the water storage variations using two approaches as mentioned above following the methodology elaborated by Frappart et al. (2008, 2012) for the multi-satellite approach and Papa et al. (2013) and Salameh et al. (2017) for the hypsometric curve approach. For the lakes, another approach has been used. It combined time series of lake surface water extent from Pekel dataset (i.e., a dataset that quantify changes in global surface water over the past 32 years at high resolution [30m] from Landsat satellite images, Pekel et al., 2016) and lake water level provided by the HydroSat database. In order to be confident with the generated water volume variations representing the hydrological dynamic of the CRB, it was crucial to provide a strong evaluation of the dataset. Here we used for the evaluation: historical and contemporary observations of in situ river discharge, Multi-Source Weighted-Ensemble Precipitation

(MSWEP) Version 2.8 and existing dataset on the SWS over the CRB over 2003-2007 (Becker et al., 2018). After evaluating the newly developed dataset, we then used it to characterize the major anomaly event related to the exceptional drought documented in 2005-2006. This is a key example of an application to which the dataset can be used for.

5.2 Preprint: " A long-term monthly surface water storage dataset for the Congo basin from 1992 to 2015"

A long-term monthly surface water storage dataset for the Congo basin from 1992 to 2015

Benjamin Kitambo[1,2,3], Fabrice Papa[1,4], Adrien Paris[5,1], Raphael M. Tshimanga[2], Frederic Frappart[6], Stephane Calmant[1], Omid Elmi[7], Ayan Santos Fleischmann[8], Melanie Becker[9], Mohammad J. Tourian[7], Rômulo A. Jucá Oliveira[1], Sly Wongchuig[1]

[1]Laboratoire d'Etudes en Géophysique et Océanographie Spatiales (LEGOS), Université de Toulouse, CNES/CNRS/IRD/UT3, Toulouse, France
[2]Congo Basin Water Resources Research Center (CRREBaC) & the Regional School of Water, University of Kinshasa (UNIKIN), Kinshasa, Democratic Republic of the Congo
[3]Faculty of Sciences, Department of Geology, University of Lubumbashi (UNILU), Route Kasapa, Lubumbashi, Democratic Republic of the Congo
[4]Institute of Geosciences, Campus Universitario Darcy Ribeiro, Universidade de Brasília (UnB), 70910-900 Brasilia (DF), Brazi
[5]Hydro Matters, 1 Chemin de la Pousaraque, 31460 Le Faget, France
[6]INRAE, Bordeaux Sciences Agro, UMR1391 ISPA, 71 Avenue Edouard Bourlaux, 33882 CEDEX Villenave d'Ornon, France
[7]Institute of Geodesy, University of Stuttgart, Germany
[8]Instituto de Desenvolvimento Sustentável Mamirauá, Tefé, AM, Brazil
[9]LIENSs/CNRS, UMR 7266, ULR/CNRS, 2 Rue Olympe de Gouges, La Rochelle, France

Correspondence to: Benjamin Kitambo (benjamin.kitambo@legos.obs-mip.fr)

Abstract. The spatio-temporal variation of surface water storage (SWS) in the Congo River basin (CRB), the second largest watershed in the world, remains widely unknown. In this study, satellite-derived observations are combined to estimate SWS dynamics at the CRB and sub-basin scales over 1992-2015. Two methods are employed. The first one combines surface water extent (SWE) from the Global Inundation Extent from Multi-Satellite (GIEMS-2) dataset and the long-term satellite-derived surface water height from multi-mission radar altimetry. The second one, based on the hypsometric curve approach, combines SWE from GIEMS-2 with topographic data from four global Digital Elevation Models (DEMs), namely The Terra Advanced Spaceborne Thermal Emission and Reflection Radiometer (ASTER), Advanced Land Observing Satellite (ALOS), Multi-Error-Removed Improved-Terrain (MERIT) and Forest And Buildings removed Copernicus DEM (FABDEM). The results provide SWS variations at monthly time step from 1992 to 2015 characterized by a strong seasonal and interannual variability with an annual mean amplitude of ~101 ± 23 km^3. Middle-Congo sub-basin shows higher mean annual amplitude (~71 ± 15 km^3). The comparison of SWS derived from the two methods and four DEMs shows an overall fair agreement. The SWS estimates are assessed against satellite precipitation data and in situ river discharge and, in general, a relatively fair agreement is found between the three hydrological variables at the basin and sub-basin scales (linear correlation coefficient > 0.5). We further characterize the spatial distribution of the major drought that occurred across the basin at the end of 2005 and early 2006. The SWS estimates clearly reveal the widespread spatial distribution of this severe event (~40% deficit as compared to their long-term average), in accordance with the large negative anomaly observed in precipitation over that period. This new SWS long-term dataset over the Congo basin is an unprecedented new source of information for improving our comprehension of hydrological and biogeochemical cycles in the basin. As the datasets used in our study are available globally, our study opens opportunities to further develop satellite-derived SWS estimates at the global scale. The dataset of the CRB's SWS and the related Python code to run the reproducibility of the hypsometric

curve approach dataset of SWS are respectively available for download at https://doi.org/10.5281/zenodo.7299823 and https://doi.org/10.5281/zenodo.8011607 (Kitambo et al., 2022b ; Kitambo et al., 2023).

1 Introduction

Freshwater on Earth's ice-free land accounts for only ~1% of the total amount of water globally (Vörösmarty et al., 2010; Steffen et al., 2015; Cazenave et al., 2016; Albert et al., 2021). However, terrestrial freshwater is essential to all human needs, ecosystem environments, and biospheric processes. Freshwater on land (excluding ice caps) is stored in various forms, including glaciers, snowpack, aquifers, root zone (upper few meters of the soil), and surface waters. The latter includes rivers, lakes, man-made reservoirs, wetlands, floodplains and inundated areas (Boberg, 2005; Zhou et al., 2016). All these continental components are permanently interacting with the atmosphere and oceans, exchanging energy and water fluxes (i.e., precipitation, evaporation, transpiration of the vegetation, heat transfer, and surface and underground runoff) through horizontal and vertical motions, characterizing the global water cycle (Trenberth et al., 2007, 2011; Good et al., 2015; Cazenave et al. 2016). These exchanges and the associated storage variations of continental freshwater, specifically surface waters, are key players in the climate system and water resources variability as well as in the global biogeochemical and hydrological cycles (Chahine, 1992; de Marsily et al., 2005; Oki and Kanae, 2006; Shelton, 2009; Stephens et al., 2020). For instance, despite their small surface coverage (~6% of the continents), wetlands and floodplains have a substantial impact on flood flow alteration, sediment stabilization, water quality, groundwater recharge, and discharge (Bullock and Acreman, 2003). The amount of water stored through large floodplains and wetlands is a key component to understand the exchange between the main river channel and the dissolved and particulate material (sediment and organic matter) (Melack and Forsberg, 2001; Ward et al., 2017). Furthermore, it also acts as a regulator for basin hydrology owning to storage effects along channel reaches (Reis et al., 2017; Wohl, 2021). Additionally, the amount of water stored and flowing through surface water bodies influences the biogeochemical and traces gas exchanges and transport between the atmosphere land and the ocean (Richey et al., 2002; Raymond et al., 2013, Hastie et al., 2021).

Surprisingly, in spite of the importance of surface water storage (SWS), our current knowledge about its spatio-temporal variability is still poorly known, especially at regional and global scales (Mekonnen and Hoekstra, 2016; Cooley et al., 2021). Therefore, there is a fundamental need for the quantification of the storage of surface freshwater on land (Alsdorf et al., 2003, 2007; Rodell et al., 2015; O'Connell, 2017).

Efforts have recently been devoted to measure SWS for large lakes, reservoirs, rivers, floodplains, and wetlands in large river basins using satellite-derived observations. Papa and Frappart (2021) provide an overview of the recent advances in the quantification of SWS in rivers, floodplains, and wetlands from Earth observations, presenting several studies (e.g., Frappart et al., 2008, 2010, 2012, 2015, 2018; Papa et al., 2013, 2015; Becker et al., 2018; Tourian et al., 2018; Normandin et al., 2018; Pham-Duc et al., 2020) that characterize the variations in SWS changes in different large river basins. For instance, Frappart et al. (2012) used continuous multi-satellite observations of surface water extent and water level from 2003 to 2007 to monitor monthly variations of SWS in the Amazon basin and the signature of the exceptional drought of 2005, when the amount of water in rivers and floodplains was found to be ~70% below its long-term average. Papa et al. (2013) developed a hypsometric curve approach to derive SWS variations by combining surface extent from the Global Inundation Extent from Multi-satellite (GIEMS; Prigent et al., 2007) and topographic data from the global digital elevation model from the

Advance Spaceborne Thermal Emission and Reflection Radiometer (ASTER). At the basin scale, they showed that the mean annual amplitude of the Amazon SWS is ~1 200 km^3 and contributes to about half of the annual terrestrial water change as detected by Gravity and Recovery Climate Experiment (GRACE) data (Papa et al., 2021).

Despite being the second largest river system in the world, both in terms of the drainage area and discharge to the ocean, the Congo River basin (CRB)'s SWS still remains widely unknown. CRB yet hosts extensive floodplains and wetlands such as the well-known Cuvette Centrale region, which stores a large amount of freshwater, playing a crucial role in the sediment dynamics of the river, as well as in the global carbon storage (Datok et al., 2020; Biddulph et al., 2021).

Crowley et al. (2006) estimated terrestrial (surface plus ground) water storage within the Congo Basin for the period of April 2002 to May 2006 using GRACE satellite gravity data. The result showed a significant seasonal (30 ± 6 mm of equivalent water thickness) and long-term trends, the latter yielding a total loss of ~280 km^3 of water over the 50-month period of analysis. Lee et al. (2011) determined the amount of water annually filling and draining the Congo main wetlands to 111 km^3. This was done by using a water balance equation combining several remotely sensed observations (i.e., GRACE, satellite radar altimeter, GPCP, JERS-1, SRTM, and MODIS). Richey et al. (2015) provided a groundwater stress assessment quantifying the relationship between groundwater use and availability in the world's 37 largest aquifer systems using GRACE data. The Congo Basin aquifer is characterized as low stress from the Renewable Groundwater Stress ratio. At the basin scale, Becker et al. (2018) further estimated the spatio-temporal variability of SWS by combining surface water extent from GIEMS and radar altimeter-derived surface water height of rivers at 350 virtual stations (VSs) from the Environmental Satellite (ENVISAT) mission over the period 2003-2007. They reported that the mean annual variations of the CRB's SWS was about 81 ± 24 km^3, contributing to $19 \pm 5\%$ of the annual variations of GRACE-derived terrestrial water storage. Recently, Frappart et al. (2021) proposed a densification of the network of VSs by including water elevation variations over the floodplains of the Cuvette Centrale and showed that SWS estimates can be much larger than when only VSs over the rivers are used. In parallel, PALSAR observations in InSAR acquisitions were used over the Cuvette Centrale of the Congo in combination to ENVISAT altimetry to establish relationships between water depth and surface water storage and derived absolute surface water storage change over 2002–2011 (Yuan et al. 2017).

Despite these efforts to characterize CRB's SWS, there is still a lot to unravel about the dynamics of SWS in the basin, leaving major questions open: What are the spatio-temporal dynamics of SWS over long-term period at CRB basin and sub-basins scales? How is these dynamics modulated by climate variability and what is the SWS behavior during exceptional drought events?

Earth observation is a unique means to answer these questions and is very useful for monitoring large drainage basin climate and hydrology where in situ information is lacking (Fassoni et al., 2021, Kitambo et al., 2021). Thus, in this study, we use two approaches to estimate, for the first time, the spatio-temporal variations of CRB's SWS over the period 1992-2015. The first approach (Frappart et al., 2008, 2011, 2012, 2019) is based on the complementarity between the spatio-temporal dynamics of the surface water extent, and satellite-derived surface water height. The second approach relies on the methodology developed by Papa et al. (2013) using the relationships between elevation from digital elevation models and surface water extent variations, called the hypsometric curve approach, that enables the estimation of SWS changes.

Section 2 presents the study area. Section 3 describes the datasets and Section 4 the methodology used in this study. Section 5 is dedicated to results and validation. An assessment is performed comparing the developed SWS with other independent datasets such as historic and contemporary river discharge and precipitation data. Section 6 presents an application case of the dataset in which the spatial distribution of the major drought that occurred across the basin at the end of 2005 and early 2006 is investigated. Section 7 presents the repository from which the SWS dataset can be accessed freely, and finally, Section 8 provides the conclusions and future perspectives.

2 Study area

The CRB (Fig. 1) represent the second largest freshwater system in the world, behind the Amazon basin, both in terms of drainage area (~3.7×10^6 km^2) and mean annual river discharge (40 500 m^3 s^{-1}) (Laraque et al., 2009, 2013). This large basin hosts the Earth's second-largest expanse of tropical forest, covering about 45% of its area and the world's largest tropical peat carbon storage (~28% of the total tropical peat carbon). The vast resources of the basin support the livelihoods of 80% of the riparian population (Verhegghen et al., 2012, Inogwabini, 2020; White et al., 2021; Crezee et al., 2022). The Congo River flows over 4 700 km from its source in the southeastern part of the Democratic Republic of Congo (DRC) to the Atlantic Ocean and its drainage area spans over nine countries, Central Africa Republic, Cameroon, Republic of the Congo, Angola, DRC, Zambia, Tanzania, Rwanda, and Burundi.

The CRB is generally divided into six main subbasins (Fig. 1) based on the physiography of the basin (Laraque et al., 2020): Lower-Congo (southwest), Middle-Congo (center), Sangha (northwest), Ubangui (northeast), Kasai (south-center), and Lualaba (southeast). The mean surface air temperature over the basin is estimated to be 25° C. The average rainfall is 2 000 mm yr^{-1} in the central part of the basin and decreases to 1 100 mm yr^{-1} away from the equator. While the peak annual potential evapotranspiration is ~1 500 mm yr^{-1} near the equator, it decreases northwards and southwards to less than 1 000 mm yr^{-1} (Sridhar et al., 2022).

The central part of the basin is characterized by an internal drainage basin and a large tropical rainforest, the Cuvette Centrale, where the river system is dominated by large wetlands and floodplains, with flat topography (Bricquet, 1993; Laraque et al., 2009, 2020). The hydrology of the CRB is also dominated by the presence of several lakes (Figure 1). The southeast Lualaba sub-basin contains the majority of them. In the highland of the Bangweulu region, there are several lakes characterized by small depths (less than 10 m) of which lake Bangweulu is the largest (~2 000 km^2) and is bordered on its east part by large wetlands (14 000 km^2) formed of large grassy swamps and floodplains. One can also find Lake Mweru (~4 413 km^2 and ~37 m depth) and Lake Mweru Wantipa with a smaller surface area (~1500 km^2). The Upemba depression contains a mosaic of lakes (e.g., Upemba Lake) and wetlands that can reach seasonally ~8 000 to ~11 840 km^2 in extent. The east part of the CRB hosts Tanganyika and Kivu Lakes. Tanganyika Lake, the second deepest (i.e., ~1 470 m) lake worldwide, contains a volume of ~18 800 km^3 and drains into the CRB system through the Lukuga River (Gasse et al., 1989; Runge, 2007; Harrison et al., 2016). In the south center region of the CRB, the Mai-Ndombe and Tumba Lakes are located in the Kasaï and Middle-Congo sub-basins, respectively.

3 Datasets

3.1 Multi-satellite-derived surface water extent

We used the estimates of surface water extent (SWE) derived from the Global Inundation Extent from Multi-Satellite (GIEMS-2) which provides global coverage at monthly time step of different water bodies including wetlands, rivers, lakes at 0.25° (~27 km) spatial resolution at the Equator (on an equal-area grid, i.e., each pixel covers 773 km^2; Prigent et al., 2007, 2020). The dataset was developed by merging observations from different sensors, as described in Prigent et al. (2007) and Papa et al. (2010). The last version used in this study, spans over a long-term period from 1992 to 2015. For more details about the technique, we refer to Prigent et al. (2007, 2020).

Several studies such as Prigent et al. (2007, 2020), Papa et al. (2008, 2010, 2013) and Decharme et al. (2011) have been assessing the interannual and seasonal dynamics of the long-term SWE in different environments against several variables, such as the in situ river discharges, in situ and satellite-derived water level in rivers, lakes, wetlands, the total water storage from GRACE, and the satellite-derived rainfall. Recently, the characterization and evaluation of the 24-year SWE from GIEMS-2 have been conducted in the CRB against the in situ river discharge and water level and the performance gave satisfactory results (see Fig. 6 to Fig. 10 of Kitambo et al., 2022a for details on the characterization and the assessment of GIEMS-2 over the CRB).

3.2 Radar-altimetry-derived surface water height

Satellite radar altimetry provides a systematic monitoring of surface water height (SWH) of large rivers, lakes, wetlands, and floodplains at the virtual station (VS), defined as the intersection of a water body with the satellite theoretical ground track. The temporal variation of SWH is retrieved according to the repeat cycle of the satellite (Da Silva et al., 2010; Cretaux et al., 2017), cycle that varies from ten to twenty-seven days for current operational satellites. Several studies, including Frappart et al. (2006), Da Silva et al. (2010), Papa et al. (2010, 2015), Kao et al. (2019), Kittel et al. (2021), Paris et al. (2022), and Kitambo et al. (2022), to name a few, have been conducted in different river basins to validate SWH variations against in situ water levels. Results generally show a good capability of radar altimeter to retrieve SWH variability with uncertainties ranging from a few centimeters to tens of centimeters, depending on the acquisition mode of the satellite and the environment characteristics (Bogning et al., 2018; Normandin et al., 2018; Jiang et al., 2020; Kittel et al., 2021; Kitambo et al., 2022a).

Over CRB, Kitambo et al. (2022) used ~2300 VSs from different satellite missions and their pooling based on the principle of the nearest neighbor (located at a minimum distance of 2 km, see Da Silva et al., 2010; Cretaux et al., 2017) to generate long-term time series with records lengths ranging from 12 to 25 years records (Fig. 2d of Kitambo et al., 2022a). A thorough assessment and validation of these long-term satellite-derived surface water height at nine in situ gauge stations provided root mean squared error ranging from 10 (with Sentinel-3A) to 75 cm (with European Remote Sensing satellite-2) (see Table 2 of Kitambo et al., 2022a).

In the current study, the satellite-derived SWH used are the ones spanning the record period 1995-2015, acquired from three satellites missions, (1) European Remote Sensing-2 satellite (ERS-2), with observations spanning April 1995 to June 2003, (2) the Environmental Satellite (ENVISAT, hereafter named ENV), with observations spanning March 2002 to June 2012, and (3) the Satellite with ARgos and ALtiKa (SARAL/Altika, hereafter named SRL), from which we use observations from February 2013 to July 2016. All the three satellite missions have 35 days repeat cycle. These datasets were made available by the Centre de Topographie des Océans et de l'Hydrosphère (CTOH, http://ctoh.legos.obs-mip.fr). They come from the Geophysical Data Records made available by space agencies. For ERS-2, land reprocessing was used (Frappart et al., 2016). These datasets were

processed using either the Multi-mission Altimetry Processing Software (MAPS, Frappart et al., 2015b) or the Altimetry Time-Series software (Frappart et al., 2021b) to generate the time series of water level. Therefore, the generated 160 VSs cover the entire CRB (see Fig. S1, in supplementary materials) and a period of ~21 years. The southern-eastern portion of the basin, including Upemba and Bangweulu Lake regions, was not covered by the SWH VSs due to the simultaneous lack of data from the three aforementioned satellite mission. Over this region, missing data were replaced by the annual cycle computed using the altimetry-based water levels available during the study period.

3.3 Digital elevation model

We used four freely available global Digital Elevation Models (DEMs) (Table 2): (1) Advanced Spaceborne Thermal Emission and Reflection Radiometer (ASTER) version 3, (2) Advanced Land Observing Satellite (ALOS), (3) Multi-Error-Removed Improved-Terrain (MERIT), and (4) Forest And Buildings removed Copernicus DEM (FABDEM).

DEMs are divided broadly in two categories based on the specific topographic surfaces they represent, which are digital surface model (DSM) and digital terrain model (DTM). DSM refers to the upper surface of natural and built or artificial features of the environment such as buildings, man-made features, and trees, while DTM represents the elevation of the earth surface removed with all natural and built features, i.e., the bare-earth surface (Guth et al., 2021; Hawker et al., 2022). Among the DEMs used, ASTER and ALOS are classified as DSM. MERIT is closer to a DTM because of the removal of tree height bias but it is not a complete DTM (Yamazaki et al., 2017; Hawker et al., 2022) due to other artifacts such as man-made features. In this study, only FABDEM can be considered as DTM (Hawker et al., 2022).

Therefore, in order to remove the presence of tree bias in DSMs, we subtract from them the forest canopy height from a global dataset (Potapov et al., 2020). For that, the global canopy height dataset, ASTER and ALOS were all resampled to 90 m spatial resolution using the nearest neighbour resampling method.

3.4 Global Forest Canopy Height

The global forest canopy height (available at https://glad.umd.edu/dataset/gedi/, last access 17 May 2023) is a global dataset developed by combining the Global Ecosystem Dynamics Investigation (GEDI) lidar forest structure measurement and Landsat analysis-ready data time series (Potapov et al., 2020). GEDI is a new spaceborne lidar instrument onboard the International Space Station collecting data on the vegetation structure since April 2019 (Dubayah et al., 2020a). The spatial resolution of the dataset is 30 m providing the global forest canopy height map for the year 2019 in WGS84 reference system. The dataset covers zones between 54°N and 52°S globally and then we use it over the CRB. For more details on the dataset, we refer to Potapov et al. (2020).

3.5 Lake water storage anomaly

Over the largest lakes of the CRB, time series of monthly water storage anomaly for Lakes Bangweulu, Kivu, Mweru, Tanganyika, Upemba (see Fig. 1 for their locations; Fig. S2 for their time series) are estimated using surface water extent and water level time series obtained from HydroSat database (accessible at http://hydrosat.gis.uni-stuttgart.de/ [Tourian et al. 2022]). After collecting the simultaneous lake water area and

height measurements, the empirical relationship between lake surface water level and area is developed. This model represents the bathymetry of the lake for the part which is captured by remote sensing observations. By assuming that the lake has a regular morphology and a pyramid shape between two consecutive measurement epochs, the lake water level-area-storage model is developed. Finally, time series of lake water storage anomaly are calculated using the developed model and lake water level or surface extent measurements.

3.6. Auxiliary data

3.6.1 In situ river discharge

We used the monthly time series of historical and contemporary observations of in situ river discharge located at the outlet of five sub-basins (see Fig. 1 for their locations and Table 2 for their characteristics) obtained from the Congo Basin Water Resources Research Center (CRREBaC, https://www.crrebac.org/), and from the Environmental Observation and Research project (SO-HyBam; https://hybam.obs-mip.fr/fr/, last access: 17 May 2023).

3.6.2 Rainfall

We used precipitation estimates from the Multi-Source Weighted-Ensemble Precipitation (MSWEP) Version 2.8 (V2.8). MSWEP is a global precipitation product with a spatial resolution of 0.1 ° at 3-hourly temporal resolution (also available at daily scale), covering the period from 1979 to present in near real-time. MSWEP precipitation estimates are derived by optimally merging multiple precipitation data sources, such as gauge, satellite, and reanalysis estimates (Beck et al., 2019a). The latest MSWEP version (V2.8) includes several changes compared to its previous version (V2.2). Among the major updates, in addition to near real-time (NRT) estimates, it also features new data sources that were defined based on their superior performances.

The historical MSWEP V2.8 considers i) one model-based precipitation product: European Centre for Medium-Range Weather Forecasts (ECMWF) ReAnalysis 5 (ERA5); ii) two satellite-based precipitation products: the Integrated Multi-satellitE Retrievals for GPM (IMERG) algorithm and the Gridded Satellite (GridSat) data; and iii) gauge observations from various sources: the Global Historical Climatology Network-Daily (GHCN-D), the Global Summary of the Day (GSOD) databases, and several national databases. On the other hand, MSWEP V2.8 NRT merges i) two model-based precipitation products: ERA5 and National Centers for Environmental Prediction (NCEP) Global Data Assimilation System (GDAS) Analysis; and ii) two satellite-based precipitation products: Global Satellite Mapping of Precipitation (GSMaP) and IMERG. MSWEP was globally and regionally assessed and it exhibits realistic spatial precipitation patterns in frequency, magnitude, and mean (Beck et al., 2017; Beck et al., 2019b). MSWEP V2.8 is available via http://www.gloh2o.org.

3.6.3 Total Water Storage Anomaly from the Gravity Recovery and Climate Experiment mission

The Gravity Recovery and Climate Experiment (GRACE) is a joint NASA and German Aerospace Center (DLR) mission launched in March 2002 (Tapley et al., 2004) and, together with its successor GRACE Follow-On (GRACE-FO) launched in 2018 (Tapley et al., 2019), provides estimates of changes in water storage at the basin scale. For the analysis in this study, we used data from GRACE/GRACE-FO Mascon data available

at http://grace.jpl.nasa.gov (Wiese et al., 2016,2018). The mascon data provides surface mass changes with a spatial sampling of 0.5 degrees in both latitude and longitude (Watkins et al., 2015). From this dataset, we obtained time series of Terrestrial Water Storage Anomaly (TWSA) over the CRB through area weighted aggregation of those grid cells in basins.

4 Methods

In order to estimate SWS variations over the CRB, two approaches are used (Figure 2): a) the multi-satellite approach following the methodology of Frappart et al. (2008, 2011) and b) the hypsometric curve approach following the methodology of Papa et al., (2013) and Salameh et al., (2017).

4.1 Multi-Satellite Approach

The multi-satellite approach (Fig. 2a) consists of the combination of the SWE and satellite-derived SWH over inland water bodies (rivers, lakes, reservoirs, wetlands, and floodplains), generally derived from radar altimetry over a common period of availability for both datasets (Frappart et al., 2008, 2011; Becker et al., 2018; Papa and Frappart, 2021). Therefore, this complementarity of multi-satellite observations offers the possibility to quantify SWS changes and water volume variations in a watershed. SWE and SWH used in this study are respectively from GIEMS-2 and the family of spaceborne radar altimeters with 35 days repeat cycle (hereafter ERS-2, ENV, and SRL). Their common period of availability is 1995-2015.

We summarize in the next sections the two-step methodology and, for more details, we refer to Frappart et al. (2008, 2011, 2012, 2019).

4.1.1 Monthly maps of surface water level anomalies

Monthly maps of water level anomalies of 0.25° spatial resolution referenced to the EGM2008 geoid are derived by combining GIEMS-2 and the combined long-term time series of ERS-2_ENV_SRL (1995-2015) satellite-derived water levels. For each given month of the water levels, these are linearly interpolated over the GIEMS-2 grid and the elevation of each pixel is provided with reference to a map of minimum surface water levels estimated over 1995–2015 using the principle of the hypsometric curve approach between SWH from radar altimetry and SWE from GIEMS-2 to take into account the difference of altitude in each cell area of GIEMS-2. (See Frappart et al., 2012 for more details).

4.1.2 Monthly time series of surface water storage variations

Following Frappart et al. (2012, 2019), the time variations of SWS are computed at the basin scale as

$$V_{SW}(t) = R_e^2 \sum_{j \epsilon S} P(\lambda_j,\varphi_j,t)(h(\lambda_j,\varphi_j,t) - h_{min}(\lambda_j,\varphi_j))\cos(\varphi_j)\Delta\lambda\Delta\varphi \quad (1)$$

where V_{SW} is the volume of surface water, R_e is the radius of the Earth (6 378 km), $P(\lambda_j,\varphi_j,t)$, $h(\lambda_j,\varphi_j,t)$, and $h_{min}(\lambda_j,\varphi_j)$ are respectively, the percentage of inundation, the water level at time t, and the minimum of water level at the pixel (λ_j,φ_j), and $\Delta\lambda$ and $\Delta\varphi$ are respectively, the grid steps in longitude and latitude.

The maximum error on the volume variation is estimated as follows:

$$\Delta V_{SW,max} \leq \Delta S_{max}\delta h_{max} + S_{max}\Delta(\delta h_{max}) \quad (2)$$

where $\Delta V_{SW,max}$ is the maximum error on the water monthly volume anomaly, S_{max} is the maximum monthly flooded surface, δh_{max} is the maximum water level variation between two consecutive months, ΔS_{max} is the maximum error for the flooded surface, and $\Delta(\delta h_{max})$ is the maximum error for the water level between two consecutive months.

Note that the volume of SWS variations in a given basin is the sum of the contributions of the water storage contained in floodplains, wetlands, rivers, and small lakes. For larger lakes, as mentioned previously, estimates of SWS are complementarily obtained by the HydroSat database (Tourian et al. 2022). Therefore, the water storage analysis takes into account variations in floodplains, wetlands, rivers, and lakes.

4.2 Hypsometric Curve Approach Using Digital Elevation Models

In complement to the multi-satellite approach, we also used the hypsometric curve approach that consists of the combination of SWE and DEM-based topographic data. Following Papa et al. (2013), we summarize here the four-step process (Fig. 2b) to estimate SWS, using as example the combination of GIEMS-2 SWE and FABDEM topography resampled at 90 m:

4.2.1 Establishment of the hypsometric curve (area – elevation relationship)

For each GIEMS-2 pixel (Fig. 3; left column), we first derived the cumulative distribution function of elevation values within the corresponding FABDEM subset (Fig. 3; center column). For each GIEMS-2 pixel, over the CRB, this corresponds to ~95 000 elevation points falling within the satellite-derived SWE pixel, from which the hypsometric curve or curve of cumulative frequencies is established. It is equivalent to the distribution of elevation values in each 773 km^2 pixel (with 773 km^2 of flood coverage at the abscissa convert into percentage 100%) sorted in ascending order to represent an area – elevation relationship (Fig. 3; right column).

4.2.2 Correction of the hypsometric curve

To avoid the overestimation of SWS at the pixel level from the unrealistic amplitude, this step corrects the behavior of the FABDEM hypsometric curve (Fig. 4). For each GIEMS-2 pixel, the established area-elevation relationship enables us to derive the elevation amplitude (i.e., Similar to the amplitude of SWH) from the corresponding difference between the average annual minimum and the average annual maximum of SWE over the period 1992-2015. The mean maximum amplitude of SWH over the CRB varies between 1.5 to ~7.5 m (see Fig. 5 of Kitambo et al., 2022a). In most cases (~90% of GIEMS-2 pixels), the elevation amplitude derived from the difference between the average minimum and maximum provides values that satisfactorily match the range of the SWH amplitude. Often, these realistic values correspond on the FABDEM hypsometric curve to the percentage of flood coverage representing the main channel or floodplains (lower part of hypsometric curve) with a smooth increase of slope (as in Fig. 4a and g). However, Fig. 4 also points out that some elevation amplitudes (from ~10% of GIEMS-2 pixels) are above the range of 1.5 to ~7.5 m. These pixels therefore present unrealistic amplitude as compared to the range of previous findings over the CRB that can lead to the overestimation of SWS at the pixel level (Fig. 4c and d). Usually, these higher values are localized above 20% of flood coverage.

For this, following Papa et al. (2013), we propose a simple procedure to correct the behavior of FABDEM hypsometric curve exceeding the range of 1.5 to ~7.5 m of elevation amplitude. For each percent increment of flood coverage area, if the corresponding value of elevation belongs to a 5% window of 773 km^2 pixel (i.e., ~35 km^2) where the standard deviation (STD) of elevation is below 0.7 m threshold, the elevation value is kept. Conversely, if the elevation value corresponding to the percent increment of flood coverage belongs to a window in which the STD is above 0.7 m, the elevation value is replaced by the fitted value based on a simple linear regression analysis using the two previous elevation values of the hypsometric curve. For instance, a given elevation value corresponding to 8% of flood coverage belonging to a window with STD (i.e., calculated using values at 8, 9, 10, 11, and 12%) greater than 0.7 m, will be replaced by the fitted value calculated using the simple linear regression equation obtained from the values at 6 and 7%. The next STD will be computed with values of elevation at 9, 10, 11,12, and 13%, and so on.

Several attempts of correction with different STD values ranging from 0.3 to 1.1 m were performed (as shown in Fig. S3 as supplementary material) and the STD 0.7 m was chosen due to the realistic comparisons with the variations of surface water heights from altimetric VS. This value is also in agreement with the one chosen for the Amazon River basin (Papa et al., 2013).

Note that there is a non-significant percentage of pixels (~1%) for which, the hypsometric curve correction results in a slight increase of elevation amplitudes instead of a decrease (Fig. S4, in supplementary materials). However, these pixels generally provide acceptable estimates of SWS, without unrealistic overestimations.

Note also that, beside this correction, the hypsometric curve obtained from ASTER and ALOS showed roughness in their curve (Fig. S5, in supplementary materials), which was smoothed out using Savitzky-Golay filter embedded in SciPy API package in python before applying the correction described above.

4.2.3 Establishment of the area – surface water storage relationship

The hypsometric curve representing the area-elevation relationship is then converted into an area-SWS relationship by estimating the surface water storage associated with an increase of the pixel fractional open water coverage (with an increment of 1%) by filling the hypsometric curve from its base level to an upward level. Here we used three formulas for comparison purposes:

$$V(\alpha) = \sum_{i=1}^{\alpha} (H_i - H_{i-1}) * S_i \quad (3)$$

$$V(\alpha) = \sum_{i=1}^{\alpha} (H_i - H_{i-1}) * \frac{S_i + S_{i-1}}{2} \quad (4)$$

$$V(\alpha) = \sum_{i=1}^{\alpha} \frac{(H_i - H_{i-1})}{3} * (S_i + S_{i-1} + \sqrt{S_i * S_{i-1}}) \quad (5)$$

where V is the surface water storage in km^3 for a percentage of flood inundation α. Note that the incrementation is on a step of 1%. S is the 773 km^2 area of GIEMS-2 pixel, and H represents the elevation (in km) for a percentage of flood inundation α given by the hypsometric curve.

Three formulas, (3), (4), and (5) used to retrieve the estimation of SWS from the hypsometric curve approach are compared in Figure 5. It shows that there is a slight difference in the SWS changes of about one hundredth after the decimal point between the three formulas (3), (4), and (5) except for Fig. 5d and g where the difference is of one-tenth after the decimal point. Overall, the difference seems negligible, and we decided to use only the formula

(5) representing a volume of a trunk or regular truncated pyramid for SWS computation based on the hypsometric curve approach.

4.2.4 Monthly time series of surface water storage variations

Finally, the hypsometric curve of the area-SWS relationship is combined with the monthly variations of SWE from GIEMS-2. This enables thus the estimation of SWS for each month by intersecting the hypsometric curve value with the GIEMS-2 estimates of pixel coverage for that month (Fig. 5). Note that with such method, the lowest level of storage refers to the level zero, determined by the minimum of SWE from GIEMS-2 observations for each pixel, from which the variation of the storage is started to be accounted for. Thus, the estimated SWS represents the increment above the minimum storage.

It is worth noting that, in the attempt of determining the extreme low storage values of exceptional drought years, it can be a potential source of uncertainties in a sense that DEM's values should have produced credible elevation data for those periods at the lower part of the hypsometric curve. Such information is unfortunately difficult to assess.

5 Results and validation

5.1 Distribution and variability of surface water storage across the Congo River basin

Figure 6 presents the characteristics of the SWS temporal dynamics at CRB scale (anomaly time series versus its long-term mean, deseasonalized anomaly, and annual cycle for SWS aggregated for the entire CRB). It shows all SWS estimates computed with both the multi-satellite (for 1995-2015) and the hypsometric curve (for 1992-2015) approaches from the use of the four DEMs (ALOS, ASTER, MERIT, and FABDEM).

Figure 6a shows, for the very first time, the long-term month-to-month variations of the CRB's SWS over a period of 24 years. It shows a strong seasonal cycle of SWS over the CRB showing a comparable behavior in the peak-to-peak SWS variations from both approaches. The SWS amplitude ranges from ~50 to ~150 km^3 over the years, showing a large year-to-year variability. The bi-modal patterns that characterizes the hydrological regime of the CRB's (Kitambo et al., 2022a), linked to the variability of the intertropical convergence zone (Kitambo et al., 2022a), is well depicted in the SWS estimates.

All SWS estimates from the different DEMs show fair agreement in their variations in between them (Fig. 6a). However, we observed that SWS from ASTER (violet color) tends to overestimate the SWS at the first peak (i.e., spanning over August-February) along the time series.

Figure 6b displays the deseasonalized anomaly (obtained by subtracting the mean monthly values over the considered period, 1992-2015, or 1995-2015 from individual months) of CRB's SWS. A similar observation about the matching of SWS anomaly from different approaches and DEMs products is observed.

These SWS estimates also show a substantial interannual variability at basin scale, especially in terms of annual maximum and minimum, pointing out extreme events in terms of droughts and floods that recently affected the CRB. Figure 6b reveals interesting and strong anomaly signals such as the large positive peaks observed in 1997-1998 and 2006-2007. These can be related to the positive Indian Ocean Dipole (pIOD) events, in combination with the El Niño events that occurred in 1997–1998 and 2006–2007 that triggered floods in western Indian Ocean

and eastern Africa (Mcphaden, 2002; Ummenhofer et al., 2009; Becker et al., 2018, Kitambo et al., 2022a). Another major event is the severe drought that occurred in 2005-2006 that is clearly depicted on the CRB's SWS time series anomaly as the minima of the record (Fig. 6b). This is in agreement with Ndehedehe et al. (2019, 2022) and Tshimanga et al. (2022) who reported that, in the 1990s and 2000s's, multi-year droughts in the CRB affected a significant part of the Congo basin. This interannual variability is also superimposed to variations at larger time scale, from few years to decadal, such as a large increase in SWS anomaly in 1996-1997, followed by a slight decrease until the minimum that occurred in 2005-2006, before SWS starts to slowly increase again after the 2007 peak, until 2015.

Figure 6c shows the CRB's SWS annual cycle (computed over 1992-2015 and 1995-2015 period for the hypsometric and multi-satellite approaches, respectively) revealing a strong seasonal variation. Both approaches present a mean annual amplitude of the same order in magnitude (Table 3) with estimates ranging around 80 ± 17, 101 ± 23, 80 ± 20 km^3 (respectively from ALOS, FABDEM and MERIT based on the hypsometric curve approach), and 70 ± 17 km^3 from the multi-satellite approach. These estimates are of the same order of magnitude with previous findings over the CRB, i.e., 81 ± 24 km^3 as in Becker et al. (2018). As a matter of comparison, the mean annual amplitude of SWS from ASTER represents ~11% of the Amazon basin's SWS mean annual amplitude of ~1200 km^3, as reported in Papa et al. (2013, 2021).

As observed in Fig. 6a, ASTER's SWS provides larger estimates, with a mean annual amplitude of ~124 ± 25 km^3 (Table 3). This can be explained by the fact that, among the four DEMs (ALOS, ASTER, FABDEM and MERIT), ASTER has a greater vertical error (i.e., 17 m, see Table 1 of Hawker et al., 2019) compared to the others and, consequently, this can impact the elevation amplitude (derived at step 2 of section 4.2 used to calculate the SWS variations (step 3 of section 4.2).

Table 3 presents also the statistics errors comparing the FABDEM's SWS dataset to other estimates and reinforce the difference highlighted in SWS magnitude between different approaches and DEMs. Note that trees and urban areas biases are only removed from FABDEM, and thus it seems to be the most adequate DEM in representing hydrology processes (Hawker et al., 2022). ALOS and MERIT have provided small errors as reflected in the mean absolute error (MAE) (9 and 5 km^3) and the root mean squared error (RMSE) values (11 and 7 km^3) compared to values greater than 15 km^3 of MAE and above 20 km^3 of RMSE from multi-satellite approach and ASTER DEM.

At the basin scale, Fig. 6c clearly depicts a double peak, with a SWS maximum reached in November for the first peak and in April for the second peak. In comparison with the annual cycle of GIEMS-2 SWE (Fig. 7c of Kitambo et al., 2022a), the first peak of SWS maximum is in phase with the maximum SWE, while for the second peak there is a one-month delay, with maximum SWE occurring in March. This can be explained by the non-linear relationship between SWE and SWS through the hypsometric curve approach.

It is important to note that SWS from FABDEM and MERIT shows a very good fit at all seasons whereas ALOS slightly underestimates the storage at the second peak. Contrary to others, ASTER shows a peculiar behavior with its SWS largely underestimating and overestimating the storage at the second and first peak of the hydrological regime, respectively.

In agreement with the results from the SWS hypsometric curve approach, SWS from the multi-satellite approach also points out the maximum SWS in November and April for the first and second peaks. However, the dynamics of SWS from the multi-satellite approach differs from the others over the period from February to May. Over that period of time, the hydrological regime of the basin is more controlled by the southeast region, especially by the

Bangweulu and Upemba Lake area (Kitambo et al., 2022a). In this region, the spatial distribution of VSs is not sufficient enough (Fig. S1, in supplementary materials) to obtain a very accurate representation of the temporal variations of the SWS even if the mean annual cycle variations of some VSs from ENV and SRL were used to account for the water level over the entire 1995-2015 period. This might explain in part the different dynamics observed in the SWS variations over February-May in the southeastern region.

In parallel to Fig. 6, Fig. 7 presents the spatial distribution of SWS dynamics (mean annual, Standard Deviation (STD), mean annual maximum, and average month of the maximum) for the entire CRB. In the following parts of the paper, the estimates obtained with the FABDEM DEM will become our reference and we will use them to display the results. This is justified by FABDEM DEM topographic characteristics and properties which makes it the closest to a DTM. The estimates obtained with the other DEM will be displayed in Supplementary Material (Fig. S6).

In agreement with the spatial distribution of SWE across CRB (Fig. 6 of Kitambo et al., 2022a), SWS (Fig. 7a and b) shows realistic spatial patterns along the Congo River and the Cuvette Centrale and depict quite well the other main structures of the basin, for instance, the main tributaries (e.g., Sangha, Ubangui, Luvua, Luapula, Lualaba Rivers) along with their large wetlands and floodplains. These are characterized by a strong variability in SWS (Fig. 7c and d).

Higher values of SWS ranging from 0.3 to 0.6 km^3 in a 773 km^2 dominate the extensive wetlands and floodplains such as the Cuvette Centrale and in the southeastern part of the basin (Upemba and Bangweulu region). These regions display a large variability as well (in terms of the STD, Fig. 7c and d) and are characterized by maximum values of surface water storage generally greater than 0.6 km^3 per pixel of 773 km^2 (Fig. 7e and f).

The heart of the Cuvette Centrale as well as the lake Mai-Ndombe (in the Kasai sub-basin) and a large part of the main channel of the Congo (up to Lomami River) present the maximum values of the SWS change in the basin. Same observation is done for the lakes in the Upemba depression (e.g., Upemba Lake), Mweru and Bangweulu. These maximum values are reached in September-October in the upper part of the Cuvette Centrale and November-December in their lower part (Fig. 7g and h). In the Lualaba sub-basin, the average month of the maximum of SWS is January-February, while in other parts, such as lake Mweru and the east part of Bangweulu, with its large grassy swamps and floodplains, it recorded in March-April. Conversely to the general trend in the Cuvette Centrale, the region of lake Tumba and Mai-Ndombe reached their maximum of SWS in July-August.

In general, the results from the hypsometric curve (Fig. 7, left column) and multi-satellite (Fig. 7, right column) approaches are quite similar in terms of spatial distribution, for both magnitude and variability of the changes. Nevertheless, as expected, the multi-satellite dataset approach shows a limitation in terms of spatial distribution caused by the reduced availability of the combined long-term VSs in some regions. For instance, there is a lack of observations on the east part of the Tanganyika Lake and in the Bangweulu region, where the spatial distribution of SWS from the multi-satellite approach is smaller than that of the FABDEM hypsometric curve approach. This is mainly explained by the sparse availability of long-term satellite-derived (ERS2-ENV-SRL) time series in that region, leading to less distributed SWS estimates in these regions.

On the other hand, SWS variations from hypsometric curve approach also present limitations, mainly on small lakes and around large lakes where there are almost no variations in elevation from the DEMs leading to flat

hypsometric curves, and therefore to the computed storage to be of zero changes. This is for instance the case around Lake Kivu in the Lualaba sub-basin. In this case, the SWS change of the lake is then added to the dataset using the Lake Water Storage Anomaly computed independently (see Data description in section 3.5).

Finally, for comparison purposes, Fig. S6 (in supplementary materials) shows the same analysis in terms of spatial distribution and variability of SWS across the basin for the other estimates based on the hypsometric curve approach (i.e., ALOS, see Fig. S6 left column; ASTER, see Fig. S6 middle column; and MERIT, see Fig. S6 right column). In general terms, results are consistent between one another. The pattern of SWS in terms of the distribution and order of magnitude of the mean annual (Fig. S6a, b, and c), variability in terms of STD (Fig. S6d, e, and f), mean annual maximum (Fig. S6g, h, and i) and average month of the maximum (Fig. S6j, k, and l) between the three DEMs and FABDEM are generally similar although results from ASTER DEM (Fig. S6b, e, and h) underestimate the storage (i.e., values ranging between 0.15-0.45 km^3) compared to other DEMs (i.e., values greater than 0.6 km^3) in the Bangweulu-Upemba region (e.g., Lake Bangweulu, Lake Upemba).

At the sub-basin scale, the mean annual amplitude for the five sub-basins is provided as follows. Middle-Congo is the sub-basin with the large amplitude (71 ± 15 km^3), associated with the strong variations of SWS anomaly observed in the Cuvette Centrale. It is followed by Lualaba sub-basin with 59 ± 15 km^3 due to the presence of major lakes (Kivu, Tanganyika, Mweru, Bangweulu) and large wetlands that show large variability and are characterized by maximum values of surface water storage generally greater than 0.6 km^3 per pixel of 773 km^2. Sangha and Kasaï show quite similar annual amplitude (i.e., respectively of 24 ± 5 and 24 ± 6 km^3). Both sub-basins are overlapped at their mouth (i.e., downstream part) by the Cuvette Centrale. Among the five sub-basins, Ubangui is the one with the smallest mean annual amplitude (13 ± 4 km^3) although it is among the two northern sub-basins (i.e., Ubangui and Sangha) with higher satellite-derived SWH mean maximum amplitude (see Fig. 5a of Kitambo et al., 2022a). As observed for Sangha and Kasaï subbasins, Ubangui subbasin is also occupied by its downstream part by the Cuvette Centrale (Fig. 1).

5.2 Evaluation against independent datasets

In order to evaluate the monthly estimates of the large-scale SWS over the CRB, we compare, at the basin and sub-basin levels, their seasonal and interannual variability against other independent hydrological variables such as precipitation data from MSWEP V2.8 and in situ discharges. For clarity purpose, only the SWS result from the hypsometric curve approach with FABDEM and from the multi-satellite approach are displayed and discussed here.

At the basin level, Fig. 8 presents the comparison of the aggregated normalized SWS anomaly variation over the entire basin against the normalized precipitation anomaly and the in situ normalized discharge anomaly at the outlet of the basin (Brazzaville/Kinshasa station, see Table 2). The normalized anomalies here are estimated by subtracting the mean value of the time series from individual months and by dividing the obtained series by the STD of the original time series). As a complement, we report in Table 4, the maximum linear Pearson correlation coefficient, along with their lag, calculated between the aggregated normalized SWS anomaly variation, the normalized precipitation anomaly, and the in situ normalized discharge anomaly, at basin and sub-basin scales.

Figure 8a presents a fair agreement between the SWS and the other two hydrological variables, with a maximum correlation coefficient r of 0.56 (lag = 0; p value < 0.01) between SWS and precipitation variations. A similar correlation coefficient (r = 0.57 with a 0-month lag; p value < 0.01) is found between normalized SWS anomaly

and in situ normalized discharge anomaly. The deseasonalized normalized anomaly (acquired by subtracting the mean monthly values over the considered period, 1992-2015 or 1995-2015 from individual months and dividing by the STD of the raw series) (Fig. 8b) show correlation coefficient of r = 0.52 (lag = 0; p value < 0.01) and r = 0.12 (lag = 0; p value < 0.05) respectively between SWS versus in situ discharge and SWS versus precipitation. Additionally, we also perform a comparison with previous estimates of SWS over the Congo basin from Becker et al. (2018), estimated using the multi-satellite approach and available over the period 2003-2007. The assessment with SWS anomaly from FABDEM shows a good agreement (Fig. 8a), with similar amplitude, with a maximum correlation coefficient of r = 0.73 (lag = 0; p value < 0.01).

At the seasonal time-scale, Fig. 8c reveals for the first peak (i.e., August-February) that SWS anomaly reaches their maximum in November, one month before the maximum of the river normalized discharge anomaly (December) and after the maximum of normalized precipitation anomaly data (October). Same observation is made in terms of the temporal shift for the second peak (i.e., March-July), where the maximum of SWS anomaly occurs in April and one month later for normalized discharge anomaly and one month before for normalized precipitation anomaly respectively in May and March.

Figure 9 displays the comparison at the basin level between the aggregated normalized SWS anomaly and TWSA from GRACE. Both variables, show a similar interannual variability during the common period of availability of data (i.e., 2002 to 2015) presenting a fair correlation of r = 0.84 (lag = 1; p value < 0.01; Fig. 9a). It is worth to mention as well that both datasets capture the bi-modal patterns. Figure 9b presents the deseasonalized normalized anomaly for the two variables (r = 0.4; lag = 0; p value < 0.01), showing quite similar variations, especially in the long-term variability. We also notice the higher magnitude of the normalized SWS anomaly as compared to the normalized TWSA. At the seasonal time-scale, Fig. 9c reveals a similar behavior, with the two peaks depicted in the two variables, one in November-December and one in April. The lowest level of the SWS happens in July that is one month ahead of TWSA minimum. Figure 10 presents the same comparison as done in Fig. 8 but at the sub-basin level (considering Ubangui, Sangha, Middle-Congo, Kasaï, and Lualaba sub-basins, see Fig.1). The seasonal variations of all sub-basins are provided in Fig. 10 (right column). The outlet of Kasaï and Lualaba sub-basins provides historical observations (i.e., data before the 1990s), thus, the comparison with its in situ normalized discharge anomaly time series was integrated only at the annual cycle. For Ubangui, Sangha, and Lualaba sub-basins, the maximum linear correlation coefficient is not significant between normalized SWS anomaly and normalized precipitation anomaly variations at the interannual level and their associated anomaly (Figs. 10a, b, d, e, m, and n, Table 4). This could be associated to the bi-modal dynamics observed in the precipitation data whereas the SWS variations do not show that behavior. Becker et al. (2018), using similar datasets (GIEMS-1 for SWE and VS from ENVISAT), reported the same observation between precipitation data with a bi-modal patterns and SWE with uni-modal patterns (Fig. 4 of Becker et al., 2018). Another reason could be that, for Ubangui and Sangha, SWS is mainly function of discharge variations, while for the Lualaba sub-basin, that encompasses many lakes and floodplains, the various processes and their link for instance with evaporation lead to an insignificant precipitation-SWS correlation. Additionally, one can observe a negative lag between normalized SWS anomaly and normalized precipitation anomaly for Ubangui and Lualaba sub-basins which is not physically acceptable since we except positive temporal shift between SWS and precipitation. This is probably due to the fact that SWS show uni-modal pattern while precipitation shows bi-modal pattern. Nevertheless, the comparison between normalized SWS anomaly versus normalized discharge anomaly for Ubangui and Sangha, except for Lualaba

sub-basin, shows fair correlation coefficient ($r > 0.7$; p value < 0.01) at the interannual time-scale (Fig. 10a and d). Their related deseasonalized normalized anomalies (Fig. 10b and e) presents lower values of correlation coefficients ($r < 0.4$; p value < 0.01). Regarding Middle-Congo and Kasaï subbasins (Fig. 10g and j), a maximum linear correlation coefficient is respectively of $r = 0.32$ and $r = 0.69$ (lag = 0; p value < 0.01) between normalized SWS anomaly and normalized precipitation anomaly. Their associated deseasonalized normalized anomaly (Fig. 10h and k) does not show significant correlation coefficient. In contrast to this, for Middle-Congo, the comparison between SWS and discharge provides moderate correlation coefficient for both interannual and deseasonalized anomaly variations ($r > 0.5$ with a delay lag of 1-month; p value < 0.01). In accordance with other results (see Fig. 10h of Kitambo et al., 2022a), the Middle-Congo appears to be the main sub-basin for which the variability of the normalized discharge anomaly at the outlet Brazzaville/Kinshasa station is fairly related (~35%) to the variations of normalized SWS anomaly in the Cuvette Centrale region due to its significant correlation coefficient of $r = 0.58$ between the deseasonalized normalized anomaly of both SWS and discharge. Northern and the Middle-Congo sub-basins reach their SWS anomaly' maximum in November (for Sangha and Middle-Congo, fig. 9f and i) and October (for Ubangui, Fig. 10c), and this is in phase with the maximum of the normalized discharge anomaly and a backward temporal shift of 1 month with the normalized precipitation anomaly. Comparatively to northern sub-basins, southern sub-basins (Kasaï and Lualaba), for the period January to May, reach their SWS anomaly' maximum in March (Fig. 10l and o) that is in phase with the occurrence of the maximum of normalized precipitation anomaly. The maximum of normalized discharge anomaly occurs two months later in May for Lualaba and one month later for Kasaï. In contrast to the other sub-basins, Kasaï and Middle-Congo have depicted the bi-modal patterns in SWS anomaly variations. For Middle-Congo, the first peak is reached in November and the second in May while for Kasaï, the first peak occurs in December and the second peak with a steadily evolution occurs in March and May. Similar results were observed in the Cuvette centrale by Frappart et al. (2021a).

The temporal patterns in Fig. 8 and 10 follow alternatively wet and dry events associated with large-scale climatic phenomena, for all dataset (SWS, precipitation and discharge). A focus on the Lualaba and Kasai deseasonalized normalized anomaly of SWS reveals that there are the two main sub-basins significantly impacted (large positive anomaly in Fig. 10k and 10n) by the major flood event triggered by the positive Indian Ocean Dipole in combination with the El Niño event that characterized the period 1997-1998. Conversely, recent studies using hydro-meteorological datasets have shown that some parts of the CRB are subjects to a long-term drying trend over the past decades (Hua et al., 2016; Ndehedehe et al., 2018). The droughts that affected large areas of CRB in recent years are amongst the most severe ones in the past decades (Ndehedehe et al., 2022), including the large anomalous event of the 2005-2006 drought (Fig. 8). This is further investigated below.

6 Application: the spatio-temporal dynamics of SWS during the 2005-2006 drought

SWS estimates are essential in the characterization of large-scale, extreme climate events such as droughts and floods (Frappart et al., 2012; Pervez and Henebry, 2015, Papa et al., 2021). Here, we investigated the spatial signature and distribution of the major drought that occurred in the end of 2005 and early 2006 across the CRB (Ndehedehe et al., 2019, 2022). During that period, SWS anomaly was at its lowest level at basin-scale (Fig. 6b). The spatial patterns of this drought are further illustrated in Fig. 11 using the FABDEM estimates. The anomaly of SWS from FABDEM in the end 2005 and early 2006 is estimated here by subtracting the November-December-

January mean values over 1992-2015 from the maximum value between November 2005 to January 2006 and by dividing the obtained value by the November-December-January mean values.

Figure 11 evidences that during that period the major part of the basin was affected by large negative anomalies of SWS, with values sometimes reaching a 50% deficit as compare to their long-term average. It clearly shows a widespread severe drought across the basin (< - 40% of the mean maximum), even if some parts of the Oubangui sub-basin and Lukenie Rivers in the north of Kasaï sub-basin are relatively less affected (> - 10% of the mean maximum of SWS). Figure 11 shows the large drought spatial signature of the southeastern wetlands/floodplains (e.g., Bangwelo, Upemba) in the Lualaba sub-basin, with SWS estimated at more than -40% of the mean maximum during that period. Notably, the heart of the Cuvette Centrale displays a stronger negative signal in terms of SWS. The hydrological dynamic in the Cuvette Centrale might explain that the mainstream that receives water from all adjacent wetlands and streams experiences a less intense impact of drought (Lee et al., 2011). This aligns with the previous findings that large parts of the CRB found to be extensively affected (Ndehedehe et al., 2019) and it is confirmed by analyzing the monthly mean spatial distribution of MSWEP precipitation anomaly (Fig. 12) around that period of time. Figure 12 shows the monthly mean spatial distribution of MSWEP precipitation anomaly at 0.25° spatial resolution from the period September 2005 to February 2006 based on the 1992-2015 climatology. Over the six months, November 2005 to January 2006 are the most impacted months (Fig. 12c, d, e). November 2005 (Fig. 12c) displays a large spread negative anomaly all over the basin whereas December 2005 (Fig. 12d) and January 2006 (Fig. 12e) show severe negative anomalies only in the southern part of the basin, in accordance with the spatial distribution of SWS across the basin as described previously. However, some parts of the Oubangui sub-basin and Lukenie Rivers in the north of Kasaï sub-basin seem to be relatively less affected by the drought in terms of SWS, even if large precipitation negative anomaly is observed of these regions. Investigating the climatic and hydrological drivers of these anomalous events in CRB is far beyond the scope of the present study, but our results point out to the capability of this new long-term estimates of SWS to be used in future studies.

7 Data availability

The SWS estimates from the multi-satellite approach (1995-2015), as well as the hypsometric curves approach providing the surface water extent area-height relationships from the four DEMs (before and after the corrections), the surface water extent area-storage relationships, along with the four SWS estimates (1992-2015) are publicly available for non-commercial use and distributed via the following URL/DOI: https://doi.org/10.5281/zenodo.7299823 (Kitambo et al., 2022b).

8 Code availability

Here we provide the Python code to run the reproducibility of the hypsometric curve approach dataset of SWS. This code allows the application of the method elsewhere and is available at Zenodo platform through the following URL/DOI link: https://doi.org/10.5281/zenodo.8011607 (Kitambo et al., 2023).

9 Conclusions and perspectives

In this study, we present an unprecedented dataset of monthly SWS anomaly of wetlands, floodplains, rivers and lakes over the entire Congo basin during the 1992-2015 period at ~ 0.25° spatial resolution. Two methods are employed, one based on a multi-satellite approach and one on a hypsometric curve approach. The multi-satellite approach consists of the combination of SWE from GIEMS-2 and satellite-derived SWH from radar altimetry (long-term series ERS-2_ENV_SRL) on the same period of availability for the two datasets, here 1995-2015. The hypsometric curve approach consists of the combination of SWE from GIEMS-2 dataset and hypsometric curves obtained from various DEMs (i.e., ASTER, ALOS, MERIT, and FABDEM). Both methods generate monthly spatio-temporal variations of SWS changes across the entire CRB, enabling for the first time the quantification of surface freshwater volume variations in the Congo basin over a long-term period (24-year). The SWS computed from different approaches, multi-satellite and hypsometric curve, and from different DEMs (ALOS, ASTER, MERIT, FABDEM), generally show good agreements between them at the interannual and seasonal scale, with minor exceptions for SWS variations from ASTER DEM due possibly to its largest vertical error. SWS variations from the multi-satellite approach show some limitations due to the spatial distribution of altimetry-derived VSs over the basin. The two approaches are complementary: the hypsometric curve approach allows to generate the SWS changes over the entire basin with limitation over lakes and in high altitude topography, while the multi-satellite one can generate SWS variations over lakes but with a spatial constraint on the availability of VSs. SWS variations from FABDEM, which is the only DTM among all the DEMs used (i.e., both biases associated with trees and building have been removed) is then used to illustrate the capability of the new dataset.

The temporal variations of SWS satisfactorily depicted the bimodal pattern at the interannual and seasonal scales, a well-known characteristic of the hydrological regime of the Congo basin. The mean annual amplitude was determined to be 101 ± 23 km³, which, in perspective, represents ~8% of the Amazon basin's mean annual amplitude. The spatial distribution of the SWS has shown a realistic pattern for major tributaries of the Congo basin and its analysis showed large SWS variability (e.g., 0.3 to 0.6 km³) over the extensive wetlands and floodplains such as the Cuvette Centrale and in the southeastern part (i.e., Bangweulu, Mweru, Upemba) of the basin. In the Cuvette Centrale, the maximum SWS values are reached in September-October in the upper part and in November-December in the lower part. The new monthly surface water storage has been compared on common period to the previous estimates over 2003-2007 showing a good agreement and a fair correlation coefficient. Furthermore, an evaluation was conducted with independent hydrological variables, precipitation from MSWEP dataset and in situ discharges from contemporary and historical observations, showing an overall good correspondence among all variables. The estimates of SWS variations also enable to depict the major anomalous events related to droughts (e.g., exceptional drought documented in 2005-2006) and floods (e.g., exceptional flood occurred in 1997-1998). We further map, across the basin, the spatial signature of the widespread drought that took place in the end of 2005 and the beginning of 2006, revealing the severity of this particular event on surface freshwater store, in agreement with satellite-derived precipitation observations, although the northeast of the Cuvette Centrale and some tributaries of the Kasaï River (in the Mai-Ndombe Lake region) were less impacted. These unique long-term monthly time series of CRB's SWS provide the broad characteristic of the variability of surface water storage anomaly at the basin and sub-basin levels over 24-year in the CRB. It opens new perspectives to move toward answering several crucial scientific questions regarding the role of SWS dynamics into the hydrological and biogeochemical cycles of CRB. For instance, SWS estimates are a relevant source of

information to make progress in the understanding of the hydrodynamic processes that drive the exchanges between rivers and floodplains, both in terms of freshwater and dissolved and particulate materials. Such datasets also enable us to explore the link between regional climate variability and water resources, especially during extreme events, and can now be used to improve our understanding of hydroclimate processes in the Congo region (Frappart et al., 2012).

Overall, these results from satellite-based observations also confirm the capability and benefits of using Earth observations in a sparse gauged basin such as the CRB to better characterize and improve our understanding of the hydrological science in ungauged basins. The information derived from SWS will therefore be very pertinent as a benchmark product regarding the calibration/validation of the future hydrology-oriented Surface Water and Ocean Topography (SWOT) satellite mission,launched on the 16th of December 2022, which will provide water storage variability of water bodies globally (Biancamaria et al., 2016). Additionally, SWS estimates provide a unique opportunity for future hydrological or climate modeling and to evaluate regional hydrological models (Scanlon et al., 2019) that still lack proper representation of surface water storage variability at large scale (Paris et al., 2022), especially in major African river basins (Papa et al., 2022).

Following previous studies (Frappart et al., 2019, Becker et al., 2018), SWS estimates also open new opportunities to generate a long-term spatio-temporal variations of sub-surface freshwater through decomposition of the Total Water Storage variations as measured by the GRACE/GRACE-FO (Gravity Recovery and Climate Experiment Follow-On) (Pham-duc et al., 2019). Such understanding of freshwater variations in the continental reservoirs has many potentials to better characterize the hydro-climate processes of the region and improve our knowledge on the water resources availability in CRB. For instance, SWS estimates are key to determine the total drainable water storage of a basin (Tourian et al., 2018, 2022), that provide essential information about the distribution and availability of freshwater in a basin.

Finally, since GIEMS-2 and the DEMS used in this study are available globally, our results thus present also a new first step toward the development of such SWS databases at the global scale. Furthermore, the proliferation of new DEMs that are proper DTMs, and the increasing availability of high-accuracy bare-earth DEMs (O'Loughlin et al., 2016; Yamazaki et al., 2017; Hawker et al., 2022) has opened new opportunities to better investigate SWS dynamics at the global scale. As highlighted in Papa and Frappart (2021), global SWS estimates and variations are crucial to understand the role of continental water in the global water cycle and global estimates will offer new opportunities for hydrological and multidisciplinary sciences, including data assimilation, land–ocean exchanges and water management.

Author contributions BK, FP, AP, RTM, and SC conceived the research design. BK processed the data and created the SWS dataset from hypsometric curve approach. FF created the SWS dataset from multi-satellite approach. OE created SWS of lakes. RJO provided precipitation data and Figure 11. BK, FP, and AP analyzed and interpreted the results and wrote the draft. FP and RTM were responsible for the data curation. All authors discussed the results and contributed to the final version of the paper.

Competing interests. The contact author declare that they have not any competing interests.

Acknowledgements. Benjamin Kitambo has been supported by a doctoral grant from the French Space Agency (CNES), Agence Française du Développement (AFD), and Institut de Recherche pour le Développement (IRD). This research has been supported by the CNES TOSCA project "DYnamique hydrologique du BAssin du CoNGO (DYBANGO)" (2020–2023). We thank Dr Catherine Prigent from Sorbonne Université, Observatoire de Paris, Université PSL Paris, France for sharing the GIEMS-2 database.

Financial support. This research has been supported by the Centre National d'Etudes Spatiales (project TOSCA DYBANGO).

References

Albert, J.S.; Destouni, G.; Duke-Sylvester, S.M.; Magurran, A.E.; Oberdorff, T.; Reis, R.E.; Winemiller, K.O.; Ripple, W.J. Scientists' warning to humanity on the freshwater biodiversity crisis. Ambio, 50, 85–94, https://doi.org/10.1007/s13280-020-01318-8, 2021

Alsdorf, D.E.; Lettenmaier, D.P. Tracking fresh water from space. Science, 301, 1492–1494, DOI: 10.1126/science.1089802, 2003.

Alsdorf, D.E.; Rodríguez, E.; Lettenmaier, D.P. Measuring surface water from space. Rev. Geophys., 45, RG2002, https://doi.org/10.1029/2006RG000197, 2007.

Becker, M., Papa, F., Frappart, F., Alsdorf, D., Calmant, S., da Silva, J. S., Prigent, C., and Seyler, F.: Satellite-based estimates of surface water dynamics in the Congo River Basin, Int. J. Appl. Earth Obs. Geoinf., 66, 196–209, https://doi.org/10.1016/j.jag.2017.11.015, 2018.

Beck, H. E., Pan, M., Roy, T., Weedon, G. P., Pappenberger, F., Dijk, A. I. J. M. Van, Huffman, G. J., Adler, R. F., and Wood, E. F. Daily evaluation of 26 precipitation datasets using Stage-IV gauge-radar data for the CONUS. *Hydrol. Earth Syst. Sci.*, *23*, 207–224. https://doi.org/https://doi.org/10.5194/hess-23-207-2019, 2019.

Beck, H. E., Vergopolan, N., Pan, M., Levizzani, V., Dijk, A. I. J. M. Van, Weedon, G. P., Brocca, L., Pappenberger, F., Huffman, G. J., and Wood, E. F. Global-scale evaluation of 22 precipitation datasets using gauge observations and hydrological modeling. *Hydrol. Earth Syst. Sci.*, *21*, 6201–6217. https://doi.org/https://doi.org/10.5194/hess-21-6201-2017, 2017.

Beck, H. E., Wood, E. F., Pan, M., Fisher, C. K., Miralles, D. G., Dijk, A. I. J. M. van, McVicar, T. R., and Adler, R. F. MSWEP V2 Global 3-Hourly 0.1° Precipitation: Methodology and Quantitative Assessment. *Bull. Am. Meteorol. Soc.*, *100*(March), 473–500. https://doi.org/https://doi.org/10.1175/BAMS-D-17-0138.1, 2019.

Becker, M., Papa, F., Frappart, F., Alsdorf, D., Calmant, S., da Silva, J. S., Prigent, C., and Seyler, F. Satellite-based estimates of surface water dynamics in the Congo River Basin. *Int. J. Appl. Earth Obs. Geoinf.*, *66* (8), 196–209. https://doi.org/10.1016/j.jag.2017.11.015, 2018.

Biancamaria, S., Lettenmaier, D. P., Pavelsky, T. M. The SWOT Mission and Its Capabilities for Land Hydrology. Surveys in Geophysics, 37(2), 307–337. https://doi.org/10.1007/s10712-015-9346-y, 2016.

Biddulph, G. E., Bocko, Y. E., Bola, P., Crezee, B., Dargie, G. C., Emba, O., Georgiou, S., Girkin, N., Hawthorne, D., Jonay Jovani-Sancho, A., Joseph Kanyama, T., Mampouya, W. E., Mbemba, M., Sciumbata, M., and Tyrrell, G. Current knowledge on the Cuvette Centrale peatland complex and future research directions. *Bois Forets des Trop.*, *350*, 3–14. https://doi.org/10.19182/bft2021.350.a36288, 2021.

Boberg, J. Freshwater Availability. In Liquid Assets: How Demographic Changes and Water Management Policies Affect Freshwater Resources; RAND Corporation: Santa Monica, CA, USA; Arlington, VA, USA; Pittsburgh, PA, USA, pp. 15–28. Available online: http://www.jstor.org/stable/10.7249/mg358cf.9 (last access on 17 May 2023), 2005.

Bogning, S., Frappart, F., Blarel, F., Niño, F., Mahé, G., Bricquet, J. P., Seyler, F., Onguéné, R., Etamé, J., Paiz, M. C., and Braun, J. J.: Monitoring water levels and discharges using radar altimetry in an ungauged river basin: The case of the Ogooué, Remote Sens., 10, 350, https://doi.org/10.3390/rs10020350, 2018.

Bricquet, J.-P.: Les écoulements du Congo à Brazzaville et la spatialisation des apports, in: Grands bassins fluviaux périatlantiques: Congo, Niger, Amazone, Paris, ORSTOM, edited by: Boulègue, J. and Olivry, J.-C., Colloques et Séminaires, Grands Bassins Fluviaux Péri-Atlantiques: Congo, Niger, Amazone, Paris, France, 1993/11/22-24, 27–38, ISBN 2-7099-1245-7, ISSN 0767-2896, 1995.

Bullock, A., Acreman, M. The role of wetlands in the hydrological cycle. Hydrol. Earth Syst. Sci., 7, 358–389. doi:10.5194/hess-7-358-2003, 2003.

Cazenave, A., Champollion, N., Benveniste, J., and Chen, J. Remote Sensing and Water Resources Management. In A. Cazenave, N. Champollion, J. Benveniste, and J. Chen (Eds.), *J. Am. Water Resour. Assoc.*,10 (4). Springer. https://doi.org/10.1111/j.1752-1688.1974.tb05660.x, 2016.

Chahine, M.T. The hydrological cycle and its influence on climate. Nature, 359, 373–380, https://doi.org/10.1038/359373a0, 1992

Cooley, S.W.; Ryan, J.C.; Smith, L.C. Human alteration of global surface water storage variability. Nature, 591, 78–81, https://doi.org/10.1038/s41586-021-03262-3, 2021.

Crétaux, J. F., Arsen, A., Calmant, S., Kouraev, A., Vuglinski, V., Bergé-Nguyen, M., Gennero, M. C., Nino, F., Abarca Del Rio, R., Cazenave, A., and Maisongrande, P. SOLS: A lake database to monitor in the Near Real Time water level and storage variations from remote sensing data. *Adv. Sp. Res.*, *47*(9), 1497–1507. https://doi.org/10.1016/j.asr.2011.01.004, 2011.

Cretaux, J., Frappart, F., Papa, F., Calmant, S., Nielsen, K., and Benveniste, J.: Hydrological Applications of Satellite Altimetry Rivers, Lakes, Man-Made Reservoirs, Inundated Areas, in: Satellite Altimetry over Oceans and Land Surfaces, edited by: Stammer, D. C. and Cazenave, A., Taylor & Francis Group, New York, 459–504, ISBN 9781315151779, https://doi.org/10.1201/9781315151779, 2017.

Crezee, B., Dargie, G. C., Ewango, C. E. N., Mitchard, E. T. A., B, O. E., T, J. K., Bola, P., Ndjango, J. N., Girkin, N. T., Bocko, Y. E., Ifo, S. A., Hubau, W., Seidensticker, D., Batumike, R., Wotzka, H., Bean, H., Baker, T. R., Baird, A. J., Boom, A., … Lewis, S. L. Mapping peat thickness and carbon stocks of the central Congo Basin using field data. Nature Geoscience, 15, 639–644. https://doi.org/10.1038/s41561-022-00966-7, 2022.

Crowley, J. W., Mitrovica, J. X., Bailey, R. C., Tamisiea, M. E., Davis, J. L. Land water storage within the Congo Basin inferred from GRACE satellite gravity data. Geophysical Research Letters, 33(19). https://doi.org/10.1029/2006GL027070, 2006.

Da Silva, J., Calmant, S., Seyler, F., Corrêa, O., Filho, R., Cochonneau, G., and João, W.: Water levels in the Amazon basin derived from the ERS 2 and ENVISAT radar altimetry missions, Remote Sens. Environ., 114, 2160–2181, https://doi.org/10.1016/j.rse.2010.04.020, 2010.

Datok, P., Fabre, C., Sauvage, S., Moukandi N'kaya, G. D., Paris, A., Dos Santos, V., Guilhen, J., Manteaux S,

Laraque, A., and Sanchez Perez, J. M. Investigating the role of the Cuvette Centrale wetlands in the hydrology, sediment and carbon fluxes of the Congo River Basin (CRB). *Earth Sp. Sci. Open Arch.*. https://doi.org/https://doi.org/10.1002/essoar.10505504.1, 2020.

Decharme, B., Alkama, R., Papa, F., Faroux, S., Douville, H., and Prigent, C.: Global off-line evaluation of the ISBA-TRIP flood model, Clim. Dynam., 38, 1389–1412, https://doi.org/10.1007/s00382-011-1054-9, 2011.

de Marsily, G.: Eaux continentales, C. R. Geosci., 337, 1–2, 2005. Decharme, B., Douville, H., Prigent, C., Papa, F., and Aires, F.: A new river flooding scheme for global climate applications: Off-line validation over South America, J. Geophys. Res., 113, D11110, doi:10.1029/2007JD009376, 2008.

Dubayah, R., Blair, J.B., Goetz, S., Fatoyinbo, L., Hansen, M., Healey, S., Hofton, M., Hurtt, G., Kellner, J., Luthcke, S. The global ecosystem dynamics investigation: high-resolution laser ranging of the Earth's forests and topography. Sci. Remote Sens. 1, 100002, https://doi.org/10.1016/j.srs.2020.100002, 2020a.

Fassoni-Andrade, A. C., Fleischmann, A. S., Papa, F., Paiva, R. C. D. d., Wongchuig, S., Melack, J. M., et al. Amazon hydrology from space: Scientific advances and future challenges. Reviews of Geophysics, 59, e2020RG000728. https://doi.org/10.1029/2020RG000728, 2021.

Frappart, F., Calmant, S., Cauhopé, M., Seyler, F., and Cazenave, A.: Preliminary results of ENVISAT RA-2-derived water levels validation over the Amazon basin, Remote Sens. Environ., 100, 252–264, https://doi.org/10.1016/j.rse.2005.10.027, 2006.

Frappart, F.; Papa, F.; Famiglietti, J.; Prigent, C.; Rossow, W.B.; Seyler, F. Interannual variations of river water storage from a multiple satellite approach: A case study for the Rio Negro River basin. J. Geophys. Res., 113, 113, https://doi.org/10.1029/2007JD009438, 2008.

Frappart, F.; Papa, F.; Güntner, A.; Werth, S.; Ramillien, G.; Prigent, C.; Rossow, W.B.; Bonnet, M.-P. Interannual variations of the terrestrial water storage in the Lower Ob' Basin from a multisatellite approach. Hydrol. Earth Syst. Sci., 14, 2443–2453, https://doi.org/10.5194/hess-14-2443-2010, 2010.

Frappart, F., Papa, F., Güntner, A., Werth, S., Santos da Silva, J., Tomasella, J., Seyler, F., Prigent, C., Rossow, W. B., Calmant, S., & Bonnet, M. P. Satellite-based estimates of groundwater storage variations in large drainage basins with extensive floodplains. Remote Sens. Environ., 115(6), 1588–1594. https://doi.org/10.1016/j.rse.2011.02.003, 2011.

Frappart, F.; Papa, F.; Da Silva, J.S.; Ramillien, G.; Prigent, C.; Seyler, F.; Calmant, S. Surface freshwater storage and dynamics in the Amazon basin during the 2005 exceptional drought. Environ. Res. Lett., 7, 7, https://iopscience.iop.org/article/10.1088/1748-9326/7/4/044010, 2012.

Frappart, F.; Papa, F.; Malbéteau, Y.; Leon, J.G.; Ramillien, G.; Prigent, C.; Seoane, L.; Seyler, F.; Calmant, S. Surface freshwater storage variations in the Orinoco floodplains using multi-satellite observations. Remote Sens., 7, 89–110, https://doi.org/10.3390/rs70100089, 2015.

Frappart, F., Papa, F., Marieu, V., Malbeteau, Y., Jordy, F., Calmant, S., Durant, F., Bala, S. Preliminary assessment of SARAL/AltiKa observations over the Ganges-Brahmaputra and Irrawaddy Rivers. Marine Geodesy, 38(sup1), 568-580, DOI: 10.1080/01490419.2014.990591, 2015b.

Frappart, F., Legrésy, B., Nino, F., Blarel, F., Fuller, N., Fleury, S., Birol, F., Calmant, S. An ERS-2 altimetry reprocessing compatible with ENVISAT for long-term land and ice sheets studies. Remote Sens. Environ., 184, 558-581, https://doi.org/10.1016/j.rse.2016.07.037, 2016.

Frappart, F.; Biancamaria, S.; Normandin, C.; Blarel, F.; Bourrel, L.; Aumont, M.; Azemar, P.; Vu, P.-L.; Le

Toan, T.; Lubac, B.; et al. Influence of recent climatic events on the surface water storage of the Tonle Sap Lake. Sci. Total. Environ., 636, 1520–1533, https://doi.org/10.1016/j.scitotenv.2018.04.326, 2018.

Frappart, F.; Papa, F.; Güntner, A.; Tomasella, J.; Pfeffer, J.; Ramillien, G.; Emilio, T.; Schietti, J.; Seoane, L.; da Silva Carvalho, J.; Medeiros Moreira, D., Bonnet, M.P., Seyler, F. The spatio-temporal variability of groundwater storage in the Amazon River Basin. Adv. Water Resour., 124, 41–52, https://doi.org/10.1016/j.advwatres.2018.12.005, 2019.

Frappart, F., Blarel, F., Fayad, I., Bergé-Nguyen, M., Crétaux, J. F., Shu, S., Schregenberger, J., Baghdadi, N. Evaluation of the performances of radar and lidar altimetry missions for water level retrievals in mountainous environment: The case of the Swiss lakes. Remote Sensing, 13(11), 2196, https://doi.org/10.3390/rs13112196, 2021b.

Good, S.P.; Noone, D.; Bowen, G. Hydrologic connectivity constrains partitioning of global terrestrial water fluxes. Science, 349, 175–177, DOI: 10.1126/science.aaa5931, 2015

Gasse, F., Ledee, V., Massauh, M., and Fontes, J. Water-level fluctuations of Lake Tanganyika in phase with oceanic changes during the last glaciation and deglaciation. *Nature*, *342*, 57–59. https://doi.org/https://doi.org/10.1038/342057a0, 1989.

Guth, P. L., Van Niekerk, A., Grohmann, C. H., Muller, J. P., Hawker, L., Florinsky, I. V., Gesch, D., Reuter, H. I., Herrera-Cruz, V., Riazanoff, S., López-Vázquez, C., Carabajal, C. C., Albinet, C., Strobl, P. Digital elevation models: Terminology and definitions. Remote Sens., 13(18), 1–19. https://doi.org/10.3390/rs13183581, 2021.

Harrison, I. J., Brummett, R., and Stiassny, M. L. J. The Congo River Basin. In C. M. Finlayson, A. A. van Dam, K. Irvine, M. Everard, R. J. McInnes, B. A. Middleton, and N. C. Davidson (Eds.), *The Wetland Book* (1). Springer Science+Business Media Dordrecht. https://doi.org/10.1007/978-94-007-6173-5, 2016.

Hastie, A., Lauerwald, R., Ciais, P., Papa, F., Regnier, P. Historical and future contributions of inland waters to the Congo Basin carbon balance. Earth System Dynamics, 12(1), 37–62. https://doi.org/10.5194/esd-12-37-2021, 2021.

Hawker, L., Neal, J., and Bates, P. Accuracy assessment of the TanDEM-X 90 Digital Elevation Model for selected floodplain sites. *Remote Sens. Environ.*, *232*(11). https://doi.org/10.1016/j.rse.2019.111319, 2019.

Hawker, L., Uhe, P., Paulo, L., Sosa, J., Savage, J., Sampson, C., Neal, J. A 30 m global map of elevation with forests and buildings removed. Environ. Res. Lett., 17(2). https://doi.org/10.1088/1748-9326/ac4d4f, 2022.

Hua, W., Zhou, L., Chen, H., Nicholson, S. E., Raghavendra, A., and Jiang, Y. Possible causes of the Central Equatorial African long-term drought Possible causes of the Central Equatorial African long-term drought. *Environ. Res. Lett.*, *11*. http://dx.doi.org/10.1088/1748-9326/11/12/124002, 2016.

Huffman, G.J., E.F. Stocker, D.T. Bolvin, E.J. Nelkin, Jackson Tan. GPM IMERG Final Precipitation L3 Half Hourly 0.1 degree x 0.1 degree V06, Greenbelt, MD, Goddard Earth Sciences Data and Information Services Center (GES DISC), Accessed: [17 May 2023], 10.5067/GPM/IMERG/3B-HH/06, 2019.

Inogwabini, B.-I.: The changing water cycle: Freshwater in the Congo, WIREs Water, 7, e1410, https://doi.org/10.1002/wat2.1410, 2020.

Jiang, L., Nielsen, K., Dinardo, S., Andersen, O. B., Bauer-Gottwein, P. Evaluation of Sentinel-3 SRAL SAR altimetry over Chinese rivers. *Remote Sensing of Environment*, *237*, 111546. https://doi.org/https://doi.org/10.1016/j.rse.2019.111546, 2020.

Kao, H., Kuo, C., Tseng, K., Shum, C. K., Tseng, T.-P., Jia, Y.- Y., Yang, T.-Y., Ali, T. A., Yi, Y., and Hussain, D.: Assessment of Cryosat-2 and SARAL/AltiKa altimetry for measuring inland water and coastal sea level variations: A case study on Tibetan Plateau Lake and Taiwan Coast, Mar. Geod., 42, 327–343, https://doi.org/10.1080/01490419.2019.1623352, 2019.

Kitambo, B., Papa, F., Paris, A., Tshimanga, R. M., Calmant, S., Fleischmann, A. S., Frappart, F., Becker, M., Tourian, M. J., Prigent, C., and Andriambeloson, J.: A combined use of in situ and satellite-derived observations to characterize surface hydrology and its variability in the Congo River basin, Hydrol. Earth Syst. Sci., 26, 1857–1882, https://doi.org/10.5194/hess-26-1857-2022, 2022a.

Kitambo, B., Papa, F., Paris, A., Tshimanga, R. M., Frappart, F., Calmant, S., Elmi, O., Fleischmann, A. S., Becker, M., Tourian, M. J., Jucá Oliveira, R. A., Wongchuig, S. A long-term monthly surface water storage dataset for the Congo basin from 1992 to 2015 [Data set]. Zenodo. https://doi.org/10.5281/zenodo.7299823, 2022b.

Kitambo, B., Papa, F., Paris, A. Surface Water Storage computation (1.0). Zenodo. https://doi.org/10.5281/zenodo.8011607, 2023.

Kittel, C. M. M., Jiang, L., Tøttrup, C., and Bauer-Gottwein, P.: Sentinel-3 radar altimetry for river monitoring - A catchmentscale evaluation of satellite water surface elevation from Sentinel-3A and Sentinel-3B, Hydrol. Earth Syst. Sci., 25, 333–357, https://doi.org/10.5194/hess-25-333-2021, 2021.

Laraque, Alain, Bricquet, J. P., Pandi, A., and Olivry, J. C.: A review of material transport by the Congo River and its tributaries, Hydrol. Process., 23, 3216–3224, https://doi.org/10.1002/hyp.7395, 2009.

Laraque, A., Bellanger, M., Adele, G., Guebanda, S., Gulemvuga, G., Pandi, A., Paturel, J. E., Robert, A., Tathy, J. P., and Yambele, A.: Evolutions récentes des débits du Congo, de l'Oubangui et de la Sangha, Geo-Eco-Trop., 37, 93–100, http://www.geoecotrop.be/uploads/publications/pub_371_06.pdf (last access on 17/05/2023), 2013.

Laraque, A., N'kaya, G. D. M., Orange, D., Tshimanga, R., Tshitenge, J. M., Mahé, G., Nguimalet, C. R., Trigg, M. A., Yepez, S., and Gulemvuga, G.: Recent budget of hydroclimatology and hydrosedimentology of the congo river in central Africa. Water, 12(9). https://doi.org/10.3390/w12092613, 2020.

Lee, H., Beighley, R. E., Alsdorf, D., Chul, H., Shum, C. K., Duan, J., Guo, J., Yamazaki, D., and Andreadis, K.: Remote Sensing of Environment Characterization of terrestrial water dynamics in the Congo Basin using GRACE and satellite radar altimetry, Remote Sens. Environ., 115, 3530–3538, https://doi.org/10.1016/j.rse.2011.08.015, 2011.

Mcphaden, M. J. El Ni no and La Ni na: Causes and Global Consequences. In Encyclopedia of Global Environmental Change (1), pp. 1–17, ISBN 0-471-97796-9, https://www.pmel.noaa.gov/gtmba/files/PDF/pubs/ElNinoLaNina.pdf (last access: 17 May 2023), 2002.

Mekonnen, M.M.; Hoekstra, A.Y. Sustainability: Four billion people facing severe water scarcity. Sci. Adv., 2, e1500323, DOI: 10.1126/sciadv.1500323, 2016.

Melack, J.M., Forsberg, B.R. Biogeochemistry of Amazon floodplain lakes and associated wetlands. In The Bio-Geochemistry of the Amazon Basin; McClain, M.E., Victoria, R.L., Richey, J.E., Eds.; Oxford University Press: New York, NY, USA, pp. 235–274, DOI: 10.1093/oso/9780195114317.001.0001, 2001.

Ndehedehe, C. E., Awange, J. L., Agutu, N. O., and Okwuashi, O. Changes in hydro-meteorological conditions

over tropical West Africa (1980 – 2015) and links to global climate. *Glob. Planet. Change*, *162* (2), 321–341. https://doi.org/10.1016/j.gloplacha.2018.01.020, 2018.

Ndehedehe, C. E., Anyah, R. O., Alsdorf, D., Agutu, N. O., and Ferreira, V. G. Modelling the impacts of glo bal multi-scale climatic drivers on hydro-climatic extremes (1901 – 2014) over the Congo basin. *Sci. Total Environ.*, *651*, 1569–1587. https://doi.org/10.1016/j.scitotenv.2018.09.203, 2019.

Ndehedehe, C. E., and Agutu, N. O. Historical Changes in Rainfall Patterns over the Congo Basin and Impacts on Runoff (1903 – 2010). In R. M. Tshimanga, G. D. M. N'kaya, & D. Alsdorf (Eds.), Congo Basin Hydrology, Climate, and Biogeochemistry A Foundation for the Future. American Geophysical Union and John Wiley and Sons, Inc. https://doi.org/10.1002/9781119657002.ch9, 2022.

Normandin, C.; Frappart, F.; Lubac, B.; Bélanger, S.; Marieu, V.; Blarel, F.; Robinet, A.; Guiastrennec-Faugas, L. Quantification of surface water volume changes in the Mackenzie Delta using satellite multi-mission data. Hydrol. Earth Syst. Sci., 22, 1543–1561, https://doi.org/10.5194/hess-22-1543-2018, 2018.

O'Connell, E. Towards Adaptation ofWater Resource Systems to Climatic and Socio-Economic Change. Water Resour. Manag., 31, 2965–2984, https://doi.org/10.1007/s11269-017-1734-2, 2017.

O'Loughlin, F. E., Paiva, R. C. D., Durand, M., Alsdorf, D. E., Bates, P. D. A multi-sensor approach towards a global vegetation corrected SRTM DEM product. Remote Sensing of Environment, 182, 49–59. https://doi.org/https://doi.org/10.1016/j.rse.2016.04.018, 2016.

Oki, T.; Kanae, S. Global Hydrological Cycles and WorldWater Resources. Science, 313, 1068–1072, DOI: 10.1126/science.1128845, 2006.

Prigent, Catherine, Papa, F., Aires, F., Rossow, W. B., and Matthews, E.: Global inundation dynamics inferred from multiple satellite observations, 1993–2000, J. Geophys. Res.-Atmos., 112, 1993–2000, https://doi.org/10.1029/2006JD007847, 2007.

Prigent, C., Jimenez, C., Bousquet, P. Satellite-derived global surface water extent and dynamics over the last 25 years (GIEMS-2). J. Geophys. Res. Atmos., 125, e2019JD030711. https://doi.org/10.1029/2019JD030711, 2020.

Papa, F, Gu, A., Frappart, F., Prigent, C., and Rossow, W. B.: Variations of surface water extent and water storage in large river basins: A comparison of different global data sources, Geophys. Res. Lett., 35, 1–5, https://doi.org/10.1029/2008GL033857, 2008.

Papa, F., Prigent, C., Aires, F., Jimenez, C., Rossow, W. B., and Matthews, E.: Interannual variability of surface water extent at the global scale, 1993–2004, J. Geophys. Res.-Atmos., 115, 1–17, https://doi.org/10.1029/2009JD012674, 2010.

Papa, F., Frappart, F., Güntner, A., Prigent, C., Aires, F., Getirana, A. C. V., and Maurer, R.: Surface freshwater storage and variability in the Amazon basin from multi-satellite observations, 1993–2007, J. Geophys. Res.-Atmos., 118, 11951–11965, https://doi.org/10.1002/2013JD020500, 2013.

Papa, F., Frappart, F., Malbeteau, Y., Shamsudduha, M., Vuruputur, V., Sekhar, M., Ramillien, G., Prigent, C., Aires, F., Pandey, R. K., Bala, S., and Calmant, S.: Satellitederived surface and sub-surface water storage in the Ganges- Brahmaputra River Basin, J. Hydrol. Reg. Stud., 4, 15–35, https://doi.org/10.1016/j.ejrh.2015.03.004, 2015.

Papa, F.; Frappart, F. SurfaceWater Storage in Rivers and Wetlands Derived from Satellite Observations: A Review of Current Advances and Future Opportunities for Hydrological Sciences. Remote Sens.,

13, 4162. https:// doi.org/10.3390/rs13204162, 2021.

Paris, Adrien, De Paiva, R. D., Da Silva, J. S., Moreira, D. M., Calmant, S., Garambois, P.-A., Collischonn, W., Bonnet, M., and Seyler, F.: Stage-discharge rating curves based on satellite altimetry and modeled discharge in the Amazon basin, Water Resour. Res., 52, 3787–3814, https://doi.org/10.1002/2014WR016618, 2016.

Paris, A., Calmant, S., Gosset, M., Fleischmann, A. S., Conchy, T. S. X., Garambois, P.-A., Bricquet, J.-P., Papa, F., Tshimanga, R. M., Guzanga, G. G., Siqueira, V. A., Tondo, B.-L., Paiva, R., da Silva, J. S., and Laraque, A.: Monitoring Hydrological Variables from Remote Sensing and Modeling in the Congo River Basin, in: Congo Basin Hydrology, Climate, and Biogeochemistry edited by: Tshimanga, R. M., N'kaya, G. D. M., and Alsdorf, D., AGU, https://doi.org/10.1002/9781119657002.ch18, 2022.

Pervez, M. S., and Henebry, G. M. Spatial and seasonal responses of precipitation in the Ganges and Brahmaputra river basins to ENSO and Indian Ocean dipole modes : implications for flooding and drought. *Nat. Hazards Earth Syst. Sci.*, *15*, 147–162. https://doi.org/10.5194/nhess-15-147-2015, 2015.

Pham-duc, B., Papa, F., Prigent, C., Aires, F., Biancamaria, S., Frappart, F. Variations of Surface and Subsurface Water Storage in the Lower Mekong Basin (Vietnam and Cambodia) from Multisatellite Observations. Water, 11(1), 1–17. https://doi.org/10.3390/w11010075, 2019.

Pham-Duc, B.; Sylvestre, F.; Papa, F.; Frappart, F.; Bouchez, C.; Crétaux, J.-F. The Lake Chad hydrology under current climate change. Sci. Rep., 10, 5498, https://doi.org/10.1038/s41598-020-62417-w, 2020.

Potapov, P., Li, X., Hernandez-Serna, A., Tyukavina, A., Hansen, M.C., Kommareddy, A., Pickens, A., Turubanova, S., Tang, H., Silva, C.E., Armston, J., Dubayah, R., Blair, J. B., Hofton, M. Mapping and monitoring global forest canopy height through integration of GEDI and Landsat data, Remote Sens. Environ., 112165. https://doi.org/10.1016/j.rse.2020.112165, 2020.

Prigent, C., Jimenez, C., and Bousquet, P.: Satellite-Derived Global Surface Water Extent and Dynamics Over the Last 25 Years (GIEMS-2), J. Geophys. Res.-Atmos., 125, 1–21, https://doi.org/10.1029/2019JD030711, 2020.

Raymond, P.A.; Hartmann, J.; Lauerwald, R.; Sobek, S.; McDonald, C.; Hoover, M.; Butman, D.; Striegl, R.; Mayorga, E.; Humborg, C.; et al. Global carbon dioxide emissions from inland waters. Nature, 503, 355–359, https://doi.org/10.1038/nature12760, 2013.

Reis, V.; Hermoso, V.; Hamilton, S.K.; Ward, D.; Fluet-Chouinard, E.; Lehner, B.; Linke, S. A Global Assessment of Inland Wetland Conservation Status. Bioscience, 67, 523–533, https://doi.org/10.1093/biosci/bix045, 2017.

Richey, J.E.; Melack, J.M.; Aufdenkampe, A.; Ballester, V.M.; Hess, L.L. Outgassing from Amazonian rivers and wetlands as a large tropical source of atmospheric CO2. Nature, 416, 617–620, https://doi.org/10.1038/416617a, 2002.

Richey, A. S., Thomas, B. F., Lo, M. H., Reager, J. T., Famiglietti, J. S., Voss, K., Swenson, S., Rodell, M. Quantifying renewable groundwater stress with GRACE. Water Resources Research, 51(7), 5217–5237. https://doi.org/10.1002/2015WR017349, 2015.

Rodell, M.; Beaudoing, H.K.; L'Ecuyer, T.S.; Olson, W.S.; Famiglietti, J.; Houser, P.R.; Adler, R.; Bosilovich, M.G.; Clayson, C.A.; Chambers, D.; et al. The Observed State of the Water Cycle in the Early Twenty-First Century. J. Clim., 28, 8289–8318, https://doi.org/10.1175/JCLI-D-14-00555.1, 2015.

Scanlon, B. R., Zhang, Z., Rateb, A., Sun, A., Wiese, D., Save, H., Beaudoing, H., Lo, M. H., Müller-Schmied,

H., Döll, P., Beek, R. van, Swenson, S., Lawrence, D., Croteau, M., Reedy, R. C. Tracking Seasonal Fluctuations in Land Water Storage Using Global Models and GRACE Satellites. Geophysical Research Letters, 46(10), 5254–5264. https://doi.org/10.1029/2018GL081836, 2019.

Shelton, M.L. Hydroclimatology, Perspectives and applications, Cambridge University Press, New York, https://assets.cambridge.org/97805218/48886/frontmatter/9780521848886_frontmatter.pdf (last accessed: 17/05/2023), 2009.

Sridhar, V., Kang, H., Ali, S. A., Bola, G. B., Tshimanga, M. R., Lakshmi, V.: Bilan hydrique et sechéresse dans les conditions ctuelles et futures dans le bassin du fleuve Congo, in: Congo Basin Hydrology, Climate, and Biogeochemistry edited by: Tshimanga, R. M., N'kaya, G. D. M., and Alsdorf, D., AGU, https://doi.org/10.1002/9781119657002.ch18, 2022.

Stephens, G.L.; Slingo, J.M.; Rignot, E.; Reager, J.T.; Hakuba, M.Z.; Durack, P.J.; Worden, J.; Rocca, R. Earth's water reservoirs in a changing climate. Proc. R. Soc. A, 476, 20190458, https://doi.org/10.1098/rspa.2019.0458, 2020.

Steffen, W.; Richardson, K.; Rockström, J.; Cornell, S.E.; Fetzer, I.; Bennett, E.M.; Biggs, R.; De Carpenter, S.R.; Carpenter, S.R.; De Vries, W.; et al. Planetary boundaries: Guiding human development on a changing planet. Science, 347, 1259855, DOI: 10.1126/science.12598, 2015.

Tapley, B. D., Bettadpur, S., Watkins, M., & Reigber, C. The gravity recovery and climate experiment: Mission overview and early results. Geophysical research letters, 31(9), https://doi.org/10.1029/2004GL019920, 2004.

Tapley, B. D., Watkins, M. M., Flechtner, F., Reigber, C., Bettadpur, S., Rodell, M., ... & Velicogna, I. Contributions of GRACE to understanding climate change. Nature climate change, 9(5), 358-369, https://doi.org/10.1038/s41558-019-0456-2, 2019.

Tourian, M.J.; Reager, J.T.; Sneeuw, N. The Total Drainable Water Storage of the Amazon River Basin: A First Estimate Using GRACE. Water Resour. Res., 54, 3290–3312, https://doi.org/10.1029/2017WR021674, 2018.

Tourian, M. J., Elmi, O., Shafaghi, Y., Behnia, S., Saemian, P., Schlesinger, R., & Sneeuw, N. HydroSat: geometric quantities of the global water cycle from geodetic satellites. Earth System Science Data, 14(5), 2463-2486, doi: 10.5194/essd-2021-174, 2022.

Tourian, M.J., Papa, F., Elmi, O., Sneeuw, N., Kitambo, B., Tshimanga, R., Paris, A., Calmant S.: Current availability and distribution of Congo Basin's freshwater resources. Commun Earth Environ 4, 174, https://doi.org/10.1038/s43247-023-00836-z, 2023.

Trenberth, K.E.; Smith, L.; Qian, T.; Dai, A.; Fasullo, J. Estimates of the global water budget and its annual cycle using observational and model data. J. Hydrometeorol., 8, 758–769, https://doi.org/10.1175/JHM600.1, 2007.

Trenberth, K.E.; Fasullo, J.; Mackaro, J. Atmospheric Moisture Transports from Ocean to Land and Global Energy Flows in Reanalyses. J. Clim., 24, 4907–4924, https://doi.org/10.1175/2011JCLI4171.1, 2011.

Tshimanga, R. M., N'kaya, G. D. M., & Alsdorf, D. Congo Basin Hydrology, Climate, and Biogeochemistry A Foundation for the Future (R. M. Tshimanga, G. D. M. N'kaya, & D. Alsdorf (eds.)). American Geophysical

Union and John Wiley and Sons, Inc., 2022.

Ummenhofer, C. C., England, M. H., Mcintosh, P. C., Meyers, G. A., Pook, M. J., Risbey, J. S., and Gupta, A. Sen. What causes southeast Australia ' s worst droughts ? *Geophys. Res. Lett.*, *36*, 1–5. https://doi.org/10.1029/2008GL036801, 2009.

Verhegghen, A., Mayaux, P., De Wasseige, C., and Defourny, P.: Mapping Congo Basin vegetation types from 300m and 1 km multi-sensor time series for carbon stocks and forest areas estimation, Biogeosciences, 9, 5061–5079, https://doi.org/10.5194/bg-9-5061-2012, 2012.

Vörösmarty, C.J.; McIntyre, P.B.; Gessner, M.O.; Dudgeon, D.; Prusevich, A.; Green, P.; Glidden, S.; Bunn, S.E.; Sullivan, C.A.; Liermann, C.R.; et al. Global threats to human water security and river biodiversity. Nature, 467, 555–561, https://doi.org/10.1038/nature09440, 2010.

Ward, N.D.; Bianchi, T.; Medeiros, P.M.; Seidel, M.; Richey, J.E.; Keil, R.G.; Sawakuchi, H.O. Where Carbon Goes WhenWater Flows: Carbon Cycling across the Aquatic Continuum. Front. Mar. Sci., 4, https://doi.org/10.3389/fmars.2017.00007, 2017.

Watkins, M. M., D. N. Wiese, D.-N. Yuan, C. Boening, and F. W. Landerer. Improved methods for observing Earth's time variable mass distribution with GRACE using spherical cap mascons, J. Geophys. Res. Solid Earth, 120, doi:10.1002/2014JB011547, 2015.

White, L. J. T., Masudi, E. B., Ndongo, J. D., Matondo, R., Soudan-Nonault, A., Ngomanda, A., Averti, I. S., Ewango, C. E. N., Sonké, B., and Lewis, S. L.: Congo Basin rainforest - invest US$150 million in science. Nature, 598(7881), 411–414. https://doi.org/10.1038/d41586-021-02818-7, 2021.

Wiese, D. N., F. W. Landerer, and M. M. Watkins. Quantifying and reducing leakage errors in the JPL RL05M GRACE mascon solution, Water Resour. Res., 52, 7490–7502, doi:10.1002/2016WR019344, 2016.

Wiese, D.-N. Yuan, C. Boening, F. W. Landerer, M. M. Watkins. JPL GRACE Mascon Ocean, Ice, and Hydrology Equivalent Water Height Release 06 Coastal Resolution Improvement (CRI) Filtered Version 1.0. Ver. 1.0. PO.DAAC, CA, USA. Dataset accessed [2023-05-17] at http://dx.doi.org/10.5067/TEMSC-3MJC6, 2018.

Wohl, E. An Integrative Conceptualization of Floodplain Storage. Rev. Geophys., 59, e2020RG000724, https://doi.org/10.1029/2020RG000724, 2021.

Yamazaki D., Ikeshima, D., Tawatari, R., Yamaguchi, T., O'Loughlin, F., Neal, J.C., Sampson, C.C., Kanae, S., Bates, P.D. A high accuracy map of global terrain elevations, Geophys. Res. Lett., 44, pp.5844-5853, doi: 10.1002/2017GL072874, 2017.

Yuan T, Lee H, Jung CH, Aierken A, Beighley E, Alsdorf DE, Tshimanga RM, Kim D. Absolute water storages in the Congo River floodplains from integration of InSAR and satellite radar altimetry. Remote Sens Environ 201:57–72. https:// doi. org/ 10. 1016/j. rse. 2017. 09. 003, 2017.

Zakharova, E., Nielsen, K., Kamenev, G., and Kouraev, A.: River discharge estimation from radar altimetry: Assessment of satellite performance, river scales and methods, J. Hydrol., 583, 124561, https://doi.org/10.1016/j.jhydrol.2020.124561, 2020.

Zhou, T.; Nijssen, B.; Gao, H.; Lettenmaier, D.P. The Contribution of Reservoirs to Global Land Surface Water Storage Variations. J. Hydrometeorol., 17, 309–325, https://doi.org/10.1175/JHM-D-15-0002.1, 2016.

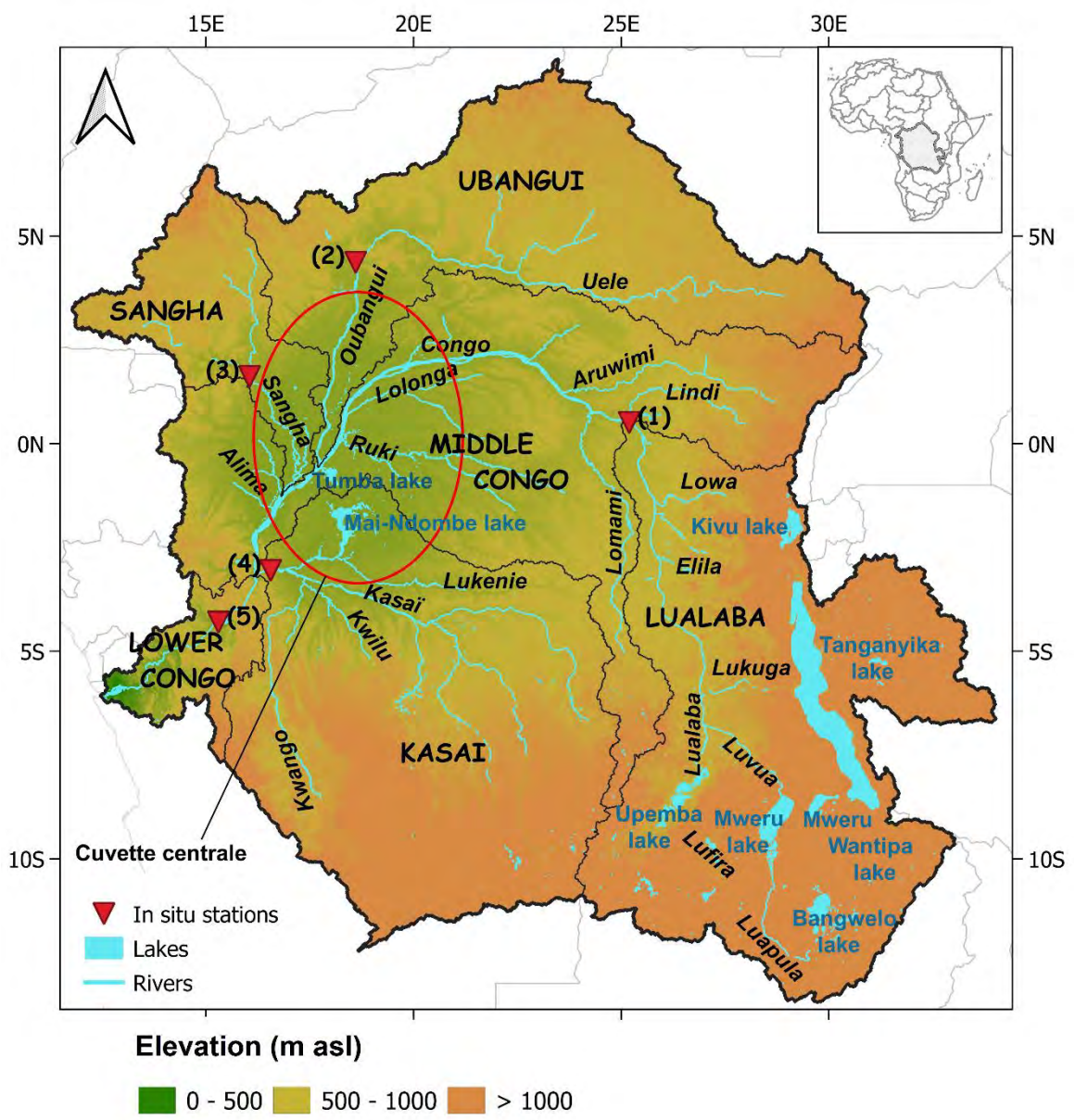

Figure 1: The Congo River basin (CRB) and its main subbasins (thin dark line), along with the major rivers and lakes (light blue color). The green portion in the central part circled by red line corresponds to the Cuvette Centrale. The background topography is derived from the Multi-Error-Removed Improved Terrain (MERIT) digital elevation model (DEM). The red triangles display the available in situ gauging stations, with their characteristics reported in Table 2.

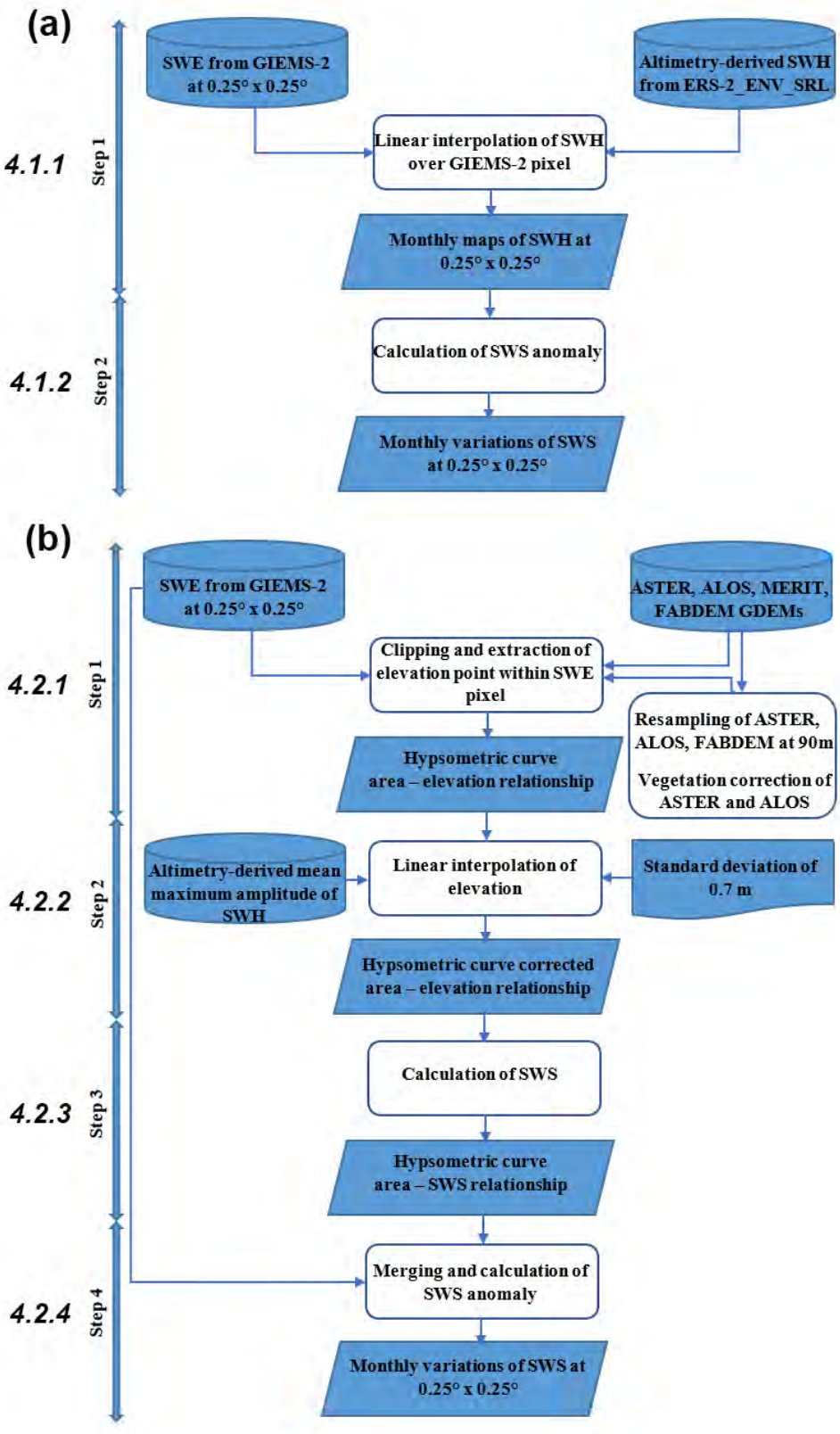

Figure 2: Schematic representation of (a) the multi-satellite and (b) hypsometric curve approaches algorithms. The numbers on the left refer to the sections where the different steps are described.

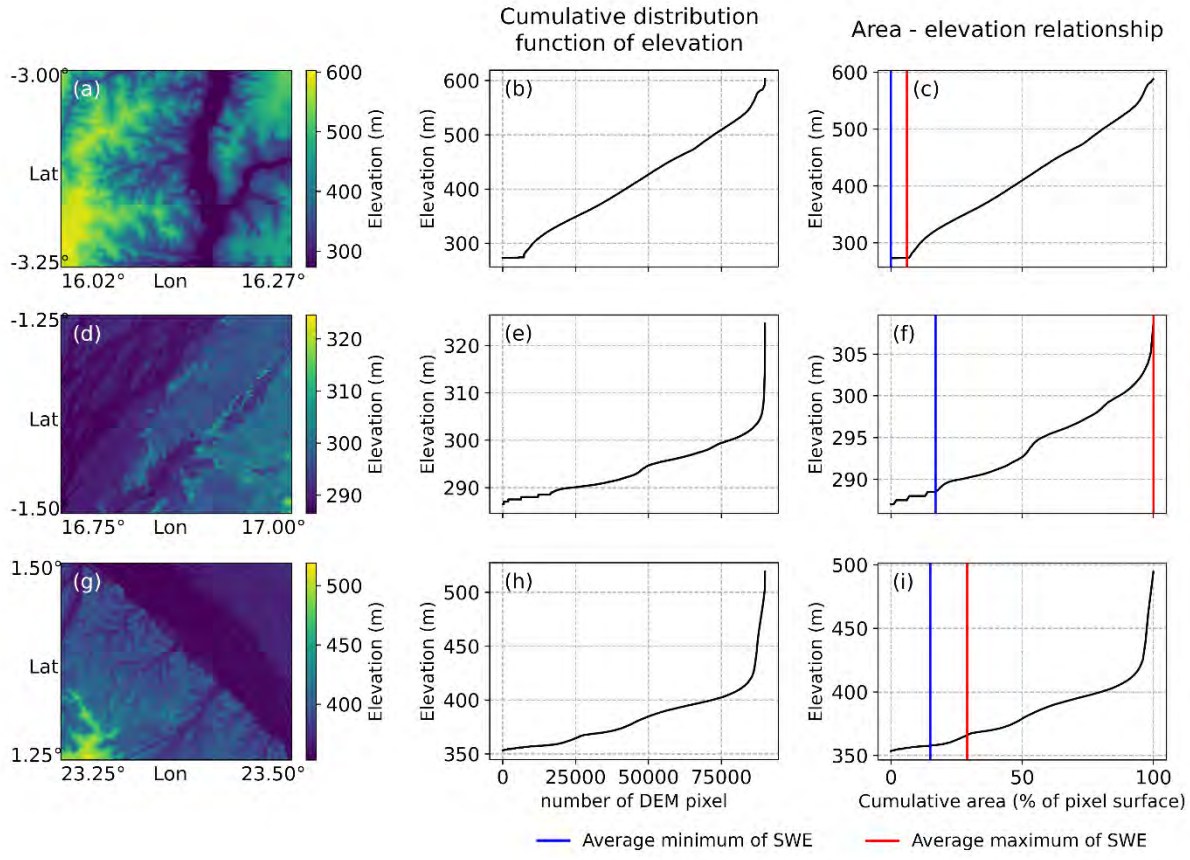

Figure 3: Hypsometric curve from FABDEM over the CRB. Left column: Map of FABDEM elevations within a 773 km^2 pixel of GIEMS-2. Middle column: The hypsometric curve from FABDEM, i.e., the distribution of elevation values in each 773 km^2 pixel sorted in ascending order. Right column: the hypsometric curve from FABDEM providing the relationship between the elevation and the inundated area of 773 km^2 pixel (as a percentage). The blue (red) line is the average minimum (maximum) coverage of SWE observed by GIEMS-2 over 1992-2015.

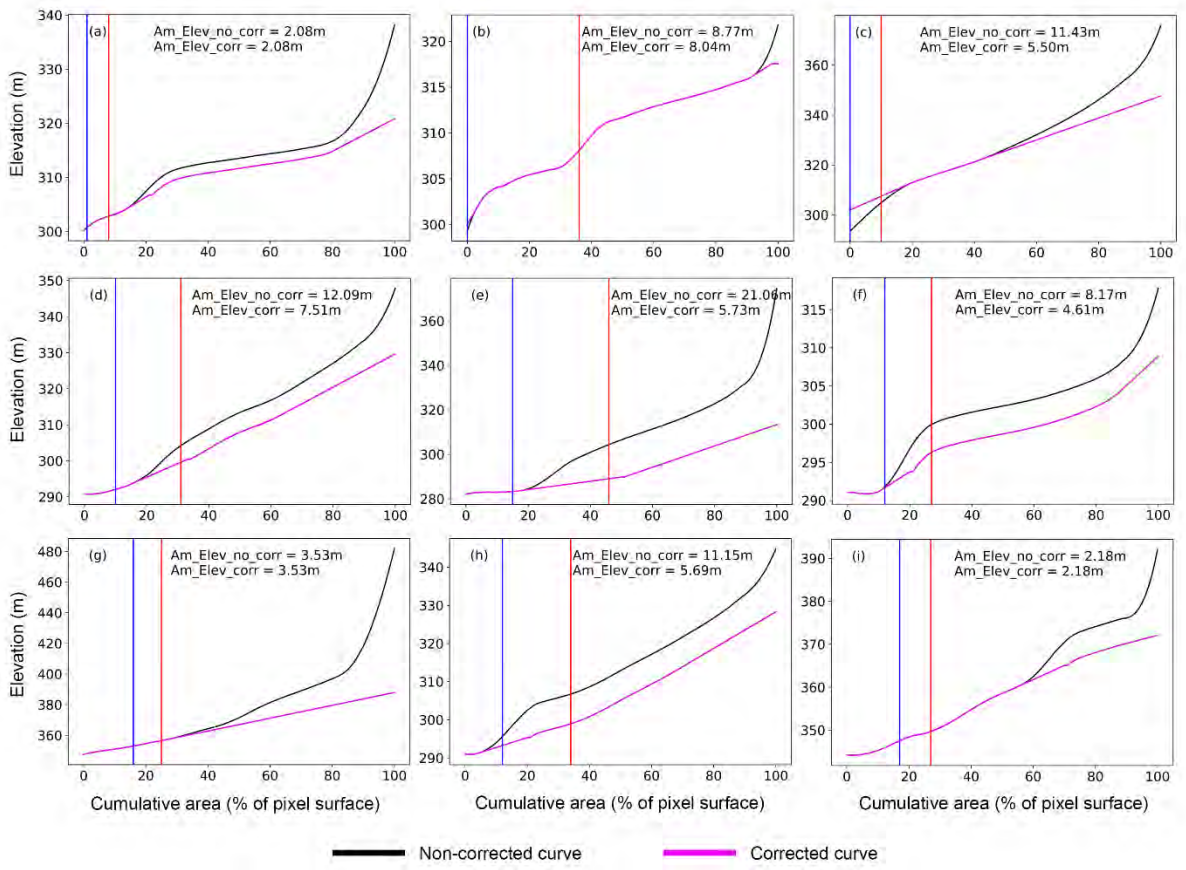

Figure 4: Correction of hypsometric curve from FABDEM by calculating the STD (m) of elevation over 5% flood coverage windows (see details of the procedure in section 4.2.2). Black and magenta curves stand respectively for non-corrected and corrected hypsometric curve. Am_Elev_no_corr (from non-corrected curve) and Am_Elev_corr (from corrected curve) are the elevation amplitude derived from the average minimum (blue line) and maximum (red line) coverage of surface water extent observed by GIEMS-2 over 1992-2015. (a) to (i) show different pixels of GIEMS-2 in which the hypsometric curve is derived.

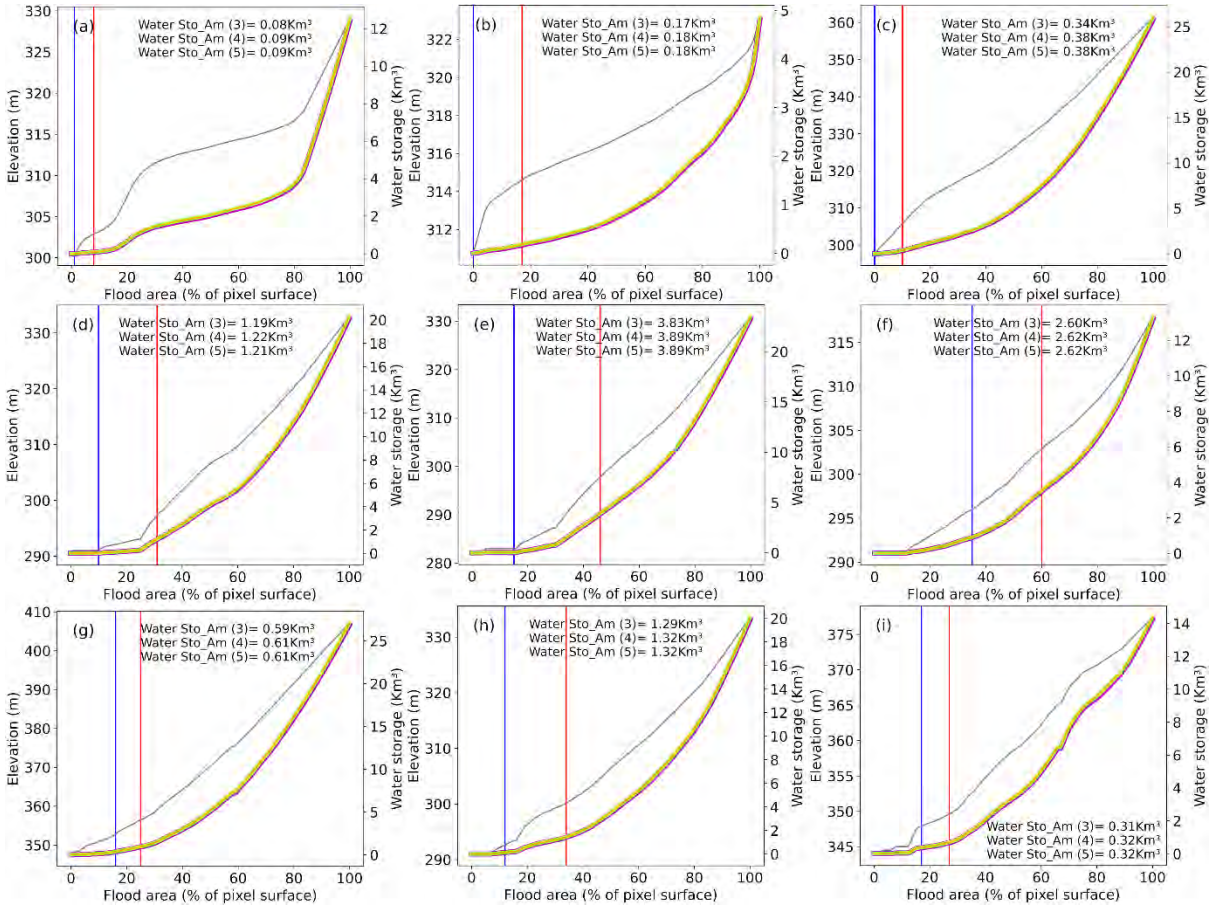

Figure 5: For the same GIEMS-2 pixel as in Fig. 3, the Surface Water Storage profile, i.e., the relationship between SWS within each GIEMS-2 pixel and the fractional inundated area of 773 km² in percentage (abscissa – right ordinate) obtained from the area-elevation relationship (abscissa – left ordinate). Magenta, green, orange colors are respectively the curve of SWS from the formulas (3), (4), and (5). The grey curve stands for the corrected FABDEM hypsometric curve. The blue (red) line is the average minimum (maximum) coverage of surface water extent observed by GIEMS-2 over 1992-2015. (a) to (i) represent different pixels of GIEMS-2 in which the hypsometric curve is derived.

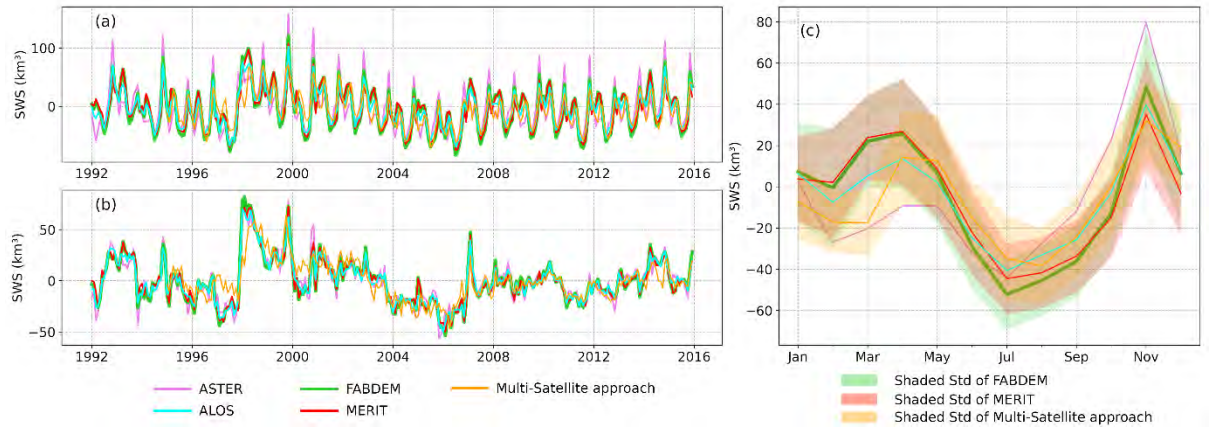

Figure 6: Long-term monthly time series of Congo River Basin's Surface Water Storage (a) and its deseasonalized anomaly (b) obtained from the hypsometric curve approach for 1992-2015 (violet for ASTER, aqua for ALOS, limegreen for FABDEM, red for MERIT) and from the multi-satellite approach for 1995-2015 (orange) (c) Annual cycles for each SWS estimate, with the shaded areas illustrating the standard deviations around their long-term mean.

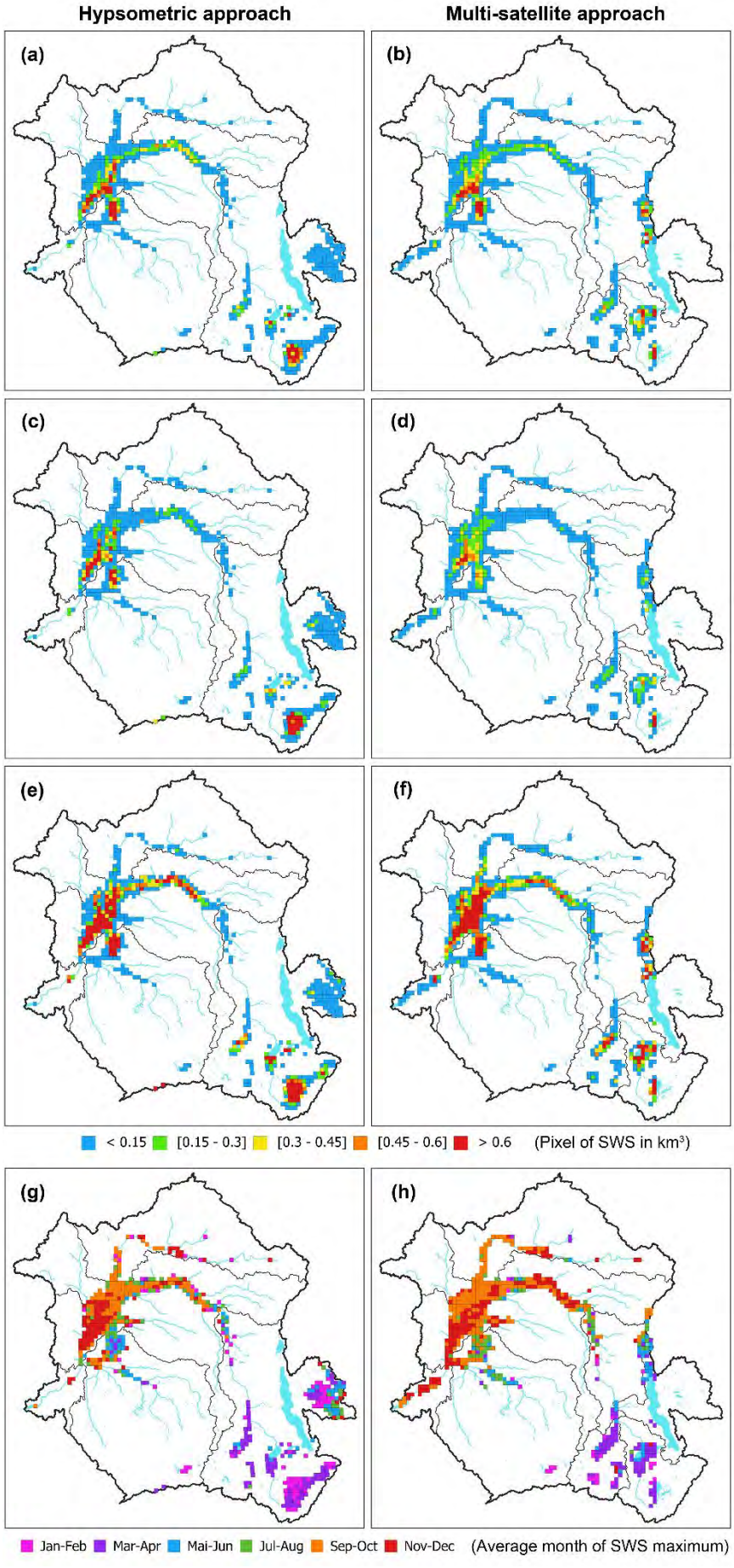
Hypsometric approach
Multi-satellite approach
(a)
(b)
(c)
(d)
(e)
(f)
(g)
(h)
< 0.15
[0.15 - 0.3]
[0.3 - 0.45]
[0.45 - 0.6]
> 0.6
(Pixel of SWS in km³)
Jan-Feb
Mar-Apr
Mai-Jun
Jul-Aug
Sep-Oct
Nov-Dec
(Average month of SWS maximum)

1150

Figure 7: Spatial characterization of the CRB's SWS variations from the FABDEM hypsometric curve approach (over 1992– 2015, left column) and from the multi-satellite approach (over 1995-2015, right column). (a, b): SWS mean annual amplitude in km^3; (c, d) Standard deviation (STD) in km^3, (e, f) mean annual maximum in km^3 and (g, h) average month of the maximum (in month).

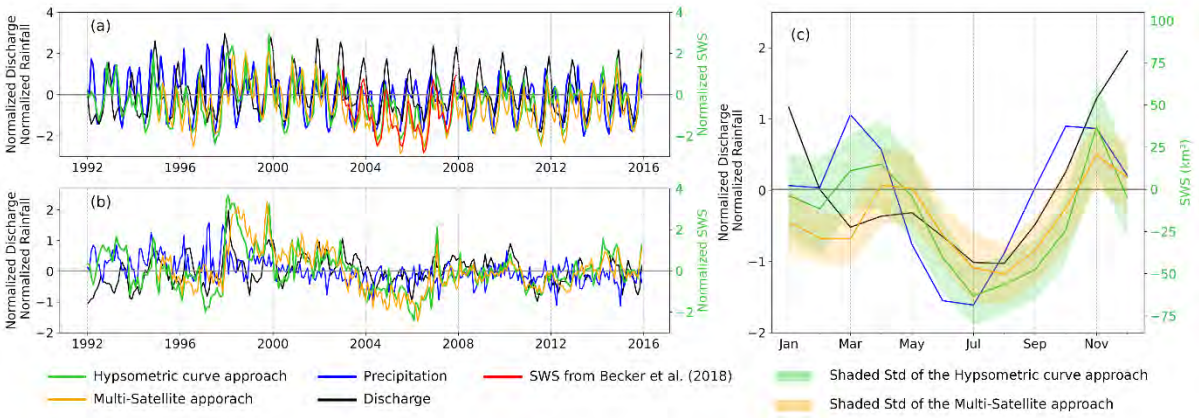

Figure 8: Comparison between the monthly aggregated normalized surface water storage anomaly, normalized precipitation anomaly over the basin and normalized discharge anomaly variations (at the outlet of CRB, Brazzaville/Kinshasa station) (for comparison purposes, SWS, precipitation and discharge were normalized by dividing their time series of anomalies by the standard deviation of the raw series). (a) For the entire Congo basin, the green and orange line represent respectively the SWS anomaly variations from hypsometric curve (over 1992-2015, from FABDEM) and multi-satellite (over 1995-2015) approaches, the red line shows SWS anomaly estimated by Becker et al. (2018) over 2003-2007, the black line is the discharge, the blue line is the normalized precipitation anomaly. (b) Deseasonalized normalized anomaly for SWS (green and orange), precipitation (blue), and discharge (black). (c) Normalized mean annual cycle for the three variables (except for the SWS), with the shaded areas depicting the standard deviations around the SWS anomaly.

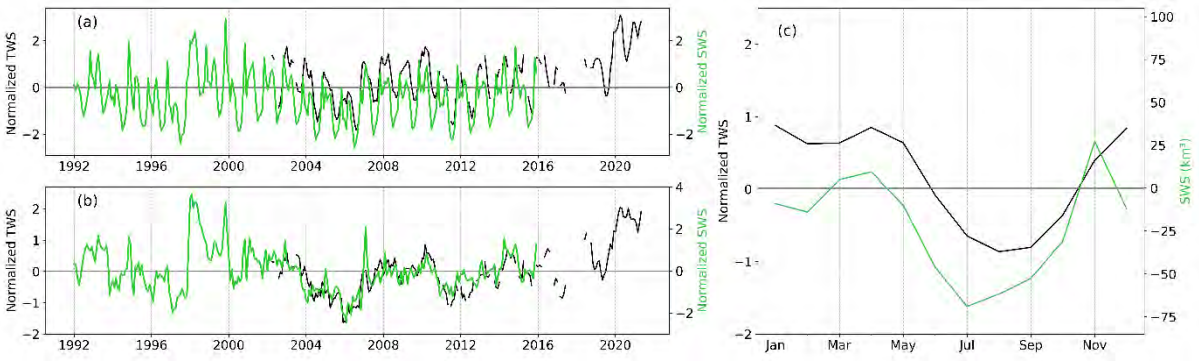

Figure 9. Comparison between the monthly aggregated normalized surface water storage anomaly and the normalized Terrestrial Water Storage Anomaly over the basin (for comparison purposes, SWS and TWSA were normalized by dividing their time series of anomalies by the standard deviation of the raw series). (a) For the entire Congo basin, the green and black line represent respectively the SWS anomaly variations from hypsometric curve approach (over 1992-2015, from FABDEM) and TWSA. (b) Deseasonalized normalized anomaly for SWS (green) and TWSA (black). (c) Normalized mean annual cycle for TWSA (black) (except for SWS, in green) calculated over the same period of data availability of the two variables, SWS and TWSA.

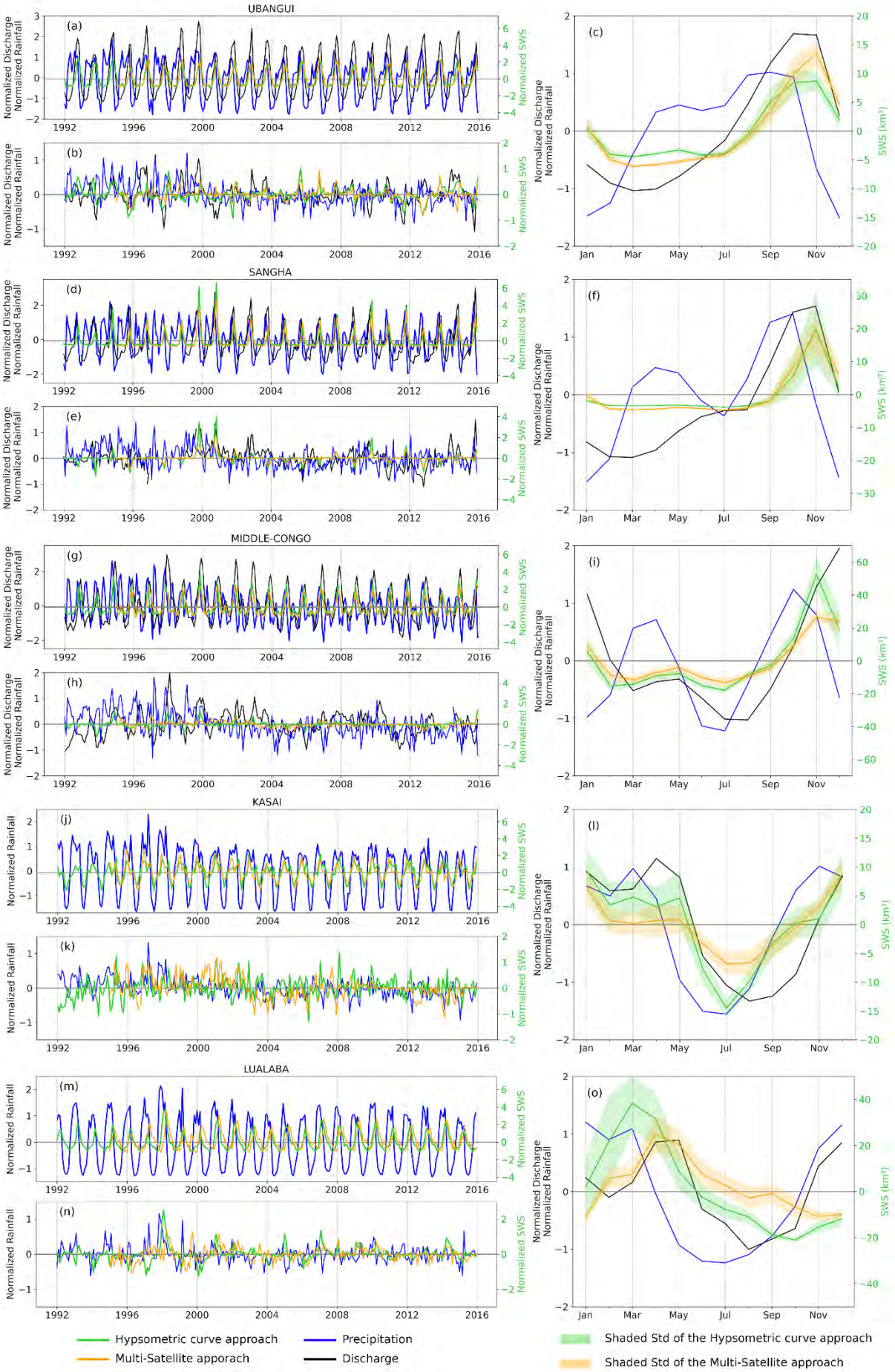
UBANGUI
(a)
(b)
(c)
SANGHA
(d)
(e)
(f)
MIDDLE-CONGO
(g)
(h)
(i)
KASAI
(j)
(k)
(l)
LUALABA
(m)
(n)
(o)
Normalized Discharge
Normalized Rainfall
Normalized SWS
SWS (km³)
1992
1996
2000
2004
2008
2012
2016
Jan
Mar
May
Jul
Sep
Nov
Hypsometric curve approach
Multi-Satellite apporach
Precipitation
Discharge
Shaded Std of the Hypsometric curve approach
Shaded Std of the Multi-Satellite approach

Figure 10: Same to Fig. 8 but the discharge is considered at the outlets of each sub-basin, and the precipitation is the estimated mean over each sub-basin, both are compared to the normalized SWS anomaly variations. (a) For each sub-basin, the green and orange line represents respectively the SWS anomaly variations from hypsometric curve (over 1992-2015, from FABDEM) and multi-satellite (over 1995-2015) approaches, the red line shows SWS anomaly from Becker et al. (2018) over 2003-2007, the black line is the normalized discharge anomaly, the blue line is the normalized precipitation anomaly. (b) Deseasonalized normalized anomaly for SWS (green and orange), precipitation (blue), and discharge (black). (c) Normalized mean annual cycle for the three variables (except for the SWS), with the shaded areas depicting the standard deviations around the SWS anomaly.

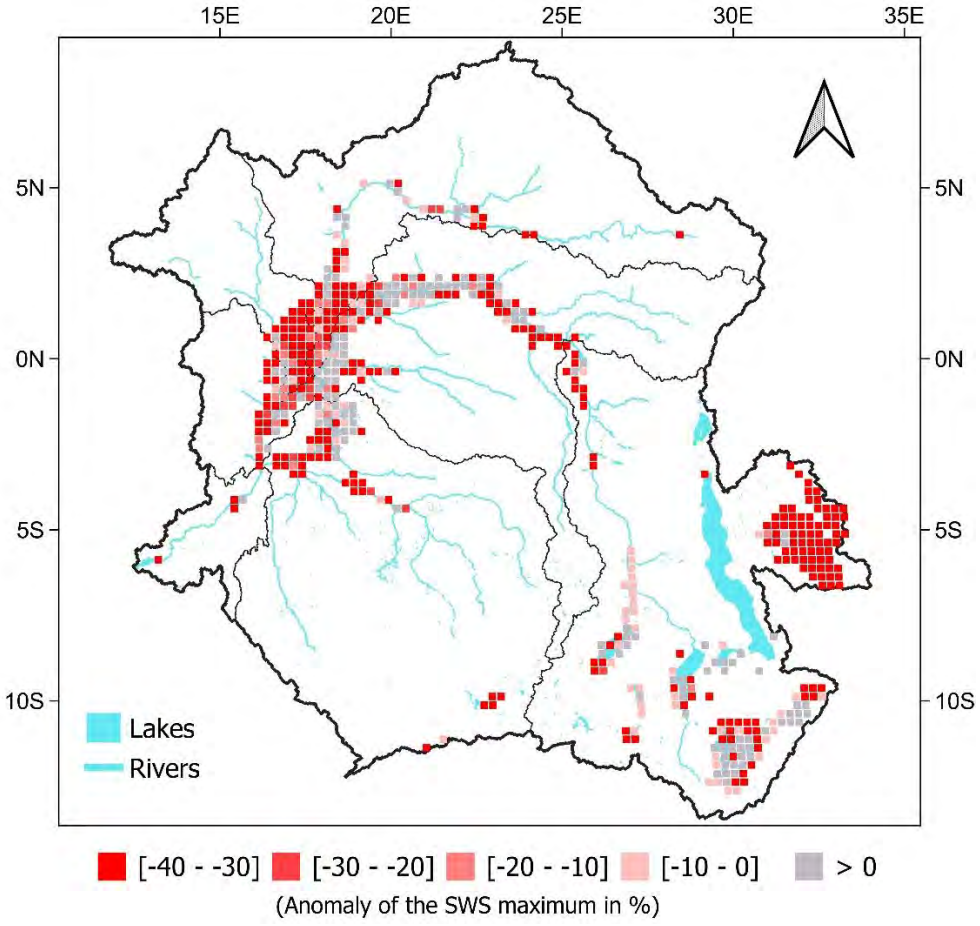

Figure 11: The 2005-2006 drought over the CRB as seen from the hypsometric curve approach SWS dataset based on FABDEM. Anomaly of the maximum SWS over November 2005 to January 2006 as compared to the 1992-2015 November-December-January mean value. The unit is in percentage of the 24-years mean monthly value.

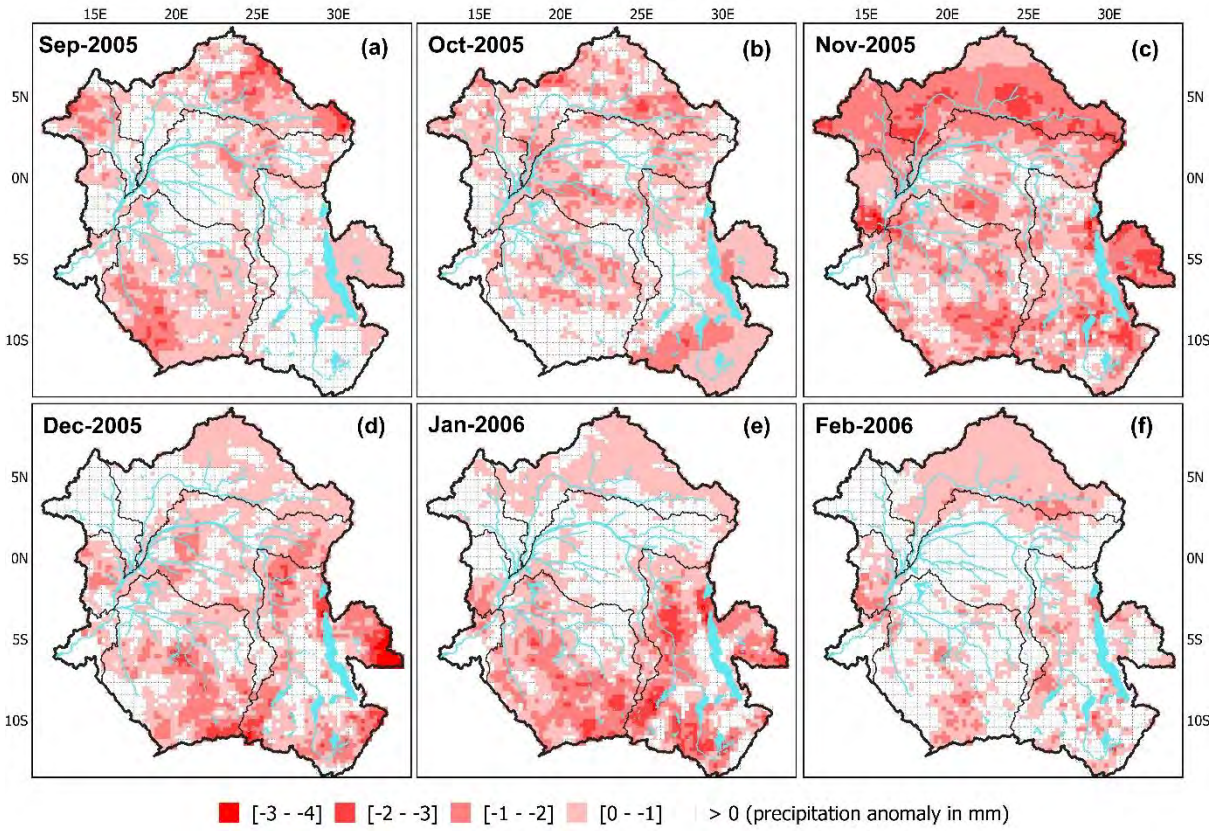

Figure 12: Monthly mean spatial distribution of MSWEP precipitation anomaly in mm (resampled at 0.25° spatial resolution) from the period September 2005 to February 2006 based on the 1992-2015 climatology.

Table 1: Characteristics of the used Digital Elevation Models.

Dataset	**ALOS AW3D30**	**ASTER**	**MERIT**	**FABDEM**
Producer	JAXA Japan Aerospace Exploration Agency	NASA & METI National Aeronautics and Space Administration (US) Ministry of Economy, Trade, and Industry (Japan)	University of Tokyo	University of Bristol
Available at	https://www.eorc.jaxa.jp/ALOS/en/aw3d30/data/index.htm, last access: 17 May 2023	https://search.earthdata.nasa.gov/search/?fst0=Land%20Surface, last access: 17 May 2023	http://hydro.iis.u-tokyo.ac.jp/~yamadai/MERIT_DEM/, last access: 17 May 2023	https://doi.org/10.5523/bris.25wfy0f9ukoge2gs7a5mqpq2j7, last access: 17 May 2023
DEM coverage	90N-90S	83N-83S	90N-60S	80N-60S
Acquisition year	2006–2011	2000–2013	2000	2011–2015

Sensor	Panchromatic Remote-sensing Instrument for Stereo Mapping	Optical	AW3D30, Shuttle Radar Topography Mission (SRTM) & Viewfinder Panorama	Synthetic Aperture Radar (SAR) interferometer
Vertical datum	Orthometric EGM96	Orthometric EGM96	Orthometric EGM96	Orthometric EGM2008
Spatial resolution	30 m	30 m	90 m	30 m

Table 2: Location and main characteristics of the in situ discharge stations used in this study. The number in the first column refers to the location of the station in Fig. 1.

N°	Name	Latitude	Longitude	Sub-basin	Period	Source
1	Kisangani	0.51	25.19	Lualaba	1950-1959	CRREBaC
2	Bangui	4.37	18.61	Ubangui	1936-2020	CRREBaC/ SO-Hybam
3	Ouesso	1.62	16.07	Sangha	1947-2020	CRREBaC/ SO-Hybam
4	Lediba	-3.06	16.56	Kasaï	1950-1959	CRREBaC
5	Brazzaville/ Kinshasa	-4.3	15.30	Middle-Congo	1903-2020	CRREBaC/ SO-Hybam

Table 3: Mean annual amplitude over the CRB calculated from multi-satellite and hypsometric curve approaches. Error statistics comparing SWS from ALOS, ASTER, MERIT, and the multi-satellite approach against SWS from FABDEM, considered here as the reference. Comparisons are done over the same period by aggregating all SWS pixels over the basin for the compared datasets. MAE stands for mean absolute error and RMSE for root mean squared error, in km^3.

Method	DEM	Time span	Mean annual amplitude (km^3)	Error in relation to SWS from FABDEM (km^3)	
				MAE	RMSE
Hypsometric curve approach	FABDEM	1992 - 2015	101 ± 23	/	/
	ALOS	1992 - 2015	80 ± 17	9	11
	ASTER	1992 - 2015	124 ± 25	22	26
	MERIT	1992 - 2015	80 ± 20	5	7
Multi-satellite approach	/	1995 - 2015	70 ± 17	18	22

Table 4: Summary of the maximum linear Pearson correlation coefficient r along with the lag for the comparison between SWS, precipitation, and discharge. Des. Ano. stands for deseasonalized anomalies. In bold are shown the

significant correlation coefficients with p value < 0.01. For Kasaï and Lualaba sub-basins no contemporary discharge data are available therefore no correlation are reported.

Basin and sub-basin	r(lag)			
	SWS vs Precipitation		SWS vs Discharge	
	Raw series	Des. Ano.	Raw series	Des. Ano.
CRB	**0.56**(0)	**0.12(0)**	**0.57**(0)	**0.52**(0)
Sangha	0.04(0)	0.15(-2)	**0.73**(0)	**0.43**(0)
Ubangui	**0.63**(-2)	-0.06(3)	**0.89**(0)	**0.39**(0)
Middle-Congo	**0.32**(0)	0(3)	**0.87**(1)	**0.58**(1)
Kasaï	**0.69**(0)	0.03(-2)	/	/
Lualaba	**0.50**(0)	**0.43**(-2)	/	/

5.3 Conclusion

The mains findings of this paper on the CRB's SWS can be resumed as follows:

- The long-term variations of the CRB's SWS over 24-year shows a strong seasonal cycle and a comparable behavior in the peak to-peak SWS variations from both approaches and different DEMs along with an amplitude ranging from ~50 to ~150 km^3 over the years. At the sub-basin scale, Middle-Congo and Lualaba sub-basins present higher amplitude (i.e., respectively 71 ± 15 km^3 and 59 ± 15 km^3) due to the presence of large wetlands in these regions.
- At the basin scale, the SWS estimates show a substantial interannual variability especially in terms of annual maximum and minimum, pointing out extreme events in terms of droughts and floods that recently affected the CRB. An example of the exceptional drought and flood documented respectively in 2005-2006 and in 1997-1998. At the sub-basin scale, Kasaï and Lualaba sub-basins are the only ones that captured the exceptional flood signal that occurred in 1997-1998.
- The spatial distribution of the SWS has shown a realistic pattern for major tributaries of the CRB and its analysis showed large SWS variability (e.g., 0.3 to 0.6 km^3) over the extensive wetlands and floodplains such as the *Cuvette Centrale* and in the southeastern part (i.e., Bangweulu, Mweru, Upemba) of the basin. In the *Cuvette Centrale*, the maximum SWS values are reached in September-October in the upper part and in November-December in the lower part.
- The spatial signature of the widespread drought that took place in the end of 2005 and the beginning of 2006 across the CRB, revealing the severity of this particular event on surface freshwater storage, in agreement with satellite-derived precipitation observations, with the northeast of the *Cuvette Centrale* and some tributaries of the Kasaï River (in the Mai-Ndombe Lake region) less impacted.

These unique long-term monthly time series of the CRB's SWS provide the broad characteristic of the variability of surface water storage anomaly at the basin and sub-basin levels over 24-year in the CRB. It opens new perspectives to move toward answering several crucial scientific questions regarding the role of SWS dynamics into the hydrological and biogeochemical cycles of the CRB. Since GIEMS-2 and the DEMs used in this study are available globally, our results thus present also a new first step toward the development of such SWS databases at the global scale. This information coupled to the output of the MGB hydrodynamic model will allow a

better representation of the local and basin scale hydrodynamics and will ensure a better real-time monitoring of the hydrological variables from space.

Chapter 6: Long-term daily simulation of hydrological variables using hydrodynamic modeling in the Congo basin

This chapter is structured as an article-based to be submitted soon. Therefore, there are some parts mentioned or treated previously to which we will be referred to.

6.1 Introduction

In the CRB, in situ hydroclimate observations are very limited (Laraque et al., 2020). For instance, the Global Data Runoff Centre (GRDC) portal that displays hydrological information related to in situ river discharge stations worldwide from different national hydrological services enables to point out a dramatically decreased of contemporary observations over Africa and Asia (https://portal.grdc.bafg.de/applications/public.html?publicuser=PublicUser#data Download /Home, last access 13 February 2023). Similar observations have been highlighted in other studies for Africa (i.e., Tramblay et al., 2021). As seen in section 3.2 dedicated to in situ data, Alsdorf et al. (2016) and Tshimanga (2022) reported that almost 400 flow monitoring gauges were installed within the CRB before the 1960s, while today, there are only 15 gauges considered operational (Laraque et al., 2020). Therefore, this critical state of the lack of in situ data limits our understanding of the major factors controlling freshwater dynamics at the adequate space and time scales and prevents the development of appropriate and sustainable strategies to manage water resources in the CRB (Tshimanga et al., 2022a). Meanwhile, the recent advances in earth observations provide an unprecedented opportunity for hydrological monitoring and predictions at finer scales in these large river basins.

To add value to the existing poor and limited in situ data as well as given the need to simulate hydrological variables at the required space and time scales of management, catchment modeling is often used to estimate different components of the hydrological cycle (Singh, 2018), as highlighted in the section 2.3 of this thesis.

As seen in section 1.2, during the past two decades, several hydrological modeling studies have been carried out in the CRB using different type of models, including statistical models, process-based hydrological models and hydrodynamic models to overcome the lack of observational data and contribute to the understanding of the CRB's hydrologic variability and processes at the large scale (Tshimanga et al., 2011; Tshimanga and Hughes, 2014; Aloysius and Saiers, 2017; Munzimi et al., 2019; O'Loughlin et al., 2019; Kabuya et al., 2020; Datok et

al., 2022; Tshimanga, 2022; Paris et al., 2022; among others. For more details about these studies, refers to the aforementioned section.

Many of these studies have been challenged by various issues, including, the lack of in situ hydrological data with sufficient spatial and temporal coverage that could reasonably enable the implementation of models in the basin, taking into consideration its geographic extent and the natural complexity of the processes to be modelled (Munzimi et al., 2019; Paris et al., 2022), processes understanding (Kabuya et al., 2020; Tshimanga, 2022), and uncertainty of model structures and parameters (Tshimanga et al., 2011). In addition, there are other many challenges that relate to the adequate representation of some dominate features of lakes and wetlands that dominate the hydrology of the CRB into model structures (Tshimanga and Hughes, 2014; Paris et al., 2022) as well as the adequate representation of the geometry of floodplains and connectivity with the large channels, specifically in the *Cuvette Centrale* (Paris et al., 2022).

It is also worth noting that many of these studies were mainly implemented in an experimental phase, attempting to explore the performance of the hydrological models in a new and tropical data-scarce environment without addressing the real issues of water resources management and support for policy decision in the basin (Tshimanga, 2022). Therefore, there is still an enormous need for the development of comprehensive modeling frameworks to address the many challenges of hydrological predictions and water resources management under the context of growing concerns for global impacts of land use and climate changes on many socio-economic and environmental sectors that depend on water resources availability. Thus, a tool that will serve to formulate policy decisions of water resources management.

This is the aim of this study that consists of developing a robust hydrological model for the CRB, taking the many issues already highlighted in terms of limitation of in situ data, incorporation of lake and wetland processes as well as uncertainty prediction – right modelling for the right reason (Tshimanga, 2022). In this regard, the existing conceptual, semi-distributed, large-scale hydrological-hydrodynamic model MGB (Paris et al., 2022) by integrating lakes and wetland features, spatial distribution vegetation parameters and an adequate representation of the geometry of floodplains in particular the *Cuvette Centrale* using the merging of finer resolution of MERIT DEM (i.e., 90m of spatial resolution) and an unprecedented in situ dataset. It is also worth noting that MGB model simulates some important aspects of river hydrodynamics in largest tropical basin such as backwater effects and flood inundation (Paiva et al., 2013).

The aim of this study is therefore threefold. First, to set-up the large-scale hydrologic-hydrodynamics MGB model at the daily time scale over the period 01 January 2001 to 31 December 2020. Secondly, to use the parameters obtained after calibration along with past climate forcing data to perform hydrological projection for the historical period from 1981 in order to better understand the historical hydroclimate variability in the basin.

Section 2 describes briefly the datasets used in this study and presents the model set-up over the basin along with the major output of the preprocessing steps. Section 3 provides the results of the calibration and validation. In addition to this, this section will present a comparison of the model output with other remotely sensed data.

6.2 Datasets and model set-up

6.2.1. In situ data

The MGB uses input forcing data to simulate hydrological variables of interest and can be calibrated using streamflow and water level data. In this study, the Climate Hazards Group InfraRed Precipitation with Station (CHIRPS) precipitation product and climatological variables such as pressure, insolation, wind, relative humidity and surface temperature from the improved spatial and temporal resolution of ERA5 reanalysis dataset are used as input model forcing data. Streamflow and water level data from nine gauging stations in the basin (Table 6-1 and Fig. 6-1 for their locations) are used for the MGB model calibration for 20 years, 01/01/2001 to 31/12/2020. The Chapter 3 of this Thesis provides details about the source and types of in situ data used (also see Kitambo et al., 2022a). Given the uncertainty surrounding some of the stations, such as the Lediba at the outlet of the Kasai sub-basin, the rating curve taken from literature was used to convert satellite-derived SWH nearby the in situ gauge station into discharge time series (Paris et al., 2022). Beside these contemporary observations overlapping the set-up period, historical observations of discharge and water level from 1981 have also been used at 21 stations (Fig. 6-1) to validate the MGB model during the projection for the historical period from 1981.

For lake calibration purposes, historical discharge time series from five stations (Table 6-1 and Fig. 6-1 for their locations) at monthly climatology time scale from 1950 to 1959 have been used. Considering the period of the hydrological modeling set up, the calibration was performed by analyzing the monthly climatology of the series.

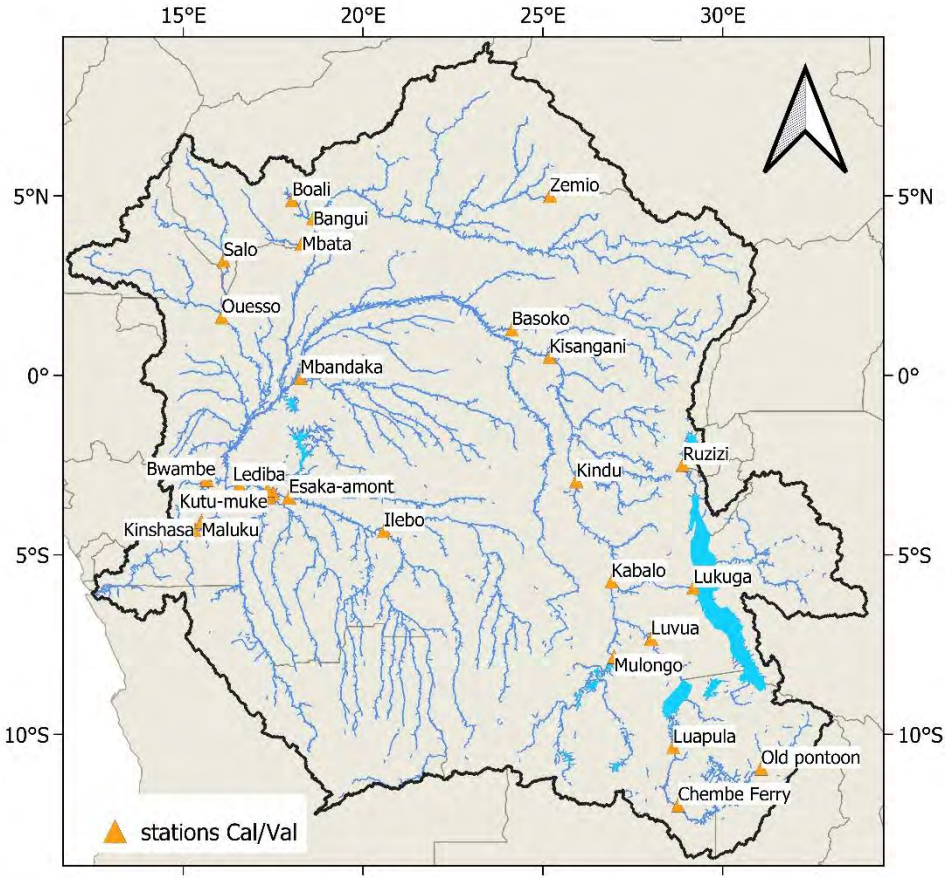

Figure 6-1. In situ stations of river discharge and water stage used for calibration/validation of MGB model.

Table 6-1. Location and main characteristics of in situ stations used for calibration and validation purposes. The locations are displayed in Fig. 6-1.

N°	Name	Lat	Lon	Sub-basin	Variable *	Period	Frequency **	Observation ***	Source
1	Bangui	4.37	18.61	Ubangui	ws/Q	1936-2020	D/M	Cal/val	CRREBaC/ SO-Hybam
2	Ouesso	1.62	16.07	Sangha		1947-2020			
3	Brazzaville/ Kinshasa	-4.3	15.30	Lower-Congo		1903-2020			
4	Lumbu-dima	-3.28	17.5	Kasaï	ws	1909-2012	D		CRREBaC
5	Kisangani	0.51	25.19	Lualaba	ws/Q	1967-2011/ 1950-1959	D/M		
6	Ilebo	-4.33	20.58	Kasaï	Q	2013-2016	D		
7	Lediba	-3.06	16.56			2011-2016		Cal	Paris et al. 2022
8	Old pontoon	-10.95	31.07	Chambeshi		1972-2004		Cal/val	GRDC

9	Bagata	-3.39	17.40	Kasaï	ws	1952-1990		val	CRREBaC
10	Bandundu	-3.30	17.37			1929-1993			
11	Basoko	1.28	24.14	Middle-Congo	ws	1972-1991	D	val	CRREBaC
12	Esaka-amont	-3.4	17.94	Kasaï		1977-2010			
13	Kabalo	-5.74	26.91	Lualaba		1975-1990			
14	Mbandaka	-0.07	18.26	Middle-Congo		1913-1984			
15	Kindu	-2.95	25.93	Lualaba	ws/Q	1960-2004/ 1933-1959	D/M	Cal/val	
16	Kutu-muke	-3.20	17.34	Kasaï	swe	2017-2020	H	Cal/val	
17	Maluku	-4.07	15.51	Lower-Congo	ws	2017-2020/ 1966-1991	H/D	Cal	
18	Mbata	3.67	18.30	Ubangui	ws/Q	2016-2018/ 1950-1994	H/M	val	
19	Zemio	5.0	25.2	Ubangui	Q	1952-1994	Monthly		
20	Salo	3.2	16.12	Sangha		1953-1994	Monthly		
21	Chembe Ferry	-11.97	28.76	Lualaba		1956-2005	D/M		GRDC/ CRREBaC
22	Boali	4.88	18.03	Ubangui		1985-1988	D		GRDC
23	Bwambe	-2.91	15.65	Middle-Congo		1978-1980			
Stations used for lakes calibration									
24	Lukuga	-5.91	29.19	Lualaba	Q	1950-1959	M	Cal climatolgy	CRREBaC
25	Mulongo	-7.84	26.98						
26	Luvua	-7.34	28.01						
27	Luapula	-10.36	28.62						
28	Ruzizi	-2.49	28.89						

*ws (water stage), Q (discharge), swe (surface water elevation)

**D (daily), M (monthly), H (Hourly)

**Cal (calibration), Val (validation)

6.2.2 Satellite-derived SWH from radar altimetry

In addition to the nine in situ gauging stations used to calibrate the model, a number of 836 VSs (Fig. 6-2) from satellite altimetry data was also used for the same purpose to calibrate the hydrological-hydrodynamic MGB model as achieved in other hydrological modeling studies (Paiva et al., 2013a; Siqueira et al., 2018; Paris et al., 2022). They are obtained from the multi-satellite missions ERS-2, ENV, J2/3, SRL, and S3A/B presented previously in chapter 3 and 4 of this thesis. ERS-2 is not involved in the calibration phase as it is not covering the simulation period 01/01/2001 to 31/12/2020. For more insight on the satellite radar altimetry dataset used in this study, refers to Kitambo et al. (2022a).

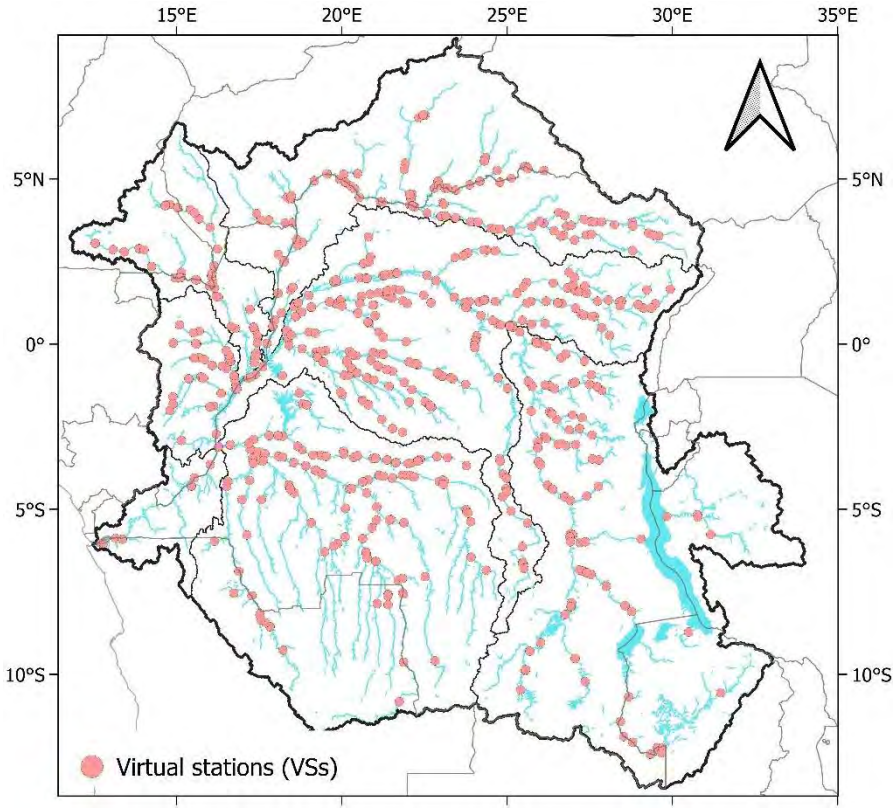

Figure 6-2. Virtual stations from ERS-2, ENV, J2/3, SRL, and S3A missions used for calibration of MGB model.

6.2.3 MGB model set-up

6.2.3.1 Model set-up

Being a conceptual and semi-distributed model, the first step in the model set-up was to discretize the basin into irregular unit catchments which were further divided into HRU. This

was achieved using the automated preprocessing steps based on MERIT DEM working under python3 environment developed by Hydro-matters company (https://www.hydro-matters.fr/) rather than the GIS-based tool namely IPH-Hydro Tools package (Siqueira et al., 2016). A threshold of 1 000 ha was adopted to consider the beginning of the drainage network. 50 sub-basins and 11580 unit-catchments (river reaches) were defined in this study during the discretization phase. Within each unit-catchment, the river reaches had a fixed-length vector-based discretization of 10 km to ensure balance between model stability and efficiency considering the numerical solution approach for hydraulic propagation (Siqueira et al., 2018; Wongchuig et al., 2019; Paris et al., 2022). It is worth noting that the number of sub-basins depended essentially on the availability of either the discharge/water level in situ gauge or satellite-derived SWH from radar altimetry at the outlet of each sub-basin and by the consideration of the physiographic of the basin. The width and depth that define the hydraulic parameters were derived respectively from MERIT Hydro dataset (http://hydro.iis.u-tokyo.ac.jp/~yamadai/ MERIT_ Hydro/, last access 13 February 2023, Yamazaki et al. [2014]) and the hydraulic geometry relationships (HG) according to drainage area (A_d) (Paiva et al., 2013b). Throughout the main stem of the Congo River, from Kisangani (further upstream) to Pool Malebo (further downstream at Brazzaville/Kinshasa), the calculated depth from the HG was replaced by the measured depth of the riverbed, thanks to the collaboration with regional partners CRREBaC. Floodplain geometry (i.e., its bathymetry) was extracted from MERIT DEM. The Manning's coefficient was set to be 0.035 which is in the range of values for different large river basins (Paiva et al., 2013b). In the CRB, there is no better alternate value known (Paris et al., 2022).

The HRU map (Fig. 6-4) at a resolution of 90m was defined by combining the vegetation map, land use-land cover (LULC) and soil map. The LULC map where six classes were defined (Fig. 6-3b), is provided by the 2019 global land cover, land use map derived from Landsat satellite imagery and topographical data at 30m of resolution (https://glad.umd.edu/dataset/global-land-cover-land-use-v1, last access 13 February 2023, Hansen et al. [2022]). For soil map (Fig. 6-3a), the latter derived from the Harmonized World Soil Database (HWSD) at 1km of resolution (https://www.fao.org/soils-portal/data-hub/soil-maps-and-databases/harmonized-world-soil-database-v12/en/, last access 13 February 2023, Fao/Iiasa/Isric/Isscas/Jrc [2012]). Among the four classes of soil map, one refers to the representation of the *Cuvette Centrale* wetland. The HRU map resulted in 10 classes (Fig. 6-4).

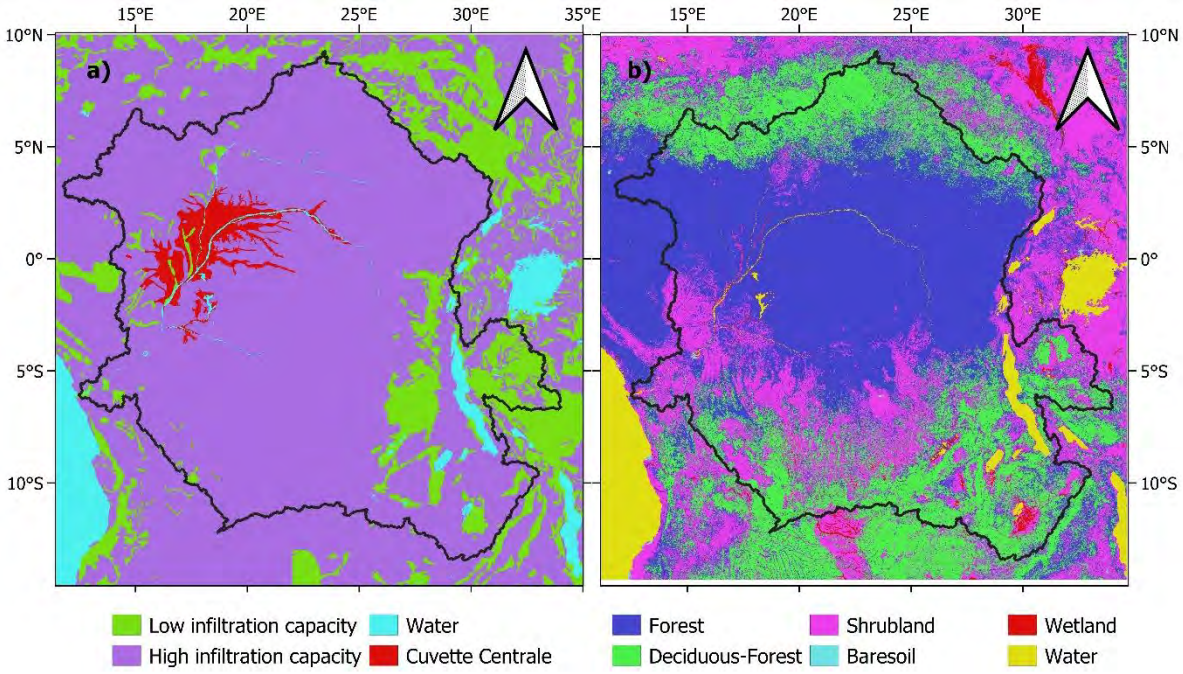

Figure 6-3. Soil (a) and land use-land cover (b) maps along with their classes considered for MGB preprocessing.

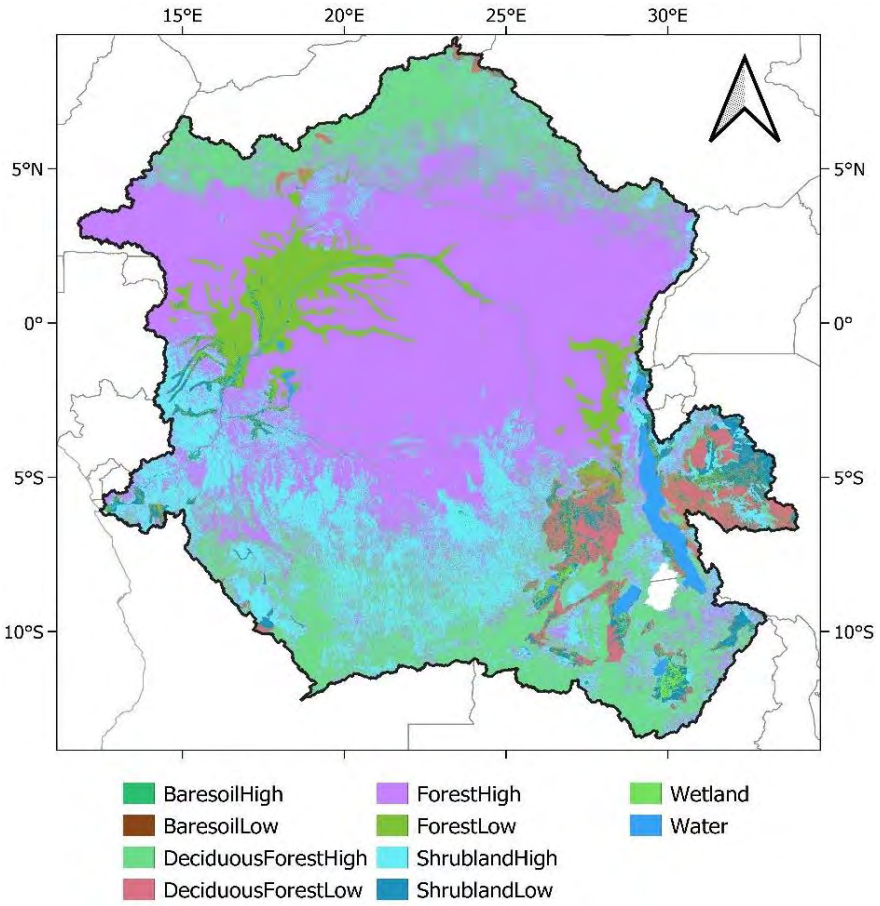

Figure 6-4. HRU map resulted from the MGB preprocessing.

The simulation period was carried out between 01 January 2001 and 31 December 2020 at daily time step. The spin-up period considered to eliminate the influence of initial conditions is two years. CHIRPS data, used as the model forcing, is based on precipitation models merged by interpolation of in situ precipitation data (Funk et al., 2015). The last version of CHIRPS v2.0 at a spatial resolution of 0.05° x 0.05° on a daily time scale was used in this study. Precipitation data for each mini-catchment was obtained by the interpolation to each CHIPRS grid, using the nearest neighbor algorithm. Dos Santos et al. (2022) reported the good performance of CHIRPS v2.0 in the Congo basin when evaluated against other satellite-based precipitation datasets into a large hydrological model. This precedent result motivated our choice for CHIRPS data. Climate variables used to compute evapotranspiration were retrieved from the ERA5 reanalysis dataset which is a global atmospheric reanalysis dataset from the European Centre for Medium-Range Weather Forecasts (ECMWF) that provide a large number of atmospheric, land and oceanic climate variables at a finer spatial resolution of 30 km and at a 1-hourly time step spanning the period 1950 to present (Tarek et al., 2020). Into MGB model, we considered the monthly climatology for each unit-catchment. It is worth nothing that both datasets, CHIRPS and ERA5 reanalysis were used for both the set-up and the hydrological projection for the historical period from 1981. River discharge and water levels are the hydrological variables considered for the calibration of the model. In order to improve agreement between observations and model results, a set of model parameters (Table 6-2) were manually adjusted. For the MGB model parameters related to soil water budget, Paris et al. (2022) reported that mainly W_m, b, K_{bas}, K_{int}, C_s, C_i, and C_b were the most sensitive parameters (see Table 6.2 for a definition of these parameters). In addition to these parameters, a manual adjustment of width and depth of the river network was also considered according to the in situ information to mainly calibrate the amplitude and shape of the water level time series. Google Earth Imagery was also used in order to compare the width obtained from MERIT Hydro (Yamazaki et al., 2014).

Table 6-2. Set of sensitive MGB model parameters.

Parameter	Description	Unit	Min	Max
W_m	Maximum water storage	mm	50	2000
b	Controls the distribution of water storage capacity of the soil	/	0.01	1.6
K_{bas}	Percolation rate from soil to groundwater	mm Δt^{-1}	0.1	4
K_{int}	Saturated soil hydraulic conductivity	mm Δt^{-1}	4.00	40.00

C_s	Adjustment factor for superficial reservoir residence time	/	1	30.00
C_i	Adjustment factor for subsurface reservoir residence time	/	50	200
C_b	Groundwater reservoir residence time	h	800	8000

6.2.3.2 Lake routing

The hydrology of the CRB is dominated by several lakes and wetlands which play an important role in the hydrologic regimes of the basin by their ability to store water inducing hydrological effect of attenuation and regulation of streamflow, delays and increased of residence time (Tshimanga, 2022). It should be noted that the MGB model was previously developed for the CRB (Paris et al., 2022), but this first development did not consider inclusion of lake and wetland processes. In this study, major features of lakes and wetlands are considered in the model, which include Bangweulu, Mweru, Tanganyika, Kivu, Zimbambo, Tumba, and Mai-Ndombe Lakes (Fig. 6-5). In this regard, a lake routing module is implemented in the model, similar to Fleischmann et al. (2019) and based on a lumped (level-pool) model defined by Fread (1992). This computes a simple and lumped continuity equation for a given reservoir assuming a horizontal water level in the respective lake which is here represented by the unit-catchment identified as the outlet of each lake.

The variation of storage within the reservoir area is computed by the continuity equation (Eq. 2) already defined in the hydrodynamic inertial propagation in the MGB model. The storage can be adjusted by replacing the respective unit-catchments' level–storage relationship by the one representing the lake. For this purpose, a preprocessing was developed in each lake's outlet in which a representative level-storage relationship was defined by using satellite altimetry and flooded area from the Theia Hydroweb database (https://hydroweb.theia-land.fr/).

The second characteristic that defines a lake representation within the MGB is its outflow equation defined here as a rectangular spillway structure, considered as an internal boundary condition, and defined as follows:

$$Q = C \times L \times H_d^{\frac{3}{2}} \quad (5)$$

where Q is the spillway outflow, C the spillway discharge coefficient, L the spillway length and H_d represents the water height above the crest of the spillway level. The C and L parameters were considered to be adjusted for calibration purposes for each lake. Normally, L is a fixed parameter obtained from satellite imagery as it represents the spillway length.

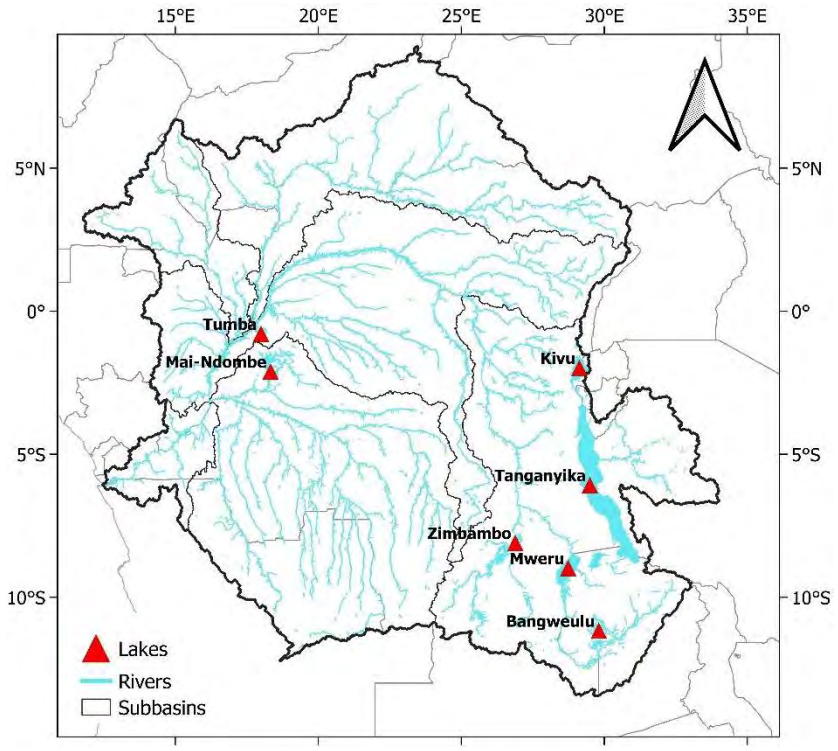

Figure 6-5. Lakes represented into MGB model for lake routing.

6.2.3.3 Metrics for assessment of results

A set of efficiency metrics (Table 6-3) were used for the assessment of model results during the calibration and validation phases as in Siqueira et al. (2018).

Table 6-3. Set of efficiency metrics used for model assessment.

Metric	Abbreviation	Assessment	variables
Pearson's correlation coefficient	r	Linear correlation	Discharge, water level, TWS
Kling–Gupta efficiency	KGE	Overall performance	Discharge
Nash–Sutcliffe efficiency	NSE	High flows	Discharge, water level
Overall BIAS (%)	Bias	Under- and overestimation (volume)	Discharge

The equations related to each of the above metrics are provided as follows:

$$r = \frac{\sum[(x_{sim} - \bar{x}_{sim})(x_{obs} - \bar{x}_{obs})]}{\sqrt{\sum(x_{sim} - \bar{x}_{sim})^2}\sqrt{\sum(x_{obs} - \bar{x}_{obs})^2}} \quad (6)$$

$$KGE = 1 - \sqrt{(1-r)^2 + \left(1 - \frac{\bar{x}_{sim}}{\bar{x}_{obs}}\right)^2 + \left(1 - \frac{CV_{sim}}{CV_{obs}}\right)^2} \quad (7)$$

$$NSE = 1 - \frac{\sum(x_{sim} - x_{obs})^2}{\sum(x_{obs} - \bar{x}_{obs})^2} \quad (8)$$

$$Bias = \left(\frac{\sum x_{sim} - \sum x_{obs}}{\sum x_{obs}}\right) \times 100 \quad (9)$$

Where x_{sim}, $\bar{x}_{sim}$, x_{obs}, $\bar{x}_{obs}$, and CV stand for the simulated and mean of simulated variable, the observed and mean of observed variable, the coefficient of variation, respectively.

6.3 Results

6.3.1 Results of the MGB Model calibration in the CRB

The MGB model calibration for the CRB involved both streamflow and water levels for the period 2001–2020. Figure 6-6 presents the comparison performed between the simulated daily discharge with in situ observations during the calibration phase for selected stations in the CRB, representing the major physiographic or hydrological units of the CRB. These are the Sangha sub-basin in the North-Ouest (Ouesso station), Ubangui sub-basin in the Northeast (Bangui station), Kasaï sub-basin in the South Ouest (Lediba and Ilebo stations), Lualaba sub-basin in the Southeast (Old-pontoon station) and Lower-Congo that drains about 98% of the whole CRB (Brazzaville/Kinshasa station). The map of performance metric in NSE as well as boxplots of different metrics (i.e., KGE, NSE and BIAS) are also presented. Overall, based on the statistical criteria used for evaluation of the model performance, it can be seen that the model performed very adequately for the different physiographic regions of the CRB, thus is able to represent the heterogeneity of the various hydrological processes in the CRB. The KGE, NSE and relative BIAS showed a median value of 0.84, 0.73 and 1.7%, respectively. The lowest values of NSE and KGE are observed at the most downstream gauge of Brazzaville/Kinshasa. This can be attributed to the overestimation of water volume by the model at the second peak (happening in March-July) of the hydrogramme. In Northern sub-basins, Ouesso and Sangha, we also observed a significant overestimation of the water volume during the years 2012 and 2013 at Ouesso station and 2011, 2012, 2017 and 2018 at Bangui station at higher flows period occurring in October-November. Part of the problem could also be attributed to unknown uncertainties in the available observed data. In comparison to previous attempt of regional hydrological modeling in the CRB, the performance found is much better than those from GW-PITMAN model (Tshimanga and Hughes, 2014), GeoSFM model (Munzimi et al., 2019), SWAT model (Datok et al., 2022; Dos Santos et al., 2022) except from the previous development of MGB model (Paris et al., 2022).

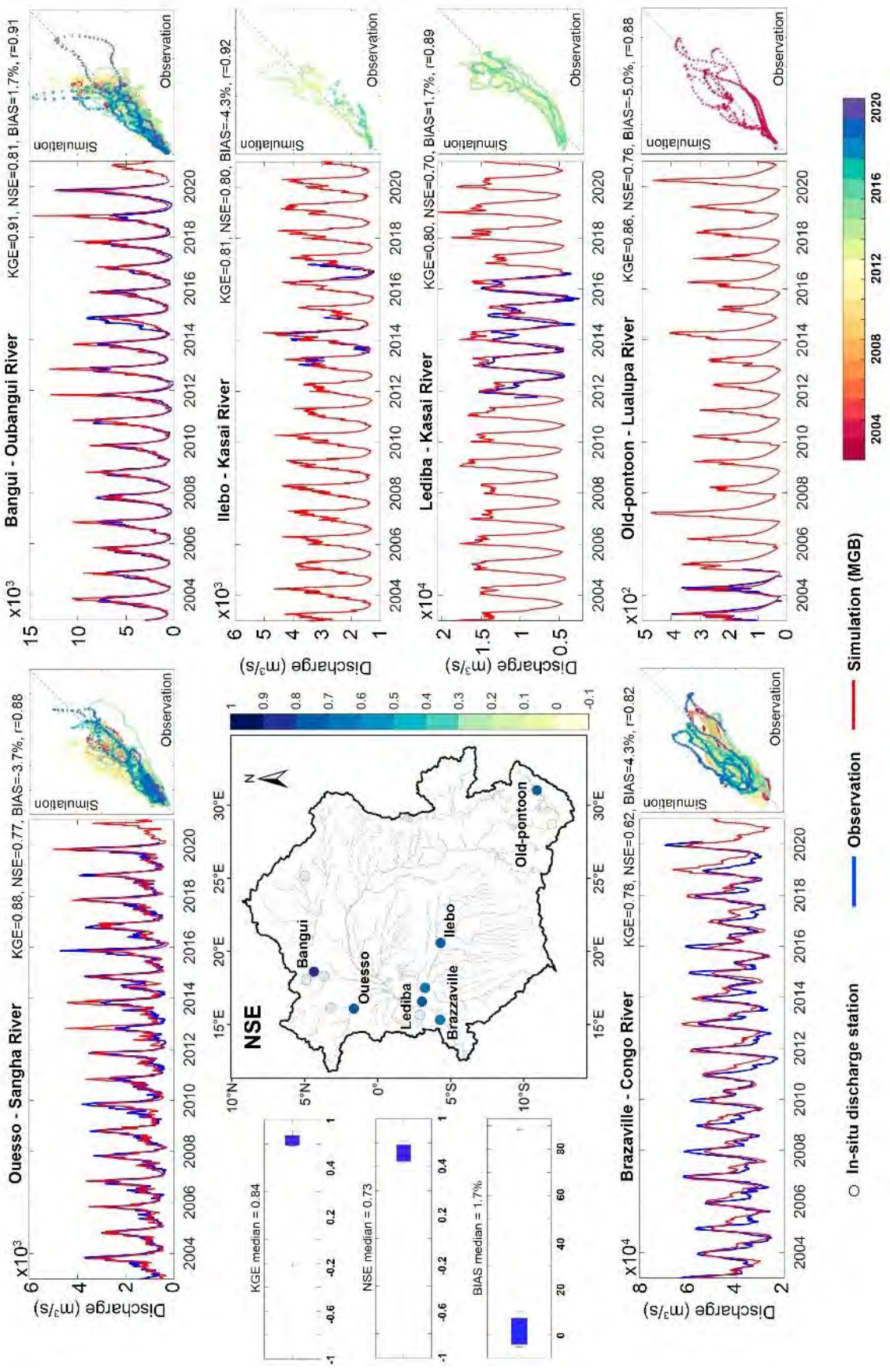
Bangui - Oubangui River
KGE=0.91, NSE=0.81, BIAS=1.7%, r=0.91
Ouesso - Sangha River
KGE=0.88, NSE=0.77, BIAS=-3.7%, r=0.88
Ilebo - Kasai River
KGE=0.81, NSE=0.80, BIAS=-4.3%, r=0.92
Lediba - Kasai River
KGE=0.80, NSE=0.70, BIAS=1.7%, r=0.89
Old-pontoon - Lualupa River
KGE=0.86, NSE=0.76, BIAS=-5.0%, r=0.88
Brazaville - Congo River
KGE=0.78, NSE=0.62, BIAS=4.3%, r=0.82
Discharge (m³/s)
Simulation
Observation
NSE
Bangui
Ouesso
Lediba
Brazzaville
Ilebo
Old-pontoon
KGE median = 0.84
NSE median = 0.73
BIAS median = 1.7%
In-situ discharge station
Observation
Simulation (MGB)

Figure 6-6. Temporal series of observed (blue line) and simulated (red line) discharge for six in situ stations for the calibration period 2001-2020. The scatterplot of the observed versus simulated daily series with the colors of each point corresponding to the respective year is placed to the right side of the time series (same unit, in m^3/s). The spatial distribution and the boxplot of the statistical performance index for in situ gauges are shown in the left-centre panel.

Similarly, the simulated daily water level was compared to the in situ water level also at six stations as for the river discharge, Ubangui (Bangui and Mbata stations), Lualaba (Kindu station), and Middle-Congo (Maluku station) sub-basins. The performance result is shown in Fig. 6-7. The NSE and Pearson coefficient r showed a median value of 0.66 and 0.86, respectively. Better performance is captured in the northern parts of the basin which are less seasonal than the southern part of the CRB. Same behavior as for discharge is observed for the most downstream station Brazzaville/Kinshasa station where the overestimation in water level is observed at the second peak. The performance of our model in simulating the timing and magnitude of high and low water level are fairly better as provided by the Pearson coefficient r. Figure 6-7 also provides the map in terms of the NSE performance.

Figure 6-8 shows the temporal series of water level anomaly (i.e., the anomaly is computed by subtracting the long-term mean to each individual values to have same reference) and the spatial distribution of the statistical indexes for 836 virtual stations during the calibration period, where the overall performance for NSE and r Pearson coefficient are 0.38 and 0.75, respectively. Better performance is shown in the northern and Kasai River (southern region) tributaries of the CRB where the model was calibrated based on the presence of in situ stations. In contrast, the central (Fimi, Ruki, Lulonga, and main-stem Congo Rivers) and east (Lowa, Elila, Lualaba Rivers) part of the basin present lower performance probably due to the lack of in situ station with data overlapping the calibration period. These two regions are also characterized by a strong seasonal variation that could not be depicted well. In general, the temporal series of water level amplitude showed an adequate agreement between MGB simulations and remote sensing-based observations, considering amplitude, interannual and seasonal representation.

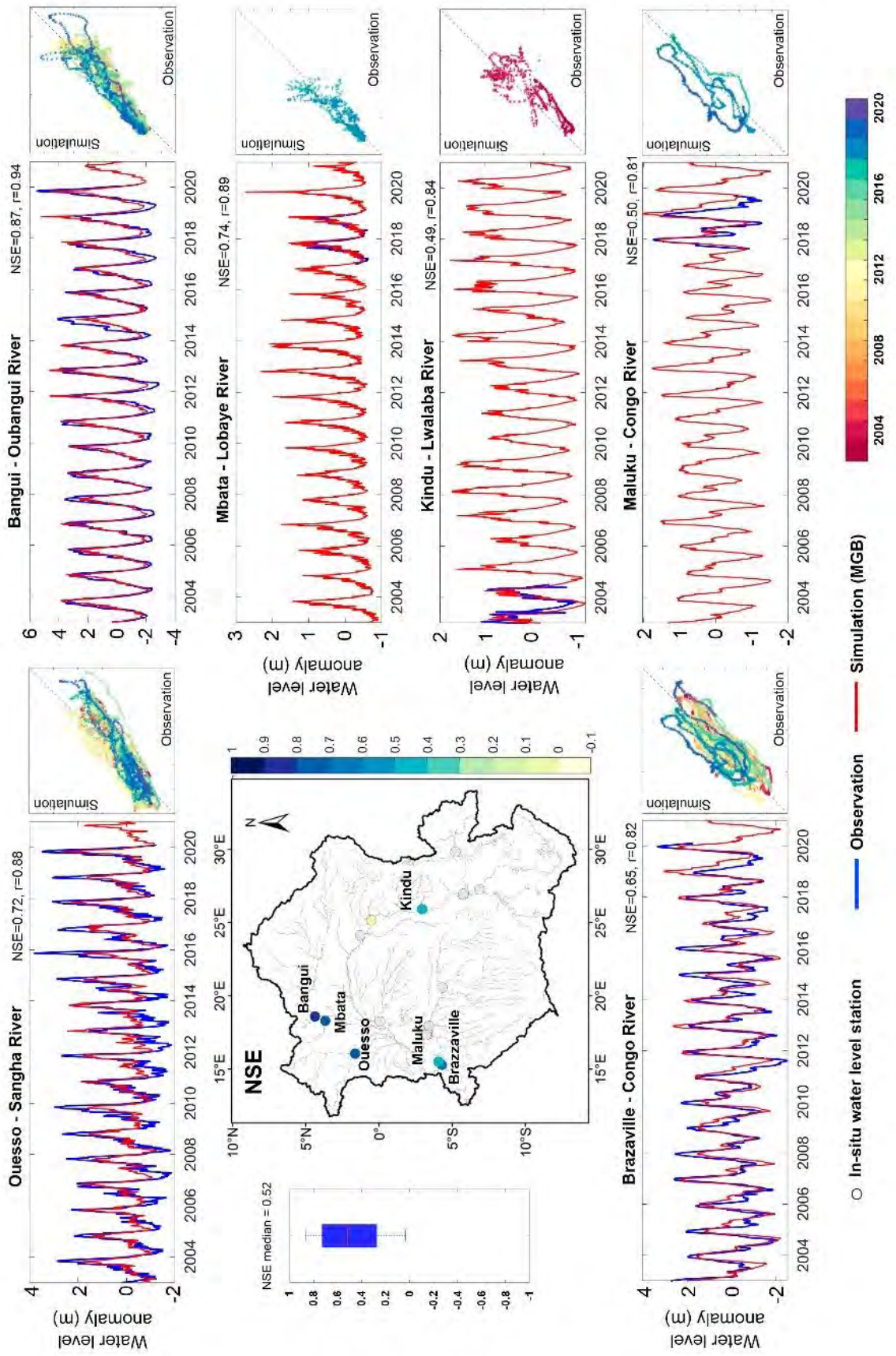
Bangui - Oubangui River
NSE=0.87, r=0.94
Mbata - Lobaye River
NSE=0.74, r=0.89
Kindu - Lwalaba River
NSE=0.49, r=0.84
Maluku - Congo River
NSE=0.50, r=0.81
Ouesso - Sangha River
NSE=0.72, r=0.88
Brazzaville - Congo River
NSE=0.85, r=0.82
Water level anomaly (m)
Simulation
Observation
NSE
Bangui
Mbata
Ouesso
Kindu
Maluku
Brazzaville
NSE median = 0.52
In-situ water level station
Observation
Simulation (MGB)

Figure 6-7. Temporal series of observed (blue line) and simulated (red line) water level for six in situ stations for the calibration period 2001-2020. The scatterplot of the observed versus simulated daily series with the colors of each point corresponding to the respective year is placed to the right side of the time series (same unit, in m). The spatial distribution and the boxplot of the statistical performance index for in situ gauges are shown in the left-centre panel.

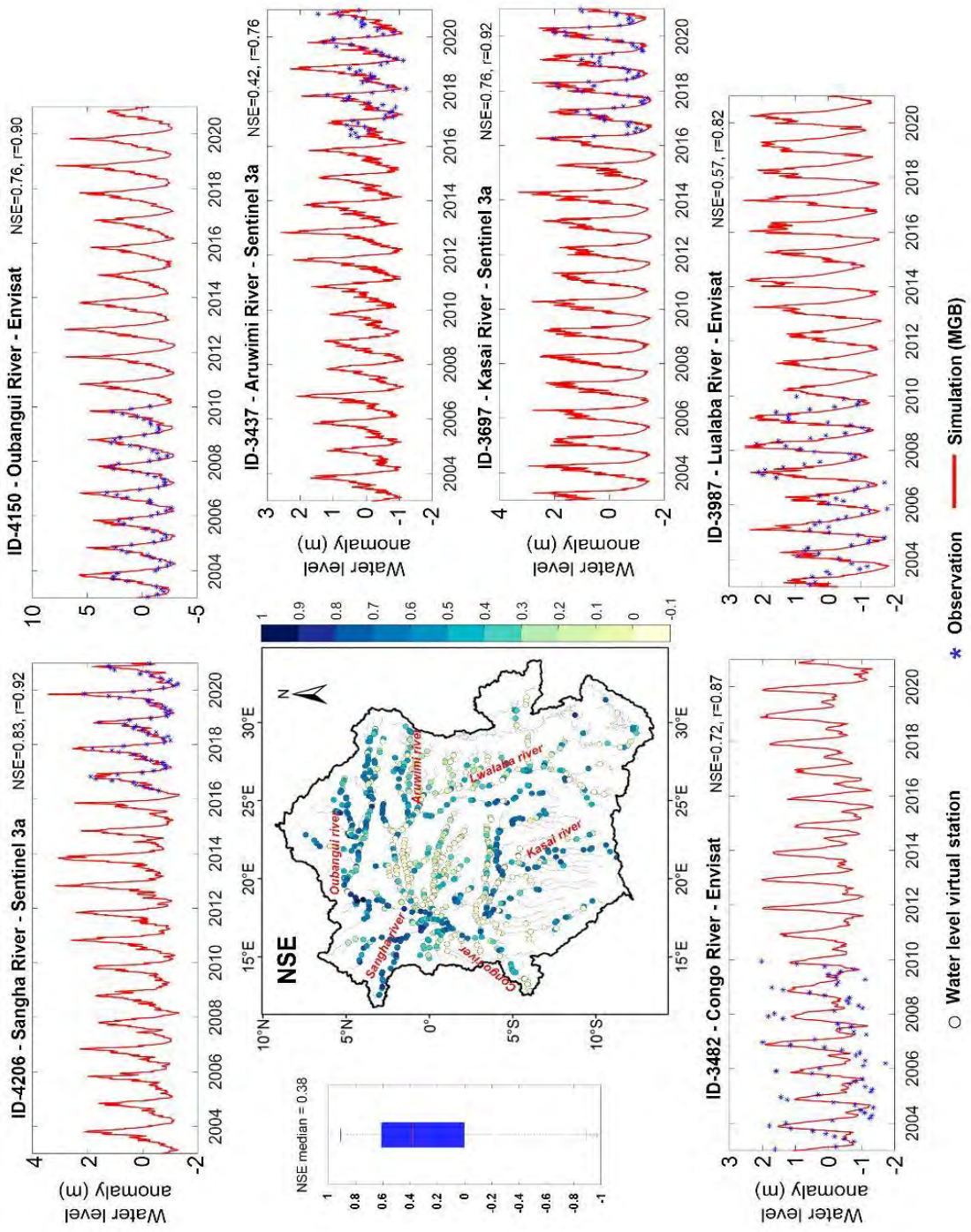

Figure 6-8. Temporal series of observed (blue dots) and simulated (red line) water level for 836 virtual stations for the calibration period 2001-2020. The spatial distribution and the

boxplot of the statistical performance index for virtual stations are shown in the left-centre panel.

6.3.2 MGB model validation in the CRB

As for the calibration, the model validation is also carried out for both river discharge and water levels, for the period 1984-2000.

Figure 6-9 shows the temporal series and spatial distribution of river discharge performance during the validation period (1981-2000). The KGE, NSE and relative Bias showed a median value of 0.71, 0.51 and -11.7%, respectively. Similar to the calibration period, the better performance is captured for the northern region of the CRB, where interannual and seasonal variability are adequately represented. At Brazzaville/Kinshasa station, the significant overestimation in the second peak is still observed underling the weakness of the model output to fairly reproduce the magnitude of discharge during the hydrological peak observed in March-July. This could also be attributed to unknown uncertainties in input data to the model as well as in the observed flow and water levels data. In addition, there is also the fact that the central part of the CRB, characterized by a bimodal hydrological regime, showed a lower performance as seen during the calibration phase with VSs (Fig. 6-8) and this region explained ~35% of discharge variability at Brazzaville/Kinshasa (Kitambo et al., 2022a). At Old-pontoon, there is a remarkable underestimation of water volume that can be related to the short period involved for calibration phase.

Figure 6-10 shows the comparison at the interannual time scale between the daily simulated and in situ water level anomaly at different places in the CRB (i.e., Ouesso, Bangui, Brazzaville/Kinshasa, Kisangani, Esaka-amont, Ilebo, to name a few). The agreement between simulated and observed water level is notable for both high and low flows in most of the cases with fairly index of NSE and Pearson correlation coefficient greater than 0.60 and 0.70, respectively. Figure 6-10 presents the map of performance metric as well in NSE where other stations are represented for which their time series are not represented.

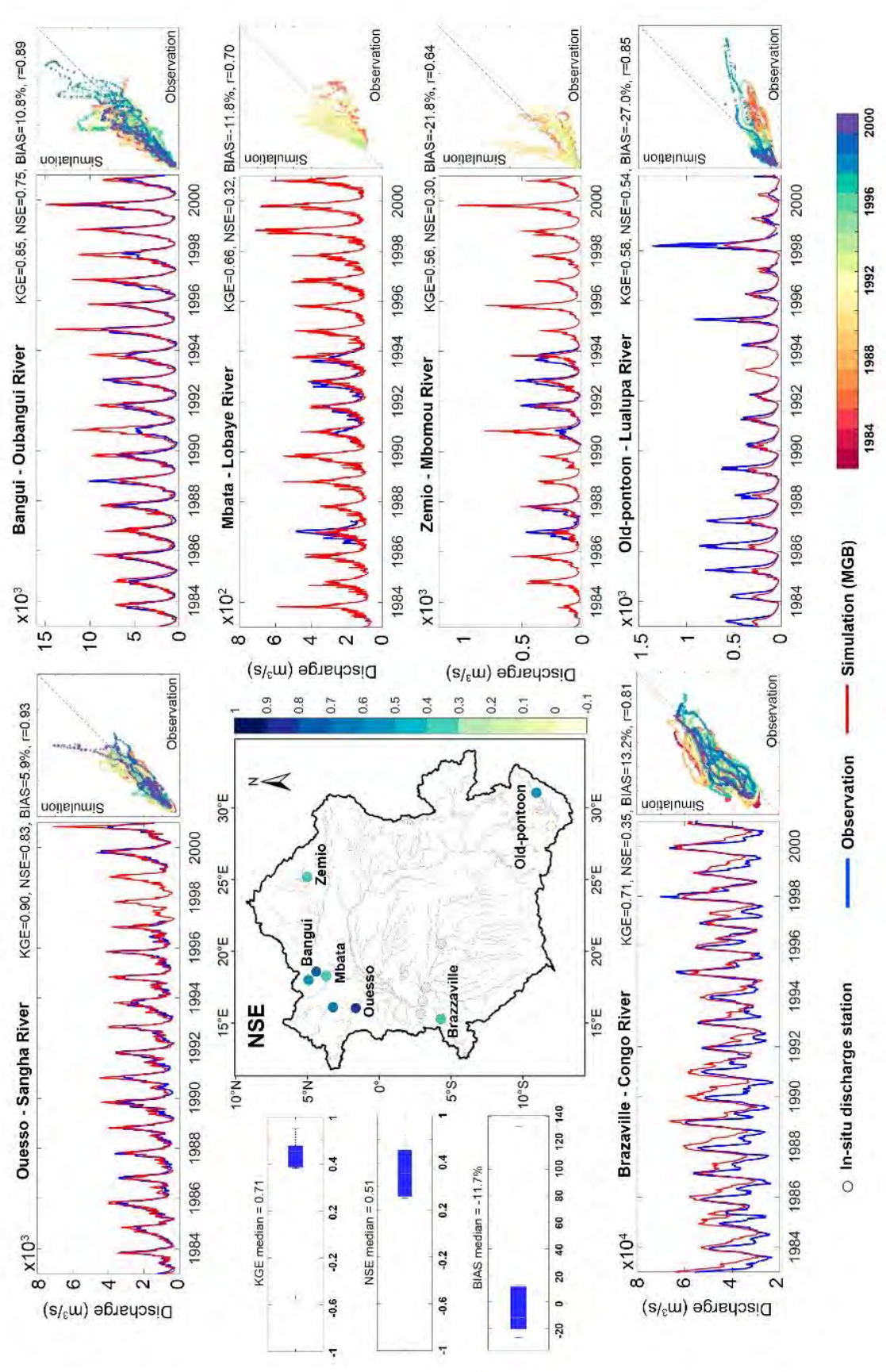

Figure 6-9. Temporal series of observed (blue line) and simulated (red line) discharge for six in situ stations for the validation period 1981-2000. The scatterplot of the observed versus

simulated daily series with the colors of each point corresponding to the respective year is placed to the right side of the time series (same unit, in m^3/s). The spatial distribution and the boxplot of the statistical performance index for in situ gauges are shown in the left-centre panel.

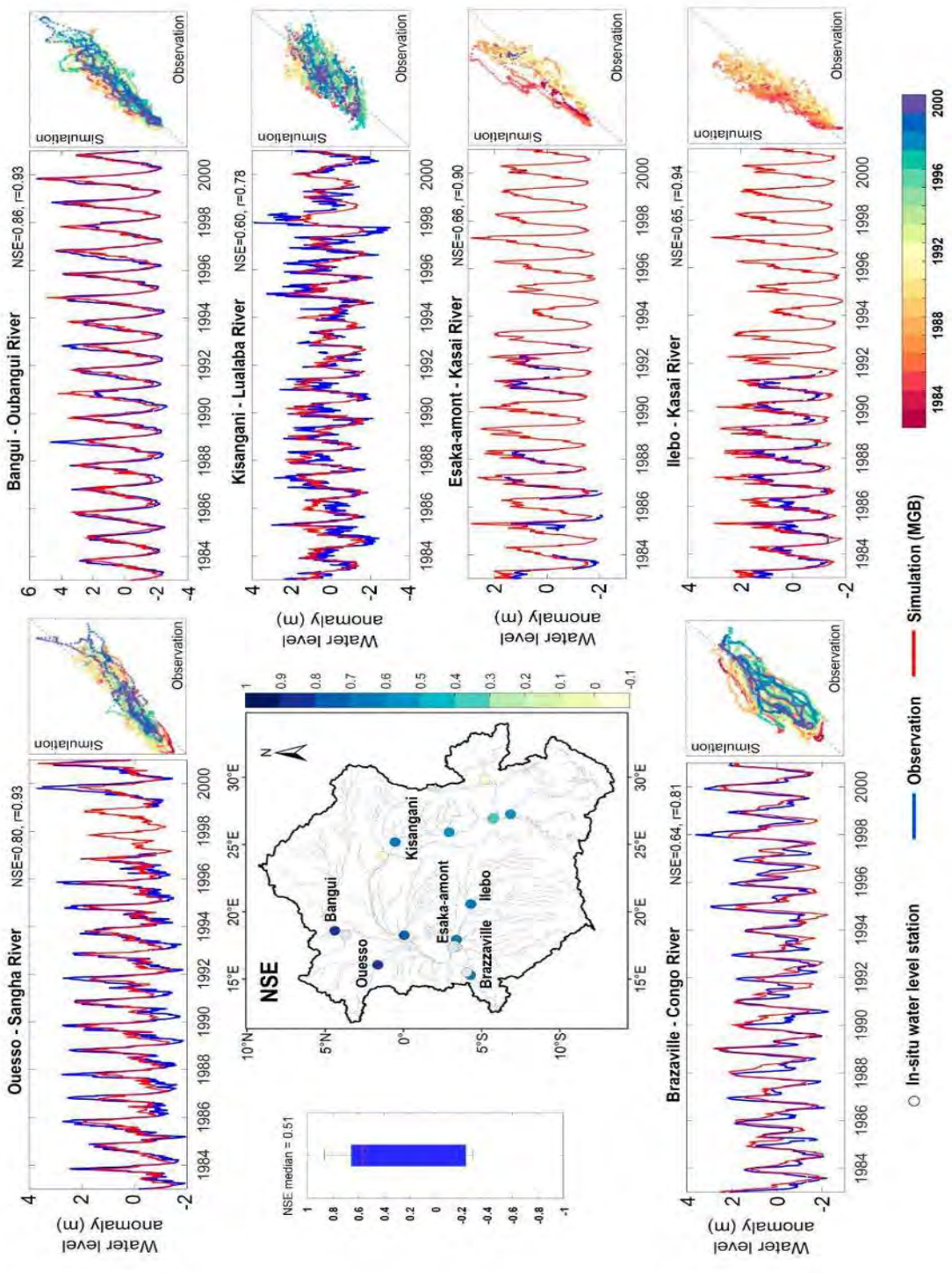

Figure 6-10. Temporal series of observed (blue line) and simulated (red line) water level anomaly for six in situ stations for the validation period 1981-2000. The scatterplot of the observed versus simulated daily series with the colors of each point corresponding to the

respective year is placed to right side of the time series (same unit, in m). The spatial distribution and the boxplot of the statistical performance index for in situ gauges are shown in the left-centre panel.

6.3.3 Application of the MGB model for simulating the special features of hydrological processes in the CRB

As previously mentioned, hydrodynamic component of the MGB model enables simulation of specific features of hydrological processes inherent to the hydrology of large rivers such as the Congo. This may include attenuation, storage and slow release of flows as well as flow routing in natural reservoirs such as large lakes, wetlands and large channels with their riparian areas. It may also include hydrological connectivity and the movement of water between the various components of the surface water storage during high flow and low flow seasons. All these processes have been considered as critical for a robust modelling of the hydrology in the CRB (Tshimanga, 2022). They are very relevant for an adequate simulation of future impacts of land use and climate changes in the CRB where natural lakes and wetlands are known to be habitats of rich aquatic biodiversity and play an important role in storing tons of carbons and nutrients. In this study, efforts have been made to parameterize the MGB model by integrating lake and wetland features, spatial distribution of vegetation parameters, and an adequate representation of the geometry of floodplains in particular the *Cuvette Centrale*.

6.3.3.1 Simulation of lake processes

A lake routing representation module was implemented in this version of MGB model and Fig. 6-11 shows the seasonal climatological time series of river discharge for historical records from in situ stations downstream of four lakes compared to the MGB simulation outputs for calibration purposes. Tanganyika lake shows the best performance considering bias and r Pearson coefficient of -1.3% and 0.97. In addition, lakes Mweru and Zimzambo manage to capture seasonality, but there is still an overestimation of discharge climatology by the MGB model. On the other hand, in Lake Kivu there is a significant underestimation of the climatological discharge, mainly in the dry period, this could be explained by the fact that Kivu is a regulated lake and therefore there is probably a flow discharge during the dry period. In general, it has been possible to capture the climatological discharge in four lakes, even considering that the errors in the bias could also be attributed to the fact that two different

periods 50 years apart have been considered. At the other three lakes, Tumba, Mai-Ndombe and Bangweulu we did not perform the comparison due the lack of in situ data.

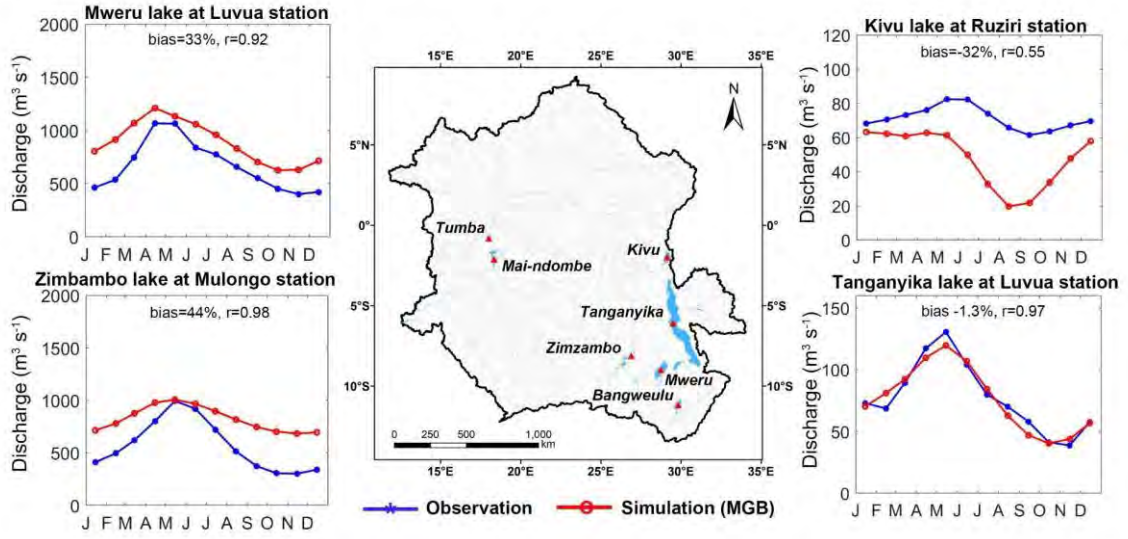

Figure 6-11. Temporal series of observed historical (blue, 1950-1959) and simulated (red, 2001-2020) river discharge climatology for four stations downstream of lakes. The location map of different lakes is shown in the centre panel.

6.3.3.2 Simulation of Terrestrial Water Storage

Regarding other water components, Figure 6-12 shows the temporal series of the terrestrial water storage (TWS) anomaly from remote sensing-derived from GRACE/GRACE-FO dataset and simulations from MGB model. The analysis was performed for six defined large sub-basins in the CRB, Sangha, Ubangui, Middle-Congo, Lualaba, Kasaï and Lower-Congo. Overall, a better performance was found with a median r Pearson coefficient of 0.81. Four sub-basins which are Sangha, Ubangui, Lualaba and Kasai out of two (i.e., Middle-Congo and Lower-Congo sub-basins) showed r Pearson coefficients greater than 0.8 and the amplitude of TWS are quite similar between the observed and the model. However, the model simulation still has some difficulties to represent (overestimate) the amplitude in many of the sub-basin's TWS observation based, specifically for the Middle-Congo that indicated the lower r Pearson coefficient. This overestimation could be explained by the different spatial resolution of the two datasets. GRACE is derived from a coarse resolution of 1° while the total water storage from the model depends on the geometry of floodplain computed from a DEM of 90 m of spatial resolution.

6.3.3.3 Simulation of flooded area extent

Figure 6-13 shows a comparison of the flooded area extent in the Congo basin between the MGB simulations and the multi-satellite dataset from GIEMS-2. Overall, the MGB simulations overestimate the estimation based on remote sensing during all the periods. It is worth noting that the SWE observations from GIEMS-2 are from a coarse spatial resolution of ~27 km while the MGB model used a finer spatial resolution DEM of 90 m from which the flooded extent is derived. This could explain the difference in amplitude while the dynamic is similar for both. Also shown on Fig. 6-13, the map of the maximum (i.e., March 2007 represented by vertical blue line) and minimum (i.e., July 2013 represented by vertical purple line) flooded months considering GIEMS-2 time series for both the model and GIEMS-2 along with a zoom on the confluence between the Fimi and Kasaï River that poured into the Congo River.

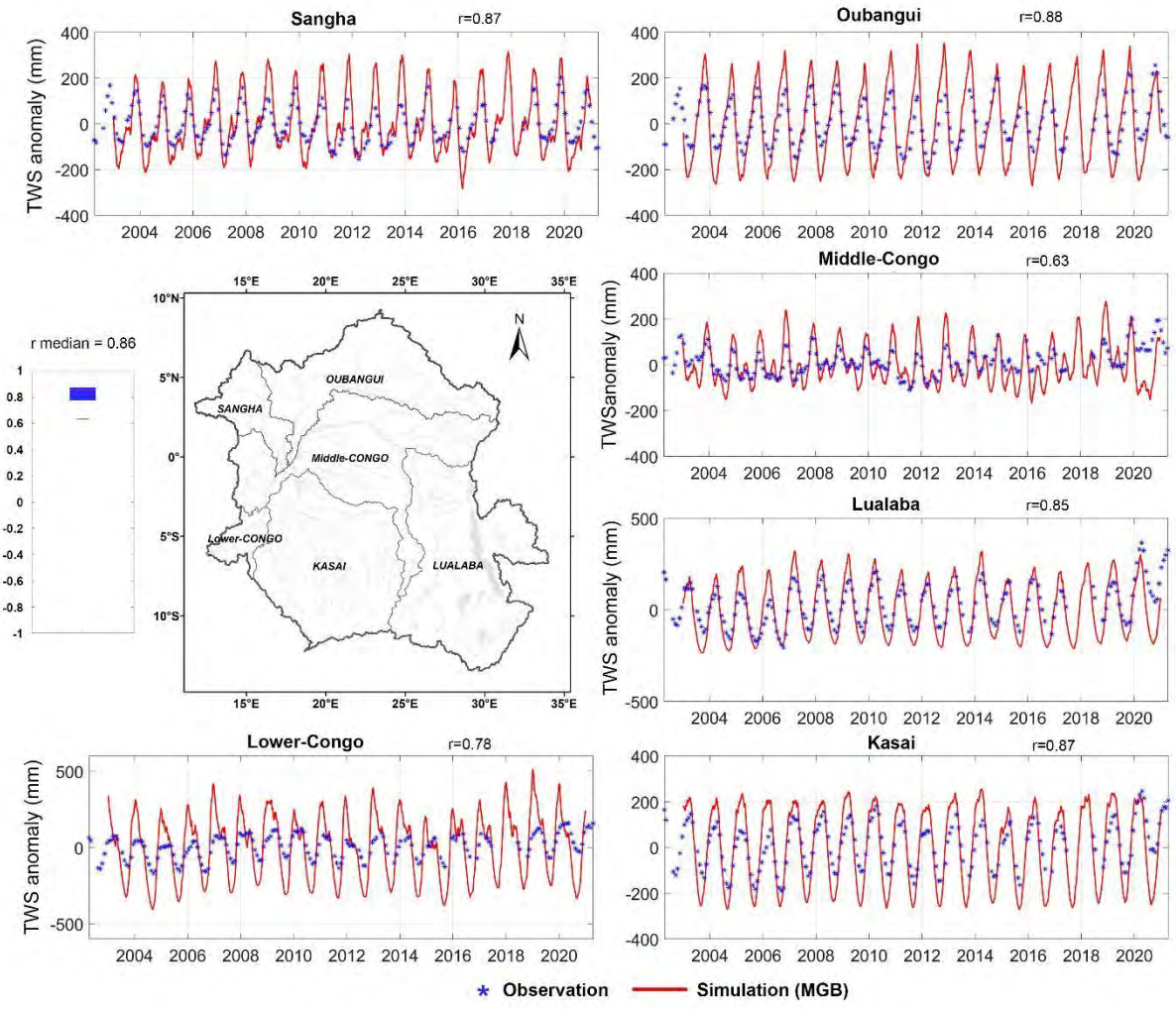

Figure 6-12. Temporal series of observed (blue dots) and simulated (red line) terrestrial water storage for six large sub-basins for the calibration period 2001-2020 for GRACE/GRACE-FO

and MGB, respectively. The spatial distribution and the boxplot of the statistical performance index for sub-basins are shown in the left-centre panel.

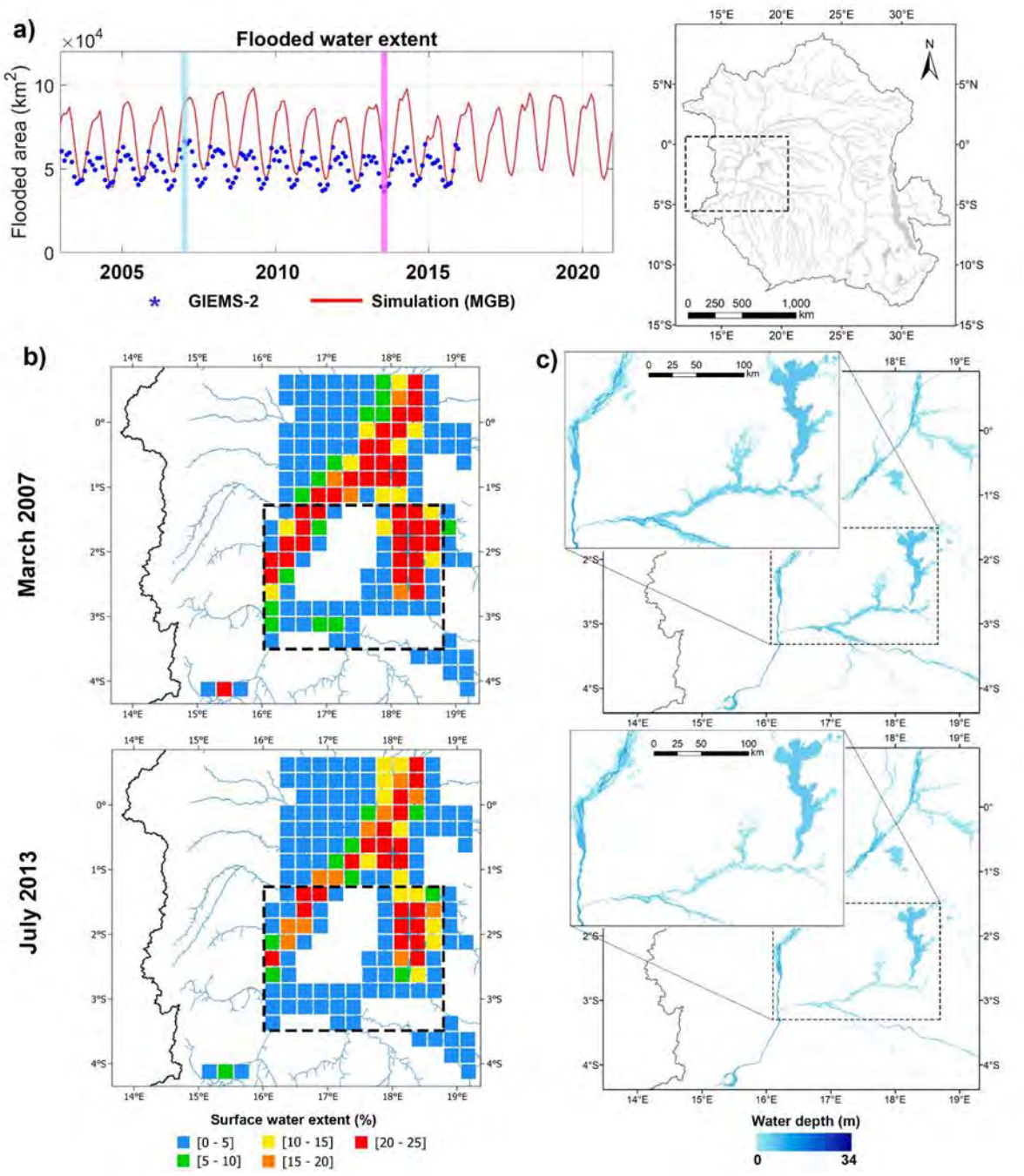

Figure 6-13. Comparison between the observed (blue dots) and simulated (red line) surface water extent for the calibration period 2001-2020 from GIEMS-2 dataset and MGB, respectively. Time series of both the total observed and simulated during 2001-2020 (a). zoom map in the Cuvette Centrale of the maximum (i.e., March 2007, expressed as a percentage of the pixel coverage size of 773 km^2) and minimum (i.e., July 2013, expressed similarly as in March 2007) flooded months from GIEMS-2 (b). Similar zoom map from the MGB model (c).

In these sections 6.3.1 and 6.3.2, we performed the calibration and validation over 2001 to 2020 and 1981 to 2000, respectively of the MGB model at the daily time scale. The simulated river discharge and water level have been compared to in situ river discharge, water level, and satellite-derived SWH. Overall, the model presented fair satisfactory statistical indexes for both variables, discharge and water level. A median value of 0.84, 0.73 and 1.7% for KGE, NSE and relative BIAS, respectively have been found during the calibration phase for discharge and 0.66 and 0.86 for NSE and r Pearson coefficient, respectively for water level.

Similar performance has been obtained in the section 6.3.3 where in addition to the discharge and water level, the simulated TWS and flooded area extent have been compared to the satellite observations TWS and SWE from GRACE/GRACE-FO and GIEMS-2 datasets.

Our daily results outperform those from the previous attempt of regional hydrological modeling in the CRB at monthly time scale. However, some inconsistencies have been pointed out during the calibration and validation phases regarding the overestimation of water volume at the second peak of the hydrogramme and during some specific years.

The satisfactory evaluation of different model outputs, river discharge, water level, TWS and flooded area extent presented in these sections, provides the confidence to further perform the long-term daily simulation from 1981 to 2020.

6.3.4 Long-term daily simulation over 1981 to 2020

Figure 6-14. shows the long-term simulation of discharge for the period 1981-2020 using both datasets, CHIRPS for precipitation and ERA5 reanalysis for climatological variables. The performance of statistical indexes for NSE, KGE and r Person coefficient are 0.61, 0.73 and 0.87, respectively. These values can be considered as an adequate performance for a 40 years' time simulation at daily time scale. Overall, the bimodal behavior of discharge series at Lediba and Brazzaville/Kinshasa stations are captured by MGB simulations. For the three stations with a long record discharge, Brazzaville/Kinshasa, Ubangui and Sangha, the model and the in situ discharge present quite well a similar behavior in the peak-to-peak discharge variations. However, there are still maximum year events in which MGB simulations overestimate the observations such as for the year 2000 in the north-west part at Salo and Ouesso, and during the year 2003 northern region at Bangui and Zemio stations. This behavior is specifically during these years, so it is probably due to poor representativeness of the CHIRPS rainfall database in

the northern region over the CRB. For many in situ stations such as Boali, Salo stations, to name a few, this unique long run completes actual temporal gaps of the in situ observations. Conversely, for Ilebo, Dima-Lumbu stations, to name a few, this unprecedented dataset completes the historical temporal gaps of many stations. Therefore, this exclusive spatiotemporal long-term dataset over 1981 to 2020 at daily time scale across the CRB bridges the gap for the very first time between the past in situ databases and current and future monitoring of the CRB as an ensemble and paves the way for several research opportunities that are presented in the perspectives section.

6.4 Conclusion

The present study presents an unprecedented dataset of simulated daily river discharge, water level, flooded area extent, TWS, among others over the entire CRB from 1981 to 2020. A hydrological-hydrodynamic model namely MGB was used for this purpose. CHIRPS and ERA5 reanalysis datasets for precipitation and climatological variables, respectively were used as model forcing to set-up the MGB model during both the calibration phase from 2001 to 2020 and the hydrological projection for the historical period from 1981 to 2000 as validation period. A unique and consolidated in situ dataset and satellite-based observations, particularly radar altimetry-derived SWH variations (a total of 836 VSs) and SWE from GIEMS-2 over the CRB have been used to assess the simulated outputs of the model. Thanks to the regional partners for in situ data and to all previous work with satellite-based observations that enables the evaluation of the MGB model. In general, the statistical indexes for both the calibration and validation indicated good performance (e.g., KGE, NSE and relative BIAS showed a median value of 0.84, 0.73 and 1.7%, respectively for river discharge) along with some inconsistencies mainly due to the overestimation in water volume of the model as compared to the in situ data during March-July corresponding to the second peak of the hydrogramme. Northern sub-basins outperformed than southern sub-basins probably due to the less seasonality that characterized them. The satisfactory results allowed to simulate a long-term daily simulation from 1981 to 2020 (i.e., ~40-year) that bridges the gap between the past in situ databases and current and future monitoring of the CRB. This unprecedented dataset of river discharge and water level, to name a few over 40-year spatially distributed across the CRB has opened several opportunities that are presented as perspectives in the next section.

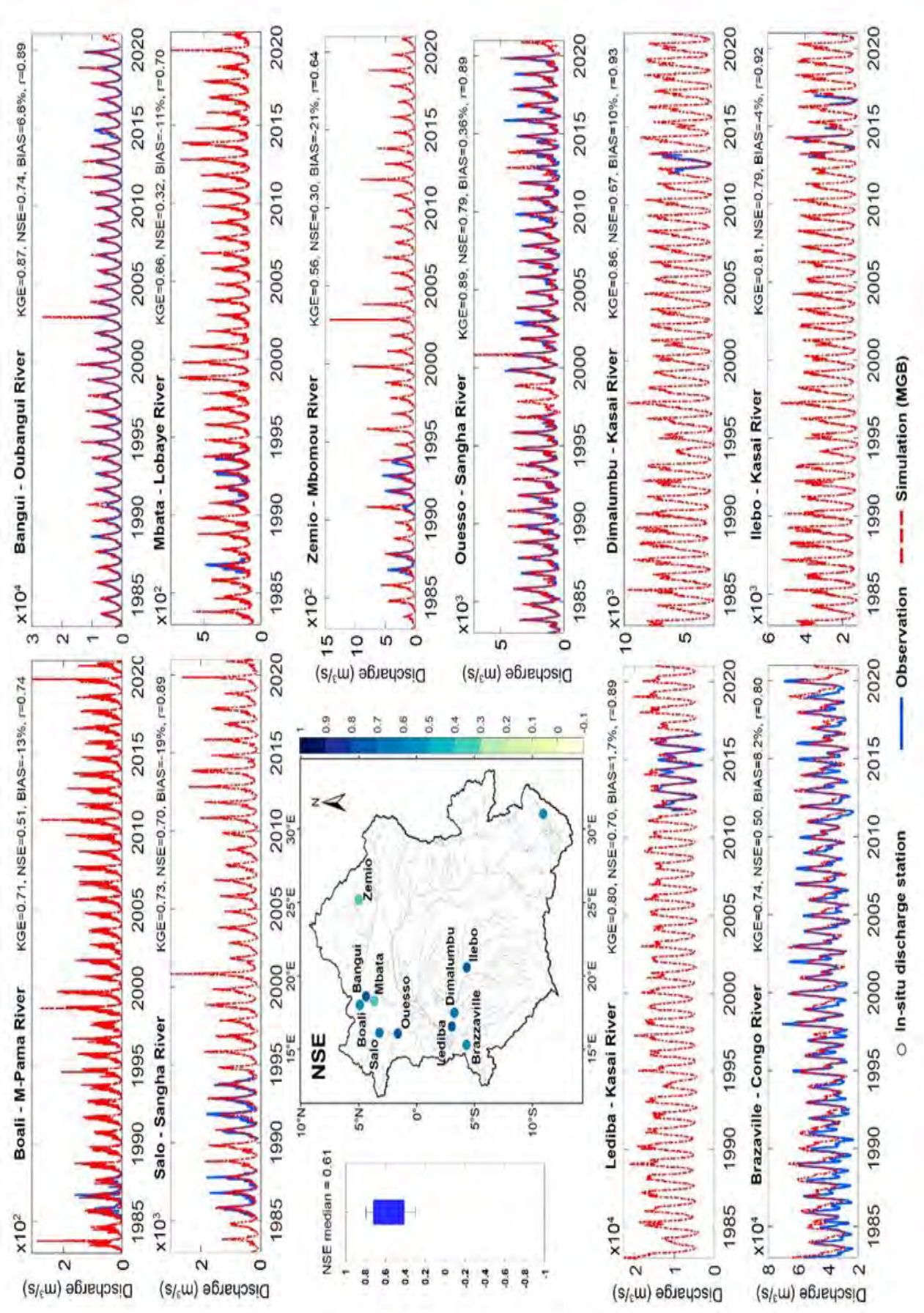
Boali - M-Pama River KGE=0.71, NSE=0.51, BIAS=-13%, r=0.74
Salo - Sangha River KGE=0.73, NSE=0.70, BIAS=-19%, r=0.89
Bangui - Oubangui River KGE=0.87, NSE=0.74, BIAS=6.6%, r=0.89
Mbata - Lobaye River KGE=0.66, NSE=0.32, BIAS=-11%, r=0.70
Zemio - Mbomou River KGE=0.56, NSE=0.30, BIAS=-21%, r=0.64
Ouesso - Sangha River KGE=0.89, NSE=0.79, BIAS=0.36%, r=0.89
Dimalumbu - Kasai River KGE=0.86, NSE=0.67, BIAS=10%, r=0.93
Ilebo - Kasai River KGE=0.81, NSE=0.79, BIAS=-4%, r=0.92
Lediba - Kasai River KGE=0.80, NSE=0.70, BIAS=1.7%, r=0.89
Brazaville - Congo River KGE=0.74, NSE=0.50, BIAS=8.2%, r=0.80
Discharge (m³/s)
NSE
NSE median = 0.61
Zemio
Bangui
Mbata
Boali
Salo
Ouesso
Lediba
Dimalumbu
Ilebo
Brazzaville
Observation
Simulation (MGB)
In-situ discharge station

Figure 6-14. Temporal series of observed (blue line) and simulated (red line) discharge for ten in situ stations for the long-term period 1981-2020. The spatial distribution and the boxplot of the statistical performance index for in situ gauges are shown in the left-centre panel.

Chapter 7: Conclusion and perspectives

7.1 Conclusion

As the second-largest river basin and tropical forest worldwide, with significant impacts on the socio-economic growth at the regional scale and of particular importance for carbon studies and in regulating Earth's climate, the CRB's hydro-climatology remained during decades among the least studied worldwide. This limits our capacity of understanding its characteristics and internal variability, and the CRB's impact on recent changes and extremes observed in the region. The low density of the hydrometeorological stations network and the occurrence of complex geomorphologic structures and processes deep inside the basin are among the causes of this critical state of knowledge in the basin. Therefore, there are still unanswered questions regarding the spatiotemporal variability of the CRB hydro-climatology and the understanding of climate impact in modulating hydrological variables in the region.
In this context, heterogeneous observations from consolidated in situ hydrometeorological stations, remote sensing databases (specifically, long-term satellite radar altimetry and SWE from multi-satellite technique), and numerical hydrological modeling were combined and analyzed to fill the gap spatial and temporal of hydrological information for the better understanding of the CRB's hydro-climatology.

To gain confidence with the long-term satellite-derived SWH from radar altimetry and SWE from GIEMS-2, an in-depth validation and assessment of these two large datasets were necessary. For the very first time, we compared radar altimetry SWH time series from ERS-2, ENV, SRL, J2/3, and S3A/B with in situ water level gauges (9 stations). A total number of ~2300 VSs were used in this study. The RMSE varied from 10 cm (with S3A) to 75 cm (ERS-2), with results in agreement with metrics from other basins and global literature, and an overall good agreement was observed. In parallel to this, the 25-year GIEMS-2 monthly SWE time series were also compared with monthly water flows and heights at the same in situ stations. Over the five major sub-basins, the comparison resulted in an overall good agreement, with a correlation coefficient ranging from 0.80 to 0.92, respectively for the Middle-Congo and the Ubangui sub-basins. The lowest correlation between SWE and discharges was observed in the Lualaba sub-basin, with a value of 0.54, probably due to its non-straightforward hydrology dominated by large lakes and their connections with floodplains. These two long-term and properly validated records were then used to analyze the spatiotemporal dynamics of surface freshwater and its propagation at the sub-basin and basin scales. SWH annual amplitude

exhibits large spatial variability across the basin. In the Ubangui and Sangha rivers, the variations can go up to more than 5 m, while in the Congo main-stream and *Cuvette Centrale* tributaries the variations are smaller (between 1.5 m to 4.5 m). At the basin scale, GIEMS-2 SWE shows that the maximum flood in the *Cuvette Centrale* occurs in October/November. The northern hemisphere part of the basin (Sangha and Ubangui basins) is flooded at its maximum in September/October, and the southern eastern part (Lwalaba basin) in January/February. At the sub-basin scale, SWE from GIEMS-2 compared well with seasonal and interannual variations of flow at the most downstream station of the basin, Brazzaville/Kinshasa station. When applying temporal shifts of 0 to 3 months on GIEMS-2 SWE time series, correlations with the flow at Brazzaville/Kinshasa ranged between 0.74 and 0.89 for the Kasaï, Ubangui, Sangha and Middle-Congo sub-basins, revealing the flood propagation dynamics and water residence time in flooded areas. Furthermore, SWH from satellite altimetry and SWE from GIEMS-2 joint analysis helped capture the relative contribution of each tributary to the flow at Brazzaville/Kinshasa station, characterized by a bimodal series. Most sub-basins showed higher correlation with the first peak that occurs between August and February at Brazzaville/Kinshasa while only the southern part (Kasaï) and Middle-Congo were more related to the second peak that occurs between March and July.

These results illustrated the capability of both long-term SWH from satellite radar altimetry and SWE from GIEMS-2 for monitoring the CRB's surface water as an ensemble and provided an inestimable insight on how floods propagate within the basin. The merging of these consolidated datasets opened an opportunity to estimate the long-term and interannual variations of freshwater SWS in the CRB.

To this end, we used two methods: the multi-satellite and hypsometric curves approaches. The multi-satellite approach combined SWE from GIEMS-2 dataset and long-term satellite-derived SWH from the multi-satellite mission with 35 days repeat cycle (ERS-2, ENV and SRL) (1995-2016) generated in the first part of this thesis. On the other hand, the hypsometric curves approach combines SWE from GIEMS-2 with topographic data acquired from four DEM (i.e., ASTER, ALOS, MERIT and FABDEM). Both methods allowed the production of an unprecedented dataset of monthly SWS anomaly over wetlands, floodplains, rivers and lakes across the entire Congo basin during the 1992-2015 period at ~0.25° spatial resolution. The SWS computed from the two methodologies and from different DEMs (four) generally showed good agreements between them at the interannual and seasonal scale, with minor exceptions for SWS variations from ASTER DEM due possibly to its largest vertical error. At the basin scale, the temporal variations of SWS satisfactorily depicted the bimodal pattern at the interannual

and seasonal scales and showed a strong seasonal variability along with the mean annual amplitude of ~101 ± 23 km^3, which, in perspective, represents ~8% of the Amazon basin's mean annual amplitude. Large SWS variability (e.g. from 0.3 to 0.6 km^3) was observed over the extensive wetlands and floodplains in the central (i.e., *Cuvette Centrale*) and the southeastern part (i.e., Bangweulu swamps and Mweru Upemba lakes) of the basin. At the sub-basin scale, the Middle-Congo and Lualaba sub-basins showed the higher mean annual amplitude (~71 ± 15 and 59 ± 15 km^3 respectively), amplitude that can be explained by the presence of lakes and their connections with floodplains within these sub-basins. Furthermore, the interannual SWS estimates were evaluated against independent datasets of satellite precipitation and in situ river discharge and, overall, a fair agreement was found, with correlation coefficients higher than 0.5 between the SWS and the two other variables. Moreover, this new dataset permits to depict the recent extreme events related to droughts and floods that occurred in the basin. As an application of this dataset, we mapped all over the basin the hydrological spatial signature of the widespread drought that took place in the end of 2005 and the beginning of 2006. Such mapping will help understand the impact of extreme events on freshwater resources.

Both methods showed limitations in their application in the CRB. Indeed, the hypsometric curves approach did not allow to generate SWS changes over lakes and in high altitude topography because of the altitude none-variation and large gradient, respectively. On the other hand, the multi-satellite approach exhibited a spatial constraint to produce the SWS changes over the entire basin due to the availability of VSs. Nevertheless, both methods are complementary. We advise using both methods in parallel. Future research may lead to identifying a way to combine both in one only process, merging the strengths of both.

This new 24-year dataset of SWS represents an unprecedented source of information for future hydrological or climate modeling and for water resources management in the Congo basin. It is worth noting that the analysis conducted with current remote sensing derived datasets still have some limitations such as temporal and spatial limitations. In order to better represent and understand the wide range of hydrological processes that occur across many spaces and timescales, also a near real-time monitoring of the CRB, these datasets were used jointly with a hydrological model.

To this end, a conceptual, semi-distributed, large-scale hydrological-hydrodynamics model, namely MGB, was set-up at daily time scale over the period 01 January 2001 to 31 December 2020 with a historical hydrological projection for the period 01 January 1981 to 31 December 2000. The simulated daily river discharge and water level showed good agreement during the

calibration and validation phases with in situ discharge and water level and satellite-derived water level from radar altimetry datasets with satisfactory statistical indexes (Kling–Gupta efficiency [KGE] of 0.84 and Nash–Sutcliffe efficiency [NSE] of 0.66 for river discharge and water level, respectively). In addition to this good performance, there is an improvement in the representation of the geometry of floodplains in particular the *Cuvette Centrale* (DEM at 90m of spatial resolution). With all the aforementioned improvement, we build for the very first time a unique spatiotemporal long-term dataset of hydrological variables over 1981 to 2020 at daily time scale across the CRB that bridges the gap between the past in situ databases and current and future monitoring of the CRB as an ensemble.

7.2 Perspectives

The development of the unprecedented SWS dataset and the hydrodynamic-hydrologic MGB model over a long-term period of more than 20 years across the CRB have paved the way for new perspectives of research in the basin.

Satellite-based estimation of a long-term variations of subsurface and groundwater storage

Following previous studies (Becker et al., 2018; Frappart et al., 2019; Pham-duc et al., 2020), SWS estimates opened new opportunities to generate a long-term (i.e., 2002 to 2015) spatio-temporal variations of subsurface and groundwater storage through decomposition of the Total Water Storage (TWS) variations as measured by the GRACE/GRACE-FO (Gravity Recovery and Climate Experiment Follow-On) knowing that the time variations of TWS are the sum of the contribution of SWS, the soil moisture and the groundwater (Pham-duc et al., 2019, 2020). Such understanding of freshwater variations in the continental reservoirs has many potentials to better characterize the hydro-climate processes of the region and improve our knowledge on the water resources availability in CRB.

Long-term spatiotemporal variations of the global surface water storage anomaly from space from 1992 to 2015

Global SWS estimates and variations are crucial to understand the role of continental water in the global water cycle (Papa and Frappart, 2021; Wu et al., 2022). Surprisingly, its knowledge about its spatiotemporal variability is still poorly known. Therefore, there is a fundamental need for the quantification of the storage of surface freshwater globally (Papa and Frappart, 2021;

Coss et al., 2023). The results of our research studies opened a new step toward the development of such a database using the hypsometric curve method since the datasets involved in the estimation of SWS are available globally (Kitambo et al., 2022b). As a first step in our attempt to compute the global SWS dataset, we devoted our effort to characterize the variations in SWS changes over the entire African (Fig. 7-1a) and South American (Fig. 7-1b) continent as shown in Fig. 7-1. To be confident with the South American's SWS estimates although there is still some ongoing work, we performed a validation with independent variables (Fig. 7-1c), here precipitation (from CHIRPS) and discharge data at Obidos. Overall, there is a fair agreement. It is worth nothing that the global estimates will offer new opportunities for hydrological and multidisciplinary sciences, including data assimilation, land–ocean exchanges and water management (Papa and Frappart, 2021). In addition, this global dataset will be a benchmark of the SWOT products in playing a key role in its evaluation and validation. Furthermore, this also paves the way for estimating long-term groundwater variations at the continental scales.

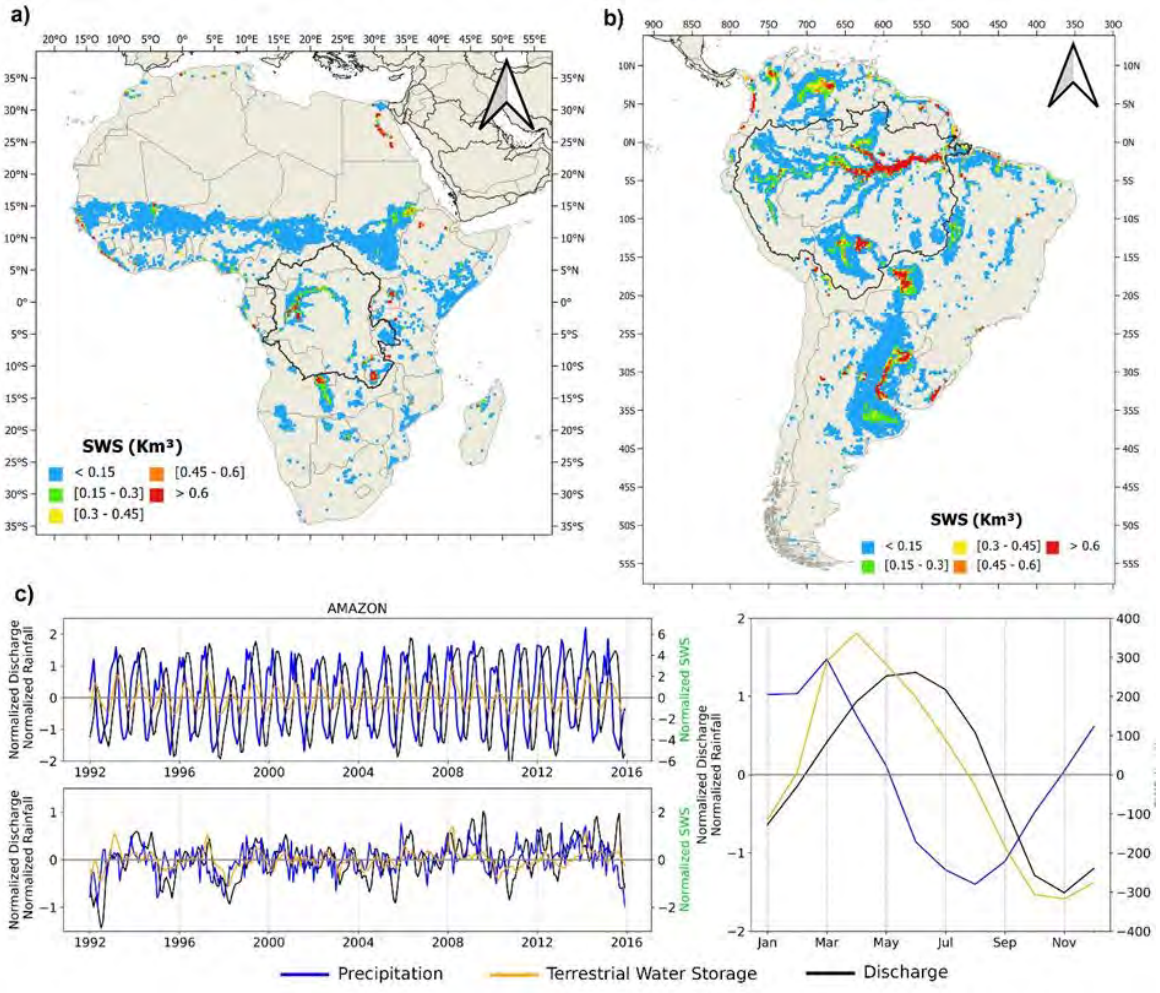

Figure 7-1. Spatial characterization of the SWS mean annual amplitude variations in km3 from the FABDEM hypsometric approach from 1992–2015. Over the African continent with the dark

bold line showing the CRB (a). Over the South American continent with the dark bold line showing the Amazon basin (b). Comparison at the entire Amazon basin between the monthly aggregated normalized surface water storage anomaly (orange line), normalized precipitation anomaly (blue line) and normalized discharge anomaly variations (dark line, at Obidos gauge station) (c). At (c), the upper panel is the interannual time series of the mentioned three variables along with their deseasonalized anomaly at the bottom panel. The right panel is the normalized mean annual cycle for the three variables (except for the SWS).

High-resolution of the estimation of the global surface water storage by SWOT satellite

Our research study (Kitambo et al., 2022b) has demonstrated as others (Papa et al., 2015; Frappart et al., 2015a; Pham-duc et al., 2019) the possibility of estimating surface freshwater storage over rivers, floodplains, and wetlands in combining different satellite observations of surface water extent and surface water level from radar altimetry or topographic data. This indirect technique was able to capture the spatial and temporal patterns of SWS at a coarse resolution of ~0.25° in different environments (i.e., Amazon basin, Congo basin, Ob River basin, Orinoco River basin, to name a few). However, there is a need for a comprehensive observation-based estimation of SWS globally (Wu et al., 2022; Coss et al., 2023). For the very first time, with its new technical concept, the wide-swath interferometric altimetry, SWOT mission will survey at higher resolution at the same time the height, area and changes in volume over time (Biancamaria et al., 2016). SWOT satellite will survey globally rivers wider than 100 metres and in general water bodies of 100 metres by 100 metres.

Understanding the hydrology of the CRB

Ndehedehe et al. (2019) evidenced the occurrence of a long-term drying trend over the past decades in the CRB. Moreover, other studies such as Kitambo et al. (2022b) and Becker et al. (2018) also highlighted the severe drought that happened in the end of 2005 and beginning of 2006 and the large flood that occurred in 1998, respectively. Little is known about their spatial signature, distribution, and severity over the basin. Therefore, this unprecedented dataset of river discharge and water level over 40-year spatially distributed across the CRB from the MGB simulation model paved the way to explore extreme events that have occurred recently in the CRB since 1981 and their link to climate.

In addition to this, some latest works on the CRB have indicated the possibility to subdivide the multi-year streamflow records into several homogeneous phases related to the hydrological

variability that affected the basin (N'kaya et al., 2022). For instance, by analyzing the annual

extremes (maximum and minimum) and daily mean discharge data over the 1911-2014 at Bangui station in the Ubangui sub-basin, Nguimalet (2017) demonstrated the noticeable difference in the hydrological response for the temporal changes in the Ubangui regime. Due to the limited in situ observations in the CRB, such studies can not be deployed all over the basin. Therefore, the long-term daily river discharge and water level of 40 years from the MGB simulation opens opportunities to conduct trend analysis studies everywhere in the CRB. Furthermore, research studies in the CRB have highlighted the importance that plays the *Cuvette Centrale* for Carbone (Crezee et al., 2022), sediment and ecology (Datok et al., 2022), and forest (Verhegghen et al., 2012). Kitambo et al. (2022a) also highlighted the strong influence of the *Cuvette Centrale* region on the flow at the most remote downstream station Brazzaville/Kinshasa, for which the variability may be explained, at ~35 %, by the variations in SWE in the large wetland region. With regard to this, there is a need therefore to better understand the processes governing the water dynamic in the *Cuvette Centrale* and examine its water balance by the means of the outputs of the MGB model. Moreover, the development of the unique spatiotemporal long-term dataset over 1981 to 2020 at daily time step across the CRB will enable the estimation on the contributions of the individual components of the water balance equation of the CRB and the partitioning between continental water storage variations (surface storage, groundwater and soil moisture), river discharge and evapotranspiration.

Hydrological reanalysis: data assimilation technique in the MGB model

In recent years, data assimilation techniques have been developed to enhance the output of hydrological variables by providing adequate and accurate hydrological data needed for water resources management (Wongchuig et al., 2019; Revel et al., 2023). The daily output of the river discharge and water level of the simulation conducted in our research thesis over 40 years showed an inconsistency mainly regarding the representation of the second peak (happening in March-July) of the hydrogramme. In general, during the calibration and validation phases, there was an overestimation of water volume by the model during this period. Based on the positive results obtained in Amazon basin when applying assimilation technique through to use of MGB model (Wongchuig et al., 2019; Revel et al., 2023), we assume that by performing a similar approach over the CRB, there will be a significant improvement in the representation of the

magnitude of water volume at the second and first peak of the hydrogramme and thus an increase in the statistical indexes.

Future assessments of hydrological variables in the context of climate change

Climate change, environmental alterations and anthropogenic pressure threaten freshwater resources availability in Africa (Papa et al., 2022). Tshimanga and Hughes (2012) had already evidenced the threat to water resources availability, including hydrological processes in the CRB due to the changes in land use practices, such as large-scale mining or deforestation. Moreover, in East Africa, climate change has affected the agriculture, water, and energy sectors and its impact is projected to increase in the future (Gebrechorkos et al., 2023). In order to allow adaptation and mitigation of the impacts in the future, the changes in climate are assessed by the means of hydrological models (Aloysius and Saiers, 2017; Gebrechorkos et al., 2023). The set-up in our thesis of the MGB model over 40-years can serve as a reference period that enables us to perform the assessment of the future changes in climate and hydroclimate extremes and their impacts on hydrology in the CRB using different global climate models and various scenarios of greenhouse gas emission and concentration evolution.

7.3 Conclusion (version française)

En tant que deuxième plus grand bassin fluviatile et forêt tropicale au monde, avec des impacts significatifs sur la croissance socio-économique à l'échelle régionale et une importance particulière pour les études sur le carbone et la régulation du climat à l'échelle globale, l'hydro-climatologie du bassin du Congo reste parmi les moins étudiées au monde, ce qui limite les connaissances sur ses caractéristiques, sa variabilité et ses changements dans la région. La faible densité du réseau de stations hydrométéorologiques est l'une des causes de cet état critique des connaissances dans le bassin. Par conséquent, il reste encore des questions sans réponse concernant la variabilité spatio-temporelle de l'hydro-climatologie du bassin du Congo et la compréhension de l'impact du climat dans la modulation des variables hydrologiques dans la région.

Dans ce contexte, différentes observations issues de la consolidation de la base de données des stations hydrométéorologiques in situ, de la télédétection, en particulier les longues séries de l'altimétrie radar satellitaire et des étendues d'eau provenant de la technique multi-satellite, et de la modélisation hydrologique ont été combinées et analysées afin de combler le manque

d'informations hydrologiques pour mieux appréhender l'hydro-climatologie du bassin du Congo.

Pour donner du crédit aux jeux de données long terme de hauteur d'eau de surface dérivées de l'altimétrie radar et des étendues d'eau issues de GIEMS-2, une validation et une évaluation approfondies de ces deux grands ensembles de données étaient nécessaires. Nous avons comparé à l'échelle interannuelle les séries temporelles de hauteur d'eau de surface issues de l'altimétrie radar des missions ERS-2, ENV, SRL, J2/3, et S3A/B avec plusieurs station in situ de niveau d'eau ou règle (7 stations). Un nombre total de ~2300 SVs a été impliqué dans cette étude. Les erreurs quadratiques moyennes ont varié de 10 cm (avec S3A) à 75 cm (ERS-2) en accord avec les résultats d'autres bassins et un bon ajustement global a été observé. Parallèlement à cela, la série temporelle mensuelle de GIEMS-2 sur 25 ans a également été comparée aux débits et hauteurs d'eau mensuels de sept stations in situ. Sur cinq sous-bassins majeurs, elle a montré une bonne concordance générale, avec un coefficient de corrélation variant de 0.80 pour le Moyen-Congo à 0.92 pour l'Oubangui. Le sous-bassin du Lualaba a présenté la plus faible corrélation de 0.54, probablement en raison de son hydrologie dominée par les lacs et leurs connexions aux plaines d'inondation. Ces deux jeux de données long terme ont ensuite été utilisés pour analyser la dynamique spatio-temporelle de l'eau de surface et sa propagation à l'échelle du sous-bassin et du bassin. L'amplitude annuelle de hauteur d'eau de surface présente une grande variabilité spatiale à travers le bassin, les rivières de l'Oubangui et de la Sangha présentant les plus grandes variations, jusqu'à plus de 5 m, tandis que les affluents du cours principal du Congo et de la *Cuvette Centrale* varient dans des proportions plus faibles (1.5 m à 4.5 m). A l'échelle du bassin, GIEMS-2 montre que la *Cuvette Centrale* est inondée à son maximum en octobre/novembre. La partie du bassin située dans l'hémisphère nord atteint son maximum en septembre/octobre, et la partie sud-est en janvier/février. A l'échelle du sous-bassin, GIEMS-2 s'est bien comparé aux variations saisonnières et interannuelles de débit de la station à l'exutoire du bassin Brazzaville/Kinshasa. En appliquant des décalages temporels de 0 à 3 mois sur les séries temporelles de GIEMS-2, les corrélations avec le débit à Brazzaville/Kinshasa ont varié entre 0.74 et 0.89 pour le Kasaï, l'Oubangui, la Sangha et le Moyen-Congo, révélant la dynamique de propagation des crues et le temps de résidence de l'eau dans les zones inondées. En outre, l'analyse conjointe de hauteur d'eau de surface et GIEMS-2 a permis de saisir la contribution relative régionale au débit à la station de Brazzaville/Kinshasa caractérisée par une série bimodale. La plupart des sous-bassins ont montré une corrélation plus élevée avec le pic qui s'est produit entre août et février à Brazzaville/Kinshasa, tandis que seule

la partie sud (Kasaï) et le Moyen-Congo étaient plus liés au pic secondaire qui s'est produit entre mars et juillet.
Ces résultats ont illustré la capacité que possède les jeux de données long terme de hauteur d'eau de surface provenant de l'altimétrie radar par satellite et des étendues d'eau provenant de GIEMS-2 à surveiller et à caractériser les eaux de surface du bassin du Congo dans son ensemble. La combinaison de ces deux ensembles de données a permis d'estimer les variations long terme et interannuelles de stock d'eau de surface dans le bassin du Congo.

Pour arriver à cette fin, deux méthodes ont été utilisées, la méthode par multi-satellite et celle des courbes hypsométriques pour estimer la dynamique des stocks d'eau de surface sur une longue période de plus de 20 ans. La méthode par multi-satellite a combiné les étendues d'eau issues de la base de données GIEMS-2 et les hauteurs d'eau de surface dérivées de l'altimétrie radar satellitaire des missions ayant un cycle de répétition de 35 jours (ERS-2, ENV et SRL, couvrant une période de 1995-2016) générées dans le premier objectif de la thèse. D'autre part, la méthode des courbes hypsométriques combine les étendues d'eau de GIEMS-2 avec les données topographiques acquises à partir de quatre MNT (ASTER, ALOS, MERIT et FABDEM). Les deux méthodes ont permis de produire un ensemble de données sans précédent sur l'anomalie mensuelle du stock d'eau de surface des zones humides, des plaines d'inondation, des rivières et des lacs sur l'ensemble du bassin du Congo pendant la période 1992-2015 à une résolution spatiale de ~0.25°. Les stocks d'eau de surface calculés à partir des deux méthodes et de différents MNT (quatre) ont généralement montré de bonnes concordances entre eux à l'échelle interannuelle et saisonnière, avec des exceptions mineures pour les variations de stock d'eau à partir du MNT d'ASTER, probablement en raison de sa plus grande erreur verticale. A l'échelle du bassin, les variations temporelles de stock d'eau de surface ont représenté de manière satisfaisante le régime bimodal du bassin à l'exutoire aux échelles interannuelle et saisonnière et ont montré une forte variabilité saisonnière ainsi qu'une amplitude annuelle moyenne de ~101 ± 23 km^3, ce qui, en perspective, représente ~8% de l'amplitude annuelle moyenne du bassin amazonien. Une grande variabilité des stocks d'eau de surface (par exemple, 0.3 à 0.6 km^3) a été observée sur les vastes zones humides et plaines d'inondation du centre (c'est-à-dire la *Cuvette Centrale*) et de la partie sud-est (c'est-à-dire Bangweulu, Mweru, Upemba) du bassin. À l'échelle des sous-bassins, les sous-bassins du Moyen-Congo et du Lualaba ont montré une amplitude annuelle moyenne plus élevée (~71 ± 15 et 59 ± 15 km^3 respectivement) due à la présence des lacs et leurs connexions avec les plaines d'inondation dans ces sous-bassins. En outre, les estimations interannuelles de stock d'eau de surface ont été

évaluées par rapport à des données indépendantes de précipitations par satellite et de débit fluvial in situ et, dans l'ensemble, un accord relativement bon a été trouvé, montrant souvent un coefficient de corrélation supérieur à 0.5. En plus, le nouvel ensemble de données a permis de capter les principaux événements extrêmes liés aux sécheresses et aux inondations. Comme application de ce jeu de données, nous avons cartographié, à travers le bassin, la signature spatiale de la sécheresse généralisée qui a eu lieu à la fin de 2005 et au début de 2006, ce qui a aidé à comprendre l'impact des événements extrêmes sur les ressources en eau douce du bassin du Congo.

Cependant, certaines limitations peuvent être soulevées pour les deux méthodes. La méthode des courbes hypsométriques n'a pas permis de générer des changements de stock d'eau de surface au-dessus des lacs et dans les régions à topographie de haute altitude, et d'autre part, la méthode de multi-satellite a présenté une contrainte spatiale pour générer les changements de stock d'eau sur l'ensemble du bassin en raison de la disponibilité limitée des SVs. Néanmoins, les deux méthodes sont complémentaires, la faiblesse de l'une étant compensée par l'autre.

Ce nouveau jeu de données de 24 ans de stock d'eau de surface représente une source d'information sans précédent pour les futures modélisations hydrologiques ou climatiques et pour la gestion des ressources en eau dans le bassin du Congo. Il convient de noter que l'analyse menée avec ces précédents ensembles de données a été réalisée à l'échelle de temps mensuelle avec des limitations spatiales. Afin de mieux représenter et comprendre le large éventail de processus hydrologiques qui se produisent à différentes échelles spatiales et temporelles, ainsi qu'un suivi en temps quasi réel des eaux de surface du bassin du Congo, ces ensembles de données ont été utilisés conjointement avec un modèle hydrologique.

A cette fin, un modèle hydrologique-hydrodynamique conceptuel, semi-distribué et à grande échelle, à savoir MGB, a été développé à l'échelle journalière sur la période du 01 janvier 2001 au 31 décembre 2020 avec une projection hydrologique pour la période historique du 01 janvier 1981 au 31 décembre 2000. Le débit et le niveau d'eau simulés au pas de temps journalier ont montré un bon accord pendant les phases de calibration et de validation avec le débit et le niveau d'eau in situ et le niveau d'eau dérivé du satellite à partir de données altimétriques radar avec des indices statistiques satisfaisants (Kling–Gupta efficiency [KGE] de 0.84 et Nash–Sutcliffe efficiency [NSE] de 0.66 pour le débit et le niveau d'eau, respectivement). En plus de cette bonne performance, il y a eu une amélioration dans la représentation de la géométrie des plaines d'inondation en particulier la *Cuvette Centrale* (DEM à 90m de résolution spatiale). Avec toutes les améliorations mentionnées ci-dessus, nous disposons pour la toute première fois d'un

ensemble unique de données spatio-temporelles à long terme de variables hydrologiques sur la période 1981 à 2020 à l'échelle journalière à travers l'ensemble du bassin du Congo qui comble le fossé entre les bases de données in situ historiques et contemporaine et future du bassin du Congo.

7.4 Perspectives (version française)

Le développement inédit du jeu de données de stock d'eau de surface et du modèle hydrodynamique-hydrologique MGB sur une période de plus de 20 ans dans le bassin du Congo a ouvert la voie à de nouvelles perspectives de recherche dans le bassin.

Estimation par satellite des variations long terme du stockage d'eau de subsurface et souterraine

Dans les études précédentes telles que Becker et al. (2018), Frappart et al. (2019), Pham-duc et al. (2020), les estimations du SWS avaient ouvert de nouvelles opportunités pour générer la variation spatio-temporelle long terme (c'est-à-dire, de 2002 jusqu'à 2015) des stocks d'eau de subsurface et souterraines par la décomposition de la variation du stock d'eau total (TWS) telles que mesurées par les satellites GRACE/GRACE-FO (Gravity Recovery and Climate Experiment Follow-On) sachant que les variations temporelles de TWS constituent la somme de la contribution du SWS, de l'humidité du sol (subsurface) et des eaux souterraines (Pham-duc et al., 2019, 2020). Une telle acquisition des variations d'eau douce dans les différents réservoirs continentaux a de nombreuses opportunités entre autres caractériser les processus hydro-climatiques de la région et améliorer nos connaissances sur la disponibilité des ressources en eau dans le bassin du Congo.

Les variations spatio-temporelles long terme de 1992 à 2015 de l'anomalie de stock d'eaux de surface à l'échelle globale depuis l'espace

Les estimations et les variations de SWS global sont cruciales pour comprendre le rôle de l'eau continentale dans le cycle global de l'eau (Papa and Frappart, 2021; Wu et al., 2022). De manière surprenante, les connaissances sur sa variabilité spatio-temporelle sont encore peu connues. Par conséquent, il existe un besoin fondamental de quantifier le stock d'eau douce de surface à l'échelle globale (Papa et Frappart, 2021 ; Coss et al., 2023). Les résultats de nos études de recherche ont ouvert une nouvelle étape vers le développement d'une telle base de

données en utilisant la méthode de la courbe hypsométrique puisque les ensembles de données impliqués dans l'estimation de SWS sont disponibles globalement (Kitambo et al., 2022b). Comme première étape dans notre tentative de calculer le jeu de données de SWS global, nous avons consacré nos efforts à caractériser les variations de SWS sur l'ensemble du continent sud-américain comme le montre la Fig.7-1. Il est à noter que les estimations globales offriront de nouvelles opportunités pour les sciences hydrologiques et multidisciplinaires, notamment l'assimilation de données, les échanges terre-océan et la gestion de l'eau (Papa et Frappart, 2021). En outre, cet ensemble de données global sera un point de référence pour les produits SWOT en jouant un rôle clé dans leur évaluation et leur validation. En plus de cela, ceci ouvre également la voie à l'estimation des variations à long terme des eaux souterraines à l'échelle continentale.

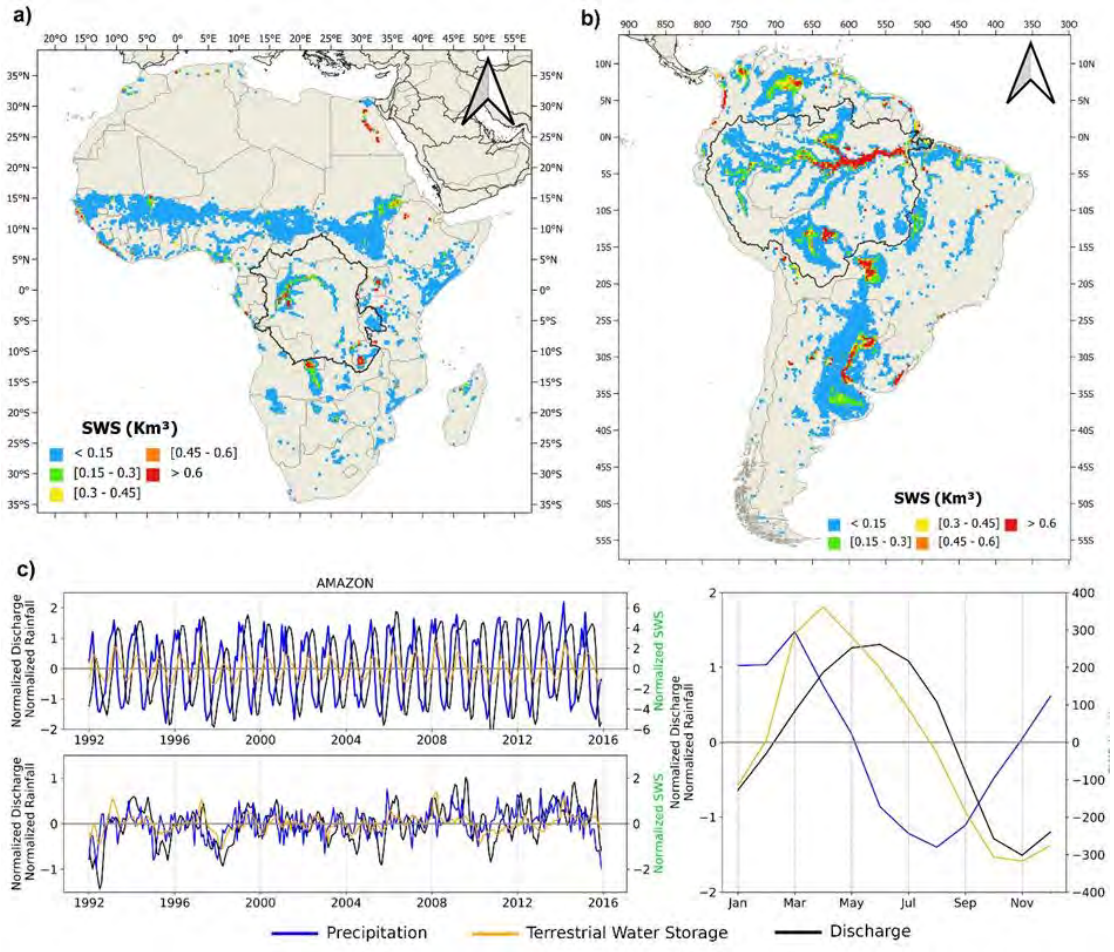

Figure 7-2. Caractérisation spatiale des variations de l'amplitude annuelle moyenne du stockage des eaux de surface en km3 à partir de l'approche hypsométrique utilisant FABDEM de 1992 à 2015. Sur le continent africain avec la ligne en gras noire montrant le bassin du Congo (a). Sur le continent sud-américain avec la ligne en gras noire montrant le bassin de l'Amazone (b). Comparaison sur l'ensemble du bassin de l'Amazone entre les variations

mensuelles agrégées de l'anomalie normalisée du stockage des eaux de surface (ligne orange), de l'anomalie normalisée des précipitations (ligne bleue) et de l'anomalie normalisée du débit (ligne noire, à la station de mesure d'Obidos) (c). Dans (c), le panneau supérieur est la série temporelle interannuelle des trois variables mentionnées ainsi que leur anomalie désaisonnalisée dans le panneau inférieur. Le panneau de droite est le cycle annuel moyen normalisé pour les trois variables (sauf pour le SWS).

Estimation à haute résolution du stock des eaux de surface à l'échelle global par le satellite SWOT

Notre étude de recherche (Kitambo et al., 2022b) a démontré comme d'autres (Papa et al., 2015 ; Frappart et al., 2015a ; Pham-duc et al., 2019) la possibilité d'estimer le stock d'eau douce de surface des rivières, des plaines inondables et des zones humides en combinant différentes observations satellitaires des étendues et du niveau d'eau de surface à partir de l'altimétrie radar ou de données topographiques. Cette technique indirecte a permis de générer les variations spatiale et temporelle du SWS à une résolution grossière de ~0.25° dans différents environnements (exemple du bassin de l'Amazone, bassin du Congo, bassin du fleuve Ob, bassin du fleuve Orinoco, etc). Cependant, il est nécessaire de disposer d'une estimation à l'échelle globale du SWS basée sur de l'observation directe pour diminuer les incertitudes (Coss et al., 2023). Pour la toute première fois, et grâce à son nouveau concept technique d'altimétrie interférométrique à large fauchée, la mission SWOT étudiera simultanément, à une résolution plus élevée, la hauteur, la superficie et les changements de volume dans le temps (Biancamaria et al., 2016). Le satellite SWOT étudiera globalement les rivières de plus de 100 mètres de large et en général les plans d'eau de 100 mètres sur 100 mètres.

Compréhension de l'hydrologie du bassin du Congo

Ndehedehe et al. (2019) ont mis en évidence l'apparition d'une tendance à l'assèchement à long terme au cours des dernières décennies dans le bassin du Congo. En outre, d'autres études telles que Kitambo et al. (2022b) et Becker et al. (2018) ont également mis en évidence respectivement la grave sécheresse survenue fin 2005 et début 2006 et la grande inondation survenue en 1998. On sait peu de choses sur leur signature spatiale, leur distribution et leur sévérité sur le bassin. Par conséquent, cet ensemble de données sans précédent sur le débit des rivières et le niveau d'eau sur 40 ans spatialement distribué à travers le bassin du Congo issu du

modèle de simulation MGB a ouvert la voie à l'exploration des événements extrêmes qui se sont produits récemment dans le bassin du Congo depuis 1981 et leur lien avec le climat.
En outre, certains travaux récents sur le bassin du Congo ont indiqué la possibilité de subdiviser les enregistrements pluriannuels de débit en plusieurs phases homogènes liées à la variabilité hydrologique qui a affecté le bassin du Congo (N'kaya et al., 2022). Par exemple, en analysant les extrêmes annuels (maximum et minimum) et les données de débit moyen journalier sur la période 1911-2014 à la station de Bangui dans le sous-bassin de l'Oubangui, Nguimalet (2017) a démontré la différence notable dans la réponse hydrologique pour les changements temporels du régime de l'Oubangui. En raison des observations in situ limitées dans le bassin du Congo, de telles études ne peuvent pas être déployées sur l'ensemble du bassin. Par conséquent, le débit journalier et le niveau d'eau à long terme de 40 ans de la simulation MGB ouvre des opportunités pour mener des études d'analyse des tendances partout dans le bassin du Congo.

Par ailleurs, des études de recherche dans le bassin du Congo ont souligné l'importance que joue la *Cuvette Centrale* pour le Carbone (Crezee et al., 2022), les sédiments et l'écologie (Datok et al., 2022), et la forêt (Verhegghen et al., 2012). Kitambo et al. (2022a) a également souligné la forte influence de la région de la *Cuvette Centrale* sur le débit de la station la plus en aval du bassin du Congo, Brazzaville/Kinshasa, dont la variabilité peut être expliquée à ~35%, par les variations des étendues d'eau dans la grande région humide de la *Cuvette Centrale*. Dans ce contexte, il est donc nécessaire de mieux comprendre les processus qui régissent la dynamique de l'eau dans la *Cuvette Centrale* et d'examiner son bilan hydrologique à l'aide des sorties du modèle MGB. De plus, le développement inédit de cet ensemble de données spatio-temporelles à long terme de 1981 à 2020 à pas de temps journalier à travers le bassin du Congo ouvre également la voix de pouvoir estimer les contributions des différents composants de l'équation du bilan hydrologique du bassin du Congo et la répartition entre les variations de stockage de l'eau dans le bassin du Congo, à savoir stockage de surface, humidité du sol et eaux souterraines, le débit des rivières et l'évapotranspiration.

Technique d'assimilation de données dans le modèle MGB

Ces dernières années, les techniques d'assimilation de données ont été développées pour améliorer la sortie des variables hydrologiques des modèles en fournissant des données hydrologiques adéquates et précises nécessaires à la gestion des ressources en eau (Wongchuig et al., 2019; Revel et al., 2023). Les sorties de débit et de niveau d'eau de la simulation réalisée dans notre thèse sur 40 ans à pas de temps journalier ont montré une incohérence principalement

concernant la représentation du deuxième pic (se produisant en mars-juillet) de l'hydrogramme. En général, pendant les phases de calibration et de validation, il y a eu une surestimation du volume d'eau par le modèle pendant cette période. Sur la base des résultats positifs obtenus dans le bassin de l'Amazone lors de l'application de la technique d'assimilation en utilisant le modèle hydrologique-hydrodynamique MGB (Wongchuig et al., 2019; Revel et al., 2023), nous supposons qu'en appliquant une approche similaire sur les sorties du modèle de notre simulation, il y aura une amélioration significative de la représentation de la magnitude du volume d'eau au deuxième et au premier pic de l'hydrogramme et donc une augmentation des indices statistiques.

Évaluations futures des variables hydrologiques dans le contexte du changement climatique

Le changement climatique, les altérations environnementales et la pression anthropique menacent la disponibilité des ressources en eau douce en Afrique (Papa et al., 2022). Tshimanga et Hughes (2012) avaient déjà mis en évidence la menace qui pèse sur la disponibilité des ressources en eau, y compris les processus hydrologiques dans le bassin du Congo, en raison des changements dans les pratiques d'utilisation des terres, comme l'exploitation minière à grande échelle ou la déforestation. En outre, en Afrique de l'Est, le changement climatique a affecté les secteurs de l'agriculture, de l'eau et de l'énergie et son impact devrait s'accroître à l'avenir (Gebrechorkos et al., 2023). Afin de permettre l'adaptation et l'atténuation des impacts dans le futur, les changements climatiques sont évalués à l'aide de modèles hydrologiques (Aloysius et Saiers, 2017 ; Gebrechorkos et al., 2023). La mise en place dans notre thèse du modèle MGB sur 40 ans peut servir de période de référence qui permettra de réaliser l'évaluation des changements futurs du climat et des extrêmes hydroclimatiques et leurs impacts sur l'hydrologie dans le bassin du Congo en utilisant différents modèles climatiques globaux et scénarios d'évolution des concentrations de gaz à effet de serre.

Appendix Publication record as co-author

1. Fabrice Papa, Jean-François Crétaux, Manuela Grippa, Elodie Robert, Mark Trigg, Raphael Tshimanga, ***Benjamin Kitambo***, Adrien Paris, Andrew Carr, Ayan Santos Fleischmann, Mathilde de Fleury, Paul Gerard Gbetkom, Beatriz Calmettes, Stephane Calmant; Water Resources in Africa under Global Change: Role of Earth Observation and Models for Monitoring Surface Waters; [Surveys in Geophysics] Published (2022); https://doi.org/10.1007/s10712-022-09700-9

Surveys in Geophysics
https://doi.org/10.1007/s10712-022-09700-9

Water Resources in Africa under Global Change: Monitoring Surface Waters from Space

Fabrice Papa[1,2] · Jean-François Crétaux[1] · Manuela Grippa[3] · Elodie Robert[4] · Mark Trigg[5] · Raphael M. Tshimanga[6], et al. ***[full author details at the end of the article]***

Received: 28 October 2021 / Accepted: 5 March 2022

Abstract
The African continent hosts some of the largest freshwater systems worldwide, characterized by a large distribution and variability of surface waters that play a key role in the water, energy and carbon cycles and are of major importance to the global climate and water resources. Freshwater availability in Africa has now become of major concern under the combined effect of climate change, environmental alterations and anthropogenic pressure. However, the hydrology of the African river basins remains one of the least studied worldwide and a better monitoring and understanding of the hydrological processes across the continent become fundamental. Earth Observation, that offers a cost-effective means for monitoring the terrestrial water cycle, plays a major role in supporting surface hydrology investigations. Remote sensing advances are therefore a game changer to develop comprehensive observing systems to monitor Africa's land water and manage its water resources. Here, we review the achievements of more than three decades of advances using remote sensing to study surface waters in Africa, highlighting the current benefits and difficulties. We show how the availability of a large number of sensors and observations, coupled with models, offers new possibilities to monitor a continent with scarce gauged stations. In the context of upcoming satellite missions dedicated to surface hydrology, such as the Surface Water and Ocean Topography (SWOT), we discuss future opportunities and how the use of remote sensing could benefit scientific and societal applications, such as water resource management, flood risk prevention and environment monitoring under current global change.

Keywords Africa · Hydrology · Surface water · Remote sensing · Modeling · Review

Article Highlights

- The hydrology of African surface water is of global importance, yet it remains poorly monitored and understood
- Comprehensive review of remote sensing and modeling advances to monitor Africa's surface water and water resources
- Future opportunities with upcoming satellite missions and to translate scientific advances into societal applications

Published online: 20 April 2022

1 Introduction

Freshwater on land is a vital resource for terrestrial life, ecosystems, biodiversity and human societies (Vörösmarty et al. 2000, 2010; Steffen et al. 2015; Seddon et al. 2016; Albert et al. 2021). Continental water is stored in various reservoirs, unevenly distributed across geophysical environments and climates (Chahine 1992; Shiklomanov and Rodda 2003). It includes seasonal ice and snow, glaciers and ice caps, aquifers, soil water and soil moisture, and surface waters (Stephens et al. 2020). The latter, comprising of rivers, lakes, man-made reservoirs, wetlands, floodplains and inundated areas (Alsdorf et al. 2007), is of particular significance as it supports diverse and dynamic environments globally and provides important benefits and services to human society and economic activities (Oki and Kanae 2006).

Surface waters are also an integral part of the global water cycle (Good et al. 2015; Trenberth et al. 2007), continuously exchanging mass with the atmosphere and the oceans, making them a key component of the climate system and its variability (Stephens et al. 2020).

However, freshwater storage and flux, their spatial distribution and variability, remain highly unknown in many regions of the world (Rodell et al. 2018), preventing the development of adequate and sustainable strategies to manage water resources (Oki and Kanae 2006; Hall et al. 2014).

This context leaves open major questions regarding the contemporary distribution of water availability across lands (Alsdorf et al. 2007): How much freshwater is stored across the surface of continents? What is the spatiotemporal dynamic of surface freshwater and how does it interact with climate variability and anthropogenic pressure?

These questions are of particular relevance for Africa, the second-largest continent in the world, both in size and population. The region occupies ~ 30 million km^2 and hosts almost 1.4 billion inhabitants as of 2022, currently ~ 18% of the global population (United Nations 2019). Africa's population is expected to double by 2050 with the share of global population projected to grow to 26% in 2050 and possibly ~ 40% by 2100 (United Nations 2019).

The African continent hosts some of the largest freshwater systems worldwide (Fig. 1), including the Nile, the longest river in the world, and the Congo River, the second-largest world's basin both in terms of drainage area and discharge to the ocean (Dai et al. 2009; Laraque et al. 2020). Three of the 10 largest freshwater lakes on Earth, in terms of area and volume, are also located in Africa, namely the Victoria, Tanganyika and Malawi Lakes (Hernegger et al 2021). Further, Africa is home to many wetlands and floodplains in the Congo, Chad, Niger, Okavango and Niles basins, which are of global significance for biodiversity and the carbon and nutrient cycles (Simaika et al. 2021; Lunt et al. 2019; Hastie et al. 2021). Some regions are also largely covered by tropical forest that harbors incredible natural resources and acts as a carbon sink that stores billions of tons of carbon (Verhegghen et al. 2012; Dargie et al. 2017). Conversely, smaller water systems, such as streams, reservoirs, ponds and tanks, are also part of the African landscapes (Gardelle et al. 2010), providing water, food and natural resources for agriculture to a large portion of the population that remains mainly rural such as in the sub-Saharan region.

The hydrology of the African continent is characterized by a wide range of processes that are under the influence of complex atmosphere–land–ocean interactions and the availability of freshwater is strongly heterogeneous, generally highly seasonal and driven primarily by local or remote rainfall (Conway 2002; Conway et al. 2009). It is subject to strong

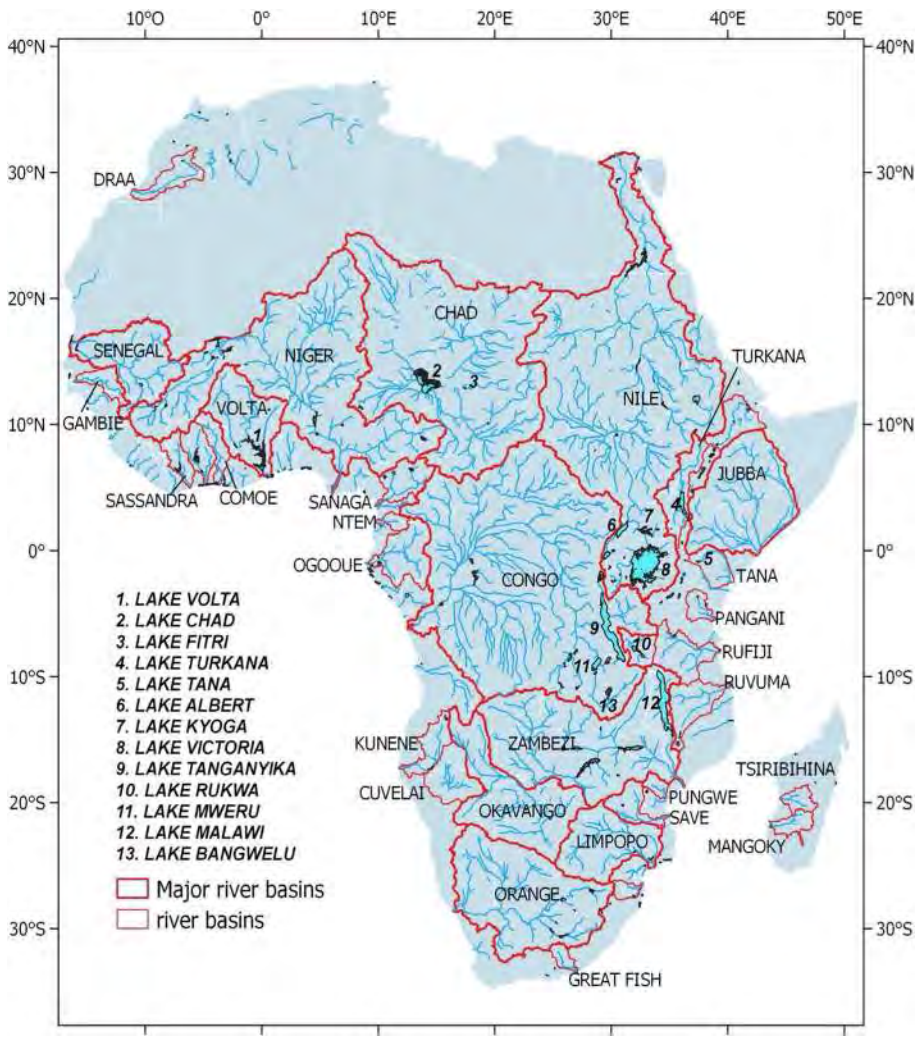

Fig. 1 Location of river basins and lakes in Africa

climate variability across timescales (Janicot, 1992; Hulme et al. 2001), from interannual to decadal changes (Ropelewski and Halpert 1996; Stager et al. 2007), with alternate periods of floods or droughts (Tierney et al. 2015; Oguntunde et al. 2018). Among many examples, Lake Chad and its dramatic shrinkage since the 1980s is obviously a symbol of how climate variability can impact African freshwater resources (Pham-Duc et al. 2020).

In the past decades, the combined effect of climate change and anthropogenic pressure made freshwater availability a current global major concern (Alcamo et al. 2007; Hoekstra et al. 2012; Famiglietti 2014; Konapala et al. 2020). In rapidly growing African economies, increasing demands for freshwater supply to sustain population growth and the needs of the agriculture and industrial sectors (Haddeland et al. 2014; Mehran et al. 2017) now pose significant threats to water resources. Environmental alterations such as land use practices, groundwater stress and deforestation, along with political conflicts, transboundary rivers,

inadequate infrastructure and low adaptive capacity in many regions, make the African population particularly vulnerable to hydro-climatic variability and to any future changes in the water cycle (Inogwabini 2020; Anderson et al. 2021).

A better understanding of hydrological processes across the continent therefore becomes fundamental for addressing these current challenges, for reducing uncertainty in future evolutions of water availability and for developing mitigation strategies (Adenuga et al. 2021).

Surprisingly, the hydrology of the African river basins remains one of the least studied worldwide and has not attracted as much attention among the scientific and international communities (Alsdorf et al. 2016) as has been, for instance, for other large tropical and subtropical regions such as the Amazon River basin (Fassoni-Andrade et al. 2021) or the Indian sub-continent with the Ganges–Brahmaputra (Papa et al. 2015 and references therein). It currently leaves an insufficient knowledge of Africa hydro-climate characteristics.

Historically, the monitoring of land surface water variability relies on in situ observations that quantify the movement (height, extent, discharge) and quality of water in river channels, lakes and wetlands. However, in situ networks are sparse, unevenly distributed globally, or even within a hydrological basin, particularly in remote areas with difficult access or security concerns. In situ gauge networks are generally costly to maintain, especially for developing countries, and the availability of ground-based hydrological information has dramatically decreased during the last decades (Fekete et al. 2012), especially over Africa (Tramblay et al. 2021). A striking example is the Congo River basin, where hydrological monitoring can be traced back to the beginning of the 20th century (Trigg and Tshimanga, 2020). Until the end of the 1960s, more than 400 gauging sites provided observations of water level and discharge (Alsdorf et al. 2016), while today, there are only 15 gauges considered as operational (Laraque et al. 2020). In addition, in many places, even when data exist, their public access can be restricted by government agencies (Chawla et al. 2020) and they are often not available to the scientific community due to political situations or transboundary water sharing conditions (Papa et al. 2010a). Finally, in situ data are not capable of monitoring all water characteristics such as large floods events, wetland-river connectivity or the variability of numerous small lakes/ponds in a same area (Alsdorf et al. 2007).

In addition to the assessment of water stock and fluxes, water quality is also a major issue. For example, cyanobacteria, often referred to as blue-green algae, are opportunistic prokaryotes with very strong adaptive capacities, some species of which can synthesize highly toxic metabolites. Cyanobacterial bloom can lead to eutrophication of water bodies. They can disrupt the dynamics of aquatic ecosystems by reducing water clarity and leading to hypoxia and therefore death of fish and benthic invertebrates following the degradation of cyanobacterial blooms. The production of toxins may disrupt irrigated crops (Mhlanga et al. 2006), recreational uses and may constitute an acute health risk (Funari and Testai 2008) by inducing digestive or neurological diseases.

Monitoring suspended particulate matter (SPM) in inland waters is also fundamental. SPM is related to the sediment fluxes in rivers, lakes, and reservoirs and can help with assessing the sediment discharge, and more generally the sediment budget within catchments, including its seasonal variability and its evolution over time. In turn, the sediment budget is controlling the silting rate of the dams, which impacts the sustainability of hydroelectric structures and the supply of water for treatment plants. SPM in surface waters also contributes to pollution and public health issues, playing an important role in the transport of nutrients and various types of contaminants (World Health Organization 2018). Indeed, SPM commonly favors bacteria development and, at the same time, decreases

their mortality through ultraviolet protection (Rochelle-Newall et al. 2015). Some of these bacteria or microbes cause widespread water diseases like diarrhea, which is one of the major causes of mortality in children under five years in developing countries (Reiner et al. 2018). Despite sub-Saharan Africa being the world region with the highest burden, few studies have analyzed the link between water quality parameters and bacteria in this area (Levy et al. 2016).

In this context, satellite remote sensing techniques offer a cost-effective means for monitoring the various components of the terrestrial water cycle, with a relatively continuous, high spatiotemporal coverage and reasonable accuracy (Chawla et al. 2020). Over the last thirty years, they have been very useful to hydrology investigations with the advent of monitoring the extent and elevation of water bodies and their changes over time from space (Alsdorf et al. 2007; Calmant et al. 2008; Chawla et al. 2020; Fassoni-Andrade et al. 2021, among others). For instance, since the late 1990s, radar altimetry missions provide observations of water levels of lakes, rivers and floodplains (Cretaux et al. 2017) under their orbit tracks, now with the potential of long-term monitoring at thousands of virtual stations (VS). In parallel, the use of satellite observations in a wide range of the electromagnetic spectrum (visible, infrared, and microwave, and their combination) has been developed to monitor the extent and quality of surface water bodies for various spatial and temporal scales (Papa et al. 2010b; Pekel et al. 2016; Prigent et al. 2016; Huang et al. 2018). They are often complementary to observations from the Gravity Recovery And Climate Experiment (GRACE) mission which provides, since 2002, long-term time series of the spatiotemporal variations in total terrestrial water storage (TWS) (Tapley et al. 2004) changes and helps to depict emerging changes in water availability at the global scale linked to environmental or human disturbances (Rodell et al. 2018).

In parallel, the availability of remote sensing observations has fostered the developments of hydrological and hydraulic modeling that helps to understand hydrological processes and their interactions and to build scenarios of past or future hydrological evolutions in the context of climate change, environmental alterations and flow/storage regulations by human interventions (Sood and Smakhtin 2015; Lettenmaier et al. 2015; Döll et al. 2016).

Earth Observation advances are therefore a game changer for surface hydrology and a unique opportunity to develop comprehensive observing systems to monitor Africa's land water and manage its water resources.

In the present paper, we review the developments and achievements of more than three decades of advances using remote sensing for surface waters in Africa (Fig. 2), highlighting the current benefits and difficulties.

Our review accounts for the various variables (water elevation, extent, storage, quality) of the surface water components including lakes, rivers, floodplains and wetlands. We analyzed approximately 200 publications. These contributions were selected using the knowledge of the experts that were reunited to make this review and using databases such as Web of Science. We mainly consider published papers in peer-reviewed journals and we do not include reports and other non-research articles and activities such as magazines, newsletters, editorials. Conference papers of notable relevance are also included. The period covered is from ~ 1990 to present. For each variable (Fig. 2), we summarized how it is retrieved from remote sensing observations, and present and discuss the advances that have been achieved from this information. Therefore, we show how the availability of a large number of sensors and observations, from low to very high resolution, coupled with models offers new possibilities to monitor a continent with scarce gauged stations. We also discuss how the use of satellite observations could benefit societal applications such as water resources management, flood risk prevention and environment monitoring. We then present

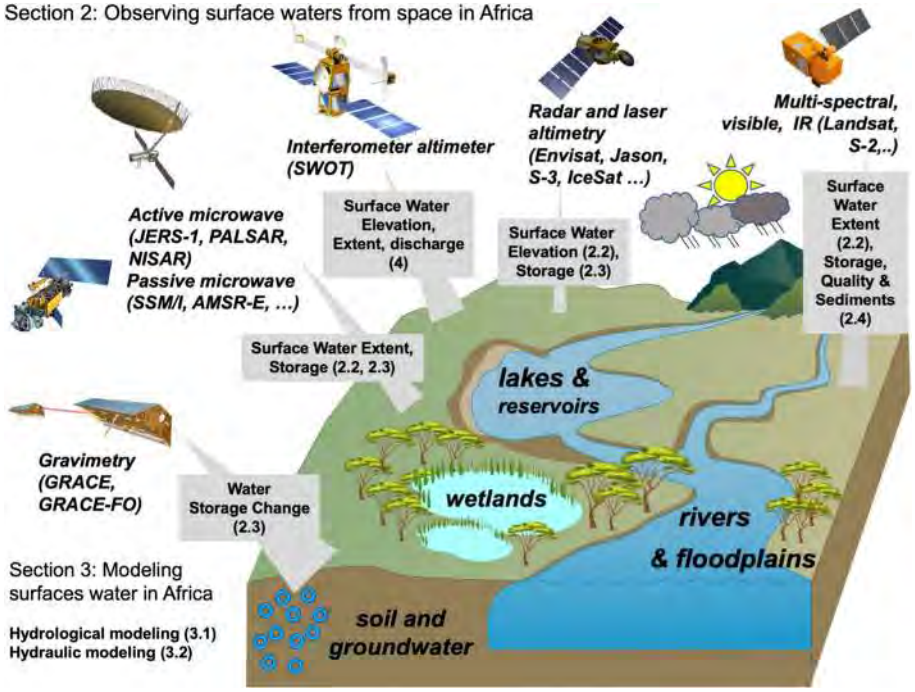

Fig. 2 Schematic representation of the outline of the review. The hydrological variables (water elevation, extent, storage, quality) of the surface water components and the main sensors/satellites that are used to monitor them are indicated. The number in bracket provides the section which addresses the respective hydrological variables and remote sensing techniques

perspectives, currently fostered by the upcoming launch of dedicated surface hydrology satellites, such as the Surface Water and Ocean Topography (SWOT) or the NASA-ISRO Synthetic Aperture Radar (SAR) mission (NISAR) or the planning of future missions for the next decade, such as the SMall Altimetry Satellite for Hydrology (SMASH) constellation and Sentinel-3 Topography New Generation (S-3 Topo NG).

The review is organized as follows (Fig. 2). Section 2 reviews the various methodologies and results in monitoring surface water from space. Section 3 deals with hydrologic and hydraulic models applied to African basins and with the use of remote sensors. Section 4 presents the current observational challenges and the future opportunities of the use of Earth Observations in hydrological sciences and multi-disciplinary sciences and for societal applications resources management. Finally, Sect. 5 concludes the study and provides recommendations.

2 Observing Surface Waters from Space in Africa

2.1 Surface Water Elevation from Earth Observation

Surface water elevation of inland water bodies is a key parameter in hydrology and water resources and has been long measured through historical gauge networks (Fekete et al.

2012). Over Africa, where traditional in situ measurements are sparse, a comprehensive monitoring of surface water elevation still remains a challenge. Moreover, the lack of fiducial in situ measurements can possibly be a limitation regarding the ground validation of remote sensing products.

Although, up to now, no satellite mission has been specifically designed to survey inland water elevations, satellite altimetry has been extensively used in the last three decades to remotely sense surface water elevation variations in lakes, rivers, reservoirs, and floodplains (Calmant et al. 2008) and improve the long-term monitoring of Africa's hydrology.

Radar altimeters onboard satellites are initially designed to measure the ocean surface topography by providing along-track nadir measurements of water surface elevation (Stammer and Cazenave 2017). Over the continents, pioneering studies in the Amazon basin (Fassoni-Andrade et al. 2021) quickly demonstrated the capacity of retrieving accurate surface water elevation from radar echoes and adapted retracking procedures at the intersection of the satellite ground track with a water body (Birkett 1998; Frappart et al. 2006; Da Silva et al. 2010). These intersections, named virtual stations (VSs), are defined by the satellite orbit configuration, the repeat cycle of which define also the temporal interval sampling of altimetric observations (generally 10, 27 or 35 days) (Normandin et al. 2018; Papa et al. 2012a). At a given VS, surface water elevation is estimated through the inversion of the signal round-trip propagation time between the satellite and the Earth's surface, which provides the range. Several corrections (in hydrology, essentially due to delayed propagation through the atmosphere or the interaction with the ionosphere and geophysical corrections due to the dynamics of Earth's surface) need to be applied to this range to retrieve the surface water elevation. The height of the reflecting surface, given in respect to the height of the satellite above the reference ellipsoid, is then corrected from the local undulation of the geoid in order to be converted into an orthometric height or geoidal altitude of the water body, the variable that is useful for hydrologists. For a detailed and complete description of the characteristics of the different satellite altimetry missions and the estimation of surface water elevation for hydrology, including the various re-trackers used, altimetric waveform description, the specific corrections (geoid gradient for lakes, hooking effect for rivers and small water bodies), the associated errors and biases, the different acquisition modes [Low-Resolution Mode (LRM), SAR, SAR Interferometric (SARIn)], we refer to Cretaux et al. (2017).

Several groups or institutions around the world provided time series of surface water elevation, covering a wide range of water bodies and applications. Table 1 provides the main sources and databases (non-exhaustive) that provide surface water elevation time series over Africa.

The in-depth assessment and validation of the water levels derived from the satellite altimeter over lakes, rivers and other inland water bodies were performed worldwide against in situ gauges (Frappart et al. 2006; Da Silva et al. 2010; Papa et al. 2010a; Ričko et al. 2012; Cretaux et al. 2018; Kao et al. 2019; Paris et al. 2022; Kittel et al. 2021a; Kitambo et al. 2021), with satisfactory results and uncertainties ranging between few centimeters to tens of centimeters, depending on the environments (Cretaux et al. 2017).

Radar altimetry over African lakes The large lakes (Fig. 1) of Central Africa (Chad, Fitri) and East Africa (in the Rift and adjacent regions, such as Lakes Victoria, Tanganyika and Malawi) are icons of Africa's tremendous water resources and valuable sentinels of the effects of climate variability and change. They remain highly dependent on the long-term rainfall characteristics (Becker et al. 2010; Hernegger et al. 2021), and they also influence the climate locally (Nicholson and Yin 2002). For instance, rainfall over Lake Victoria was found to be 30% higher than in the surrounding land areas, since part of the evaporation

Table 1 List of main databases providing surface water elevation time series over inland water bodies from radar altimetry

Name of the database (types of water body)	Producer (reference)	Website
River & Lake (Rivers, Lakes, reservoirs)	De Montfort University (Berry et al. 2005)	http://altimetry.esa.int/riverlake/continent/africa.html
Hydroweb (Rivers, lakes reservoirs)	IRD/LEGOS, CNES (French Space Agency), and Universidade do Estado de Amazonas (Cretaux et al. 2011; Da Silva et al. 2010)	http://hydroweb.theia-land.fr/
DAHITI (Rivers, lakes reservoirs)	German Geodetic Research Institute (Schwatke et al. 2015)	https://dahiti.dgfi.tum.de/en/
G-REALM (Lakes and reservoirs)	USDA NASA (Birkett et al. 2017)	https://ipad.fas.usda.gov/cropexplorer/global_reservoir/
GRRATS (Rivers)	Ohio State University (Coss et al. 2020)	http://research.bpcrc.osu.edu/grrats

returns directly to the lake through precipitation (Asnani 1993; Anyah et al. 2006). Synchronous variations in water level records on the three largest lakes in the Rift region are explained by large-scale climate mechanisms associated with oscillations of warm and cold phases of El Niño (Ogallo 1988; Nicholson 1996; Ropelewski and Halpert 1996; Stager et al. 2007) or the Indian Ocean Dipole (IOD) (Hastenrath et al. 1993; Marchant et al. 2006), or the Atlantic SST (Sea Surface Temperature) anomaly patterns (Janicot 1992). The IOD is also partly driving the lake water level over East Africa, modulated by El Niño-Southern Oscillation (ENSO) events (Mistry and Conway 2003; Birkett et al. 1999). Tierney and Russell (2007) further highlighted the significant influence of the Indian Monsoon variability and the migration of the Inter Tropical Convergence Zone (ITCZ) on African lake levels. The use of an 80 year-record of in situ level data at Lake Malawi (1916–1995) helped with identifying the links with the rainfall variability over the catchment and the flows of the Zambezi River (Jury and Gwazantini 2002), consistent with large-scale climate variability that helps the prediction of lake levels a year in advance. Finally, other studies have shown that global warming has an impact on precipitation and temperature variations with consequent changes in African lake levels (Xu et al. 2005; De Wit and Stankiewicz 2006).

Despite the importance of a regular monitoring of lake levels in Central and East Africa, very few lakes of this region are instrumented with level gauges allowing long-term monitoring.

Radar altimetry helps to fill this gap and has contributed to a better understanding of the processes that drive water level variations in these lakes. For example, Mercier et al (2002) used seven years of radar altimetry data with TOPEX/Poseidon (T/P) over the Great Lakes and large-scale rainfall measurements to reveal the links between SST (Sea Surface Temperature) in the Indian Ocean and rainfall over East Africa, which generated the consequent variations in the levels of these lakes. Combining satellite altimetry with GRACE observations and rainfall data, Becker et al (2010) confirmed that the variation in total water content over East African watersheds and lakes (Victoria, Tanganyika, Malawi and Turkana) was closely linked to the IOD and ENSO, confirming early results from Birkett et al (1999).

Using radar altimetry observations among other data, Swenson and Wahr (2009) evidenced a larger impact of human activities (such agriculture practices and the construction of dams) on Lake Victoria, between 2002 and 2008, as compared to other natural lakes in the region. They also showed that only 50% of Lake Victoria's water level variations could be explained by natural causes, while the other half is entirely due to discharges into Lake Kyoga directly downstream. In particular, radar altimetry data revealed that between 2002 and 2008, Lake Victoria's water level decreased about 40% faster than that in Lakes Tanganyika or Malawi.

Ahmed and Wiese (2019) also used GRACE data in combination with time series of lake water level changes from the Hydroweb database (Cretaux et al. 2011) to determine how much of the Total Water Storage (TWS) variability in East Africa and in the Zambezi basin comes from the lakes, including Lake Malawi. For the period 2002–2018, they report an increase in the water volume of eight lakes, which contributes to ~ 60% of the overall TWS increased over the Rift zone. This change is largely driven by the water volume variations over Lake Victoria. On the contrary, the region of Lake Malawi experienced a decrease in TWS over the same period, but with a large interannual variability, alternating water mass loss and gain over the catchment. Lake Malawi variations explain 50% of these regional changes, mainly due to natural climate variability.

Recently, Hernegger et al. (2021) used in situ data and satellite altimetry from the Database for Hydrological Time Series of Inland Waters (DAHITI) database (Schwatke et al. 2015) to evidence very high-water levels on six Kenyan lakes in the central rift valley, linked with the very high positive rainfall anomalies during the 2010–2020 decade, especially after 2018. This study, which covered a very long period (1984–2020), concluded that the recent water levels have reached record highs, due to very high rainfalls over the region in the past years.

Over Central Africa, in the Lake Chad basin, the origins of the lake level variations are different and have been directly influenced over the last decades by the succession of drier and wetter periods, but tempered by a strong interaction between surface water and groundwater (Pham-Duc et al. 2020).

To illustrate the use of radar altimetry over the lakes, Fig. 3 shows water level variations for eight large lakes across Africa (see Fig. 1 for their locations) over 20 years (2001–2020) derived from observations available on Hydroweb (Table 1). For lakes of such large size, many studies have evaluated the accuracy of altimetry-derived water level variations using field data at several locations worldwide in different environments. It showed that altimetry makes it possible to obtain long time series with a temporal resolution of a few days, and an accuracy of a few centimeters (Ričko et al. 2012; Cretaux et al. 2018).

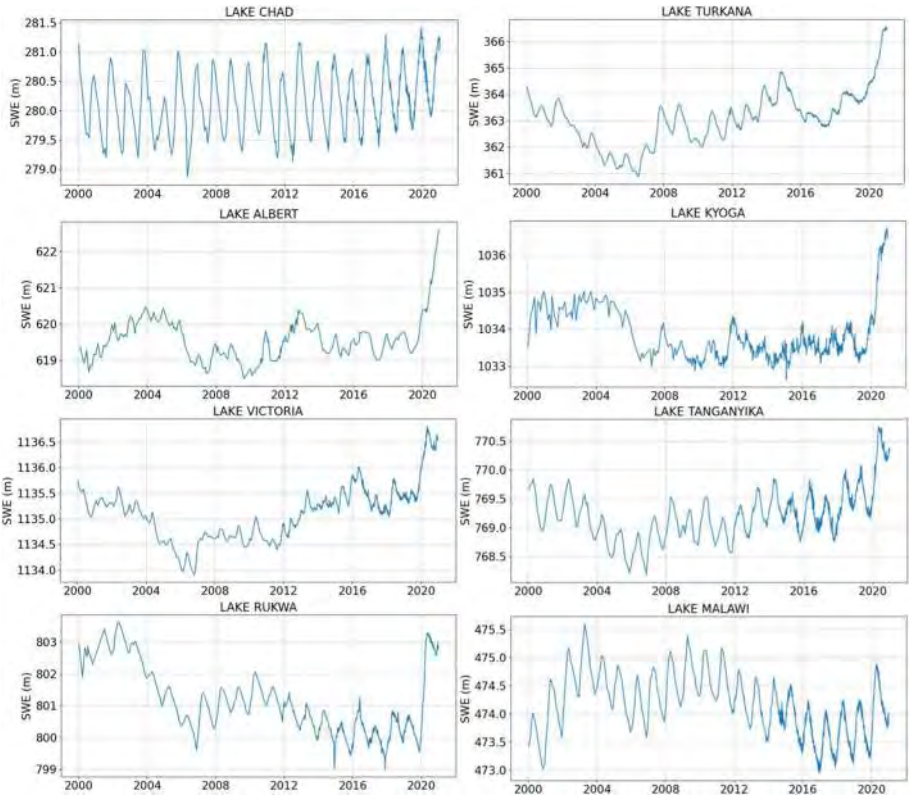

Fig. 3 Surface water elevation for 2000–2020 for a selection of eight large lakes in Central, East and Southern Africa (See Fig. 1 for their locations), extracted from the Hydroweb database (hydroweb.theia.land.fr) indicates the square of Pearson's correlation coefficient

Figure 3 shows a strong seasonal signal on Lakes Chad and Malawi, whereas for the Rift lakes, the signal is primarily dominated by multi-annual variability. Three generic behaviors are observed. For the first one (Lake Chad), we observed a gradual increase in water level, more pronounced at the end of the period (2019–2020). The second behavior, for the lakes in the Rift Valley (Victoria, Tanganyika and Turkana), is characterized by a very sharp increase at the end of the period. Finally, Lakes Rukwa, Kyoga, and Albert show a strong positive anomaly during the years 2001 to 2005, and in 2019–2020.

This can be explained by increasing rainfall observed in all central and east Africa over the last two years, generating a dramatic jump in water levels. It confirms the results found for lakes in Kenya by Hernegger et al. (2021) linked to rainfall excess. For the biggest lake of the region, Lake Victoria, with a total area of ~ 68,000 km^2, the increase in water storage for a level increase of ~ 1.5 m in one year is nearly 100 km^3. Lake Malawi, located within the Zambezi basin, presents over the whole period two positive anomalies, in 2002–2005 and 2008–2010, followed by a constant shrinkage until 2016, then a quasi-constant water level, only varying at seasonal scale, with a significant but not drastic increase as for the Rift valley lakes. This was in part observed in Ahmed and Wiese (2019) and fully linked to spatial patterns of the rainfall over the period of observation.

Other recent studies showed the potentials for retrieving water levels over smaller lakes, especially in western Africa, such as Lake Volta (Ni et al. 2017) and lakes in Nigeria (Okeowo et al. 2017). As discussed in Cretaux et al (2016) and Biancamaria et al (2016), one of the major limitations of satellite altimetry is its partial spatial coverage due to the satellite intertrack distance that leaves large regions with no observations, especially in the tropics (at the equator the intertrack can vary from tens of kilometers to few hundreds of kilometers), and prevent monitor of small lakes in between the tracks. This has improved with the tandem interleaved orbit configuration of Sentinel-3A/B (since 2018) which allows the densification of the Earth's coverage and therefore targets a much larger number of lakes and significantly improves the survey of narrow reservoirs. More recently, laser altimetry techniques, such as measurements by ICESat-2, proved useful to monitor water levels and water storage variability in reservoirs and lakes at the global scale and allow highlighting the important contribution of human management in Southern and Eastern Africa (Cooley et al. 2021).

Over the next few years, as discussed later in Sect. 4, major improvements to monitor surface water elevation are expected from SWOT which, thanks to his wide swath coverage will observe all lakes with an area bigger than 250 m × 250 m globally.

Radar altimetry over African River basins In parallel to applications over lakes, radar altimetry has been long used for monitoring the river systems of Africa. Many studies were conducted over African river basins to evaluate the capability of radar altimetry to retrieve the variations in water river elevation, and validate the estimates with the available in situ networks or dedicated field campaigns to overcome the lack of ground measurements. These studies contributed to the global effort to assess the potential of the technique and foster methodological developments. Michailovsky and Bauer-Gottwein (2014) used ENVIronment SATellite (ENVISAT)-derived water level variations along the Zambezi River and obtained a root-mean-square error (RMSE) of 32–72 cm with respect to in situ gauge data. Evaluations have also been reported over the Congo (Becker et al. 2014; Paris et al. 2022), the Nile (Eldardiry and Hossain 2019), the Niger (Schröder et al. 2019) and the Ogooué river basins (Bogning et al. 2018), with relative error and uncertainties in the same range as for other basins worldwide (Frappart et al. 2006; Da Silva et al. 2010; Papa et al. 2012b). Normandin et al (2018), focusing over the Niger River, is probably the most comprehensive evaluation of the performance of altimetry missions over Africa, assessing

seven satellite missions (i.e., European Remote Sensing Satellite-2 (ERS-2), ENVISAT, Satellite with Argos and ALtika (SARAL), Jason-1, Jason-2, Jason-3 and Sentinel-3A), against in situ records at 19 gauging stations in the Inner Niger Delta (IND) from 1995 to 2017. It reported an overall very good agreement between altimetry-based and in situ water levels with RMSE generally lower than 0.4 m. Better performances are reported for the recently launched missions such as SARAL, Jason-3 and Sentinel-3A than for former missions, suggesting improved results thanks to the use of the Ka-band for SARAL and of the SAR mode for Sentinel-3A. Similar conclusions regarding the improved performances of radar altimetry over time in a multi-mission context are also reported in the Congo Basin (Kitambo et al. 2021) where comparisons with long-term in situ water stages (1995–2020) provide RMSE reducing from 75 cm with ERS-2 to 10 cm with Sentinel-3A. We refer to Cretaux et al (2017) for a description of the recent missions and the advantages of the SAR mode as compared to the previous low-resolution data acquisition modes.

In recent years, many efforts have been seen carried out to increase the number of altimeric observations available across the African continent, fostered by the launch of new missions and as the result of almost thirty years of research and developments. But it is also a willingness of the scientific community, in agreement with local water agencies, to engage new studies specifically over Africa. Therefore, from several VSs a few years ago, there are now thousands of VSs available across the river basins of the continent, freely accessible on websites (Table 1), with potentially hundreds more of long-term observations. This is shown in Fig. 4 which displays the maximum amplitude of surface water elevation estimated for all available SV over Africa obtained from the Hydroweb database (see Table 1).

Note that all available VSs are displayed independently of the altimetry mission. So, it is worth noting that all SVs which are displayed don't necessarily cover the same period of time and don't have the same record length. Here, we used a total of 2157 VSs, including

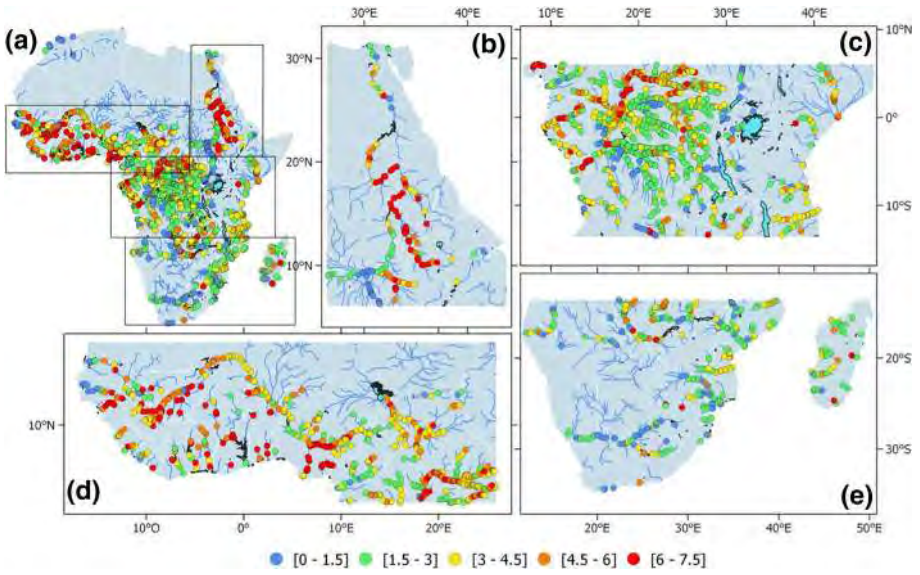

Fig. 4 River maximum amplitude of surface water elevation at altimetry-derived virtual stations **a** over Africa (in meters) and zoom in over **b** the Nile region, **c** the Congo River Basin and Central Africa, **d** the Sahelian region, **e** Southern Africa and Madagascar

173 VSs from ENVISAT (2002–2010), 204 VSs from Jason-2 (2008–2019), 230 VSs for Jason-3 (2016-present), 960 VSs for Sentinel-3/A (2016-present) and 797 VSs for Sentinel-3/B (2018-present). Moreover, for some VSs, the maximum amplitude is calculated from a time series with a 35-day interval sampling (ENVISAT), while others are estimated from observations with a 27-day (Sentinel-3A/B) or a 10-day (Jason-2/3) interval sampling. However, Fig. 4 clearly shows the high spatial coverage achieved over certain large river basins, but also on secondary size rivers.

To further illustrate the potential of radar altimetry measurements over the rivers of Africa, Fig. 5 shows examples of long-term time series of altimetry-derived river water elevation at several VSs in Africa obtained from the combination multi-mission observations.

The altimetry time series in Fig. 5 are composed from all the individual series collected by the successive altimetry missions since 1995, in a same reach. Bias between series due to river slope is taken into account to refer to a same location. Examples are provided for various environments and various types of rivers and geomorphological characteristics. For

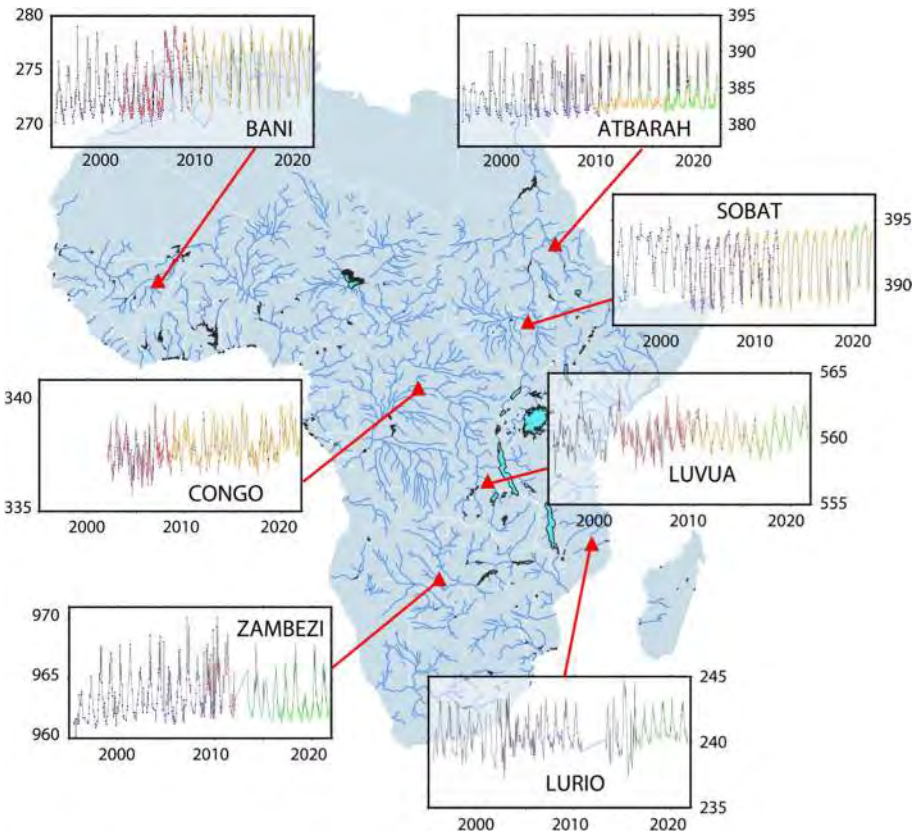

Fig. 5 Examples of long-term time series of altimetry-derived river water elevation (in meters) at several locations in Africa from multi-mission observations. Dark blue stands for ERS-2 measurements (every 35 days from 1995 to 2002), blue for ENVISAT (every 35 days from 2002 to 2012), light blue for SARAL (every 35 days from 2013 to 2016), red for Jason-1 (every 10 days from 2001 to 2008), orange for Jason-2 and Jason-3 (every 10 days since 2008), green for Sentinel-3A (every 27 days since 2016) and Sentinel-3B (every 27 days since 2018)

instance, the Atbarath River, a tributary of the Nile River, shows an example of river flowing in a desert environment and is characterized by reach width that varies largely between the low and high-water seasons (the minor bed is less than 100 m wide when the major bed is around 600 m). The Sobat river, also located in the Nile River Basin, is flowing in a vegetated area, with river width varying seasonally between ~ 100 and ~ 800 m. Over the Congo River, the time series illustrates the water elevation variability in the Cuvette Centrale, 1650 km upstream of the river mouth, characterized by a dense forest environment, frequently inundated. Luvua is a tributary of the Lwalaba River, in the Upper Congo, carrying waters from Lake Mweru to the Congo fluvial system. The reach is about 400 m wide, laterally bordered by seasonal inundated floodplains that can extent over several kilometers. As another example of large river, Fig. 5 also shows a reach of the Zambezi River located just downstream of the Sioma Falls, 2000 km upstream the river mouth, in a rare vegetation environment. The river It is well channelized with a width of ~ 1200–1300 m that stays almost constant over the seasons. Lurio is chosen as an example of small coastal river, flowing is a low vegetation environment, with a width seasonally varying between ~ 60 m and more than 800 m. Finally, the Bani River, a right-hand tributary of the Upper Niger river, upstream the Inner Delta is flowing in a quasi-desert environment. Its width can vary significantly, from 350 m at low waters to 1500 m at high waters when the major bed is temporarily inundated.

Altimetry data are extremely useful to better understand the processes that drive the hydrological variability across scales. Using T/P radar altimetry over the Chad Basin, Coe and Birkett (2004) demonstrated that river discharge upstream of the lake could be estimated from space, therefore, the lake and marsh height could be predicted in advance.

Becker et al. (2014) used radar altimetry-derived water levels at 140 VSs from ENVISAT to classify groups of hydrologically similar catchments in the CRB. In the Inner Niger Delta, cross-correlation analysis among water levels from the altimetry mission identifies time-lags between the upstream and the downstream part of the region of around two months that could be related to the residence time of water in the drainage area (Normandin et al. 2018).

In the Congo Basin, Lee et al. (2011) characterized the variability of terrestrial water dynamics in the Congo Basin using a combination of GRACE and satellite radar altimetry, while satellite altimetry-derived observations recently revealed the full range of variability of water surface elevation across the various rivers and wetlands of the Congo system (Carr et al. 2019). Now, more than 2000 VSs are available in the Congo Basin, sometimes covering almost 25 years of observations, thanks to multi-mission analysis (Kitambo et al. 2021). This has helped to reveal the seasonal dynamics of the Congo annual flood pulse, along with the relative contributions of the Congo sub-basins to the entire basin hydrology and the link with large-scale climate variability, including the annual bimodal pattern observed in the rainfall and discharge (Laraque et al. 2020). Smaller and ungauged basins are also strongly benefiting from the use of satellite altimetry observations such that the Ogooué River Basin in Central Africa (Bogning et al. 2018) or the so-called abandoned basins in terms of monitoring such as in Madagascar (Andriambeloson et al. 2020).

Finally, in addition to the most used missions for hydrology (such as Jason-2/3, ERS-2, ENVISAT, SARAL, Sentinel-3A/B), some studies are now making use of observations from Cryosat-2 and IceSat satellites to retrieve much detailed hydraulic characterization of the reaches such as over the middle Congo River (O'Loughlin et al. 2013) or the Zambezi River (Kittel et al. 2021a) or to take advantage of the drifting orbits (Bogning et al. 2018).

In addition to nadir altimetry, SAR Interferometry (InSAR) is another technique that can be used to estimate changes in water level by determining phase differences of more than

two complex SAR images obtained at different angles and/or at different times (Alsdorf et al. 2000). As firstly demonstrated over the Amazon, the technique provides water level changes in inundated floodplain vegetation under vegetation owing to the double-bounce effect (see Mohammadimanesh et al. (2019) for a review of the InSAR technique and its applications). Using this technique, Jung et al (2010) revealed strikingly different flood behaviors between the Amazon and the Congo systems, with the Congo system having less connectivity between the main channel, floodplains and interfluvial areas than in the Amazon. The complementarity between InSAR and ENVISAT radar altimetry has been also used in the wetland region of the Cuvette Centrale in the Congo Basin to derive surface water level from images from the Phased Array L-band Synthetic Aperture Radar (PALSAR) onboard the Advanced Land Observing Satellite-1 (ALOS) acquired from 2007 to 2010 (Lee et al. 2015) and to study the hydraulics characteristics of the Congo floodplain (Yuan et al. 2017a).

The new availability of such a large amount of altimetric-derived data over the African rivers opens new perspectives of scientific advances in hydrology, such as that in the Amazon Basin over the last decades. Among many examples, we can mention the use of satellite altimetry to derive altimetric profiles of rivers throughout the African river basins and provision of spatiotemporal variations in the water surface slopes which are useful to study backwater effects and their impacts on flows. Altimetry can also be very useful to observe channel-floodplain connectivity and study the role of channelized flows and of overbank flows, which contributes to surface water storage that has a crucial role in floodplain ecological productivity. The perspective to develop VSs over wetlands and flooded areas, far from river main channels, which seems now possible with Sentinel-3 SAR mode, will open new perspectives.

Further use of radar altimetry observations in hydrologic and hydraulic models is discussed in Sect. 3, while the role of water level derived from space to derive river discharge over Africa is discussed by Tarpanelli et al. (2021).

2.2 Surface Water Extent from Earth Observation

The extent of surface water bodies and their variation is of primary importance to the water, energy and biogeochemical cycles and the maintenance of biodiversity of the African continent. In many regions of Africa, water bodies cover a large portion land's surface area, with strong seasonal and interannual variability that play a key role in the carbon cycle (Hastie et al. 2021; Hubau et al. 2020), biogeochemistry processes (Borges et al. 2015) and the occurrence of water-related disasters such as flood risk in populated areas.

Measuring the distribution and variability in the extent of surface waters across different spatial and temporal scales has always faced great difficulties, especially using the in situ networks. It is indeed very difficult to estimate on the ground the variations in surface water extent in large floodplains and wetlands, especially under vegetation or during extreme events such as inundation. Even in the era of remote sensing observations, it still remains a challenge.

A variety of remote sensing techniques employing a wide range of observations in the electromagnetic spectrum, including visible, infrared, or microwave observations (Alsdorf et al. 2007; Prigent et al. 2016; Huang et al. 2018), have been developed in the last decades to estimate the distribution of surface water from very fine spatial resolution (few meters) to coarser ones (~ 50 km) covering various temporal scales and periods. These remote sensing techniques are now widely used in hydrology and water resource research.

Depending on the sensors or the applications they are developed for, these observations include a large range of space/time resolutions, most of the time resulting from a trade-off between temporal and spatial coverages and sampling (Chawla et al. 2020). For instance, SARs show very large capabilities to measure surface water extent at high resolution (10–100 m) but often suffer from a low temporal revisit time, making them not suitable to monitor rapid hydrological processes. In one hand, optical and infrared sensors have good spatial/temporal resolution, sometimes with ~ 10 m resolution and a few days revisit, but their capabilities are limited in tropical and subtropical Africa regions because of dense clouds and vegetation. On the other hand, passive microwave sensors offer frequent temporal sampling, sometime twice daily, but the observations are generally at low spatial resolution (~ 10–50 km) thus limiting their use to the monitoring of large surface water areas. As already mentioned in the previous section regarding surface water elevation, many methodologies regarding the monitoring of surface water extent from space in tropical environments have been originally conducted in the Amazon Basin (Fassoni-Andrade et al. 2021); with the African river basins only recently benefiting from these advances.

Following the use of SARs to delineate surface water extent in the Amazon floodplains and tropical forest environments (Hess et al. 1995, 2003), efforts have been carried out to undertake similar studies in the Congo River Basin that hosts several seasonally or permanently flooded areas, such as the Bangwelu and Upemba swamps or the Cuvette Centrale in the Middle Congo. Seasonal flooding dynamics and vegetation types were thus derived from the Japanese Earth Resources Satellite-1 (JERS-1) (Rosenqvist and Birkett 2002) or the use of multi-temporal SAR coverage, such as the ScanSAR mode of ALOS/PALSAR SAR data (Lee et al. 2011). They conclude that the JERS-1 SAR mosaics may serve well to appraise the maximum extents of flooding in the Congo River basin, but perform poorly to assess the dynamics and ranges of the variations. Bwangoy et al (2010) and Betbeder et al (2014) employed a combination of SAR L-band and optical imagery to characterize the Cuvette Centrale land cover. They estimated the wetland extent to reach more than 360,000 km^2, representing about 32% of the total area.

Nevertheless, these datasets generally represent large data volumes and suffer from low temporal frequency observations that limit these monitoring to a few samples of a few basins, preventing systematic, long-term assessments of inundation dynamics. This context is changing and SAR observations with a high resolution in the order of 10 m are becoming a very powerful tool to be used for monitoring flood risk and for managing disasters (Alfieri et al. 2018; Lindersson et al. 2020; Matgen et al. 2020). The case studies over Africa are becoming more relevant such as over Uganda (Barasa and Wanyama 2020), Namibia (Long et al. 2014) or the Zambezi region (Refice et al. 2020), even if SAR satellite missions, such as the Copernicus Sentinel-1 SAR (launched in 2014, global revisit of 6–12 days), still need to be fully exploited over Africa.

Passive microwave sensors [e.g., Special Sensor Microwave/Imager (SSM/I), Advanced Microwave Scanning Radiometer (AMSR-E)] have long demonstrated their capability for observing surface water and flood extent given the sensitivity of brightness temperatures and emissivities to the presence of surface water (Sippel et al. 1998; Prigent et al. 2007) and the different dielectric properties among water, soil and vegetation. They are not limited by cloud cover, with a near-daily revisit time (D'Addabbo et al. 2018), but suffer from a relatively low radiation intensity in the microwave spectrum that causes the spatial resolution of the data to be generally low (10–50 km), often insufficient to observe small water bodies. Floods can be assessed using passive microwave brightness temperatures (Brakenridge et al. 2007) calibrated with a ratio of dry/wet areas and river discharges to delineate flood plain extent and its variability and provide a fraction of surface water within an area.

It was specifically applied for flood detection in some regions in Africa, and forecasting has been investigated in the Zambezi watershed (De Groeve 2010) using AMSR-E imagery or in smaller scale watersheds with sparse observations in Malawi, East Africa (Mokkenstorm et al. 2021). Products making use of passive microwave-derived observations have been also specifically developed to monitor surface water extent over large African basins, such as the Surface Water Fraction (SWAF) product based on multi-angular and dual polarization passive L-band (1.4 GHz) microwave signal from Soil Moisture Ocean Salinity (SMOS) (Fatras et al. 2021). This product has been recently used to map the spatiotemporal variability of water bodies in the Congo River basin at ~ 50 km spatial resolution and weekly temporal resolution from 2010 to 2017, with the ability of the L-Band frequency to retrieve water under dense canopy (Parrens et al. 2017). They reported that the mean flooded area of the Congo extent was between 2 and 3% of the entire basin. The dataset was also helpful to characterize flood and drought events in the basin during the last 10 years.

The development of specific products for Africa remains limited and many studies over this continent rely on the use of products originally designed for global scale applications. These products are generally based on multi-satellite methodologies that combine the complementary strengths of the information provided by passive microwave observations with other types of satellite observations (Papa et al. 2010b). It includes the Surface WAter Microwave Product Series (SWAMPS) Inundated Area Fraction (Schroeder et al. 2015) and the Global Inundation Extent from Multi-Satellite (GIEMS; Prigent et al. 2007; Papa et al. 2010b) that quantify the variability of surface water extent at ~ 25 km over long periods (Papa et al. 2008; Prigent et al. 2012). The most recent version of GIEMS covers the period 1992 to 2015 on a monthly basis (GIEMS-2, Prigent et al. 2020), whereas SWAMPS now currently offers near-real-time information (Jensen et al. 2018). Figure 6 shows the distribution and temporal evolution of surface water extent estimated from GIEMS-2 (25 km, monthly) and GIEMS-D15 (500 m, static, see further below) over Africa, as well as their variability at seasonal and interannual timescales.

Over Africa, GIEMS was used to characterize the flood dynamics and seasonal flood wave in the Congo main steam and sub-basins (Becker et al. 2018; Kitambo et al. 2021). These studies also contributed to characterize basin scale water extent variability, including its link with large-scale climate modes (Becker et al. 2018), such as positive Indian Ocean Dipole events in conjunction with the El Niño event (especially the notable events in 1997–1998 and 2006–2007) that triggered major floods in the Congo Basin. It is worth noting that the estimates of surface water extent from SMOS, SWAMPS or GIEMS show an overall similar spatial distribution and variability in the Congo Basin. Their cross-evaluation against other products, such as the ESA-CCI (European Space Agency-Climate Change Initiative), and IGBP water bodies products also shows a fair agreement among the estimates. Nevertheless, an assessment of these products against high-resolution SAR map over the region, as performed for example over the Amazon Basin (Prigent et al. 2007; Fassoni-Andrade et al. 2021), has not been done yet, leaving open the question of whether the maximum surface water extent from passive microwave products in the Congo is largely underestimating the actual water extent.

GIEMS was also used to monitor the extent variation in the Inner Niger Delta (Aires et al. 2014) and was the reference for water extent variability in climate studies over African wetlands (Taylor et al. 2018; Prigent et al. 2011). These studies analyzed the influence of wetlands on rainfall patterns across sub-Saharan Africa and demonstrated that rainfall in the vicinity of major wetlands was locally suppressed as compared to nearby drier areas, especially during the afternoon, highlighting the influence of sub-Saharan Africa wetlands on local rainfall patterns.

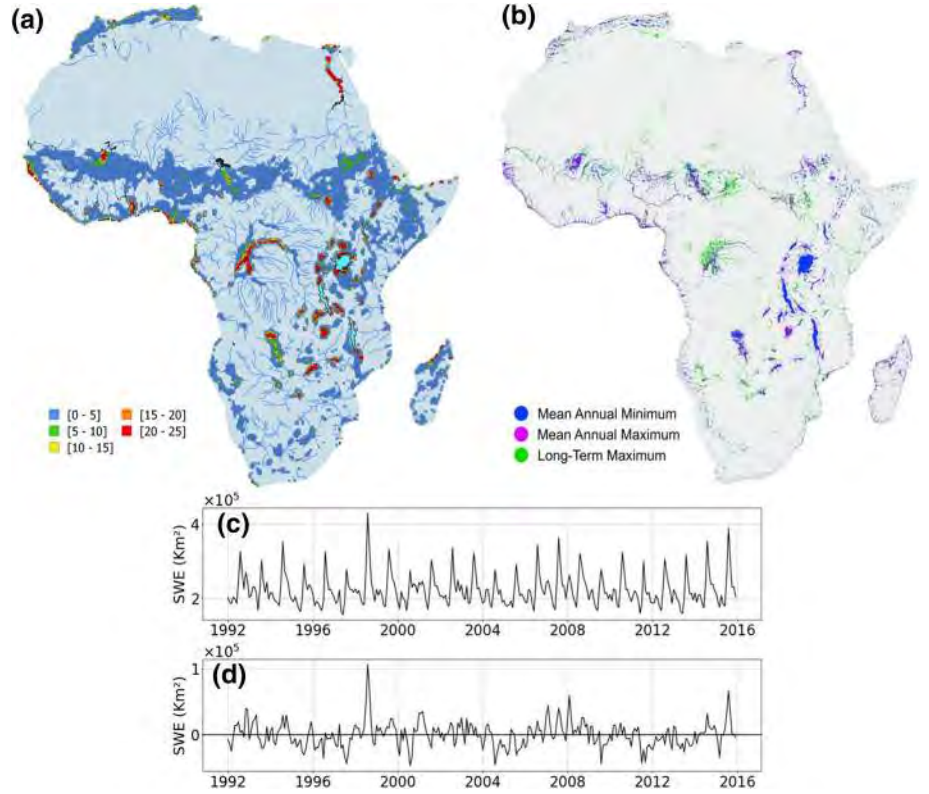

Fig. 6 Characterization of surface water extent from multi-satellite techniques over Africa. **a** Mean surface water extent (1992–2015) from GIEMS-2 expressed in percentage of the pixel coverage size of 773 km^2 (for visual purpose, only pixels with a value > 0.1% are displayed). **b** Surface water extent at 500 m spatial resolution from GIEMS-D15. **c** Time series of surface water extent aggregated over Africa, and **d** Corresponding deseasonalized anomalies obtained by subtracting the 24-year mean monthly value from individual months

Estimations of surface water extent can also be retrieved using observations in the visible and infrared domain (such as from Landsat, Advanced Very High-Resolution Radiometer (AVHRR), Moderate Resolution Imaging Spectroradiometer (MODIS) or Sentinel-2A/B to name only the most relevant) which offer moderate to high spatial (~ 5–500 m) and temporal (daily to weekly) resolutions. However, in tropical and subtropical environments, these observations potentially show strong limitations for detecting surface water beneath clouds or dense vegetation. As a consequence, obtaining cloud-free data during the flood season of tropical Africa is a challenge (Klein et al. 2015; Huang et al. 2018; Mayr et al. 2021).

The potential for using the MODIS Terra instrument to monitor changes in flooding was demonstrated over specific regions such as the arid Inner Niger Delta (Bergé-Nguyen and Crétaux 2015). Weekly estimates make it possible to describe the process of inundation in the delta and to quantify the flooded scenes in terms of open water and a mixture of water, dry land and aquatic vegetation. More importantly, the study showed there was an increase in vegetation over the 14 years of study (2000–2013) and a slight open water

decrease over the region. Pham-Duc et al. (2020) also used times series of the surface water extent derived from multispectral MODIS over the Lake Chad to show that the lake extent has remained stable during the last two decades (2000–2020) and has not been affected by drastic changes since the 2000s, despite some large year to year variations. However, this study also highlighted the need to provide a clearer definition of the observed target to accurately delineate water and water under vegetation, as differences between estimates across studies can remain large.

More recent satellite missions, such as Landsat 8 (since 2013), which carries the Operational Land Imager (OLI), Landsat 9 (since 2021, carrying OLI-2), Sentinel-2A (since 2015) and Sentinel-2B (since 2017), both carrying the MultiSpectral Instrument (MSI) (Drusch et al. 2012) offer new opportunities to study fine scale surface water extent variability. As proposed by Ogilvie et al (2020), the emergences of all these observations from Landsat 7/8, Sentinel-2 and MODIS offer new opportunities for multi-sensor approaches to long-term water monitoring of temporary water bodies, as demonstrated over the Senegal River floodplain. Their results provide important implications to guide the development of multi-sensor products to monitor large wetlands, floodplains and water bodies of Africa.

Finally, there is a strong need to accurately monitor the extent and variability of small water bodies, particularly in semiarid areas of Africa where these small water bodies, being widely spread all over the landscape, provide a critical resource to rural population. Small water bodies are very reactive to climate variability and can exhibit complex and sometimes unexpected dynamics, such the paradoxical increase in surface and volume during and after big Sahelian droughts (Gal et al. 2017). Optical sensors have proved successful to monitor their dynamics in different semiarid regions as for example the Sahel (Haas et al. 2009, 2011; Gardelle et al. 2010; Gal et al. 2016; Grippa et al. 2017), Tunisia (Ogilvie et al. 2018) and Namibia (Naidoo et al. 2020). Using Landsat, Pekel et al (2016) provided a detailed dataset, the Global Surface Water (GSW) of open inland water worldwide at 30 m resolution, that include the characteristics of the seasonal cycles and trends over the last 30 years. Although open water can be easily detected using the middle infrared bands, the retrieval of water areas is more difficult when aquatic vegetation or trees are present. Indeed, most small water bodies are not permanent and several of them are covered by aquatic vegetation and/or trees which requires the development of specific algorithms to take them into account. For example, a supervised classification (here, the Active Learning for Cloud Detection (ALCD) from Baetens et al. 2019) using Sentinel-2 over the Gourma region in the Sahelian Mali (Fig. 7, based on the T30PXC tile in the Sentinel-2 US-Military Grid Reference System (MGRS) naming convention) illustrates well the high number of small temporary lakes. In the middle of the dry season (Fig. 6a), only 158 lakes are depicted, mainly open water (150 open water, 8 with vegetation) for a total water area of 29,9211 km^2. At the end of the wet season (Fig. 7b), 337 lakes have been detected, about half of them being covered with vegetation (177 open water, 160 with vegetation) for a total water area of 96,1802 km^2. Only half of the detected lakes in Fig. 7b are included in GSW (Pekel et al. 2016), mainly due to the fact that this database focuses on open water and misses most of the lakes covered by vegetation. Maximum water area over the 1984–2019 period in this database is equal to only 67,3585 km^2.

To conclude this section, it is also worth mentioning the efforts developed to take advantage of the combination of the various observations we described above. For instance, the low resolution but long-term estimates of passive microwave can be combined to optical data, such as those from MODIS with higher spatial resolution, but limited in time, via downscaling methodologies that combine both estimates into long-term, high-resolution products, such as the inundation extent product proposed over the Inner Niger Delta (Aires

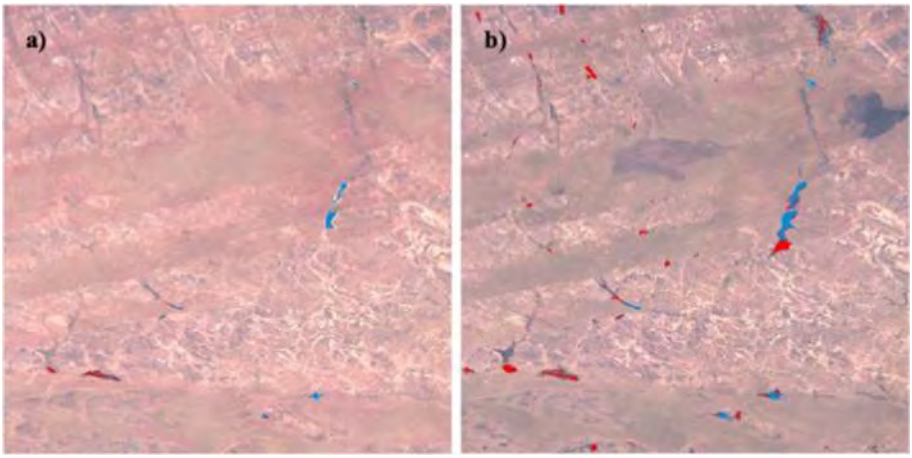

Fig. 7 Sahelian small water bodies from Sentinel-2 and supervised classification in Gourma, Mali. **a** dry season (16/03/2018), and **b** rainy season (11/11/2018). Red: lakes with vegetation, Blue: open water

et al. 2014). This was one of the starting points of several other studies using downscaling approaches based on topography and floodability index, that now provide global maps of surface water coverage at high spatial resolution, such as GIEMS-D15 (Fluet-Chouinard et al. 2015; ~500 m spatial resolution) and GIEMS-D3 (Aires et al. 2017, 90 m) that can be extremely useful for African water bodies.

It is obvious that more investigations are required to fully characterize the diversity and variability in the extent of African water bodies, especially in relation to the physical processes driving this dynamic. Great opportunities, as discussed further in Sect. 4, will emerge with the upcoming launch of the SWOT (Biancamaria et al. 2016; Grippa et al. 2019) and L-band SAR from NASA/ISRO SAR (NISAR) missions which will provide improved monitoring of African surface water across many scales.

2.3 Surface Water Storage in Lakes, Rivers, Wetlands and Reservoirs

Surface water storage, which represents the amount of freshwater stored in surface water bodies, is also a very important quantity to be estimated for hydrology and water resources (Schumann et al. 2016; Papa and Frappart 2021). As surface water storage is, by definition, linked to the variations in surface water level (Sect. 2.1) and extent (Sect. 2.2), it is similarly challenging to quantify at adequate time/space sampling.

The Gravity Recovery And Climate Experiment (GRACE) observations (and its follow-on mission GRACE-FO) provide, since 2002, estimates of the spatiotemporal variations in total terrestrial water storage (Tapley et al. 2004; Rodell et al. 2018) with an accuracy of ~1.5 cm of equivalent water thickness when averaged over surfaces of a few hundred square-kilometers. This quantity results from the changes in groundwater storage, soil moisture storage and surface water storage (it also includes ice and snow changes, but this is not applicable over Africa). Quantifying the storage of surface water is key to partition the GRACE-derived estimates in its different water storage contributions and to better quantify groundwater storage changes (Frappart et al. 2019). GRACE data also proved

successful in estimating water stock changes over the Sahel (Grippa et al. 2011). In tropical and subtropical humid environments, the contribution of surface water storage to total terrestrial water storage can be substantial, sometimes up to 50% (Kim et al. 2009; Getirana et al. 2017a), and the lack of information at the surface prevents an estimate of groundwater/subsurface storage changes from GRACE data.

The estimation of surface water storage from space is generally based on multi-satellite approaches that use the complementarity between products which provide the dynamic of the surface water extent and observations of surface water elevation. Thus, their combination offers the possibility to estimate surface water volume changes (Cretaux et al. 2016; Papa and Frappart 2021).

Over lakes and reservoirs, satellite altimetry and satellite imagery together are now commonly used to calculate water storage changes in order to study their dynamic and water balance. For a detailed description of the concept that establishes the relationship between water level, extent and water volume changes in lakes and reservoirs using a hypsometry approach, we refer to Cretaux et al. (2016), Gao et al. (2012), Duan and Bastiaanssen (2013) and Gal et al. (2016). If the bathymetry of the lake or reservoir is known, this can also be used in combination with water level estimation to infer surface water storage variations.

Several databases, generally the ones that also provide water level from altimetry (Sect. 2.1), now make water storage change estimates in lakes and reservoirs available (Hydroweb and DAHITI for instance), including several water bodies in Africa. Notably, Tortini et al (2020) and Tusker et al. (2019) built on relationships between elevation and surface area from multiple satellite altimetry missions and surface water extent estimated from Terra/Aqua MODIS or Landsat (such as GSW). They estimate continuous surface water storage changes in large lakes and reservoirs globally for 1992–2019, with many targeted lakes in Africa.

Over rivers, given the heterogeneity of channels, streams and terrain, estimating surface water storage variations is very difficult and there are only several studies worldwide and over Africa (Papa and Frappart 2021) that have been performed so far. The estimation is based on the combination of inundation extent products with surface water elevation from altimetry, similar to lakes and reservoirs, but the difference in elevation within the basin or between rivers and floodplains needs to be taken into account. Over Africa, the studies were mainly focused over the Congo River Basin, considering surface water extent maps from high to low spatial resolution products, depending on the applications.

Becker et al. (2018) combined GIEMS observations with altimetry-derived water levels from ENVISAT at 350 VSs to estimate monthly surface water storage change over the period 2003–2007 (Fig. 8) following the development of the methodology over other river basins (Frappart et al. 2008, 2012; Papa et al. 2015). In general, the uncertainties associated with the method (calculated by taking into account the uncertainties on both the water level from altimetry and GIEMS surface water extent) is ~25% in tropical river basins (Frappart et al. 2008; Papa et al. 2015; Papa and Frappart 2021). Over the entire Congo Basin, Becker et al. (2018) reported that the mean annual variation in surface water storage change amounts to $\sim 81 \pm 24$ km^3 (with an estimated uncertainty of 26%). This variation accounts for 19 ± 5% of the annual variations in GRACE-derived total terrestrial water storage.

Lee et al. (2011) used a combination of several observations (including total water storage, water level from radar altimetry, precipitation and imagery from JERS-1 and MODIS) in a frame of a water balance study to estimate the amount of freshwater entering and exiting Congo wetlands. They showed that 111 km^3 of water were flowing through the Congo

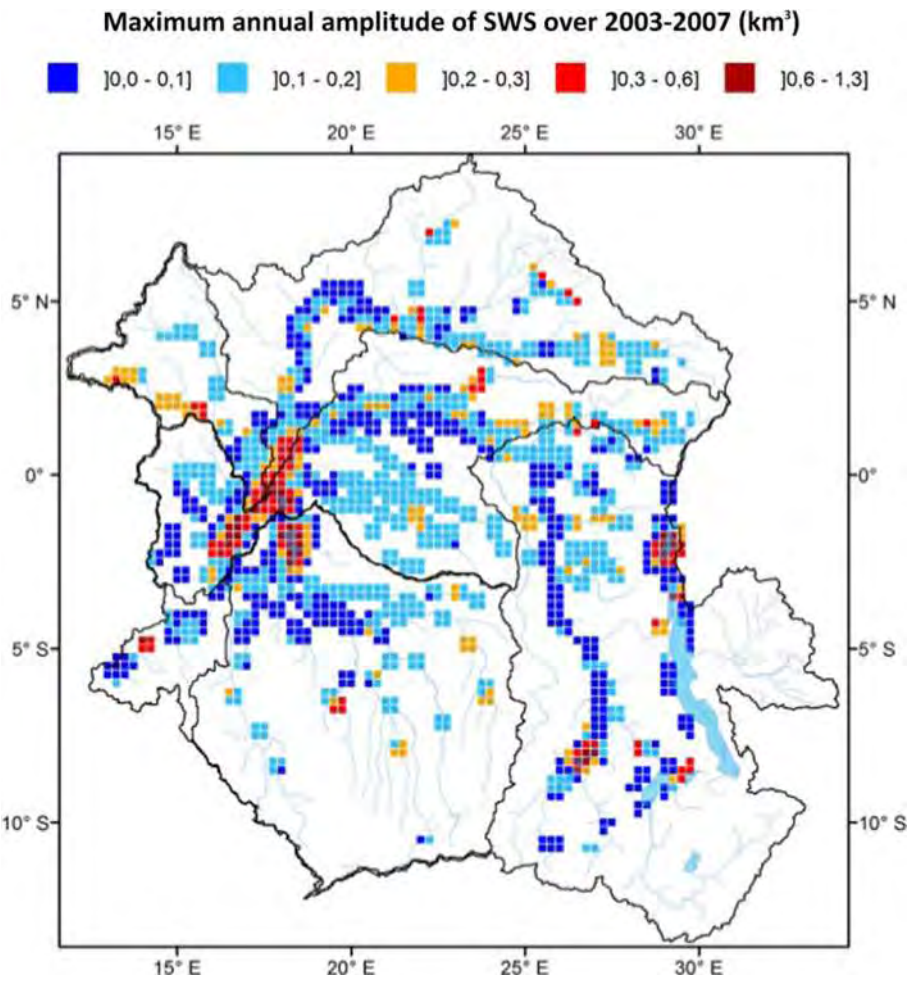

Fig. 8 Maximum annual surface water storage amplitudes (in km^3) over the Congo Basin. The estimates are obtained from a combination of surface water extent maps from GIEMS and water elevation from ENVISAT radar altimeter, over 2003–2007 (from Becker et al. 2018)

wetlands each year. Over the Cuvette Centrale of the Congo (an area covering ~7800 km^2), PALSAR observations in InSAR acquisitions were used in combination to ENVISAT altimetry to establish relationships between water depth and surface water storage and derived absolute surface water storage change over 2002–2011, with uncertainties of water storages ranging from 8 to 14% (Yuan et al. 2017b). But the difference in water storage and their variations in the region still vary depending on the methodology. For instance, the estimates of Yuan et al. (2017b) can differ up to 50% (average of ~30%) with the estimates from Lee et al. (2015). Frappart et al. (2021) suggested that the densification of the VS network over the Cuvette Centrale by including water elevation variations over the floodplains could impact the surface water storage by a factor four as compared to if only VSs over the rivers are used.

Over the Lake Chad region, Pham-Duc et al. (2020) combined MODIS-derived surface water extent of the lake and floodplains with water level from altimetry to estimate the variations in surface water storage in the area to be ~ 1.2 km^3 annually (with a maximum error of 8.5% on this estimate). In combination with GRACE data, the study further showed that groundwater (estimated with a maximum uncertainty of 23%), which contributes ~ 70% of Lake Chad's annual water storage change, is increasing since the 2000s, mainly because of sustained water supply provided by the two main tributaries of the lake. As a result, over the last two decades, Lake Chad is not shrinking thanks to groundwater and the tropical origin of water supply and is recovering seasonally its surface water extent and volume.

As we can see, most of these studies have been performed for large spatial scales and with temporal scales of monthly to seasonal changes and is restricted in general the data to capture only wide rivers, lakes and basin systems. Moreover, the spatial resolution of current gravimetry missions (generally hundreds of kilometers) is not adequate to infer changes in freshwater quantities at scales meaningful for to societal applications and water resources management. Nevertheless, these missions remain a powerful tool to study hydroclimatology and large-scale freshwater variability.

The forthcoming mission SWOT is expected to change the way surface water storage is observed globally, as it will provide, for the first time, direct estimates with an unprecedented spatial resolution (~ 100 m), even if the set of observables in floodplains and wetlands is still uncertain. A preliminary work carried out in the Gourma region lake (Grippa et al. 2019) has shown the potential of SWOT to follow the seasonal dynamics of water volumes in ponds and lakes in this area. However, deriving water masks in the Sahel may be difficult given that backscattering coefficients from water and land are sometimes close. In this case, coupling water levels by SWOT to water extent estimated by optical sensors could be a good option.

2.4 Surface Water Quality from Water Color Measurements from Remote Sensing

While the above variables are more related to water quantity, Earth Observation can also be a powerful tool to monitor the quality of inland water, including sediments (suspended particulate matter-SPM), chlorophyll *a* (chl-a), cyanobacteria and colored dissolved organic matter (CDOM). In this section, we deal with water color techniques to monitor these parameters. Previous studies provided a comprehensive review of past, present, and new satellite sensors available for deriving water quality information in inland waters (Dörnhöfer and Oppelt 2016; Dube et al. 2015; Martinez et al. 2009; Pahlevan et al. 2017). Water color measurements are particularly challenging in Africa given on the one hand the atmospheric conditions (water vapor, desert dust, and biomass fires) which disturb the optical reflectance and on the other hand the strong seasonal dynamics of surface waters and the extremely high values of certain parameters, such as for example SPM (Robert et al. 2017).

CDOM CDOM is calculated based on absorption for a specific wavelength, often 440 nm. It is an indicator of the carbon content of surface water, so it plays a major role in understanding the role of surface water in the carbon cycle, particularly in the context of climate change (Kutser 2012; Williamson et al. 2009). However, in Africa, there are few studies on the satellite monitoring of this parameter.

Chlorophyll a Chl-a is an indicator of phytoplankton, and therefore of the primary productivity of lakes and it is one of the most monitored parameters using water color techniques in Africa (Shi et al. 2019; Dube et al. 2015). It provides information on the trophic state of the water and the risks of eutrophication. Mapping chlorophyll *a* (chl-a) is crucial

for water quality management. Chl-a has absorption bands between 440 and 560 as well as at 670 nm (red band) and a strong reflectance at 500 and 700 nm. In inland waters, it seems preferable to use the red and Near InfraRed (NIR) bands and not the blue to limit interference with CDOM and SPM (Shi et al. 2019; Obaid et al. 2021). In Africa, chl-a studies have developed especially since the 2010s, particularly in the Great Lakes (Bergamino et al. 2010; Horion et al. 2010; Loiselle et al. 2014) and in southern Africa (Chavula et al. 2009; Chawira et al. 2013; Dlamini et al. 2016; Masocha et al. 2018) but more specifically in South Africa (Matthews et al. 2010; Matthews 2014; Malahlela et al. 2018; Sakuno et al. 2018; Obaid et al. 2021; Bande et al. 2018) and its use has since spread to other African countries. More recently, Buma and Lee (2020) showed the interest of using a 3-band algorithm to monitor chl-a in the Chad Lake with Sentinel-2 (Red bands and NIR band are used) and Landsat 8 (blue, green and red band) satellite data. Obaid et al (2021) on the Vaal Dam used a blue-green ratio for Landsat and red-NIR ratio for Sentinel-2 to retrieve chl-a. Gidudu et al (2021) on the Lake Victoria used a 488 nm/645 nm ratio with MODIS data. Normalized Difference Vegetation Index (NDVI) was also employed to monitor water hyacinth (Kiage and Obuoyo 2011; Dube et al. 2014; Shekede et al. 2008).

Cyanobacteria The use of the quantification of chl-a as an indicator of the abundance of cyanobacteria is problematic because this pigment exists for phytoplankton communities. Thus, PhycoCyanin (PC) is preferred, which is the unique pigment of cyanobacteria with an absorption at 620–630 nm. Finally, vegetation indexes can also be used [NDVI, Floating Algae Index (FAI), etc.] Despite the growing interest in estimating cyanobacteria in Africa (Dalu and Wasserman 2018; Ndlela et al. 2016), few studies focus on their monitoring by satellite (Stumpf et al. 2016), except in South Africa (Matthews 2014; Oberholste and Botha 2010). Matthews (2014) used the Maximum Peak Heigh (MPH) algorithm (Matthews et al. 2012) link to chl-a using Medium Resolution Imaging Spectrometer (MERIS) data to detect cyanobacterial blooms. The FAI (Hu 2009) is the most widely used spectral index for detecting dense cyanobacterial blooms (Shi et al. 2019).

Sediments The use of satellite data to monitor SPM was first applied to temperate coastal areas, and then ocean water followed by tropical areas. In Africa, its application to inland surface waters is very recent. Kaba et al (2014) and Robert et al (2016) used MODIS data to document SPM in the Tana (Ethiopia) and Bagré (Burkina Faso, north of Lake Volta in the Volta basin, see Fig. 1) lakes, respectively. Robert et al. (2017) assessed the capability of high (Landsat 7/8) and medium (MODIS) resolution satellite sensors to monitor SPM in extremely turbid waters in the Gourma region (Mali). Sentinel-2 data were also found to provide good results for SPM monitoring in Burkina Faso (Robert et al. 2021), over the middle Niger River and over the Lake Chad.

All these studies are based on in situ measurements in order to identify the best corresponding band or ratio band to monitor the dynamics of SPM: Depending on the site, this is either the NIR/R ratio or most often the NIR band which seems the best to retrieve SPM values, in particular for high values. However, there is a limit at about 2500 mg/l above which reflectance reaches saturation. An example of the capability of Sentinel-2 to monitor SPM spatiotemporal variability in the Bagré Lake in Burkina Faso is shown in Fig. 9.

The NIR band derived from Sentinel-2 was used to study the SPM dynamics of the Bagré Lake (Fig. 9a–g). Before the start of the rainy season, low SPM values are observed throughout the lake. Then, the onset of the rainy season is synonymous with an increase in values in the upstream part of the lake. Then, it is like a wave of SPM which moves from upstream to downstream areas between the months of May and September. The usable images of 2019 make it possible to see this dynamic from the end of May to the beginning of July: with the highest values around 1000–1200 mg/l in the upstream part, 600–800 mg/l

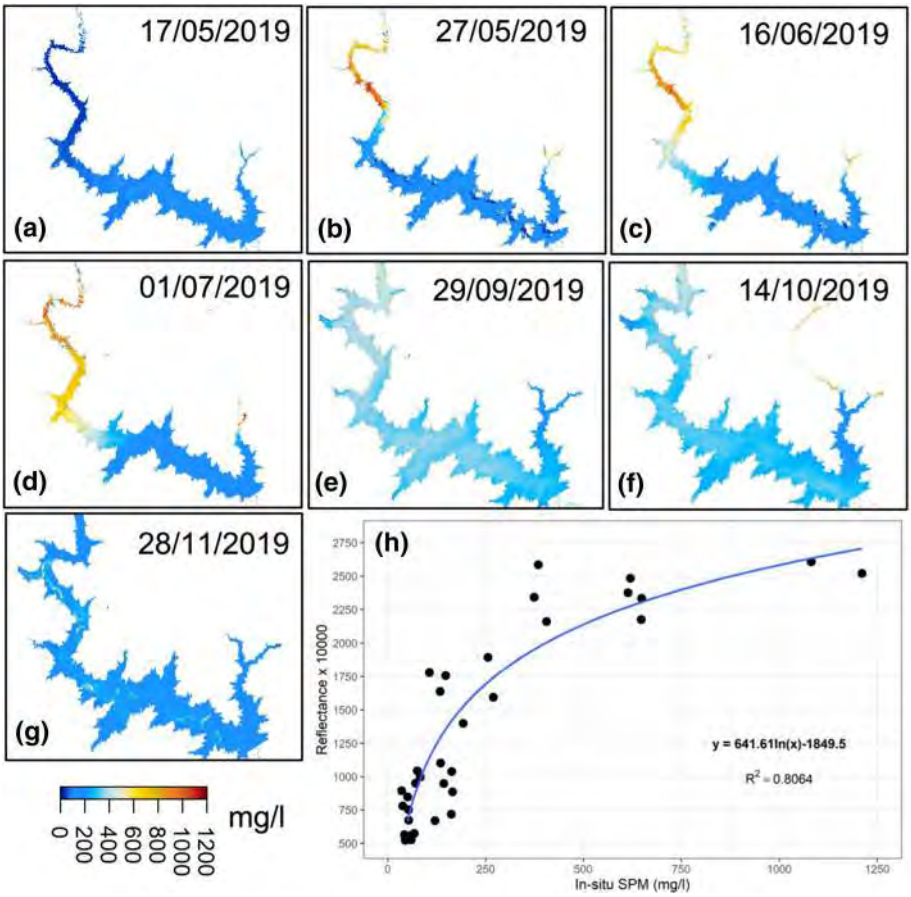

Fig. 9 **a–g** Spatiotemporal evolution of suspended particulate matter (SPM) (mg/l) in the Bagré Lake (Near InfraRed (NIR) band inversed from Sentinel-2 images; **h** Sentinel-2 NIR band as a function of SPM in log *x*-axis scale. R^2 indicates the Pearson's correlation

in the middle part, and lower values in the downstream part. The images of the end of September and the middle of October show a homogenization of the amount of suspended matter (400 mg/l) present in the lake. The rest of the year, the values are lower (less than 200 mg/l). It was also found that surface reflectance produced by the French Data Center THEIA provided better relationships to in situ SPM than surface reflectance produced by Copernicus which shows the importance of atmospheric corrections for water color-based applications (Fig. 9h). Finally, Robert et al (2021) highlighted that *E. coli* and diarrheal disease are strongly correlated with in situ SPM, and reflectance in the NIR which makes water color satellite approaches suited to monitor health hazard.

3 The Use of Earth Observations for Modeling Surface Waters and Hydrological Processes in Africa

3.1 Hydrological Modeling

Hydrological models are employed to numerically reproduce the hydrological functional behaviors and the water cycle processes through sets of mathematical equations. This representation of the processes related to the transition of rainfall to runoff through channels occurring at the land surface is termed hydrological modeling, which can also be understood as a means of quantitative prediction for decision-making (Tshimanga 2022). Hydrological modeling is commonly used to understand hydrological process, to predict hydrological variables, particularly when and where they are not currently measured in situ, and/or to predict the effects of future climate and explore "what-if" scenarios to understand the impacts of other changes, such as land use, dam building or urbanization. Quantifying all these processes is of paramount importance for hydrological prediction and water resources management under both stationary and non-stationary conditions, further complicated by our limited ability to measure or assess the subsurface interactions where many complex water fluxes take place.

In the African continent, a number of hydrological model applications have been initiated to meet the purpose of processes understanding and predictions across different scales, as well as water resources management plans. Some of these initiatives include the development of new models that are fit for purpose in the context of the African hydrology. Particular reference is made to the Pitman model (Pitman 1973; Hughes et al. 2007), the Agricultural Catchment Research Unit (ACRU) model (Schulze and George 1987) and a Hybrid Atmospheric and Terrestrial Water Balance (HATWAB) model (Alemaw and Chaoka 2003) that have been developed and used for simulating hydrological processes under different African hydro-climatic conditions.

A large number of hydrological modeling structures are currently available, but they differ in the degree of detail of the description of processes, the manner in which processes are conceptualized, the requirements for input and output data, and the possible spatial and temporal resolution. The common practice now in hydrological modeling communities is to use or adapt model structures that have been relatively successfully performed elsewhere. In this regard, a large number of global or land surface models have been used under different conditions and for different purposes across the African continent (Trambauer et al. 2013; Hughes et al. 2015; Boone et al. 2009; Grippa et al. 2017; Getirana et al. 2017b). Here, we do not intend to provide a classification of hydrological models, so more detailed information about the classification of these models can be referred to in the references cited.

Overall, several approaches have been used for hydrological models' applications across the African continent. These approaches vary from parameter estimation (Nyabeze 2005; Kapangaziwiri and Hughes 2008), regionalization (e.g., Love et al. 2011), assimilation of new data types into hydrological models (Mekonnen et al. 2009; Milzow et al. 2011) and model uncertainty prediction (e.g., Katambara and Ndiritu 2009; Kapangaziwiri et al. 2012). Models have also been applied at different spatial scales from the relatively small to medium catchments (Hamlat et al. 2013; Gal et al. 2017; Nonki et al. 2021) to large rivers (Tshimanga and Hughes 2014; Casse et al. 2016; Munzimi et al. 2019) and even continental scales (Alemaw and Chaoka 2003; Trambauer et al. 2013). Apart from the general catchment water balance modeling, progress has also been made in the use of models

for more specific processes such as flooding (Yawson et al. 2005; Ngongondo et al. 2013; Smithers et al. 2013) and drought assessments (Nyabeze 2004), modeling of floodplains (Birkhead et al. 2007; Unami et al. 2009), sediment yields (Ndomba et al. 2008) groundwater surface water interactions (Ayenew et al. 2008; Tanner and Hughes 2015). Models have also been used to address the purpose of water allocation (McCartney and Arranz 2007; Mwebaze et al. 2021).

In a review of the 16 most widely used hydrological models for water resources applications worldwide, with the purpose of assessing their suitability for drought forecasting in Africa, Trambauer et al. (2013) noticed that not all of these models sufficiently represent all the important water balance components for African semiarid areas. This is partly due to the fact that most models do not represent relevant hydrological processes that could be significant in these areas, such as transmission losses along the river channel, re-infiltration and subsequent evaporation of surface runoff, and interception of the wet surface, as well as the high temporal and spatial variability of rainfall. Out of the 16 well known hydrological and land surface models that were reviewed, they concluded that only five (i.e., PCRaster Global Water Balance (PCR-GLOBWB), Global Water Availability Assessment (GWAVA), land surface Hydrology Tiled European Centre for Medium-Range Weather Forecasts (ECMWF) Scheme for Surface Exchanges over Land (HTESSEL), Distributed Water Balance and Flood Simulation Model (LISFLOOD) and the Soil and Water Assessment Tool (SWAT)) were suitable for hydrological drought forecasting in Africa.

Results from the African Monsoon Multidisciplinar Analysis (AMMA) Land Surface Intercomparison Project carried out in West Africa have shown that general Land Surface Models (LSMs) have difficulties in representing surface runoff over the different West African soils and slow reservoirs (Boone et al. 2009; Grippa et al. 2017; Getirana et al. 2017b).

With a rapidly growing population and low level of water utilization, Africa's economic development continues to be hampered by water policies and management decisions that are based on sparse and unreliable information (Guzinski et al. 2014) and a severe lack of in situ network already highlighted. Hydrological models have a particularly important role to play in water management in Africa in filling some of these data gaps. However, the lack of in situ data also severely hampers the development of reliable hydrological models, mainly due to the lack of calibration and validation data. This has been a continued challenge for hydrologists, even with advances in methods developed through the Prediction in Ungauged BasinS (PUBS) efforts (Hrachowitz et al. 2013).

Earth Observations have demonstrated their value globally in improving hydrological modeling (Lettenmaier et al. 2015), but in Africa, they play an even more crucial role. Almost all hydrological modeling undertaken on the continent now relies on Earth Observation for many of its data needs (Paris et al. 2022). While the growth in utilizing Earth Observation in hydrological studies only really took off in earnest since 2000, mainly due to the advent of satellite-derived data products (see Sect. 2), it has now become so ubiquitous to use Earth Observation in these studies that many hydrology papers no longer mention Earth Observation in the title (Lettenmaier et al. 2015).

Here, we provide some examples to illustrate the role Earth Observation currently plays in hydrological modeling at different scales and for differing applications over Africa. We use this to highlight some of the successes of applying these data in hydrological modeling of the continent.

One of the significant benefits of using satellite observations in hydrological modeling is the large spatial scale of what can be measured and used, although often at increased computational modeling cost. However, there are very few examples of hydrology modeling specifically for the African continental scale. This may in part be

due to regional technical capacity issues, as well as data availability for such studies, but there has also been a tendency for researchers to develop global hydrology models, rather than just at a continental scale. Nevertheless, Earth Observation has contributed to studies specific to the African continent scale. One example of continent scale modeling is the use of daily remotely sensed surface water extent assimilated in the LISFLOOD hydrology model at the continental spatial scale in Africa and South America, with the conclusion that remotely sensed surface water extent improves streamflow simulations, potentially leading to a better forecast of the peak flow in ungauged regions (Revilla-Romero et al. 2016). These models have also been used to explore explicit links between hydrology and malaria transmission across the African continent (Smith et al. 2020).

Unsurprisingly, as observed in Sect. 2, Earth Observation has had much more research focus on hydrology at a large basin scale in Africa including Niger, Nile, Congo, Chad basins. This is perhaps the ideal scale for the use of satellite data in hydrology modeling, where the large scale of the basins makes in situ observations of sufficient detail hard to gather, as well as there being a better performance of hydrology modeling due to the longer timescale responses of such large basins. These large basins are also important transboundary river systems that require multi-country management and Earth Observation has played an important nonpartisan role in a more transparent understanding of the hydrology and water availability of these rivers (Ekeu-wei and Blackburn 2018; Guzinski et al. 2014).

A particularly well documented basin in Africa is the Niger River Basin, for which there have been many hydrology studies that benefited from satellite data. This basin is very particular and heterogeneous in terms of hydrological processes, since it involves tropical areas (e.g., the Guinean highlands), complex river floodplain systems (e.g., the Inner Niger Delta and the Niger river delta) and semiarid regions (e.g., the Red Flood tributaries). Pedinotti et al. (2012) for instance used satellite-derived observations of surface water (altimetry and GIEMS, see Sect. 2) to develop an improved version of the Interaction Sol-Biosphère-Atmosphère-Total Runoff Integrating Pathways (ISBA-TRIP) continental hydrologic system for the Niger basin, including a flooding scheme. As well as direct observations of surface water (see Sect. 2), Earth Observation is also crucial for primary model build datasets such as land use observations and for model driver datasets such rainfall. These models have used Earth Observation in the Niger Basin to explore a range of issues, such as the use of MODIS and Landsat for vegetation and surface water in groundwater recharge processes (Leblanc et al. 2007), and satellite rainfall products such as ECMWF Re-Analysis (ERA)-Interim for runoff estimation (Oyerinde et al. 2017) and the Climate Prediction Center morphing method (CMORPH), the near-real-time legacy product of Tropical Rainfall Measuring Mission Multi-satellite Precipitation Analysis (TMPA 3B42RT) and the Precipitation Estimation from Remotely Sensed Information using Artificial Neural Networks (PERSIANN) for flood forecasting (Casse et al. 2015). Casse et al. (2016) have employed the ISBA-TRIP model to investigate the long-term changes along the Red Flood tributaries, which are located in the Sahel region and have been facing intensified flood hazard over the last decades. A recent application for the Upper Niger River basin of the MGB model (MGB is the acronym in Portuguese for "Large Scale Hydrological Model", Fleischmann et al. 2018) presented a two-way coupling of large-scale hydrological and hydraulic models over the basin and highlighted the importance of representing the interactions between floodplains and unsaturated soils during the annual flood wave propagation across the Inner Niger Delta.

The Nile Basin is another well-studied large basin in Africa, with many studies focusing on water resource management and rift valley lakes management issues. Digital elevation models (DEM) derived from radar observations (e.g., the Shuttle Radar Topography Mission, SRTM) have been used for basin delineation and flow routing to study lake hydrology in the upper Nile Basin (Bastawesy et al. 2013). Thermal infrared remote sensing data from AVHRR are used to estimate evaporation fluxes from the large Sudd wetland (Mohamed et al. 2006). Surface water extent observations from Landsat have been used to improve hydrology modeling of the lower Nile (Gleason et al. 2018). Recently, altimetry-derived surface water storage was assimilated into the World-Wide Water Resources Assessment (W3RA) model using the ensemble Kalman filter (EnKF) for the period of 2003 to 2016 (Khaki and Awange 2020), which improved model outputs, especially the surface water discharge RMSE which is reduced by approximately 33%.

Smaller African basins are also benefiting from modeling with a significant reliance on satellite dataset due to data scarcity, for example for modeling of flood hydrology and the subsequent flood hazard in the Oti River Basin (Komi et al. 2017), for water availability modeling in the Rokel-Seli catchment in Sierra Leone (Masafu et al. 2016) or for developing a water balance model for Lake Turkuna in East Africa (Velpuri et al. 2012), calibrated with a composite series of water level from T/P, Jason-1 and ENVISAT satellite altimetry data.

3.2 Hydraulic Modeling

Although hydrological modeling includes the transport of water through rivers, either implicitly or explicitly, there is still a need for more specialist models that simulate in detail the flow transport in channels and floodplains. These hydraulic models, also commonly referred to as hydrodynamic models, generally utilize some derivative of the Saint–Venant shallow water flow equations and are used to model river channel and floodplain processes more explicitly and in higher detail than would typically be undertaken with a hydrological model. Importantly, they provide spatiotemporal predictions of water levels and velocities, which allows the mapping of floodplain inundation dynamics and simulate sediment transport characteristics. Satellite-derived observations of these parameters have also advanced our understanding of these processes and allowed calibration and validation where in situ data are sparce (Schumann et al. 2009).

Over the last decade, there have been an increasing number of Earth Observation-based hydraulic modeling studies carried out on large African rivers that can be more easily observed from space. These models have been used to investigate inundation dynamics, map flood hazard, and to advance flood modeling methods in data sparse contexts. Generally, the models utilize a global DEM to represent terrain and map floodplain and main river channels and rely on remotely sensed observations of water surface elevation and/or extent for model calibration and validation. Typically, these models also involve estimation of river channel bathymetry, often by treating it as a parameter to be calibrated alongside the friction coefficient. While the representation of bathymetry is crucial to the hydraulic model performance, observed bathymetry data are seldom available, which presents a key challenge of modeling large rivers in this data sparse context. The river flow data used to drive these models are acquired using a variety of methods, which are covered in the previous hydrological modeling section.

The Niger River again is a prime example of an African river whose study has been significantly enhanced by satellite data, having been the subject of no less than four

hydrodynamic modeling studies within the last decade. The upper Niger, including the Inner Niger Delta, has been simulated with multiple models all of which make extensive use of satellite-derived water surface elevation and extent data, as described in Sect. 2 (Neal et al. 2012; Fleischmann et al. 2018; Haque et al. 2019; Getirana et al. 2021). Landsat imagery of water extents was used to estimate river channel width and validate modeled flood extents. Neal et al. (2012) also used water surface elevation observations from the Ice, Cloud, and land Elevation Satellite (ICESat) altimeter to calibrate their model's friction and bathymetry parameters and showed the model was able to predict water surface elevation at altimeter VSs with a RMSE of 1.21 m. Fleischmann et al (2018) drew on water surface elevations from the Jason-2, ENVISAT and SARAL altimeters as part of their model validation process and found RMSE in modeled water surface elevation at altimeter VSs to be 0.95 m. The lower reaches of the Niger River including the Niger Delta have also been modeled hydraulically by Ekeu-wei and Blackburn (2020). They used ICESat altimetry to estimate bathymetry where observations were lacking and validated their model using flood extents from both MODIS and SAR observations. Their 'percentage flood extent capture' validation metric ranged from 70 to 92%.

Hydraulic modeling efforts on the Zambezi have also benefited from Earth Observation data. The Lower Zambezi flood forecasting model produced by Schumann et al (2013) is another example of a hydraulic model calibrated by varying channel friction and bathymetry parameters to fit water surface elevation observations from the ICESat altimeter. Model validation using flood extents obtained from Landsat imagery showed the predicted correct flood area to be 86%. Reaches of the Upper Zambezi and associated tributaries have also recently been modeled hydraulically by Kittel et al (2021b). In this instance, friction and bathymetry parameters were calibrated to observations of water surface elevation from CryoSat-2, and the model evaluated according to its ability to predict water surface elevation observed by the Sentinel-3 altimeter. The resulting RMSE values ranged from 0.6 to 1.31 m. Over the Congo River, the hydraulic modeling study by O'Loughlin et al. (2020) covers the Congo middle reach and major tributaries, where surface water elevation from the ERS-2 and ENVISAT altimeters were used to calibrate the friction and bathymetry parameters and validate the model (RMSE in modeled water surface elevation was 0.84 m). Landsat imagery was also used to obtain channel width estimates. Flood inundation fractions produced globally at 25 km spatial resolution from GIEMS (Prigent et al. 2007) were used to evaluate modeled flood extents, the dense rainforest here having prevented routine acquisition of higher resolution flood extents from satellite imagery. Also, Paris et al. (2022) presented the MGB hydrologic-hydraulic model for the whole Congo River basin, which was validated with several satellite-derived surface water elevation and extent datasets.

Published Earth Observation-based hydraulic modeling studies of rivers other than the principal African rivers described above are scarce but do exist. For example, Komi et al (2017) used the Oti River, a tributary of the Volta River in West Africa, as a case study for flood modeling of mid-size rivers in data sparse contexts. This river is typically around 60 m along the 140 km long modeled study reach, which is not wide enough to accommodate the footprint of a satellite altimeter. However, flood extents were observed by MODIS and were used to calibrate the model's friction and bathymetry parameters. Fernández et al (2016) developed a LISFLOOD-FP (FP for FloodPlain) hydraulic model for the Logone floodplain in the Lake Chad basin, which was validated with 52 Landsat-based flood extent maps.

There is a natural water cycle overlap between hydrology and hydraulic modeling and many studies that benefit from Earth Observation combine both approaches, for example

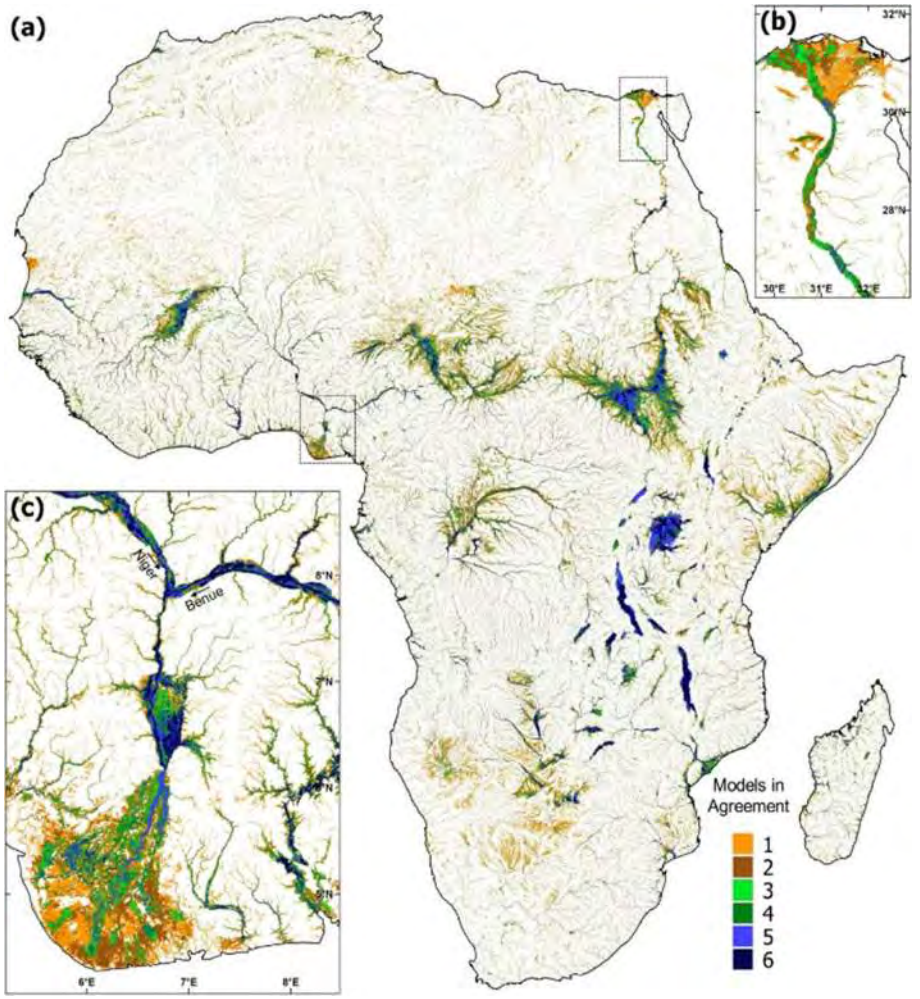

Fig. 10 **a** agreement of Global Flood Models (GFMs) in Africa **b** Nile River, **c** Niger River (from Trigg et al. 2016)

for floodplain wetland management in Africa (Chomba et al. 2021). At the global scale, this can be seen through the development of Global Flood Models (GFMs) (Trigg et al. 2021), which would not be possible without increasing availability of satellite-derived open datasets. These GFMs have been a valuable source of currently missing flood risk information in Africa, nonetheless, these methods are still relatively new and there is some way to go before models consistently predict similar areas of flood hazard (Trigg et al. 2016; Bernhofen et al. 2018), as demonstrated in Fig. 10. In many locations, GFMs provide the best available information on flood hazard. However, these models are applied in an automated fashion and are generally not calibrated or validated, and their coarse scale can miss many smaller rivers (Bernhofen et al. 2021).

Despite the current limitations of GFMs, they can be of use to decision-makers, as documented by Emerton et al. (2020) in their evaluation of the use of GFMs in the

emergency response to cyclones in Mozambique. This evaluation concluded that real-time hazard and risk information from a GFM provided a successful proof of concept with a positive real-world impact.

Specifically, the emergency flood bulletins derived directly from the GFM supported critical actions such as sending an assessment team to the region most likely to be affected. These extreme hydrological events are likely to become more common with climate change, and while Earth Observation cannot predict future climate change, it has been crucial for the development of models for predicting future impacts and will also be essential for monitoring the changing impacts over the coming decades (Guo et al. 2015).

There is no doubt that Earth Observation data have transformed hydrology and hydrodynamic modeling across Africa in the last few decades. With the development of new data sources, e.g., SWOT, NISAR, CubeSats, Unmanned Aerial Vehicles (UAVs) and smartphones, the future of modeling looks likely to continue this advance. This future will generate petabytes of data accessed through cloud storage and will require new methods of interpretation (McCabe et al. 2017).

4 Observational Challenges and Future Opportunities to Monitor African Surface Waters: Way Forward to Water Resources Management

African surface hydrology and terrestrial water cycle have undoubtedly benefited from more than 30 years of developments and studies using Earth Observation and models, as demonstrated and discussed in the previous sections.

The use of remote sensing data has helped to improve our overall knowledge and understanding of the variability and changes of surface water across the African continent, as well as the processes and mechanisms that drive them at various scales.

Remote sensing data now represent a powerful complement to "classical" observations, and the synergy of both means is key to overcome difficulties in a region with sparse in situ networks and where many basins are still ungauged. This complementary exist in many aspects, since satellites often brings a mean to spatialize observations, over large-scale regions and sometimes at fine spatial resolution, while ground observations bring very accurate measurements with often high temporal frequency that no current satellite can compete with. Conversely, satellites give access to new quantities such as the inundated area, which are almost impossible to collect from the ground.

Therefore, remote sensing data dedicated to hydrology have strongly contributed to filling some gaps in the observational systems needed to accurately and comprehensively monitor the environment of Africa. Our review thus highlighted the main remote sensing products that are now available to study African surface water and how their use has contributed to new findings and advances in hydrology across the region.

Current limitations However, there are still many gaps that can be identified regarding our current knowledge of African surface water and the scientific community will need to tackle them in the near future to ensure a comprehensive monitoring and understanding of African hydrology. Some of these basic questions were listed in a community-based effort that synthetized 23 Unsolved Problems in Hydrology (Blöschl et al. 2019) which was recently further developed for Africa specifically through the "23 Unsolved Problems in Hydrology in Africa" initiative (https://www.researchgate.net/project/23-UPH-in-Africa).

Without the pretention of making an exhaustive list of these incomplete knowledges, one can note from our review analysis some obvious and important gaps regarding surface water. For instance, many water bodies are still left with no observations or are monitored with temporal/spatial sampling which are not adequate to capture their characteristics or dynamics. Our review clearly demonstrated that radar altimetry is a very powerful for monitoring water bodies such as lakes and reservoirs located under the satellite tracks, but it is still blind to many smaller lakes and reservoirs that stand in between the ground-tracks. Some processes and mechanisms that drive the variability of water bodies also require observations with high temporal frequency which most current satellite missions don't offer. These limitations therefore prevent a better understanding of the variability of water level and extent in small lakes, reservoirs, rivers and wetlands and how these water bodies interact in complex systems such as in the river floodplain and in river–lake continuums. Additionally, there is still a very limited knowledge of water level and slopes at fine spatiotemporal resolution over African surface water, as well as topography in floodplains and flooded forests, preventing to significant improvements in hydraulic modeling of the systems. Similarly, river discharge, which was historically one of the first variables measured in hydrology and the most used to develop and calibrate models, is still not properly measured from space, as discussed in Tarpanelli et al. (2021). This review stresses a need to accurately estimate river discharge across the continent with fine spatial and temporal resolutions.

Our review also emphasized that, surprisingly, despite its importance, surface water storage in lakes, reservoirs, rivers and floodplains and its variations and changes still remain widely unknown in many parts of Africa. Such a conclusion regarding the surface freshwater reservoir is all the more striking given that, already more than fifteen years ago, Alsdorf et al. (2007) emphasized that "*Given societies' basic need for freshwater, perhaps the most important hydrologic observations that can be made are of the temporal and spatial variations in water stored in rivers, lakes, reservoirs, floodplains, and wetlands.*" Lacking information on the amount of water stored and moving through surface water bodies prevents progresses in understanding their role in transporting sediment and organic matter, especially between channels and floodplains and how they impact the carbon balance, biogeochemical cycle and river ecology. The amount of water transported through floodplains, wetlands and lakes also impacts basin hydrology due to storage effects and regulates the size and timing of the river flood waves. Water storage is also key for water resources management and, as already mentioned, accurate partitioning of GRACE-derived total water storage into groundwater estimates requires measurements of surface water storage variations. Furthermore, it requires better spatial and temporal resolution than what is currently available in order to infer changes in freshwater storages at scales meaningful for to societal applications.

Finally, we identified a strong need for monitoring water quality through remote sensing, which remains challenging especially given the complexity of African inland waters. Using recent optical sensors, suspended sediment concentration could be retrieved with promising results over specific sites, but developing general algorithms to estimate this variable at the regional or continental scale remains a challenge. As part of river hydrology that involves flood dynamics, surface types and complex interactions, sedimentation processes need to be properly monitored to assess geomorphological changes in floodplain and river channels. Improving the observations of phytoplankton and the chlorophyll a dynamic using satellites is also identified as key since they contribute to healthy ecosystems, biodiversity and water security.

A better characterization of these components from space in the near future could foster new developments and improvements in modeling, especially regarding flood storage, parameterization of surface/subsurface processes and wetlands/rivers/lakes connectivity.

Satellite observations are also very important to quantify and understand how the hydrological cycle responds to environmental changes and alterations, due to climate change and anthropogenic pressure. For instance, human activities can alter the ecological services of rivers, lakes and floodplains by modifying their connectivity and the role of storage in modulating fluxes of waters, sediment and nutrients, with strong impacts on the environment. The construction of dams, the impacts of deforestation, and the alteration of flowing rivers (Grill et al. 2019) can also have strong implications on surface water and hydrology. Unlike the Amazon Basin (Fassoni-Andrade et al. 2021), where many studies have been conducted to investigate the interplay between environmental impacts and the water cycle, the African river basins still suffer from a lack of such assessments. Such investigations need to be developed and required long-term monitoring in addition to local assessment achieved on the ground. Satellite observations dedicated to hydrology could offer this unique opportunity for a continuous and long-term monitoring of environmental changes.

Future opportunities In the coming years, new opportunities will soon emerge thanks to an unprecedented and increasing monitoring of African surface water as upcoming and future satellite missions dedicated to surface hydrology will be launched.

The upcoming Surface Water and Ocean Topography (SWOT) satellite mission (Biancamaria et al. 2016) is now planned to be launched at the end of 2022, in collaboration between the United States National Aeronautics and Space Administration (NASA), the Centre National d'Études Spatiales (CNES, the French Spatial Agency), the Canadian Space Agency (CSA) and the United Kingdom Space Agency (UKSA). SWOT can be seen as a "topographic imager" satellite mission that offers observations at ~ 100 m spatial resolution thanks to its SAR interferometry technique and will provide measurements of surface water elevation, slope and water mask, with a temporal resolution of two measurements every cycle of 21 days, almost globally. More details about the mission and SAR interferometry and the KaRIn measurements on board SWOT can be found in (BIancamaria et al. 2016). Its capability to measure height and surface changes will help characterize variations in river discharge and lake water storage in all rivers wider than 100 m and water bodies greater than 250 m × 250 m in area under the swath coverage. A preliminary study on SWOT applicability over Sahelian lake has indeed shown promising results (Grippa et al. 2019). SWOT could also potentially provide measurements in wetlands and floodplains, even in regions with denser vegetation, although it is still unknown to what extent the observations will be affected. The mission will open new perspectives in a large range of applications, from scientific studies to water management since, for the first time, components of the water cycle such as global discharge of rivers, water storage changes in natural and artificial reservoirs, and the dynamic of floodplain storage will be observed jointly. In addition, SWOT data will offer new opportunities in the fields of data assimilation into models (Wongchuig-Correa et al. 2020) or across interfaces to study land–ocean exchanges (Stephens et al. 2020).

Because SWOT data will be freely accessible, as altimetry has always been, a major advantage of SWOT mission will also reside in the possibility to propose an independent, reliable, and accurate measurement system to scientists and water management authorities over an entire basin. This is of particular importance in Africa given the transboundary character of many of its river basins making Earth Observation a fundamental tool to fulfill the disparity in data availability among countries. Nevertheless, it should also be noticed that the SWOT mission will still face some limitations, especially regarding its use

for water resource management or when it comes to the monitoring of surface water bodies such as wetlands, floodplains or inundated area with vegetation. SWOT will indeed provide water stage and discharge measurements on a global scale every 21 days (thanks to its wide swath technique, this revisit time will be reduced to 10–11 days in tropical regions) with a possible latency time of 3 days. This is a major improvement as compared to current observations but such temporal revisit might not be adequate for applications such as flood forecasting (Falck et al. 2021) or reservoir/dam operating. Moreover, in floodplains and wetlands environments, characterized by large extents of open water and sparse vegetation, SWOT will potentially provide observations of water surface elevation, extent and storage. However, in regions with denser vegetation, to what extent SWOT observations will be affected by vegetation is still largely unknown and more investigations are required. Therefore, studies that use the synergy with other satellite observations, which will be simultaneously available with SWOT, should be encouraged and supported to improve our understanding of the entire continental water extent and storage variability.

The capability of measuring surface water from space will also expand soon with the upcoming launch of the NASA-ISRO SAR mission (NISAR), a mission with an ability to map the extent of surface water in lakes and rivers, track floods, even under cloud cover and vegetation canopies and measure changes in the water surface height. SWOT and NISAR will complement the current capability offered by the COPERNICUS program to monitor surface water over long time periods.

As already stated, finer temporal sampling of the estimates of surface water elevation, ideally daily, should also be achieved for a better understanding of hydrological variability and causality at all space and timescales. This could be done thanks to the future capabilities of the next generation of radar altimetry mission aiming at daily revisit, such as the SMall Altimetry Satellite for Hydrology (SMASH) constellation currently under study by the scientific community with the support of CNES.In the future, we should consider to combine the strengths of SWOT swath global measurements with a high temporal sampling of SMASH-like constellation to define a new SWOT-like satellite constellation providing global and daily to sub-daily observations.

An ongoing trend, motivated by the amount of satellite records, now covering multiple decades, along with advances in data storage and computation, has resulted in a more integrated use of satellite observations, based on synergy or data fusion techniques. A comprehensive monitoring of surface water could only benefit from integrating and merging various satellite observations with complementary strengths, such as proposed for instance in Pham-Duc et al. (2020) who combined altimetry, imagery and gravimetry observations to reveal that over the last twenty years Lake Chad is not drying.

At several points in our review, we also stressed the paucity of in situ observations in Africa. The lack of in situ observations, with a good coverage of the large spectrum of the natural variability of hydrological variable, is a limiting factor in the validation of Earth Observation products. Therefore, collection and long-term maintenance of in situ measurement networks should be supported by the agencies and service providers of satellite data, along with the development of open source-based tools to facilitate intercomparison efforts among the scientific community.

Finally, new Earth Observation techniques and methodologies are continuously being developed to help monitor surface waters and will benefit the African continent. For instance, program such the PlanetScope constellation (CubeSats, available since 2014, Cooley et al. 2019) is still underexploited and could bring new opportunities to monitor fine scale African surface water characteristics and process thanks to their capacity to provide ultra-high (3–5 m) resolution observations on a daily basis. The Global Navigation

Satellite System-Reflectometry (GNSS-R) also offers new promising potentials (Chew and Small 2020) with the use of Cyclone GNSS (CYGNSS) constellation to capture surface water dynamic. Besides the concept of satellite missions, the advent of new space-borne measurements, such as real-time high-definition video for monitoring the environment, including surface water and flood for instance, or measurements from unmanned aerial vehicles (UAVs) or small unmanned drones offer great upcoming opportunities. In the near future, this will probably push back the current spatiotemporal constraints and will deliver new hydrological process insights (McCabe et al. 2017). Nevertheless, the unprecedented availability of information, with the possible production of petabytes of data will challenge the current storage and analysis capabilities. This will require new analytical approaches and capacities to interpret such massive data volumes. New tools or fusion techniques based on artificial intelligence and increased computing power will be needed. Such new opportunities will require the joint effort of space agencies, the commercial sector and start-up companies.

Way forward Monitoring and modeling the components of the hydrological cycle with Earth Observation have now become a reality and this will be reinforced further in the coming years. However, there is still an open path to bring all these scientific advances forward into effective applications in water resources management and related decision-making. Africa, like many regions worldwide, is currently facing an extensive human footprint on its freshwater which raises a new set of needs in this context. Complex water management problems thus call for integrated planning using Earth Observation monitoring tools. Remote sensing has the potential to emulate essential information for decision-makers (Fassoni-Andrade et al. 2021) and is bringing new ways to monitor "politically ungauged" regions where information is not publicly available as advocate by Gleason and Durand (2020). But these Earth Observation advances need to translate into real support to water and environmental governance. Thus, the remote sensing community is now facing real challenges as it needs to promote these new knowledges and datasets in a manner that is more useful for societies and to pave the way for innovation and decision support in Africa.

Potential actions to take include to reducing the gap between scientific communities, by promoting interdisciplinary approaches toward more inclusive water systems, by training decision-makers to Earth Observation current progress and advances, by promoting open access datasets, tools and repositories. These actions should also include a better integration and support of African scientists in future programs related to water in order to reduce the disparity of opportunity and access to resources. Investment in science, from national and international communities, is also needed to fill these gaps, as demonstrated for the Congo Basin (White et al. 2021).

Initiatives such as Earth Observation Science for Society from the European Space Agency (https://eo4society.esa.int/) or NASA-SERVIR, especially its declination over Africa (https://www.nasa.gov/mission_pages/servir/africa.html), are useful tools for such promotion so that remote sensing could be incorporated into applications.

Earth Observation brings also large opportunities for operational monitoring, i.e., providing observations in real time (or near real time), simulating the potential of the water resource for hydropower plants, irrigation systems, fluvial transport and freight, and we expect these capabilities to be an area of great development and application interest in the coming years. New progress is expected, especially when integrating such information into existing tools and platforms dedicated to the planning and management of water resources, such as for instance the Congo Basin Catchment Information System (https://cbcis.info/), or the Satellite-based water monitoring and flow forecasting for the Niger River Basin project (http://www.sath.abn.ne/index.html).

Acknowledgements This work is partially funded by the Centre National d'Etude Spatiale (CNES) through the TOSCA project "DYnamique hydrologique du BAssin du CoNGO (DYBANGO)" (2020–2023). BK is supported by a PhD grant from the CNES, Agence Française du Développement (AFD) and Institut de Recherche pour le Développement (IRD). FP, AP, SC, BK and RT are supported by the IRD Groupement De Recherche International SCaHyLab. The work on African Lakes by JFC, PGG and BC is supported by the European Space Agency (ESA) through project Lakes of the Climate Change Initiative program. Funding for MT, AC and RT was provided by the Royal Society-DFID Africa Capacity Building Initiative (grants AQ150005, FLR\R1\192057, FCG\R1\201027). This work was supported by the French Centre National d'Etudes Spatiales (CNES) through the TELESSAO project and the SPLASH (APR TOSCA). ER, MG and MdF would like to thanks Laurent Kergoat (GET) for helpful discussion on remote sensing of small waterbodies in West Africa, Hediwge Nikiema (University Joseph Ki-zerbo, Burkina Faso) for help with the in situ SPM measurements in the Bagré Lake (Burkina Faso) and Santiago Pena Luqe (CNES) for help with the ALCD algorithm. We thank the International Space Science Institute (ISSI, Switzerland) for organizing the workshop "Global Change in Africa: Role of Space Observations" and for coordinating the publication of this special issue. We thank the two anonymous reviewers for they constructive comments and the assessment of our work

Data Availability Statement This is a review paper for which no new data were generated. Data supporting the figures are available via the cited references.

Declarations

Conflict of Interest The authors declare no conflicts of interest. The funders had no role in the design of the study; in the collection, analyses, or interpretation of data; in the writing of the manuscript, or in the decision to publish the results.

References

Adenuga KI, Mahmoud AS, Dodo YA, Albert M, Kori SA, Danlami NJ (2021) Climate change adaptation and mitigation in sub-Saharan African countries. In: Asif M (ed) Energy and environmental security in developing countries. Advanced sciences and technologies for security applications. Springer, Cham. https://doi.org/10.1007/978-3-030-63654-816

Ahmed M, Wiese DN (2019) Short-term trends in Africa's freshwater resources: rates and drivers. Sci Total Environ. https://doi.org/10.1016/j.scitoenv.2019.133843

Aires F, Prigent C, Papa F, Cretaux J-F, Berge-Nguyen M (2014) Characterization and space-time downscaling of the inundation extent over the inner Niger delta using GIEMS and MODIS data. J Hydrometeorol 15:171–192. https://doi.org/10.1175/JHM-D-13-032.1

Aires F, Miolane L, Prigent C, Pham-Duc B, Fluet-Chouinard E, Lehner B, Papa F (2017) A global dynamic and long-term inundation extent dataset at high spatial resolution derived through downscaling of satellite observations. J Hydrometeorol 18:1305–1325. https://doi.org/10.1175/JHM-D-16-0155.1

Albert JS, Destouni G, Duke-Sylvester SM et al (2021) Scientists' warning to humanity on the freshwater biodiversity crisis. Ambio 50:85–94. https://doi.org/10.1007/s13280-020-01318-8

Alfieri L, Cohen S, Galantowicz J, Schumann GJP, Trigg MA et al (2018) A global network for operational flood risk reduction. Environ Sci Policy 84:149–158. https://doi.org/10.1016/j.envsci.2018.03.014

Alcamo J, Flörkeand M, Märker M (2007) Future long-term changes in global water resources driven by socio-economic and climatic changes. Hydrol Sci J 52(2):247–275. https://doi.org/10.1623/hysj.52.2.247

Alsdorf DE, Rodríguez E, Lettenmaier DP (2007) Measuring surface water from space. Rev Geophys 45:RG2002. https://doi.org/10.1029/2006RG000197

Alsdorf DE, Beighley E, Laraque A, Lee H, Tshimanga R, O'Loughlin F et al (2016) Opportunities for hydrologic research in the Congo Basin. Rev Geophys 54(2):378–409. https://doi.org/10.1002/2016RG000517

Alsdorf DE, Melack JM, Dunne T, Mertes LAK, Hess LL, Smith LC (2000) Interferometric radar measurements of water level changes on the Amazon flood plain. Nature 404:174–177. https://doi.org/10.1038/35004560

Anderson W, Taylor C, McDermid S et al (2021) Violent conflict exacerbated drought-related food insecurity between 2009 and 2019 in sub-Saharan Africa. Nat Food 2:603–615. https://doi.org/10.1038/s43016-021-00327-4

Andriambeloson JA, Paris A, Calmant S, Rakotondraompiana S (2020) Re-initiating depth-discharge monitoring in small-sized ungauged watersheds by combining remote sensing and hydrological modelling: a case study in Madagascar. Hydrol Sci J 65:2709–2728. https://doi.org/10.1080/02626667.2020.1833013

Anyah RO, Semazzi FHM, Xie L (2006) Simulated physical mechanisms associated with climate variability over Lake Victoria Basin in East Africa. Mon Weather Rev 134(12):3588–3609. https://doi.org/10.1175/MWR3266.1

Alemaw B, Chaoka T (2003) A continental scale water balance model: a GIS-approach for Southern Africa. Phys Chem Earth Parts a/b/c 28:957–966. https://doi.org/10.1016/j.pce.2003.08.040

Asnani GC (1993) Tropical meteorology, vols 1 and 2. Indian Institute of Tropical Meteorology, 1012 pp

Ayenew T, Demlie M, Wohnlich S (2008) Hydrogeological framework and occurrence of groundwater in the Ethiopian aquifers. J Afr Earth Sci 52(3):97–113. https://doi.org/10.1016/j.jafrearsci.2008.06.006

Baetens L, Desjardins C, Hagolle O (2019) Validation of Copernicus Sentinel-2 cloud masks obtained from MAJA, Sen2Cor, and FMask processors using reference cloud masks generated with a supervised active learning procedure. Remote Sens 11(4):433. https://doi.org/10.3390/rs11040433

Bande P, Adam E, Elbasi MAMA, Adelabu S (2018) Comparing Landsat 8 and Sentinel-2 in mapping water quality at Vaal dam. In: 2018 IEEE International geoscience and remote sensing symposium, 9280–9283, IGARSS 2018, Valencia, Spain, July 22–27, 2018. IEEE 2018, ISBN 978-1-5386-7150-4

Barasa B, Wanyama J (2020) Freshwater lake inundation monitoring using Sentinel-1 SAR imagery in Eastern Uganda. Ann GIS 26(2):191–200. https://doi.org/10.1080/19475683.2020.1743754

Bastawesy ME, Gabr S, White K (2013) Hydrology and geomorphology of the Upper White Nile Lakes and their relevance for water resources management in the Nile basin. Hydrol Process 27(2):196–205. https://doi.org/10.1002/hyp.9216

Becker M, Llowel W, Cazenave A, Güntner A, Crétaux J-F (2010) Recent hydrological behaviour of the East African Great Lakes region inferred from GRACE, satellite altimetry and rainfall observations. C R Geosciences 342(3):223–233. https://doi.org/10.1016/j.crte.2009.12.010,2010

Becker M, Papa F, Frappart F, Alsdorf D, Calmantt S, da Silva JS, Prigent C, Seyler F (2018) Satellite-based estimates of surface water dynamics in the Congo River Basin. Int J Appl Earth Obs Geoinf 66:196–209. https://doi.org/10.1016/j.jag.2017.11.015

Becker M, Santos J, Calmant S, Robinet V, Linguet L, Seyler F (2014) Water level fluctuations in the Congo Basin derived from ENVISAT satellite altimetry. Remote Sens 6:9340–9358. https://doi.org/10.3390/rs6109340

Bergamino N, Horion S, Stenuite S, Cornet Y, Loiselle S, Plisnier PD, Descy JP (2010) Spatio-temporal dynamics of phytoplankton and primary production in Lake Tanganyika using a MODIS-based bio-optical time series. Remote Sens Environ 114:772–780. https://doi.org/10.1016/j.rse.2009.11.013

Bergé-Nguyen M, Crétaux J-F (2015) Inundations in the Inner Niger Delta: Monitoring and analysis using MODIS and global precipitation datasets. Remote Sens 7(2):2127–2151. https://doi.org/10.3390/rs70202127

Bernhofen MV, Trigg MA, Sleigh PA, Sampson CC, Smith AM (2021) Global flood exposure from different sized rivers. Nat Hazards Earth Syst Sci 21:2829–2847. https://doi.org/10.5194/nhess-21-2829-2021

Bernhofen MV, Whyman C, Trigg MA, Sleigh PA, Smith AM, Sampson CC, Yamazaki D, Ward PJ, Rudari R, Pappenberger F (2018) A first collective validation of global fluvial flood models for major floods in Nigeria and Mozambique. Environ Res Lett 13(10):104007. https://doi.org/10.1088/1748-9326/aae014

Berry PAM, Garlick JD, Freeman JA, Mathers EL (2005) Global inland water monitoring from multi-mission altimetry. Geophys Res Lett 32(16). https://doi.org/10.1029/2005GL022814

Betbeder J, Gond V, Frappart F, Baghdadi NN, Briant G, Bartholomé E (2014) Mapping of Central Africa forested wetlands using remote sensing. IEEE J Sel Top Appl Earth Obs Remote Sens 7(2):531–542. https://doi.org/10.1109/JSTARS.2013.2269733

Biancamaria S, Lettenmaier DP, Pavelsky TM (2016) The SWOT mission and its capabilities for land hydrology. Surv Geophys 37(2):307–337. https://doi.org/10.1007/s10712-015-9346-y

Birkhead A, James C, Kleynhans M (2007) Hydrological and hydraulic modelling of the Nyl River floodplain Part 2: Modelling hydraulic behaviour. Water SA 33(1). doi:https://doi.org/10.4314/wsa.v33i1.47866

Birkett CM (1998) Contribution of the TOPEX NASA Radar Altimeter to the global monitoring of large rivers and wetlands. Water Resour Res 34(5):1223–1239. https://doi.org/10.1029/98WR00124

Birkett CM, Murtugudde R, Allan T (1999) Indian Ocean climate event brings floods to East Africa's lakes and the Sudd Marsh. Geophys Res Lett 26:1031–1034. https://doi.org/10.1029/1999GL900165
Birkett CM, Ricko M, Beckley, BD, Yang X, Tetrault RL (2017) G-REALM: a lake/reservoir monitoring tool for drought monitoring and water resources management. In: AGU fall meeting abstracts, vol 2017, pp H23P–02
Blöschl G, Bierkens MFP et al (2019) Twenty-three unsolved problems in hydrology (UPH)—a community perspective. Hydrol Sci J 64(10):1141–1158. https://doi.org/10.1080/02626667.2019.1620507
Boone A, De Rosnay P, Balsamo G, Beljaars A, Chopin F, Decharme B, Delire C, Ducharne A, Gascoin S, Grippa M, Guichard F (2009) The AMMA Land Surface Model Intercomparison Project (ALMIP). Bull Am Meteorol Soc 90(12):1865–1880. https://doi.org/10.1175/2009BAMS2786.1
Bogning S, Frappart F, Blarel F, Niño F, Mahé G, Bricquet J-P, Seyler F, Onguéné R, Etamé J, Paiz M-C, Braun J-J (2018) Monitoring Water levels and discharges using radar altimetry in an Ungauged River Basin: the case of the Ogooué. Remote Sens 10(2):350. https://doi.org/10.3390/rs10020350
Borges AV, Darchambeau F, Teodoru CR, Marwick TR, Tamooh F, Geeraert N, Omengo FO, Guérin F, Lambert T, Morana C, Okuku E, Bouillon S (2015) Globally significant greenhouse-gas emissions from African inland waters. Nat Geosci 8:637–642. https://doi.org/10.1038/ngeo2486
Brakenridge GR, Nghiem SV, Anderson E, Mic R (2007) Orbital microwave measurement of river discharge and ice status. Water Resour Res 43(4):W04405. https://doi.org/10.1029/2006WR005238
Buma WG, Lee SI (2020) Evaluation of Sentinel-2 and Landsat 8 images for estimating chlorophyll-a concentrations in Lake Chad, Africa. Remote Sens 12(15):2437. https://doi.org/10.3390/rs12152437
Bwangoy JRB, Hansen MC, Roy DP, De Grandi G, Justice CO (2010) Wetland mapping in the Congo Basin using optical and radar remotely sensed data and derived topographical indices. Remote Sens Environ 114(1):73–86. https://doi.org/10.1016/j.rse.2009.08.004
Calmant S, Seyler F, Cretaux JF (2008) Monitoring continental surface waters by satellite altimetry. Surv Geophy 29(4–5):247–269. https://doi.org/10.1007/s10712-008-9051-1
Carr AB, Trigg MA, Tshimanga RM, Borman DJ, Smith MW (2019) Greater water surface variability revealed by new Congo River field data: implications for satellite altimetry measurements of large rivers. Geophys Res Lett 46:8093–8101. https://doi.org/10.1029/2019GL083720
Casse C, Gosset M, Peugeot C, Pedinotti V, Boone A, Tanimoun BA, Decharme B (2015) Potential of satellite rainfall products to predict Niger River flood events in Niamey. Atmos Res 163:162–176. https://doi.org/10.1016/j.atmosres.2015.01.010
Casse C, Gosset M, Vischel T, Quantin G, Tanimoun BA (2016) Model-based study of the role of rainfall and land use–land cover in the changes in the occurrence and intensity of Niger red floods in Niamey between 1953 and 2012. Hydrol Earth Syst Sci 20:2841–2859. https://doi.org/10.5194/hess-20-2841-2016
Chahine MT (1992) The hydrological cycle and its influence on climate. Nature 359:373–380
Chavula G, Brezonik P, Thenkabail P, Johnson T, Bauer M (2009) Estimating the surface temperature of Lake Malawi using AVHRR and MODIS satellite imagery. Phys Chem Earth Parts a/b/c 34:749–754. https://doi.org/10.1016/j.pce.2009.08.001
Chawla I, Karthikeyan L, Mishra AKA (2020) Review of remote sensing applications for water security: quantity, quality, and extremes. J Hydrol 585:124826. https://doi.org/10.1016/j.jhydrol.2020.124826
Chawira M, Dube T, Gumindoga W (2013) Remote sensing based water quality monitoring in Chivero and Manyame lakes of Zimbabwe. Phys Chem Earth Parts a/b/c 66:38–44. https://doi.org/10.1016/j.pce.2013.09.003
Chew C, Small E (2020) Estimating inundation extent using CYGNSS data: a conceptual modelling study. Remote Sens Environ 246:111869. https://doi.org/10.1016/j.rse.2020.111869
Chomba IC, Banda KE, Winsemius HC, Chomba MJ, Mataa M, Ngwenya V, Sichingabula HM, Nyambe IA, Ellender B (2021) A review of coupled hydrologic-hydraulic models for floodplain assessments in Africa: opportunities and challenges for floodplain wetland management. Hydrology 8(1):44. https://doi.org/10.3390/hydrology8010044
Coe MT, Birkett CM (2004) Calculation of river discharge and prediction of lake height from satellite radar altimetry: example for the Lake Chad basin. Water Resour Res 40:W10205. https://doi.org/10.1029/2003WR002543
Cooley SW, Smith LC, Ryan JC, Pitcher LH, Pavelsky TM (2019) Arctic-Boreal Lake dynamics revealed using CubeSat imagery. Geophys Res Lett 46(4):2111–2120. https://doi.org/10.1029/2018GL081584
Cooley SW, Ryan JC, Smith LC (2021) Human alteration of global surface water storage variability. Nature 591:78–81. https://doi.org/10.1038/s41586-021-03262-3
Conway D (2002) Extreme rainfall events and lake level changes in East Africa: Recent events and historical precedents. In: Odada EO, Olago DO (eds) The East African Great Lakes: limnology, palaeolimnology and biodiversity. Advances in global change research series, vol 12. Kluwer, pp 63–92

Conway D, Persechino A, Ardoin-Bardin S, Hamandawana H, Dieulin C, Mahé G (2009) Rainfall and water resources variability in sub-Saharan Africa during the Twentieth Century. J Hydrometeorol 10(1):41–59. https://journals.ametsoc.org/view/journals/hydr/10/1/2008jhm10041.xml

Coss S, Durand M, Yi Y, Jia Y, Guo Q, Tuozzolo S et al (2020) Global river radar altimetry time series (GRRATS): new river elevation earth science data records for the hydrologic community. Earth Syst Scie Data 12(1):137–150. https://doi.org/10.5194/essd-12-137-2020

Cretaux J-F, Jelinski W, Calmant S, Kouraev AV, Vuglinski V, Bergé-Nguyen M, Gennero M-C, Nino F, Abarca-Del-Rio R, Cazenave A, Maisongrande P (2011) SOLS: a lake database to monitor in near real time water level and storage variations from remote sensing data. J Adv Space Res 47(9):1497–1507. https://doi.org/10.1016/j.asr.2011.01.004

Cretaux J-F, Frappart F, Papa F, Calmant S, Nielsen K, Benveniste J (2017) Hydrological applications of satellite Altimetry rivers, lakes, man-made reservoirs, inundated areas. In: Stammer DC, Cazenave A (eds) Satellite altimetry over oceans and land surfaces. Taylor & Francis Group, New York, pp 459–504

Cretaux J-F, Bergé-Nguyen M, Calmant S, Jamangulova N, Satylkanov R, Lyard F, Perosanz F, Verron J, Montazem AM, Leguilcher G, Leroux D, Barrie J, Maisongrande P, Bonnefond P (2018) Absolute calibration/validation of the altimeters on Sentinel-3A and Jason-3 over the lake Issykkul. Remote Sens 10:1679. https://doi.org/10.3390/rs10111679

Cretaux J-F, Abarca-del-Río R, Bergé-Nguyen M et al (2016) Lake volume monitoring from space. Surv Geophys 37:269–305. https://doi.org/10.1007/s10712-016-9362-6

D'Addabbo A, Capolongo D, Refice A (2018) Flood monitoring through remote sensing. Springer, Cham

Dai A, Qian T, Trenberth KE, Milliman JD (2009) Changes in continental freshwater discharge from 1948 to 2004. J Clim 22(10):2773–2792. https://doi.org/10.1175/2008JCLI2592.1

Dalu T, Wasserman RJ (2018) Cyanobacteria dynamics in a small tropical reservoir: understanding spatio-temporal variability and influence of environmental variables. Sci Total Environ 643:835–841. https://doi.org/10.1016/j.scitotenv.2018.06.256

Dargie GC, Lewis SL, Lawson IT, Mitchard ETA, Page SE, Bocko YE, Ifo SA (2017) Age, extent and carbon storage of the central Congo Basin peatland complex. Nature 542:86–90. https://doi.org/10.1038/nature21048

Da Silva JS, Calmant S, Seyler F, Rotunno Filho OC, Cochonneau G, Mansur WJ (2010) Water levels in the Amazon basin derived from the ERS 2 and ENVISAT radar altimetry missions. Remote Sensing Environ 114(10): 2160–2181. https://doi.org/10.1016/j.rse.2010.04.020.

De Groeve T (2010) Flood monitoring and mapping using passive microwave remote sensing in Namibia. Geomat Nat Hazards Risk 1(1):19–35. https://doi.org/10.1080/19475701003648085

De Wit M, Stankiewicz J (2006) Changes in surface water supply across Africa with predicted climate change. Science 311(5769):1917–1921. https://doi.org/10.1126/science.1119929

Dlamini S, Nhapi I, Gumindoga W, Nhiwatiwa T, Dube T (2016) Assessing the feasibility of integrating remote sensing and in-situ measurements in monitoring water quality status of Lake Chivero, Zimbabwe. Phys Chem Earth 93:2–11. https://doi.org/10.1016/j.pce.2016.04.004

Döll P, Douville H, Güntner A et al (2016) Modelling freshwater resources at the global scale: challenges and prospects. Surv Geophys 37:195–221. https://doi.org/10.1007/s10712-015-9343-1

Dörnhöfer K, Oppelt N (2016) Remote sensing for lake research and monitoring—recent advances. Ecol Ind 64:105–122. https://doi.org/10.1016/j.ecolind.2015.12.009

Drusch M, Del Bello U, Carlier S, Colin O, Fernandez V, Gascon F, Hoersch B, Isola C, Laberinti P, Martimort P, Meygret A, Spoto F, Sy O, Marchese F, Bargellini P (2012) Sentinel-2: ESA's optical high-resolution mission for GMES operational services. Remote Sens Environ 120:25–36. https://doi.org/10.1016/j.rse.2011.11.026

Duan Z, Bastiaanssen WGM (2013) Estimating water volume variations in lakes and reservoirs from four operational satellite altimetry databases and satellite imagery data. Remote Sens Environ 134:403–416. https://doi.org/10.1016/j.rse.2013.03.010

Dube T, Mutanga O, Seutloali K, Adelabu S, Shoko C (2015) Water quality monitoring in sub-Saharan African lakes: a review of remote sensing applications. Afr J Aquat Sci 40(1):1–7. https://doi.org/10.2989/16085914.2015.1014994

Dube T, Gumindoga W, Chawira M (2014) Detection of land cover changes around Lake Mutirikwi, Zimbabwe based on traditional remote sensing image classification techniques. Afr J Aquat Sci 39:1–7. https://doi.org/10.2989/16085914.2013.870068

Eldardiry H, Hossain F (2019) Understanding reservoir operating rules in the transboundary Nile river basin using macroscale hydrologic modeling with satellite measurements. J Hydrometeorol 20(11):2253–2269. https://journals.ametsoc.org/view/journals/hydr/20/11/jhm-d-19-0058_1.xml

Ekeu-wei IT, Blackburn GA (2018) Applications of open-access remotely sensed data for flood modelling and mapping in developing regions. Hydrology 5(3):39. https://doi.org/10.3390/hydrology5030039
Ekeu-wei IT, Blackburn GA (2020) Catchment-scale flood modelling in data-sparse regions using open-access geospatial technology. ISPRS Int J Geo Inf 9(9):512. https://doi.org/10.3390/ijgi9090512
Emerton R, Cloke H, Ficchi A, Hawker L, de Wit S, Speight L, Prudhomme C, Rundell P, West R, Neal J (2020) Emergency flood bulletins for Cyclones Idai and Kenneth: a critical evaluation of the use of global flood forecasts for international humanitarian preparedness and response. Int J Disaster Risk Reduct 50:101811. https://doi.org/10.1016/j.ijdrr.2020.101811
Falck AS, Tomasella J, Papa F (2021) Assessing the potential of upcoming satellite altimeter missions in operational flood forecasting systems. Remote Sens 13(21):4459. https://doi.org/10.3390/rs13214459
Famiglietti JS (2014) The global groundwater crisis. Nat Clim Chang 14:945–948. https://doi.org/10.1038/nclimate2425)
Fassoni-Andrade A, Fleischmann A, Papa F, Paiva R, Wongchuig S, Melack JM et al (2021) Amazon hydrology from space: scientific advances and future challenges. Rev Geophys 59:e2020RG000728. https://doi.org/10.1029/2020RG000728
Fatras C, Parrens M, Peña Luque S, Al Bitar A (2021) Hydrological dynamics of the Congo Basin from water surfaces based on L-band microwave. Water Resour Res. https://doi.org/10.1029/2020wr027259
Fekete BM, Looser U, Pietroniro A, Robarts RD (2012) Rationale for monitoring discharge on the ground. Jf Hydrometeorol 13:1977–1986. https://doi.org/10.1175/jhm-d-11-0126.1
Fernández A, Najafi MR, Durand M, Mark BG, Moritz M, Jung HC, Neal J, Shastry A, Laborde S, Phang SC, Hamilton IM, Xiao N (2016) Testing the skill of numerical hydraulic modeling to simulate spatiotemporal flooding patterns in the Logone floodplain, Cameroon. J Hydrol 539:265–280. https://doi.org/10.1016/j.jhydrol.2016.05.026
Fleischmann A, Siqueira V, Paris A, Collischonn W, Paiva R, Pontes P, Crétaux J-F, Bergé-Nguyen M, Biancamaria S, Gosset M (2018) Modelling hydrologic and hydrodynamic processes in basins with large semi-arid wetlands. J Hydrol 561:943–959. https://doi.org/10.1016/j.jhydrol.2018.04.041
Fluet-Chouinard E, Lehner B, Rebelo LM, Papa F, Hamilton SK (2015) Development of a global inundation map at high spatial resolution from topographic downscaling of coarse-scale remote sensing data. Remote Sens Environ 158:348–361. https://doi.org/10.1016/j.rse.2014.10.015
Frappart F, Calmant S, Cauhopé M, Seyler F, Cazenave A (2006) Preliminary results of ENVISAT RA-2-derived water levels validation over the Amazon basin. Remote Sens Environ 100:252–264. https://doi.org/10.1016/j.rse.2005.10.027
Frappart F, Papa F, Guentner A, Tomasella J, Pfeffer J, Ramillien G, Emilio T, Schietti J, Seoane L, da Silva CJ, Medeiros Moreira D, Bonnet M-P, Seyler F (2019) The spatio-temporal variability of groundwater storage in the Amazon River Basin. Adv Water Res 124:41–52. https://doi.org/10.1016/j.advwatres.2018.12.005
Frappart F, Zeiger P, Betbeder J, Gond V, Bellot R, Baghdadi N, Blarel F, Darrozes J, Bourrel L, Seyler F (2021) Automatic detection of inland water bodies along altimetry tracks for estimating surface water storage variations in the Congo Basin. Remote Sens 13(19):3804. https://doi.org/10.3390/rs13193804
Frappart F, Papa F, Famiglietti JS, Prigent C, Rossow WB, Seyler F (2008) Interannual variations of river water storage from a multiple satellite approach: a case study for the Rio Negro River basin. J Geophys Res 113:D21104. https://doi.org/10.1029/2007JD009438
Frappart F, Papa F, Santos da Silva J, Ramillien G, Prigent C, Seyler F, Calmant S (2012) Surface freshwater storage and dynamics in the Amazon basin during the 2005 exceptional drought. Environ Res Lett 7:044010. https://doi.org/10.1088/1748-9326/7/4/044010
Funari E, Testai E (2008) Human health risk assessment related to cyanotoxins exposure. Crit Rev Toxicol 38(2):97–125. https://doi.org/10.1080/10408440701749454
Good SP, Noone D, Bowen G (2015) Hydrologic connectivity constrains partitioning of global terrestrial water fluxes. Science 349:175–177. https://doi.org/10.1126/science.aaa593
Gao H, Birkett CM, Lettenmeir DP (2012) Global monitoring of large reservoir storage from satellite remote sensing. Water Resour Res 48:W09504. https://doi.org/10.1029/2012WR012063
Gardelle J, Hiernaux P, Kergoat L, Grippa M (2010) Less rain, more water in ponds: a remote sensing study of the dynamics of surface waters from 1950 to present in pastoral Sahel (Gourma region, Mali). Hydrol Earth Syst Sci 14:309–324. https://doi.org/10.5194/hess-14-309-2010
Gal L, Grippa M, Kergoat L, Hiernaux P, Peugeot C, Mougin E (2016) Changes in ponds water volume and runoff coefficients over ungauged sahelian watersheds. J Hydrol 540:1176–1188. https://doi.org/10.1016/j.jhydrol.2016.07.035

Gal L, Grippa M, Hiernaux P, Pons L, Kergoat L (2017) Modeling the paradoxical evolution of runoff in pastoral Sahel. The case of the Agoufou watershed, Mali. Hydrol Earth Syst Sci 21:4591–4613. https://doi.org/10.5194/hess-2016-623

Getirana A, Kumar S, Girotto M, Rodell M (2017a) Rivers and floodplains as key components of global terrestrial water storage variability. Geophys Res Lett 44:10359–10368. https://doi.org/10.1002/2017GL074684

Getirana A, Boone A, Peugeot C et the ALMIP2 Working Group (2017b) Streamflows over a West African Basin from the ALMIP2 model ensemble. J Hydrometeorol 18(7):1831–1845. https://doi.org/10.1175/JHM-D-16-0233.1

Getirana A, Kumar S, Konapala G, Ndehedehe CE (2021) Impacts of fully coupling land surface and flood models on the simulation of large wetland's water dynamics: the case of the Inner Niger Delta. J Adv Model Earth Syst 13(5):e2021MS002463. https://doi.org/10.1029/2021MS002463

Gidudu A, Letaru L, Kulabako RN (2021) Empirical modeling of chlorophyll a from MODIS satellite imagery for trophic status monitoring of Lake Victoria in East Africa. J Great Lakes Res 47(4):1209–1218. https://doi.org/10.1016/j.jglr.2021.05.005

Gleason CJ, Wada Y, Wang J (2018) A hybrid of optical remote sensing and hydrological modeling improves water balance estimation. J Adv Model Earth Syst 10(1):2–17. https://doi.org/10.1002/2017MS000986

Gleason CJ, Durand MT (2020) Remote sensing of river discharge: a review and a framing for the discipline. Remote Sens 12(7):1–28. https://doi.org/10.3390/rs12071107

Grill G, Lehner B, Thieme M et al (2019) Mapping the world's free-flowing rivers. Nature 569:215–221. https://doi.org/10.1038/s41586-019-1111-9

Grippa M, Kergoat L, Frappart F, Araud Q, Boone A, De Rosnay P, Lemoine JM, Gascoin S, Balsamo G, Ottlé C, Decharme B, Saux-Picart S, Ramillien G (2011) Land water storage changes over West Africa estimated by GRACE and land surface models. Wat Res 47:W05549. https://doi.org/10.1029/2009WR008856

Grippa M, Rouzies C, Biancamaria S, Blumstein D, Cretaux J-F, Gal L, Robert E, Gosset M, Kergoat L (2019) Potential of SWOT for monitoring water volumes in Sahelian ponds and lakes. IEEE J Sel Top Appl Earth Obs Remote Sens 12(7):2541–2549. https://doi.org/10.1109/JSTARS.2019.2901434

Grippa M, Kergoat L, Boone A, Peugeot C, Demarty J, Cappelaere B, Gal L, Hiernaux P, Mougin E, Ducharne A, Dutra E, Hain C, Anderson M, The ALMIP2 Working group Modelling (2017) Surface runoff and water fluxes over contrasted soils in pastoral Sahel: evaluation of the ALMIP2 land surface models over the Gourma region in Mali. J Hydrometeorol 18(7). https://doi.org/10.1175/JHM-D-16-0170.1

Guo HD, Zhang L, Zhu LW (2015) Earth observation big data for climate change research. Adv Clim Chang Res 6(2):108–117. https://doi.org/10.1016/j.accre.2015.09.007

Guzinski R, Kass S, Huber S, Bauer-Gottwein P, Jensen IH, Naeimi V, Doubkova M, Walli A, Tottrup C (2014) Enabling the use of earth observation data for integrated water resource management in Africa with the water observation and information system. Remote Sens 6(8):7819–7839. https://doi.org/10.3390/rs6087819

Haas EM, Bartholomé E, Combal B (2009) Time series analysis of optical remote sensing data for the mapping of temporary surface water bodies in sub-Saharan western Africa. J Hydrol 370(1–4):52–63. https://doi.org/10.1016/j.jhydrol.2009.02.052

Haas EM, Bartholomé E, Lambin EF, Vanacker V (2011) Remotely sensed surface water extent as an indicator of short-term changes in ecohydrological processes in sub-Saharan Western Africa. Remote Sens Environ 115(12):3436–3445. https://doi.org/10.1016/j.rse.2011.08.007

Haddeland I, Heinke J, Biemans H, Eisner S, Flörke M, Hanasaki N, Konzmann M, Ludwig F, Masaki Y, Schewe J, Stacke T, Tessler ZD, Wada Y, Wisser D (2014) Water, human impacts, and climate change. Proc Natl Acad Sci USA 111(9):3251–3256. https://doi.org/10.1073/pnas.1222475110

Haque MM, Seidou O, Mohammadian A, Djibo AG, Liersch S, Fournet S, Karam S, Perera EDP, Kleynhans M (2019) Improving the accuracy of hydrodynamic simulations in data scarce environments using Bayesian model averaging: a case study of the inner Niger Delta, Mali, West Africa. Water 11(9):1766. https://doi.org/10.3390/w11091766

Hall JW, Grey D, Garrick D, Fung F, Brown C, Dadson SJ, Sadoff CW (2014) Coping with the curse of freshwater variability: institutions, infrastructure, and information for adaptation. Science 346(6208):429–443. https://doi.org/10.1126/science.1257890

Hamlat A, Errih M, Guidoum A (2013) Simulation of water resources management scenarios in western Algeria watersheds using WEAP model. Arab J Geosci 6(7):2225–2236. https://doi.org/10.1007/s12517-012-0539-0

Hastenrath S, Nicklis A, Greischar L (1993) Atmospheric–hydrospheric mechanisms of climate anomalies in the western equatorial Indian Ocean. J Geophys Res 98:20219–20235

Hastie A, Lauerwald R, Ciais P, Papa F, Regnier P (2021) Historical and future contributions of inland waters to the Congo basin carbon balance. Earth Syst Dyn 12:37–62. https://doi.org/10.5194/esd-12-37-2021

Hernegger M, Stecher G, Schwatke C, Olang L (2021) Hydroclimatic analysis of rising water levels in the Great rift Valley lakes of Kenya. J Hydrol Reg Stud. https://doi.org/10.1016/j.ejrh.2021.100857

Hess LL, Melack JM, Filoso S, Wang Y, Wang Y (1995) Delineation of inundated area and vegetation along the Amazon floodplain with the SIR-C synthetic aperture radar. IEEE Trans Geosci Remote Sens 33(4):896–904. https://doi.org/10.1109/36.406675

Hess LL, Melack JM, Novo EMLM, Barbosa CCFF, Gastil M (2003) Dual-season mapping of wetland inundation and vegetation for the central Amazon basin. Remote Sens Environ 87(4):404–428. https://doi.org/10.1016/j.rse.2003.04.001

Hoekstra AY, Mekonnen MM, Chapagain AK, Mathews RE, Richter BD (2012) Global monthly water scarcity: blue water footprints versus blue water availability. PLoS ONE 7(2):e32688. https://doi.org/10.1371/journal.pone.0032688

Horion S, Bergamino N, Stenuite S, Descy J-P, Plisnier P-D, Loiselle SA, Cornet Y (2010) Optimized extraction of daily bio-optical time series derived from MODIS/aqua imagery for Lake Tanganyika, Africa. Remote Sens Environ 114(4):781–791. https://doi.org/10.1016/j.rse.2009.11.012

Hrachowitz M, Savenije H, Blöschl G, McDonnell J, Sivapalan M, Pomeroy J, Arheimer B, Blume T, Clark M, Ehret U (2013) A decade of predictions in Ungauged Basins (PUB)—a review. Hydrol Sci J 58(6):1198–1255. https://doi.org/10.1080/02626667.2013.803183

Hu CM (2009) A novel ocean color index to detect floating algae in the global oceans. Remote Sens Environ 113:2118–2129. https://doi.org/10.1016/j.rse.2009.05.012

Huang C, Chen Y, Zhang S, Wu J (2018) Detecting, extracting, and monitoring surface water from space using optical sensors: a review. Rev Geophys 56:333–360. https://doi.org/10.1029/2018RG000598

Hughes D, Jewitt G, Mahé G, Mazvimavi D, Stisen S (2015) A review of aspects of hydrological sciences research in Africa over the past decade. Hydrol Sci J 60(11):1865–1879. https://doi.org/10.1080/02626667.2015.1072276

Hughes DA, Parsons R, Conrad JE (2007) Quantification of the groundwater contribution to baseflow. Water Res Comm

Hulme M, Doherty R, Ngara T, New M, Lister D (2001) African climate change: 1900–2100. Clim Res 17:145–168. https://doi.org/10.3354/cr017145

Hubau W, Lewis SL, Phillips OL, Affum-Baffoe K, Beeckman H, Cuní-Sanchez A, Daniels AK, Ewango CE, Fauset S, Mukinzi JM, Sheil D (2020) Asynchronous carbon sink saturation in African and Amazonian tropical forests. Nature 579(7797):80–87. https://doi.org/10.1038/s41586-020-2035-0

Inogwabini BI (2020) The changing water cycle: freshwater in the Congo. Wires Water 7:e1410. https://doi.org/10.1002/wat2.1410

Janicot S (1992) Spatio-temporal variability of West African rainfall. J Clim 5:489–551

Jensen K, McDonald K, Podest E, Rodriguez-Alvarez N, Horna V, Steiner N (2018) Assessing L-Band GNSS-reflectometry and imaging radar for detecting sub-canopy inundation dynamics in a tropicalwetlands complex. Remote Sens 10(9):1431. https://doi.org/10.3390/rs10091431

Jung HC, Hamski J, Durand M, Alsdorf D, Hossain F, Lee H, Hossain AKM, Hasan K, Khan AS, Hoque AKM (2010) Characterization of complex fluvial systems using remote sensing of spatial and temporal water level variations in the Amazon, Congo, and Brahmaputra Rivers. Earth Surf Process Landf 35:294–304

Jury MR, Gwazantini E (2002) Climate variability in Malawi, Part 2: sensitivity and prediction of lake levels. Int J Climatol 22:1303–1312. https://doi.org/10.1002/joc.772,2002

Kaba E, Philpot W, Steenhuis T (2014) Evaluating suitability of MODIS-Terraimages for reproducing historic sediment concentrations in water bodies: lake Tana, Ethiopia. Int J Appl Earth Obs Geoinform 26:286–297. https://doi.org/10.1016/j.jag.2013.08.001

Kao H, Kuo C, Tseng K, Shum CK, Tseng TP, Jia YY, Yang TY, Al TA, Yi Y, Hussain D (2019) Assessment of Cryosat-2 and SARAL/AltiKa altimetry for measuring inland water and coastal sea level variations: a case study on Tibetan Plateau Lake and Taiwan Coast. Mar Geod 42:327–343. https://doi.org/10.1080/01490419.2019.1623352

Kapangaziwiri E, Hughes D, Wagener T (2012) Incorporating uncertainty in hydrological predictions for gauged and ungauged basins in southern Africa. Hydrol Sci J 57(5):1000–1019. https://doi.org/10.1080/02626667.2012.690881

Kapangaziwiri E, Hughes DA (2008) Towards revised physically based parameter estimation methods for the Pitman monthly rainfall-runoff model. Water SA 34(2):183–192. https://doi.org/10.4314/wsa.v34i2.183638

Katambara Z, Ndiritu J (2009) A fuzzy inference system for modelling streamflow: case of Letaba River, South Africa. Phys Chem Earth Parts a/b/c 34(10–12):688–700. https://doi.org/10.1016/j.pce.2009.06.001

Khaki M, Awange J (2020) Altimetry-derived surface water data assimilation over the Nile Basin. Sci Total Environ 735:139008. https://doi.org/10.1016/j.scitotenv.2020.139008

Kiage L, Obuoyo J (2011) The potential link between El Niño and water hyacinth blooms in Winam Gulf of Lake Victoria, East Africa: evidence from satellite imagery. Water Resour Manag 25:3931–3945. https://doi.org/10.1007/s11269-011-9895-x

Kim H, Yeh PJF, Oki T, Kanae S (2009) Role of rivers in the seasonal variations of terrestrial water storage over global basins. Geophys Res Lett 36:L17402. https://doi.org/10.1029/2009GL039006

Kitambo B, Papa F, Paris A, Tshimanga R, Calmant S, Fleischmann AS, Frappart F, Becker M, Tourian MJ, Prigent C, Andriambeloson J (2021) A combined use of in situ and satellite-derived observations to characterize surface hydrology and its variability in the Congo River Basin. Hydrol Earth Syst Sci Discuss. https://doi.org/10.5194/hess-2021-315

Kittel CM, Jiang L, Tøttrup C, Bauer-Gottwein P (2021a) Sentinel-3 radar altimetry for river monitoring—a catchment-scale evaluation of satellite water surface elevation from Sentinel-3A and Sentinel-3B. Hydrol Earth Syst Sci 25:333–357. https://doi.org/10.5194/hess-25-333-2021

Kittel CM, Hatchard S, Neal JC, Nielsen K, Bates PD, Bauer-Gottwein P (2021b) Hydraulic model calibration using CryoSat-2 observations in the Zambezi catchment. Water Resour Res 57(9):e2020WR029261. https://doi.org/10.1029/2020WR029261

Klein I, Dietz A, Gessner U, Dech S, Kuenzer C (2015) Results of the Global WaterPack: a novel product to assess inland water body dynamics on a daily basis. Remote Sens Lett 6(1). https://doi.org/10.1080/2150704X.2014.1002945

Komi K, Neal J, Trigg MA, Diekkrüger B (2017) Modelling of flood hazard extent in data sparse areas: a case study of the Oti River basin, West Africa. J Hydrol Reg Stud 10:122–132. https://doi.org/10.1016/j.ejrh.2017.03.001

Konapala G, Mishra AK, Wada Y et al (2020) Climate change will affect global water availability through compounding changes in seasonal precipitation and evaporation. Nat Commun 11:3044. https://doi.org/10.1038/s41467-020-16757-w

Kutser T (2012) The possibility of using the Landsat image archive for monitoring long time trends in coloured dissolved organic matter concentration in lake waters. Remote Sensing Environ 123:334–338. https://doi.org/10.1016/j.rse.2012.04.004

Loiselle S, Cózar A, Adgo E, Ballatore T, Chavula G, Descy JP, Harper DM, Kansiime F, Kimirei I, Langenberg V (2014) Decadal trends and common dynamics of the bio-optical and thermal characteristics of the African Great Lakes. PLoS ONE 9:e93656. https://doi.org/10.1371/journal.pone.0093656

Laraque A, N'kaya GDM, Orange D, Tshimanga R, Tshitenge JM, Mahé G, Nguimalet CR, Trigg MA, Yepez S, Gulemvuga G (2020) Recent budget of hydroclimatology and hydrosedimentology of the congo river in central Africa. Water 12:2613. https://doi.org/10.3390/w12092613

Leblanc M, Favreau G, Tweed S, Leduc C, Razack M, Mofor L (2007) Remote sensing for groundwater modelling in large semiarid areas: Lake Chad Basin, Africa. Hydrogeol J 15(1):97–100. https://doi.org/10.1007/s10040-006-0126-0

Lee H, Beighley RE, Alsdorf DE, Jung HC, Shum CK, Duan J, Guo J, Yamazaki D, Andreadis K (2011) Characterization of terrestrial water dynamics in the Congo Basin using GRACE and satellite radar altimetry. Remote Sens Environ 115:3530–3538. https://doi.org/10.1016/j.rse.2011.08.015

Lee H, Yuan T, Jung HC, Beighley E (2015) Mapping wetland water depths over the central Congo Basin using PALSAR ScanSAR, Envisat altimetry, and MODIS VCF data. Remote Sens Environ 159:70–79. https://doi.org/10.1016/j.rse.2014.11.030

Lettenmaier DP, Alsdorf DE, Dozier J, Huffman GJ, Pan M, Wood EF (2015) Inroads of remote sensing into hydrologic science during the WRR era. Water Resour Res 51(9):7309–7342. https://doi.org/10.1002/2015WR017616

Levy K, Woster AP, Goldstein RS, Carlton EJ (2016) Untangling the impacts of climate change on waterborne diseases: a systematic review of relationships between diarrheal diseases and temperature, rainfall, flooding, and drought. Environ Sci Technol 50(10):4905–4922. https://doi.org/10.1021/acs.est.5b06186

Lindersson S, Brandimarte L, Mård J, Di Baldassarre G (2020) A review of freely accessible global datasets for the study of floods, droughts and their interactions with human societies. Wires Water 7:e1424. https://doi.org/10.1002/wat2.1424

Long S, Fatoyinbo TE, Policelli F (2014) Flood extent mapping for Namibia using change detection and thresholding with SAR. Environ Res Lett 9:035002. https://doi.org/10.1088/1748-9326/9/3/035002

Love D, Uhlenbrook S, van der Zaag P (2011) Regionalising a meso-catchment scale conceptual model for river basin management in the semi-arid environment. Phys Chem Earth Parts a/b/c 36(14–15):747–760. https://doi.org/10.1016/J.PCE.2011.07.005

Lunt MF, Palmer PI, Feng L, Taylor CM, Boesch H, Parker RJ (2019) An increase in methane emissions from tropical Africa between 2010 and 2016 inferred from satellite data. Atmos Chem Phys 19:14721–14740. https://doi.org/10.5194/acp-19-14721-2019

Malahlela OE, Oliphant T, Tsoeleng LT, Mhangara P (2018) Mapping chlorophyll-a concentrations in a cyanobacteria- and algae-impacted Vaal Dam using Landsat 8 OLI data. S Afr J Sci 114(9/10). https://doi.org/10.17159/sajs.2018/4841

Marchant R, Mumbi C, Behera S, Yamagata T (2006) The Indian Ocean dipole—the unsung driver of climatic variability in East Africa. Afr J Ecol 45(1):4–16. https://doi.org/10.1111/j.1365-2028.2006.00707.x

Martinez JM, Guyot JL, Filizola N, Sondag F (2009) Increase in suspended sediment discharge of the Amazon River assessed by monitoring network and satellite data. CATENA 79:257–264. https://doi.org/10.1016/j.catena.2009.05.011

Masocha M, Dube T, Nhiwatiwa T, Choruma D (2018) Testing utility of Landsat 8 for remote assessment of water quality in two subtropical African reservoirs with contrasting trophic states. Geocarto Int 33(7):667–680. https://doi.org/10.1080/10106049.2017.1289561

Masafu CK, Trigg MA, Carter R, Howden NJK (2016) Water availability and agricultural demand: an assessment framework using global datasets in a data scarce catchment, Rokel-Seli River, Sierra Leone. J Hydrol Reg Stud 8:222–234. https://doi.org/10.1016/j.ejrh.2016.10.001

McCabe MF, Rodell M, Alsdorf DE, Miralles DG, Uijlenhoet R, Wagner W, Lucieer A, Houborg R, Verhoest NE, Franz TE (2017) The future of Earth observation in hydrology. Hydrol Earth Syst Sci 21(7):3879–3914. https://doi.org/10.5194/hess-21-3879-2017

McCartney MP, Arranz R (2007) Evaluation of historic, current and future water demand in the Olifants River Catchment, South Africa. IWMI

Matgen P, Martinis S, Wagner W, Freeman V, Zeil P, McCormick N (2020) Feasibility assessment of an automated, global, satellite-based flood-monitoring product for the Copernicus Emergency Management Service. EUR 30073 EN, Publications Office of the European Union, Luxembourg ISBN 978-92-76-10254-0. https://doi.org/10.2760/653891, JRC119812, Ispra

Matthews MW, Bernard S, Winter K (2010) Remote sensing of cyanobacteria-dominant algal blooms and water quality parameters in Zeekoevlei, a small hypertrophic lake. Using MERIS Remote Sens Environ 114(9):2070–2087. https://doi.org/10.1016/j.rse.2010.04.013

Matthews MW (2014) Eutrophication and cyanobacterial blooms in South African inland waters: 10 years of MERI observations. Remote Sens Environ 155:161–177. https://doi.org/10.1016/j.rse.2014.08.010

Matthews MW, Bernard S, Robertson L (2012) An Algorithm for detecting trophic status (chlorophyll-a), cyanobacterial- dominance, surface scums and floating vegetation in inland and coastal waters. Remote Sens Environ 124:637–652. https://doi.org/10.1016/j.rse.2012.05.032

Mayr S, Klein I, Rutzinger M, Kuenzer C (2021) Systematic water fraction estimation for a global and daily surface water time-series. Remote Sens 13(14):2675. https://doi.org/10.3390/rs13142675

Mehran A, AghaKouchak A, Nakhjiri N et al (2017) Compounding impacts of human-induced water stress and climate change on water availability. Sci Rep 7:6282. https://doi.org/10.1038/s41598-017-06765-0

Mekonnen MA, Wörman A, Dargahi B, Gebeyehu A (2009) Hydrological modelling of Ethiopian catchments using limited data. Hydrol Process 23(23):3401–3408

Mercier F, Cazenave A, Maheu C (2002) Interannual lake level fluctuations in Africa from TOPEX-Poseidon: connections with ocean-atmosphere interactions over the Indian ocean. Glob Planet Chang 32:141–163. https://doi.org/10.1016/S0921-8181(01)00139-4

Mhlanga L, Day J, Cronberg G, Chimbari M, Siziba N, Annadotter H (2006) Cyanobacteria and Cyanotoxins in the source water from Lake Chivero, Harare, Zimbabwe, and the presence of Cyanotoxins in drinking water. Afr J Aquat Sci 31(2):165–173. https://doi.org/10.2989/16085910609503888

Michailovsky CI, Bauer-Gottwein P (2014) Operational reservoir inflow forecasting with radar altimetry: the Zambezi case study. Hydrol Earth Syst Sci 18:997–1007. https://doi.org/10.5194/hess-18-997-2014

Milzow C, Krogh PE, Bauer-Gottwein P (2011) Combining satellite radar altimetry, SAR surface soil moisture and GRACE total storage changes for hydrological model calibration in a large poorly gauged catchment. Hydrol Earth Syst Sci 15(6):1729–1743. https://doi.org/10.5194/hess-15-1729-2011

Mistry V, Conway D (2003) Remote forcing of East African rainfall and relationships with fluctuations in levels of Lake Victoria. Int J Climatol 23(1):67–89. https://doi.org/10.1002/joc.861

Mohamed Y, Savenije H, Bastiaanssen W, Hurk B (2006) New lessons on the Sudd hydrology learned from remote sensing and climate modeling. Hydrol Earth Syst Sci 10(4):507–518. https://doi.org/10.5194/hess-10-507-2006

Mohammadimanesh F, Salehi B, Mahdianpari M, Brisco B, Mn M (2019) Wetland water level monitoring using interferometric synthetic aperture radar (InSAR): a review. Can J Remote Sens 44:247–262. https://doi.org/10.1080/07038992.2018.1477680

Mokkenstorm LC, van den Homberg MJC, Winsemius H, Persson A (2021) River flood detection using passive microwave remote sensing in a data-scarce environment: a case study for two river Basins in Malawi. Front Earth Sci 9:670997. https://doi.org/10.3389/feart.2021.670997

Munzimi YA, Hansen MC, Asante KO (2019) Estimating daily streamflow in the Congo Basin using satellite-derived data and a semi-distributed hydrological model. Hydrol Sci J 64(12):1472–1487. https://doi.org/10.1080/02626667.2019.1647342

Mwebaze CE, Majaliwa JGM, Wanyama J, Gabiri G (2021) Assessing the impact of management options on water allocation in River Mubuku-Sebwe Sub-Catchments of Lake Edward-George Basin, Western Uganda. Water 13(15):2009. https://doi.org/10.3390/w13152009

Naidoo R, Brennan A, Shapiro AC, Beytell P, Aschenborn O, Du Preez P, Kilian JW, Stuart-Hill G, Taylor RD (2020) Mapping and assessing the impact of small-scale ephemeral water sources on wildlife in an African seasonal savannah. Ecol Appl 30(8). https://doi.org/10.1002/eap.2203

Ndlela LL, Oberholster PJ, Van Wyk JH, Cheng PH (2016) An overview of cyanobacterial bloom occurrences and research in Africa over the last decade. Harmful Algae 60:11–26. https://doi.org/10.1016/j.hal.2016.10.001

Ndomba PM, Mtalo FW, Killingtveit Å (2008) A guided SWAT model application on sediment yield modeling in Pangani river basin: lessons learnt. J Urban Environ Eng 2(2):53–62

Neal J, Schumann G, Bates P (2012) A subgrid channel model for simulating river hydraulics and floodplain inundation over large and data sparse areas. Water Resour Res 48(11). https://doi.org/10.1029/2012WR012514

Ngongondo C, Li L, Gong L, Xu CY, Alemaw BF (2013) Flood frequency under changing climate in the upper Kafue River basin, southern Africa: a large scale hydrological model application. Stoch Env Res Risk Assess 27(8):1883–1898. https://doi.org/10.1007/s00477-013-0724-z

Ni S, Chen J, Wilson CR, Hu X (2017) Long-term water storage changes of lake Volta from GRACE and satellite altimetry and connections with regional climate. Remote Sens 9(8):842. https://doi.org/10.3390/rs9080842

Nicholson SE (1996) A review of climate dynamics and climate variability in eastern Africa. In: Johnson T, Odada E (eds) The limnology, climatology and paleoclimatology of the East African Lakes. Gordon and Breach, pp 25–56

Nicholson SE, Yin X (2002) Mesoscale patterns of rainfall, cloudiness and evaporation over the Great lakes of East Africa. In: The East African great lakes: limnology, paleolimnology and biodiversity. Advance in global change research, vol 12. Kluwer Academic Publishers

Nonki RM, Lenouo A, Tshimanga RM, Donfack FC, Tchawoua C (2021) Performance assessment and uncertainty prediction of a daily time-step HBV-Light rainfall-runoff model for the Upper Benue River Basin, Northern Cameroon. J Hydrol Reg Stud 36:100849. https://doi.org/10.1016/j.ejrh.2021.100849

Normandin C, Frappart F, Diepkilé AT, Marieu V, Mougin E, Blarel F, Lubac B, Braquet N, Ba A (2018) Evolution of the performances of radar altimetry missions from ERS-2 to Sentinel-3A over the Inner Niger Delta. Remote Sens 10(6):833. https://doi.org/10.3390/rs10060833

Nyabeze WR (2005) Calibrating a distributed model to estimate runoff for ungauged catchments in Zimbabwe. Phys Chem Earth Parts a/b/c 30(11–16):625–633

Nyabeze WR (2004) Estimating and interpreting hydrological drought indices using a selected catchment in Zimbabwe. Phys Chem Earth Parts a/b/c 29(15–18):1173–1180. https://doi.org/10.1016/j.pce.2005.08.001

Obaid AA, Ali KA, Abiye TA, Adam EM (2021) Assessing the utility of using current generation high-resolution satellites (Sentinel 2 and Landsat 8) to monitor large water supply dam in South Africa. Remote Sens Appl Soc Environ 22:100521. https://doi.org/10.1016/j.rsase.2021.100521

Oberholste PJ, Botha AM (2010) Use of remote sensing and molecular markers to detect toxic cyanobacterial hyperscum crust: a case study on Lake Hartbeespoort, South Africa. Afr J Biotechnol 95(1):8791–8799

Ogallo LJ (1988) Relationships between seasonal rainfall in East Africa and the southern oscillation. J Climatol 8:31–43. https://doi.org/10.1002/joc.3370080104

Ogilvie A, Belaud G, Massuel S, Mulligan M, Le Goulven P, Calvez R (2018) Surface water monitoring in small water bodies: potential and limits of multi-sensor Landsat time series. Hydrol Earth Syst Sci 22:4349–4380. https://doi.org/10.5194/hess-22-4349-2018

Ogilvie A, Poussin J-C, Bader J-C, Bayo F, Bodian A, Dacosta H, Dia D, Diop L, Martin D, Sambou S (2020) Combining multi-sensor satellite imagery to improve long-term monitoring of temporary surface water bodies in the Senegal River floodplain. Remote Sens 12(19):3157. https://doi.org/10.3390/rs12193157

Oguntunde PG, Lischeid G, Abiodun BJ (2018) Impacts of climate variability and change on drought characteristics in the Niger River Basin, West Africa. Stoch Environ Res Risk Assess 32:1017–1034. https://doi.org/10.1007/s00477-017-1484-y

Okeowo MA, Lee H, Hossain F, Getirana A (2017) Automated generation of lakes and reservoirs water elevation changes from satellite radar altimetry. IEEE J Sel Top Appl Earth Obs Remote Sens 10(8):3465–3481. https://doi.org/10.1109/JSTARS.2017.2684081

Oki T, Kanae S (2006) Global hydrological cycles and world water resources. Science 313(5790):1068–1072. https://doi.org/10.1126/science.1128845

O'Loughlin FE, Trigg MA, Schumann GP, Bates PD (2013) Hydraulic characterization of the middle reach of the Congo River. Water Resour Res 49:5059–5070. https://doi.org/10.1002/wrcr.20398

O'Loughlin FE, Neal J, Schumann GP, Beighley E, Bates PD (2020) A LISFLOOD-FP hydraulic model of the middle reach of the Congo. J Hydrol 580:124203. https://doi.org/10.1016/j.jhydrol.2019.124203

Oyerinde GT, Fademi IO, Denton OA (2017) Modeling runoff with satellite-based rainfall estimates in the Niger basin. Cogent Food Agric 3(1):1363340. https://doi.org/10.1080/23311932.2017.1363340

Pahlevan N, Sarkar S, Franz BA, Balasubramanian SV, He J (2017) Sentinel-2 multispectral instrument (MSI) data processing for aquatic science applications: demonstrations and validations. Remote Sens Environ 201:47–56. https://doi.org/10.1016/j.rse.2017.08.033

Papa F, Frappart F, Malbeteau Y, Shamsudduha M, Vuruputur V, Sekhar M et al (2015) Satellite-derived surface and sub-surface water storage in the Ganges–Brahmaputra River Basin. J Hydrol Reg Stud 4:15–35. https://doi.org/10.1016/j.ejrh.2015.03.004

Papa F, Durand F, Rossow WB, Rahman A, Bala and SK (2010a) Seasonal and interannual variations of the Ganges–Brahmaputra river discharge, 1993–2008 from satellite altimeters J Geophys Res 115:C12013. https://doi.org/10.1029/2009JC006075

Papa F, Prigent C, Aires F, Jimenez C, Rossow WB, Matthews E (2010b) Interannual variability of surface water extent at the global scale, 1993–2004. J Geophys Res 115:D12111. https://doi.org/10.1029/2009JD012674

Papa F, Biancamaria S, Lion C, Rossow WB (2012a) Uncertainties in mean river discharge estimates associated with satellite altimeters temporal sampling intervals: a case study for the annual peak flow in the context of the future SWOT hydrology mission. IEEE Geosci Remote Sens Lett 9(4):569–573. https://doi.org/10.1109/LGRS.2011.2174958

Papa F, Bala SK, Pandey RK, Durand F, Gopalakrishna VV, Rahman A, Rossow WB (2012b) Ganga–Brahmaputra river discharge from Jason-2 radar altimetry: an update to the long-term satellite-derived estimates of continental freshwater forcing flux into the Bay of Bengal. J Geophys Res 117:C11021. https://doi.org/10.1029/2012JC008158

Papa F, Güntner A, Frappart F, Prigent C, Rossow WB (2008) Variations of surface water extent and water storage in large river basins: a comparison of different global data sources. Geophys Res Lett 35:L11401. https://doi.org/10.1029/2008GL033857

Papa F, Frappart F (2021) Surface Water Storage in Rivers and Wetlands derived from Satellite Observations: a review of current advances and future opportunities for hydrological sciences. Remote Sens 13(20):4162. https://doi.org/10.3390/rs13204162

Paris A, Calmant S, Gosset M, Fleischmann A, Conchy T, Garambois P et al (2022) Monitoring hydrological variables from remote sensing and modelling in the Congo River basin. In: Tshimanga RM, N'kaya GDM, Alsdorf D (eds) Congo Basin hydrology, climate, and biogeochemistry. https://doi.org/10.1002/9781119657002.ch18

Parrens M, Al Bitar A, Frappart F, Papa F, Calmant S, Crétaux JF, Wigneron JP, Kerr Y (2017) Mapping dynamic water fraction under the tropical rain forests of the Amazonian Basin from SMOS brightness temperatures. Water 9(5):350. https://doi.org/10.3390/w9050350

Pedinotti V, Boone A, Decharme B, Cretaux JF, Mognard N, Panthou G, Papa F, Tanimoun BA (2012) Evaluation of the ISBA-TRIP continental hydrologic system over the Niger basin using in situ and satellite derived datasetsh. Hydrol Earth Syst Sci 16:1745–1773. https://doi.org/10.5194/hess-16-1745-201

Pekel JF, Cottam A, Gorelick N, Belward AS (2016) High-resolution mapping of global surface water and its long-term changes. Nature 540(7633):418–422. https://doi.org/10.1038/nature20584

Pham-Duc B, Sylvestre F, Papa F, Frappart F, Bouchez C, Crétaux JF (2020) The Lake Chad hydrology under current climate change. Sci Rep 10:5498. https://doi.org/10.1038/s41598-020-62417-w

Pitman WV (1973) A mathematical model for generating monthly river flows from meteorological data in South Africa. University of the Witwatersrand, Department of Civil Engineering

Prigent C, Lettenmaier DP, Aires F, Papa F (2016) Towards a high resolution monitoring of continental surface water extent and dynamics, at global scale: from GIEMS (Global Inundation Extent from Multi-Satellites) to SWOT (Surface Water Ocean Topography). Surv Geophys 37(2):339–355. https://doi.org/10.1007/s10712-015-9339-x

Prigent C, Papa F, Aires F, Rossow WB, Matthews E (2007) Global inundation dynamics inferred from multiple satellite observations, 1993–2000. J Geophys Res Atmos 112(12). https://doi.org/10.1029/2006JD007847

Prigent C, Papa F, Aires F, Jimenez C, Rossow WB, Matthews E (2012) Changes in land surface water dynamics since the 1990s and relation to population pressure. Geophys Res Lett 39(8). https://doi.org/10.1029/2012GL051276

Prigent C, Jimenez C, Bousquet P (2020) Satellite-derived global surface water extent and dynamics over the last 25 years (GIEMS-2). J Geophys Res Atmos 125(3). https://doi.org/10.1029/2019JD030711

Prigent C, Rochetin N, Aires F, Defer E, Grandpeix JY, Jimenez C, Papa F (2011) Impact of the inundation occurrence on the deep convection at continental scale from satellite observations and modeling experiments. J Geophys Res 116:D24118. https://doi.org/10.1029/2011JD016311

Refice A, Zingaro M, D'Addabbo A, Chini M (2020) Integrating C- and L-band SAR imagery for detailed flood monitoring of remote vegetated areas. Water 12(10):2745. https://doi.org/10.3390/w12102745

Reiner Jr RC, Graetz N, Casey DC, Troeger C, Garcia GM, Mosser JF, Deshpande A, Swartz SJ, Ray SE, Blacker BF, Rao PC (2018) Variation in childhood diarrheal morbidity and mortality in Africa 2000–2015. New England J Med 379(12): 1128–1138. https://doi.org/10.1056/NEJMoa1716766

Revilla-Romero B, Wanders N, Burek P, Salamon P, de Roo A (2016) Integrating remotely sensed surface water extent into continental scale hydrology. J Hydrol 543:659–670. https://doi.org/10.1016/j.jhydrol.2016.10.041

Ričko M, Birkett CM, Carton JA, Cretaux JF (2012) Intercomparison and validation of continental water level products derived from satellite radar altimetry. J Appl Remote Sens 6:061710. https://doi.org/10.1117/1.JRS.6.061710

Robert E, Grippa M, Nikiema DE, Kergoat L, Koudougou H, Auda Y et al (2021) Environmental determinants of E. coli, link with the diarrheal diseases, and indication of vulnerability criteria in tropical West Africa (Kapore, Burkina Faso). PLoS Negl Trop Dis 15(8):e0009634. https://doi.org/10.1371/journal.pntd.0009634.

Robert E, Grippa M, Kergoat L, Pinet S, Gal L, Cochonneau G et al (2016) Monitoring water turbidity and surface suspended sediment concentration of the Bagre Reservoir (Burkina Faso) using MODIS and field reflectance data. Int J Appl Earth Obs Geoinf 52:243–251. https://doi.org/10.1016/j.jag.2016.06.016

Robert E, Kergoat L, Soumaguel N, Merlet S, Martinez JM, Diawara M et al (2017) Analysis of suspended particulate matter and its drivers in Sahelian ponds and lakes by remote sensing (Landsat and MODIS): Gourma Region, Mali. Remote Sens 9(12):1272. https://doi.org/10.3390/rs9121272

Rochelle-Newall E, Nguyen TMH, Le TPQ, Sengtaheuanghoung O, Riblozi O (2015) A short review of fecal indicator bacteria in tropical aquatic ecosystem: knowledge gaps and future directions. Front Microbiol 6:1–15. https://doi.org/10.3389/fmicb.2015.00308

Rodell M, Famiglietti JS, Wiese DN et al (2018) Emerging trends in global freshwater availability. Nature 557:651–659. https://doi.org/10.1038/s41586-018-0123-1

Ropelewski CF, Halpert MS (1996) Quantifying southern oscillation–precipitation relationships. J Clim 9:1043–1059. https://doi.org/10.1175/1520-0442

Rosenqvist AA, Birkett CM (2002) Evaluation of JERS-1 SAR mosaics for hydrological applications in the Congo River Basin. Int J Remote Sens 23:1283–1302. https://doi.org/10.1080/01431160110092902

Sakuno Y, Yajima H, Yoshioka Y, Sugahara S, Abd Elbasit M, Adam E, Chirima J (2018) Evaluation of unified algorithms for remote sensing of chlorophyll-a and turbidity in Lake Shinji and Lake Nakaumi of Japan and the Vaal Dam Reservoir of South Africa under eutrophic and ultra-turbid conditions. Water 10(5):618. https://doi.org/10.3390/w10050618

Seddon A, Macias-Fauria M, Long P et al (2016) Sensitivity of global terrestrial ecosystems to climate variability. Nature 531:229–232. https://doi.org/10.1038/nature16986

Schulze R, George W (1987) A dynamic, process-based, user-oriented model of forest effects on water yield. Hydrol Process 1(3):293–307

Schröder S, Springer A, Kusche J, Uebbing B, Fenoglio-Marc L, Diekkrüger B, Poméon T (2019) Niger discharge from radar altimetry: bridging gaps between gauge and altimetry time series. Hydrol Earth Syst Sci 23:4113–4128. https://doi.org/10.5194/hess-23-4113-2019

Schroeder R, McDonald KC, Chapman BD, Jensen K, Podest E, Tessler ZD et al (2015) Development and evaluation of a multi-year fractional surface water data set derived from active/passive microwave remote sensing data. Remote Sens 7(12):16688–16732. https://doi.org/10.3390/rs71215843

Schumann GP, Bates PD, Horritt MS, Matgen P, Pappenberger F (2009) Progress in integration of remote sensing–derived flood extent and stage data and hydraulic models. Rev Geophys 47(4). https://doi.org/10.1029/2008RG000274

Schumann GP, Neal JC, Voisin N, Andreadis KM, Pappenberger F, Phanthuwongpakdee N, Hall AC, Bates PD (2013) A first large-scale flood inundation forecasting model. Water Resour Res 49(10):6248–6257. https://doi.org/10.1002/wrcr.20521

Schumann GP, Stampoulis D, Smith AM, Sampson CC, Andreadis KM, Neal JC, Bates PD (2016) Rethinking flood hazard at the global scale. Geophys Res Lett 43:10249–10256. https://doi.org/10.1002/2016GL070260

Schwatke C, Dettmering D, Bosch W, Seitz F (2015) DAHITI–an innovative approach for estimating water level time series over inland waters using multimission satellite altimetry. Hydrol Earth Syst Sci 19:4345–4364. https://doi.org/10.5194/hess-19-4345-2015

Shekede M, Kusangaya S, Schmidt K (2008) Spatio-temporal variations of aquatic weed abundance and coverage in Lake Chivero, Zimbabwe. Phys Chem Earth Parts a/b/c 33:714–721. https://doi.org/10.1016/j.pce.2008.06.052

Shi K, Zhang Y, Qin B, Zhou B (2019) Remote sensing of cyanobacterial blooms in inland waters: present knowledge and future challenges. Sci Bull 64(20):1540–1556. https://doi.org/10.1016/j.scib.2019.07.002

Shiklomanov IA, Rodda JC (2003) World water resources at the beginning of the twenty-first century. Cambridge University Press, Cambridge

Simaika JP, Chakona A, van Dam AA (2021) Editorial: towards the sustainable use of African Wetlands. Front Environ Sci 9:658871. https://doi.org/10.3389/fenvs.2021.658871

Sippel SJ, Hamilton SK, Melack JM, Novo EMM (1998) Passive microwave observations of inundation area and the area/stage relation in the Amazon River floodplain. Int J Remote Sens 19(16):3055–3074. https://doi.org/10.1080/014311698214181

Smith M, Willis T, Alfieri L, James W, Trigg M, Yamazaki D, Hardy A, Bisselink B, De Roo A, Macklin M (2020) Incorporating hydrology into climate suitability models changes projections of malaria transmission in Africa. Nat Commun 11(1):1–9. https://doi.org/10.1038/s41467-020-18239-5

Smithers J, Chetty K, Frezghi M, Knoesen D, Tewolde M (2013) Development and assessment of a daily time-step continuous simulation modelling approach for design flood estimation at ungauged locations: ACRU model and Thukela Catchment case study. Water SA 39(4):467–476. https://doi.org/10.4314/wsa.v39i4.4

Sood A, Smakhtin V (2015) Global hydrological models: a review. Hydrolog Sci J 60(4):549–565. https://doi.org/10.1080/02626667.2014.950580

Stager JC, Ruzmaikin A, Conway D, Verburg P, Mason PJ (2007) Sunspots, El Niño, and the levels of Lake Victoria, East Africa. J Geophys Res 112:D15106. https://doi.org/10.1029/2006JD008362

Stammer D, Cazenave A (2017) Satellite altimetry over oceans and land surfaces, 1st edn. Taylor & Francis Group, CRC Press, New York. https://doi.org/10.1201/9781315151779

Stumpf RP, Davis TW, Wynne TT, Graham JL, Loftin KA, Johengen TH, Gossiaux D, Palladino D, Burtner A (2016) Challenges for mapping cyanotoxin patterns from remote sensing of cyanobacteria. Harmful Algae 54:160–173. https://doi.org/10.1016/j.hal.2016.01.005

Steffen W, Richardson K, Rockström J, Cornell SE, Fetzer I, Bennett EM, Biggs R, De Carpenter SR et al (2015) Planetary boundaries: guiding human development on a changing planet. Science 347:1259855. https://doi.org/10.1126/science.1259855

Stephens GL, Slingo JM, Rignot E, Reager JT, Hakuba MZ, Durack PJ, Worden J, Rocca R (2020) Earth's water reservoirs in a changing climate. Proc R Soc A 476:20190458. https://doi.org/10.1098/rspa.2019.0458

Swenson S, Wahr J (2009) Monitoring the water balance of Lake Victoria, East Africa, from space. J Hydrol 370:163–176. https://doi.org/10.1016/j.jhydrol.2009.03.008

Tanner J, Hughes D (2015) Surface water–groundwater interactions in catchment scale water resources assessments—understanding and hypothesis testing with a hydrological model. Hydrol Sci J 60(11):1880–1895. https://doi.org/10.1080/02626667.2015.1052453

Tapley BD, Bettadpur S, Ries JC, Thompson PF, Watkins M (2004) GRACE measurements of mass variability in the earth system. Science 305:503–505. https://doi.org/10.1126/science.1099192

Tarpanelli A, Paris A, Sichangi AW, O'Loughlin F, Papa F (2021) Water resources: Role of earth observations data to hydrodynamic modelling and to derive river discharge. Sur Geo submitted (this issue)
Taylor CM, Prigent C, Dadson SJ (2018) Mesoscale rainfall patterns observed around wetlands in sub-Saharan Africa. Q J R Meteorol Soc 144:2118–2132. https://doi.org/10.1002/qj.3311
Tierney JE, Russell JM (2007) Abrupt climate change in southeast tropical Africa influenced by Indian monsoon variability and ITCZ migration. Geophys Res Lett 34:L15709. https://doi.org/10.1029/2007GL029508
Tierney JE, Ummenhofer CC, deMenocal PB (2015) Past and future rainfall in the Horn of Africa. Sci Adv. https://doi.org/10.1126/sciadv.1500682
Tortini R, Noujdina N, Yeo S, Ricko M, Birkett CM, Khandelwal A, Kumar V, Marlier ME, Lettenmaier DP (2020) Satellite-based remote sensing data set of global surface water storage change from 1992 to 2018. Earth Syst Sci Data 12:1141–1151. https://doi.org/10.5194/essd-12-1141-2020
Trambauer P, Maskey S, Winsemius H, Werner M, Uhlenbrook S (2013) A review of continental scale hydrological models and their suitability for drought forecasting in (sub-Saharan) Africa. Phys Chem Earth Parts a/b/c 66:16–26. https://doi.org/10.1016/j.pce.2013.07.003
Tramblay Y, Rouché N, Paturel JE, Mahé G, Boyer J-F, Amoussou E, Bodian A, Dacosta H, Dakhlaoui H, Dezetter A, Hughes D, Hanich L, Peugeot C, Tshimanga R, Lachassagne P (2021) ADHI: the African database of hydrometric indices (1950–2018). Earth Syst Sci Data 13:1547–1560. https://doi.org/10.5194/essd-13-1547-2021
Trenberth KE, Smith L, Qian T, Dai A, Fasullo J (2007) Estimates of the global water budget and its annual cycle using observational and model data. J Hydrometeorol 8:758–769. https://doi.org/10.1175/JHM600.1
Trigg MA, Bernhofen M, Marechal D, Alfieri L, Dottori F, Hoch J, Horritt M, Sampson C, Smith A, Yamazaki D (2021) Global flood models 181-200. In: Global drought and flood: observation, modeling, and prediction edited by G. Schumann. Elsevier
Trigg MA, Birch CE, Neal JC, Bates PD, Smith A, Sampson CC, Yamazaki D, Hirabayashi Y, Pappenberger F, Dutra E, Ward PJ, Winsemius HC, Salamon P, Dottori F, Rudari R, Kappes MS, Simpson AL, Hadzilacos G, Fewtrell TJ (2016) The credibility challenge for global fluvial flood risk analysis. Environ Res Lett 11(9). https://doi.org/10.1088/1748-9326/11/9/094014
Trigg MA, Tshimanga RM (2020) Capacity building in the Congo Basin: rich resources requiring sustainable development. One Earth 2(3):207–210. https://doi.org/10.1016/j.oneear.2020.02.008
Tshimanga RM, Hughes DA (2014) Basin-scale performance of a semidistributed rainfall-runoff model for hydrological predictions and water resources assessment of large rivers: the Congo River. Water Resour Res 50(2):1174–1188. https://doi.org/10.1002/2013WR014310
Tshimanga, RM (2022) Two decades of hydrologic modeling and predictions in the Congo River Basin. In: Tshimanga RM, N'kaya GDM, Alsdorf D (eds) Congo Basin hydrology, climate, and biogeochemistry. https://doi.org/10.1002/9781119657002.ch12
Tusker T, de Roo A, Gelati E, Schwatke C, Adamovic M, Bisselink B, Pekel J-F, Cottam A (2019) A global lake and reservoir volume analysis using a surface water dataset and satellite altimetry. Hydrol Earth Syst Sci 23:669–690. https://doi.org/10.5194/hess-23-669-2019
Unami K, Kawachi T, Berisavljevic GK, Kofi A, Maeda S, Takeuchi J (2009) Case study: hydraulic modeling of runoff processes in Ghanaian inland valleys. J Hydraul Eng 135(7):539–553. https://doi.org/10.1061/(ASCE)HY.1943-7900.0000041
United Nations (2019) Department of Economic and Social Affairs, Population Division. World Population Prospects 2019: Volume I: Comprehensive Tables. https://population.un.org/wpp/Publications/Files/WPP2019Volume-IComprehensive-Tables.pdf. Accessed 1 Oct 2021
Velpuri NM, Senay GB, Asante KO (2012) A multi-source satellite data approach for modelling Lake Turkana water level: calibration and validation using satellite altimetry data. Hydrol Earth Syst Sci 16(1):1–18. https://doi.org/10.5194/hess-16-1-2012
Verhegghen A, Mayaux P, De Wasseige C, Defourny P (2012) Mapping Congo Basin vegetation types from 300 m and 1 km multi-sensor time series for carbon stocks and forest areas estimation. Biogeosciences 9:5061–5079. https://doi.org/10.5194/bg-9-5061-2012
Vörösmarty CJ, Green P, Salisbury J, Lammers RB (2000) Global water resources: vulnerability from climate change and population growth. Science 289(5477):284–288. https://doi.org/10.1126/science.289.5477.284
Vörösmarty CJ, McIntyre PB, Gessner MO, Dudgeon D, Prusevich A, Green P, Glidden S, Bunn SE, Sullivan CA, Reidy Liermann C, Davies PM (2010) Global threats to human water security and river biodiversity. Nature 467:555–561. https://doi.org/10.1038/nature09440
Williamson CE, Saros JE, Vincent WF, Smol JP (2009) Lakes and reservoirs as sentinels, integrators, and regulators of climate change. Limnol Oceanogr 54. https://doi.org/10.4319/lo.2009.54.6_part_2.2273

White LJT, Masudi EB, Ndongo JD, Matondo R, Soudan-Nonault A, Ngomanda A, Averti IS, Ewango CEN, Sonke B, Lewis SL (2021) Congo Basin rainforest—invest US$150 million in science. Nature 598:411–414. https://doi.org/10.1038/d41586-021-02818-7

Wongchuig-Correa S, Paiva RCD, Biancamaria S, Collischonn W (2020) Assimilation of future SWOT-based river elevations, surface extent observations and discharge estimations into uncertain global hydrological models. J Hydrol 590:125473. https://doi.org/10.1016/j.jhydrol.2020.125473

World Health Organization (2018) Global health estimates 2016: deaths by cause, age, sex, by country and by region, 2000–2016. Geneva

Xu CY, Widen E, Halldin S (2005) Modelling hydrological consequences of climate change—progress and challenges. Adv Atmos Sci 22(6):789–797. https://doi.org/10.1007/BF02918679

Yawson D, Kongo V, Kachroo R (2005) Application of linear and nonlinear techniques in river flow forecasting in the Kilombero River basin, Tanzania. Hydrol Sci J 50(5). https://doi.org/10.1623/hysj.2005.50.5.783

Yuan T, Lee H, Jung HC (2017a) Congo floodplain hydraulics using PALSAR InSAR and Envisat altimetry data. In: Remote sensing of hydrological extremes. Springer, Cham, pp 65–81

Yuan T, Lee H, Jung CH, Aierken A, Beighley E, Alsdorf DE, Tshimanga RM, Kim D (2017b) Absolute water storages in the Congo River floodplains from integration of InSAR and satellite radar altimetry. Remote Sens Environ 201:57–72. https://doi.org/10.1016/j.rse.2017.09.003

Authors and Affiliations

Fabrice Papa[1,2] · Jean-François Crétaux[1] · Manuela Grippa[3] · Elodie Robert[4] · Mark Trigg[5] · Raphael M. Tshimanga[6] · Benjamin Kitambo[1,6,7] · Adrien Paris[1,8] · Andrew Carr[5] · Ayan Santos Fleischmann[9,10] · Mathilde de Fleury[3] · Paul Gerard Gbetkom[1] · Beatriz Calmettes[11] · Stephane Calmant[1,12]

✉ Fabrice Papa
fabrice.papa@ird.fr

1 LEGOS, Université de Toulouse, IRD, CNES, CNRS, UPS, 31400 Toulouse, France

2 Institute of Geosciences, Universidade de Brasília (UnB), 70910-900 Brasília, Brazil

3 GET, Université de Toulouse, IRD, CNES, CNRS, UPS, 31400 Toulouse, France

4 LETG, CNRS, Université de Nantes, 44312 Nantes, France

5 School of Civil Engineering, University of Leeds, Leeds LS2 9DY, United Kingdom

6 Congo Basin Water Resources Research Center (CRREBaC) and Department of Natural Resources Management, University of Kinshasa (UNIKIN), Kinshasa, Democratic Republic of the Congo

7 Department of Geology, University of Lubumbashi (UNILU), Route Kasapa, Lubumbashi, Democratic Republic of the Congo

8 Hydro Matters, 31460 Le Faget, France

9 Hydraulic Research Institute (IPH), Federal University of Rio Grande do Sul (UFRGS), 91501-970 Porto Alegre, Brazil

10 Instituto de Desenvolvimento Sustentável Mamirauá, 69553-225 Tefé, AM, Brazil

11 Collecte Localisation Satellites (CLS), 31520 Ramonville Saint-Agne, France

12 Institute de Recherche pour le Développement (IRD), Cayenne IRD Center, 97323 French Guiana, France

2. Tourian, M.J., Papa, F., Elmi, O., Sneeuw, N., Kitambo, B., Tshimanga, R., Paris, A., Calmant, S. Current availability and distribution of Congo Basin's freshwater resources. Commun Earth Environ 4, 174 (2023). https://doi.org/10.1038/s43247-023-00836-z

communications earth & environment

Article | Open Access | Published: 22 May 2023

Current availability and distribution of Congo Basin's freshwater resources

Mohammad J. Tourian ✉, Fabrice Papa, Omid Elmi, Nico Sneeuw, Benjamin Kitambo, Raphael M. Tshimanga, Adrien Paris & Stéphane Calmant

Communications Earth & Environment **4**, Article number: 174 (2023) | Cite this article

Abstract

The Congo Basin is of global significance for biodiversity and the water and carbon cycles. However, its freshwater availability and distribution remain relatively unknown. Using satellite data, here we show that currently the Congo Basin's Total Drainable Water Storage lies within a range of 476 km^3 to 502 km^3, unevenly distributed throughout the region, with 63% being stored in the southernmost sub-basins, Kasaï (220–228 km^3) and Lualaba (109–169 km^3), while the northern sub-basins contribute only 173 ± 8 km^3. We further estimate the hydraulic time constant for draining its entire water storage to be 4.3 ± 0.1 months, but, regionally, permanent wetlands and large lakes act as resistors resulting in greater time constants of up to 105 ± 3 months. Our estimate provides a robust basis to address the challenges of water demand for 120 million inhabitants, a population expected to double in a few decades.

Bibliography

Abdalla, S., Abdeh Kolahchi, A., Ablain, M., Adusumilli, S., Aich Bhowmick, S., Alou-Font, E., Amarouche, L., Andersen, O. B., Antich, H., Aouf, L., Arbic, B., Armitage, T., Arnault, S., Artana, C., Aulicino, G., Ayoub, N., Badulin, S., Baker, S., Banks, C., … Zlotnicki, V. (2021). Altimetry for the future: Building on 25 years of progress. *Advances in Space Research*, *68*(2), 319–363. https://doi.org/https://doi.org/10.1016/j.asr.2021.01.022

Aloysius, N., & Saiers, J. (2017). Simulated hydrologic response to projected changes in precipitation and temperature in the Congo River basin. *Hydrology and Earth System Sciences*, *21*, 4115–4130. https://doi.org/https://doi.org/10.5194/hess-21-4115-2017

Alsdorf, D., Beighley, E., Laraque, A., Lee, H., Tshimanga, R., O'Loughlin, F., Mahé, G., Dinga, B., Moukandi, G., & Spencer, R. G. M. (2016). Opportunities for hydrologic research in the Congo Basin. *Reviews of Geophysics*, *54*(2), 378–409. https://doi.org/10.1002/2016RG000517

Alsdorf, D. E., Rodríguez, E., & Lettenmaier, D. P. (2007). Measuring surface water from space. *Reviews of Geophysics*, *45*(2), 1–24. https://doi.org/10.1029/2006RG000197

Andersen, J., Refsgaard, J. C., & Jensen, K. H. (2001). Distributed hydrological modelling of the Senegal River Basin — model construction and validation. *Journal of Hydrology*, *247*(3), 200–214. https://doi.org/https://doi.org/10.1016/S0022-1694(01)00384-5

Andersen, O. B., & Knudsen, P. (2000). The role of satellite altimetry in gravity field modelling in coastal areas. *Physics and Chemistry of the Earth, Part A: Solid Earth and Geodesy*, *25*(1), 17–24. https://doi.org/https://doi.org/10.1016/S1464-1895(00)00004-1

Barzaghi, R., Migliaccio, F., Reguzzoni, M., & Albertella, A. (2015). The Earth gravity field in the time of satellites. *Rendiconti Lincei*, *26*(1), 13–23. https://doi.org/10.1007/s12210-015-0382-9

Bates, P. D., Horritt, M. S., & Fewtrell, T. J. (2010). A simple inertial formulation of the shallow water equations for efficient two-dimensional flood inundation modelling. *Journal of Hydrology*, *387*(1), 33–45. https://doi.org/https://doi.org/10.1016/j.jhydrol.2010.03.027

Becker, M., Papa, F., Frappart, F., Alsdorf, D., Calmant, S., da Silva, J. S., Prigent, C., & Seyler, F. (2018). Satellite-based estimates of surface water dynamics in the Congo River Basin. *International Journal of Applied Earth Observation and Geoinformation*, *66*(August

2017), 196–209. https://doi.org/10.1016/j.jag.2017.11.015

Becker, Mélanie, Santos, J., Calmant, S., Robinet, V., Linguet, L., & Seyler, F. (2014). *Water Level Fluctuations in the Congo Basin Derived from ENVISAT Satellite Altimetry*. *6*, 9340–9358. https://doi.org/10.3390/rs6109340

Bele, Y., Mulotwa, E., Bokoto de Semboli, B., Sonwa, D., & Tiani, A. . (2010). *Afrique centrale: Les effets du changement climatique dans le Bassin du Congo: la nécessité de soutenir les capacités adaptatives locales*.

Bengtsson, L., Bonnet, R.-M., Calisto, M., Destouni, G., Gurney, R., Johannessen, J., Kerr, Y., Lahoz, W. A., & Rast, M. (2014). *The Earth's Hydrological Cycle* (L. Bengtsson, R.-M. Bonnet, M. Calisto, G. Destouni, R. Gurney, J. Johannessen, Y. Kerr, W. A. Lahoz, & M. Rast (eds.)). Springer. https://doi.org/10.1007/978-94-017-8789-5

Berry, P. A. M., Garlick, J. D., Freeman, J. A., & Mathers, E. L. (2005). Global inland water monitoring from multi-mission altimetry. *Geophysical Research Letters*, *32*(16). https://doi.org/https://doi.org/10.1029/2005GL022814

Betbeder, J., Gond, V., Frappart, F., Baghdadi, N. N., Briant, G., & Bartholomé, E. (2014). Mapping of Central Africa Forested Wetlands Using Remote Sensing. *IEEE Journal of Selected Topics in Applied Earth Observations and Remote Sensing*, *7*(2), 531–542. https://doi.org/10.1109/JSTARS.2013.2269733

Biancamaria, S., Lettenmaier, D. P., & Pavelsky, T. M. (2016). The SWOT Mission and Its Capabilities for Land Hydrology. *Surveys in Geophysics*, *37*(2), 307–337. https://doi.org/10.1007/s10712-015-9346-y

Biddulph, G. E., Bocko, Y. E., Bola, P., Crezee, B., Dargie, G. C., Emba, O., Georgiou, S., Girkin, N., Hawthorne, D., Jonay Jovani-Sancho, A., Joseph Kanyama, T., Mampouya, W. E., Mbemba, M., Sciumbata, M., & Tyrrell, G. (2021). Current knowledge on the Cuvette Centrale peatland complex and future research directions. *Bois et Forets Des Tropiques*, *350*, 3–14. https://doi.org/10.19182/bft2021.350.a36288

Birkett, C. M. (1994). Radar altimetry: A new concept in monitoring lake level changes. *Eos, Transactions American Geophysical Union*, *75*(24), 273–275. https://doi.org/https://doi.org/10.1029/94EO00944

Birkett, C. M. (1995). The contribution of TOPEX/POSEIDON to the global monitoring of

climatically sensitive lakes. *Journal of Geophysical Research: Oceans*, *100*(C12), 25179–25204. https://doi.org/https://doi.org/10.1029/95JC02125

Birkett, C., Reynolds, C., Beckley, B., & Doorn, B. (2011). *From Research to Operations: The USDA Global Reservoir and Lake Monitor BT - Coastal Altimetry* (S. Vignudelli, A. G. Kostianoy, P. Cipollini, & J. Benveniste (eds.); pp. 19–50). Springer Berlin Heidelberg. https://doi.org/10.1007/978-3-642-12796-0_2

Brêda, J. P. L. F., de Paiva, R. C. D., Collischon, W., Bravo, J. M., Siqueira, V. A., & Steinke, E. B. (2020). Climate change impacts on South American water balance from a continental-scale hydrological model driven by CMIP5 projections. *Climatic Change*, *159*(4), 503–522. https://doi.org/10.1007/s10584-020-02667-9

Bremicker, M., Homagk, P., & Ludwig, K. (2004). *Operational low-flow-forecast for the Neckar river basin*. Wasserwirtschaft.

Bricquet, J. P. (1993). Les Ecoulements Du Congo a Brazzaville Et La Spatialisation Des Apports. *Grands Bassins Fluviaux*, *800 m*, 22–24.

Burnett, M., Quetin, G., & Konings, A. (2020). Data-driven estimates of evapotranspiration and its drivers in the Congo Basin. *Hydrology and Earth System Sciences*, *24*, 4189–4211. https://doi.org/10.5194/hess-2020-186

Calmant, S., & Seyler, F. (2006). Continental surface waters from satellite altimetry. *Comptes Rendus Geoscience*, *338*(14), 1113–1122. https://doi.org/https://doi.org/10.1016/j.crte.2006.05.012

Calmant, S., Seyler, F., & Cretaux, J. F. (2008). Monitoring Continental Surface Waters by Satellite Altimetry. *Surveys in Geophysics*, *29*(4), 247–269. https://doi.org/10.1007/s10712-008-9051-1

Carabajal, C. C., & Boy, J.-P. (2021). Lake and reservoir volume variations in South America from radar altimetry, ICESat laser altimetry, and GRACE time-variable gravity. *Advances in Space Research*, *68*(2), 652–671. https://doi.org/https://doi.org/10.1016/j.asr.2020.04.022

Carr, A. B., Trigg, M. A., Tshimanga, R. M., Borman, D. J., & Smith, M. W. (2019). Greater Water Surface Variability Revealed by New Congo River Field Data : Implications for Satellite Altimetry Measurements of Large Rivers. *Geophysical Research Letters*, *46*(14),

8093–8101. https://doi.org/10.1029/2019GL083720

Cazenave, A., Palanisamy, H., & Ablain, M. (2018). Contemporary sea level changes from satellite altimetry: What have we learned? What are the new challenges? *Advances in Space Research*, *62*(7), 1639–1653. https://doi.org/https://doi.org/10.1016/j.asr.2018.07.017

Chawla, I., Karthikeyan, L., & Mishra, A. K. (2020). A review of remote sensing applications for water security: Quantity, quality, and extremes. *Journal of Hydrology*, *585*, 124826. https://doi.org/https://doi.org/10.1016/j.jhydrol.2020.124826

Collischonn, w., Allasia, d., Da silva, b. c., & Tucci, c. e. m. (2007). The MGB-IPH model for large-scale rainfall—runoff modelling. *Hydrological Sciences Journal*, *52*(5), 878–895. https://doi.org/10.1623/hysj.52.5.878

Corbari, C., Huber, C., Yesou, H., Huang, Y., & Su, Z. (2019). Multi-Satellite Data of Land Surface Temperature , Lakes Area , and Water Level for Hydrological Model Calibration and Validation in the Yangtze River Basin. *Water*, *11*(12). https://doi.org/10.3390/w11122621

Coss, S, Durand, M., Yi, Y., Jia, Y., Guo, Q., Tuozzolo, S., Shum, C. K., Allen, G. H., Calmant, S., & Pavelsky, T. (2020). Global River Radar Altimetry Time Series (GRRATS): new river elevation earth science data records for the hydrologic community. *Earth System Science Data*, *12*(1), 137–150. https://doi.org/10.5194/essd-12-137-2020

Coss, Stephen, Durand, M. T., Shum, C. K., Yi, Y., Yang, X., Pavelsky, T., Getirana, A., & Yamazaki, D. (2023). Channel Water Storage Anomaly: A New Remotely Sensed Quantity for Global River Analysis. *Geophysical Research Letters*, *50*(1), e2022GL100185. https://doi.org/https://doi.org/10.1029/2022GL100185

Crawford, N. H., & Linsley, R. K. (1966). *Digital Simulation in Hydrology'Stanford Watershed Model 4*.

Cretaux, J.-F. (2022). Inland Water Altimetry: Technological Progress and Applications. In A. Di Mauro, A. Scozzari, & F. Soldovieri (Eds.), *Instrumentation and Measurement Technologies for Water Cycle Management* (pp. 111–139). Springer International Publishing. https://doi.org/10.1007/978-3-031-08262-7_6

Cretaux, J.-F., Nielsen, K., Frappart, F., Papa, F., Calmant, S., & Benveniste, J. (2017).

Hydrological applications of satellite altimetryrivers, lakes, man-made reservoirs, inundated areas. In *Satellite altimetry over oceans and land surfaces* (pp. 459–504). CRC Press.

Crétaux, J. F., Arsen, A., Calmant, S., Kouraev, A., Vuglinski, V., Bergé-Nguyen, M., Gennero, M. C., Nino, F., Abarca Del Rio, R., Cazenave, A., & Maisongrande, P. (2011). SOLS: A lake database to monitor in the Near Real Time water level and storage variations from remote sensing data. *Advances in Space Research*, *47*(9), 1497–1507. https://doi.org/10.1016/j.asr.2011.01.004

Crezee, B., Dargie, G. C., Ewango, C. E. N., Mitchard, E. T. A., B, O. E., T, J. K., Bola, P., Ndjango, J. N., Girkin, N. T., Bocko, Y. E., Ifo, S. A., Hubau, W., Seidensticker, D., Batumike, R., Wotzka, H., Bean, H., Baker, T. R., Baird, A. J., Boom, A., … Lewis, S. L. (2022). Mapping peat thickness and carbon stocks of the central Congo Basin using field data. *Nature Geoscience*, *15*, 639–644. https://doi.org/10.1038/s41561-022-00966-7

Crowley, J. W., Mitrovica, J. X., Bailey, R. C., Tamisiea, M. E., & Davis, J. L. (2006). Land water storage within the Congo Basin inferred from GRACE satellite gravity data. *Geophysical Research Letters*, *33*(19). https://doi.org/10.1029/2006GL027070

Da Silva, J.S, Calmant, S., Seyler, F., Corrêa, O., Filho, R., Cochonneau, G., & João, W. (2010). Water levels in the Amazon basin derived from the ERS 2 and ENVISAT radar altimetry missions. *Remote Sensing of Environment*, *114*, 2160–2181. https://doi.org/10.1016/j.rse.2010.04.020

da Silva, Joecila Santos, Calmant, S., Seyler, F., Lee, H., & Shum, C. K. (2012). Mapping of the extreme stage variations using ENVISAT altimetry in the Amazon basin rivers. *International Water Technology Journal*, *2*(1), 14–25.

da Silva, Joecila Santos, Calmant, S., Seyler, F., Moreira, D. M., Oliveira, D., & Monteiro, A. (2014). Radar Altimetry Aids Managing Gauge Networks. *Water Resources Management*, *28*(3), 587–603. https://doi.org/10.1007/s11269-013-0484-z

Dargie, G. C., Lewis, S. L., Lawson, I. T., Mitchard, E. T. A., Page, S. E., Bocko, Y. E., & Ifo, S. A. (2017). Age, extent and carbon storage of the central Congo Basin peatland complex. *Nature*, *542*(7639), 86–90. https://doi.org/10.1038/nature21048

Datok, P., Fabre, C., Sauvage, S., N'kaya, G. D. M., Paris, A., Santos, V. Dos, Laraque, A., & Sánchez-Pérez, J. (2022). Investigating the Role of the Cuvette Centrale in the Hydrology

of the Congo River Basin. In Raphael M. Tshimanga, G. D. M. N'kaya, & D. Alsdorf (Eds.), *Congo Basin Hydrology, Climate, and Biogeochemistry A Foundation for the Future* (pp. 247–273). American Geophysical Union and John Wiley and Sons, Inc. https://doi.org/10.1002/9781119657002.ch14

de Paiva, Rodrigo Cauduro Dias, Buarque, D. C., Collischonn, W., Bonnet, M.-P., Frappart, F., Calmant, S., & Bulhões Mendes, C. A. (2013). Large-scale hydrologic and hydrodynamic modeling of the Amazon River basin. *Water Resources Research*, *49*(3), 1226–1243. https://doi.org/https://doi.org/10.1002/wrcr.20067

Decharme, B., Alkama, R., Papa, F., Faroux, S., Douville, H., & Prigent, C. (2011). Global off-line evaluation of the ISBA-TRIP flood model. *Climate Dynamics*, *38*(7–8), 1389–1412. https://doi.org/10.1007/s00382-011-1054-9

Decharme, Bertrand, Douville, H., Prigent, C., Papa, F., & Aires, F. (2008). A new river flooding scheme for global climate applications : Off-line evaluation over South America. *Journal of Geophysical Research Atmospheres*, *113*(11), 1–11. https://doi.org/10.1029/2007JD009376

Devia, G. K., Ganasri, B. P., & Dwarakish, G. S. (2015). A Review on Hydrological Models. *Aquatic Procedia*, *4*, 1001–1007. https://doi.org/https://doi.org/10.1016/j.aqpro.2015.02.126

Döll, P., Douville, H., Güntner, A., Müller Schmied, H., & Wada, Y. (2016). Modelling Freshwater Resources at the Global Scale: Challenges and Prospects. *Surveys in Geophysics*, *37*(2), 195–221. https://doi.org/10.1007/s10712-015-9343-1

Dos Santos, V., Oliveira, R. A. J., Datok, P., Sauvage, S., Paris, A., Gosset, M., & Sánchez-Pérez, J. M. (2022). Evaluating the performance of multiple satellite-based precipitation products in the Congo River Basin using the SWAT model. *Journal of Hydrology: Regional Studies*, *42*, 101168. https://doi.org/https://doi.org/10.1016/j.ejrh.2022.101168

Fan, F. M., Collischonn, W., Quiroz, K. J., Sorribas, M. V, Buarque, D. C., & Siqueira, V. A. (2016). Flood forecasting on the Tocantins River using ensemble rainfall forecasts and real-time satellite rainfall estimates. *Journal of Flood Risk Management*, *9*(3), 278–288. https://doi.org/https://doi.org/10.1111/jfr3.12177

Fan, L., Wigneron, J.-P., Ciais, P., Chave, J., Brandt, M., Fensholt, R., Saatchi, S. S., Bastos, A., Al-Yaari, A., Hufkens, K., Qin, Y., Xiao, X., Chen, C., Myneni, R. B., Fernandez-

Moran, R., Mialon, A., Rodriguez-Fernandez, N. J., Kerr, Y., Tian, F., & Peñuelas, J. (2019). Satellite-observed pantropical carbon dynamics. *Nature Plants*, *5*(9), 944–951. https://doi.org/10.1038/s41477-019-0478-9

Fao/Iiasa/Isric/Isscas/Jrc. (2012). *Harmonized world soil database (version 1.2)*. FAO, Rome, Italy and IIASA, Laxenburg, Austria.

Fassoni-Andrade, A. C., Fleischmann, A. S., Papa, F., Paiva, R. C. D. de, Wongchuig, S., Melack, J. M., Moreira, A. A., Paris, A., Ruhoff, A., Barbosa, C., Maciel, D. A., Novo, E., Durand, F., Frappart, F., Aires, F., Gabriel Medeiros Abrahão, J. F.-F., Jhan Carlo Espinoza, L. L., Costa, M. H., Raul Espinoza-Villar, S. C., & Pellet, V. (2021). Amazon Hydrology From Space: Scientific Advances and Future Challenges. *Reviews of Geophysics*, 1–97. https://doi.org/10.1029/2020RG000728

Fatras, C., Parrens, M., Peña Luque, S., & Al Bitar, A. (2021). Hydrological Dynamics of the Congo Basin From Water Surfaces Based on L-Band Microwave. *Water Resources Research*, *57*(2). https://doi.org/10.1029/2020wr027259

Fekete, B. M., Looser, U., Pietroniro, A., & Robarts, R. D. (2012). Rationale for Monitoring Discharge on the Ground. *Journal of Hydrometeorology*, *13*(6), 1977–1986. https://doi.org/https://doi.org/10.1175/JHM-D-11-0126.1

Femenias P., Baker S., Brockley D. J., B., M., F.-H., M., M., O., B., P., Roca M., S., R., R., S., F., S., P., V., F., P., & P., F. (2014). Reprocessing of the ERS-1 and ERS-2 altimetry missions. The REAPER project. *Ocean Surface Topography Science Team Meeting*.

Fisher, R. A., & Koven, C. D. (2020). Perspectives on the Future of Land Surface Models and the Challenges of Representing Complex Terrestrial Systems. *Journal of Advances in Modeling Earth Systems*, *12*(4), e2018MS001453. https://doi.org/https://doi.org/10.1029/2018MS001453

Fleischmann, A., Collischonn, W., Paiva, R., & Tucci, C. E. (2019). Modeling the role of reservoirs versus floodplains on large-scale river hydrodynamics. *Natural Hazards*, *99*(2), 1075–1104. https://doi.org/10.1007/s11069-019-03797-9

Frappart, F., Papa, F., Famiglietti, J. S., Prigent, C., Rossow, W. B., & Seyler, F. (2008). Interannual variations of river water storage from a multiple satellite approach : A case study for the Rio Negro River basin. *Journal of Geophysical Research*, *113*, 1–12. https://doi.org/10.1029/2007JD009438

Frappart, F, Legrésy, B., Niño, F., Blarel, F., Fuller, N., Fleury, S., Birol, F., & Calmant, S. (2016). An ERS-2 altimetry reprocessing compatible with ENVISAT for long-term land and ice sheets studies. *Remote Sensing of Environment*, *184*, 558–581. https://doi.org/https://doi.org/10.1016/j.rse.2016.07.037

Frappart, F, Papa, F., Marieu, V., Malbeteau, Y., Jordy, F., Calmant, S., Durand, F., & Bala, S. (2015). Preliminary Assessment of SARAL/AltiKa Observations over the Ganges-Brahmaputra and Irrawaddy Rivers. *Marine Geodesy*, *38*(sup1), 568–580. https://doi.org/10.1080/01490419.2014.990591

Frappart, Frédéric, Blarel, F., Fayad, I., Bergé-Nguyen, M., Crétaux, J.-F., Shu, S., Schregenberger, J., & Baghdadi, N. (2021). Evaluation of the Performances of Radar and Lidar Altimetry Missions for Water Level Retrievals in Mountainous Environment: The Case of the Swiss Lakes. In *Remote Sensing* (Vol. 13, Issue 11). https://doi.org/10.3390/rs13112196

Frappart, Frédéric, Calmant, S., Cauhopé, M., Seyler, F., & Cazenave, A. (2006). Preliminary results of ENVISAT RA-2-derived water levels validation over the Amazon basin. *Remote Sensing of Environment*, *100*(2), 252–264. https://doi.org/https://doi.org/10.1016/j.rse.2005.10.027

Frappart, Frédéric, Papa, F., Güntner, A., Werth, S., Santos da Silva, J., Tomasella, J., Seyler, F., Prigent, C., Rossow, W. B., Calmant, S., & Bonnet, M. P. (2011). Satellite-based estimates of groundwater storage variations in large drainage basins with extensive floodplains. *Remote Sensing of Environment*, *115*(6), 1588–1594. https://doi.org/10.1016/j.rse.2011.02.003

Frappart, Frédéric, Papa, F., Malbeteau, Y., León, J. G., Ramillien, G., Prigent, C., Seoane, L., Seyler, F., & Calmant, S. (2015a). Surface freshwater storage variations in the Orinoco floodplains using multi-satellite observations. *Remote Sensing*, *7*(1), 89–110. https://doi.org/10.3390/rs70100089

Frappart, Frédéric, Papa, F., Malbeteau, Y., León, J. G., Ramillien, G., Prigent, C., Seoane, L., Seyler, F., & Calmant, S. (2015b). Surface Freshwater Storage Variations in the Orinoco Floodplains Using Multi-Satellite Observations. In *Remote Sensing* (Vol. 7, Issue 1, pp. 89–110). https://doi.org/10.3390/rs70100089

Frappart, Frédéric, Papa, F., Santos Da Silva, J., Ramillien, G., Prigent, C., Seyler, F., &

Calmant, S. (2012). Surface freshwater storage and dynamics in the Amazon basin during the 2005 exceptional drought. *Environmental Research Letters*, *7*(4). https://doi.org/10.1088/1748-9326/7/4/044010

Frappart, Frédéric, Zeiger, P., Betbeder, J., Gond, V., Bellot, R., Baghdadi, N., Blarel, F., Darrozes, J., Bourrel, L., & Seyler, F. (2021). Automatic Detection of Inland Water Bodies along Altimetry Tracks for Estimating Surface Water Storage Variations in the Congo Basin. In *Remote Sensing* (Vol. 13, Issue 19). https://doi.org/10.3390/rs13193804

Fread, D. L. (1992). Flow routing. In *Handbook of hydrology* (Vol. 10). McGraw-Hill.

Funk, C., Peterson, P., Landsfeld, M., Pedreros, D., Verdin, J., Shukla, S., Husak, G., Rowland, J., Harrison, L., Hoell, A., & Michaelsen, J. (2015). The climate hazards infrared precipitation with stations—a new environmental record for monitoring extremes. *Scientific Data*, *2*(1), 150066. https://doi.org/10.1038/sdata.2015.66

Gallucci, M. (2021). How to measure all the world's freshwater. *MIT Technology Review*, 1–10. https://www.technologyreview.com/2021/12/22/1041323/remote-sensing-freshwater-climate-hydrologist/

Garambois, P. A., Calmant, S., Roux, H., Paris, A., Monnier, J., Finaud-Guyot, P., Samine Montazem, A., & Santos da Silva, J. (2017). Hydraulic visibility: Using satellite altimetry to parameterize a hydraulic model of an ungauged reach of a braided river. *Hydrological Processes*, *31*(4), 756–767. https://doi.org/10.1002/hyp.11033

Gardner, A. S., Moholdt, G., Cogley, J. G., Wouters, B., Arendt, A. A., Wahr, J., Berthier, E., Hock, R., Pfeffer, W. T., Kaser, G., Ligtenberg, S. R. M., Bolch, T., Sharp, M. J., Hagen, J. O., van den Broeke, M. R., & Paul, F. (2013). A Reconciled Estimate of Glacier Contributions to Sea Level Rise: 2003 to 2009. *Science*, *340*(6134), 852–857. https://doi.org/10.1126/science.1234532

Gebrechorkos, S. H., Taye, M. T., Birhanu, B., Solomon, D., & Demissie, T. (2023). Future changes in climate and hydroclimate extremes in East Africa. *Earth's Future*, *n/a*(n/a), e2022EF003011. https://doi.org/https://doi.org/10.1029/2022EF003011

Getirana, A. C. V, Bonnet, M.-P., Calmant, S., Roux, E., Rotunno Filho, O. C., & Mansur, W. J. (2009). Hydrological monitoring of poorly gauged basins based on rainfall–runoff modeling and spatial altimetry. *Journal of Hydrology*, *379*(3), 205–219. https://doi.org/https://doi.org/10.1016/j.jhydrol.2009.09.049

Ghosh, S., Thakur, P. K., Sharma, R., Nandy, S., Garg, V., Amarnath, G., & Bhattacharyya, S. (2017). The Potential Applications of Satellite Altimetry with SARAL/AltiKa for Indian Inland Waters. *Proceedings of the National Academy of Sciences, India Section A: Physical Sciences*, *87*(4), 661–677. https://doi.org/10.1007/s40010-017-0463-5

Gudmundsson, L., Wagener, T., Tallaksen, L. M., & Engeland, K. (2012). Evaluation of nine large-scale hydrological models with respect to the seasonal runoff climatology in Europe. *Water Resources Research*, *48*(11). https://doi.org/https://doi.org/10.1029/2011WR010911

Gumbricht, T., Román-Cuesta, R. M., Verchot, L. V, Herold, M., Wittmann, F., Householder, E., Herold, N., & Murdiyarso, D. (2017). *Tropical and Subtropical Wetlands Distribution* (V7 ed.). Center for International Forestry Research (CIFOR). https://doi.org/doi:10.17528/CIFOR/DATA.00058

Guo, S., Wang, J., Xiong, L., Ying, A., & Li, D. (2002). A macro-scale and semi-distributed monthly water balance model to predict climate change impacts in China. *Journal of Hydrology*, *268*(1), 1–15. https://doi.org/https://doi.org/10.1016/S0022-1694(02)00075-6

Hansen, M. C., Potapov, P. V, Pickens, A. H., Tyukavina, A., Hernandez-Serna, A., Zalles, V., Turubanova, S., Kommareddy, I., Stehman, S. V, Song, X.-P., & Kommareddy, A. (2022). Global land use extent and dispersion within natural land cover using Landsat data. *Environmental Research Letters*, *17*(3), 34050. https://doi.org/10.1088/1748-9326/ac46ec

Hastenrath, S. (1985). Climate and circulation of the tropics, D. Reidel Publishing Company, Holland, https://doi.org/10.1007/978-94-009-5388-8

Hastie, A., Lauerwald, R., Ciais, P., Papa, F., & Regnier, P. (2021). Historical and future contributions of inland waters to the Congo Basin carbon balance. *Earth System Dynamics*, *12*(1), 37–62. https://doi.org/10.5194/esd-12-37-2021

Huang, C., Chen, Y., Zhang, S., & Wu, J. (2018). Detecting, Extracting, and Monitoring Surface Water From Space Using Optical Sensors: A Review. *Reviews of Geophysics*, *56*(2), 333–360. https://doi.org/https://doi.org/10.1029/2018RG000598

Ingram, V., Tieguhong, J. C., Schure, J., Nkamgnia, E., & Tadjuidje, M. H. (2011). Where artisanal mines and forest meet: Socio-economic and environmental impacts in the Congo Basin. *Natural Resources Forum*, *35*(4), 304–320. https://doi.org/10.1111/j.1477-8947.2011.01408.x

Inogwabini, B. (2020). The changing water cycle: Freshwater in the Congo. *WIREs Water*, *7*(2), 1–17. https://doi.org/10.1002/wat2.1410

Jajarmizadeh, M., Harun, S., & Salarpour, M. (2012). A review on theoretical consideration and types of models in hydrology. *Journal of Environmental Science and Technology*, *5*(5), 249–261.

Jiang, L., Nielsen, K., Dinardo, S., Andersen, O. B., & Bauer-Gottwein, P. (2020). Evaluation of Sentinel-3 SRAL SAR altimetry over Chinese rivers. *Remote Sensing of Environment*, *237*, 111546. https://doi.org/https://doi.org/10.1016/j.rse.2019.111546

Jiang, L., Schneider, R., Andersen, O. B., & Bauer-Gottwein, P. (2017). CryoSat-2 Altimetry Applications over Rivers and Lakes. In *Water* (Vol. 9, Issue 3). https://doi.org/10.3390/w9030211

Kabuya, P., Hughes, D., Tshimanga, R., & Trigg, M. (2020). Understanding factors influencing the wetland parameters of a monthly rainfall-runoff model in the Upper Congo River basin. *EGU General Assembly Conference Abstracts*, 642. https://doi.org/10.5194/egusphere-egu2020-642

Karamouz, M., Nazif, S., & Falahi, M. (2013). *Hydrology and Hydroclimatology: Principles and Applications* (M. Karamouz, S. Nazif, & M. Falahi (eds.)). CRC Press, Taylor and Francis Group.

Khan, S. A., Colgan, W., Neumann, T. A., Broeke, M. R. Van Den, Brunt, K. M., Noël, B., Bamber, J. L., Hassan, J., & Bjørk, A. A. (2022). Accelerating ice loss from peripheral glaciers in North Greenland. *Geophysical Research Letters*, *49*. https://doi.org/10.1029/2022GL098915

Kitambo, B. M., Papa, F., Paris, A., Tshimanga, R. M., Frappart, F., Calmant, S., Elmi, O., Fleischmann, A. S., Becker, M., Tourian, M. J., Jucá Oliveira, R. A., & Wongchuig, S. (2022b). A long-term monthly surface water storage dataset for the Congo basin from 1992 to 2015. *Earth System Science Data Discussions*, *2022*, 1–39. https://doi.org/10.5194/essd-2022-376

Kitambo, B., Papa, F., Paris, A., Tshimanga, R. M., Calmant, S., Fleischmann, A. S., Frappart, F., Becker, M., Tourian, M. J., Prigent, C., & Andriambeloson, J. (2022a). A combined use of in situ and satellite-derived observations to characterize surface hydrology and its variability in the Congo River basin. *Hydrology and Earth System Sciences*, *26*(7), 1857–

1882. https://doi.org/10.5194/hess-26-1857-2022

Kittel, C. M. M., Jiang, L., Tøttrup, C., & Bauer-Gottwein, P. (2021). Sentinel-3 radar altimetry for river monitoring - A catchment-scale evaluation of satellite water surface elevation from Sentinel-3A and Sentinel-3B. *Hydrology and Earth System Sciences*, *25*(1), 333–357. https://doi.org/10.5194/hess-25-333-2021

Klein, P., Lapeyre, G., Siegelman, L., Qiu, B., Fu, L.-L., Torres, H., Su, Z., Menemenlis, D., & Le Gentil, S. (2019). Ocean-Scale Interactions From Space. *Earth and Space Science*, *6*(5), 795–817. https://doi.org/https://doi.org/10.1029/2018EA000492

Kouraev, A. V, Zakharova, E. A., Samain, O., Mognard, N. M., & Cazenave, A. (2004). Ob' river discharge from TOPEX/Poseidon satellite altimetry (1992–2002). *Remote Sensing of Environment*, *93*(1), 238–245. https://doi.org/https://doi.org/10.1016/j.rse.2004.07.007

Lakshmi, V., Alsdorf, D., Anderson, M., Biancamaria, S., Cosh, M., Entin, J., Huffman, G., Kustas, W., Oevelen, P. van, Painter, T., Parajka, J., Rodell, M., & Rüdiger, C. (2015). *Remote Sensing of the Terrestrial Water Cycle* (V. Lakshmi, D. Alsdorf, M. Anderson, S. Biancamaria, M. Cosh, J. Entin, G. Huffman, W. Kustas, P. van Oevelen, T. Painter, J. Parajka, M. Rodell, & C. Rüdiger (eds.)). American Geophysical Union & John Wiley & Sons, Inc.

Laraque, A., Bellanger, M., Adele, G., Guebanda, S., Gulemvuga, G., Pandi, A., Paturel, J. E., Robert, A., Tathy, J. P., & Yambele, A. (2013). Evolutions récentes des débits du Congo, de l'Oubangui et de la Sangha. *Geo-Eco-Trop*, *37*(1), 93–100.

Laraque, Alain, Bricquet, J. P., Pandi, A., & Olivry, J. C. (2009). A review of material transport by the Congo River and its tributaries. *Hydrological Processes*, *23*(22), 3216–3224. https://doi.org/10.1002/hyp.7395

Laraque, Alain, N'kaya, G. D. M., Orange, D., Tshimanga, R., Tshitenge, J. M., Mahé, G., Nguimalet, C. R., Trigg, M. A., Yepez, S., & Gulemvuga, G. (2020). Recent budget of hydroclimatology and hydrosedimentology of the congo river in central Africa. *Water*, *12*(9). https://doi.org/10.3390/w12092613

Lee, H., Beighley, R. E., Alsdorf, D., Chul, H., Shum, C. K., Duan, J., Guo, J., Yamazaki, D., & Andreadis, K. (2011). Remote Sensing of Environment Characterization of terrestrial water dynamics in the Congo Basin using GRACE and satellite radar altimetry. *Remote Sensing of Environment*, *115*(12), 3530–3538. https://doi.org/10.1016/j.rse.2011.08.015

Leon, J. G., Seyler, F., & Calmant, S. (2012). Application de l'altimétrie radar pour le suivie des eaux de surface: Tout un outil en hydrologie. Editions Universitaires Européenes.

Lettenmaier, D. P., Alsdorf, D., Dozier, J., Huffman, G. J., Pan, M., & Wood, E. F. (2015). Inroads of remote sensing into hydrologic science during the WRR era. *Water Resources Research*, *51*(9), 7309–7342. https://doi.org/https://doi.org/10.1002/2015WR017616

Li, J., Ma, R., Cao, Z., Xue, K., Xiong, J., Hu, M., & Feng, X. (2022). Satellite Detection of Surface Water Extent: A Review of Methodology. In *Water* (Vol. 14, Issue 7). https://doi.org/10.3390/w14071148

Linsley, R. K., Kohler, M. A., & Paulhus, J. L. H. (1975). *Hydrology for engineers, 2nd edn McGraw*. Hill Kogakusha Press, Tokyo.

Ludwig, K., & Bremicker, M. (2006). *The Water Balance Model LARSIM - Design , Content and Applications*.

Łyszkowicz, A. B., & Bernatowicz, A. (2017). Current state of art of satellite altimetry. *Geodesy and Cartography*, *66*(No 2). https://doi.org/10.1515/geocart-2017-0016

M.E. Noorbakhsh, Rahnama, M. B., & Montazeri, S. (2005). Estimation of Instantaneous Unit Hydrograph with Clark`s Method Using GIS Techniques. *Journal of Applied Sciences*, *5*(3), 455–458. https://doi.org/10.3923/jas.2005.455.458

Maillard, P., Bercher, N., & Calmant, S. (2015). New processing approaches on the retrieval of water levels in Envisat and SARAL radar altimetry over rivers: A case study of the São Francisco River, Brazil. *Remote Sensing of Environment*, *156*, 226–241. https://doi.org/https://doi.org/10.1016/j.rse.2014.09.027

Matheussen, B., Kirschbaum, R. L., Goodman, I. A., O'Donnell, G. M., & Lettenmaier, D. P. (2000). Effects of land cover change on streamflow in the interior Columbia River Basin (USA and Canada). *Hydrological Processes*, *14*(5), 867–885. https://doi.org/https://doi.org/10.1002/(SICI)1099-1085(20000415)14:5<867::AID-HYP975>3.0.CO;2-5

Meijerink, A. M. J., Bannert, D., Batelaan, O., Lubczynski, M., & Pointet, T. (2007). *REMOTE SENSING APPLICATIONS to GROUNDWATER* (IHP-VI Ser). UNESCO. http://unesdoc.unesco.org/images/0015/001563/156300e.pdf

Munzimi, Y. A., Hansen, M. C., & Asante, K. O. (2019). Estimating daily streamflow in the Congo Basin using satellite-derived data and a semi-distributed hydrological model. *Hydrological Sciences Journal*, *64*(12), 1472–1487.

https://doi.org/10.1080/02626667.2019.1647342

N'kaya, G. D. M., Laraque, A., Paturel, J.-E., Guzanga, G. G., Mahé, G., & Tshimanga, R. M. (2022). A New Look at Hydrology in the Congo Basin, Based on the Study of Multi-Decadal Time Series. In *Congo Basin Hydrology, Climate, and Biogeochemistry* (pp. 121–143). https://doi.org/https://doi.org/10.1002/9781119657002.ch8

Ndehedehe, C. E., & Agutu, N. O. (2022). Historical Changes in Rainfall Patterns over the Congo Basin and Impacts on Runoff (1903 – 2010). In Raphael M. Tshimanga, G. D. M. N'kaya, & D. Alsdorf (Eds.), *Congo Basin Hydrology, Climate, and Biogeochemistry A Foundation for the Future*. American Geophysical Union and John Wiley and Sons, Inc. https://doi.org/10.1002/9781119657002.ch9

Ndehedehe, C. E., Anyah, R. O., Alsdorf, D., Agutu, N. O., & Ferreira, V. G. (2019). Modelling the impacts of global multi-scale climatic drivers on hydro-climatic extremes (1901 – 2014) over the Congo basin. *Science of the Total Environment*, *651*, 1569–1587. https://doi.org/10.1016/j.scitotenv.2018.09.203

Nguimalet, C. (2017). Changements enregistrés sur les extrêmes hydrologiques de l'Oubangui à Bangui (République centrafricaine) : analyse des tendances. *Revue des sciences de l'eau / Journal of Water Science*, *30*(3), 183–196. https://doi.org/https://doi.org/10.7202/1044246ar

Nogherotto, R., Coppola, E., Giorgi, F., & Mariotti, L. (2013). Impact of Congo Basin deforestation on the African monsoon. *Atmospheric Science Letters*, *14*(1), 45–51. https://doi.org/10.1002/asl2.416

Nouel, F., Bardina, J., Jayles, C., Labrune, Y., & Truong, B. (1988). DORIS - A precise satellite-positioning Doppler system. *Astrodynamics 1987*, 311–320. https://ui.adsabs.harvard.edu/abs/1988asdy.conf..311N

O'Loughlin, F. ., Neal, J., Schumann, G. J., Beighley, R. E., & Bates, P. D. (2019). A LISFLOOD-FP hydraulic model of the middle reach of the Congo. *Journal of Hydrology*. https://doi.org/https://doi.org/10.1016/j.jhydrol.2019.124203

OMM. 2010. CONGO-HYCOS, Organisation météorologique mondiale, 101 pp., https://library.wmo.int/doc_num.php?explnum_id=4883 (last access: 13 Feb 2023)

Paiva, Rodrigo Cauduro Dias de, Buarque, D. C., Collischonn, W., Bonnet, M., Frappart, F.,

Calmant, S., & Mendes, C. A. B. (2013). Large-scale hydrologic and hydrodynamic modeling of the Amazon River basin. *Water Resources Research*, *49*, 1226–1243. https://doi.org/10.1002/wrcr.20067

Paiva, Rodrigo C D, Collischonn, W., & Buarque, D. C. (2013). Validation of a full hydrodynamic model for large-scale hydrologic modelling in the Amazon. *Hydrological Processes*, *27*(3), 333–346.

Paiva, Rodrigo C D, Collischonn, W., & Tucci, C. E. M. (2011). Large scale hydrologic and hydrodynamic modeling using limited data and a GIS based approach. *Journal of Hydrology*, *406*(3), 170–181. https://doi.org/https://doi.org/10.1016/j.jhydrol.2011.06.007

Papa, F., Prigent, C., Aires, F., Jimenez, C., Rossow, W. B., & Matthews, E. (2010). Interannual variability of surface water extent at the global scale, 1993-2004. *Journal of Geophysical Research Atmospheres*, *115*(12), 1–17. https://doi.org/10.1029/2009JD012674

Papa, F, Prigent, C., Aires, F., Jimenez, C., Rossow, W. B., & Matthews, E. (2010). Interannual variability of surface water extent at the global scale, 1993–2004. *Journal of Geophysical Research: Atmospheres*, *115*(D12). https://doi.org/https://doi.org/10.1029/2009JD012674

Papa, Fabrice, Bala, S. K., Pandey, R. K., Durand, F., Gopalakrishna, V. V, Rahman, A., & Rossow, W. B. (2012a). Ganga-Brahmaputra river discharge from Jason-2 radar altimetry : An update to the long-term satellite-derived estimates of continental freshwater forcing flux into the Bay of Bengal. *Journal of Geophysical Research*, *117*, C11021. https://doi.org/10.1029/2012JC008158

Papa, Fabrice, Bala, S. K., Pandey, R. K., Durand, F., Gopalakrishna, V. V, Rahman, A., & Rossow, W. B. (2012b). Ganga-Brahmaputra river discharge from Jason-2 radar altimetry: An update to the long-term satellite-derived estimates of continental freshwater forcing flux into the Bay of Bengal. *Journal of Geophysical Research: Oceans*, *117*(C11). https://doi.org/https://doi.org/10.1029/2012JC008158

Papa, Fabrice, Crétaux, J.-F., Grippa, M., Robert, E., Trigg, M., Tshimanga, R. M., Kitambo, B., Paris, A., Carr, A., Fleischmann, A. S., de Fleury, M., Gbetkom, P. G., Calmettes, B., & Calmant, S. (2022). Water Resources in Africa under Global Change: Monitoring Surface Waters from Space. *Surveys in Geophysics*. https://doi.org/10.1007/s10712-022-09700-9

Papa, Fabrice, Durand, F., Rossow, W. B., Rahman, A., & Bala, S. K. (2010). Satellite altimeter

- derived monthly discharge of the Ganga - Brahmaputra River and its seasonal to interannual variations from 1993 to 2008. *Journal of Geophysical Research*, *115*, C12013. https://doi.org/10.1029/2009JC006075

Papa, Fabrice, & Frappart, F. (2021). Surface water storage in rivers and wetlands derived from satellite observations: A review of current advances and future opportunities for hydrological sciences. *Remote Sensing*, *13*(20). https://doi.org/10.3390/rs13204162

Papa, Fabrice, Frappart, F., Güntner, A., Prigent, C., Aires, F., Getirana, A. C. V., & Maurer, R. (2013a). Surface freshwater storage and variability in the Amazon basin from multi-satellite observations, 1993-2007. *Journal of Geophysical Research Atmospheres*, *118*(21), 11,951-11,965. https://doi.org/10.1002/2013JD020500

Papa, Fabrice, Frappart, F., Güntner, A., Prigent, C., Aires, F., Getirana, A. C. V, & Maurer, R. (2013b). Surface freshwater storage and variability in the Amazon basin from multi-satellite observations , 1993 – 2007. *Journal of Geophysical Research: Atmospheres*, *118*(11), 1993–2007. https://doi.org/10.1002/2013JD020500

Papa, Fabrice, Frappart, F., Malbeteau, Y., Shamsudduha, M., Vuruputur, V., Sekhar, M., Ramillien, G., Prigent, C., Aires, F., Pandey, R. K., Bala, S., & Calmant, S. (2015). Satellite-derived surface and sub-surface water storage in the Ganges-Brahmaputra River Basin. *Journal of Hydrology: Regional Studies*, *4*(April), 15–35. https://doi.org/10.1016/j.ejrh.2015.03.004

Paris, A., Calmant, S., Gosset, M., Fleischmann, A. S., Sampaio, T., Conchy, X., Garambois, P., Bricquet, J., Papa, F., Tshimanga, R. M., Guzanga, G. G., Siqueira, V. A., Tondo, B., Paiva, R., da Silva, J. S., & Laraque, A. (2022). Monitoring Hydrological Variables from Remote Sensing and Modeling in the Congo River Basin. In Raphael M. Tshimanga, G. D. M. N'kaya, & D. Alsdorf (Eds.), *Congo Basin Hydrology, Climate, and Biogeochemistry A Foundation for the Future* (pp. 339–366). American Geophysical Union and John Wiley and Sons, Inc. https://doi.org/10.1002/9781119657002.ch18

Paris, A., De Paiva, R. D., Da Silva, J. S., Moreira, D. M., Calmant, S., Garambois, P.-A., Collischonn, W., Bonnet, M., & Seyler, F. (2016). Stage-discharge rating curves based on satellite altimetry and modeled discharge in the Amazon basin. *Water Resources Research*, *52*, 3787–3814. https://doi.org/10.1002/2014WR016618.Received

Park, E. (2020). Characterizing channel- fl oodplain connectivity using satellite altimetry :

Mechanism , hydrogeomorphic control , and sediment budget. *Remote Sensing of Environment*, *243*(February), 111783. https://doi.org/10.1016/j.rse.2020.111783

Pechlivanidis, I. G., Jackson, B. M., Mcintyre, N. R., Wheater, H. S., & others. (2011). Catchment scale hydrological modelling: A review of model types, calibration approaches and uncertainty analysis methods in the context of recent developments in technology and applications. *Global NEST Journal*, *13*(3), 193–214.

Pekel, J.-F., Cottam, A., Gorelick, N., & Belward, A. S. (2016). High-resolution mapping of global surface water and its long-term changes. *Nature*, *540*(7633), 418–422. https://doi.org/10.1038/nature20584

Petry, I., Fan, F. M., Siqueira, V. A., Collischonn, W., & Paiva, R. (2022). Predictability of daily streamflow for the great rivers of South America based on a simple metric. *Hydrological Sciences Journal*, 1–15. https://doi.org/10.1080/02626667.2022.2139620

Pham-duc, B., Papa, F., Prigent, C., Aires, F., Biancamaria, S., & Frappart, F. (2019). Variations of Surface and Subsurface Water Storage in the Lower Mekong Basin (Vietnam and Cambodia) from Multisatellite Observations. *Water*, *11*(1), 1–17. https://doi.org/10.3390/w11010075

Pham-duc, B., Sylvestre, F., Papa, F., Frappart, F., Bouchez, C., & Cr, J. (2020). The Lake Chad hydrology under current climate change. *Scientific Reports*, *10*(5498), 1–10. https://doi.org/10.1038/s41598-020-62417-w

Plisnier, P. D., Nshombo, M., Mgana, H., & Ntakimazi, G. (2018). Monitoring climate change and anthropogenic pressure at Lake Tanganyika. *Journal of Great Lakes Research*, *44*(6), 1194–1208. https://doi.org/10.1016/j.jglr.2018.05.019

Pontes, P. R. M., Fan, F. M., Fleischmann, A. S., de Paiva, R. C. D., Buarque, D. C., Siqueira, V. A., Jardim, P. F., Sorribas, M. V., & Collischonn, W. (2017). MGB-IPH model for hydrological and hydraulic simulation of large floodplain river systems coupled with open source GIS. *Environmental Modelling & Software*, *94*, 1–20. https://doi.org/https://doi.org/10.1016/j.envsoft.2017.03.029

Prigent, C., Jimenez, C., & Bousquet, P. (2020). Satellite-Derived Global Surface Water Extent and Dynamics Over the Last 25 Years (GIEMS-2). *Journal of Geophysical Research: Atmospheres*, *125*(3), 1–21. https://doi.org/10.1029/2019JD030711

Prigent, Catherine, Lettenmaier, D. P., Aires, F., & Papa, F. (2016). Toward a High-Resolution Monitoring of Continental Surface Water Extent and Dynamics, at Global Scale: from GIEMS (Global Inundation Extent from Multi-Satellites) to SWOT (Surface Water Ocean Topography). *Surveys in Geophysics*, *37*(2), 339–355. https://doi.org/10.1007/s10712-015-9339-x

Prigent, Catherine, Matthews, E., Aires, F., & Rossow, W. B. (2001). Remote sensing of global wetland dynamics with multiple satellite data sets. *Geophysical Research Letters*, *28*(24), 4631–4634. https://doi.org/https://doi.org/10.1029/2001GL013263

Prigent, Catherine, Papa, F., Aires, F., Rossow, W. B., & Matthews, E. (2007). Global inundation dynamics inferred from multiple satellite observations, 1993-2000. *Journal of Geophysical Research Atmospheres*, *112*(12), 1993–2000. https://doi.org/10.1029/2006JD007847

Pujol, L., Garambois, P. A., Finaud-Guyot, P., Monnier, J., Larnier, K., Mosé, R., Biancamaria, S., Yesou, H., Moreira, D., Paris, A., & Calmant, S. (2020). Estimation of multiple inflows and effective channel by assimilation of multi-satellite hydraulic signatures: The ungauged anabranching Negro river. *Journal of Hydrology*, *591*, 125331. https://doi.org/10.1016/j.jhydrol.2020.125331

Rast, M., Johannessen, J., & Mauser, W. (2014). Review of Understanding of Earth's Hydrological Cycle: Observations, Theory and Modelling. *Surveys in Geophysics*, *35*(3), 491–513. https://doi.org/10.1007/s10712-014-9279-x

Refsgaard, J. C., & Storm, B. (1996). Construction, Calibration And Validation of Hydrological Models BT - Distributed Hydrological Modelling. In M. B. Abbott & J. C. Refsgaard (Eds.), *Distributed Hydrological Modelling* (pp. 41–54). Springer Netherlands. https://doi.org/10.1007/978-94-009-0257-2_3

Revel, M., Zhou, X., Yamazaki, D., & Kanae, S. (2023). Assimilation of transformed water surface elevation to improve river discharge estimation in a continental-scale river. *Hydrology and Earth System Sciences*, *27*(3), 647–671. https://doi.org/10.5194/hess-27-647-2023

Ringeval, B., De Noblet-Ducoudré, N., Ciais, P., Bousquet, P., Prigent, C., Papa, F., & Rossow, W. B. (2010). An attempt to quantify the impact of changes in wetland extent on methane emissions on the seasonal and interannual time scales. *Global Biogeochemical Cycles*,

24(2). https://doi.org/10.1029/2008GB003354

Rodell, M., Famiglietti, J. S., Wiese, D. N., Reager, J. T., Beaudoing, H. K., Landerer, F. W., & Lo, M.-H. (2018). Emerging trends in global freshwater availability. *Nature*, *557*(7707), 651–659. https://doi.org/10.1038/s41586-018-0123-1

Rosenqvist, Å., & Birkett, C. M. (2002). Evaluation of JERS-1 SAR mosaics for hydrological applications in the Congo river basin. *International Journal of Remote Sensing*, *23*(7). https://doi.org/10.1080/01431160110092902

Rybushkina, G., Troitskaya, Y., & Soustova, I. (2012). Jason-2 sattelite water level monitoring in the volga reservoirs. *2012 IEEE International Geoscience and Remote Sensing Symposium*, 786–789. https://doi.org/10.1109/IGARSS.2012.6351444

Salameh, E., Frappart, F., Papa, F., Güntner, A., Venugopal, V., Getirana, A., Prigent, C., Aires, F., Labat, D., & Laignel, B. (2017). Fifteen Years (1993–2007) of Surface Freshwater Storage Variability in the Ganges-Brahmaputra River Basin Using Multi-Satellite Observations. In *Water* (Vol. 9, Issue 4). https://doi.org/10.3390/w9040245

Scherer, D., Schwatke, C., Dettmering, D., & Seitz, F. (2022). ICESat-2 Based River Surface Slope and Its Impact on Water Level Time Series From Satellite Altimetry. *Water Resources Research*, *58*(11), e2022WR032842. https://doi.org/https://doi.org/10.1029/2022WR032842

Schmitt Quedi, E., & Mainardi Fan, F. (2020). Sub seasonal streamflow forecast assessment at large-scale basins. *Journal of Hydrology*, *584*, 124635. https://doi.org/https://doi.org/10.1016/j.jhydrol.2020.124635

Schwatke, C., Dettmering, D., Bosch, W., & Seitz, F. (2015). DAHITI – an innovative approach for estimating water level time series over inland waters using multi-mission satellite altimetry. *Hydrology and Earth System Sciences*, *19*(10), 4345–4364. https://doi.org/10.5194/hess-19-4345-2015

Seyler, F., M.-P. Bonnet, S. Calmant, et al. 2005. «CASH « Contribution de l'Altimetrie Spatiale a l'hydrologie, Rapport intermediaire d'operation d'une recherche financee par le Ministere de la Recherche, Octobre 2005, Decision d'aide n: 04 T 131.

Seyler, F., Calmant, S., Silva, J., Filizola, N., Roux, E., Cochonneau, G., Vauchel, P., Bonnet, M., Seyler, F., Calmant, S., Silva, J., Filizola, N., Roux, E., Seyler, F., Calmant, S., Silva,

J., Filizola, N., & Roux, E. (2008). Monitoring water level in large trans-boundary ungauged basins with altimetry : the example of ENVISAT over the Amazon basin To cite this version : HAL Id : hal-01370629 Monitoring water level in large trans-boundary ungauged basins with altimetry : the e. *Journal of Applied Remote Sensing-SPIE*, *7150*.

Shelton, M. L. (2009). *Hydroclimatology: Perspectives and applications* (M. L. Shelton (ed.)). Cambridge Univerity Press.

Shepherd, A., Gilbert, L., Muir, A. S., Konrad, H., McMillan, M., Slater, T., Briggs, K. H., Sundal, A. V, Hogg, A. E., & Engdahl, M. E. (2019). Trends in Antarctic Ice Sheet Elevation and Mass. *Geophysical Research Letters*, *46*(14), 8174–8183. https://doi.org/https://doi.org/10.1029/2019GL082182

Silberstein, R. P. (2006). Hydrological models are so good, do we still need data? *Environmental Modelling & Software*, *21*(9), 1340–1352. https://doi.org/https://doi.org/10.1016/j.envsoft.2005.04.019

Singh, V. P. (1995). *Computer models of watershed hydrology*. Water Resources Publications.

Singh, V. P. (2018). Hydrologic modeling: progress and future directions. *Geoscience Letters*, *5*(1), 15. https://doi.org/10.1186/s40562-018-0113-z

Siqueira, V A, Paiva, R. C. D., Fleischmann, A. S., Fan, F. M., Ruhoff, A. L., Pontes, P. R. M., Paris, A., Calmant, S., & Collischonn, W. (2018). Toward continental hydrologic--hydrodynamic \hack{\break} modeling in South America. *Hydrology and Earth System Sciences*, *22*(9), 4815–4842. https://doi.org/10.5194/hess-22-4815-2018

Siqueira, Vin\'\icius Alencar, Collischonn, W., Fan, F. M., & Chou, S. C. (2016). Ensemble flood forecasting based on operational forecasts of the regional Eta EPS in the Taquari-Antas basin. *RBRH*, *21*, 587–602.

Siqueira, Vin\'\icius Alencar, Fleischmann, A., Jardim, P. F., Fan, F. M., & Collischonn, W. (2016). IPH-Hydro Tools: a GIS coupled tool for watershed topology acquisition in an open-source environment. *Rbrh*, *21*, 274–287.

Sood, A., & Smakhtin, V. (2015). Global hydrological models : a review. *Hydrological Sciences Journal*, *60*(4), 549–565. https://doi.org/10.1080/02626667.2014.950580

Sorribas, M. V., Paiva, R. C. D., Melack, J. M., Bravo, J. M., Jones, C., Carvalho, L., Beighley, E., Forsberg, B., & Costa, M. H. (2016). Projections of climate change effects on discharge

and inundation in the Amazon basin. *Climatic Change*, *136*(3), 555–570. https://doi.org/10.1007/s10584-016-1640-2

Spencer, R. G. M., Hernes, P. J., Dinga, B., Wabakanghanzi, J. N., Drake, T. W., & Six, J. (2016). Origins, seasonality, and fluxes of organic matter in the Congo River. *Global Biogeochemical Cycles*, *30*(7), 1105–1121. https://doi.org/https://doi.org/10.1002/2016GB005427

Sridhar, V., Kang, H., Ali, S. A., Bola, G. B., Tshimanga, R. M., & Lakshmi, V. (2022). Water Budgets and Droughts under Current and Future Conditions in the Congo River Basin. In Raphael M. Tshimanga, G. D. M. N'kaya, & D. Alsdorf (Eds.), *Congo Basin Hydrology, Climate, and Biogeochemistry A Foundation for the Future* (pp. 165–185). American Geophysical Union and John Wiley and Sons, Inc. https://doi.org/10.1002/9781119657002.ch10

Stammer, D., & Cazenave, A. (2017). *Satellite Altimetry over Oceans and Land Surfaces*. Taylor & Francis Group.

Sun, W., Ishidaira, H., & Bastola, S. (2012). Calibration of hydrological models in ungauged basins based on satellite radar altimetry observations of river water level. *Hydrological Processes*, *26*(23), 3524–3537. https://doi.org/10.1002/hyp.8429

Tapley, B. D., Bettadpur, S., Ries, J. C., Thompson, P. F., & Watkins, M. M. (2004). GRACE Measurements of Mass Variability in the Earth System. *Science*, *305*(5683), 503–505. https://doi.org/10.1126/science.1099192

Tapley, B. D., Born, G. H., & Parke, M. E. (1982). The SEASAT altimeter data and its accuracy assessment. *Journal of Geophysical Research: Oceans*, *87*(C5), 3179–3188. https://doi.org/https://doi.org/10.1029/JC087iC05p03179

Tarek, M., Brissette, F. P., & Arsenault, R. (2020). Evaluation of the ERA5 reanalysis as a potential reference dataset for hydrological modelling over North America. *Hydrology and Earth System Sciences*, *24*(5), 2527–2544. https://doi.org/10.5194/hess-24-2527-2020

Tarpanelli, A., Barbetta, S., Brocca, L., & Moramarco, T. (2013). River Discharge Estimation by Using Altimetry Data and Simplified Flood Routing Modeling. In *Remote Sensing* (Vol. 5, Issue 9, pp. 4145–4162). https://doi.org/10.3390/rs5094145

Tarpanelli, A., Paris, A., Sichangi, A. W., O`Loughlin, F., & Papa, F. (2022). Water Resources

in Africa: The Role of Earth Observation Data and Hydrodynamic Modeling to Derive River Discharge. *Surveys in Geophysics*. https://doi.org/10.1007/s10712-022-09744-x

Thiery, D. (1993). Calage automatique des modèles hydrodynamiques maillés. Détermination de zones géographiques homogènes et des paramètres optimaux associés. Application à 5 systèmes aquifères. *Hydrogéologie*, *4*, 281–291.

Todd, D. K., & Mays, L. W. (2005). *Groundwater hydrology* (J. Welter, V. A. Vargas, & T. Kulesa (eds.); Third Edit). John Wiley and Sons, Inc.

Tramblay, Y., Rouché, N., Paturel, J.-E., Mahé, G., Boyer, J.-F., Amoussou, E., Bodian, A., Dacosta, H., Dakhlaoui, H., Dezetter, A., Hughes, D., Hanich, L., Peugeot, C., Tshimanga, R., & Lachassagne, P. (2021). ADHI: the African Database of Hydrometric Indices (1950--2018). *Earth System Science Data*, *13*(4), 1547–1560. https://doi.org/10.5194/essd-13-1547-2021

Trigg, M. A., & Tshimanga, R. M. (2020). Capacity Building in the Congo Basin: Rich Resources Requiring Sustainable Development. *One Earth*, *2*(3), 207–210. https://doi.org/https://doi.org/10.1016/j.oneear.2020.02.008

Tshimanga, R. M., & Hughes, D. A. (2012). Climate change and impacts on the hydrology of the Congo Basin: The case of the northern sub-basins of the Oubangui and Sangha Rivers. *Physics and Chemistry of the Earth*, *50–52*, 72–83. https://doi.org/10.1016/j.pce.2012.08.002

Tshimanga, R M, & Hughes, D. A. (2014). Basin-scale performance of a semi-distributed rainfall-runoff model for hydrological predictions and water resources assessment of large rivers: the Congo River. *Water Resources Research*, *50*, 1174–1188. https://doi.org/10.1002/2013WR014310.Received

Tshimanga, R M, Hughes, D. A., & Kapangaziwiri, E. (2011). Initial calibration of a semi-distributed rainfall runoff model for the Congo River basin. *Physics and Chemistry of the Earth*, *36*(14–15), 761–774. https://doi.org/10.1016/j.pce.2011.07.045

Tshimanga, R M, Tshitenge, J. M., Kabuya, P., Alsdorf, D., Mahe, G., Kibukusa, G., & Lukanda, V. (2016). A Regional Perceptive of Flood Forecasting and Disaster Management Systems for the Congo River Basin. In T. E. Adams & T. C. B. T.-F. F. Pagano (Eds.), *Flood Forecasting A Global Perspective* (pp. 87–124). Academic Press. https://doi.org/https://doi.org/10.1016/B978-0-12-801884-2.00004-9

Tshimanga, Raphael M. (2022). Two Decades of Hydrologic Modeling and Predictions in the Congo River Basin. In Raphael M. Tshimanga, G. D. M. N'kaya, & D. Alsdorf (Eds.), *Congo Basin Hydrology, Climate, and Biogeochemistry A Foundation for the Future* (pp. 205–236). American Geophysical Union and John Wiley and Sons, Inc. https://doi.org/10.1002/9781119657002.ch12

Tshimanga, Raphael M., N'kaya, G. D. M., & Alsdorf, D. (2022). *Congo Basin Hydrology, Climate, and Biogeochemistry A Foundation for the Future* (Raphael M. Tshimanga, G. D. M. N'kaya, & D. Alsdorf (eds.)). American Geophysical Union and John Wiley and Sons, Inc.

Tshimanga, Raphael M., Trigg, M. A., Neal, J., Ndomba, P. M., Hughes, D. A., Carr, A. B., Kabuya, P. M., Bola, G. B., Mushi, C. A., Beya, J. T., Ngandu, F. K., Mokango, G. M., Mtalo, F., & Bates, P. D. (2022). New Measurements of Water Dynamics and Sediment Transport along the Middle Reach of the Congo River and the Kasai Tributary. In Raphael M. Tshimanga, G. D. M. N'kaya, & D. Alsdorf (Eds.), *Congo Basin Hydrology, Climate, and Biogeochemistry A Foundation for the Future* (pp. 447–467). American Geophysical Union and John Wiley and Sons, Inc. https://doi.org/10.1002/9781119657002.ch23

Tshimanga, Raphael M, Trigg, M. A., Neal, J., Ndomba, P. M., Hughes, D. A., Carr, A. B., Kabuya, P. M., Bola, G. B., Mushi, C. A., Beya, J. T., Ngandu, F. K., Mokango, G. M., Mtalo, F., & Bates, P. D. (2022). New Measurements of Water Dynamics and Sediment Transport along the Middle Reach of the Congo River and the Kasai Tributary. In *Congo Basin Hydrology, Climate, and Biogeochemistry* (pp. 447–467). https://doi.org/https://doi.org/10.1002/9781119657002.ch23

Tucci, C. E. M. (1986). Modelos matemáticos em hidrologia e hidráulica. *Revista Brasileira de Engenharia*, *2*.

United Nations (2019) Department of Economic and Social Affairs, Population Division. World Population Prospects 2019: Volume I: Comprehensive Tables. https:// popul ation. un. org/ wpp/ Publi catio ns/ Files/WPP20 19Vol ume- IComp rehen sive- Tables. pdf. Accessed 13 Feb 2023

Verhegghen, A., Mayaux, P., De Wasseige, C., & Defourny, P. (2012). Mapping Congo Basin vegetation types from 300 m and 1 km multi-sensor time series for carbon stocks and forest areas estimation. *Biogeosciences*, *9*(12), 5061–5079. https://doi.org/10.5194/bg-9-5061-

2012

Viessman, W., & Lewis, G. L. (1995). *Introduction to Hydrology (4th Edition)* (W. Viessman & G. L. Lewis (eds.); 4th Editio). Harpercollins College Div.

Vörösmarty, C. J., & Sahagian, D. (2000). Anthropogenic Disturbance of the Terrestrial Water Cycle. *BioScience*, *50*(9), 753–765. https://doi.org/10.1641/0006-3568(2000)050[0753:ADOTTW]2.0.CO;2

Ward, N. D., Bianchi, T. S., Medeiros, P. M., Seidel, M., Richey, J. E., Keil, R. G., & Sawakuchi, H. O. (2017). Where Carbon Goes When Water Flows: Carbon Cycling across the Aquatic Continuum. *Frontiers in Marine Science*, *4*. https://doi.org/10.3389/fmars.2017.00007

White, L. J. T., Masudi, E. B., Ndongo, J. D., Matondo, R., Soudan-Nonault, A., Ngomanda, A., Averti, I. S., Ewango, C. E. N., Sonké, B., & Lewis, S. L. (2021). Congo Basin rainforest - invest US$150 million in science. *Nature*, *598*(7881), 411–414. https://doi.org/10.1038/d41586-021-02818-7

Wohl, E. (2021). An Integrative Conceptualization of Floodplain Storage. *Reviews of Geophysics*, *59*(2), e2020RG000724. https://doi.org/https://doi.org/10.1029/2020RG000724

Wongchuig Correa, S., Paiva, R. C. D. de, Espinoza, J. C., & Collischonn, W. (2017). Multi-decadal Hydrological Retrospective: Case study of Amazon floods and droughts. *Journal of Hydrology*, *549*, 667–684. https://doi.org/https://doi.org/10.1016/j.jhydrol.2017.04.019

Wongchuig, S. C., de Paiva, R. C. D., Siqueira, V., & Collischonn, W. (2019). Hydrological reanalysis across the 20th century: A case study of the Amazon Basin. *Journal of Hydrology*, *570*, 755–773. https://doi.org/https://doi.org/10.1016/j.jhydrol.2019.01.025

Woolway, R. I., Kraemer, B. M., Lenters, J. D., Merchant, C. J., O'Reilly, C. M., & Sharma, S. (2020). Global lake responses to climate change. *Nature Reviews Earth & Environment*, *1*(8), 388–403. https://doi.org/10.1038/s43017-020-0067-5

Wu, G., Xiao, X., & Liu, Y. (2022). Satellite-Based Surface Water Storage Estimation: Its history, current status, and future prospects. *IEEE Geoscience and Remote Sensing Magazine*, *10*(3), 10–31. https://doi.org/10.1109/MGRS.2022.3175159

Yamazaki, D., Kanae, S., Kim, H., & Oki, T. (2011). A physically based description of

floodplain inundation dynamics in a global river routing model. *Water Resources Research*, *47*(4). https://doi.org/https://doi.org/10.1029/2010WR009726

Yamazaki, D., O'Loughlin, F., Trigg, M. A., Miller, Z. F., Pavelsky, T. M., & Bates, P. D. (2014). Development of the Global Width Database for Large Rivers. *Water Resources Research*, *50*(4), 3467–3480. https://doi.org/https://doi.org/10.1002/2013WR014664

Yoosefdoost, I., Bozorg-Haddad, O., Singh, V. P., & Chau, K. W. (2022). Hydrological Models BT - Climate Change in Sustainable Water Resources Management. In O. Bozorg-Haddad (Ed.), *Climate Change in Sustainable Water Resources Management* (pp. 283–329). Springer Nature Singapore. https://doi.org/10.1007/978-981-19-1898-8_8

Zakharova, E. A., Kouraev, A. V, Cazenave, A., & Seyler, F. (2006). Amazon River discharge estimated from TOPEX/Poseidon altimetry. *Comptes Rendus Geoscience*, *338*(3), 188–196. https://doi.org/https://doi.org/10.1016/j.crte.2005.10.003

Zheng, Y., Niu, Z., Gong, P., & Wang, J. (2015). A database of global wetland validation samples for wetland mapping. *Science Bulletin*, *60*(4), 428–434. https://doi.org/10.1007/s11434-014-0717-4

Etude de la ressource en eau en lien avec le climat dans le bassin du Congo : Approche intégrée utilisant des données in situ, la télédétection et la modélisation hydrologique

Résumé – Le bassin du Congo est le deuxième plus grand au monde en termes de débit fluvial et d'aire de drainage. Pourtant, ses caractéristiques hydrodynamiques et hydro-climatiques restent relativement mal connues, principalement en raison de sa complexité et du manque d'observations in situ adéquates. Une approche robuste basée sur une combinaison de mesures in situ et issues de la télédétection, associées à la modélisation hydrologique, est ainsi proposée pour caractériser l'hydrologie de surface du bassin du Congo et sa variabilité. Un nombre sans précédent de mesures in situ et d'observations satellites est traité et validé, puis utilisé pour améliorer notre compréhension de l'hydrodynamique et de l'hydro-climatologie du bassin. Les résultats sont ensuite intégrés dans le développement d'un modèle hydrologique dont l'utilisation s'avère précieuse à différentes échelles pour la prévision et la gestion des ressources en eau du bassin.

Mots-clés: Bassin du Congo, Altimétrie spatiale, Étendue des eaux de surface, Stockage des eaux de surface et souterraines, modélisation hydrodynamique

Study of water resources in relation with climate in the Congo River basin: integrated approach using in situ observations, remote sensing, and hydrological modeling

Abstract – The Congo River basin (CRB) is the world's second largest in terms of river discharge and drainage area. Yet, its hydrodynamic and hydroclimatic characteristics remained relatively poorly known mainly due to its complexity and a lack of adequate in situ observations. To overcome this challenge, a robust approach based on a combination of in situ measurement, remote sensing techniques associated with hydrological modeling is proposed for a comprehensive characterization of the CRB surface hydrology at large scale. An unprecedented and consistent number of in situ measurement and satellite derived observation is processed and validated, which is then used to develop an understanding of the basin hydrodynamics and hydro-climatology. This understanding is later integrated into the development of a hydrological model that can be used for prediction and water resources management across different scales in the basin.

Keywords: Congo River basin, Radar Altimetry, Surface Water Extent, Surface and Sub-surface water storage, Hydrodynamic modeling